Hazardous Emissions from Co – Combustion of Coal, Biomass and Waste

Brendon Miller

Imperial College of Science, Technology and Medicine
University of London

Thesis submitted in partial fulfilment of the requirements of the degree of Doctor of Philosophy.

Univ.

ABSTRACT

Combustion is a convenient method for waste disposal. It reduces the volume of waste, and the resulting heat can be used for district heating, or for generating electricity. In either application, utilisation of waste could supplant fossil fuels. Waste fuels, however, vary in quality and availability. These variations can be 'buffered' by co-combusting waste with a supporting fuel.

In this study, hazardous emissions from co-combustion were measured in a novel quartz "suspension-firing" reactor under conditions relevant to fluidised bed combustors. The design of the suspension-firing reactor allowed examination of fuel particle combustion in the absence of added bed solids. Experiments have been conducted using two coals (Polish and Colombian), four biomass fuels (wood-bark, straw, pulp sludge and paper sludge) and three wastes (agricultural waste, sewage sludge and plastic waste).

Concentrations of eighteen trace elements were measured in the raw fuels and ashes. Sewage sludge had the highest trace element content of the fuels studied, whilst straw the lowest. After combustion sewage sludge also retained the greatest proportion of its trace elements in ash, paper sludge retained the lowest proportion. Based on their average retention in ashes the trace elements have been ranked. The most volatile trace elements were Hg and Se, followed by Cd, Tl, Pb and As. More of the Zn, Sb, Cr, V, Cu, Sr, Mo, Mn and Ba contained in the fuel were retained in ash. Be, Co and Ni were retained in ash to the highest degree.

Twenty-one trace element – fuel combinations that are potentially problematic if burnt in fluidised bed combustors have been identified. Fuels potentially most problematic were plastic waste (Cd, Cu, Pb and Zn), agricultural waste (Hg, V and Zn), paper sludge (Cr, Pb and Zn) and pulp sludge (Cd, Cu and Zn).

One fuel sample, wood-bark, was burnt in the presence of injected HCl and SO_2 gases. The presence of injected HCl decreased the retention of Cd, Cu, Zn, Mn and Ba in ash compared to combustion without either gas being injected. Injection of SO_2 increased the retention of As and Hg in ash and decreased that of Cd.

NOx and N_2O emissions from co-combustion of the fuel samples were also measured. The highest NOx emissions were from combustion of the Polish coal / sewage sludge blends (up to 560 mg/m^3 at 6% oxygen), whilst the lowest were from wood-bark, approximately 300 mg/m^3. N_2O was emitted from the combustion of Polish coal (75 mg/m^3) and Colombian coal (125 mg/m^3). Emissions fell when Colombian coal was blended with paper sludge or straw, but appeared unchanged by Polish coal / sewage sludge blending. N_2O concentrations were generally higher during combustion at 800 °C than at 900 °C; however, the influence of combustion temperature on NOx emissions appeared insignificant.

For my parents, Karen and Bruce

ACKNOWLEDGEMENTS

Finally! This thesis is finished. That I have got this far is thanks to the many people who have given their assistance and advice during the last three and one half years. I don't have space to name all of you here, but your effort is appreciated, thank you.

Firstly, I would like to thank my PhD supervisors Dr Denis Dugwell and Professor Raphael Kandiyoti for their help and support during this project. Thanks also to the other senior members of the Fuel Processing group, Drs Nigel Patterson, Graham Reed and Alan Herod for giving me the benefit of their long (but not too long!) years of experience in coal research. Thanks also to Trevor Morgan, the Fuel Processing Group's Technician, for his patience in analysing samples, assistance in running the suspension reactor and company in the student union (Dr Carlos Islas is also included in the last comment!).

I must also thank members of the technical staff for their help. To Bob King and his workshop staff, especially Richard Wallington and Ken Guernsey for their help taking my rough sketches and my impractical ideas and suggesting improvements to turn them into physical reality. Thanks also to Colin Smith, the glassblower, for his patience with my frequent experiments into finding the fracture toughness of glass and quartz.

Thanks also to all the other students of the Fuel Processing group, during my time at Imperial, not just for your help in the lab and during thesis preparation, but also for your friendship and understanding when things weren't going to plan for me.

Finally, I would like to thank someone, not for his contribution to the thesis, but for his friendship, his understanding and for being there for me. Thanks Darrell. I wish you, Emma and your soon to be born child the best luck for your future together.

TABLE OF CONTENTS

ABSTRACT **2**

ACKNOWLEDGEMENTS **5**

TABLE OF CONTENTS **6**

LIST OF FIGURES **11**

LIST OF TABLES **20**

LIST OF ABBREVIATIONS **21**

1.0 INTRODUCTION **22**

2.0 BACKGROUND **25**

2.1 TRACE ELEMENTS IN COAL, BIOMASS AND WASTES 25
2.2 ORIGINS AND MODES OF OCCURRENCE OF TRACE ELEMENTS 26
2.2.1 Trace Elements in Coal *26*
2.2.2 Trace Elements in Biomass *28*
2.2.3 Trace Elements in Wastes *29*
2.3 COMBUSTION BEHAVIOUR OF TRACE ELEMENTS 32
2.4 THERMODYNAMIC EQUILIBRIUM MODELLING OF TRACE ELEMENTS 35
2.4 FORMATION OF NITROGEN OXIDES DURING COMBUSTION 36
2.4.1 Mechanisms of NO and N_2O Formation *37*

3.0 EXPERIMENTAL **40**

3.1 REACTOR DEVELOPMENT 40
3.1.1 Fuel Feeding *42*
3.1.2 Fuel Flow on Injection *43*
3.1.3 Retention of Fuel and Ash Within the Suspension-Firing Reactor *44*
3.1.4 Temperature Profile, Measurement and Control *45*
3.2 REACTOR PREPARATION AND ASH COLLECTION 48
3.3 ANALYSIS TECHNIQUES 49
3.3.1 Digestion of Samples for Trace and Minor Element Analysis *50*
3.3.3 Analysis of NOx, N_2O and O_2 In Flue Gas *53*
3.3.4 Ultimate Analysis of Raw Fuel Samples *54*
3.3.5 Proximate Analysis of Raw Fuel Samples *54*
3.3.6 Raw Fuel Volatile Matter Content and Char Reactivity *55*
3.3.7 Measurement of Raw Fuel and Ash Mercury Contents *55*
3.3.8 Calculation of Air / Fuel Ratio *56*
3.4 THERMODYNAMIC EQUILIBRIUM MODELLING OF TRACE ELEMENT BEHAVIOUR .. 56
3.4.1 Thermodynamic Equilibrium Model *57*
3.5 PRESENTATION OF TRACE ELEMENT RESULTS 60
3.6 EXPERIMENTAL ERROR IN TRACE ELEMENT MEASUREMENTS 62

4.0 CHARACTERISATION OF THE RAW FUELS **63**

4.1 ORIGINS OF THE RAW FUELS 63

4.2 MAJOR, MINOR, PROXIMATE AND REACTIVITY ANALYSES OF THE RAW FUELS ... 64
4.3 TRACE ELEMENTS CONTENTS OF THE RAW FUELS ... 68

5.0 RESULTS ... 74

5.0.1 The Influence of Combustion Temperature ... 75
5.0.2 Retention of Trace Elements Predicted to Volatilise ... 75
5.0.3 Volatilisation of Trace Elements Predicted to Remain Completely in Ash ... 76
5.0.4 Compounds not Included in Thermodynamic Equilibrium Modelling ... 76
5.1 TRACE ELEMENT RESULTS FOR MAIN FUELS ... 77
5.2 POLISH COAL AND SEWAGE SLUDGE CO-COMBUSTION ... 89
5.2.1 Arsenic ... 94
5.2.2 Cadmium ... 96
5.2.3 Mercury ... 98
5.2.4 Selenium ... 99
5.2.5 Lead ... 99
5.2.6 Chromium ... 105
5.2.7 Copper ... 105
5.2.8 Nickel ... 108
5.2.9 Vanadium ... 108
5.2.10 Zinc ... 108
5.2.11 Beryllium ... 112
5.2.12 Manganese ... 113
5.2.13 Molybdenum ... 113
5.2.14 Thallium ... 113
5.2.15 Barium ... 117
5.2.16 Cobalt ... 117
5.2.17 Antimony ... 118
5.2.18 Strontium ... 119
5.3 COLOMBIAN COAL AND PAPER SLUDGE CO-COMBUSTION ... 120
5.3.1 Arsenic ... 123
5.3.2 Cadmium ... 125
5.3.3 Mercury ... 126
5.3.4 Selenium ... 126
5.3.5 Lead ... 127
5.3.6 Chromium ... 131
5.3.7 Copper ... 131
5.3.8 Nickel ... 133
5.3.9 Vanadium ... 133
5.3.10 Zinc ... 134
5.3.11 Beryllium ... 138
5.3.12 Manganese ... 139
5.3.13 Molybdenum ... 139
5.3.14 Thallium ... 140

5.3.15 Barium *143*
5.3.16 Cobalt *143*
5.3.17 Antimony *145*
5.3.18 Strontium *146*
5.4 COLOMBIAN COAL, STRAW AND PAPER SLUDGE CO COMBUSTION 147
5.4.1 Arsenic *149*
5.4.2 Cadmium *149*
5.4.3 Mercury *149*
5.3.4 Selenium *150*
5.4.5 Lead *150*
5.4.6 Chromium *152*
5.4.7 Copper *152*
5.4.8 Nickel *152*
5.4.9 Vanadium *153*
5.4.10 Zinc *153*
5.4.11 Beryllium *156*
5.4.12 Manganese *156*
5.4.13 Molybdenum *157*
5.4.14 Thallium *157*
5.4.15 Barium *160*
5.4.16 Cobalt *160*
5.4.17 Antimony *161*
5.4.18 Strontium *162*
5.5 WOOD-BARK AND AGRICULTURAL WASTE CO-COMBUSTION 164
5.5.1 Arsenic *167*
5.5.2 Cadmium *168*
5.5.3 Mercury *171*
5.5.4 Selenium *171*
5.5.5 Lead *172*
5.5.6 Chromium *175*
5.5.7 Copper *175*
5.5.8 Nickel *177*
5.5.9 Vanadium *179*
5.5.10 Zinc *179*
5.5.11 Beryllium *183*
5.5.12 Manganese *185*
5.5.13 Molybdenum *185*
5.5.14 Thallium *185*
5.5.15 Barium *189*
5.5.16 Cobalt *189*
5.5.17 Antimony *190*
5.5.18 Strontium *190*

5.6 CO-COMBUSTION OF WOOD – BARK AND PULP SLUDGE 192
5.6.1 Arsenic *195*
5.6.2 Cadmium *196*
5.6.3 Mercury *197*
5.6.4 Selenium *197*
5.6.5 Lead *197*
5.6.6 Chromium *201*
5.6.7 Copper *201*
5.6.8 Nickel *202*
5.6.9 Vanadium *203*
5.6.10 Zinc *203*
5.6.11 Beryllium *206*
5.6.12 Manganese *206*
5.6.13 Molybdenum *207*
5.6.14 Thallium *207*
5.6.15 Barium *210*
5.6.16 Cobalt *210*
5.6.17 Antimony *211*
5.6.18 Strontium *212*
5.7 CO- COMBUSTION OF WOOD-BARK AND PLASTIC WASTE 213
5.7.1 Arsenic *216*
5.7.2 Cadmium *217*
5.7.3 Mercury *217*
5.7.4 Selenium *218*
5.7.5 Lead *218*
5.7.6 Chromium *222*
5.7.7 Copper *222*
5.7.8 Nickel *223*
5.7.9 Vanadium *224*
5.7.10 Zinc *225*
5.7.11 Beryllium *228*
5.7.12 Manganese *228*
5.7.13 Molybdenum *229*
5.7.14 Thallium *229*
5.7.15 Barium *232*
5.7. 16 Cobalt *232*
5.7.17 Antimony *233*
5.7.18 Strontium *234*
5.8 COMBUSTION OF WOOD-BARK IN THE PRESENCE OF INJECTED HCL AND SO_2 235
5.8.1 Arsenic *237*
5.8.2 Cadmium *237*
5.8.3 Mercury *238*

5.8.4 Selenium *239*
5.8.5 Lead *239*
5.8.6 Chromium *242*
5.8.7 Copper *242*
5.8.8 Nickel *243*
5.8.9 Vanadium *243*
5.8.10 Zinc *244*
5.8.11 Beryllium *246*
5.8.12 Manganese *246*
5.8.13 Molybdenum *247*
5.8.14 Thallium *247*
5.8.15 Barium *249*
5.8.16 Cobalt *249*
5.8.17 Antimony *250*
5.8.18 Strontium *250*
5.9 NOx AND N_2O EMISSIONS FROM CO-COMBUSTION 251
5.9.1 Polish Coal and Sewage Sludge Blends *253*
5.9.2 Colombian Coal and Paper Sludge Blends *255*
5.9.3 Colombian Coal/Straw and Paper Sludge Blends *257*
5.9.4 Wood-Bark and Agricultural Waste Blends *259*
5.9.5 Wood-Bark and Pulp Sludge Blends *261*
5.9.6 Wood-Bark and Plastic Waste Blends *262*

6.0 SUMMARY AND DISCUSSION OF TRACE ELEMENT RESULTS 264

6.1 TRACE ELEMENT CONTENTS OF THE RAW FUELS 265
6.2 BEHAVIOUR OF TRACE ELEMENTS DURING CO-COMBUSTION 266
6.3 INFLUENCE OF FUEL TYPE ON TRACE ELEMENT RETENTION 273
6.4 POSSIBLE PROBLEMATICAL TRACE ELEMENT EMISSIONS DURING COMBUSTION. 274

7.0 CONCLUSIONS 276

7.1 Trace Element Contents of the Raw Fuels *276*
7.2 Trace Element Behaviour During Co-Combustion *276*
7.3 Influence of Fuel Type on Trace Element Retention *277*
7.4 Possible Problematical Trace Elements Emissions from Combustion *277*
7.5 NOx and N_2O Emissions from Co-Combustion *278*

8.0 RECOMMENDATIONS FOR FUTURE WORK 279

REFERENCES 280

APPENDIX A: RAW TRACE ELEMENT RESULTS ..... CD

APPENDIX B: SYNERGY DIAGRAMS ..... CD

APPENDIX C: SPECIES INCLUDED IN THERMODYNAMIC MODELS ..... CD

Appendices included on the CD inside the back cover

List of Figures

Figure 1 Partitioning of Trace Elements During Pulverised Coal Combustion..... 33
Figure 2 The Suspension-Firing Reactor 41
Figure 3 Fuel Addition from Feeding System 42
Figure 4 Consecutive Photographs of Fuel Flow Penetration During Injection..... 43
Figure 5 Particle Size Distributions of Sinter and Bottom Ash 44
Figure 6 Sintered Quartz Plate and Top Closure Details..... 45
Figure 7 Axial Temperature Distribution at Reactor Centre and Walls, Without Fuel, 800 and 900°C 46
Figure 8 Temperature Distribution Inside the Suspension-Firing Reactor..... 47
Figure 9 Thermodynamic Equilibrium Prediction for Arsenic During Wood-Bark Combustion..... 61
Figure 10 Percentage Retention of As, Cd, Hg, Se and Pb in Ash After Combustion of the Main Fuels 78
Figure 11 Relative Enrichment of As, Cd, Hg, Se and Pb in Sinter Ash During Combustion of the Main Fuels..... 79
Figure 12 Percentage Retention of Cr, Cu, Ni, V and Zn in Ash After Combustion of the Main Fuels 81
Figure 13 Relative Enrichment of Cr, Cu, Ni, V and Zn in Sinter Ash During Combustion of the Main Fuels..... 82
Figure 14 Percentage Retention of Be, Mn, Mo and Tl in Ash After Combustion of the Main Fuels 84
Figure 15 Relative Enrichment of Be, Mn, Mo and Tl in Sinter Ash During Combustion of the Main Fuels 85
Figure 16 Percentage Retention of Ba, Co, Sb and Sr in Ash After Combustion of the Main Fuels 87
Figure 17 Relative Enrichment of Ba, Co, Sb and Sr in Sinter Ash During Combustion of the Main Fuel..... 88
Figure 18 Percentage Retention of As, Cd, Hg, Se and Pb in Ash After Polish Coal / Sewage Sludge Co-Combustion 92
Figure 19 Relative Enrichment of As, Cd, Hg, Se and Pb in Sinter Ash During Polish Coal / Sewage Sludge Co-Combustion..... 93

Figure 20 Synergy for Arsenic Retention by Polish Coal / Sewage Sludge Blends..... 94
Figure 21 Thermodynamic Equilibrium Prediction for Arsenic During Polish Coal Combustion..... 95
Figure 22 Thermodynamic Equilibrium Prediction for Arsenic During 70 % Polish Coal / 30 % Sewage Sludge Combustion..... 95
Figure 23 Thermodynamic Equilibrium Prediction for Arsenic During Sewage Sludge Combustion..... 96
Figure 24 Thermodynamic Equilibrium Prediction for Cadmium During Polish Coal Combustion..... 97
Figure 25 Thermodynamic Equilibrium Prediction for Cadmium During Sewage Sludge Combustion..... 97
Figure 26 Possible Synergy in Retention of Lead by Polish Coal / Sewage Sludge 100
Figure 27 Lead Concentration in Bottom Ash of Polish Coal / Sewage Sludge Blends 100
Figure 28 Thermodynamic Equilibrium Prediction for Lead During Polish Coal Combustion..... 101
Figure 29 Thermodynamic Equilibrium Prediction for Lead During 70 % Polish Coal / 30 % Sewage Sludge Combustion..... 102
Figure 30 Thermodynamic Equilibrium Prediction for Lead During Sewage Sludge Combustion..... 102
Figure 31 Percentage Retention of Cr, Cu Ni, V and Zn in Ash After Polish Coal / Sewage Sludge Co-Combustion 103
Figure 32 Relative Enrichment of Cr, Cu, Ni, V and Zn in Sinter Ash During Polish Coal / Sewage Sludge Co-Combustion..... 104
Figure 33 Thermodynamic Equilibrium Model for Copper During Combustion of Polish Coal..... 106
Figure 34 Thermodynamic Equilibrium Model for Copper During Combustion of 70 % Polish Coal / 30 % Sewage Sludge..... 107
Figure 35 Thermodynamic Equilibrium Model for Copper During Combustion of Sewage Sludge..... 107
Figure 36 Thermodynamic Equilibrium Model for Zinc During Polish Coal Combustion 109
Figure 37 Percentage Retention of Be, Mn, Mo and Tl in Ash During Polish Coal / Sewage Sludge Co-Combustion 110

Figure 38 Relative Enrichment of Be, Mn, Mo and Tl in Sinter Ash During Combustion of Polish Coal and Sewage Sludge 111
Figure 39 Thermodynamic Equilibrium Model for Beryllium During Polish Coal Combustion 112
Figure 40 Percentage Retention of Ba, Co, Sb and Sr in Ash After Polish Coal / Sewage Sludge Co-Combustion 115
Figure 41 Relative Enrichment of Ba, Co, Sb and Sr in Sinter Ash During Combustion of Polish Coal and Sewage Sludge 116
Figure 42 Thermodynamic Equilibrium Prediction for Cobalt During Polish Coal Combustion 117
Figure 43 Thermodynamic Equilibrium Model for Antimony During Polish Coal Combustion 118
Figure 44 Percentage Retention of As, Cd, Hg, Se and Pb During Colombian Coal / Paper Sludge Co-Combustion 121
Figure 45 Relative Enrichment of As, Cd, Hg, Se and Pb in Sinter Ash During Colombian Coal / Paper Sludge Co- Combustion 122
Figure 46 Thermodynamic Equilibrium Prediction for Arsenic During Colombian Coal Combustion 124
Figure 47 Thermodynamic Equilibrium Prediction for Arsenic During 70 % Colombian Coal / 30 % Paper Sludge Combustion 124
Figure 48 Thermodynamic Equilibrium Prediction for Cadmium During Colombian Coal Combustion 125
Figure 49 Thermodynamic Equilibrium Model for Lead During Colombian Coal Combustion 127
Figure 50 Percentage Retention of Cr, Cu Ni, V and Zn During Colombian Coal / Paper Sludge Co-Combustion 129
Figure 51 Relative Enrichments of Cr, Cu, Ni, V and Zn in Sinter Ash During Combustion of Colombian Coal and Paper Sludge 130
Figure 52 Thermodynamic Equilibrium Prediction for Copper During Colombian Coal Combustion 132
Figure 53 Thermodynamic Equilibrium Prediction for Copper During 70 % Colombian Coal / 30 % Paper Sludge Combustion 132
Figure 54 Thermodynamic Equilibrium Prediction for Zinc During Colombian Coal Combustion 134

Figure 55 Thermodynamic Equilibrium Prediction for Zinc During 70 % Colombian Coal / 30 % Paper Sludge Combustion..... 135
Figure 56 Percentage Retention of Be, Mn, Mo and Tl in Ash After Colombian Coal / Paper Sludge Co-Combustion..... 136
Figure 57 Relative Enrichments of Be, Mn, Mo and Tl in Sinter Ash During Colombian Coal / Paper Sludge Co-Combustion..... 137
Figure 58 Thermodynamic Equilibrium Prediction for Beryllium During Colombian Coal Combustion..... 138
Figure 59 Thermodynamic Equilibrium Prediction for Beryllium During 70 % Colombian Coal / 30 % Paper Sludge Combustion..... 139
Figure 60 Partitioning of Ba, Co, Sb and Sr During Colombian Coal and Paper Sludge Co-Combustion..... 141
Figure 61 Relative Enrichments of Ba, Co, Sb, and Sr in Sinter Ash During Combustion of Colombian Coal and Paper Sludge..... 142
Figure 62 Thermodynamic Equilibrium Prediction for Cobalt During Colombian Coal Combustion..... 144
Figure 63 Thermodynamic Equilibrium Prediction for Cobalt During 70 % Colombian Coal / 30 % Paper Sludge Combustion..... 144
Figure 64 Thermodynamic Equilibrium Prediction for Antimony During Colombian Coal Combustion..... 145
Figure 65 Percentage Retention of As, Cd, Hg, Se and Pb in Ash After Colombian Coal / Straw and Paper Sludge Co -Combustion..... 148
Figure 66 Percentage Retention of Cr, Cu Ni, V and Zn in Ash After Colombian Coal / Straw and Paper Sludge Co-Combustion..... 151
Figure 67 Thermodynamic Equilibrium Prediction for Zinc During Colombian Coal / Straw Combustion..... 154
Figure 68 Thermodynamic Equilibrium Prediction for Zinc During Combustion of 70 % Colombian Coal / Straw with 30 % Paper Sludge..... 154
Figure 69 Percentage Retention of Be, Mn, Mo and Tl in Ash After Colombian Coal / Straw and Paper Sludge Co-Combustion..... 155
Figure 70 Thermodynamic Equilibrium Prediction for Beryllium During Colombian Coal / Straw Combustion..... 156
Figure 71 Percentage Retention of Ba, Co, Sb and Sr in Ash After Colombian Coal / Straw and Paper Sludge Co-Combustion..... 159

Figure 72 Thermodynamic Equilibrium Prediction for Cobalt During Colombian Coal / Straw Combustion 161
Figure 73 Thermodynamic Equilibrium Prediction for Cobalt During 70 % Colombian Coal / Straw with 30 % Paper Sludge Combustion 161
Figure 74 Thermodynamic Equilibrium Prediction for Antimony During Combustion of Colombian Coal / Straw 162
Figure 75 Percentage Retention of As, Cd, Hg, Se and Pb in Ash After Wood-Bark / Agricultural Waste Co-Combustion 165
Figure 76 Relative Enrichment of As, Cd, Hg, Se and Pb in Sinter Ash During Wood-Bark / Agricultural Waste Co- Combustion 166
Figure 77 Thermodynamic Equilibrium Prediction for Arsenic During Wood-Bark Combustion 167
Figure 78 Thermodynamic Equilibrium Prediction for Arsenic During Agricultural Waste Combustion 168
Figure 79 Thermodynamic Equilibrium Prediction for Cadmium During Wood-Bark Combustion 169
Figure 80 Thermodynamic Equilibrium Prediction for Cadmium During 70 % Wood-Bark / 30 % Agricultural Waste Combustion 170
Figure 81 Thermodynamic Equilibrium Prediction for Cadmium During Agricultural Waste Combustion 170
Figure 82 Thermodynamic Equilibrium Predictions for Lead During Wood-Bark Combustion 172
Figure 83 Percentage Retention of Cr, Cu Ni, V and Zn in Ash After Wood-Bark / Agricultural Waste Co-Combustion 173
Figure 84 Relative Enrichment of Cr, Cu, Ni, V and Zn in Sinter Ash During Wood-Bark / Agricultural Waste Combustion 174
Figure 85 Thermodynamic Equilibrium Model of Copper During Wood-Bark Combustion 176
Figure 86 Thermodynamic Equilibrium Model of Copper During Agricultural Waste Combustion 177
Figure 87 Thermodynamic Equilibrium Model of Nickel During Wood-Bark Combustion 178
Figure 88 Thermodynamic Equilibrium Model of Nickel During Agricultural Waste Combustion 178

Figure 89 Percentage Retention of Be, Mn, Mo and Tl in Ash After Wood-Bark / Agricultural Waste Co-Combustion 181
Figure 90 Relative Enrichment of Be, Mn, Mo and Tl in Sinter Ash During Combustion of Wood-Bark and Agricultural Waste 182
Figure 91 Thermodynamic Equilibrium Prediction for Beryllium During Wood-Bark Combustion 183
Figure 92 Thermodynamic Equilibrium Prediction for Beryllium During 70 % Wood-Bark / 30 % Agricultural Waste Combustion 184
Figure 93 Thermodynamic Equilibrium Prediction for Beryllium During Agricultural Waste Combustion 184
Figure 94 Percentage Retention of Ba, Co, Sb and Sr in Ash After Wood-Bark / Agricultural Waste Co-Combustion 187
Figure 95 Relative Enrichment of Ba, Co, Sb and Sr in Sinter Ash During Wood-Bark / Agricultural Waste Co-Combustion 188
Figure 96 Thermodynamic Equilibrium Prediction for Co During Wood-Bark Combustion 190
Figure 97 Percentage Retention of As, Cd, Hg, Se and Pb in Ash After Wood-Bark / Pulp Sludge Co-Combustion 193
Figure 98 Relative Enrichment of As, Cd, Hg, Se and Pb in Sinter Ash During Wood-Bark / Pulp Sludge Co-Combustion 194
Figure 99 Thermodynamic Equilibrium Prediction for Arsenic During 70 % Wood-Bark / 30 % Pulp Sludge Combustion 195
Figure 100 Thermodynamic Equilibrium Prediction for Cadmium During 70 % Wood-Bark / 30 % Pulp Sludge Combustion 196
Figure 101 Thermodynamic Equilibrium Prediction for Lead During 70 % Wood-Bark / 30 % Pulp Sludge Combustion 198
Figure 102 Percentage Retention of Cr, Cu, Ni, V and Zn in Ash After Wood-Bark / Pulp Sludge Co-Combustion 199
Figure 103 Relative Enrichment of Cr, Cu, Ni, V and Zn in Sinter Ash During Wood-Bark / Pulp Sludge Co-Combustion 200
Figure 104 Thermodynamic Equilibrium Model of Copper During Combustion of 70 % Wood-Bark / 30 % Pulp Sludge 202
Figure 105 Percentage Retention of Be, Mn, Mo and Tl in Ash After Wood-Bark / Pulp Sludge Co-Combustion 204

Figure 106 Relative Enrichment of Be, Mn, Mo and Tl in Sinter Ash During Wood-Bark / Pulp Sludge Co-Combustion 205
Figure 107 Thermodynamic Equilibrium Model for Beryllium During Combustion of 70 % Wood-Bark / 30 % Pulp Sludge 206
Figure 108 Percentage Retention of Ba, Co, Sb and Sr in Ash After Wood-Bark / Pulp Sludge Co-Combustion 208
Figure 109 Relative Enrichment of Ba, Co, Sb and Sr in Sinter Ash During Wood-Bark / Pulp Sludge Co-Combustion 209
Figure 110 Thermodynamic Equilibrium Prediction for Cobalt During 70 % Wood-Bark / 30 % Pulp Sludge Combustion 211
Figure 111 Thermodynamic Equilibrium Prediction for Antimony During 70 % Wood-Bark / 30 % Pulp Sludge Combustion 212
Figure 112 Percentage Retention of As, Cd, Hg, Se and Pb in Ash After Wood-Bark / Plastic Waste Co-Combustion 214
Figure 113 Relative Enrichment of As, Cd, Hg, Se and Pb in Sinter Ash During Wood-Bark / Plastic Waste Co-Combustion 215
Figure 114 Thermodynamic Equilibrium Prediction for Arsenic During 70 % Wood-Bark / 30 % Plastic Waste Combustion 216
Figure 115 Thermodynamic Equilibrium Prediction for Lead During 70 % Wood-Bark / 30 % Plastic Waste Combustion 219
Figure 116 Percentage Retention of Cr, Cu Ni, V and Zn in Ash After Wood-Bark / Plastic Co-Combustion 220
Figure 117 Relative Enrichment of Cr, Cu, Ni, V and Zn in Sinter Ash During Wood-Bark / Plastic Waste Co-Combustion 221
Figure 118 Thermodynamic Equilibrium Prediction for Copper During 70 % Wood-Bark / 30 % Plastic Waste Combustion 223
Figure 119 Thermodynamic Equilibrium Prediction for Nickel During 70 % Wood-Bark / 30 % Plastic Waste Combustion 224
Figure 120 Thermodynamic Equilibrium Prediction for Zinc during 70 % Wood-Bark / 30 % Plastic Waste Combustion 225
Figure 121 Percentage Retention of Be, Mn, Mo and Tl in Ash After Wood-Bark / Plastic Waste Co-Combustion 226
Figure 122 Relative Enrichment of Be, Mn, Mo and Tl in Sinter Ash Wood-Bark and Plastic Waste Co-Combustion 227

Figure 123 Thermodynamic Equilibrium Prediction of Beryllium During Combustion of 70 % Wood-Bark / 30 % Plastic Waste 228
Figure 124 Percentage Retention of Ba, Co, Sb and Sr in Ash After Wood-Bark / Plastic Waste Co-Combustion 230
Figure 125 Relative Enrichment of Ba, Co, Sb and Sr in Sinter Ash During Wood-Bark / Plastic Waste Co-Combustion 231
Figure 126 Thermodynamic Equilibrium Prediction for Cobalt During Combustion of 70 % Wood-Bark / 30 % Plastic Waste 233
Figure 127 Thermodynamic Equilibrium Prediction for Antimony During 70 % Wood-Bark / 30 % Plastic Waste Combustion 234
Figure 128 The Effect of HCl and SO_2 on the Behaviour of As, Cd, Hg, Se and Pb During Combustion of Wood-Bark at 800 °C 236
Figure 129 Thermodynamic Equilibrium Prediction for Cadmium During Wood-Bark Combustion in the Presence of Injected Sulphur Dioxide 238
Figure 130 Thermodynamic Equilibrium Prediction for Lead During Wood-Bark Combustion in the Presence of Injected Sulphur Dioxide 240
Figure 131 The Effect of HCl and SO_2 on the Behaviour of Cr, Cu, Ni, V and Zn During Combustion of Wood-Bark at 800 °C 241
Figure 132 Thermodynamic Equilibrium Prediction for Copper During Wood-Bark Combustion in the Presence of Injected Sulphur Dioxide 242
Figure 133 Thermodynamic Equilibrium Prediction for Nickel During Wood-Bark Combustion in the Presence of Injected Hydrogen Chloride 243
Figure 134 The Effect of HCl and SO_2 on the Behaviour of Be, Mn, Mo and Tl During Combustion of Wood-Bark at 800 °C 245
Figure 135 Thermodynamic Equilibrium Prediction for Manganese During Wood-Bark Combustion in the Presence of Injected Hydrogen Chloride 247
Figure 136 The Effect of HCl and SO_2 on the Behaviour of Ba, Co, Sb and Sr During Combustion of Wood-Bark at 800 °C 248
Figure 137 NOx Emissions from Polish Coal and Sewage Sludge Co-Combustion 253
Figure 138 Conversion of Polish Coal and Sewage Sludge Fuel Nitrogen to NO 254
Figure 139 N_2O Emissions from Polish Coal and Sewage Sludge Co-Combustion 254
Figure 140 NOx Emissions from Colombian Coal and Paper Sludge Co-Combustion 255
Figure 141 Conversion of Colombian Coal and Paper Sludge Fuel Nitrogen to NO ... 255
Figure 142 N_2O Emissions from Colombian Coal and Paper Sludge Co-Combustion 256

Figure 143 NOx Emissions from Colombian Coal/Straw/Paper Sludge Co-Combustion 257
Figure 144 Conversion of Colombian Coal / Straw / Paper Sludge Fuel Nitrogen to NO 258
Figure 145 N_2O Emissions from Colombian Coal / Straw / Paper Sludge Co-Combustion 258
Figure 146 NOx Emissions from Wood-Bark and Agricultural Waste Co-Combustion 259
Figure 147 Conversion of Wood-Bark and Agricultural Waste Fuel Nitrogen to NO. 260
Figure 148 NOx Emissions Wood-Bark and Pulp Sludge from Co-combustion 261
Figure 149 Conversion of Wood-Bark and Pulp Sludge Fuel Nitrogen to NO 261
Figure 150 NOx Emissions from Wood-Bark and Plastic Waste Co-Combustion 262
Figure 151 Conversion of Wood-Bark and Plastic Waste Fuel Nitrogen to NO 263

List of Tables

Table 1 Trace Element Classification 25
Table 2 Trace Element Emission Limits From Waste Incineration 26
Table 3 Trace Element Isotopes Measured by ICP-MS 52
Table 4 Gas Chromatograph Details 53
Table 5 Major Element Compounds in the Thermodynamic Equilibrium Model 58
Table 6 Major and Minor Constituents of the Raw Fuel Samples 66
Table 7 Proximate Analyses of the Raw Fuels 67
Table 8 Characterisation of Fuel Reactivity 67
Table 9 Trace Element Contents of Wood – Bark, Straw, Colombian Coal and Polish Coal 71
Table 10 Trace Element Contents of Sewage Sludge, Paper Sludge, Agricultural Waste and Pulp Sludge 72
Table 11 Trace Element Content of Plastic Waste 73
Table 12 Ratios of Trace Element Concentrations in Melted and Bulk Ashes 90
Table 13 Ratios of Minor Element Concentrations in Melted and Bulk Ashes 91
Table 14 Weight Fractions of Auxiliary Fuels in Combusted Blends 251
Table 15 Trace Element Concentrations in the Raw Fuels 265
Table 16 Retention of Trace Elements in Ash 273
Table 17 Relative Volatility of Trace Elements During Combustion of the Present Set of Fuels at Temperatures Between 800 and 900 °C 274
Table 18 Potentially Problematic Fuel - Trace Element Combinations 275

List of Abbreviations

AAS	Atomic Absorption Spectroscopy
BGS	British Geological Survey, Keyworth, Nottinghamshire
CFD	Computational Fluid Dynamics
FBC	Fluidised Bed Combustion
ICP-AES	Inductively Coupled Plasma Atomic Emission Spectroscopy
ICP-MS	Inductively Coupled Plasma Mass Spectrometry
IVD	University of Stuttgart, Stuttgart, Germany
LOQ	Limit of Quantification
SIMS	Secondary Ion Mass Spectrometry
TGA	Thermogravimetric Analyser
VTT	Valtion Teknillinen Tutkimuskeskus, Jyväskylä, Finland
XRF	X – Ray Fluorescence
XAFS	X-Ray Fine Structure Spectroscopy

1.0 INTRODUCTION

The environmental consequences of waste treatment and disposal are of increasing public concern. In the past, waste disposal methods such as land filling and dumping at sea have been used in an attempt to cheaply 'hide' the problem.

Dumping of sewage sludge at sea has been banned in Europe. Whilst negative public perception of landfills and concern about their noxious emissions has constrained the opening of new landfill sites and increased the cost of waste disposal in this manner.

Effort should be made to reduce the generation of waste, but it cannot be eliminated entirely. Recycling can be employed to increase the useful life of some materials, but for others it is not practical, or economically viable. Waste from one process may be reused in another, however this may not consume or be suitable for all waste materials produced.

Combustion greatly reduces the volume of waste that must be disposed of. In addition the resulting ash need not be land filled, but put to good use in construction. Also, heat from waste combustion can be harnessed to raise steam, and generate electricity or provide district heating in the same way as coal and gas fired thermal power stations are currently used. Replacement of fossil fuel derived energy with that from waste would reduce dependence on expensive, and often imported fossil fuels.

Combustion in fluidised beds is a convenient route for the disposal of wastes whilst generating energy. There are, however, problems associated with changes in the calorific values of different wastes and seasonal variations in available total tonnages. Co-combustion with coal - a readily available source of energy, has emerged as a practical solution, to compensate for changes in waste quality and availability.

Co-combustion will allow existing equipment to be utilised with minimum alteration. This is being to be put into practice at Grenå, Denmark where coal and straw are co-

combusted in a $79MW_{th}$ fluidised bed combustor and at Gardanne, France where sawdust and sewage sludge are co-combusted with coal.

Use of biomass fuels will also reduce net carbon dioxide emissions to the atmosphere. A similar amount of carbon dioxide to that released by combustion of biomass is sequestered from the atmosphere by growing plant material. This is in strict contrast to the release of carbon from coal, which has been trapped underground for several hundred million years and is not replaced as quickly as it is burned.

Combustion of any fuel produces gaseous emissions other than carbon dioxide. Of particular interest because of their environmental effects are the nitrogen oxides. Nitrogen oxide (NO) and nitrogen dioxide (NO_2) form smog in urban areas. The sum of their concentrations (NOx) is normally regulated. Fluidised bed combustion also generates significant amounts of a third nitrogen oxide, nitrous oxide (N_2O), which contributes to possible global warming.

Less is known about the environmental effects of trace metals liberated by solid and liquid fuel combustion. However, of those released by combustion, As, Cd, Cr and Ni have been found to be human carcinogens, while Be, Cd, Co, Cr, Mn, Ni, Pb, Ti and Zn are reported to be carcinogenic in animals (Sunderman, 1979). Other elements such as As, Cd, Cr, Hg and Pb are highly toxic.

Trace elements released from fuels during combustion may exit combustors as gases or as condensed species on fly ash. Efficient modern flue gas treatment removes greater than 99.9% (by weight) of fly ash from the flue gas. Small fly ash particles of less than a micron in diameter are most likely to avoid capture and be emitted into the environment. These sub micron fly ash particles are also the most environmentally harmful. They have been found to carry a disproportionate amount of the trace metals compared with larger fly ash particles and to be mutagenic as a result (Fisher et al 1979). As biomass fuels generally contain lower concentrations of trace elements than coal, their replacement of coal would reduce trace element emissions considerably.

Co-combustion of biomass and waste with coal is still at the experimental stage. Few combustors of commercial size are operating. With this limited experience, plant

operators are reluctant to try co-combustion of new types of biomass and waste fuels, because of the risk of damage to their combustor, or excessive gaseous emissions.

The present study had two aims, both of which relate to gaseous emissions from co-combustion. The first aim was to investigate release of trace elements from coal, biomass and waste blends under fluidised bed combustion conditions. These results have been compared to thermodynamic equilibrium predictions to gain some understanding of the behaviour of the trace elements during co-combustion. The second project aim was to measure the emissions of nitrogen oxides from combustion of the fuel blends.

2.0 BACKGROUND

2.1 Trace Elements in Coal, Biomass and Wastes

Solid fuels contain most of the elements in the periodic table, although many at very low concentrations. Elements present at concentrations of less than 1000 ppm (0.1 wt %) are classified as trace elements (Swaine, 1990). It is these elements that are of most interest in the current project.

The toxicity of some trace elements has focused attention on the possible consequences of their release into the environment during combustion. The US National Research Council has classified trace elements in degrees of 'concern' about their release into the environment from coal combustion. 'Concern' takes into account each element's toxicity, the possibility of release during combustion and typical concentration in coal. Trace elements have been classified by the US National Research Council (1980) into four categories:

Elements of Greatest Concern:	As, *B*, Cd, Hg, Mo, Pb, Se
Elements of Moderate Concern:	Cr, Cu, Ni, V, Zn
Elements of Minor Concern:	Ba, Co, *Ge*, *Li*, Mn, Sb, Sr
Elements of Concern, But Only Present in Very Low Concentrations:	Be, *Sn*, *Te*, Tl

Table 1 Trace Element Classification
Elements not investigated in this project are italicised.

The emission of some of these trace elements of 'concern' has been regulated (Table 2). At present, regulations only cover trace element emissions from waste incineration. Of the fuels burnt in this study, sewage sludge, agricultural waste and plastic waste are classified for this purpose as waste, and emissions from their co-combustion must be monitored. The other auxiliary fuels, paper sludge and pulp sludge have been classified

by the EU as 'uncontaminated biomass' thus their co-combustion is not subject to trace element emissions monitoring.

Trace Element(s)	UK emission limit (mg/m^3)	EU emission limit (mg/m^3)
Hg	-	0.05
Sum of Hg and Cd	0.15	-
Sum of Cd and Tl	-	0.05
Sum of As, Co, Se and Ni	1.5	-
Sum of As, Cr, Co, Cu, Mn, Ni, Pb, Sb and V	-	0.5
Sum of Pb, Cr, Cu and Zn	1.5	-

Table 2 Trace Element Emission Limits From Waste Incineration
(Emission limits expressed at 6% oxygen, UK limits converted from 11 % oxygen)

2.2 Origins and Modes of Occurrence of Trace Elements

How a trace element is incorporated into the fuel, its mode of occurrence, can greatly affect its behaviour during combustion. Release of an otherwise volatile trace element can be hindered because it is incorporated into a refractory mineral. Conversely, non-volatile elements can be released into the gas phase by decomposition or burn out of their host material.

Just as the distribution of major and minor elements in solid fuels is inhomogeneous, trace elements are also unevenly distributed. They can be present as their own discrete mineral, incorporated as minor components of other minerals, or bound to the organic matrix. In the following section the origins and modes of occurrence of trace elements in coal, biomass (wood-bark and straw) and wastes (sewage sludge, plastic waste, agricultural waste, pulp sludge and paper sludge) will be reviewed.

2.2.1 Trace Elements in Coal

Coal is formed from ancient plant material. This has first decomposed into peat and then over millions of years further transformed by pressure and heat into coal. Trace elements present in the original biomass may remain in the coal. Additional elements

can be brought in by the inclusion or formation of minerals within the coal seam, and subsequently mined with the coal. Ground water could also deposit other elements, or leach those already present from the coal seam. The trace elements included by these mechanisms and their relative contributions will be greatly effected by the geology of the locality. As a result, the concentrations of trace elements in coal varies widely with source, and even within an individual coal seam (Swaine, 1994).

Trace elements can be associated with the organic (carbon and hydrogen matrix) or mineral fraction of coal. Trace elements in the organic fraction of coal can be further categorised by the way they are included in the organic fraction. They could be:

- Bonded to the organic matrix,
- Ionically bound, or
- Dissolved in pore water inside the organic matrix.

Organic functional groups that could bind trace elements include carboxylic (-COOH), phenolic hydroxyl (-OH), (Davidson, 1993, 1994).

Trace elements bound to mineral matter (inorganically associated) are subdivided into those that are present in their own discrete mineral (i.e. Pb in galena [PbS]) or substituted into other minerals (i.e. As in pyrite [FeS]). Trace elements in the latter category are further classified as being *chalcophilic* or *lithophilic*.

Chalcophile trace elements have an affinity for sulphur and are typically associated with sulphide minerals such as pyrite [FeS]. Lithophile elements are those with affinity for oxygen, and are often associated with aluminosilicate minerals. The most common being illite [$(HO)_4K_2(Si_6Al_2)Al_4O_{20}$] and kaolinite [$Al_2(Si_2O_5)(OH)_4$]. Carbonate minerals like calcite [$CaCO_3$], ankerite [$CaCO_3.(Mg, Fe, Mn)CO_3$] and siderite [$FeCO_3$] may also contain specific trace elements.

Direct evidence for the mode of occurrence of a trace element is difficult to obtain. Most researchers have separated coal by density and analysed the resulting fractions. They have then correlated trace element concentration with the presence of mineral or

organic matter in the density fractions. A large amount of research has been carried out in this manner, results of which are summarised in the literature reviews of Raask (1985) and Swaine (1990).

The modes of occurrence of eleven elements (As, Be, Cd, Cr, Co, Hg, Mn, Ni, Pb, Sb and Se) were reviewed by Finkelman (1994). He applied a level of confidence to the correct establishment of the mode of occurrence of these elements. Finkelman was most confident in the establishment of As occuring in pyrite, Cd in sphalerite [ZnS], Pb in galena, Mn in carbonates (including siderite and ankerite) and Se in the organic fraction, with a small amount in pyrite, accessory sulphides (galena) and selenides (clausthalite [PbSe]).

The most rigorous work is performed with direct analysis methods, such as Secondary Ion Mass Spectrometry (SIMS) (Wiese, 1990) and X -ray Absorption Fine Structure spectroscopy (XAFS) (Huggins et. al, 1994). These direct methods are extremely time consuming, hence few samples have been analysed.

A review of the literature indicates that for a small number of trace elements their mode of occurrence in coal is quite well determined (i.e. As in pyrite). Most trace elements, however, can be present in several different modes of occurrence, the proportion of the trace element contained in each varying with the coal sample.

2.2.2 Trace Elements in Biomass

Less research is available on the determination of the modes of occurrence of trace elements in biomass and waste fuels than for coal. Organically associated trace elements in forest residue (a mixture of bark, leaves and wood) were investigated by Richaud et al (1999). They dissolved the organic fraction of the forest residue by leaching with NMP (1-methyl 2-pyrrolidinone) at room temperature and at 202°C. Subsequent analysis of the NMP showed that significant proportions of the Ba, Cu, Mn, Pb and Zn were extracted.

Some of these organically associated elements may be present as enzymes and porphyrins. For example, Co is present in vitamin B12 and similar co-enzymes

(Kendrick et. al, 1992, p 71). Mn is contained in a variety of enzymes including a porphyrin required for photosynthesis and Mo is required for fixing nitrogen as ammonia (Kendrick et. al, 1992, p 61).

Trace elements in wood can also be found with the ash forming elements. Bailey and Reeve (1994 and 1996) investigated the spatial distributions of elements in black spruce and jack pine. They found that calcium was concentrated in the cell walls with manganese and iron. In a deposit found inside the black spruce, where calcium, manganese and iron levels were all very high, chromium and zinc were also found.

In the only investigation of trace element modes of occurrence in straw known to the author, Ihnat and Fernandes (1996) leached straw with water and nitric acid. Water removed all of the cadmium present, and partially removed Ba, Mn, Sr and Zn. Leaching with nitric acid, which should remove organically bound trace elements, removed all Ba, Mn, Ni, Sr and Zn. A quarter or less of the original Cu and Mo were removed by the acid.

2.2.3 Trace Elements in Wastes

Sewage Sludge

Sewage sludge is the residue remaining from the treatment of waste water from industry, sewage and in some places storm water runoff. Generally, it contains trace elements at higher concentrations than found in coal. These concentrations vary depending on the community the treatment plant serves and the proportion and types of local industry (Angelidis and Gibbs, 1989).

Several investigations have examined trace element modes of occurrence in sewage sludge using sequential leaching procedures. However, each investigating group has chosen different leaching reagents and determined slightly different modes of occurrence (Angelidis and Gibbs 1989, Chu et al. 1998, Kawasaki et al 2000).

Angelidis and Gibbs (1989) investigated the modes of occurrence of five trace metals (Cd, Cr, Pb, Cu and Zn) in sewage sludge from four treatment plants in New York. They divided the trace element modes of occurrence into, acid reducible (containing

carbonates, acid soluble sulphides and strongly adsorbed metals), oxidisable (containing organically bound elements and those present as sulphides) and crystallic (remaining mineral fraction digested using HF, HNO_3 and $HClO_4$). None of the elements were found in the adsorbed mode. They found small amounts (>20%) of Cd, Cr and Zn in the acid reducible phase. The major portion of all of the elements studied (65-92%) were in the oxidisable fraction, with between 8 and 15% of all elements remaining in the crystallic fraction.

Chu et al. (1998) investigated the modes of occurrence of trace elements in three digested sludges from Hong Kong. They separated the modes of occurrence into 6 fractions: adsorbed, carbonate bound, organically bound (including association with Fe-Mn oxides), exchangeable, sulphide bound, and forms not extracted (mostly alumino silicates and clays). All of the elements investigated (Cd, Cr, Cu, Ni, Pb and Zn) had a significant presence in the non extracted mode. The other significant modes of occurrence for each trace element were: Cd, adsorbed and organically bound, Cr, organic and sulphide phases, Cu in the sulphide phase, Pb organically bound and exchangeable, Ni exchangeable and sulphide fractions, and Zn was present in the organic and carbonate phases.

Kawasaki et al (2000) performed a similar procedure to that of Chu et al, in their survey of seven Japanese sewage sludges. They separated the modes of occurrence into: exchangeable, carbonate bound, Fe-Mn oxide bound, organic matter bound (also including sulphides), and the residual fraction. For Be and Pb the major portion of that element was found in the residual fraction (80% or greater). A significant proportion (20 – 60%) of the elements As, Cu, Ni, Sb, V and Zn was found in the organic matter / sulphide phase. Greater than 20% of As, Cd, Co, Ni, Sr, U and Zn was also found in the Fe-Mn oxide bound fraction. The only elements to have a reasonable (10 – 20%) proportion occurring in the carbonate fraction were Cd, Sb, Sr and Zn. The exchangeable fraction claiming only 13% of Co, 19% of Cu, 12% of Ni, 18% Sr and 11% of Tl.

Plastic Waste

Plastic waste for combustion usually consists of a mixture of different types of plastic. Plastics can contain significant concentrations of trace elements, either added deliberately to modify polymer properties (fillers, pigments, stabilisers), or catalyst residues and redox initiators inadvertently added during manufacture (Mascia, 1974, p 23 and Nomura et al, 2000).

Filler materials are often used to increase the volume of expensive polymers. Commonly these are alumino silicate minerals (kaolinite, quartz, mica) (Hancock and Rothon, 1995). Any trace element impurities present in the original mineral will also be present in the final polymer.

Pigments often contain trace elements. Titanium dioxide is used to prepare white polymers. Cadmium sulphide, sulpho-selenides, lead chromate and lead molybdate are all yellow pigments. Whilst green and blue plastics are sometimes prepared with chromium oxide and copper organo metallics respectively (Mascia, 1974, p127).

Stabilisers are also commonly trace element compounds. Frequently poly vinyl chloride is stabilised by cadmium, barium and zinc stearates or laurates. In other plastics tin carboxylates and lead salts are used (Mascia, 1974, p 27).

Plastic waste forms between five and ten percent of Municipal Solid Waste (MSW) (Landsberger and Chichester, 1995). In an effort to identify the sources of trace metals in MSW, Landsberger and Chichester (1995) and Nomura et al (2000) have characterised trace element concentrations in waste plastics by Neutron Activation Analysis (NAA).

They found poly ethyl terephalate plastics were contained high levels of Sb, a catalyst residue from its manufacture (Nomura et al, 2000). Co was found in some blue plastics, Ti in some white and Cd in some red. However, contrary to their expectations, the composition of few plastics followed these or any trend.

Agricultural Waste

Organic matter bound trace elements in poultry litter (similar to the agricultural waste used in the present study) were investigated by Ihnat and Fernandes (1996). They found that cadmium was readily leached by water, suggesting it was very weakly bound, while small proportions of copper, molybdenum, nickel, lead and strontium were also liberated. During leaching with 1N nitric acid, barium and zinc were also extensively liberated suggesting a substantial proportion of these elements were present in the organic fraction.

Pulp Sludge and Paper Sludge

Pulp sludge and paper sludge are by-products of the recycling of water during the paper making process. They are mostly wood-derived, and can contain significant amounts of clay minerals kaolinite ($Al_2O_3.2SiO_2.H_2O$), calcite ($CaCO_3$) and talc ($3MgO.4SiO_2.H_2O$), Latva-Somppi et al (1998). Skipperud et al (1998) investigated the fate of trace elements during the paper making process. They found that the pulp sludge contained more nickel and less cadmium than the wood originally processed. Bleaching the pulp leached copper, strontium, lead and zinc. Cobalt was unaffected by the process.

2.3 Combustion Behaviour of Trace Elements

The release of trace elements from solid fuels during combustion depends mainly on their mode of occurrence and temperature. After release, their chemistry, the gas composition, temperature and the presence of fly ash influence their behaviour.

The fate of trace elements in coal combustion has been summarised by the diagram (Figure 1) compiled by Clarke and Sloss (1992). This summary is compiled from many mass balances and observations of trace element behaviour on full-scale pulverised fuel coal fired power stations.

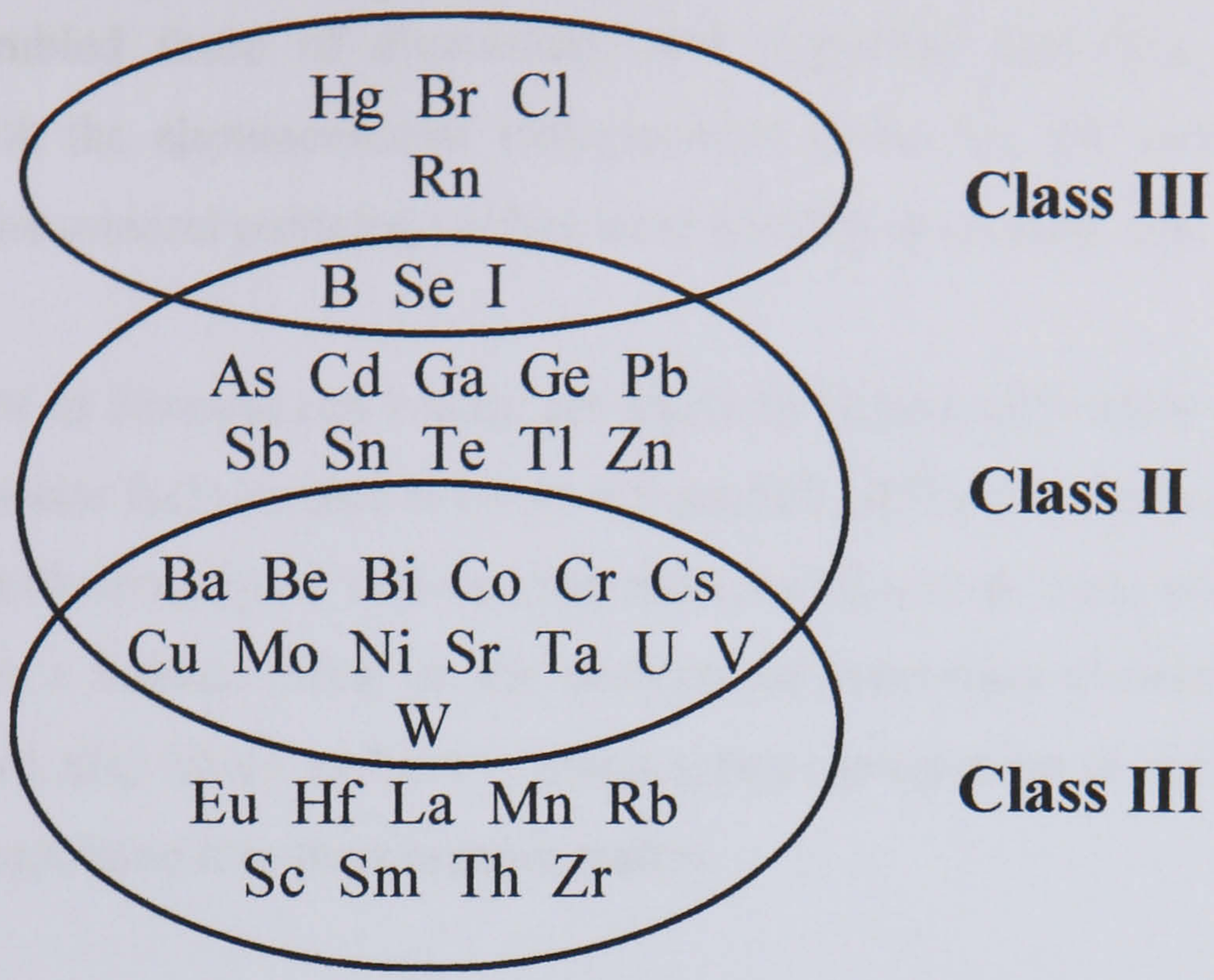


Figure 1 Partitioning of Trace Elements During Pulverised Coal Combustion

Elements in the top group (Class III) are gases at combustion temperatures, and almost completely liberated from the fuel. These elements remain gaseous at normal flue gas stack temperatures (120 °C and above).

Class II elements are concentrated on small fly ash particles. They volatilise during combustion but condense on fly ash as the flue gas cools. Preferential condensation on the smallest size fractions of fly ash occurs because the ratio of surface area to particle weight is greatest for these fractions.

Class I elements are usually lithophilic (e.g. Ba, Ce, Cs, Mg, Mn, Th) and do not vaporize during combustion. Thus they mainly remain in the bottom ashes although elutriated fines will carry some to the gas cleaning plant.

The summary of the fate of trace elements was complied by Clarke and Sloss from work carried out on pulverised fuel combustors burning coal where combustion temperatures in excess of 1600 °C occur. In one of the few studies carried out into trace element partitioning in fluidised bed combustion, Lind et al (1994) burnt Venezuelan coal in a CFBC. They found that only partial volatilisation of trace metals had occurred at the lower temperatures prevalent (typically 850 – 1000 °C). No metal showed the inverse relationship with particle size that would indicate complete volatilisation and subsequent recondensation. The distributions of Sr, Sc, V, Zn, Ga, Cs, Ba, La, Sm, Lu

and Th resembled those of aluminium, and suggested that these elements were associated with the aluminosilicate rich particles in the fly ash, either because they reacted with the mineral particles, or they were initially associated with them.

Trace elements in biomass and wastes are likely to behave differently to those in coal. Biomass and waste fuels contain not only substantially different mineral matter, but also significantly different sulphur and chlorine contents from coal: these minor elements are known to have a marked effect on the mobility of some trace elements. Biomass and waste fuels are also likely to have a much greater proportion of their trace element inventory incorporated into their organic matter.

Sewage sludge was found to inhibit trace metal loss into the gas phase by Cenni et al (1998) during pulverised fuel combustion. They could not find the cause, but gave several possibilities for this result.

- Lower flame temperature of sewage sludge had reduced metal volatilisation,
- The lower chlorine and higher sulphur content of sewage sludge had reduced metal volatilisation,
- Volatilised trace metals were adsorbed by sewage sludge mineral matter
- The large amount of small particles resulting from combustion of the sewage sludge increased trace metal condensation.

Mode of occurrence was found to have a significant impact on trace element behaviour by Bool and Helble (1995). Their conclusions were that elements that are organically bound or associated with pyrite (As, Se, Hg and Sb) vaporise extensively during combustion of bituminous and sub bituminous coals at 1450 °C. Other elements associated with silicates or oxides (Zn, Cr) tend to interact with other coal minerals without vaporising.

2.4 Thermodynamic Equilibrium Modelling of Trace Elements

Solid fuels are mixtures of a large number of organic and mineral compounds which undergo complex transformations during combustion. Modelling of the formation of NOx and N_2O has been undertaken using the comprehensive reaction rate data that are available for the important reactions in that system (Kilpin and Hupa, 1991, Jones et al, 1999). In the case of modelling the reactions involved in trace element behaviour, little or no kinetic data exist for the species that are likely to form. However, although this lack of chemical kinetic data prevents investigation of trace element behaviour through a kinetic model, we may still gain some understanding of the system by predicting the thermodynamic equilibrium composition.

Thermodynamic modelling is undertaken assuming that the system is at chemical equilibrium at a particular temperature and pressure. There are several limitations as a result:

1. No account is taken of any kinetic hindrance to chemical reaction. In low temperature systems, the rates for some reactions, especially those in the solid phase, may prevent formation of products expected from equilibrium considerations. In addition, incomplete mixing may cause local species concentrations to deviate significantly from the average values used in the thermodynamic modelling.

2. Misleading predictions may also result because data are not available for all important chemical species in a system.

3. The mode of occurrence of a particular trace element in a solid fuel may influence its volatility. Trace elements strongly held in untransformed minerals may not be released; conversely organically bound trace elements may be released by consumption of their organic host. In either case possibly at variance with their predicted behaviour.

Despite these limitations, thermodynamic equilibrium modelling provides a useful method of predicting the fate of trace elements and interpreting experimental data.

Thermodynamic calculations on trace element behaviour during coal combustion have been performed by Frandsen et al (1994), Linak and Wendt (1994) and Mojtahedi (1989). These researchers used models comprising one trace element with and the elements C, H, N, O, S, Cl. Each condensed species was assumed to form a separate phase (i.e. no mixing of the condensed phases) and the gases to behave ideally. No account was taken of the minor ash forming elements which could interact with the trace elements in several ways i.e. by forming compounds with them, competing for chlorine and sulphur with them, or dissolving them in any melts which form.

A comprehensive model of trace element behaviour during the combustion of coal, a lignite, wood and a 70 % coal / 30 % wood mixture has been developed by Thompson and Argent (1995). Their model included provision to predict the formation of fused salt and oxide melt phases. Oxide melt phases were predicted at 1300 K and atmospheric pressure for lignite and for the 70 % coal 30 % wood mixture. Further calculations showed that considerable proportions of the arsenic and zinc remained in the oxide melt. Fused salt melts were predicted for all fuels; no data are available for the solubility of trace element compounds in these phases.

Thermodynamic equilibrium modelling has been utilised by several researchers to predict trace element behaviour from fuels other than coal and wood. Trace element behaviour in coal / sewage sludge systems was investigated by Yousif (2000) and Reed et al. (2001), in clinical waste combustion by Delay et al (1999) and in municipal solid waste combustion by Durlak et al (1997).

2.4 Formation of Nitrogen Oxides During Combustion

Coal typically contains 1.2 - 1.6 wt% of nitrogen, mostly in the form of cyclic pyridinic and pyrollic groups (Molina et al, 2000). During combustion these groups undergo ring scission, releasing nitrogen compounds to react with the combustion gases. In oxidising systems, they undergo several reactions to eventually form N_2 or one of the three species of nitrogen oxides emitted from combustion: N_2O, NO, and NO_2. NO and NO_2 are known collectively as NOx. Their role in acid rain has lead to widespread regulation.

More recently N_2O has come under scrutiny, because it is thought to contribute to the greenhouse effect. The global warming potential of N_2O is thought to be 190 – 270 times that of carbon dioxide on an equivalent mass basis (Watt, 1997).

Low combustion temperature favours N_2O formation. Therefore N_2O emission is especially high from fluidised bed combustion (800 – 900 °C). Emission levels as high as 500 ppm have been reported (Amand et al 1989, Moritomi et al 1991). These values may be inaccurate, due to the potential formation of significant amounts of N_2O during storage of samples which also contain water, SO_2 and NOx (Muzio and Kramlich 1988). This sampling artefact only affects samples stored before analysis, N_2O measurement by continuous analysis methods such as Fourier Transform Infra Red spectroscopy (FTIR) are unaffected.

2.4.1 Mechanisms of NO and N_2O Formation

Most research has focused on determination of the mechanisms of formation of NO and N_2O during combustion of coal. These mechanisms are equally applicable to biomass combustion, although the relative proportions of the active species will change.

NO_2 forms from NO when the flue gas cools after combustion and constitutes at most 10 % of total NOx in the flue gas. Three mechanisms, thermal NOx, prompt NOx, and fuel NOx are used to explain the formation of NO in flames.

Thermal NOx results from the breakdown of atmospheric nitrogen at high temperatures and its subsequent reaction with molecular oxygen. NOx formation by this mechanism is only a significant at temperatures of 1500 °C and above (Morrison, 1980). Thermal NOx does not make a significant contribution to NOx emissions from fluidised bed combustion carried out at between 800 and 1000°C.

Prompt NOx can form under certain conditions of low temperature, fuel rich stochiometry and low residence times (Fenimore, 1971). It occurs through hydrocarbon free radical attack on gaseous nitrogen. Under such conditions the nitrogen atom can be oxidised (even with fuel rich conditions) to form NO. The products of this mechanism

rarely exceed 5 % of the total fuel NOx. As a result of the above, fuel nitrogen is the primary source of NOx, and probably also N_2O, from fluidised bed combustion.

Formation of NOx from Fuel Nitrogen

Nitrogen is partially released during fuel devolatilisation. This could be in small molecules (NO, HCN, N_2O, NH_3 and N_2), or in tars. The nitrogenous constituents of tars usually fragment after devolatilisation and the majority of tar nitrogen forms NH_3 or HCN.

Once in the gas phase, NH_3 will be partially converted to NO in an oxidising system (Miller and Bowman, 1989, Hulgaard et al, 1991). HCN will also be converted to NO, though for this gas N_2O is a more significant oxidation product (Kramlich, 1989).

NO can also be produced by the fuel nitrogen remaining in the char. Most of the nitrogen released from this process is in N_2, N_2O and NO. However, once formed, NO can then be reduced by subsequent reaction with either char or CO, or both together. The primary product of either reaction is N_2 though reaction with char can also produce N_2O (De Soete, 1990). NO can also be reduced by reaction with NH_3 (Miller and Bowman, 1989), which is used in some Thermal DeNOx processes.

Formation of N_2O

There are three mechanisms known for N_2O formation during combustion (Gulyurtlu, 1995). The first is heterogeneous oxidation of char nitrogen to N_2O. This route is generally less important for N_2O formation than NO, as char is usually found to be more active in reducing N_2O than it is for NO, causing lower conversion of char nitrogen to N_2O than found for NO (De Soete, 1990).

The second mechanism for N_2O formation is homogeneous oxidation of nitrogen compounds in volatiles. Most probably N_2O formed in the gas phase is produced by the oxidation of HCN (Kramlich et al, 1989), since almost no N_2O results from NH_3 oxidation (Hulgaard, 1991).

The final mechanism is heterogeneous reaction between NO and char nitrogen. This is probably by the formation and reaction of a surface –CNO site with gaseous NO (Croiset et al, 1998)

N_2O emissions from combustion are only significant in the temperature window 1050 – 1400 K (Kramlich et.al, 1989). In FBC the peak temperature in the combustor has been found to be the most significant temperature in determining the amount of N_2O emitted (Bonn et al, 1995). At high temperatures N_2O can be destroyed by reaction with hydrogen (Roby and Bowman, 1987) or decompose (Hulgaard et al, 1991). N_2O can also be destroyed by heterogeneous reduction to N_2 on char (De Soete, 1990).

3.0 EXPERIMENTAL

3.1 Reactor Development

Originally built to investigate the calcination of limestone by Khraisha (1988), the suspension-firing reactor developed in this laboratory has been extensively modified for investigating trace element release and recondensation, during the co-combustion of coal, biomass and waste.

The reactor tube is a 1260 mm long, 48 mm ID quartz tube divided into two sections by internal cones, 750 mm from the top of the reactor. Suspension gas (5 lpm, measured by a KDG 1100 rotameter) entered the suspension-firing reactor through the horizontal arm of the T-junction, beneath the base and travelled upward though the first reactor section, where it was preheated (Figure 2). The suspension gas then entered the second section of the reactor, the combustion zone, where it contacted the fuel, introduced from the top.

A rotary valve at the base of the feed hopper metered the fuel. This was transported into the combustion zone through a water-cooled (5 mm ID) quartz feeder tube with the aid of a 0.5 lpm of flow of nitrogen (measured by a Brooks Instruments BV 1355/D1B4A1D00000 rotameter). Once in the combustion zone the incoming suspension gas and fuel mixed and combusted.

Fuel and ash particles were prevented from falling into the lower, pre-heating section of the reactor by the high velocity of suspension gas entering the combustion through the cone at the bottom. Elutriation of fine particles was prevented by a quartz sinter located at the top of the combustion zone. Flue gas passed through the sinter and exited the reactor, where it was dried and the concentrations of O_2, NOx and N_2O measured.

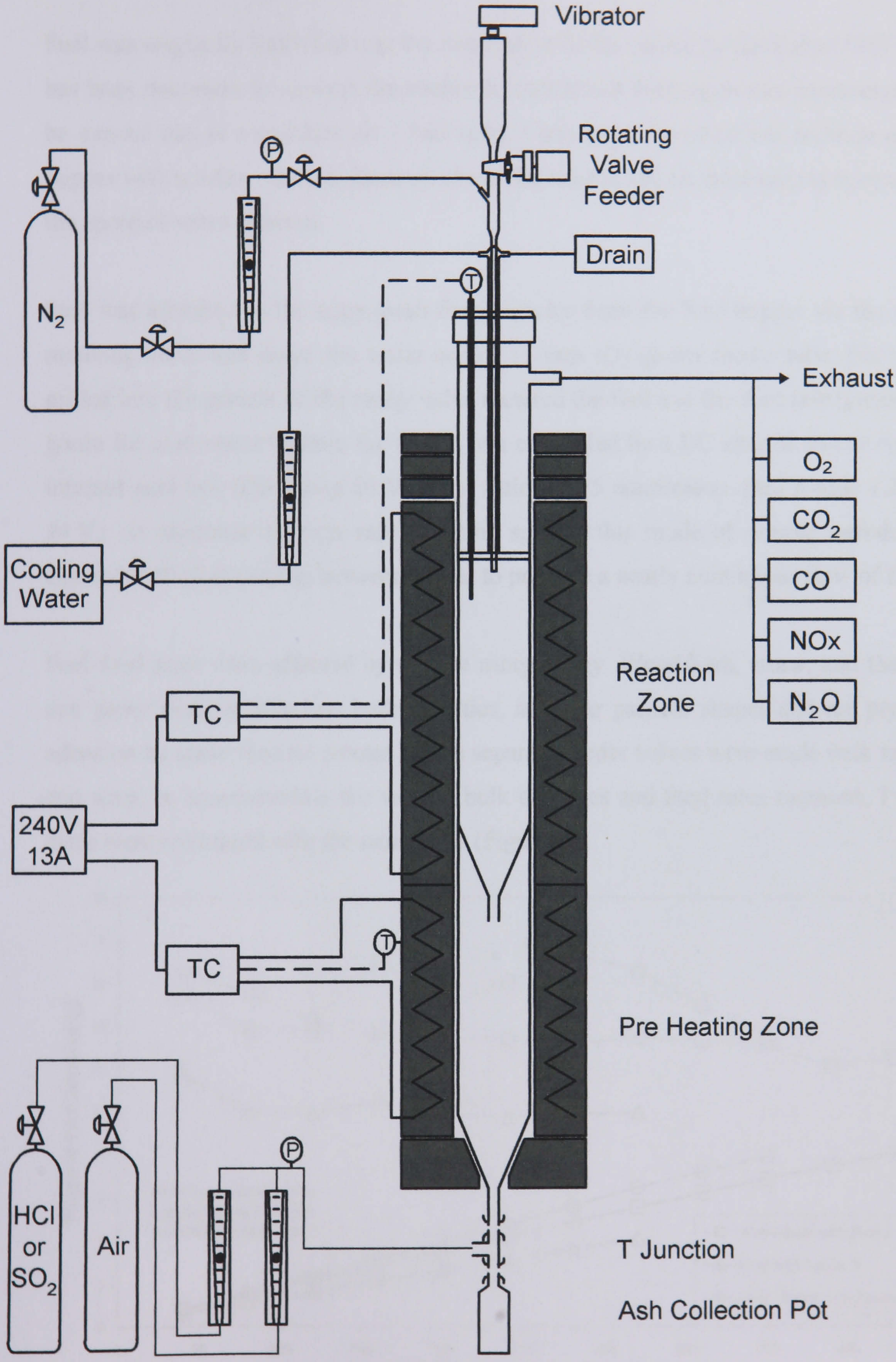


Figure 2 The Suspension-Firing Reactor

3.1.1 Fuel Feeding

Fuel was originally batch fed into the suspension-firing reactor by Khraisha (1987). Here it has been necessary to convert the reactor to continuous feeding so that experiments could be carried out at a constant air / fuel ratio. Conversion involved the addition of a feed hopper with a rotary valve at the base above the reactor and an electronic system to control the speed of valve rotation.

Fuel was admitted to the suspension-firing reactor from the feed hopper via the rotary metering valve and down the water cooled (5 mm ID) quartz feeder tube. Six 'cups' milled into the spindle of the rotary valve metered the fuel and the feed rate (around 0.5 g/min for coal and 0.9 g/min for wood) was controlled by a DC electric motor with an internal gear box (Portescap 80 W, Gear ratio 1:65.5 continuous rated torque 1.2 Nm, 24 V). At moderate to high valve rotating speeds, this mode of sample introduction ensured sufficient overlap between pulses to produce a nearly continuous flow of fuel.

Fuel feed rates were affected by sample morphology. Wood-bark, straw, and the pulp and paper sludges have low bulk densities, irregular particle shapes and are prone to adhesion by static electric charge. Three separate feeder valves were made with various cup sizes, to accommodate the various bulk densities and feed rates required. Two of these were calibrated with the main fuels (Figure 3).

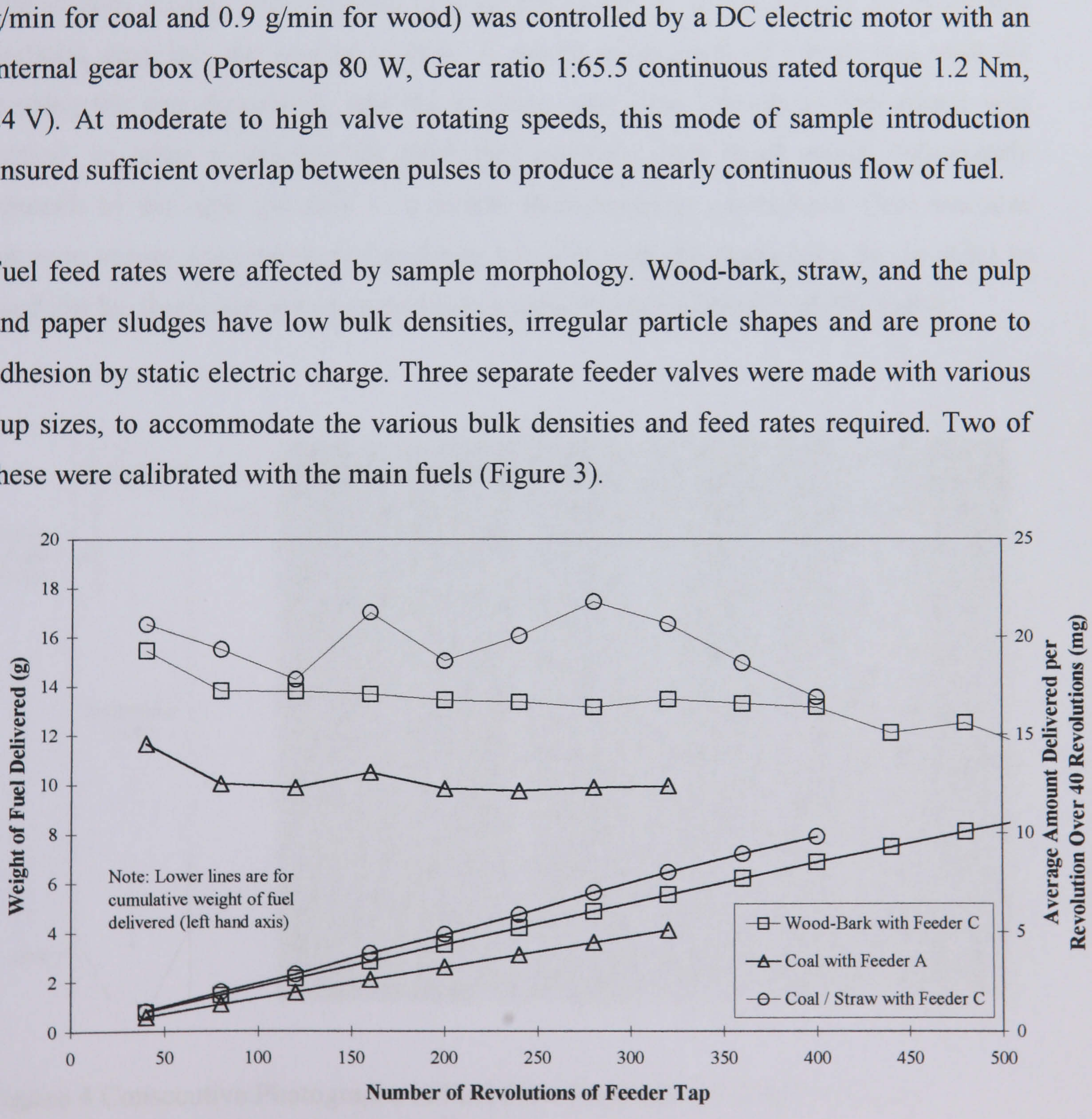


Figure 3 Fuel Addition from Feeding System

The rotary valve spindles were made from poly ether ether ketone (PEEK) an electrically conductive plastic which allowed any static electric charge to leak to earth. A vibrator was also mounted on top of the feed hopper to prevent sample bridging here. Though these alterations improved feeding immensely, neither the paper sludge nor pulp sludge could be fed from the hopper if they were not mixed with another fuel. Both neat fuels bridged the hopper just above the rotary value after approximately one minute of operation.

3.1.2 Fuel Flow on Injection

In order to prevent evolving volatiles from short-circuiting the combustion zone and immediately exiting uncombusted through the sinter, it was necessary to inject fuel particles deep into the reactor section. A stream of nitrogen (0.5 lpm) was used for pushing the fuel downward, into the reaction zone. The velocity of this stream was critical, in order to prevent the finer fuel particles from being swept immediately upwards by the main gas flow - i.e. before their complete combustion. Care was also taken to ensure good mixing of evolving volatiles with the suspension air, in order to suppress the formation of hot spots due to localised combustion of volatile matter.

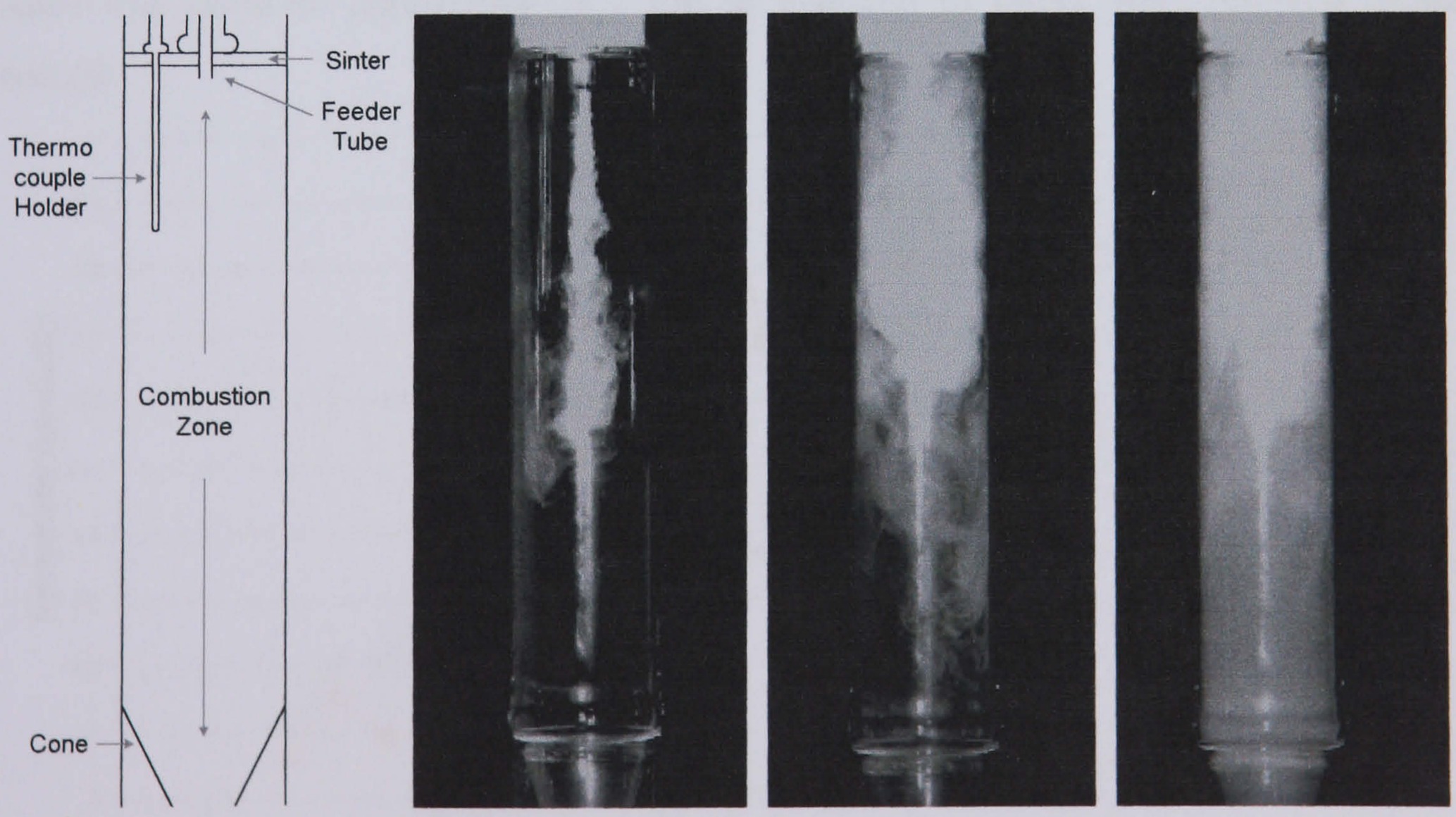


Figure 4 Consecutive Photographs of Fuel Flow Penetration During Injection

Smoke tests performed at ambient conditions have shown that immediately after injection, the flow from the feeder tube penetrates halfway down the reactor, before slowly spreading out and mixing with the suspension gas (Figure 4). Under these conditions, volatiles would not be expected to bypass the reactor, but to diffuse and combust over most of the available volume.

3.1.3 Retention of Fuel and Ash Within the Suspension-Firing Reactor

Fuel and ash particles were prevented from falling from the combustion zone into the preheating zone below by the high velocity of suspension gas entering from the preheating section. At the top of the reactor elutriating fine ash and char particles were retained inside the suspension-firing reactor by the quartz sintered-disc (porosity grade 3, QSP, Essex), which served to filter them from the flue gas. This escaped through the top (cold) section of the reactor tube for gas analysis and eventual exhausting. The sinter was sealed by a ~ 5 cm deep bed of saffal wool packed on top.

Some of the ash particles were held against the sinter by the upward flow of suspension gas and remained there when the suspension gas was turned off. Particle size distributions of this 'sinter ash' and the bulk 'bottom ash' from Colombian coal combustion (Figure 5) show that particles approximately 2 μm in diameter or larger were retained inside the reactor.

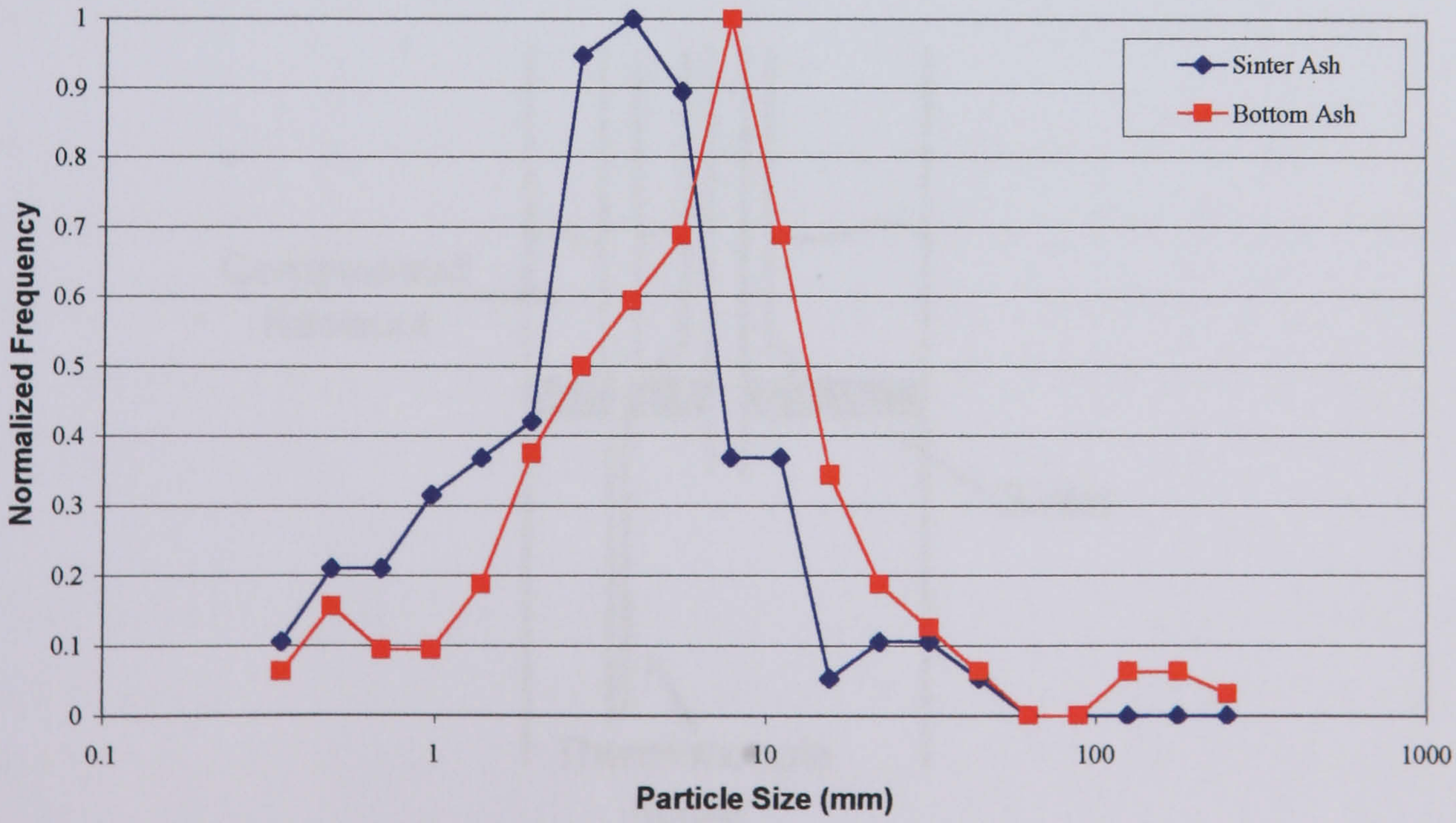


Figure 5 Particle Size Distributions of Sinter and Bottom Ash

3.1.4 Temperature Profile, Measurement and Control

The suspension-firing reactor was heated by two independently controlled elements (Figure 2). Power supplied to the bottom element (2 kW) determined the temperature of the suspension gas entering the combustion zone from the preheater. The top element (1 kW) set the temperature in the combustion zone before fuel was fed. The temperature was measured using a K-type thermocouple placed inside a quartz sheath, and protruding by 100 mm into the reaction zone (Figure 6).

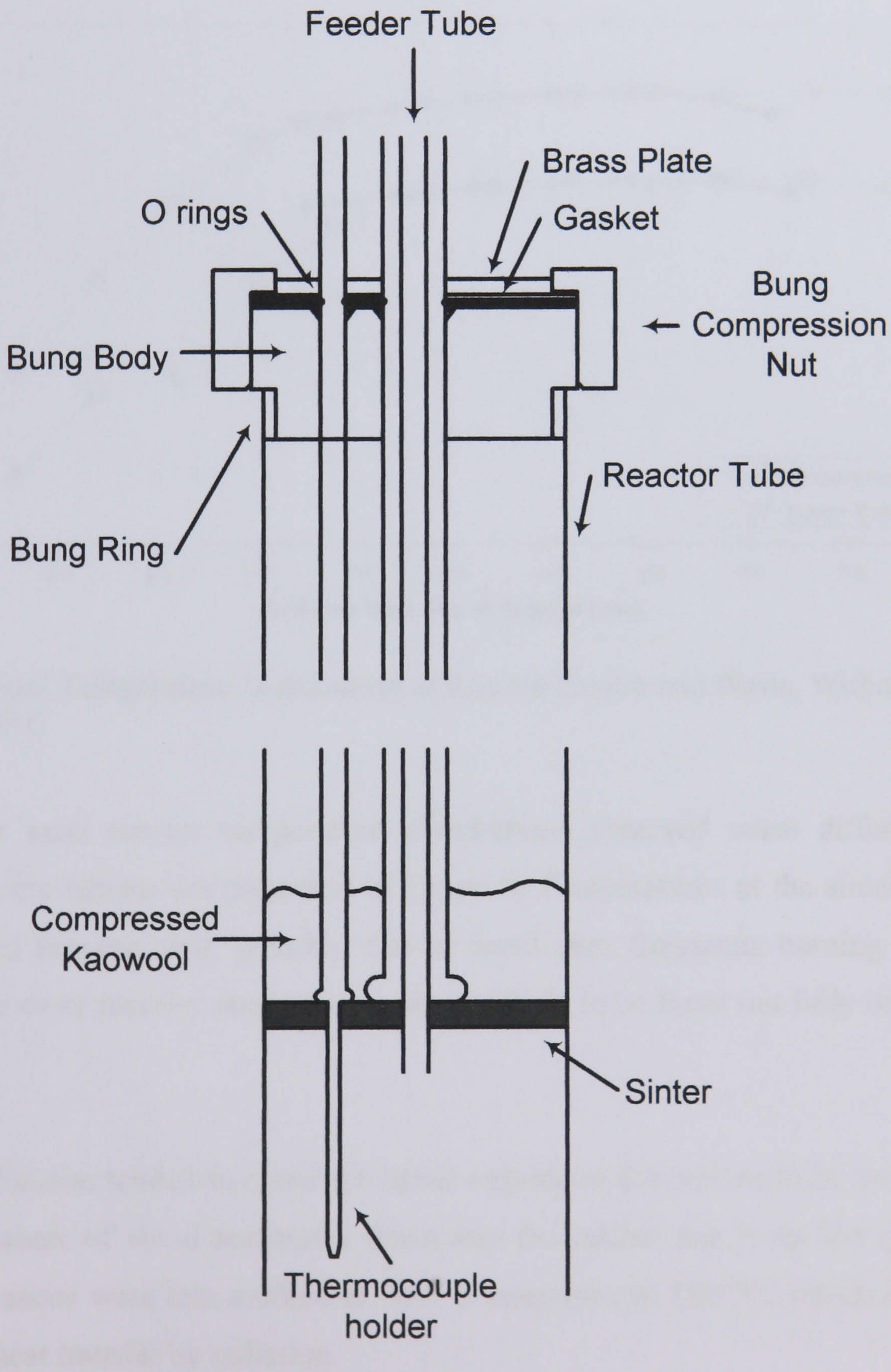


Figure 6 Sintered Quartz Plate and Top Closure Details

Axial temperature variations at the furnace wall and within the reactor are shown in Figure 7, where the position of the quartz sinter marks the top of the reaction zone (at 400 mm from the top of the reactor) and the bottom of the conical constriction at around 750 mm (from the top of the reactor) marks the bottom of the combustion zone (cf. Figure 2). Figure 7 shows that both the furnace wall and reactor temperatures were reasonably constant (400 - 700 mm from top), falling off just before the top sintered quartz plate at 400 mm. The saffal wool compressed behind the sintered disk appeared to reduce heat losses and ensure a reasonably isothermal reactor zone.

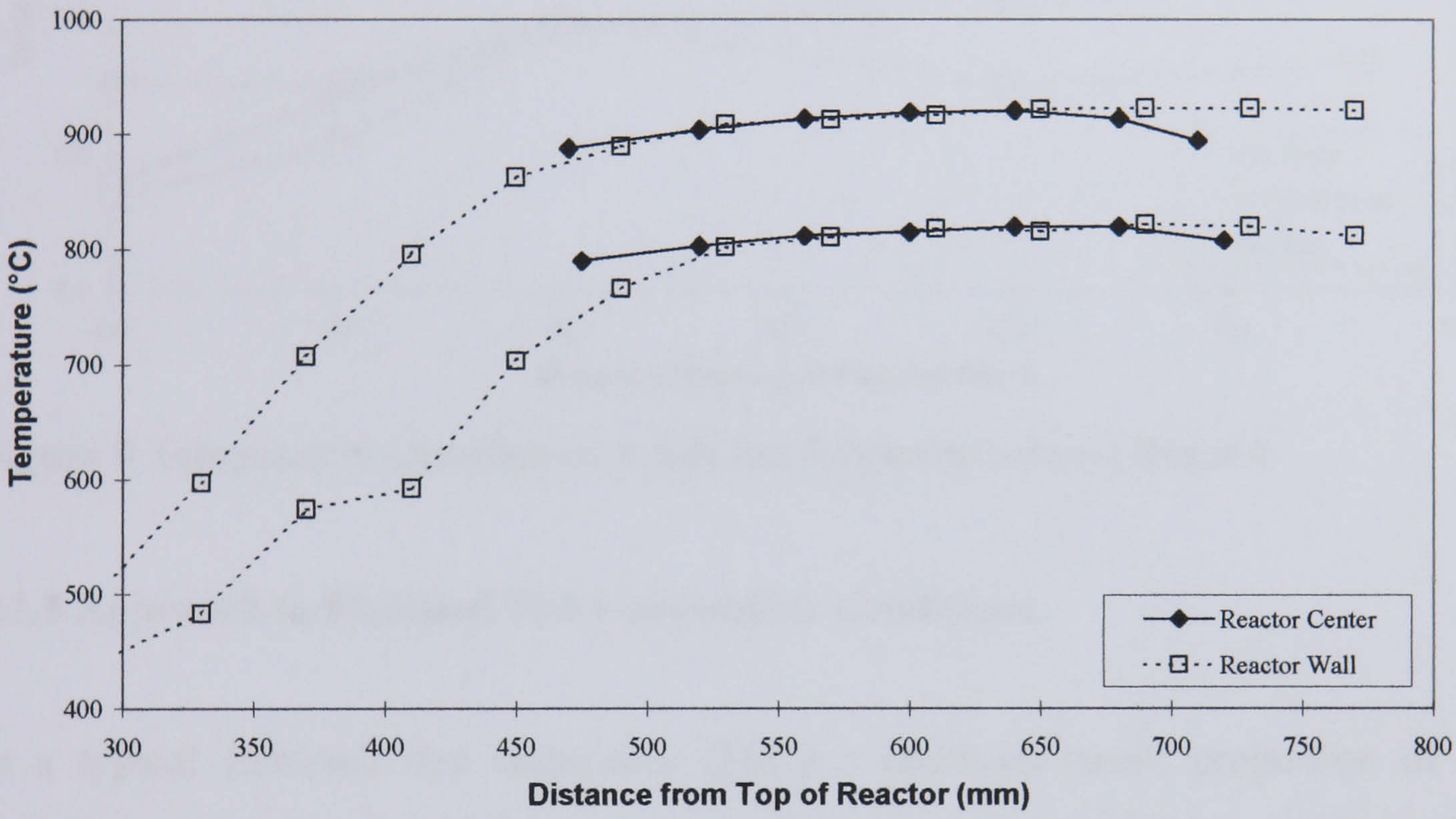


Figure 7 Axial Temperature Distribution at Reactor Centre and Walls, Without Fuel, 800 and 900°C

Changes in axial reactor temperature distributions observed when different fuels are supplied to the reactor are presented in Figure 8. Temperatures at the sintered disk were higher when burning coal, possibly due to small char fragments burning slowly there, whereas the more reactive straw and wood are likely to be burnt out fully before reaching the sinter.

Wood combustion tended to cause the lower regions of the reactor to be cooler. Probably smaller amounts of wood penetrated down into the reactor due to its low density. All of these differences were less marked at 900 °C compared to 800 °C, which may be due to increasing heat transfer by radiation.

During experiments the inlet gas temperature was set to either 800 or 900 °C and the top furnace temperature set between 20 and 50 °C below the required reaction temperature, the difference being made up by the combusting fuel.

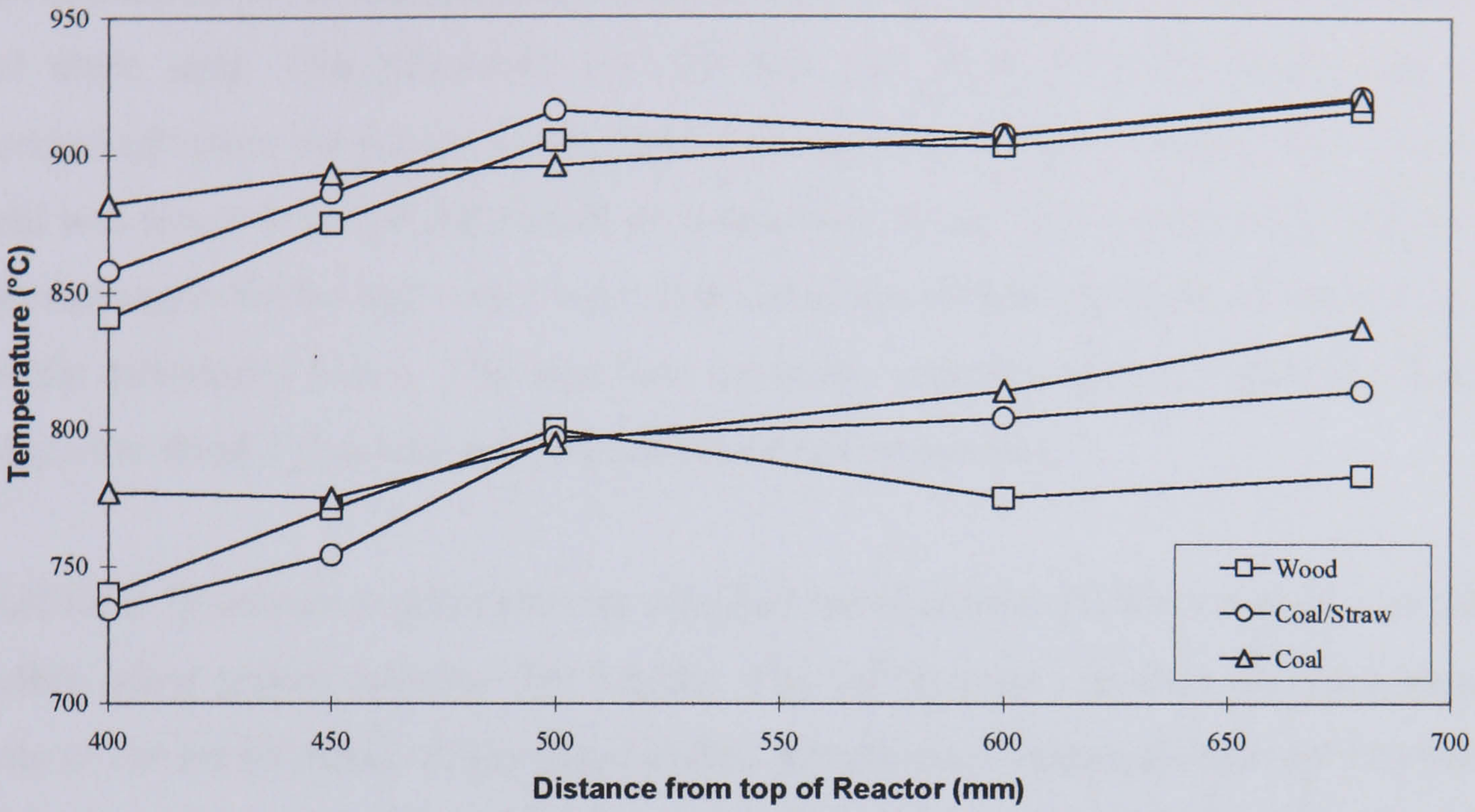


Figure 8 Temperature Distribution Inside the Suspension-Firing Reactor

3.1.5 Approach to Fluidised Bed Combustion Conditions

In a typical fluidised bed combustor (FBC) a relatively small proportion of the bed inventory (1-3 %) consists of fuel, with the balance made up of ash or deliberately added solids (e.g. sorbent or sand). Among other functions, the bed material serves as a diluent and as a heat transfer medium; most excess heat is lost from burning particles by collisions with colder particles in the bed (Hoy and Gill, 1987). Rapid mixing distributes the generated heat efficiently and macroscopic temperature gradients greater than 30 °C are uncommon, even in large diameter combustors.

This mode of heat transfer was not available in the suspension-firing reactor, due to the absence of a dense bed of solids. Thus burning particles are thought to reach somewhat higher temperatures, making trace elements slightly more likely to volatilise than in a standard FBC. Furthermore, without the large surface area of the bed material, trace elements are less likely to condense within the reactor itself. To minimise the difference in particle temperature between the suspension-firing reactor and fluidised bed combustion, relatively small particles have been used in these experiments (100 - 200 μm).

3.2 Reactor Preparation and Ash Collection

Before use, the reactor tube, feeder tube, thermocouple holder, sinter, T-junction and ash collection pot of the suspension reactor were kept immersed overnight in dilute (10 %) nitric acid. This procedure ensured that any trace elements which may have condensed inside the reactor during previous runs were completely removed. The nitric acid was rinsed from the equipment with deionised water. The reactor tube, feeder tube, thermocouple holder and sinter were then dried and assembled with the retaining bung on the laboratory bench. The complete assembly was then placed inside the furnace, where the dried T-junction and ash collection pot were added.

Fuel for a 10 minute experiment was weighed out (Sartorius R300S balance) and mixed before being placed into the fuel hopper. The fuel hopper was then clamped securely onto to the feeder stand, which also held the vibrator and rotary valve drive. The bottom of the hopper was connected to the top of the feeder tube using heat shrink rubber tubing which was discarded after every experiment.

Suspension air (zero grade air, BOC gases) was supplied to the reactor at a rate of 5 lpm and 0.5 lpm of nitrogen (oxygen free nitrogen, BOC) flowed down the feeder tube to assist fuel flow. In experiments where hydrogen chloride or sulphur dioxide were added to the suspension gas, these were supplied from bottles containing 3 % of either gas in air (Air Products Special Gases Group). These gases were metered though a separate rotameter (Brooks Instruments BV, 1355/D2F2A1D6A020) before mixing with the suspension gas.

The rate of fuel addition was controlled by the speed of the rotating valve and adjusted to maintain the selected 1.2 air / fuel ratio. Gas flows were maintained for a further two minutes after the completion of fuel feeding to allow any char remaining in the reactor to burn out.

At the completion of combustion, the furnace was turned off to cool overnight. The next day, the sinter was carefully removed and the ash brushed and washed into a beaker. The fine ash recovered from the sintered-disc was recovered and analysed separately.

When the suspension-gas flow was turned off, some of the ash fell through the reactor section into the catch pot at the bottom of the reactor tube. However, the greater part of the 'product' ash adhered loosely to reactor walls. This ash was recovered by removing the ash pot and T-junction and rinsing through the reactor with deionised water into a beaker. Ash that adhered more strongly to the reactor walls was removed with a long handled brush. This ash and that from the ash pot were added to the bottom ash beaker. Both beakers were placed on hot plates and 90 % of the water evaporated. The ash samples were then transferred onto watchglasses and dried completely at 150 °C on a hotplate (Fisher Scientific).

Blank runs were performed to establish whether the reactor body or the ash collection procedure introduced significant contamination. Quartz sand of low trace element content was introduced into the reactor when hot and then collected as ash in the normal way. To test whether there was any mercury contamination, activated carbon was introduced into the cold reactor, left overnight and then collected dry. Both blanks showed no significant increase in trace element content, giving confidence that measurements will be free from significant contamination.

To ascertain whether significant proportions of any trace element were left behind on the beaker or watchglass, the watchglasses were washed with 10 % nitric acid, and the solution analysed by ICP-MS. Very small amounts of V, Mo and Sr were detected, however no trace elements appeared at concentrations greater than the limit of quantification.

3.3 Analysis Techniques

During this project raw fuel samples were analysed for their ultimate (Section 3.3.4) and proximate (Section 3.3.5) analyses, their volatile yields and char reactivities (Section 3.3.6). Together with ash samples the trace and minor element contents of raw fuels were measured. Gases from the combustion of these fuels and their blends were analysed for NOx, N_2O and oxygen.

3.3.1 Digestion of Samples for Trace and Minor Element Analysis

Two distinct digestion methods were used to prepare the samples in a nitric acid solution for ICP-MS and ICP-AES analyses (inductively coupled plasma - mass spectrometry and - atomic emission spectrometry). The establishment and adaptation of the techniques for small (10 mg) solid samples by the 'wet ashing' and 'microwave' digestion methods have already been described by Lachas et al (1999) and Richaud (1999) and will be briefly outlined.

During wet ashing, raw fuel samples were first weighed out into platinum crucibles and 'ashed' by adding 100 μL of H_2SO_4 (Aristar Grade, BDH) with deionised water and heated to 150 °C for three hours. Samples were then placed in a muffle furnace at 520 °C overnight to breakdown the hydrocarbon matrix of the fuel. Ash samples from the suspension reactor were not subject to the 'ashing' procedure and were immediately weighed into platinum crucibles. Samples of either origin were then treated with 300 μl of perchloric acid and 500 μl of hydrofluoric acid (both Aristar Grade, BDH) to breakdown silicate minerals and returned to the hot plate until all HF had been boiled off. The residue was then dissolved in dilute Aristar grade nitric acid (10 % for ash samples, 2 % for raw fuels) and made up to a 10 ml solution. Dilution was necessary to bring the concentrations of trace elements into the range of linear response of the ICP-MS instrument. Taking the dilution factor as the solution volume in millilitres over sample weight in grams the solutions prepared from ashes were analysed at a dilution factor of 5000, those prepared from raw fuels at 1000.

Wet ashing breaks downs the entire sample, completely releasing all trace elements into solution. However, some of the more volatile elements (e.g. As, Se) can be lost during digestion. In addition, the use of perchloric acid contributes to the release of chloride ions into the final sample solution. In the ICP-MS plasma these can form polyatomic ions, which interfere with the measurements of V, As and Se.

The 'softer' microwave digestion method has thus been used for As and Se determinations, without involving the use of chlorine containing acids (Lachas et al, 1999) and Richaud et al, 1999). In this preparation, solid sample is placed inside a small PTFE vessel with 1 ml

of nitric acid (ash samples) or 0.2 ml of nitric acid and 0.2 ml of hydrogen peroxide (raw fuel samples). The vessel is then placed inside a larger PTFE vessel with 10 ml of nitric acid and locked into a microwave carousel. The acid, heat and subsequent pressure serve to leach trace elements from the organic substrate and breakdown some of the ash constituents. However, silicates in the fuels remain undissolved since no HF is used. Trace elements associated with this mineral matter and any other mineral matter insoluble in nitric acid are not expected to be liberated. The difference in results reported by the wet ashing and microwave digestion methods for a particular element can give important information on the way trace elements are bound in the raw fuels.

Each digestion run (8 samples) was accompanied by a blank sample, and a certified standard ash sample. Successful completion of the digestion was confirmed by validation of the known composition of this certified standard ash sample.

3.3.2 Analysis of Solutions for Trace and Minor Elements

Two ICP-MS facilities have been used for analysis of the trace element solutions, each with slightly different analysis techniques. Initial work was performed on a machine at the Imperial College facility at Silwood Park, Sunningdale, Berkshire, although this was relocated to Kingston University, Kingston upon Thames, Surrey. Intermediate work was performed at the British Geological Survey (BGS) at Keyworth, Nottinghamshire. At both facilities, ash samples were run at a dilution factor of 5000 (made by diluting the digestion solution fivefold) and raw fuel samples at between 500 and 1000. The main difference in technique between the two laboratories was in the determination of limits of quantification (LOQ). At BGS LOQ's were determined by taking ten times the standard deviation of the results for blanks from all digestions using the same method, whereas at Silwood Park and Kingston the blank for each particular batch was analysed five times and ten times the standard deviation of this was taken as the LOQ.

In most cases, the most abundant isotope of each trace element was chosen for analysis; however there are several exceptions where strong interferences exist. For example, ^{82}Se was analysed for in samples prepared by 'wet-ashing' (though usually below the LOQ), as the presence of chlorine interferes with the detection of ^{77}Se. Both isotopes could be

determined by microwave digestion. A full list of elements and isotopes measured is presented in Table 3, below.

^{9}Be	^{63}Cu	^{107}Ag
^{47}Ti	^{65}Cu	^{111}Cd
^{49}Ti	^{66}Zn	^{118}Sn
^{50}Ti	^{71}Ga	^{121}Sb
^{51}V	^{73}Ge	^{137}Ba
^{52}Cr	^{75}As	^{184}W
^{53}Cr	^{77}Se	^{205}Tl
^{55}Mn	^{82}Se	^{208}Pb
^{59}Co	^{86}Sr	^{232}Th
^{60}Ni	^{95}Mo	^{238}U

Table 3 Trace Element Isotopes Measured by ICP-MS

Multiple isotopes were measured for several elements. ^{52}Cr was found to be more reliable than ^{53}Cr and ^{63}Cu was favoured over ^{65}Cu. For titanium, three isotopes were examined. The least abundant isotope, ^{49}Ti (5% of Ti) was found to be the most reliable. The high levels recorded for the other Ti isotopes caused saturation of the mass spectrometer detector.

Titanium, along with other trace elements zinc and manganese were often found at high concentrations. Measurement of these metals in ash was performed by ICP-AES. This technique was also used to determine the minor element concentrations in the raw fuels and for measurement of vanadium, as the chlorine from wet ashing interferes in ICP-MS.

ICP-AES and ICP-MS have similar requirements for liquid sample dilution factor and nitric acid matrix. This allowed the solutions prepared for ICP-MS to also be analysed on the ICP-AES. Solutions of ash samples were run on ICP-AES at their initial dilution factor of 1000 as the ICP-AES is more tolerant of dissolved solids in samples. This improved the ICP-AES limits of detection. Raw fuel sample solutions were run at the same dilution factor on both machines.

3.3.3 Analysis of NOx, N_2O and O_2 In Flue Gas

Flue gas from the suspension reactor was analysed for oxygen to determine the air / fuel ratio during combustion, and the pollutants NOx and N_2O. To prevent damage to instruments and ensure measurements were carried out on dry gas, the flue gas was passed through a drying tube containing magnesium perchlorate. All instruments took flue gas samples in parallel and excess flues gas was vented to a fume cupboard.

The oxygen content of the flue gas was measured using a Telegan Tempest fuel cell based analyser. This was calibrated on room air and oxygen free nitrogen (BOC gases) before use. NOx emitted from the reactor was measured by chemi-luminescence in a Signal Series 4000 NOx meter. This instrument was calibrated before each experimental run with 500 ppm NOx (balance nitrogen) from a standard gas bottle (BOC Special Gases). Nitrous oxide in the flue gas was measured using a gas chromatograph (GC) fitted with an electron capture detector. Details of the manufacture and operation of the GC are presented in Table 4 below.

Make	Carlo Erba Strumentazione
Model	Fracto Vap Series 4160
Column Material	
Length (m)	
Pressure	2 kg/cm^2
Carrier Gas	N_2 (oxygen free, BOC)
Oven Temperature	40°C
Detector Temperature	250°C
Mode	Constant Current
	580 V
	5μs Pulse Width

Table 4 Gas Chromatograph Details

The GC was calibrated daily using a standard gas 219 ppm N_2O in Nitrogen (BOC Special Gases). Initially this was also checked using 0.98 % N_2O from another standard bottle (Jones Chromatography). To avoid the N_2O sample storage artefact leading to the

formation and measurement of additional N_2O, the dried gas sample was injected into the GC immediately (<5 s) after sampling.

Destruction of NOx and N_2O inside the reactor and sampling train was considered a possibility. To investigate this possibility for both gases, a measured flow of gas from the standard bottle was introduced into the reactor with the suspension air. The concentration of NOx and N_2O could be calculated and in both cases a similar concentration was measured.

3.3.4 Ultimate Analysis of Raw Fuel Samples

Measurements of the raw fuel ultimate analysis, moisture content and ash content were performed by TES Bretby, Burton-on-Trent, UK. Carbon, hydrogen and nitrogen contents were measured using an Exeter CE440 Elemental Analyser. Measurements of the sulphur contents were made using LECO SC 132 and SC 432 analysers. Chlorine and phosphorous contents of the fuels were measured by X-ray reflectance (XRF). Sample moisture and ash contents were measured by oven drying and combustion of a known sample weight in accordance with BS 1016 part 104 section 104.1:1991.

3.3.5 Proximate Analysis of Raw Fuel Samples

Micro scale proximate analysis of the fuel was carried out in a thermogravimetric analyser (TGA) using the method described by Cai (1995). The sample was placed in the TGA crucible and held at 30 °C for 30 - 40 minutes in an inert atmosphere to stabilise. It was then heated at 20 °C/min to 105 °C, and that temperature held for 20 minutes. The weight loss was taken as the moisture content of the sample. The temperature was then ramped at 100 °C/min to 900 °C where it was held for 7 minutes while the sample devolatilised. The difference between this weight and that after drying corresponds to the volatile matter content. The furnace was then cooled to 850 °C whilst the gas supply was switched to air and the sample burned. The final weight is the ash content, the difference between this and the weight after devolatilisation is the amount of fixed carbon.

3.3.6 Raw Fuel Volatile Matter Content and Char Reactivity

Characterisation of the fuel volatile content and char reactivity was carried out using a wire mesh reactor and a TGA. In the wire mesh reactor the sample is held between two layers of fine molybdenum mesh. An electric current is passed through the mesh, heating both it and the sample, which is pyrolyzed. The gaseous devolatilisation products being swept from the mesh by an inert gas flow. The loss in weight represents the total volatile yield, from which the volatile matter content is calculated; allowing for the water and ash contents. The very high heating rates achievable by the wire mesh reactor (up to 10^4 K/s) simulate rapid heating and combustion inside a fluidised bed.

Combustion reactivity of the char recovered from the wire mesh reactor is measured in the TGA by pre-heating a small amount of char to 500 °C in a nitrogen atmosphere and then combusting isothermally in air. At this relatively low temperature, the burning of the sample is controlled by chemical kinetics. The highest rate of weight loss under these conditions is taken as a measure of the char reactivity.

3.3.7 Measurement of Raw Fuel and Ash Mercury Contents

Mercury is difficult to measure by ICP-MS, because it is lost during preparation of the necessary acid solution. Samples were thus analysed separately for mercury using a LECO AMA 254 mercury analyser. Twenty milligram samples were combusted under a pure oxygen atmosphere inside the analyser. Mercury vapour released from the sample was captured by a gold amalgam. After purging the flue gases from the unit, the mercury is released into the gas flow from the gold amalgam by heating to 500 °C. The amount of Hg vapour present was measured by the absorbance of light at 254 nm. This method could determine mercury contents to within 20 % at concentrations as low as 0.01 ppm.

3.3.8 Calculation of Air / Fuel Ratio

Experiments in this study were carried out at an air / fuel ratio of 1.2. This was calculated in the following way:

$$A/F = \frac{N_{O,air} + N_{o,fuel}}{2N_C + \frac{N_H}{2} + N_N + 2N_S}$$

Where N_C, N_H, N_N, N_S and $N_{O,fuel}$ are the molar amounts of carbon, hydrogen, nitrogen, sulphur and oxygen in the fuel, respectively. Whilst, $N_{O,air}$ is the molar amount of oxygen supplied by the suspension gas.

For all of the fuels and blends combusted in this study, an air / fuel ratio of 1.2 resulted in an oxygen concentration in flue gas of approximately four percent.

3.4 Thermodynamic Equilibrium Modelling of Trace Element Behaviour

Thermodynamic equilibrium modelling of trace element behaviour was carried out using the computer program MTDATA (National Physical Laboratory, Teddington, London). MTDATA performs Gibbs free energy minimisation calculations to find equilibrium compositions for a variety of physical situations. In this study only two of MTDATA's modules were used; ACCESS, the database search program and MULTIPHASE, the module that performs Gibbs free energy minimisation calculations for systems containing mixtures of condensed phases and gases.

Several databases of thermodynamic data are supplied with MTDATA for various types of thermodynamic equilibrium modelling situations. During this project only data from the Scientific Thermodata Group Europe (STGE) database was used. This database was too large to perform calculations with. To prepare a smaller datafile suitable for performing calculations, the elements of interest were entered into the ACCESS module. ACCESS searched the database for all compounds that were combinations of the elements of interest. At the end of the search the retrieved compounds were listed and any not required removed. The datafile was then saved before use.

The datafile created by ACCESS supplied the selected compounds' thermodynamic data to the MULTIPHASE module. In this module the simulation conditions of temperature (900 to 1400 K in 20 K steps), pressure (1 atmosphere) and system composition (variable) were set and the calculations run.

3.4.1 Thermodynamic Equilibrium Model

Most previous models of thermodynamic equilibrium of trace elements during combustion have focused on the behaviour of one trace element when subjected to the major (here C,H,N,O,S and Cl), but not the minor elements (here Na, K, Ca, Mg, Fe, Al, Si and P). Minor elements can influence trace element behaviour directly by forming compounds with the trace element, or competing with the trace element for reaction with scarce third elements, e.g. chlorine, which often increases mobility through formation of volatile chlorides.

Entering all of the major and minor elements into ACCESS with the trace elements of interest would result in an extremely large and unwieldy datafile. However, many of the compounds contained in the datafile are unlikely to form under the combustion conditions modelled (e.g. complex hydrocarbons). Removal of these compounds increased the rate at which the model solved and decreased the size of the result files.

Initially only the elements C, H, N, O, Cl and S were modelled. Results from this preliminary run showed that many compounds included by the ACCESS database search were not predicted to form at significant concentrations. Those compounds predicted at concentrations four or more orders of magnitude below that of the most significant compound of each major element were listed. Approximately two hundred compounds were identified and excluded from the model in this way. The process was repeated with silicon and the major elements. A further thirty compounds were excluded as a result.

Compounds of major elements that have been included in models are presented in Table 5, together with the upper temperature limit for their thermodynamic data. Elemental species are also included, though not predicted to occur in significant concentrations.

The inclusion of the elemental species simplified entry of the fuel composition into the model. Without these species the composition would have had to be specified in terms of amounts of compounds.

Table 5 Major Element Compounds in the Thermodynamic Equilibrium Model

Compound and Phase	Maximum Temperature (K)
C	6000
CO<g>	6000
CO_2<g>	10000
Cl<g>	10000
Cl_2<g>	10000
HCl<g>	6000
H<g>	6000
H_2O	601
H_2O<g>	20000
N_2<g>	6000
NO<g>	20000
NO_2<g>	6000
N_2O<g>	6000
O<g>	6000
O_2<g>	20000
S<g>	10000
SO_2<g>	6000
SO_3<g>	6000

Note: all gaseous species are denoted by <g>, all other species are condensed. Compound thermodynamic data is valid from 298 K to the temperature given (note as all calculations were performed at atmospheric pressure. Liquid water data were not required above 100 °C!).

Further preliminary runs with the inclusion of the minor elements predicted several compounds to form at temperatures above the upper temperature limit for their thermodynamic data. These species included potassium phosphate, sodium phosphate and potassium hydrogen phosphate. Their upper temperature limits were 1000, 900 and 593 K respectively. Extrapolation of their thermodynamic data by MTDATA predicted their formation at temperatures of up to 1400 K. These species are not expected to form

at this temperature in reality; their prediction probably results from erroneous extrapolation of their thermodynamic data outside the valid range. Exclusion of these species from the thermodynamic equilibrium model resulted in prediction of apatite (calcium phosphate) formation. A magnesium alumino silicate ($Al_4H_2Mg_2O_{19}Si_5$) was also predicted for some fuels at temperatures above the upper temperature limit. Exclusion of this species brought the prediction of diopside ($CaMgSi_2O_6$) formation.

To model trace elements, datafiles were prepared of compounds containing the major elements: C, H, N, O, S and Cl, the minor elements Na, K, Mg, Ca, Al, Fe, Si and P, and up to 5 trace elements of interest. The organic and silicon compounds that were not predicted to form earlier were removed. Thermodynamic equilibrium models were run for the combustion of the main fuels (wood-bark, coal or coal/straw), 70 % main fuel 30 % auxiliary fuel blends and where it had been experimentally investigated, the auxiliary fuel alone.

The system composition for thermodynamic equilibrium calculation was entered into MULTIPHASE on a molar basis. Using the weight of feed burnt in the suspension reactor (maximum fuel 10 g) results in very small numbers of moles for the trace elements. These very small numbers are slower for the computer to manipulate, more prone to rounding error, and can prevent an otherwise well-specified problem from being solved. To overcome this problem, the system was scaled up to a 100 kg basis. This increases the molar amounts by about 10,000 times. This has no effect on the results of simulations as only the proportion of trace element in each species was examined.

Thermodynamic equilibrium compositions of a fuel or fuel blend have been calculated between the temperatures of 900 to 1400 K. When five trace elements were included this took around 2 hours on a 750 MHz personal computer. Batch files were run overnight to enable investigation of up to seven fuels and blends.

Predicted compounds for some trace elements included minor elements. In reality the formation of these compounds may be limited by the low probability of the trace element and minor element coming into contact, hence resulting in less than the equilibrium amount of the compound forming. When the predicted trace element specie

involved a minor element, the model was rerun without this specie being allowed to form. This showed any other compounds with could be formed. The process of excluding the predicted minor and trace element containing compound was continued until no more were predicted inside the temperature range.

When the predicted compound contained another trace element the compound was excluded from the model, because of the very small concentrations of the constituents and hence likelihood of formation. The same rational was applied to two compounds that contained multiple atoms of the same element, V_4O_{10} and Sb_4O_6. They are very unlikely to form because of their requirement of the interaction of four atoms of the trace element.

3.5 Presentation of Trace Element Results

Results for the behaviour of trace elements are presented in four types of diagram:

- Partitioning diagrams
- Enrichment diagrams
- Synergy diagrams
- Thermodynamic Equilibrium Predictions

Partitioning diagrams plot the percentage retention of each trace element in the ash. This is derived from the total amount of trace element from the combined ash fractions, divided by the amount of the element contained in the raw fuel. Results for runs at 800 °C are shown at the top of each diagram, while those for 900 °C are shown beneath. 100 % recovery of an element in the ash residue clearly corresponds to complete retention of that element in the ash. Elements that are completely retained can appear above 100 % retention because of experimental error in the results.

Enrichment diagrams plot the relative enrichment of each trace element on sinter ash. This is calculated from the concentration in the sinter ash divided by that in the bottom ash. If the enrichment is significantly above one then that element can be said to be concentrated in the sinter ash, while if it is significantly less than one that element is preferentially

retained in the bottom ash. Results for runs at 800 °C are shown above, those for 900 °C below, as for partitioning diagrams.

Synergy diagrams plot the amount of trace element retained in ash (per gram of raw fuel) against the weight fraction of auxiliary fuel in the fuel blend. Synergy is identified when the results for blends deviate significantly from that expected from the behaviour of the two pure fuels. Where more of the trace element is retained in the fuel blends than expected, there was a synergy between the fuels for retention of that trace element. If less of the trace element was retained then there was a synergy between the fuels for release of that trace element. The diagram also shows the upper and lower bounds of the trace element concentration in the raw fuel blends.

Thermodynamic equilibrium predictions present the proportion of the trace element contained in each predicted compound plotted against the temperature (as in Figure 9).

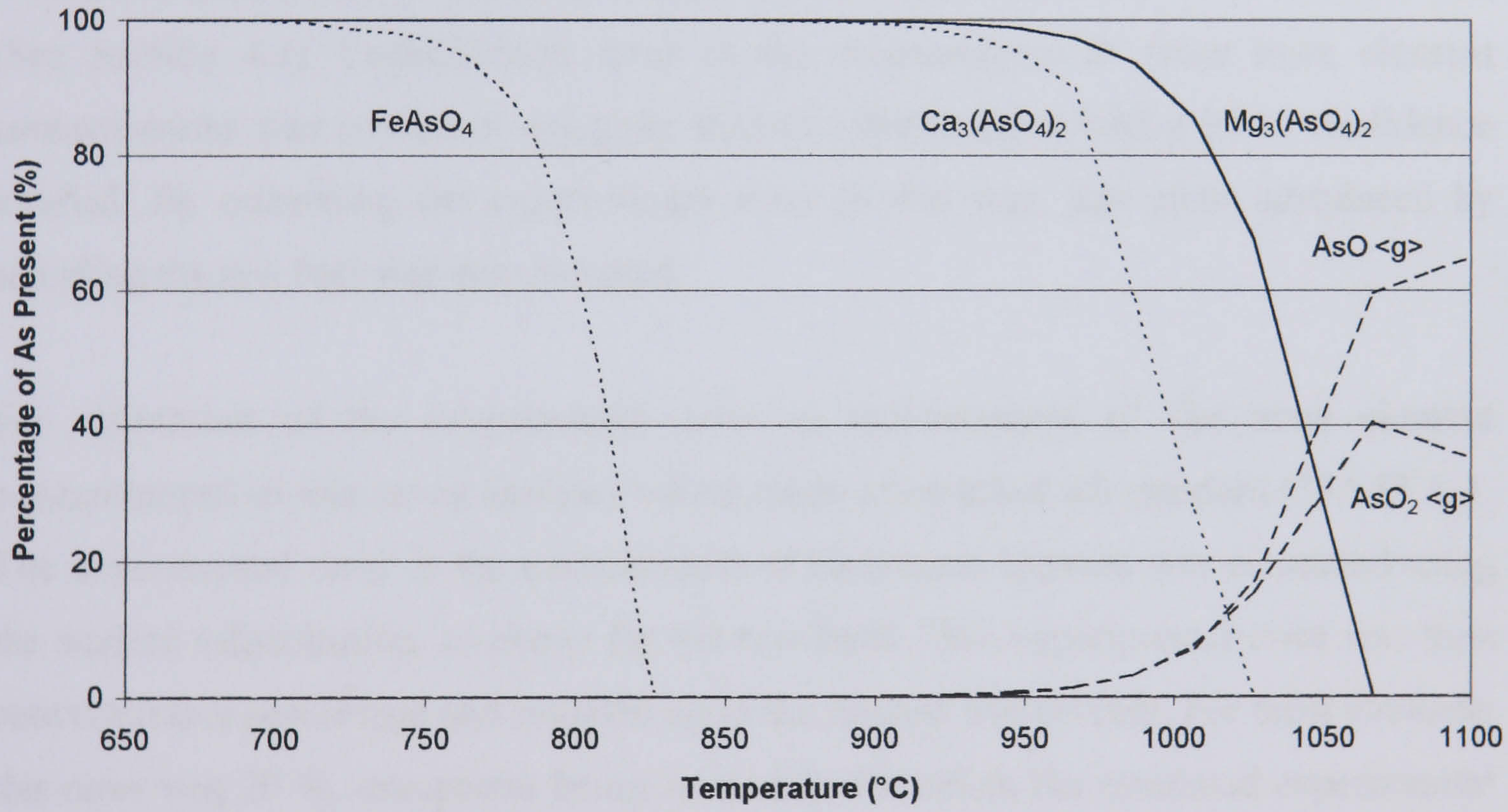


Figure 9 Thermodynamic Equilibrium Prediction for Arsenic During Wood-Bark Combustion

In this example, $Mg_3(AsO_4)_2$ is the condensed phase predicted to exist at the highest temperature. The proportion of arsenic in this compound is plotted with a solid line. Condensed species predicted if more stable compounds are excluded (here calcium and iron arsenates) are plotted with dotted lines. Those gaseous species predicted when no condensed phases are excluded are plotted with a dashed line and <g> follows their chemical formula.

3.6 Experimental Error in Trace Element Measurements

Experimental error in the investigation of trace element behaviour came from:

- Trace element concentrations in the raw fuels
- Weighing the raw fuel before combustion
- Trace element concentrations in the ash
- Weighing the ash collected from the suspension firing reactor

Measurements of weight were carried out using a Sartorius R300S balance. This balance was calibrated regularly and weighed 0.1 mg accurately. As the experimental error introduced by weighing was insignificant compared to that from measurement of the trace element concentrations it was neglected.

Multiple measurements were made of the trace element concentrations in the raw fuels (See Section 4.3). Experimental error in the measurement of these trace element concentrations was estimated using the student t-distribution, with a 95 % confidence interval. By estimating the experimental error in this way, any error introduced by sampling the raw fuel was also included.

For estimation of the experimental error in measurement of the trace element concentrations in ash, seven analyses where made of certified ash standard CTA-FFA-1. The experimental error in the measurement of each trace element was estimated using the student t-distribution, as above for the raw fuels. This experimental error was then converted to a percentage and rounded up to the nearest five percent. For most elements this error was 20 %, exceptions being As and Se for which the estimated experimental error was 25 %.

These experimental error estimates were used to determine the experimental error in the percentage retention and relative enrichment results. For percentage retention, the error was the square root of the sum of the squares of the percentage error in measurement of the trace element contents of the ash and trace element concentration in the raw fuel. For relative enrichment, the error was the square root of twice the square of the percentage error in measurement of the trace element concentration in the ash.

4.0 CHARACTERISATION OF THE RAW FUELS

In this study four main fuels were co-combusted with 10, 20 and 30 % (energy basis) of waste fuel. The main fuels for this project were wood-bark, Polish coal, Colombian coal and a 50:50 (energy basis) mixture of Colombian coal with straw.

Wood-bark was combusted with agricultural waste, pulp sludge and plastic waste, while Polish coal was burnt with sewage sludge and the Colombian coal and Colombian coal/straw mixture were co-combusted with paper sludge.

4.1 Origins of the Raw Fuels

Wood-bark was a mixture of spruce wood and bark from the UPM-Kaipola paper mills in Finland. The sample was taken directly from the de-barking plant. In normal operation it would be mixed with various plant sludges for combustion in their 77 MW_{th} BFB. Before drying, the bulk density of the sample was approximately 360 kg/m^3 and moisture content around 60 %.

Colombian high volatile bituminous coal was supplied by Midtkraft, the Danish power generator and is representative of the coal usually burnt with straw in their bubbling fluidised bed at Grenå. The straw was also supplied by Midtkraft and originates from wheat cultivation in Denmark.

The agricultural waste came from a chicken farm in Vippula, Finland. This particular hen house uses cutter chips as litter on the floor. The fuel is 40 - 50% manure and has a bulk density of around 300 kg/m^3. This type of waste fuel is thought to be very demanding to burn, with some of the ash constituents being liable to promote bed sintering and corrosion.

Paper sludge was supplied from a paper mill at Grenå, Denmark. This sample was examined as a possible fuel for Midtkraft's nearby power station. The pulp sludge was

also a waste from paper making. The sample used in this study was taken from a Kvaerner paper mill at Oulu, Finland.

The plastic waste was from the Norske Skog paper mill at Golbey, France. It was mechanically separated from paper brought to the mill for recycling. Normally this reject plastic waste is crushed and then burnt in the mill's boiler.

Polish coal was supplied by Chalmers University, Sweden and is a blend of coal from seams around Krakow, Poland. The sewage sludge sample was also supplied by Chalmers University. It is from the wastewater treatment plant at Himmerfjärdsverket, Sweden, which treats wastewater from Södertälje and southwestern Stockholm.

4.2 Major, Minor, Proximate and Reactivity Analyses of the Raw Fuels

All samples have been dried, ground and sieved to 100-200 μm. Their ultimate and minor element analyses are presented in Table 6. The analysis techniques used to obtain these results were described in section 3.3.4. Also included in Table 6 are results for silicon contents and lower heating valves of the fuels performed by VTT and the IVD on larger size fractions of the same fuel samples.

Chlorine and sulphur have a major influence on trace element behaviour. Plastic waste has the highest chlorine concentration of the samples analysed. High levels of chlorine are also recorded for straw, paper sludge (possibly from bleaching) and agricultural waste. The highest sulphur concentration was that of sewage sludge. Apart from sewage sludge, both coal samples also contained more sulphur than the other samples analysed.

The highest levels of sodium and potassium were found in the agricultural waste. The largest concentrations of magnesium and calcium of the samples analysed were recorded for sewage sludge. Plastic waste contained the highest concentration of aluminium.

Measurement of the sample proximate analyses were carried in a TGA, (see Section 3.3.5). Pulp sludge, paper sludge and plastic waste are extremely volatile (Table 8) with greater than 85 % of their weight being lost on heating (volatile matter and water together). Only the coal samples had considerable (>20 %) fixed carbon contents.

The characterisation of the fuel volatiles content and reactivity has been carried out using a wire mesh reactor and TGA (Section 3.3.6). In the wire mesh reactor the finely ground (100 – 200 μm) samples were heated to 950 °C at 5000 K/s in helium. Three of the samples were also analysed at a hold temperature of 700 °C. Table 8 combines these results with those at 950 °C.

The almost complete devolatilisation of the biomass samples, and their very low ash content, meant that the yield of char from the wire mesh was less than 1 mg in some cases. Furthermore, there was a tendency for waste residues to adhere strongly to the mesh. It thus proved impossible to recover some biomass and waste chars for TGA analysis.

The results from the wire mesh show that all of the samples except coal have 85 % or more volatile matter at 950 °C. Results from the Colombian coal, plastic and agricultural wastes indicate that, devolatilisation was essentially completed by 700 °C. The coal samples had a lower volatile yield, probably due to their more compressed structure and more tightly bound constituents.

As most of the solid residue left after pyrolysis of the biomass samples was ash, it might be expected that they would show a very low reactivity. However, this was not the case, probably due to the relatively loose structure of the biomass chars, which allowed efficient escape of volatiles and allows oxygen ingress into the char.

Table 6 Major and Minor Constituents of the Raw Fuel Samples

	Wood-Bark	Straw	Colombian Coal	Polish Coal	Sewage Sludge	Paper Sludge	Agric. Waste	Pulp Sludge	Plastic Waste
Elemental Analysis					% dry ash free				
C	53.1	49.3	80.6	85.0	52.5	54.3	50.2	48.5	67.9
H	6.00	6.10	5.31	4.81	6.61	7.57	6.23	6.49	10.0
N	0.45	0.68	1.64	1.24	7.23	0.46	4.11	1.31	0.35
O (by diff)	40.3	43.4	11.5	7.9	26.3	37.0	37.3	42.9	20.4
S	0.07	0.15	0.90	0.84	2.91	0.21	0.63	0.52	0.38
Cl	0.01	0.26	0.04	0.11	0.06	0.39	0.39	0.12	0.98
P	0.04	0.07	0.01	0.02	4.32	0.01	1.06	0.08	0.01
					% as received				
Ash	6.9	2.8	6.2	16.2	41.4	5.1	12.8	3.6	10.2
Moisture	3.0	8.7	7.9	2.9	11.0	7.0	4.0	4.3	2.6
Minor Elements					g/kg as received				
Na	1.35	0.09	0.21	0.67	2.21	1.26	4.03	3.06	1.91
K	2.26	8.86	0.87	2.89	3.90	0.27	27.1	0.87	0.25
Mg	0.79	0.38	0.45	3.14	3.17	0.65	4.28	2.04	1.18
Ca	7.98	1.83	0.70	4.94	18.8	7.82	16.4	2.37	9.43
Al	2.99	0.23	5.66	16.1	24.6	5.15	0.35	2.32	24.9
Fe	1.52	0.18	2.75	7.52	77.6	0.90	0.54	0.84	1.71
Si	9.7	8.7	24.2	33.4*	61.6*	10.3*	3.6	9.9	9.4
Lower Heating	18.6†	17.8†	29.5†	28.6‡	8.4‡	21.1†	15.7†	18.2†	29.7†

* by AAS, at IVD Stuttgart, Germany other Si results by XRF at VTT, Jyväskylä, Finland. Lower heating values in MJ/kg, † by VTT, ‡ by IVD

Table 7 Proximate Analyses of the Raw Fuels

Fuel	Moisture (wt%)	Volatile Matter (wt%)	Fixed Carbon (wt%)	Ash (wt%)
Wood-Bark	3.0	72.8	17.3	6.9
Straw	8.7	76.9	11.6	2.8
Colombian Coal	7.9	36.4	49.5	6.2
Polish Coal	2.9	30.3	50.6	16.2
Sewage Sludge	11.0	45.2	2.4	41.4
Paper Sludge	7.0	82.3	5.6	5.1
Agric. Waste	4.0	68.9	14.3	12.8
Pulp Sludge	4.3	85.4	6.7	3.6
Plastic Waste	2.6	83.9	3.3	10.2

Table 8 Characterisation of Fuel Reactivity

Fuel	Volatile Content (wt% daf)	Char Reactivity (wt%/min)
Bark / Wood	89.1	-
Straw	89.9	23.22
Colombian Coal	47.1	1.518
Colombian Coal (700°C)	41.9	1.68
Polish Coal	39.3	1.39
Sewage Sludge	93.5	16.3
Paper Sludge	91.4	11.84
Agric. Waste	87.5	8.47
Agric Waste (700°C)	84.4	15.88
Pulp Sludge	87.4	14.56
Plastic Waste	96.5	-
Plastic Waste (700°C)	94.3	-

Volatile matter contents on a dry and ash free basis. Results at 950 °C unless stated.

4.3 Trace Elements Contents of the Raw Fuels

Measurements of the trace elements in the fuel samples were carried out by ICP-MS and LECO mercury analyser. Both techniques where described earlier in section 3.3. The raw fuels where prepared for ICP-MS analysis by the wet ashing and microwave digestion methods (refer section 3.3.1). A minimum of six wet ashing and three microwave digestions were performed on each sample, to obtain an accurate estimate of the trace element concentration. If there was significant variation in these results further digestions were made. Normally 20 mg of sample was digested, the straw and paper sludge samples proved inhomogeneous at this scale. For both fuels 100 mg samples were digested.

As wet ashing is a complete digestion of the sample these results have been taken as the overall content, except for:

- As - where chlorine interference from the perchloric acid prevents measurement of the small amounts involved
- Se - where wet ashing LOQs are usually too high for measurement with the 82 isotope, the only one free from chlorine interference, and
- Hg - which was measured using the LECO analyser.

Average results from analyses are presented with a 95% confidence interval (refer Section 3.6) for the measurement. For some elements the difference in overall and microwave results was not within experimental error. This suggests these elements may be bound to the raw fuels in silicates or alumino silicates that were not broken down by the microwave digestion.

This was often the case for Titanium. However, this is may be due to the presence of TiO_2, which would not break down during microwave digestion.

Wet ashing results considerably exceed those from microwave digestion for Be, Cr and Ni in the wood-bark, indicating that these elements are partly contained in the ash fraction which are not broken down by microwave digestion. Some of the Co, Cu, Sr

and Pb may also be included in that fraction. Wood-bark also contained very large amounts of Zn, Ba and Mn, the manganese sometimes exceeding 1% in the ash, requiring the less sensitive Inductively Coupled Plasma Atomic Emission Spectroscopy (ICP-AES) to be used.

The trace element content of the straw were much lower than the other fuels with As, Be, Cd and Se all below their limit of quantification. Straw was also heterogeneous with wide variation in measurements for almost all elements. The small ash content of straw is expected to be composed mostly of silicates. No elements were found bound with this ash.

Differences between the microwave and overall results are noted for the Colombian coal, where a proportion of the Cr and Sb were not extracted by the microwave digestion. The same elements were also not extracted from the Polish coal, probably because they are included in silicate or alumino silicate material.

Of the samples measured, sewage sludge had the highest concentrations of As, Co, Cr, Cu, Hg, Ni, Mo, Sr, and Zn. This is partially because it had the highest ash content. Only Be, Ni and Sr appeared to be in modes of occurrence not extracted by the microwave digestion.

The organic fraction of paper sludge originates from wood with additional minerals added during the paper making process. Extraction of some elements from the paper sludge by microwave digestion was very low. Considerably more Ba, Sr, and Ti were measured by wet ashing indicating that these elements were not completely extracted by the microwave procedure. The difference between overall and microwave results for Ti was particularly large. The titanium probably comes from TiO_2, applied to make the finished paper surface scatter light. TiO_2 would not breakdown during microwave digestion, leading to the much lower Ti measurement.

Agricultural waste contains high concentrations of Mn and Zn. These elements were measured in similar concentrations overall and by microwave digestion. Be, Cr, and Ti, were measured in higher concentrations overall than by microwave digestion. Apart

from Ti, this suggests that these elements are held in silicate and alumino silicate minerals.

Pulp sludge comes from the same industry as the paper sludge. It was taken from an earlier stage in the paper making process. Only Ti was measured at a considerably lower concentration by microwave digestion than overall. The overall Ti concentration is much lower than that measured for paper sludge. It is probable that this sample came from a point prior to the addition of any minerals needed to change the finished paper properties.

Plastic waste contains very high concentrations of Cd, Pb, and Ti, possibly from pigments used to colour or print on the plastic, or mineral fillers. The mineral fillers may contain Be, Cd, Ni, Sb and Ti which are measured in lower concentrations by microwave digestion than overall. Some plastics (i.e. Teflon) are not broken down by the application of nitric acid and microwaves. Trace elements contained in these plastics may not have been measured.

Thus the highest concentrations of As, Co, Cr, Cu, Hg, Ni, Mo, Sr and Zn were found in the sewage sludge. The highest concentrations of Cd, Pb and Ti in the plastic waste. While the most Ba, Be, Tl and V were found in Polish coal, and the highest Se and Sb in Colombian coal and paper sludge respectively.

Beryllium and Nickel were not fully extracted by microwave digestion of the wood-bark, sewage sludge, agricultural waste (Be only) or plastic waste. Chromium was also incompletely extracted from wood-bark, as well as agricultural waste and the Polish and Colombian coals. Antimony may have been silicate or alumino silicate bound in the Polish coal, Colombian coal and plastic waste, whilst Sr may have been also in the sewage and paper sludges.

Table 9 Trace Element Contents of Wood – Bark, Straw, Colombian Coal and Polish Coal

	Wood - Bark		**Straw**		**Colombian Coal**		**Polish Coal**	
	Overall	Microwave	Overall	Microwave	Overall	Microwave	Overall	Microwave
As[a]	0.44 ± 0.95	0.44 ± 0.95	<0.1	<0.1	1.75 ± 0.79	1.75 ± 0.79	1.83 ± 0.54	1.83 ± 0.54
Ba	156 ± 14	133 ± 67	13 ± 2	12 ± 5	49 ± 8	41 ± 28	376 ± 74	281 ± 28
Be	0.07 ± 0.01	<0.03	<0.1	<0.05	0.40 ± 0.07	0.44 ± 0.10	1.30 ± 0.12	1.26 ± 0.12
Cd	0.20 ± 0.05	0.26 ± 0.13	<0.15	<0.1	0.26 ± 0.25	0.22 ± 0.14	0.21 ± 0.07	0.32 ± 0.13
Co	0.72 ± 0.06	0.51 ± 0.25	0.08 ± 0.05	0.08	1.63 ± 0.17	1.82 ± 0.44	6.0 ± 1.1	7.8 ± 0.6
Cr	26 ± 5	11 ± 8	2.5 ± 1.1	1.0 ± 0.6	11 ± 2	6.2 ± 0.6	24 ± 2	12.6 ± 1.8
Cu	87 ± 37	68 ± 42	3.2 ± 1.6	2.4 ± 2.2	5.8 ± 1.0	5.3 ± 1.3	25 ± 3	38 ± 28
Hg[b]	0.033 ± 0.001	NM	0.009 ± 0.002	NM	0.031 ± 0.001	NM	0.058 0.010	NM
Ni	10.0 ± 1.8	3.1 ± 1.8	0.90 ± 0.95	1.24	6.5 ± 0.8	7.2 ± 1.2	17.3 ± 3.0	19.7 ± 1.6
Mn	414 ± 68	403 ± 189	20 ± 2	15 ± 5	27 ± 3	30 ± 10	176 ± 9	182 ± 10
Mo	1.26 ± 0.44	1.1 ± 0.5	0.42 ± 0.03	0.34 ± 0.06	1.51 ± 0.14	1.85 ± 0.53	0.98 ± 0.09	1.02 ± 0.30
Pb	3.1 ± 0.4	2.3 ± 1.3	2.6 ± 1.1	3.3 ± 3.3	1.94 ± 0.55	2.6 ± 2.5	34 ± 4	30 ± 6
Sb	0.21 ± 0.10	0.05 ± 0.19	0.08 ± 0.06	0.04 ± 0.10	0.57 ± 0.10	0.18 ± 0.05	1.67 ± 0.38	0.14 ± 0.04
Se[a]	<0.8	<0.8	<0.2	<0.2	5.1 ± 1.0	5.1 ± 1.0	2.4 ± 0.8	2.4 ± 0.8
Sr	51 ± 4	33 ± 43	11 ± 1	9 ± 28	22 ± 2	24 ± 21	85 ± 7	82 ± 8
Ti	94 ± 34	39 ± 66	29 ± 6	<20	251 ± 46	96 ± 25	780 ± 18	207 ± 39
Tl	0.09 ± 0.03	0.12 ± 0.14	0.002 ± 0.005	<0.05	0.11 ± 0.02	0.16 ± 0.12	0.33 ± 0.08	0.25 ± 0.03
V	2.8 ± 0.6	NE	0.82 ± 0.44	NE	11.8 ± 2.0	NE	24 ± 1	NE
Zn	150 ± 21	152 ± 71	31 ± 13	21 ± 8	17.6 ± 6.6	32 ± 28	43 ± 10	70 ± 37

All trace element concentrations in parts per million (ppm)

Values in the centre column indicate only one measurement for that element above the LOQ

a Overall value taken from ICP-MS of microwave digestion

b AAS with LECO Hg analyser

NM – Not Measured

NE – Not Extracted

Table 10 Trace Element Contents of Sewage Sludge, Paper Sludge, Agricultural Waste and Pulp Sludge

	Sewage Sludge		Paper Sludge		Agricultural Waste		Pulp Sludge	
	Overall	Microwave	Overall	Microwave	Overall	Microwave	Overall	Microwave
As[a]	3.8 ± 0.5	3.8 ± 0.5	0.53 ± 0.94	0.53 ± 0.94	0.34 ± 0.13	0.34 ± 0.13	0.50 ± 0.46	0.50 ± 0.46
Ba	266 ± 49	190 ± 23	143 ± 17	72 ± 45	13.3 ± 1.2	11.7 ± 4.6	45 ± 6	42 ± 23
Be	0.49 ± 0.08	0.29 ± 0.12	0.05 ± 0.03	<0.05	0.18 ± 0.07	0.04 ± 0.03	<0.03	<0.05
Cd	2.3 ± 1.7	0.93 ± 0.19	0.77 ± 0.19	0.44 ± 0.31	0.36 ± 0.09	0.34 ± 0.06	1.99 ± 0.32	2.14 ± 0.87
Co	9.6 ± 2.3	8.4 ± 0.8	0.89 ± 0.41	0.45 ± 0.27	0.40 ± 0.07	0.36 ± 0.22	0.45 ± 0.08	0.33 ± 0.14
Cr	143 ± 30	92 ± 6	11.3 ± 2.3	7.8 ± 6.8	8.8 ± 3.7	3.8 ± 0.8	25 ± 4	22 ± 10
Cu	283 ± 45	262 ± 32	16.3 ± 1.6	17 ± 10	38.2 ± 3.9	47 ± 35	14.7 ± 7.1	13 ± 4
Hg[b]	0.85 ± 0.13	NM	0.083 ± 0.016	NM	0.95 ± 0.03	NM	0.083 ± 0.004	NM
Ni	51 ± 14	33 ± 3	2.9 ± 0.9	2.4 ± 3.8	10.6 ± 2.2	10.3 ± 3.8	10.1 ± 1.8	7.5 ± 3.3
Mn	396 ± 66	299 ± 39	62 ± 8	35 ± 24	240 ± 48	217 ± 180	137 ± 22	137 ± 62
Mo	18.7 ± 4.1	16 ± 2	1.18 ± 0.31	0.73 ± 0.14	9.1 ± 0.9	10.3 ± 4.0	0.97 ± 0.25	1.0 ± 0.5
Pb	32 ± 8	26 ± 5	21 ± 3	18 ± 2	0.86 ± 0.33	1.24 ± 1.59	2.3 ± 0.8	2.8 ± 0.9
Sb	3.3 ± 1.0	1.05 ± 0.16	6.6 ± 1.3	3.3 ± 4.4	0.08 ± 0.02	0.06 ± 0.06	0.17 ± 0.30	0.03 ± 0.01
Se[a]	<1.30	<1.30	<0.80	<0.80	<0.8	<0.8	<0.80	<0.8
Sr	120 ± 19	96.5 ± 15.3	16.7 ± 1.5	2.74	19.0 ± 1.7	23.6	13.1 ± 1.6	11 ± 15
Ti	2743 ± 38	468 ± 57	755 ± 246	1.5	26.3 ± 24.5	2.0	40 ± 13	8 ± 13
Tl	0.19 ± 0.05	0.10 ± 0.02	0.010 ± 0.004	<0.05	0.007 ± 0.005	0.01	0.13 ± 0.04	0.24 ± 0.01
V	14.8 ± 3.4	NE	2.3 ± 0.2	NE	4.2 ± 1.0	NE	5.3 ± 1.2	NE
Zn	556 ± 90	546 ± 97	132 ± 26	104 ± 85	252 ± 44	295 ± 116	200 ± 31	220 ± 90

All trace element concentrations in parts per million (ppm)

Values in the centre column indicate only one measurement for that element above the LOQ

a Overall value taken from ICP-MS of microwave digestion

b AAS with LECO Hg analyser

NE – Not Extracted

NM – Not Measured

Table 11 Trace Element Content of Plastic Waste

	Plastic Waste	
	Overall	Microwave
As[a]	0.31 ± 0.02	0.31 ± 0.02
Ba	263 ± 39	253 ± 113
Be	0.11 ± 0.03	0.04 ± 0.02
Cd	4.1 ± 0.2	2.9 ± 0.8
Co	4.6 ± 1.3	3.2 ± 1.5
Cr	33 ± 4	30 ± 10
Cu	65 ± 31	51 ± 7
Hg[b]	0.055 ± 0.003	NM
Ni	5.5 ± 0.6	2.70 ± 0.50
Mn	26 ± 4	22.1 ± 1.9
Mo	1.10 ± 0.21	0.89 ± 0.36
Pb	35 ± 18	17.5 ± 13.7
Sb	3.5 ± 0.4	0.62 ± 0.75
Se[a]	<0.60	<0.60
Sr	17.1 ± 2.2	17.8 ± 1.9
Ti	2993 ± 359	18.4 ± 2.6
Tl	0.03 ± 0.01	0.02 ± 0.02
V	3.3 ± 1.0	NE
Zn	501 ± 85	942 ± 2029

All trace element concentrations in parts per million (ppm)

a Overall value taken from ICP-MS of microwave digestion

b AAS with LECO Hg analyser

NM – Not Measured

NE – Not Extracted

5.0 RESULTS

In this section, results for trace element behaviour and emissions of NOx and N_2O are presented. Data on trace elements are presented in four groups. These categorises (described below) are based on the elements of concern to the US National Research Council (1980) and the list of trace elements whose emission from waste combustion is controlled by EU directive 2000/76/EC.

The first group consists of those trace elements thought to be most toxic: As, Cd, Hg, Se and Pb. The second group contains the less toxic elements Cr, Cu, Ni, V and Zn, whilst results for elements of moderate concern Be, Mn, Mo and Tl are in the third group. The remaining elements studied (Ba, Co, Sb and Sr) are presented in the fourth group, elements of minor concern.

For each group of trace elements, results are presented for "percentage retention" in ash and for their relative enrichment on sinter ash. In both cases two figures are presented, showing results obtained during experiments at 800 °C above and those at 900 °C below. Trace element concentrations in the raw fuels are also included in a table below the "percentage retention" results.

In analysing these data, percentage retention of trace elements in ash has been divided into three categories. The first category consists of those elements considered as almost completely volatilised during combustion, where less than 20 % of the amounts originally present in the fuel were retained in ash. In the second category were elements considered as having been almost completely retained, i.e. those with greater than 80 % retention in the ash. In the final category were elements that were partially volatilised.

Due to limitations of space, the raw trace element concentration data used to calculate the results presented in this chapter have been included on the CD inside the back cover of this thesis. "Synergy diagrams" – plots of the amount of a trace element retained in ash plotted against the weight fraction of auxiliary fuel are also only included in the main text in cases where they help describe the results. "Synergy diagrams" for all

elements and fuel blends have been prepared and are included on the CD inside the back cover of this thesis.

Thermodynamic equilibrium predictions of trace element behaviour have been made for each main fuel, mixtures of 70 % main fuel with 30 % auxiliary fuel and where auxiliary fuels have been combusted alone. Predictions were possible for all elements except molybdenum, where a lack of thermodynamic data prevented simulation.

Compounds predicted by MTDATA to be present were only described by the number of atoms of each element they contained. Normally rearrangement into common compounds was not difficult (i.e. $O4PbS \rightarrow PbSO_4$). However, several solid compounds have been predicted which contain two metallic elements and oxygen. These have been presented as mixed oxides, this has been done for convenience and does not imply that a particular form was being suggested. There are several points common to the behaviour of multiple trace elements. These are summarised below.

5.0.1 The Influence of Combustion Temperature

The difference in temperature between 800 and 900 °C is relatively small compared to the temperature ranges over which trace element behaviour often varies. For many trace elements the difference between the results obtained after combustion at 800 °C are little changed from those obtained at 900 °C. Where this is the case it has not been explicitly mentioned in the text. Only cases where the combustion temperature was influential are noted.

5.0.2 Retention of Trace Elements Predicted to Volatilise

Some trace elements were predicted to volatilise to a greater degree than actually observed. This may have been because a proportion of these trace elements were prevented volatilising because they could not escape from their original modes of occurrence in the fuels. This could be because the mode of occurrence does not decompose at the combustion temperature, or because of a kinetic limitation of the time at that temperature being too short for breakdown of the original or intermediate mode of occurrence. MTDATA does not take into account the original modes of the trace

elements in the raw fuels, hence causing the difference in predicted and measured behaviour.

The modes of occurrence that prevent trace elements from being released have not been investigated in this study. The possible modes of occurrence of each trace element are numerous and complex. Their determination in the fuels used here would be a suitable topic for further study.

5.0.3 Volatilisation of Trace Elements Predicted to Remain Completely in Ash

Some trace elements (including Ba, Co, Mn and Sr) were volatilised during combustion, contrary to the prediction of thermodynamic equilibrium modelling. This is likely to occur where the trace element was present in the organic matrix of the fuel. During combustion the organic matrix is burnt away. Any trace elements dispersed inside that matrix will be released into the gas phase when the atoms holding them are burnt away. The released trace element may immediately recondense on ash particles, if thermodynamically favoured to form a solid. There is, however, only a short time (< 2 s) for this to occur. Trace element atoms that have not recondensed in this time will exit the suspension-firing reactor with the flue gas.

Trace elements bound in other modes of occurrence maybe similarly volatilised if these decompose during combustion (e.g. pyrite). The extent to which these original forms decompose is likely to be smaller than that of organic matrices so they may not release their trace elements to the same extent.

5.0.4 Compounds not Included in Thermodynamic Equilibrium Modelling

Only compounds for which there was thermodynamic data could be included in thermodynamic equilibrium models. Actual and predicted trace element behaviours could differ where an important compound, for which there is no thermodynamic data, has not been included in the model. Lack of thermodynamic data for molybdenum compounds prevented thermodynamic modelling of this trace element from being undertaken.

5.1 Trace Element Results for Main Fuels

This section describes the trace element results obtained for the combustion of the four main fuels. These were: wood-bark, Colombian coal / straw, Colombian coal and Polish coal. Results for wood-bark, Colombian coal / straw and Colombian coal are based on the average of two runs. Polish coal data are derived from single runs.

Arsenic was only partially released from either coal sample, between 15 and 80 % of their original contents remaining with the ash (Figure 10). Results for wood-bark and Colombian coal / straw indicate that at 800 °C arsenic was partially volatilised from these fuels. Estimation of the proportion remaining in ash is hindered by large experimental error in the measurement of arsenic in the wood-bark and straw, compared to their low original contents. Volatilised arsenic from 'Colombian-coal' recondensed on the 'sinter-ash' during combustion at 800 °C, enriching the 'sinter-ash' with arsenic (Figure 11). This was not observed at 900 °C, or for any other fuel.

Cadmium was partially volatilised from the wood-bark (20 – 75 %), 'Colombian-coal' (at least 25 %) and 'Polish-coal' (15 – 100 %). Cadmium was enriched on sinter-ash from the 'Colombian-coal'. Some enrichment on 'sinter-ash' from coal/straw may be discerned during combustion at 800 °C (but not at 900 °C), but differences were small. Since the Cd concentration in the straw sample was very low, the LOQ (0.15 ppm) was taken as the maximum possible value. The maximum possible level of cadmium release from coal/straw combustion could then be calculated and is presented in Figure 10.

Mercury was almost completely released from all the fuels studied. Recondensation of a small amount of the volatilised mercury released from Colombian coal/straw and 'Polish- coal' has resulted in extensive enrichment on the 'sinter-ashes' of these fuels.

Selenium almost completely volatilised from coal/straw, 'Colombian-coal' and 'Polish-coal'. In pf-combustion, selenium was expected to be one of two most volatile elements, together with mercury (Clarke and Sloss, 1992). However, a minimum of fifteen percent of the selenium in wood-bark was retained in the ash. Calculation of the actual percentage retention was hindered by the very low level present in the raw wood-bark (< 0.8 ppm).

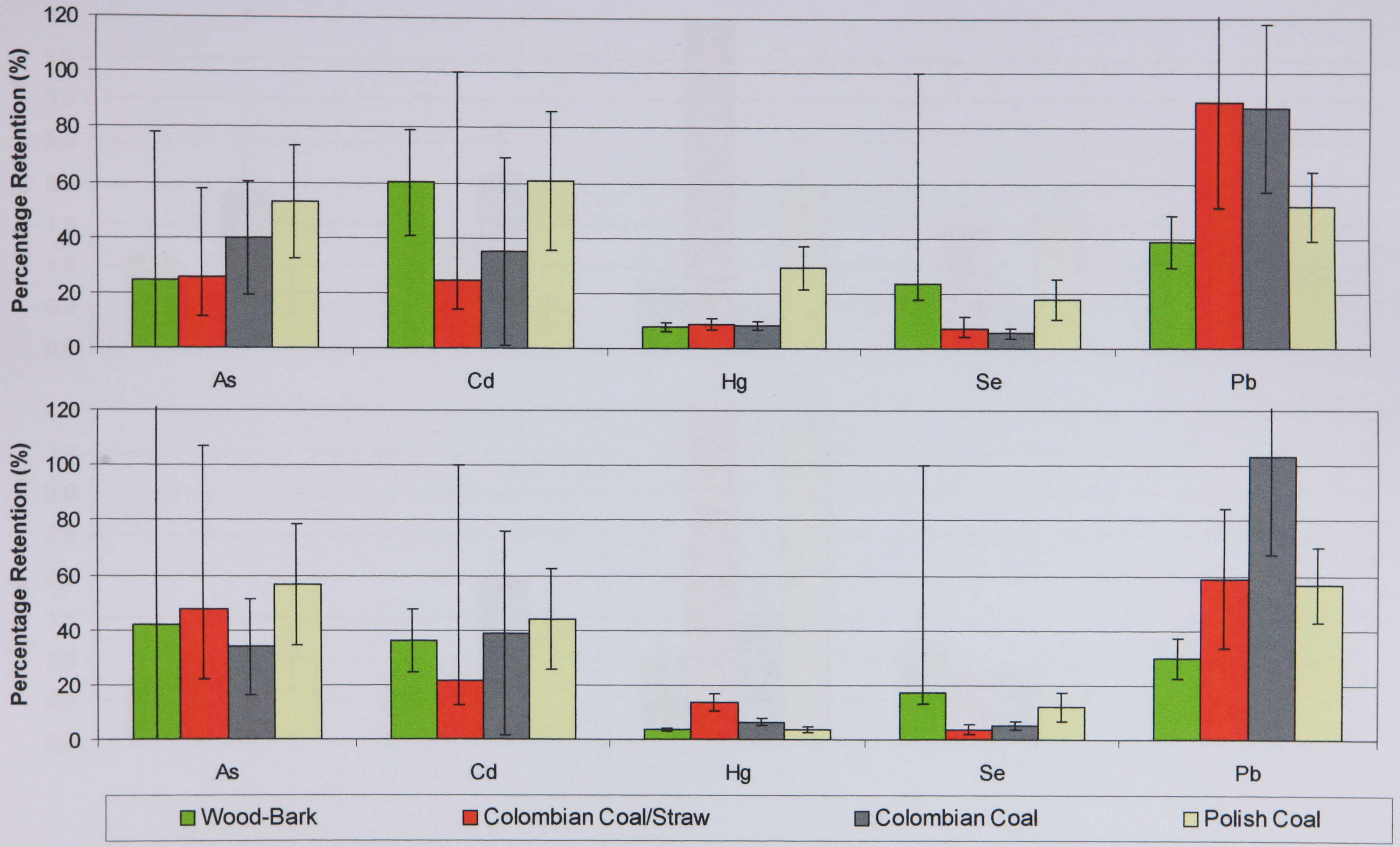


Figure 10 Percentage Retention of As, Cd, Hg, Se and Pb in Ash After Combustion of the Main Fuels

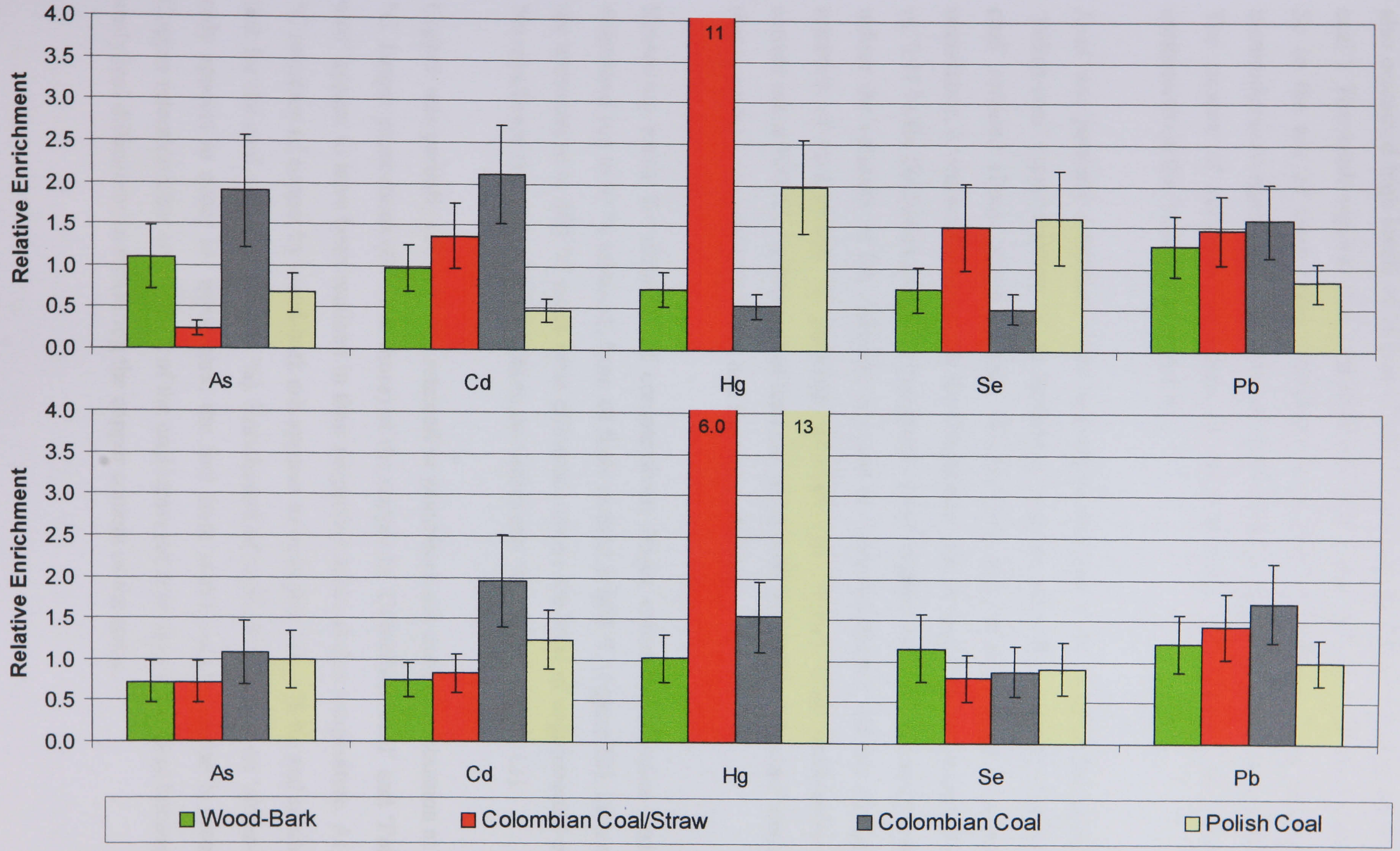


Figure 11 Relative Enrichment of As, Cd, Hg, Se and Pb in Sinter Ash During Combustion of the Main Fuels

'Polish-coal' and wood-bark retained similar proportions of their selenium. Both fuels also contained high levels of calcium (7.98 g/kg for wood-bark, 4.94 g/kg for 'Polish-coal'). The result suggests that formation of $CaSeO_4$ may have caused the retention of Se in the ash of these fuels. However, there does not appear to be data in the thermodynamic equilibrium database to check whether this is indeed a likely pathway. The capture of volatilised selenium by calcium might also explain the selenium enrichment on the 'sinter-ash' (Figure 9).

Lead was partially volatilised from wood-bark (residue < 50 % of initial total) and 'Polish-coal' (approximately 60 % remaining with the ash). By contrast, 'Colombian-coal' retained almost all of its lead. Whilst there may be differences in modes of occurrence, it was worth noting that the Colombian coal contained less chlorine (0.04 % vs. 0.11 % for the Polish coal) and marginally more sulphur. Both factors would tend to reduce the volatility of Pb. Addition of straw to 'Colombian-coal' did not change the retention of lead at 800 °C, although retention was reduced when combustion was carried out at 900 °C. Enrichment of lead on 'sinter-ash' for 'Colombian-coal' indicates that some lead was also volatilised and then recondensed.

Reviewing result for elements of comparatively lesser concern, c*hromium* partially volatilised (up to 65 % released) from all fuels studied at 800 °C (Figure 12). Increasing the temperature to 900 °C made little difference above the level of experimental error. No significant enrichment of chromium on 'sinter-ash' was found (Figure 13).

Copper was partially (20 – 55 %) retained in wood-bark ash during combustion at 900 °C. Larger proportions (60 % or more) of the copper in 'Colombian coal' and 'Polish-coal' appear to have been retained in their respective ashes at this temperature. At 800 °C retention of copper by wood-bark ash appears to be higher (25 – 75 %) and similar to that for the coal samples (40 – 95 %). Enrichment of volatilised copper on 'sinter-ash' only appears to occur for wood-bark, the fuel from which copper release is greatest. Copper retention after combustion of the coal/straw mixture does not appear because of analytical difficulties in measuring the copper content of the straw.

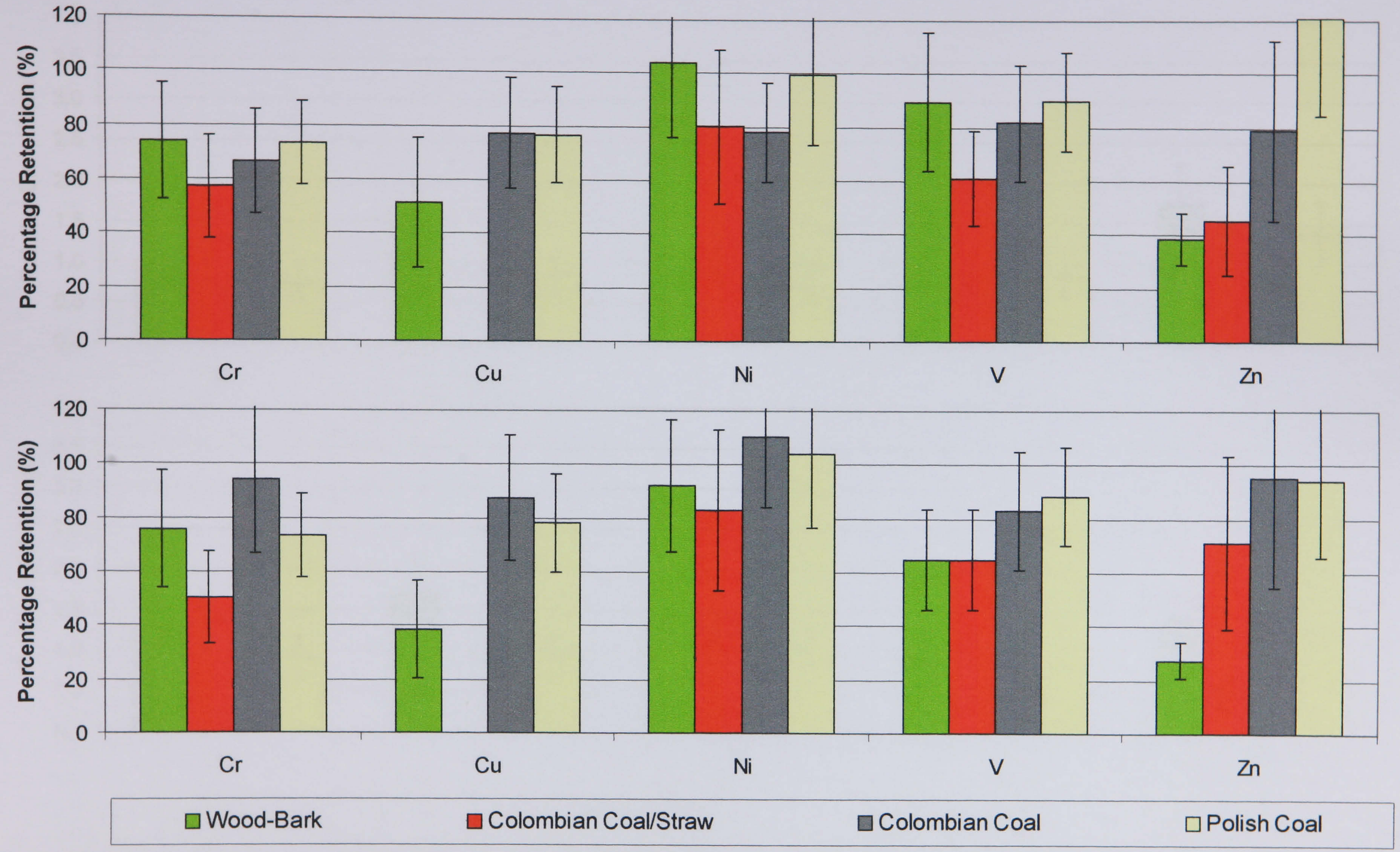


Figure 12 Percentage Retention of Cr, Cu, Ni, V and Zn in Ash After Combustion of the Main Fuels

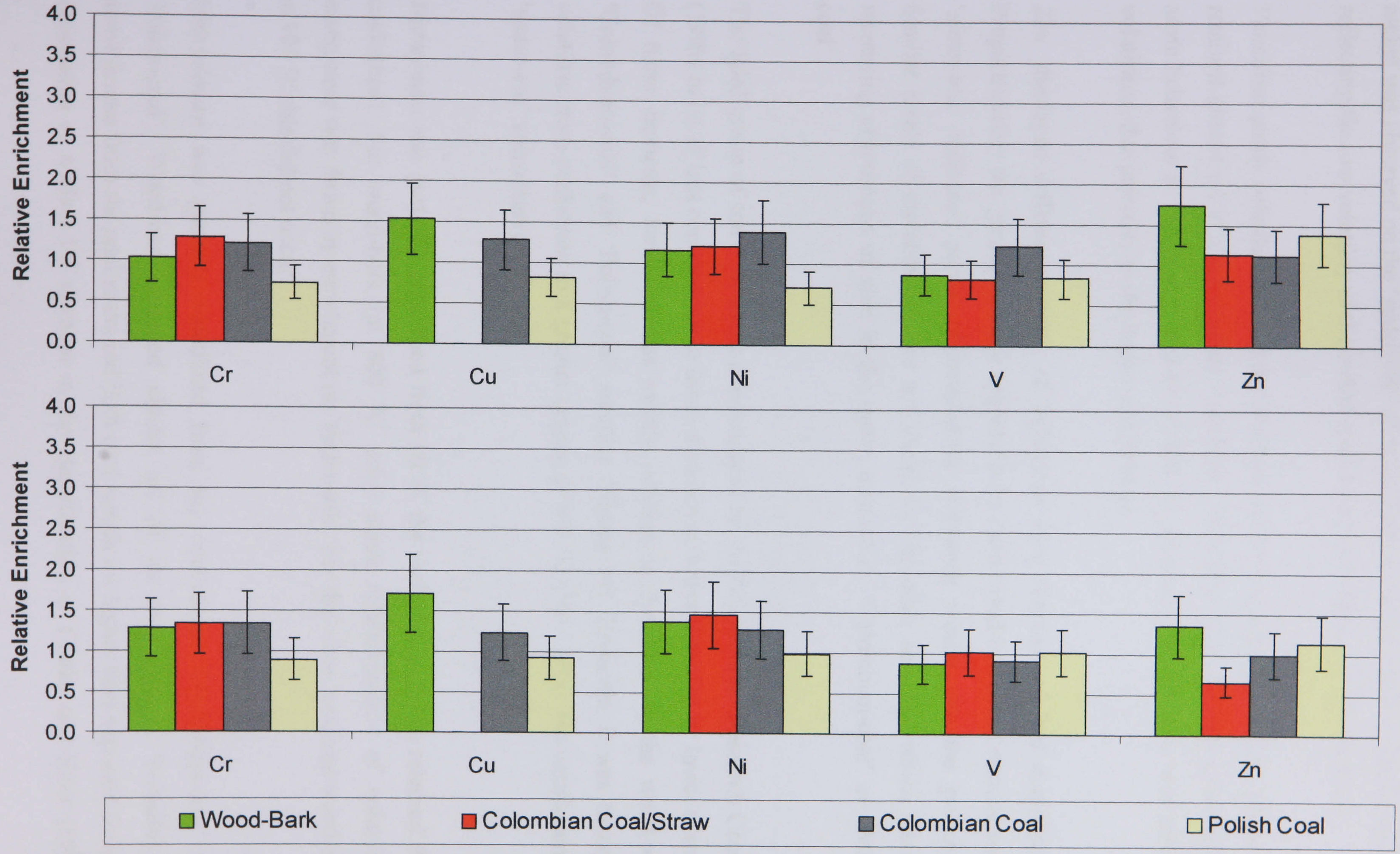


Figure 13 Relative Enrichment of Cr, Cu, Ni, V and Zn in Sinter Ash During Combustion of the Main Fuels

Nickel was mostly retained in the fuel ashes, for all fuels studied. Slight enrichment of nickel was observed on the 'sinter-ash' of wood-bark, coal/straw and 'Colombian-coal', reflecting the low volatility of the nickel species in the combustion environment.

Vanadium partly volatilised during the combustion of the coal/straw mixture. Both coals retained almost all of their original vanadium. Vanadium in wood-bark exhibited the same behaviour as that from the coals at 800 °C. However, at 900 °C it was partially volatilised, due probably to the higher temperature.

Zinc displayed different patterns of behaviour as a function of fuel composition. Proportionately the greatest release appears to be from wood-bark; zinc enrichment on 'sinter-ash' indicated partial recondensation following release into the gas phase. Similar levels of enrichment were not found for the other samples, which retained increasing proportions of zinc in the order: coal/straw, 'Colombian-coal' or 'Polish-coal'.

The third group of trace elements is considered by the US National Research Council (1980) to be of less concern due to lower abundance, lower volatility *or* lower toxicity. Of these elements, *beryllium* was mostly retained in the ashes of the wood-bark, 'Colombian-coal' and 'Polish-coal' samples (Figure 14). However, it was found to volatilise from coal/straw to a greater degree at 900 °C (30 – 70%). No enrichment of 'sinter-ash' was observed.

Manganese was partially volatilised from all of the fuels (up to 50 % released from coal/straw). For wood-bark (at 800 °C only) some recondensation of volatilised manganese was found by enrichment on 'sinter-ash'. For the other fuels and wood-bark at 900 °C this did not occur.

Molybdenum was partially volatilised from the coal/straw, 'Colombian-coal' and 'Polish-coal'. Wood-bark retained almost all of its molybdenum. Volatility of molybdenum from the coal/straw and both coal samples is higher than expected from its designation as a class I/II element in the classification of Clarke and Sloss (1992).

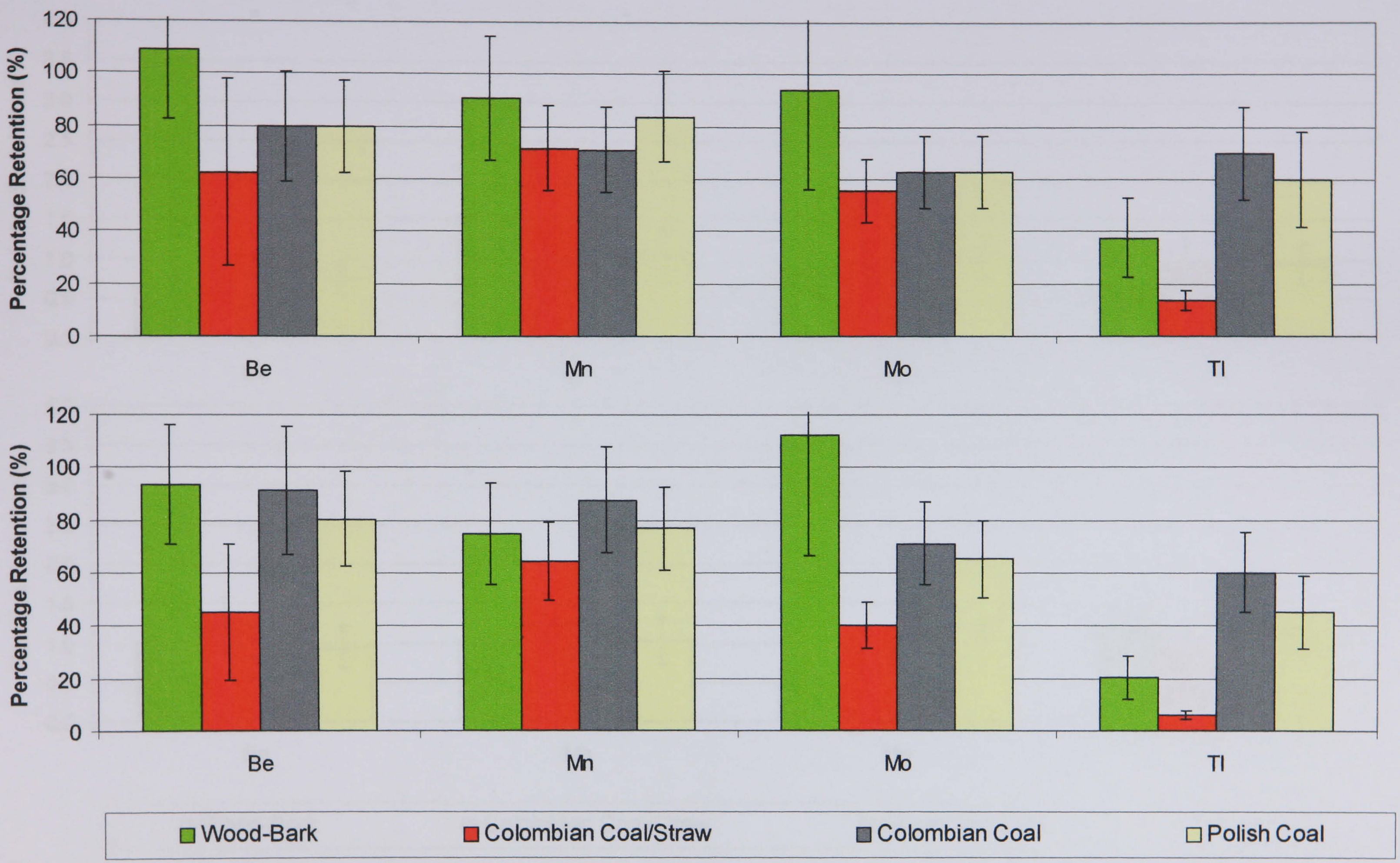


Figure 14 Percentage Retention of Be, Mn, Mo and Tl in Ash After Combustion of the Main Fuels

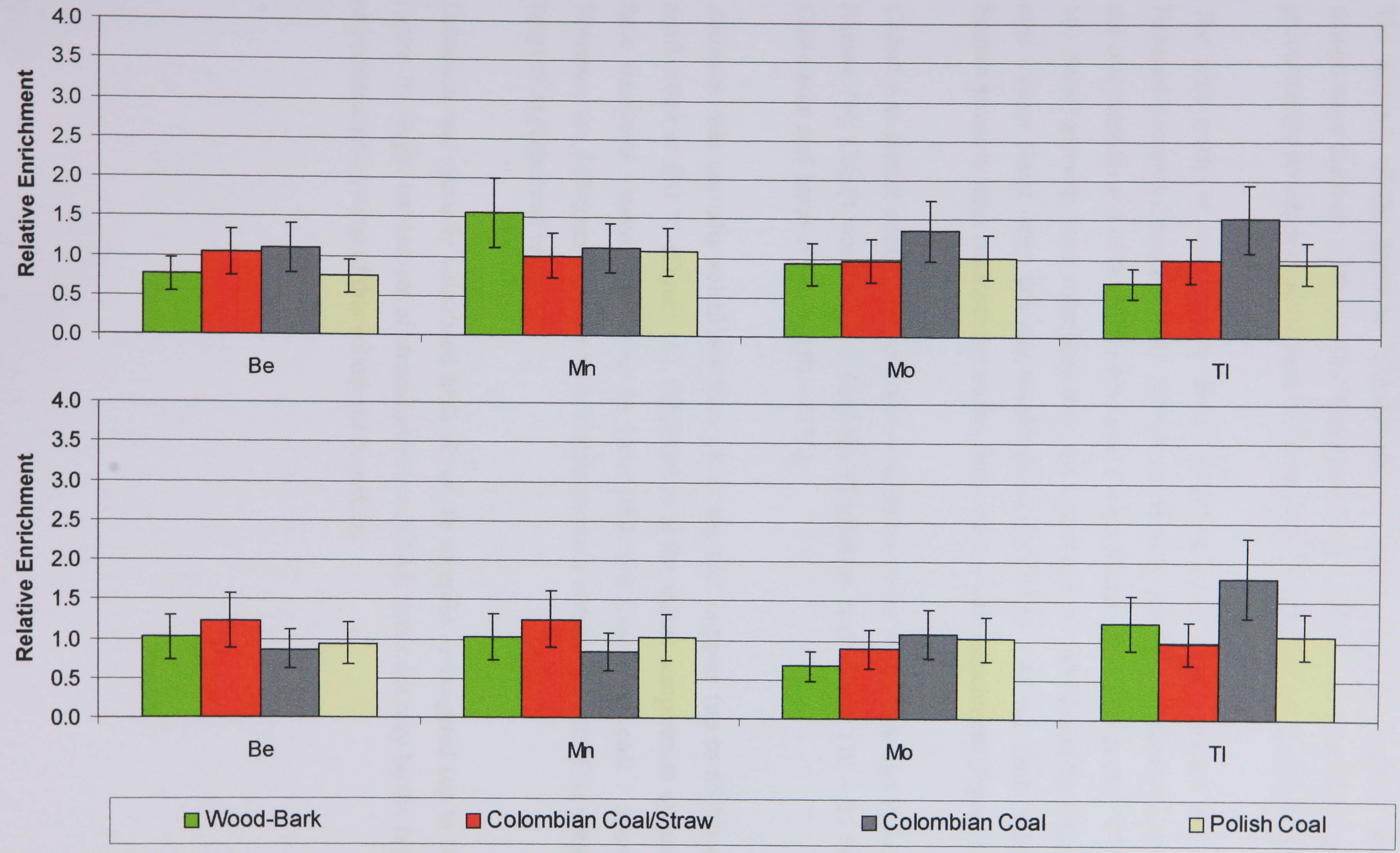


Figure 15 Relative Enrichment of Be, Mn, Mo and Tl in Sinter Ash During Combustion of the Main Fuels

Thallium was almost completely volatilised from the coal/straw. More was retained in wood-bark ash whilst thallium was only partially volatilised from both coal samples. The addition of the straw to 'Colombian-coal' greatly reduced thallium retention, though most thallium (<90 %) was 'Colombian-coal' derived. Straw addition has also prevented the enrichment of thallium on 'sinter-ash', as recorded for 'Colombian-coal'.

The final group of elements are those thought to be of minor concern by the US National Research Council (1980). *Barium* was almost completely retained in the ash of the coal samples and of the Colombian coal / straw blend when burnt at 800 °C (Figure 16). Small amounts were volatilised from the wood-bark (5 – 45 %) and the Colombian coal / straw blend when this was combusted at 900 °C (5 – 45 %). Little volatilised barium seems to have recondensed on the sinter ash to cause enrichment (Figure 17).

Cobalt was almost completely retained in the ashes of the wood-bark and Polish coal (Figure 16). Cobalt was liberated from the Colombian coal / straw (10 – 55 %) and Colombian coal burnt at 800 °C (10 – 45 %).

Antimony was partially volatilised from all of the fuel samples (up to 65 %) during combustion at 800 °C (Figure 16). Combustion at the higher temperature appeared to have increased antimony retention by wood-bark and Colombian coal / straw ash. However, the difference between these results as those obtained at 800 °C is within the range of experimental error.

Strontium was partially volatilised from all of the samples investigated (up to 55 %), Figure 16. Slight enrichment of strontium on wood-bark sinter ash may be the result of recondensation of some of this volatilised strontium.

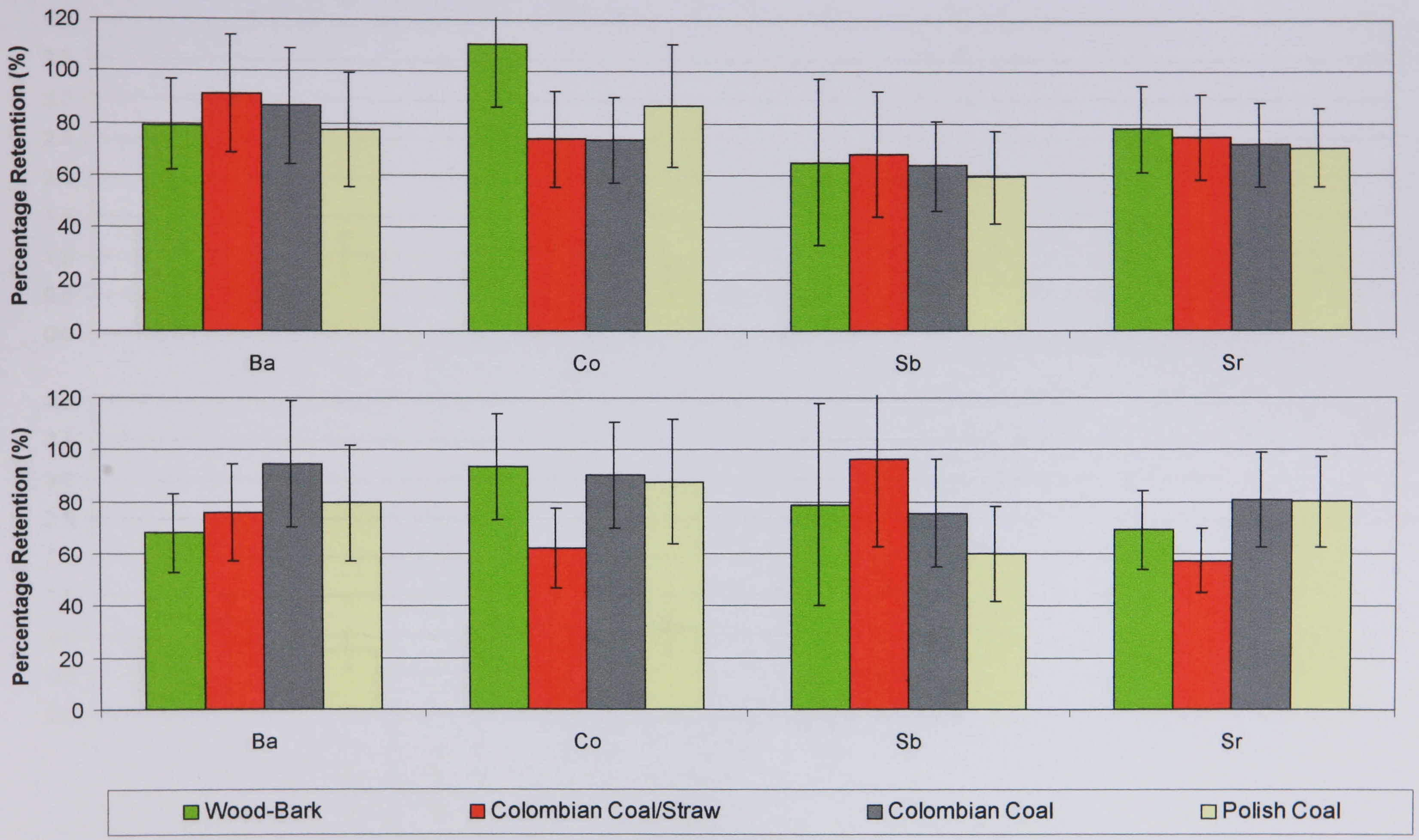


Figure 16 Percentage Retention of Ba, Co, Sb and Sr in Ash After Combustion of the Main Fuels

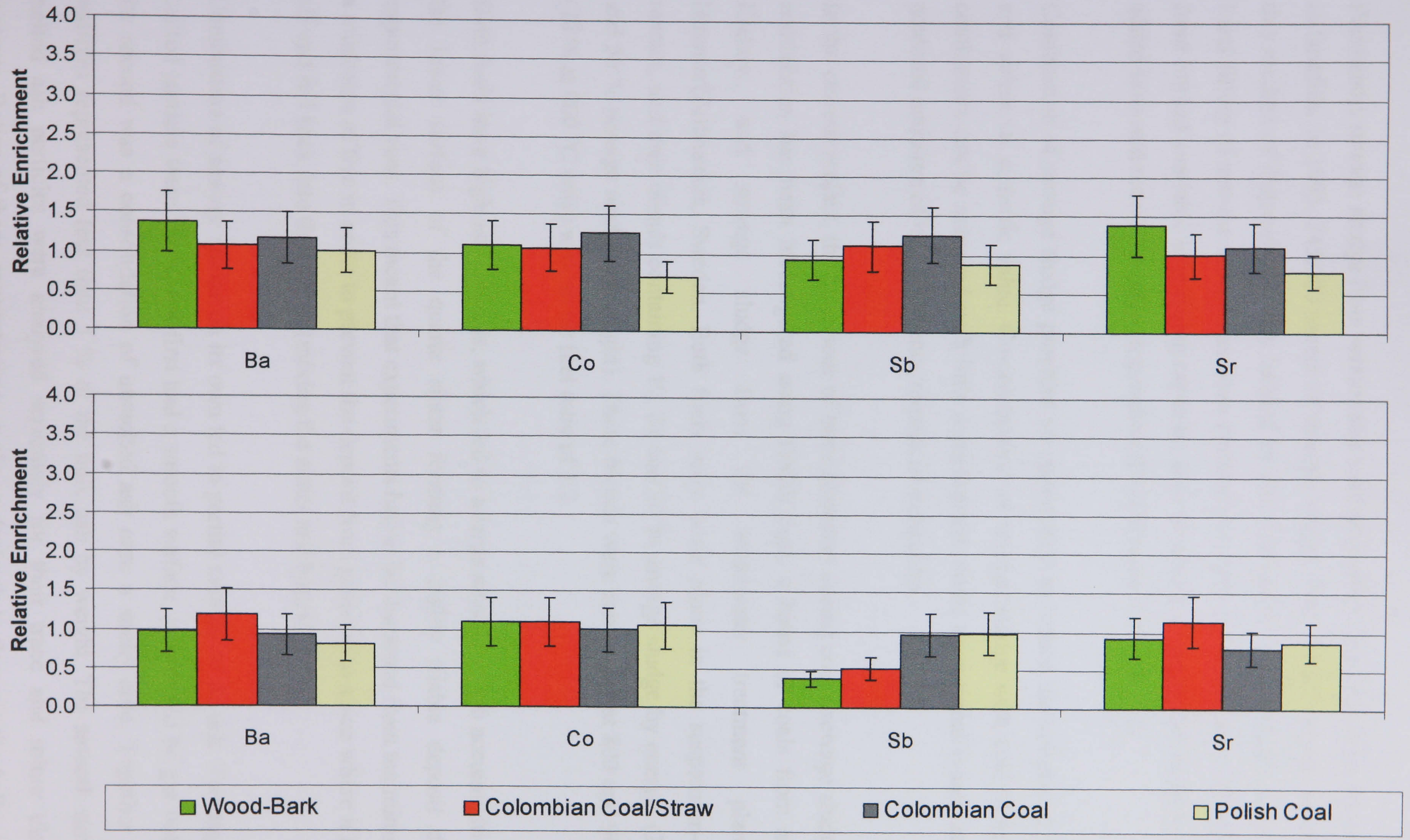


Figure 17 Relative Enrichment of Ba, Co, Sb and Sr in Sinter Ash During Combustion of the Main Fuel

5.2 Polish Coal and Sewage Sludge Co-Combustion

Previously, sewage sludge from wastewater treatment plants has been dumped at sea or in landfills. In 1995, 245,000 tonnes of sewage sludge were dumped at sea. Since 1998 this method of disposal has been banned by the Conference on the North Sea (1990). Land filling of sewage sludge has been curtailed recently by rising costs. These result from limited available land filling capacity, poor prospects of additional capacity being added soon and recent European legislation (EU Directive 1999/31/EC).

Combustion of sewage sludge provides an opportunity to reduce the volume of sludge and utilize its calorific value. Co-combustion of sewage sludge with coal in existing combustors can be achieved with little modification. Some operational issues, such as potential emission of trace elements, require investigation.

In the current project, the behaviour of trace elements during coal / sewage sludge co-combustion has been investigated using Polish coal, a blend of coals from around Krakow, and sewage sludge from the wastewater treatment plant at Himmerfjärdsverket, Sweden. Both fuels were burnt alone in the suspension-firing reactor, and then blends containing 10, 20 and 30 % sewage sludge by energy, (25, 43 and 56 % sewage sludge by weight). These blends were combusted at 800 and 900 °C (20 % at 800 °C only) with an air fuel ratio of 1.2.

Both fuels have high ash contents, which led to a large amount of ash accumulating on the lower surface of the quartz sinter forming a highly friable deposit during experimental runs. This meant that experiments had to be shortened from ten minutes to a minimum of five in order to prevent the deposit from growing to a size where it broke off and fell back into the reactor (mixing the sinter and bottom ashes).

Combustion of sewage sludge on its own led to partial melting of the ash. Two types of melted particle were found, the first had a smooth surface, punctuated by gas bubbles, the second was a consolidation of unmelted ash onto a sticky core. Together these particles represented less than 5 % of the bulk ash by weight. The smooth surfaced melted ash particles were analysed separately for their trace and minor element contents. Ratios of these concentrations in the melted ash to those in the bulk ash are

presented in Table 12 (trace elements) and Table 13 (minor elements). Nominally, a ratio > 1 indicates the element is found preferentially in the melted ash and a ratio < 1 that it is depleted. However, the enrichment or depletion of a minor element such as silicon can greatly affect the ratios recorded for trace elements. To determine enrichment or depletion the ratio for the element in question must be compared to that of other elements in the same ash.

Table 12 Ratios of Trace Element Concentrations in Melted and Bulk Ashes

Trace Element	Ratio at 800°C	Ratio at 900°C
Ba	0.77	0.92
Be	0.73	0.90
Cd	0.31	0.34
Co	0.77	1.13
Cr	0.80	1.10
Cu	0.76	1.06
Mn	0.98	1.42
Mo	0.77	1.23
Ni	0.75	1.24
Pb	0.81	0.58
Sb	0.73	0.73
Se	0.42	0.58
Sr	0.86	1.00
Tl	0.44	0.36
V	0.86	1.11
Zn	0.93	0.79

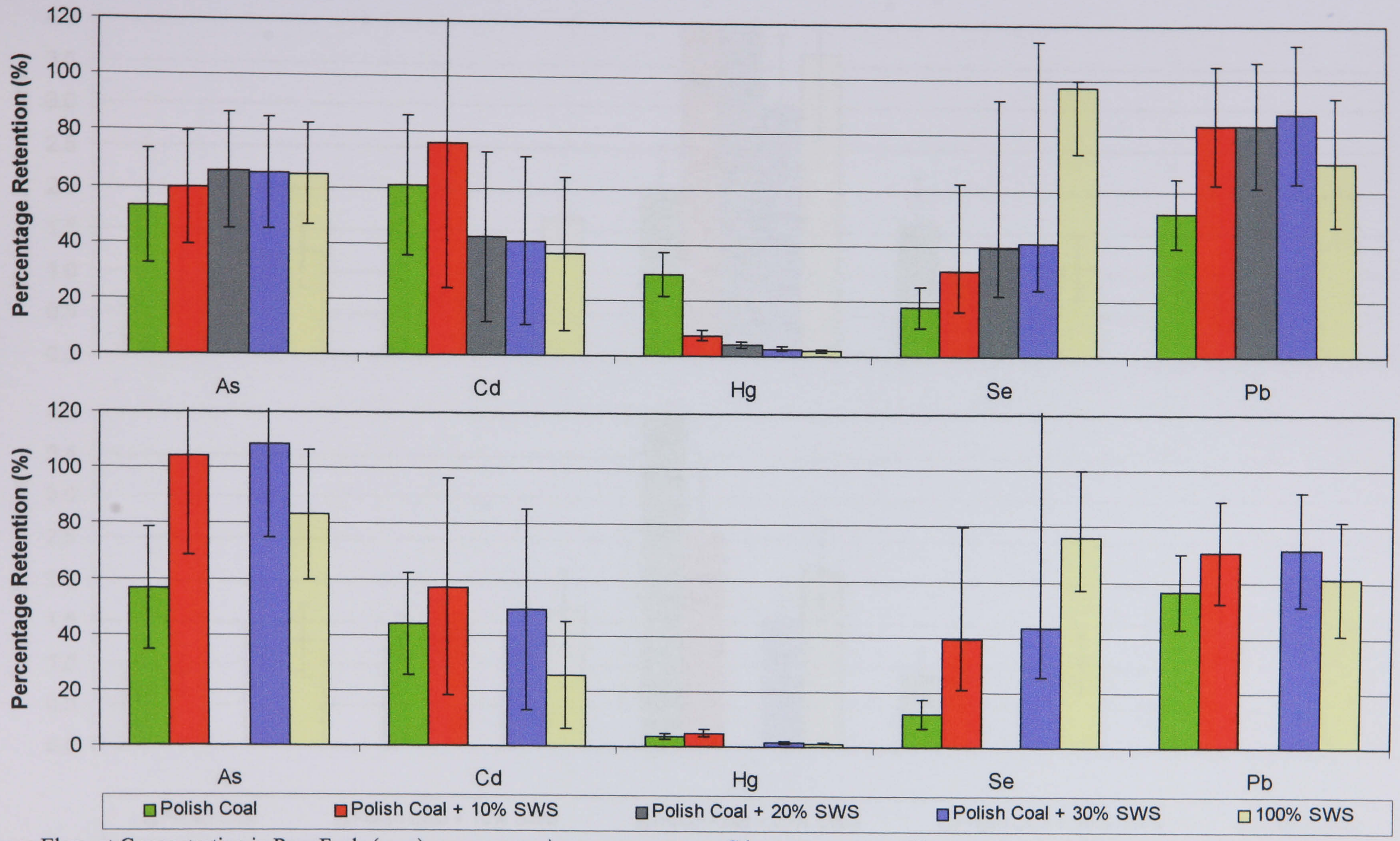
Note: the small amount of sample prevented measurement of arsenic and mercury concentrations in the melted ash.

Table 13 Ratios of Minor Element Concentrations in Melted and Bulk Ashes

Minor Element	Ratio at 800°C	Ratio at 900°C
Al	0.88	1.02
Ca	0.88	0.94
Fe	1.01	1.31
K	1.06	1.42
Mg	0.91	1.06
Na	1.06	1.64
Ti	0.93	1.10

Partial melting of the sewage sludge ash does not appear to have had a significant influence on trace element behaviour. The proportion of each trace element incorporated (or not) in the melted ash was small, as all of the ratios of element concentrations in the melted and bulk ash were less than two and the melted fraction represented less than 5 % of the ash weight.

Manganese, molybdenum and nickel however, were found preferentially in the melted ash after combustion at 900 °C. No trace elements were preferentially contained in the 800 °C melted ash although cadmium, selenium and thallium were depleted from this ash. Also depleted from the melted phase at 900 °C was lead. The alkali metals sodium and potassium were enriched in ashes at either temperature, as was iron (900 °C only).



Trace Element Concentration in Raw Fuels (ppm):	As	Cd	Hg	Se	Pb
Polish Coal	1.8 ± 0.6	0.21 ± 0.07	0.06 ± 0.01	2.4 ± 0.8	34 ± 4
Swedish Sewage Sludge	3.8 ± 0.5	2.3 ± 1.7	0.85 ± 0.13	<1.3	32 ± 8

Figure 18 Percentage Retention of As, Cd, Hg, Se and Pb in Ash After Polish Coal / Sewage Sludge Co-Combustion

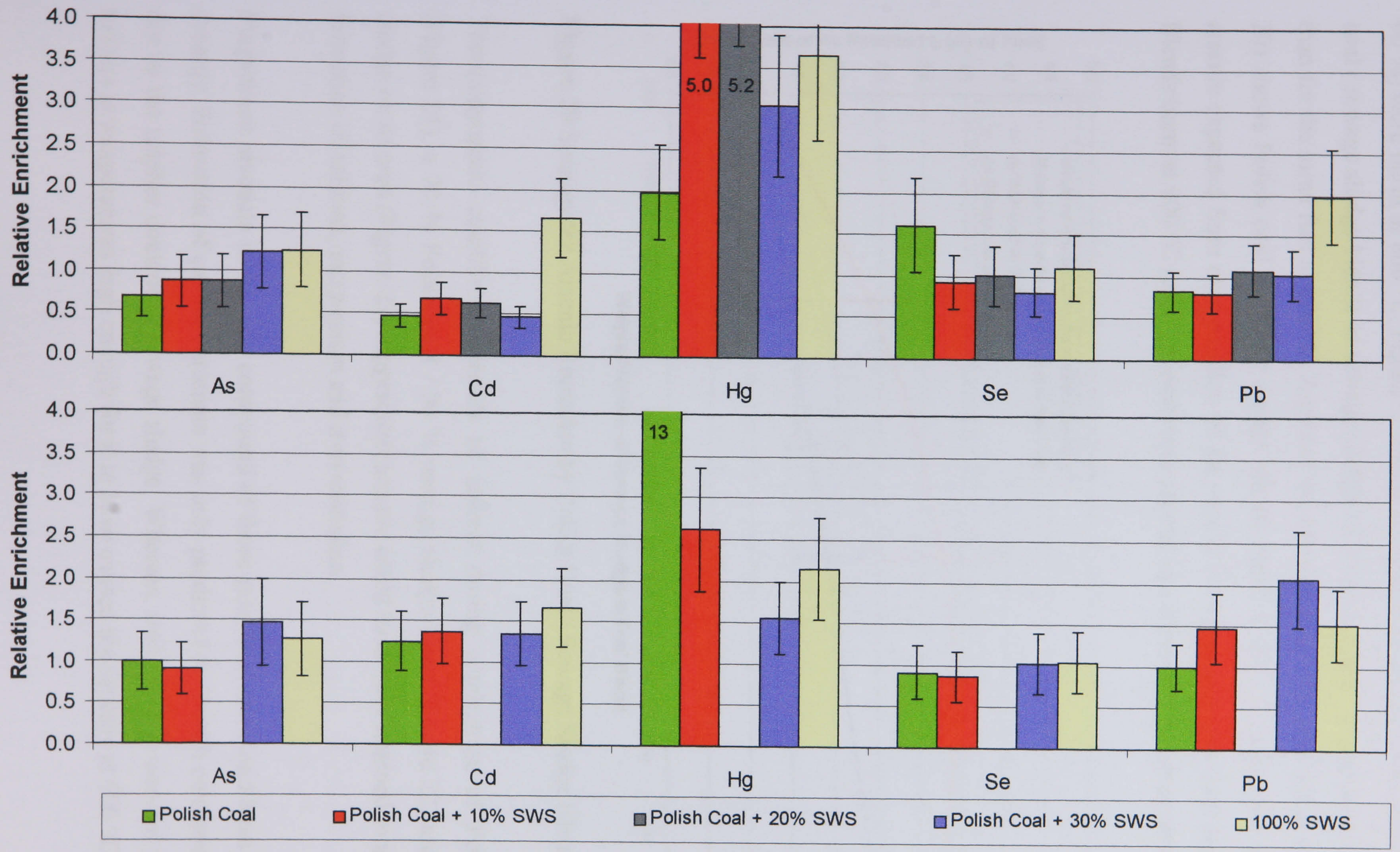


Figure 19 Relative Enrichment of As, Cd, Hg, Se and Pb in Sinter Ash During Polish Coal / Sewage Sludge Co-Combustion
Note: A relative enrichment of one corresponds to being found in equal concentrations in the sinter and bottom ashes.

5.2.1 Arsenic

Arsenic was partially volatilised when Polish coal (20 – 70 %) or sewage sludge (15 – 60 %) were burnt at 800 °C, Figure 1. Retention of arsenic during combustion of Polish coal / sewage sludge blends or sewage sludge on its own at 900 °C appears to be greater than for the same fuel at 800 °C. A plot of the amount of arsenic retained in ash (Figure 20) shows Polish coal / sewage sludge blends burnt at 800 °C retain the amount of arsenic expected from extrapolation of the results for the constituent fuels burnt alone. Blends burnt at 900 °C have retained more arsenic in a synergy for arsenic retention.

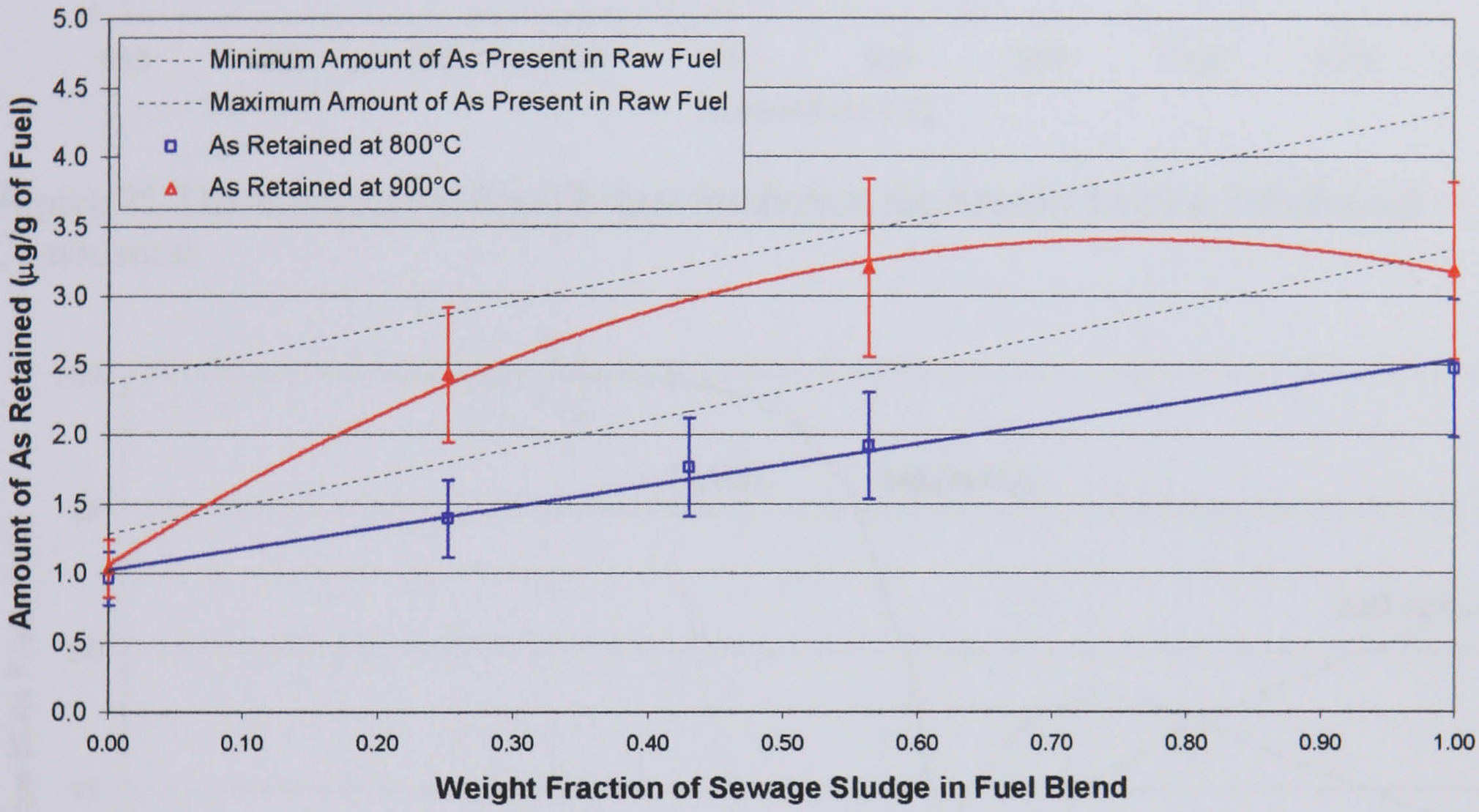


Figure 20 Synergy for Arsenic Retention by Polish Coal / Sewage Sludge Blends

Thermodynamic equilibrium models of arsenic during combustion of Polish coal (Figure 21), a 70 % Polish coal / 30 % sewage sludge blend (Figure 22) and sewage sludge on its own (Figure 23) suggest that arsenic could have been retained in ash by the formation of calcium, magnesium and iron arsenates.

Magnesium arsenate is the only compound of those predicted that could have caused a synergy. Formation of calcium arsenate was only predicted for Polish coal combustion, due to the sulphur content of sewage sludge. Whereas, iron arsenate was not predicted to form at temperatures high enough for it to have caused the synergy at 900 °C.

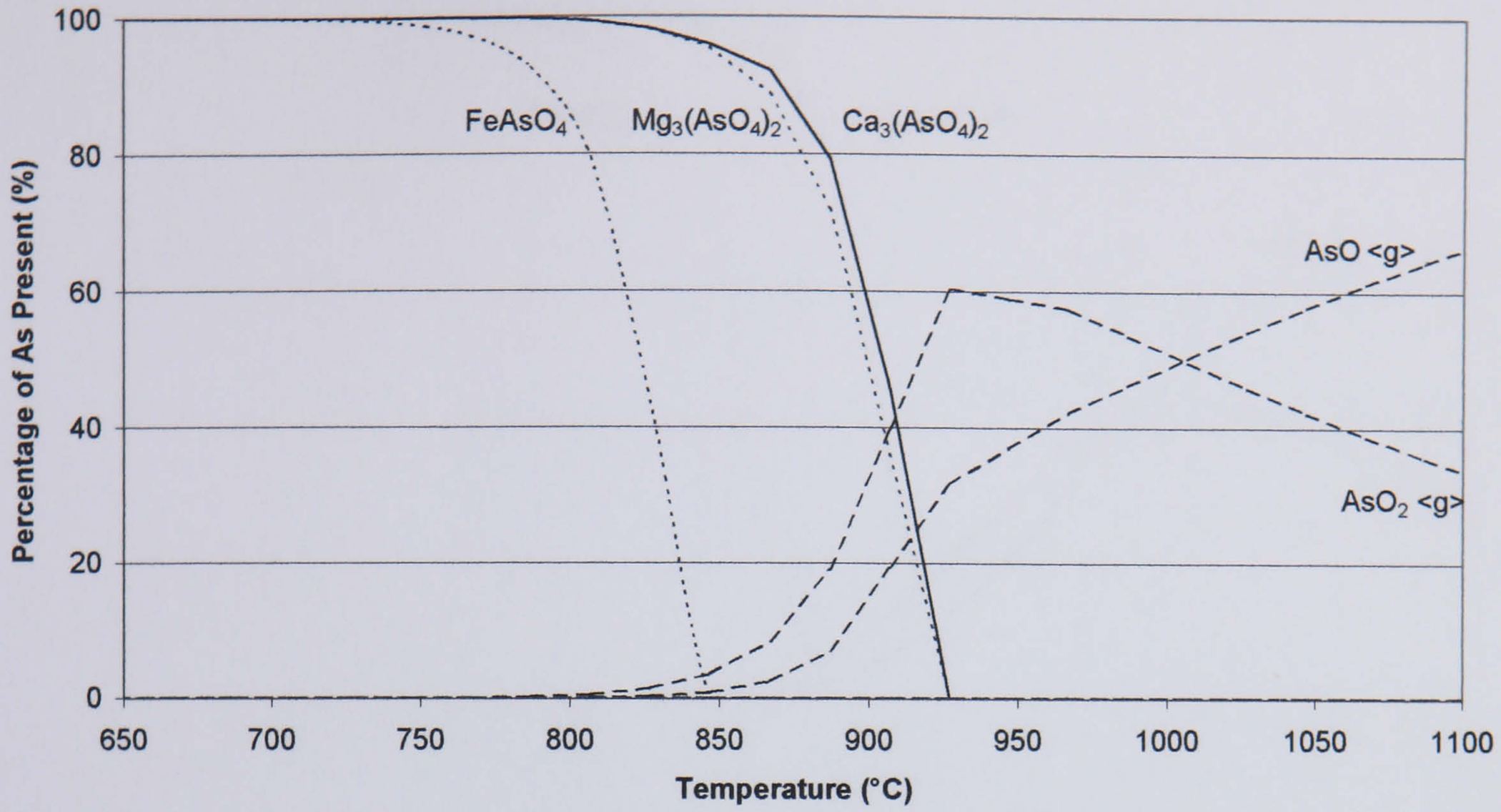


Figure 21 Thermodynamic Equilibrium Prediction for Arsenic During Polish Coal Combustion

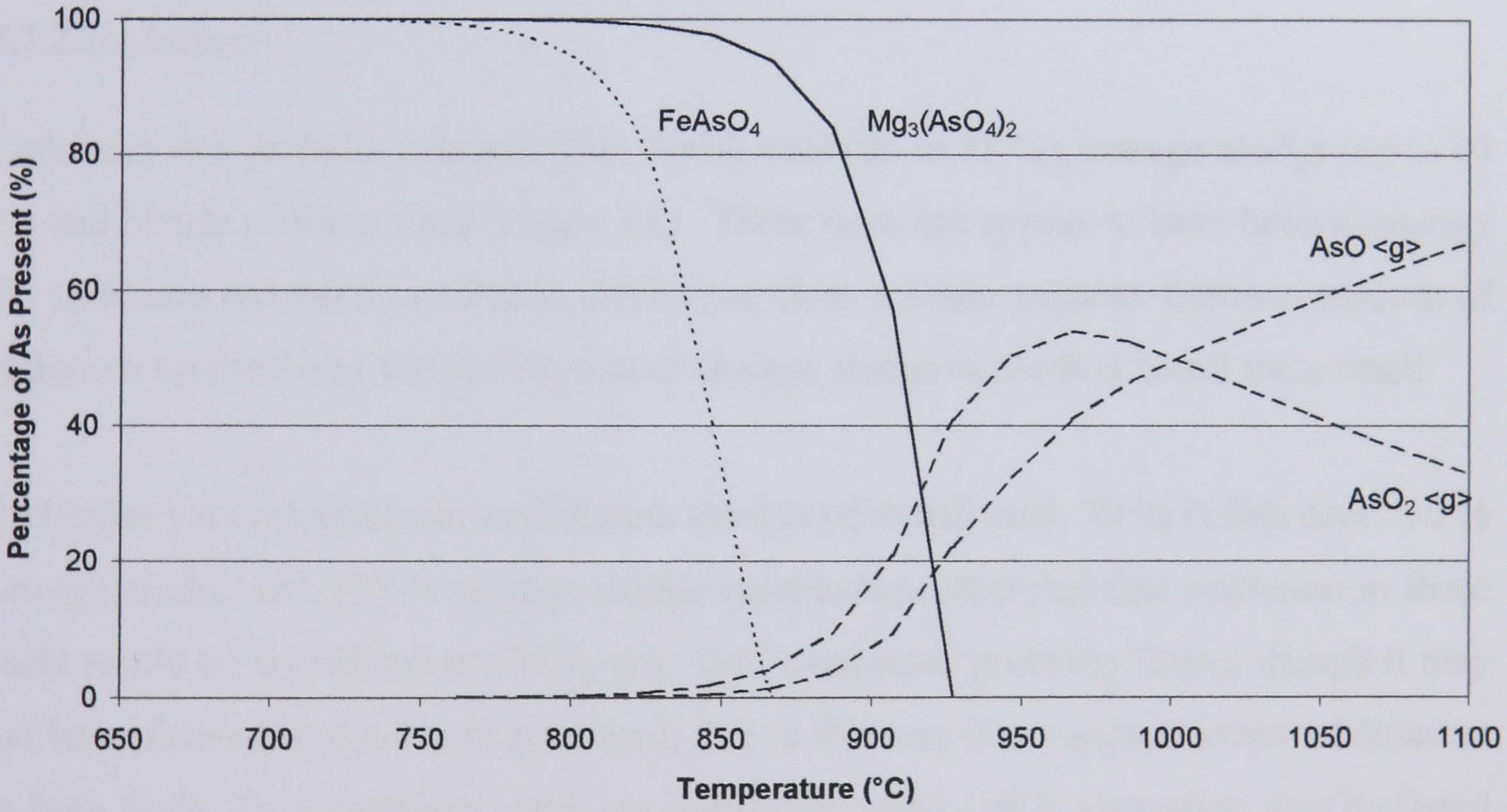


Figure 22 Thermodynamic Equilibrium Prediction for Arsenic During 70 % Polish Coal / 30 % Sewage Sludge Combustion

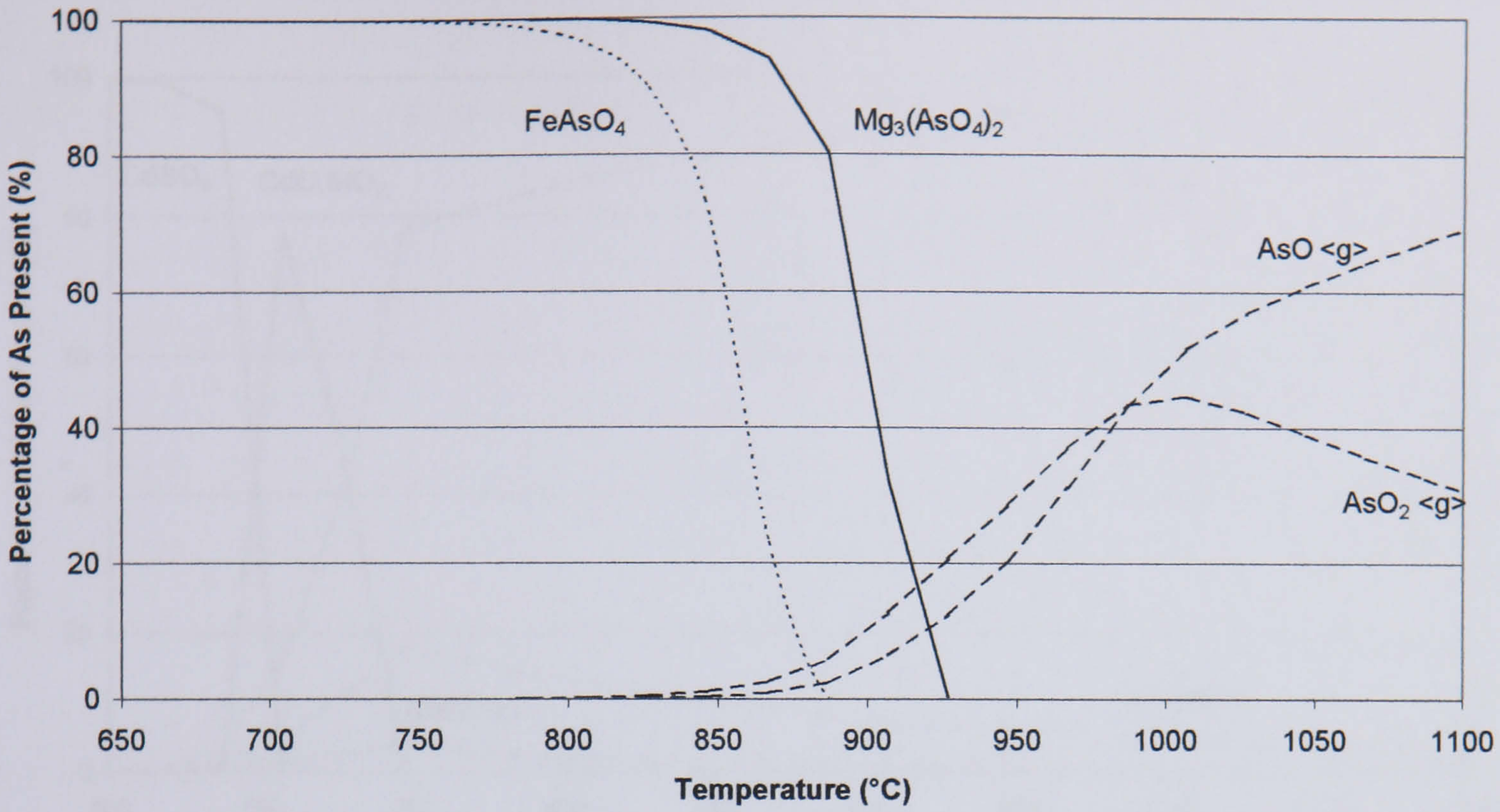


Figure 23 Thermodynamic Equilibrium Prediction for Arsenic During Sewage Sludge Combustion

5.2.2 Cadmium

Cadmium was partially released from Polish coal (up to 75 %), sewage sludge (up to 90 %) and blends of these fuels (Figure 18). There does not appear to have been a synergy for cadmium retention or release; deviations from a linear relation between amount of cadmium retained and weight fraction of sewage sludge in the fuel blend were small.

Preliminary thermodynamic equilibrium models of Polish coal, 70 % Polish coal / 30 % sewage sludge and 100 % sewage sludge combustion predicted that cadmium in these fuels would be volatilised as $CdCl_2$ gas. This compound probably forms, though it may not have formed to the extent predicted, due to the very low concentrations of chlorine in both fuels. To investigate cadmium behaviour when $CdCl_2$ formation was hindered by the low concentration of chlorine the thermodynamic equilibrium models were rerun with $CdCl_2$ excluded from prediction.

Without $CdCl_2$ gas formation allowed, solid cadmium compounds are predicted to form. Cadmium silicate was predicted to be stable at up to 750 °C during combustion of Polish coal (Figure 24) and 845 °C during combustion of sewage sludge (Figure 25).

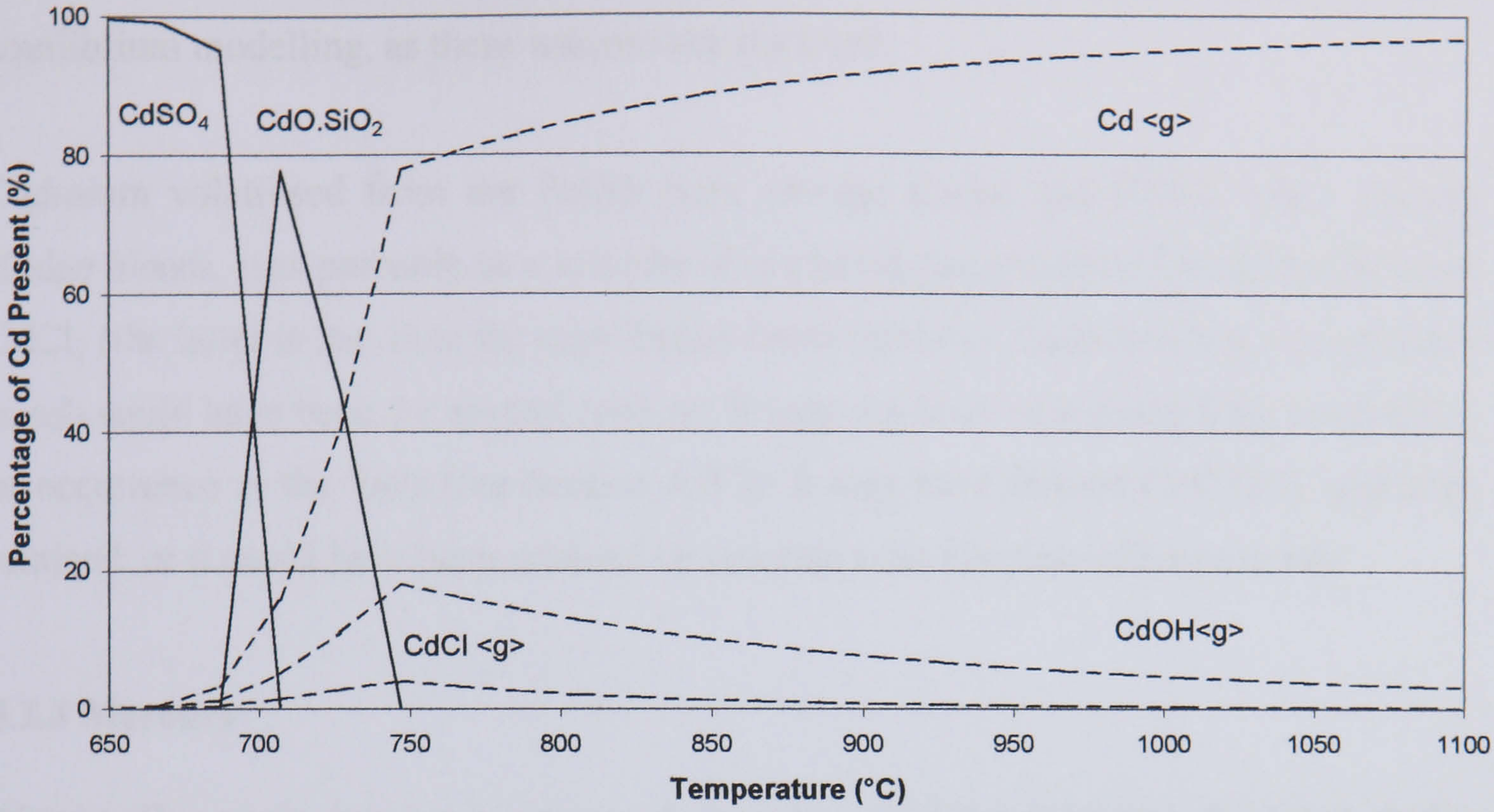


Figure 24 Thermodynamic Equilibrium Prediction for Cadmium During Polish Coal Combustion

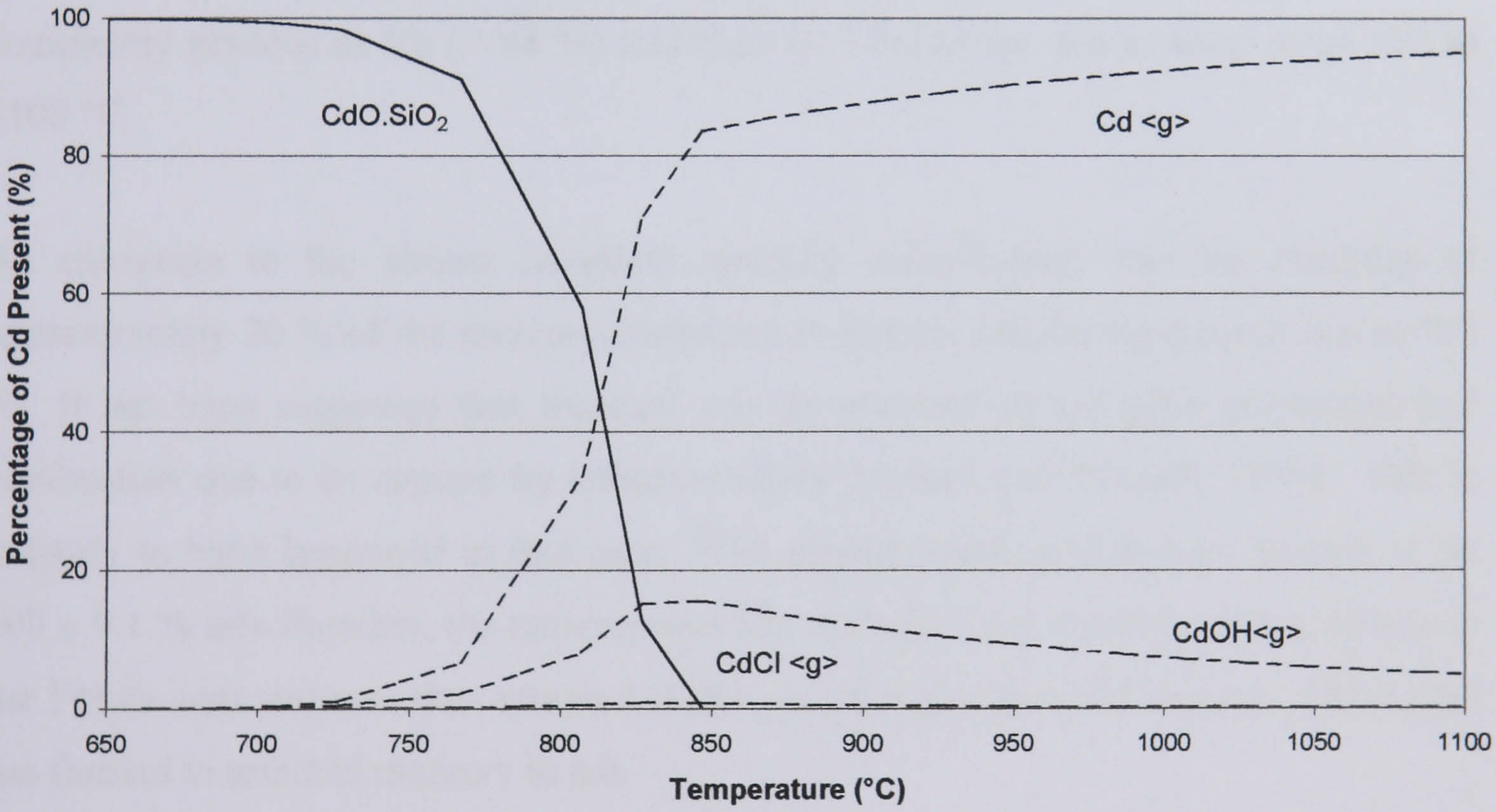


Figure 25 Thermodynamic Equilibrium Prediction for Cadmium During Sewage Sludge Combustion

Formation of this compound from volatilised cadmium may have caused the enrichment of cadmium on sewage sludge sinter ash (Figure 19). However, this enrichment may also have been caused by reaction of cadmium with other mineral matter. Kaolin in mineral matter can capture volatilised cadmium at temperatures as low as 600 °C (Lachas 1999), while bauxite and alumina can scavenge cadmium at 800 °C (Scotto et

al, 1993). The products of these reactions were not predicted by thermodynamic equilibrium modelling, as there was no data for them.

Cadmium volatilised from the Polish coal, sewage sludge and Polish coal / sewage sludge blends, was probably as a mixture of predicted gas species Cd, CdOH, CdCl and $CdCl_2$ (the latter in less than the equilibrium concentration). Cadmium that was retained in ash could have been for several reasons. It may not have volatilised from its mode(s) of occurrence in the fuels (see Section 5.0.2). It may have formed $CdO.SiO_2$ and been retained, or it could have been retained by reaction with alumino silicates in ash.

5.2.3 Mercury

Almost all mercury present in sewage sludge (95 – 98 %) and blends of sewage sludge with Polish coal (90 – 98 %) was volatilised during combustion (Figure 18). This correlates well with thermodynamic equilibrium predictions for mercury to be completely gaseous as Hg (> 98 %) and HgO (< 2 %) in the temperature range 650 to 1100 °C.

An exception to the almost complete mercury volatilisation was the retention of approximately 20 % of the mercury contained in Polish coal during combustion at 800 °C. It has been suggested that mercury can be retained on ash after pulverised fuel combustion due to its capture by unburnt carbon (Hassett and Eylands, 1999). This is unlikely to have happened in this case. TGA measurement revealed the sample to be 100 ± 0.1 % ash. Possibly, the mercury was not released from its mode of occurrence in the Polish coal and was thus retained in ash, or an unknown solid mercury compound has formed to retained mercury in ash.

An unknown solid mercury compound appears to have formed and recondensed, causing enrichment of mercury on sinter ash (Figure 19). Sinter ashes from combustion at 900 °C were, within experimental error (± 0.1 %), 100 % ash. Thus it is unlikely that carbon in ash was the cause of this enrichment either. Sinter ashes from 800 °C runs did exhibit a small (0 - 3 %) losses of weight, this was attributed slow mineral transformations not completed at this lower temperature whilst inside the suspension reactor.

5.2.4 Selenium

Selenium was mostly volatilised during combustion of Polish coal (5 – 25 % remaining in ash). The proportion retained in ash increased with the addition of sewage sludge to Polish coal. Selenium was almost completely retained in the ash when sewage sludge was burnt on its own at 800 °C. Some (up to 45 %) may have been volatilised by combustion at 900 °C (Figure 18).

Thermodynamic equilibrium modelling predicts selenium to be gaseous as either SeO (< 1 %) or SeO_2 (> 99 %) during combustion of Polish coal, 70 % Polish coal / 30 % sewage sludge or 100 % sewage sludge.

These predictions do not explain the high degree of selenium retention in sewage sludge ash. There are two possible explanations for this. Selenium may not have been released from its mode (or modes) of occurrence in the sewage sludge to volatilise and thus remained with the ash (see Section 5.0.2). Alternately, the retained selenium may have formed a compound not included in the equilibrium model. Calcium selenate formation is one possibility; this has been suggested to retain selenium in ash of a high calcium coal (Clements et al, 1999). Perhaps the same compound formed in the high calcium (1.9 %) sewage sludge.

5.2.5 Lead

Lead was partially volatilised during combustion of Polish coal (35 – 60 %) and of sewage sludge (5 – 60 %), Figure 18. Although the differences are small and within the range of experimental error, blends of these fuels appeared to have retained a higher proportion of their lead than either constituent fuel. A plot of the amount of lead retained (per gram of fuel) against the weight fraction of sewage sludge in the fuel shows a peak at around 55 % sewage sludge by weight (Figure 26). Lead concentrations in bottom ash from Polish coal / sewage sludge co-combustion also showed a peak for 800 °C results (Figure 27). Whilst lead concentrations in bottom ashes from co-combustion at 900 °C were a simple mixture of those from combustion of the fuels separately.

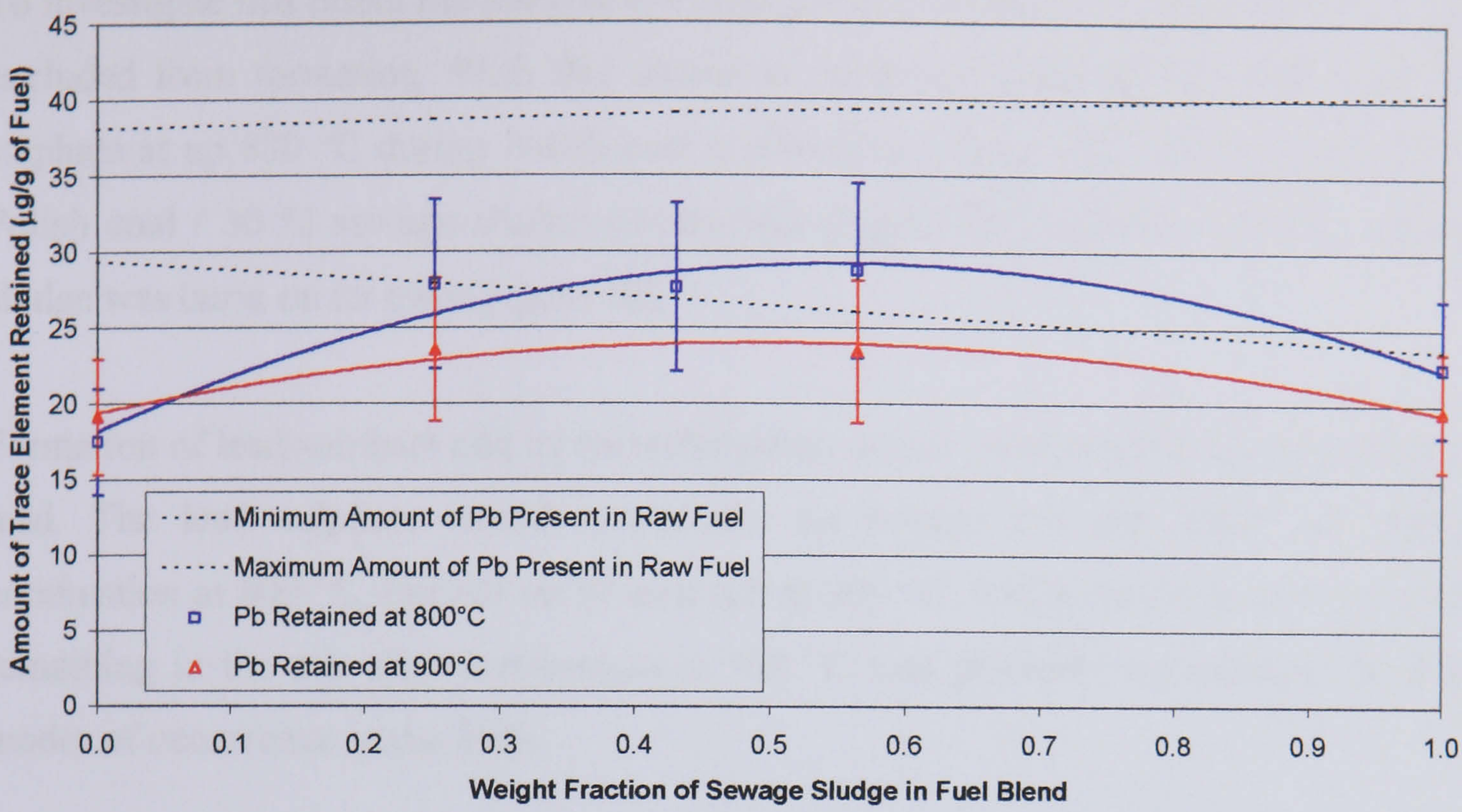


Figure 26 Possible Synergy in Retention of Lead by Polish Coal / Sewage Sludge

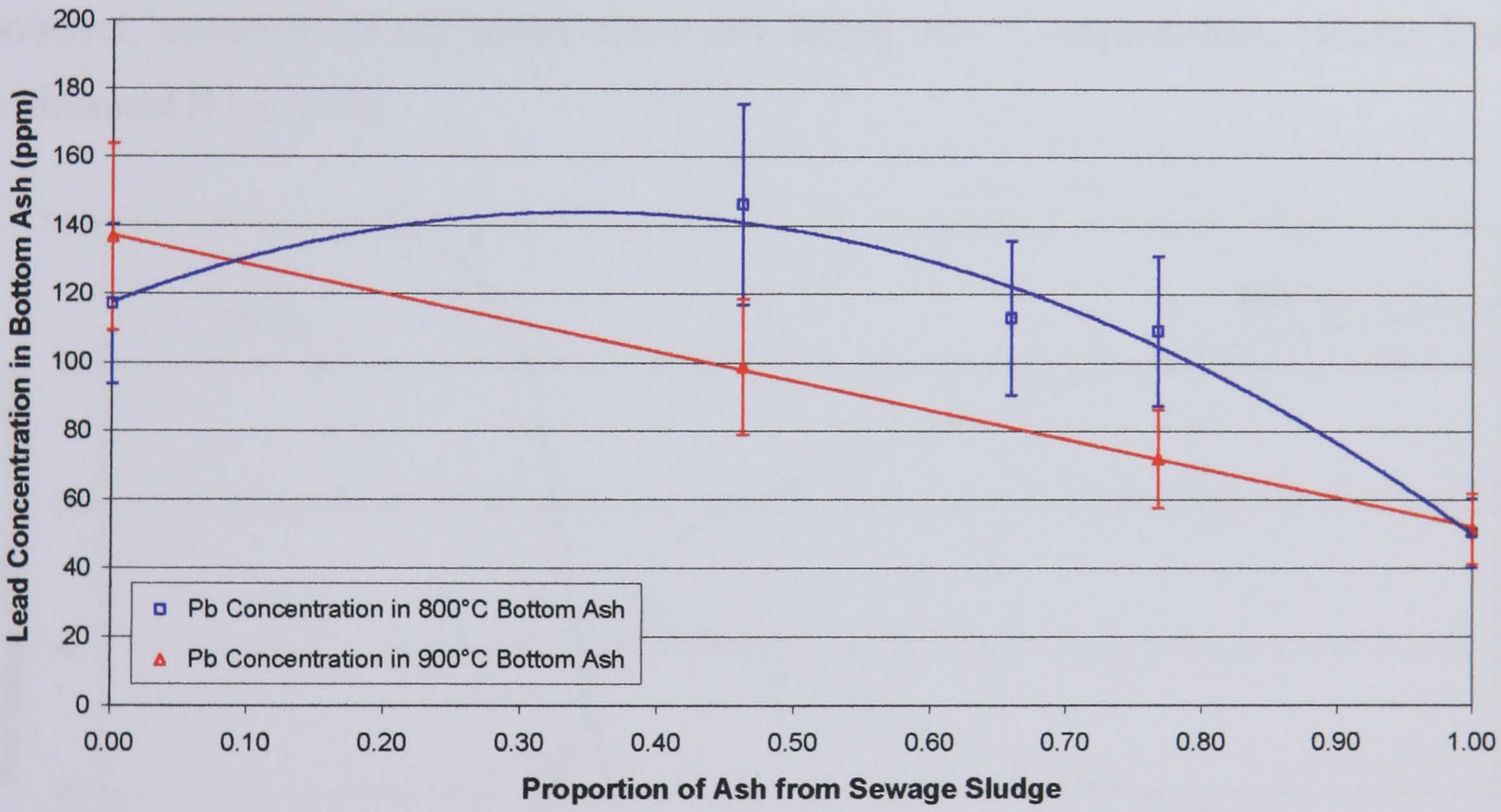


Figure 27 Lead Concentration in Bottom Ash of Polish Coal / Sewage Sludge Blends

Preliminary thermodynamic equilibrium models of lead during combustion of Polish coal, a 70 % Polish coal / 30 % sewage sludge blend and of sewage sludge on its own predicted all lead to have been volatilised as $PbCl_2$ gas. The concentrations of chlorine in the Polish coal (0.09 % as received) and sewage sludge (0.03 % as received) are low. This may have limited the formation of $PbCl_2$ due to the low probability of combining lead with two chlorine atoms.

To investigate this effect thermodynamic equilibrium models were rerun with $PbCl_2$ gas excluded from formation. With this alteration, lead was predicted to form solid lead sulphate at up 830 °C during Polish coal combustion (Figure 28), 870 °C during 70 % Polish coal / 30 % sewage sludge combustion (Figure 29) and 890 °C when sewage sludge was burnt on its own (Figure 30).

Formation of lead sulphate and its recondensation on ash could explain the behaviour of lead. The lead sulphate would recondense on bottom ash and sinter ash during combustion at 800 °C, but not on bottom ash at 900 °C, which would be too hot. Lead remaining in the ash after combustion at 900 °C was probably not released from its modes of occurrence in the fuels.

Possibly, volatilised lead formed the thermodynamically predicted lead sulphate. This could recondense on bottom ash at 800 °C, but 900 °C would be too hot. Lead could, however, condense on the cooler sinter ash during 900 °C experiments, causing lead enrichment (Figure 19).

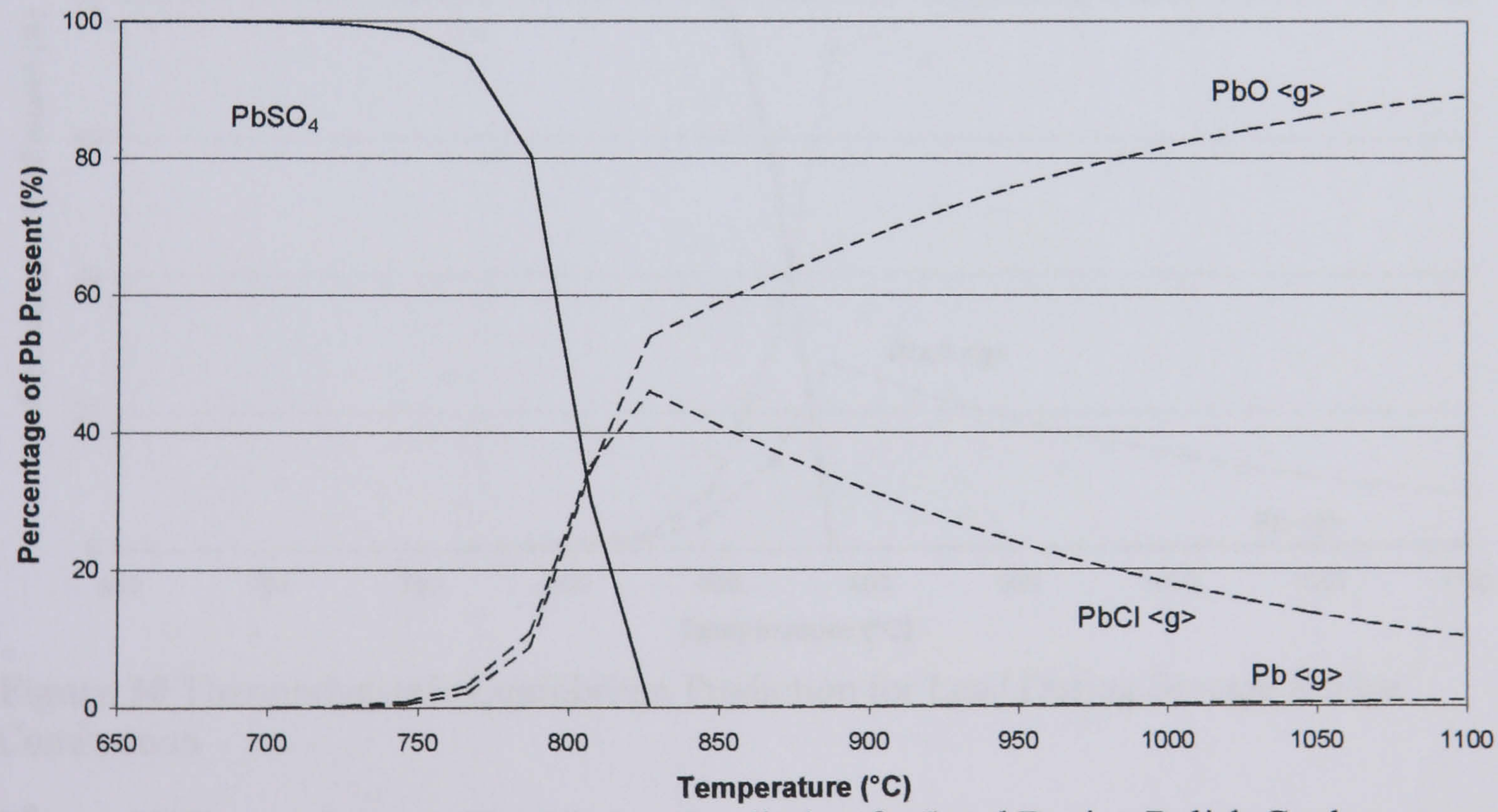


Figure 28 Thermodynamic Equilibrium Prediction for Lead During Polish Coal Combustion

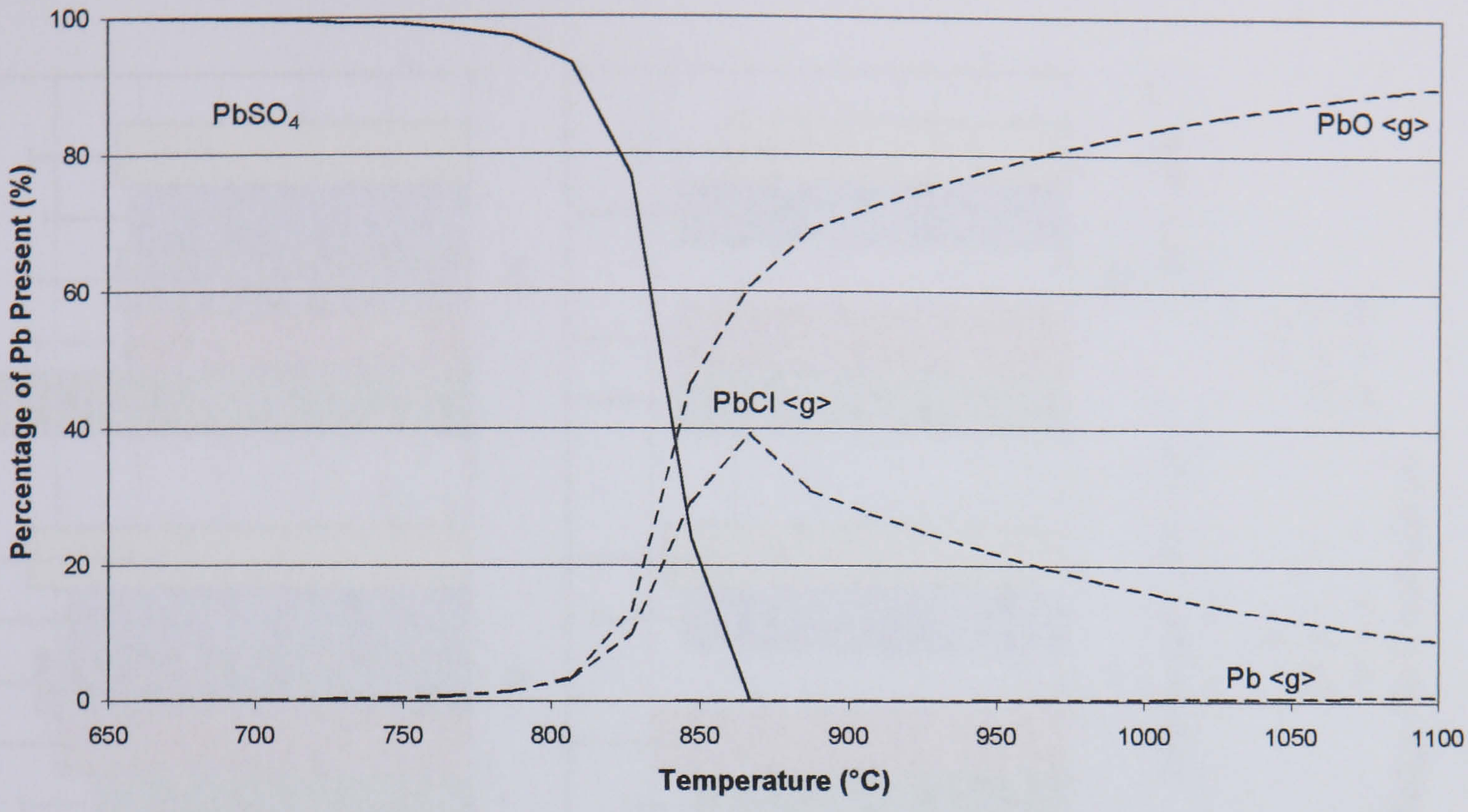


Figure 29 Thermodynamic Equilibrium Prediction for Lead During 70 % Polish Coal / 30 % Sewage Sludge Combustion

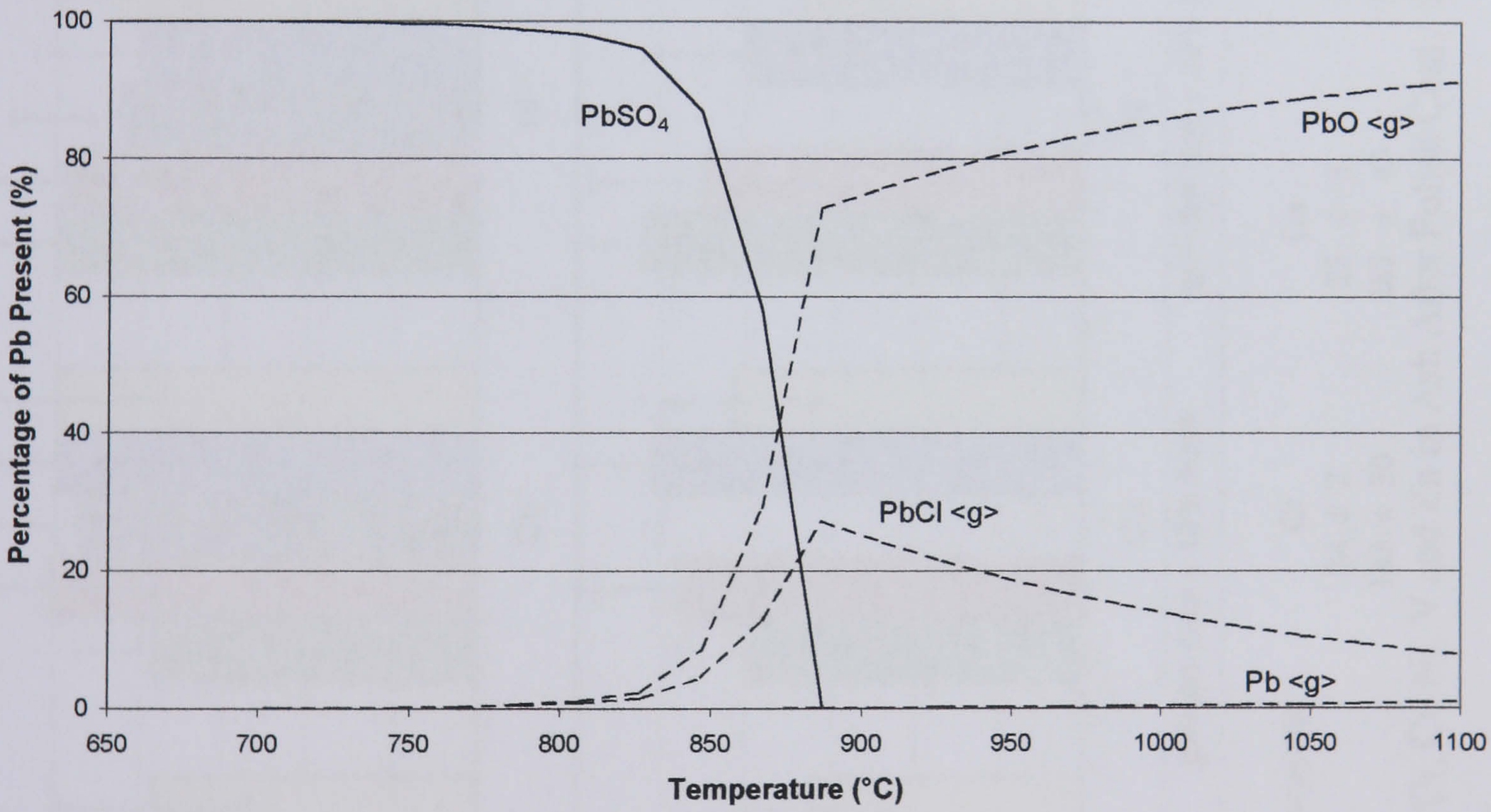
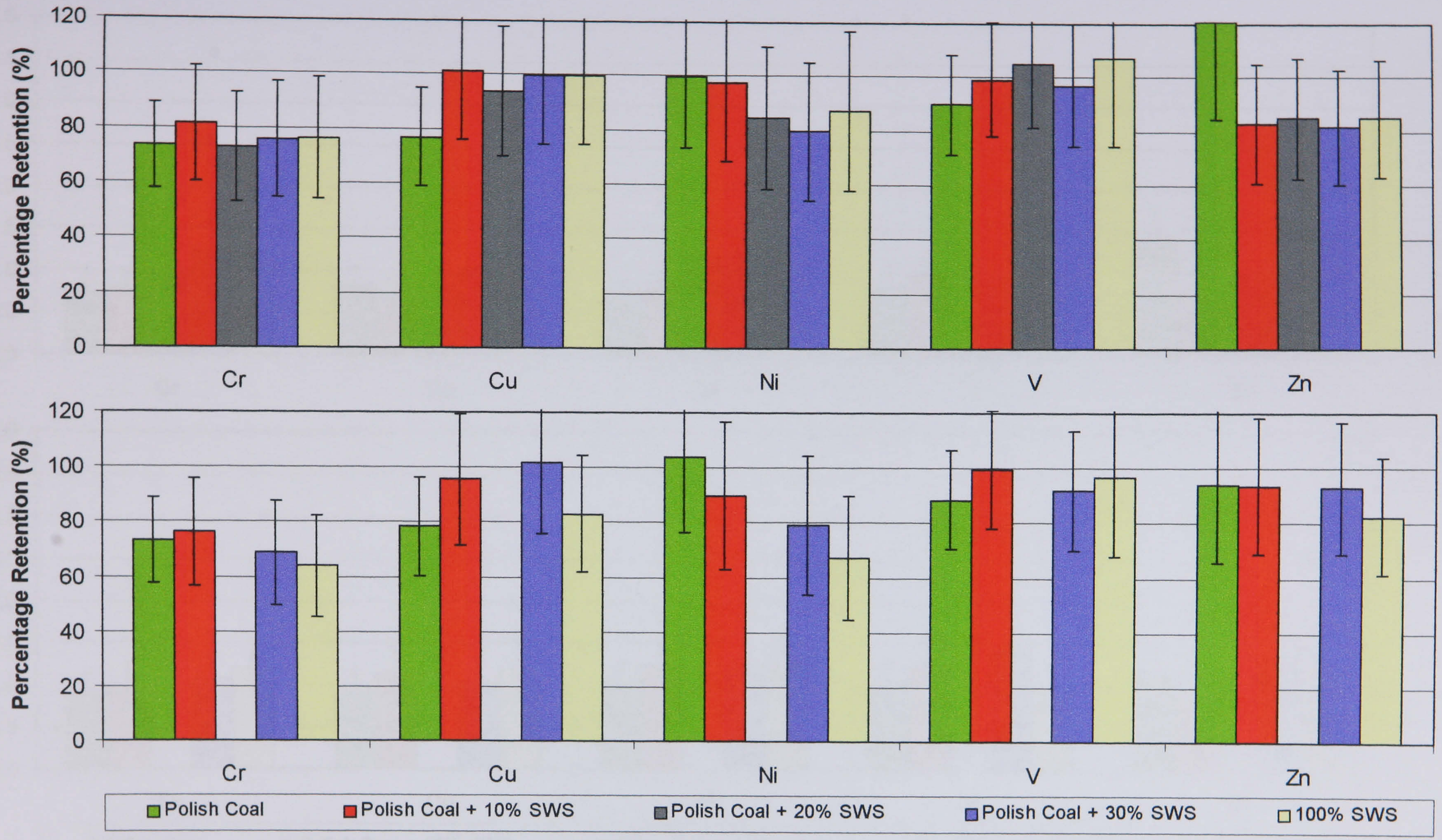


Figure 30 Thermodynamic Equilibrium Prediction for Lead During Sewage Sludge Combustion



Trace Element Concentration in Raw Fuels (ppm):	Cr	Cu	Ni	V	Zn
Polish Coal	24 ± 2	25 ± 3	17 ± 3	24 ± 1	44 ± 10
Swedish Sewage Sludge	143 ± 30	283 ± 45	52 ± 14	15 ± 3	556 ± 90

Figure 31 Percentage Retention of Cr, Cu Ni, V and Zn in Ash After Polish Coal / Sewage Sludge Co-Combustion

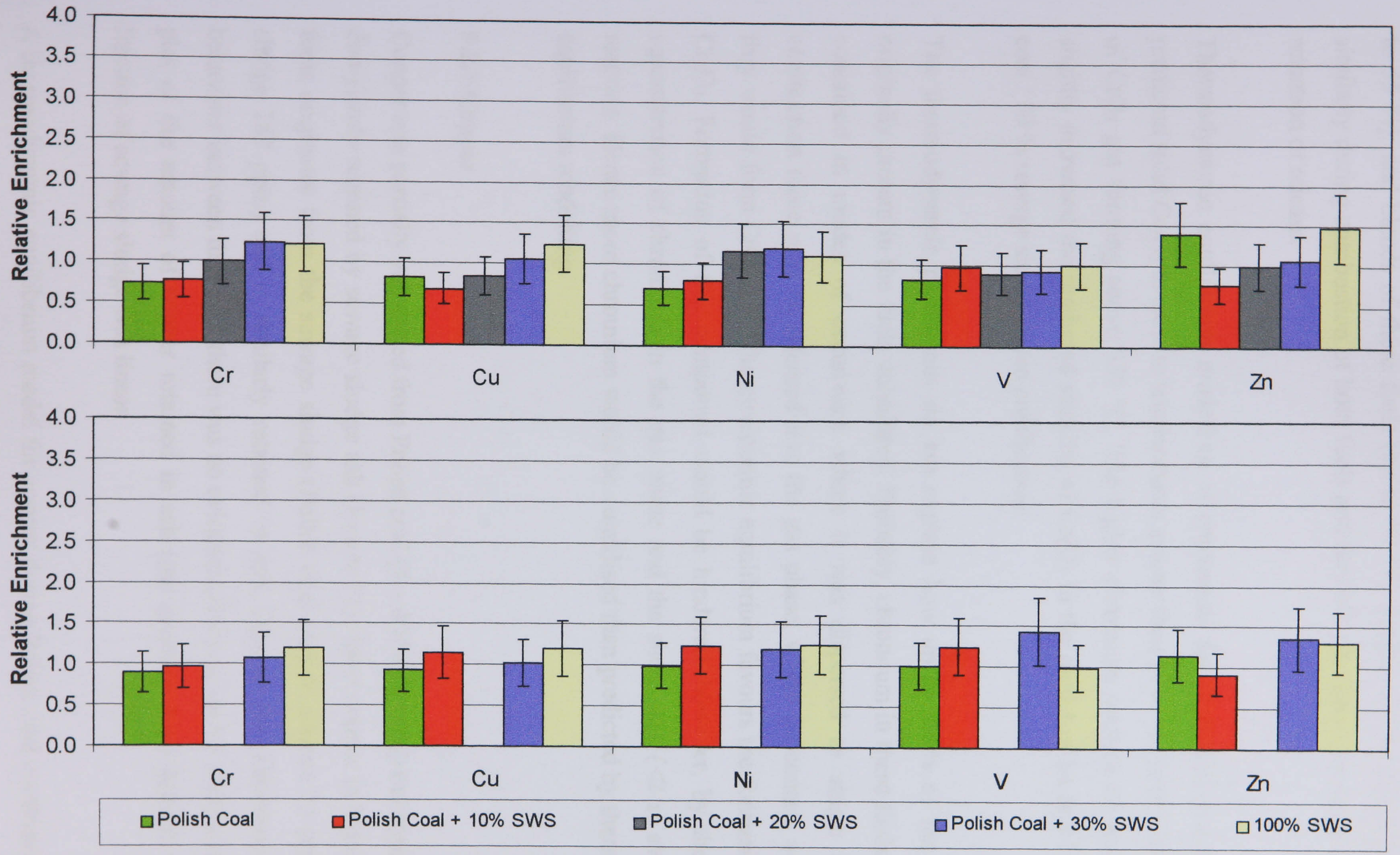


Figure 32 Relative Enrichment of Cr, Cu, Ni, V and Zn in Sinter Ash During Polish Coal / Sewage Sludge Co-Combustion
Note: A relative enrichment of one corresponds to being found in equal concentrations in the sinter and bottom ashes.

5.2.6 Chromium

Chromium was partially volatilised from the Polish coal (10 – 45 %), sewage sludge (up to 55 %), and blends of these fuels (up to 50 %), Figure 31. As chromium behaved similarly during combustion of both fuels and fuel blends, there was no synergy for its retention or release.

Thermodynamic equilibrium modelling of chromium during Polish coal combustion predicted solid Cr_2O_3 to exist to temperatures greater than 1100 °C, with minor amounts of CrO_3 gas forming above 930 °C. The higher chromium content of sewage sludge slightly increased the predicted stability of Cr_2O_3 in the model of its and 70 % Polish coal / 30 % sewage sludge blend combustion.

The thermodynamic predictions do not explain how up to 55 % of the chromium originally present in the fuels volatilised. Probably, chromium in these fuels was partly contained in modes of occurrence where it was dispersed as single atoms. On combustion these may be released into the gas phase, where on contact with oxygen they would form CrO_3 gas. Thermodynamic equilibrium favours the formation of solid Cr_2O_3. Formation of this compound would be hindered, however, by the very low concentration of chromium in the gas phase and the short time (<2 s) available for reaction. Hence more chromium would be volatilised than predicted by thermodynamic equilibrium modelling.

5.2.7 Copper

Copper was partially volatilised from Polish coal (5 – 40 % released) but appears almost completely retained by sewage sludge ash (Figure 31). Most copper in blends of these fuels originates from the sewage sludge (Polish coal copper content 25 ppm, sewage sludge 283 ppm) and is similarly retained in ash. Despite the difference in copper behaviour between the fuels, there was no evidence of a synergy for copper retention. A plot of the amount of copper retained in ash (per gram of fuel) against the weight fraction of sewage sludge was linear.

A thermodynamic equilibrium model for copper during Polish coal combustion (Figure

33) predicted its complete retention by formation of $CuO.Al_2O_3$. If $CuO.Al_2O_3$ was excluded from the thermodynamic equilibrium model formation of $CuO.Fe_2O_3$ and CuO were predicted as well as copper volatilisation as CuCl gas. The stability and number of solid phases predicted was increased by blending sewage sludge with the Polish coal (Figure 34) and burning sewage sludge on its own (Figure 35)

The partial volatilisation of copper from Polish coal (Figure 31) indicates that not all copper formed $CuO.Al_2O_3$. Probably copper retained in ash was a mixture of the predicted species ($CuO.Al_2O_3$, $CuO.Fe_2O_3$, $Cu_2O.Fe_2O$, CuO.FeO, CuO and Cu_2O) and copper which was not released from its modes of occurrence in the fuels (Section 5.0.2). Whilst that volatilised was a mixture of CuCl and CuO that did not recondense before exiting the suspension reactor (Section 5.0.3).

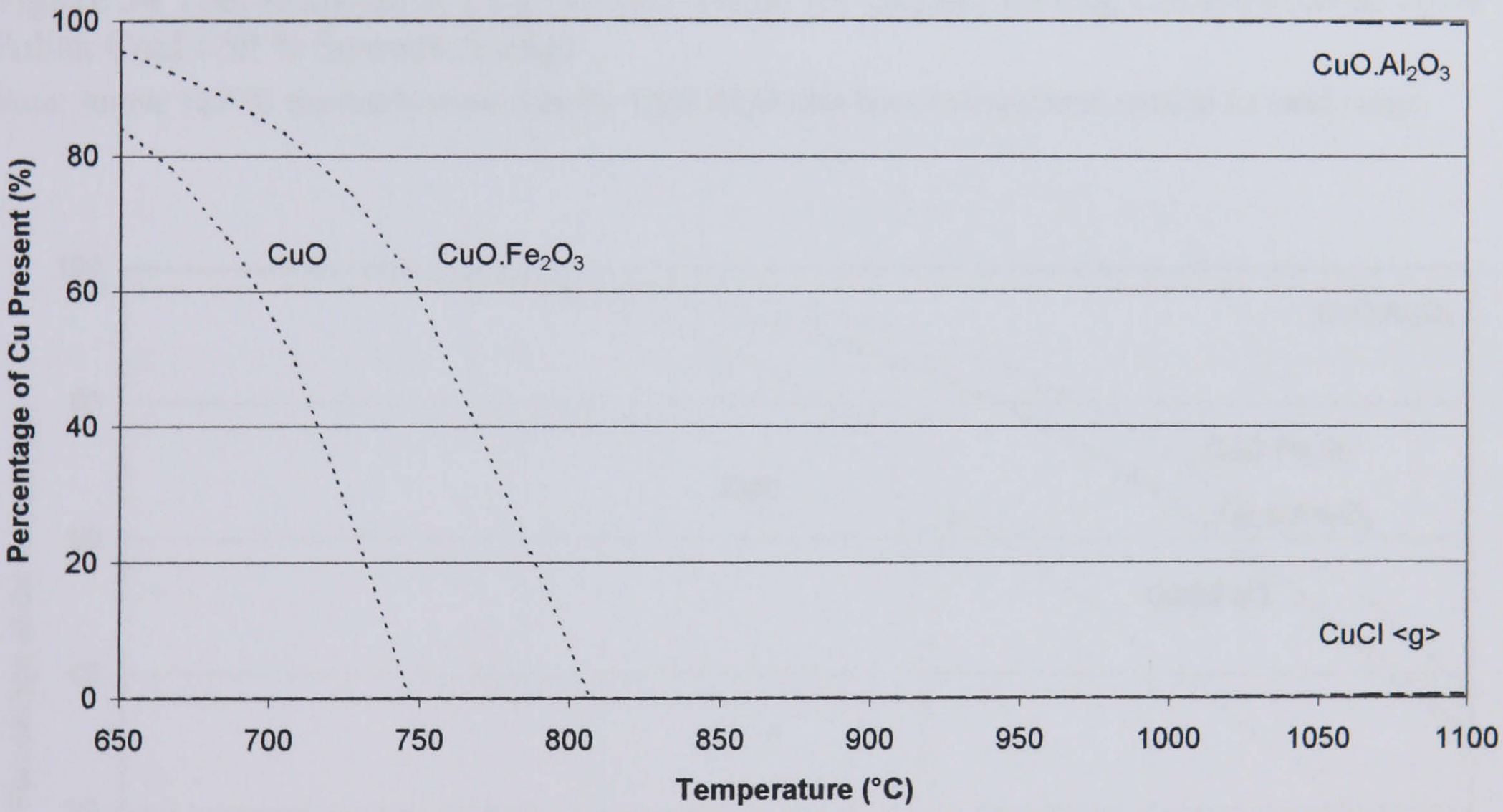


Figure 33 Thermodynamic Equilibrium Model for Copper During Combustion of Polish Coal

Note: Above 927 °C thermodynamic data for $CuO.Al_2O_3$ has been extrapolated outside its valid range.

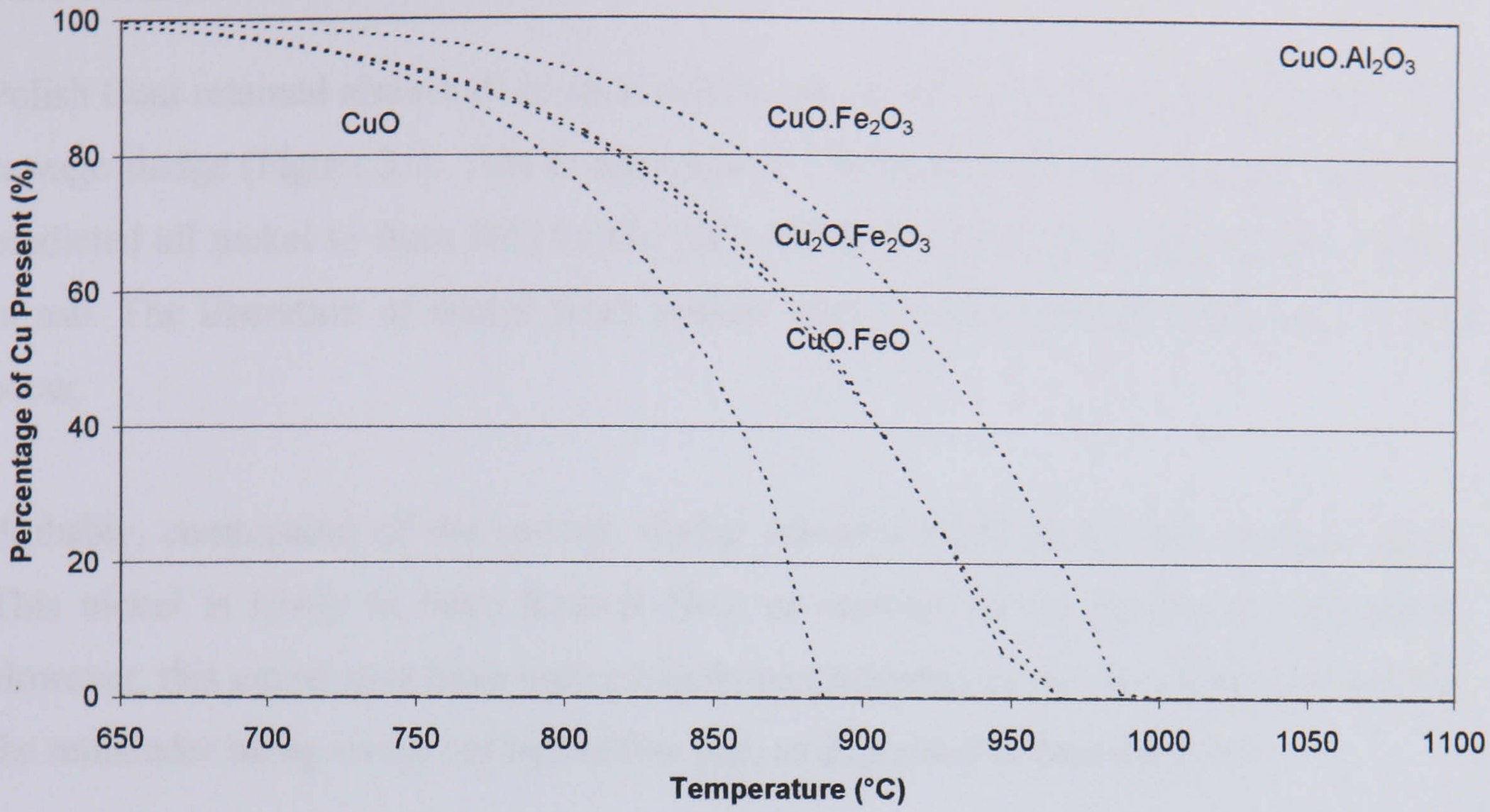


Figure 34 Thermodynamic Equilibrium Model for Copper During Combustion of 70 % Polish Coal / 30 % Sewage Sludge

Note: Above 927 °C thermodynamic data for $CuO.Al_2O_3$ has been extrapolated outside its valid range.

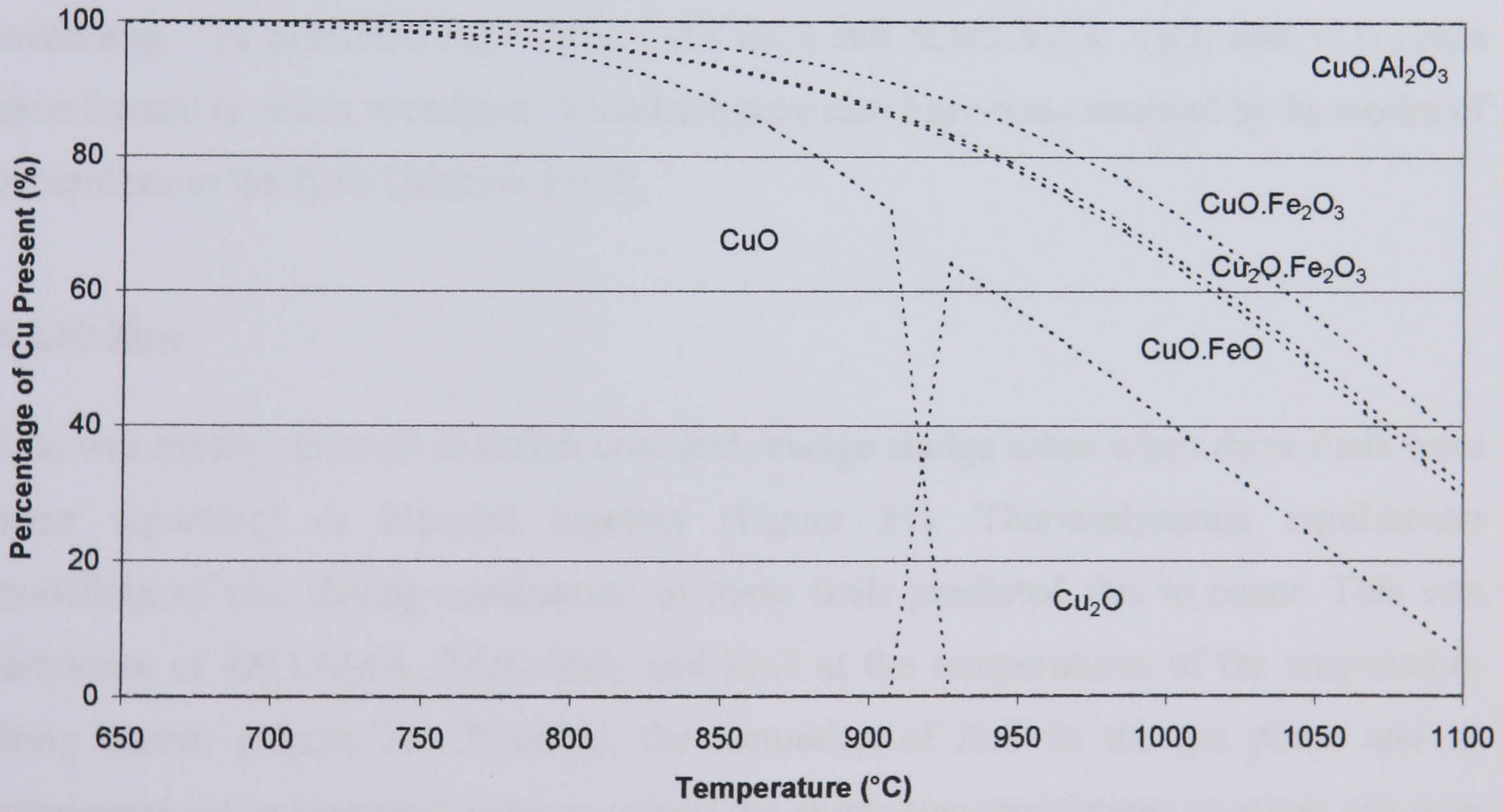


Figure 35 Thermodynamic Equilibrium Model for Copper During Combustion of Sewage Sludge

Note: Above 927 °C thermodynamic data for $CuO.Al_2O_3$ has been extrapolated outside its valid range.

5.2.8 Nickel

Polish Coal retained almost all of its nickel in ash, while up to 60 % was liberated from sewage sludge (Figure 31). This is unexpected. Thermodynamic equilibrium modelling predicted all nickel to form $NiO.Fe_2O_3$, $NiO.Al_2O_3$, $2NiO.SiO_2$ or NiO and be retained in ash. The liberation of nickel from sewage sludge shows that this does not always occur.

Probably, combustion of the sewage sludge released some nickel into the gas phase. This nickel is likely to have formed NiO, or another of the predicted compounds. However, this nickel may have only partially recondensed inside the suspension reactor, the remainder being swept out by the flue gas, as described in Section 5.0.3.

5.2.9 Vanadium

Vanadium was almost completely retained in ash of Polish coal, sewage sludge and blends of these fuels (Figure 31). This was predicted by thermodynamic equilibrium modelling. The predicted $FeO.V_2O_5$, $CaO.V_2O_5$ and $2CaO.V_2O_5$, V_2O_5 and VO_2 could have formed to retain vanadium. Vanadium may also have been retained by its modes of occurrence in the fuels (Section 5.0.2).

5.2.10 Zinc

Zinc was mostly retained in Polish coal and sewage sludge ashes when these fuels were burnt separately or blended together (Figure 31). Thermodynamic equilibrium modelling of zinc during combustion of these fuels predicted this to occur. This was formation of $ZnO.Al_2O_3$, $2ZnO.SiO_2$ and ZnO at the temperatures of the suspension-firing reactor (Figure 36). Possibly, the formation of ZnO in the gas phase and its subsequent recondensation perhaps caused the slight zinc enrichment on sinter ash seen in Figure 32.

The results suggest that zinc was either retained in ash by the formation of the predicted compounds ($ZnO.Al_2O_3$, $2ZnO.SiO_2$ and ZnO) or because it was not released from its mode(s) of occurrence in the raw fuels (see Section 5.0.2).

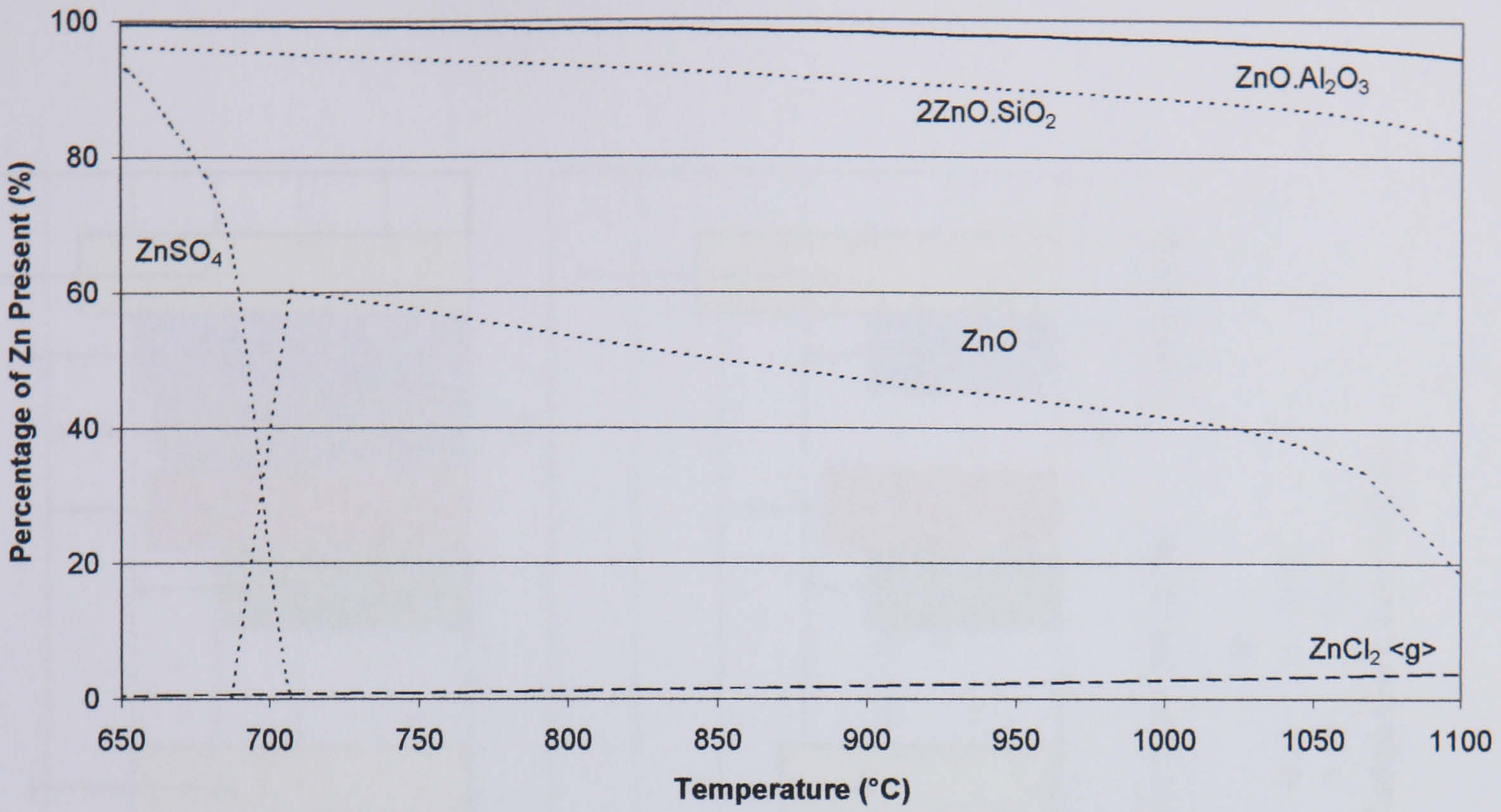
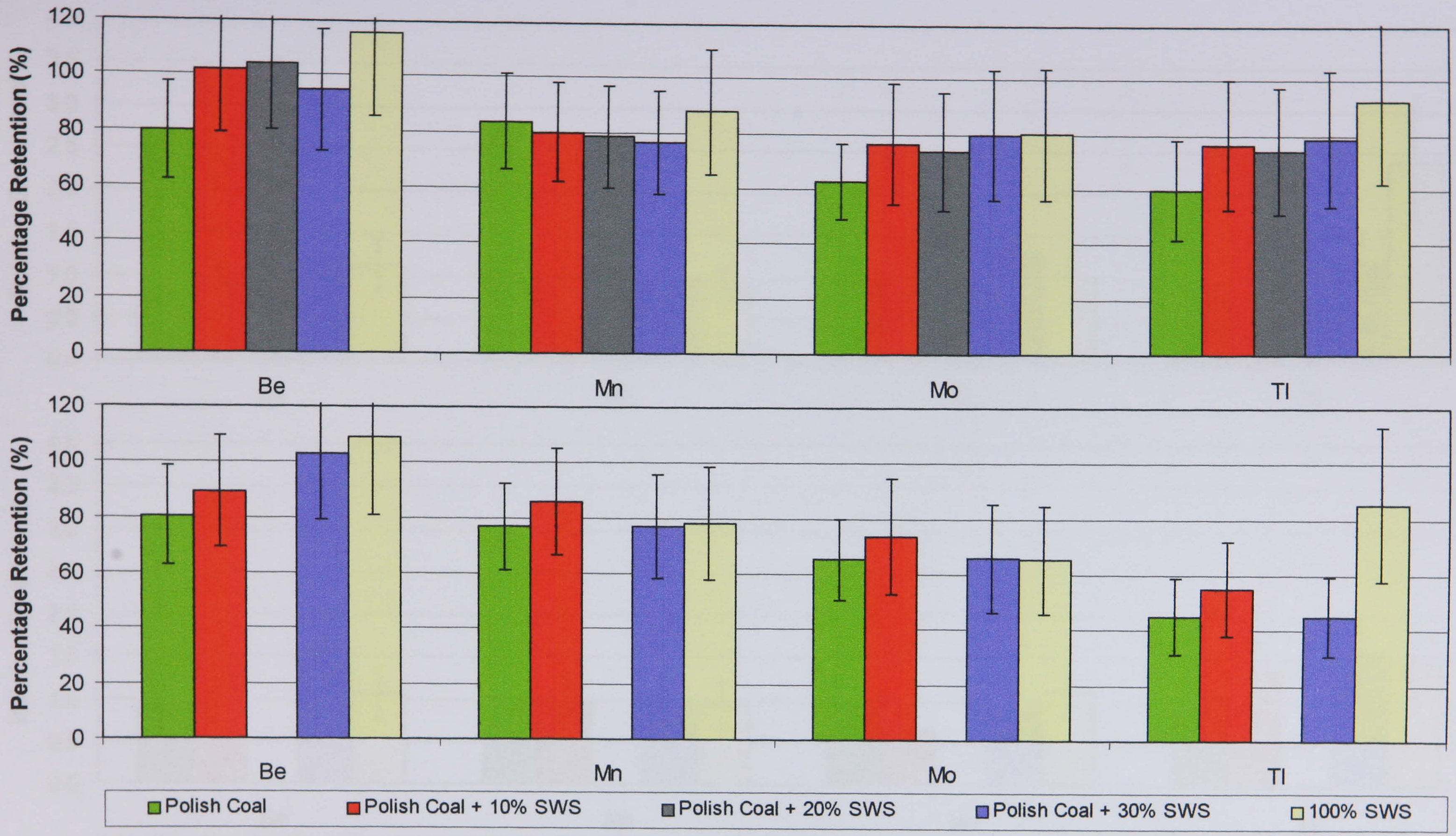


Figure 36 Thermodynamic Equilibrium Model for Zinc During Polish Coal Combustion



Trace Element Concentration in Raw Fuels (ppm):	Be		Mn		Mo		Tl	
Polish Coal	1.3	± 0.1	176	± 9	0.98	± 0.09	0.33	± 0.08
Swedish Sewage Sludge	0.49	± 0.08	396	± 66	19	± 4.1	0.19	± 0.05

Figure 37 Percentage Retention of Be, Mn, Mo and Tl in Ash During Polish Coal / Sewage Sludge Co-Combustion

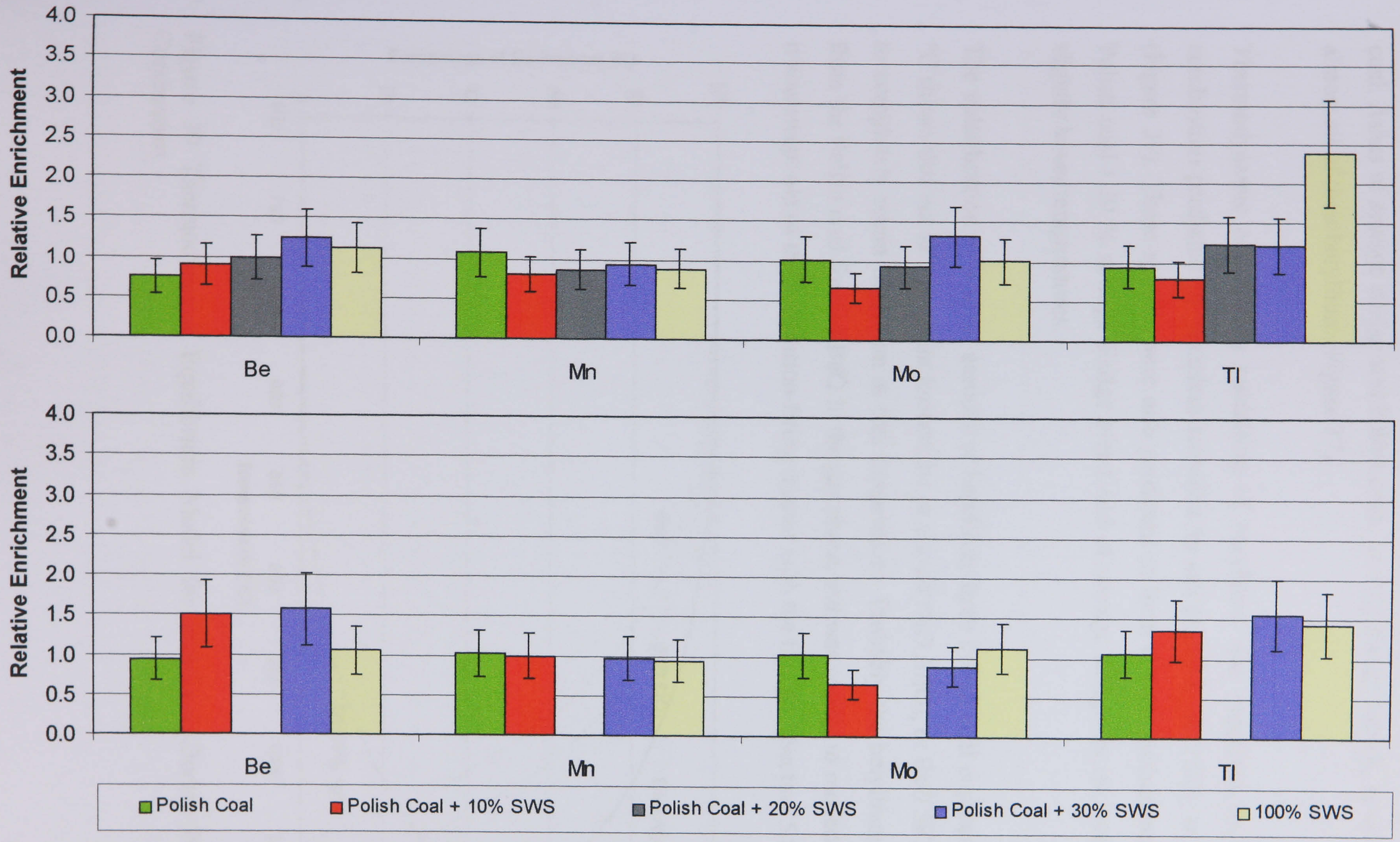


Figure 38 Relative Enrichment of Be, Mn, Mo and Tl in Sinter Ash During Combustion of Polish Coal and Sewage Sludge

5.2.11 Beryllium

A small amount (5 – 35 %) of beryllium was volatilised during the combustion of Polish coal. Ashes of sewage sludge and Polish coal / sewage sludge blends, however retained almost all of their beryllium (Figure 37).

Thermodynamic equilibrium modelling of beryllium was predicted by Polish coal combustion predicted its complete retention in ash as BeO, $BeO.SiO_2$ or $BeO.Al_2O_3$ (Figure 39). These species were also predicted to form during combustion of a 70 % Polish coal / 30 % sewage sludge blend and of sewage sludge on its own, though to slightly lower temperatures.

The volatilisation of a small amount of beryllium from Polish coal combustion at 800 °C shows that not all beryllium formed the predicted $BeO.Al_2O_3$, or $BeO.SiO_2$ predicted to completely retain beryllium at this temperature. Probably the beryllium volatilised from the Polish coal formed BeO in the gas phase, but was unable to recondense before it was swept out of the suspension-firing reactor with the flue gas (Section 5.0.3).

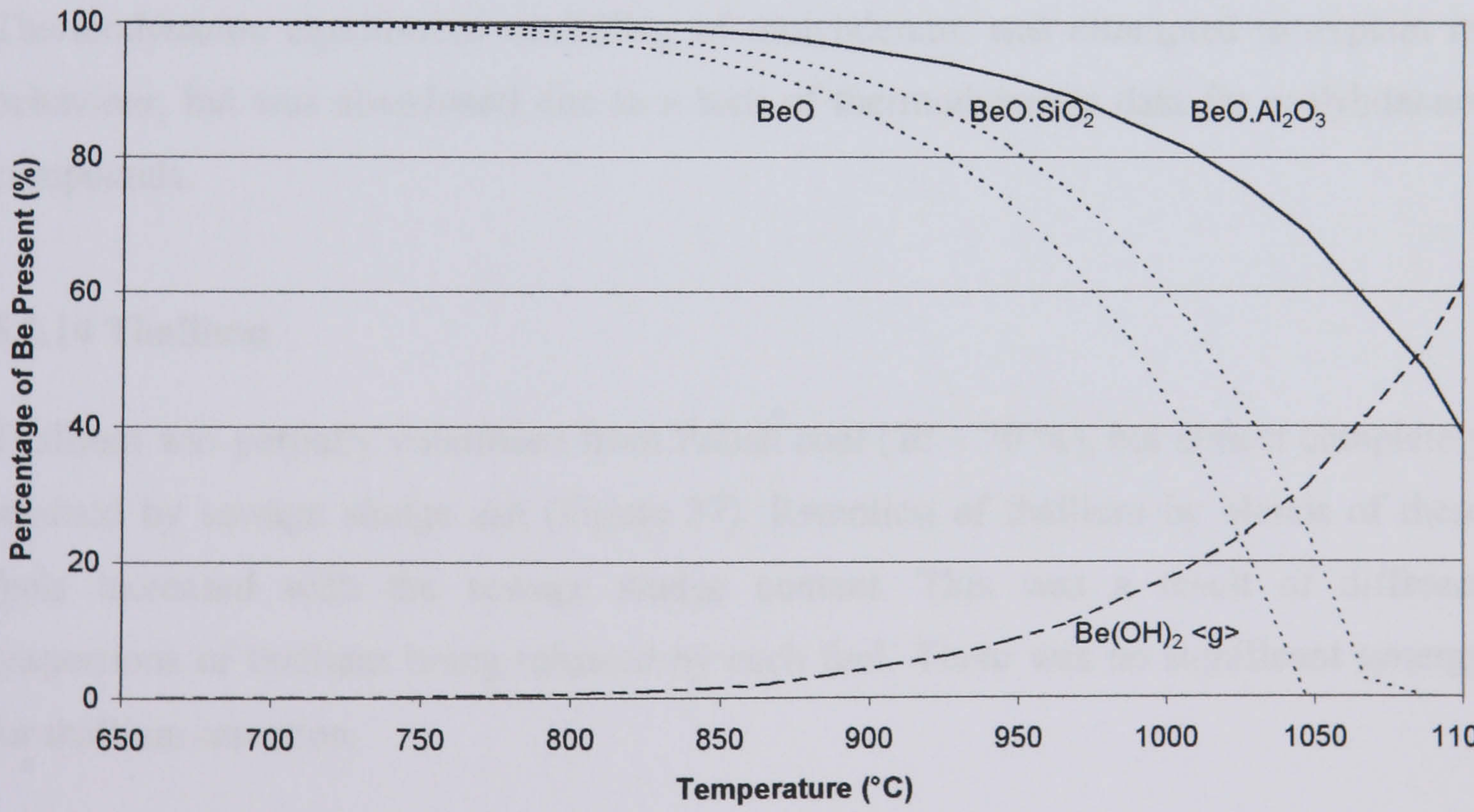


Figure 39 Thermodynamic Equilibrium Model for Beryllium During Polish Coal Combustion

5.2.12 Manganese

Up to 40 % of the manganese in Polish coal, sewage sludge and blends of these fuels may have been volatilised during combustion (Figure 37). For these fuels thermodynamic equilibrium models predicted manganese to have been completely retained in ash, by the formation of $MnO.Al_2O_3$, $MnO.SiO_2$, Mn_2O_3 and Mn_3O_4. Perhaps some of the manganese in either fuel was released during combustion and could not recondense before being swept out of the reactor (Section 5.0.3).

5.2.13 Molybdenum

Molybdenum was partially volatilised from Polish coal (20 – 50 %) and sewage sludge (0 – 55 %) during combustion (Figure 37). Molybdenum was also liberated during the combustion of Polish coal and sewage sludge blends (0 – 55%). Its behaviour during blend appears to have been an 'additive' mixture of that displayed during separate combustion of the constituent fuels. Little of the liberated molybdenum has recondensed on sinter ash (Figure 38).

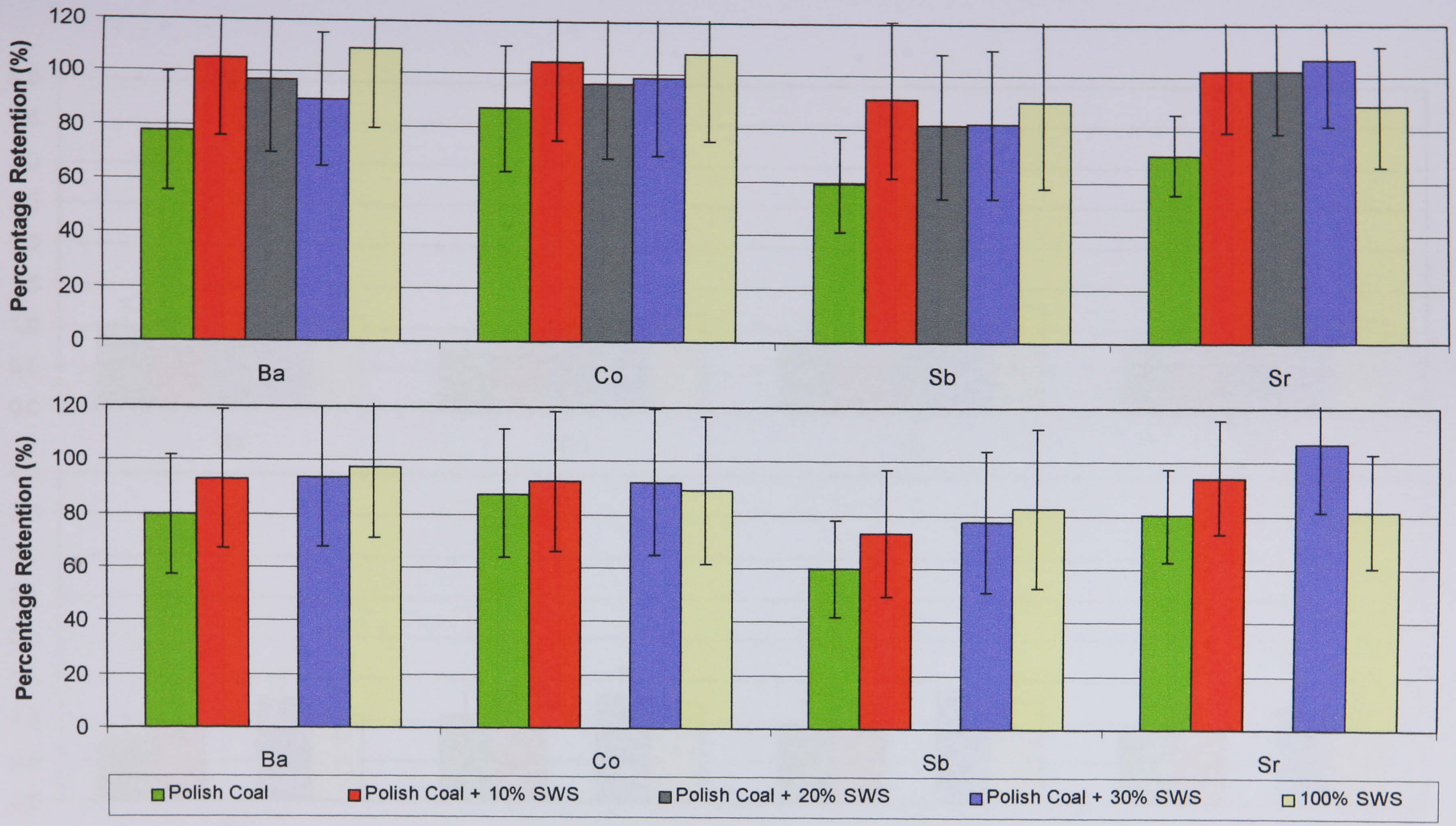
Thermodynamic equilibrium modelling of molybdenum was attempted to explain its behaviour, but was abandoned due to a lack of thermodynamic data for molybdenum compounds.

5.2.14 Thallium

Thallium was partially volatilised from Polish coal (20 – 70 %), but almost completely retained by sewage sludge ash (Figure 37). Retention of thallium by blends of these fuels increased with the sewage sludge content. This was a result of different proportions of thallium being released by each fuel. There was no significant synergy for thallium retention.

Thermodynamic equilibrium modelling predicted thallium to be completely released into as a mixture of TlCl, TlOH and Tl gases during the combustion of either fuel and a 70 % Polish coal / 30 % sewage sludge blend.

Thallium was enriched on sinter ash during combustion of sewage sludge (800 and 900 °C) and the 30 % sewage sludge blend (900 °C only). This suggests a solid thallium compound has recondensed from the gas phase. No solid thallium compounds were predicted by thermodynamic modelling to form. These results suggest an unknown thallium compound, not present in the thermodynamic database has formed during combustion of these fuels. Most of the thallium, however, was probably retained in ash because it could not escape its mode of occurrence in the fuels (Section 5.0.2).



Trace Element Concentration in Raw Fuels (ppm):	Ba	Co	Sb	Sr
Polish Coal	376 ± 74	6.0 ± 1.1	1.7 ± 0.4	85 ± 7
Swedish Sewage Sludge	267 ± 49	10 ± 2	3.3 ± 1.0	120 ± 19

Figure 40 Percentage Retention of Ba, Co, Sb and Sr in Ash After Polish Coal / Sewage Sludge Co-Combustion

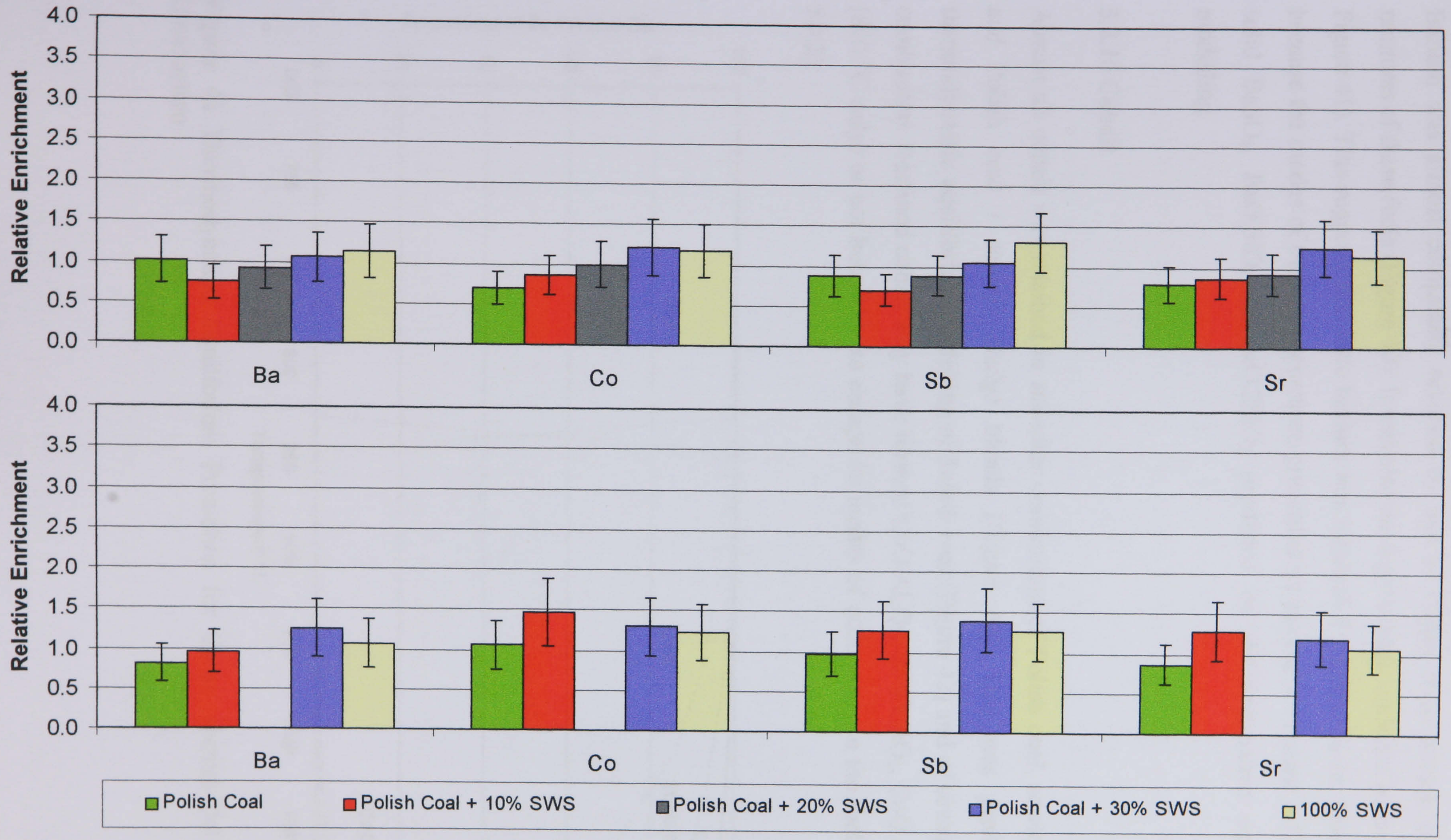


Figure 41 Relative Enrichment of Ba, Co, Sb and Sr in Sinter Ash During Combustion of Polish Coal and Sewage Sludge

5.2.15 Barium

Barium was almost completely retained by ash of Polish coal, sewage sludge and mixtures of these fuels (Figure 40). It was also not significantly enriched on sinter ash (Figure 41). This suggests that little barium was released from these fuels. This could be because the modes of barium occurrence prevented its release or because it formed the solid $BaSO_4$, $BaO.SiO_2$ or $BaO.2SiO_2$ predicted by thermodynamic equilibrium modelling.

5.2.16 Cobalt

Almost all cobalt was retained in ash after combustion of Polish coal, sewage sludge and Polish coal / sewage sludge blends (Figure 40). This was predicted by thermodynamic equilibrium modelling of Polish coal (Figure 42) and of sewage sludge combustion. Retained cobalt may have formed $CoO.Al_2O_3$, $2CoO.SiO_2$, CoO or Co_3O_4 (800 °C only) or not been able to escape its modes of occurrence in the fuel (Section 5.0.2).

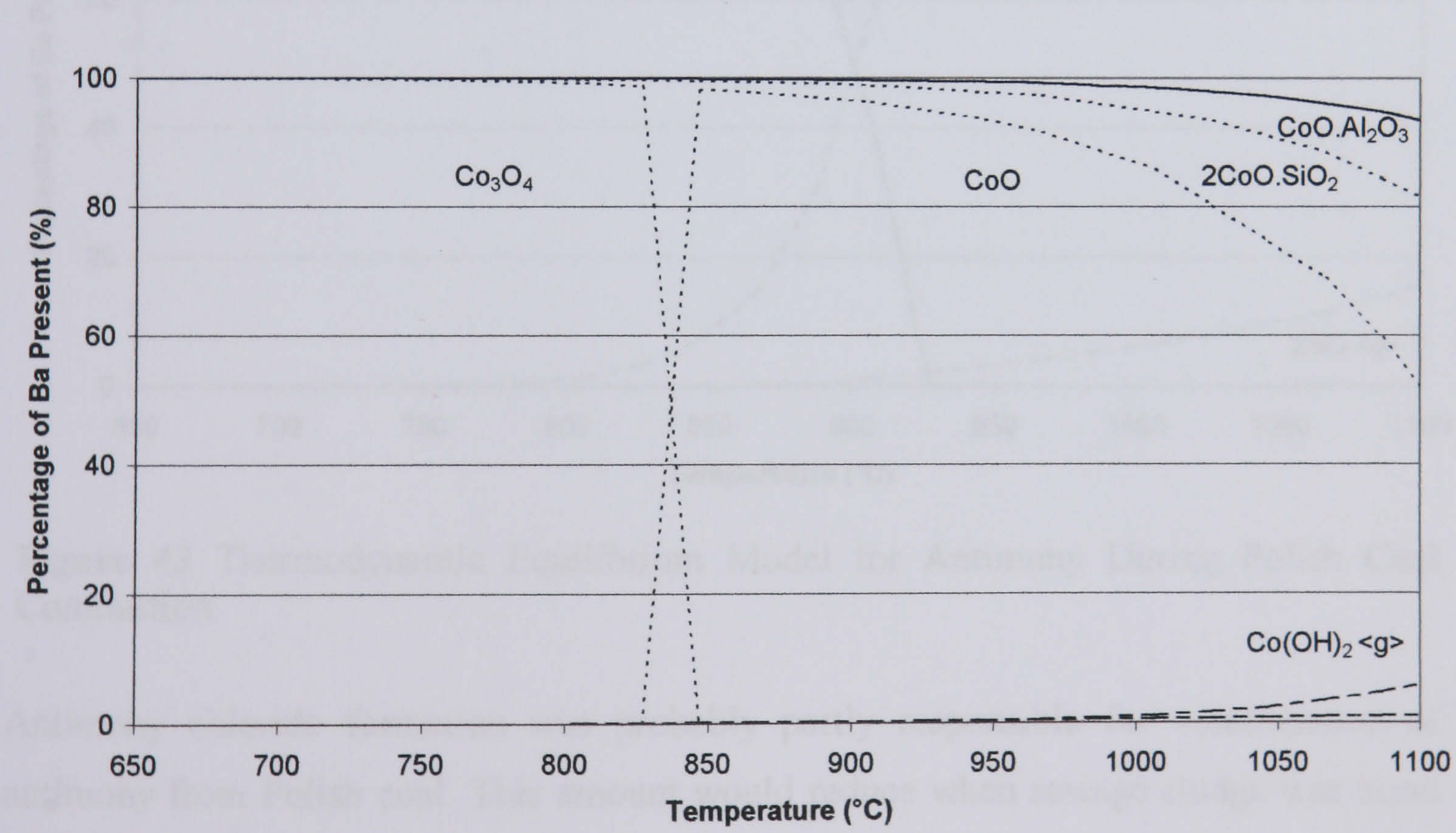


Figure 42 Thermodynamic Equilibrium Prediction for Cobalt During Polish Coal Combustion

5.2.17 Antimony

Antimony was partially volatilised (20 – 60 %) during Polish coal combustion, more was retained on sewage sludge ash. Blends of these fuels retained antimony in proportions intermediate to their constituent fuels. There was no significant synergy for antimony release or retention.

Thermodynamic equilibrium calculations predicted antimony to be partly retained in ash as antimony oxide during combustion of Polish coal (Figure 43). Predictions for sewage sludge combustion were similar, though the highest temperature to which antimony oxide was predicted to exist to increase by 50 °C due to its lower chlorine content inhibiting SbCl formation.

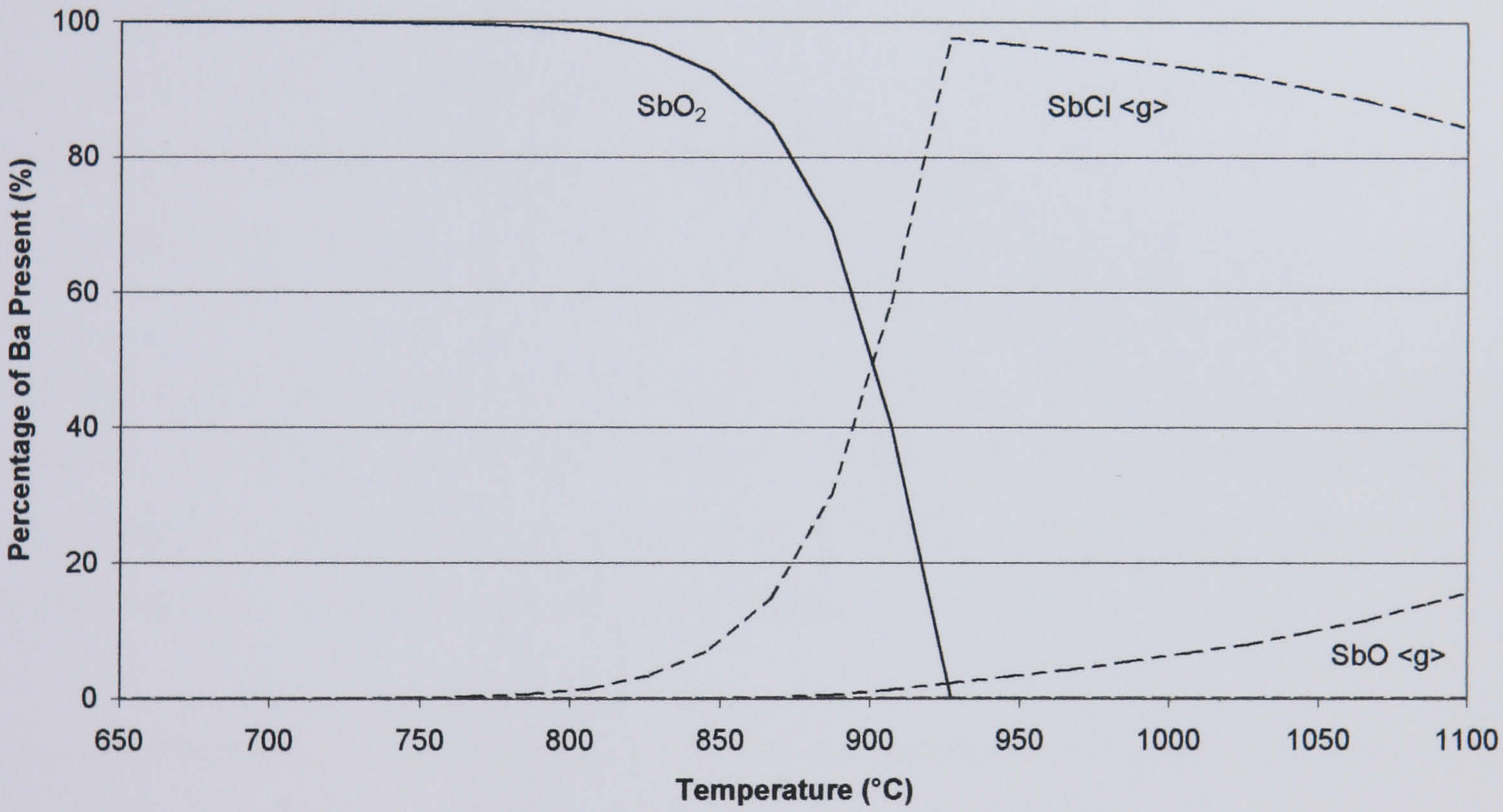


Figure 43 Thermodynamic Equilibrium Model for Antimony During Polish Coal Combustion

Antimony chloride formation was probably partly responsible for volatilisation of antimony from Polish coal. This amount would reduce when sewage sludge was burnt because of this fuel's lower chlorine content. Antimony may have also been volatilised because some SbO_2 formed in the gas phase did not recondense before being swept from the suspension-firing reactor by the flue gas (Section 5.0.3).

Partial recondensation of SbO_2 has probably caused the slight enrichment of antimony on sinter ash after combustion at 900 °C (Figure 41). At 800 °C SbO_2 could have

recondensed on bottom ash circulating inside the suspension reactor or the sinter ash, preventing antimony enrichment on sinter ash at this temperature.

5.2.18 Strontium

Strontium remained almost completely with the sewage sludge ash (Figure 40), but was partially volatilised (5 – 45 %) when Polish coal was burnt alone. Blends of these fuels retained strontium to a high degree. This was as predicted by thermodynamic equilibrium modelling, through the formation of $SrSO_4$, $SrO.SiO_2$ and $SrO.2SiO_2$. Strontium volatilised from Polish coal, may have formed these compounds, but failed to recondense before it was swept out of the suspension-firing reactor by the flue gas, as described in Section 5.0.3.

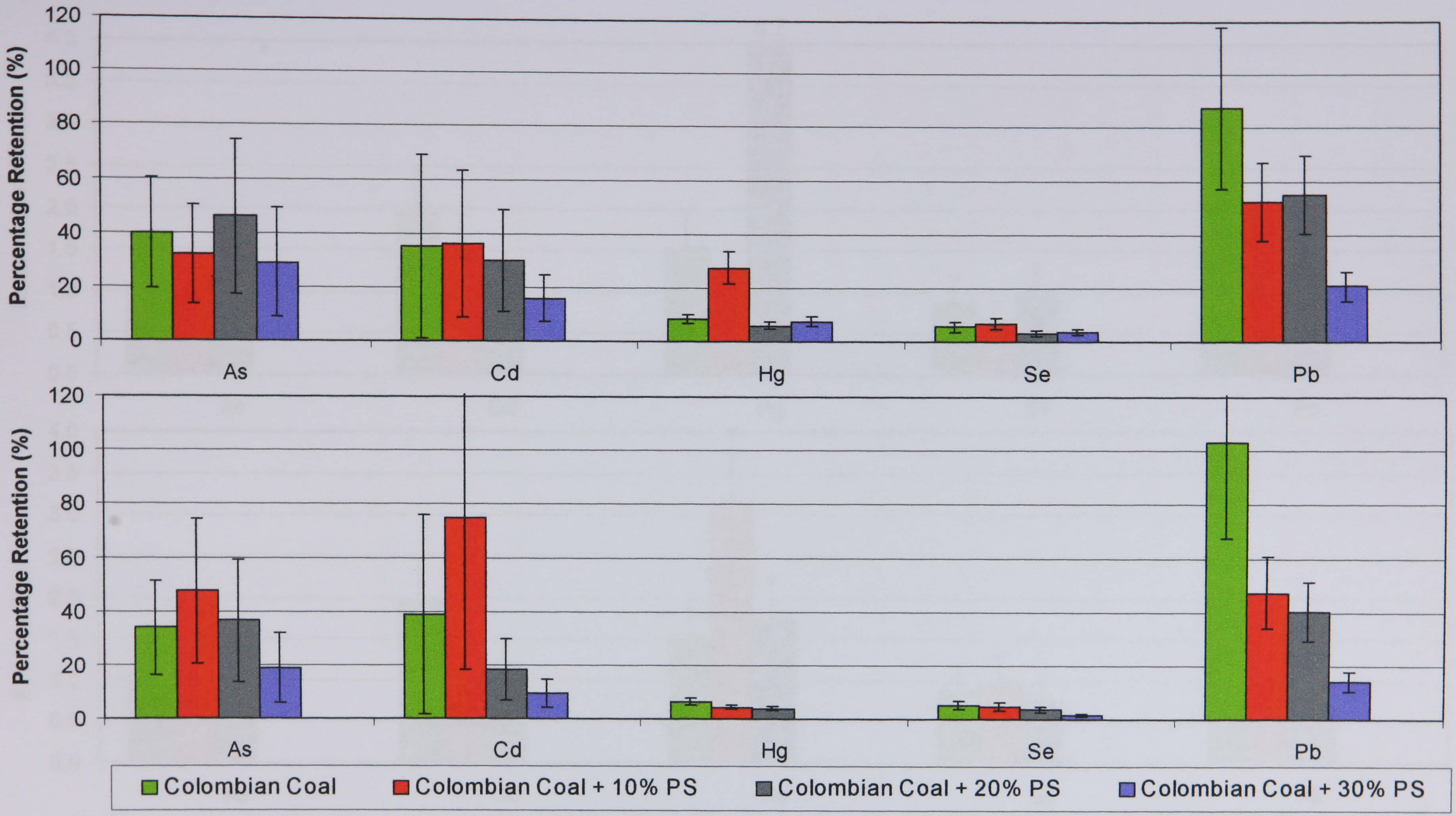
5.3 Colombian Coal and Paper Sludge Co-Combustion

Paper sludge is a by-product of paper making, separated from recycled water in paper mills. It is mostly bleached wood pulp, but also contains kaolinite, calcite and talc, minerals added during the paper making process (Latva-Sommppi et al, 1998). For the purpose of determining the trace metal emission limits from its combustion, paper sludge has been classified as biomass when burnt at the site of production (EU Directive 2000/76/EC). This classification is beneficial, it reduces the amount and cost of emissions monitoring that must be carried out during paper sludge firing alone, with other biomass fuels or with coal.

Paper sludge used in this study was supplied Midtkraft from their paper mill at Grenå, Denmark. This sludge may, in the future, be combusted in a nearby 79 MW_{th} bubbling fluidised bed power station. Therefore, paper sludge has been co-combusted with fuels representative of those usually burnt at Grenå: High volatile Colombian bituminous coal and Danish wheat straw.

It was not possible to burn paper sludge in the suspension reactor on its own due to difficultly in feeding it from the feed hopper. The absence of these results has limited the possibility of determining the existence of synergies for trace element retention or release between Colombian coal and paper sludge.

The co-combustion of paper sludge with coal produced only small amounts of sinter ash. For the 70 % Colombian coal / 30 % paper sludge blends (energy basis) the amount was insufficient to perform all of the trace element analyses. Thus, for these runs, the bottom and sinter ash were mixed and analysed together and calculation of relative enrichment on sinter ash was not possible.



Trace Element Concentration in raw fuels (ppm):	As	Cd	Hg	Se	Pb
Colombian Coal	1.8 ± 0.8	0.26 ± 0.25	0.031 ± 0.001	5.1 ± 1.0	1.9 ± 0.5
Paper Sludge	0.53 ± 0.94	0.77 ± 0.19	0.083 ± 0.016	<0.8	21 ± 3

Figure 44 Percentage Retention of As, Cd, Hg, Se and Pb During Colombian Coal / Paper Sludge Co-Combustion

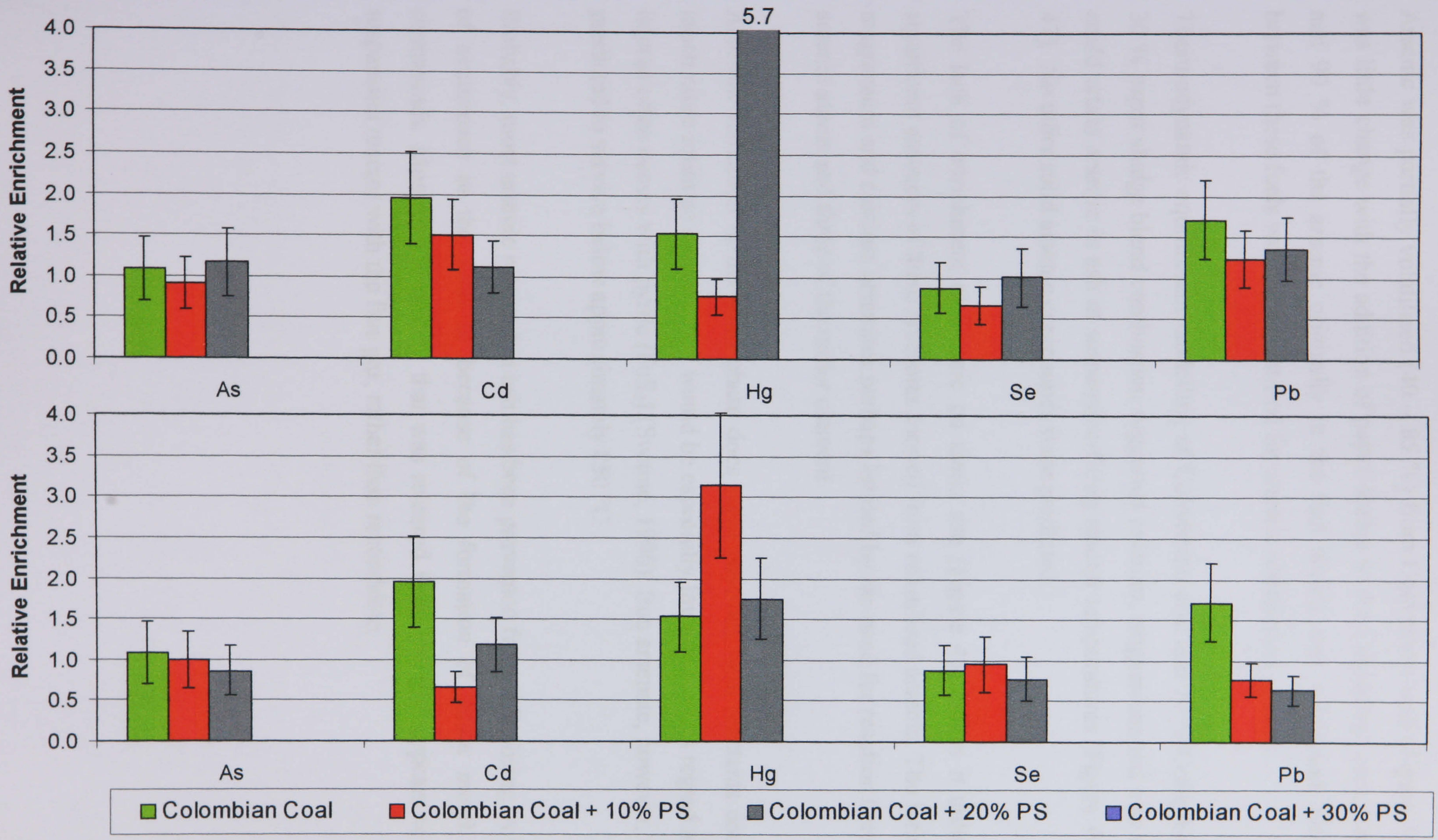


Figure 45 Relative Enrichment of As, Cd, Hg, Se and Pb in Sinter Ash During Colombian Coal / Paper Sludge Co- Combustion

Note: A relative enrichment of one corresponds to that element being found in equal concentrations in the sinter and bottom ashes

5.3.1 Arsenic

Arsenic was partially volatilised (40 – 85 %) from Colombian coal (Figure 44). There was little change with the addition of paper sludge to the Colombian coal, between 25 and 90 % of the arsenic originally in the fuel blends was volatilised. No synergy between these fuels would be identified for arsenic retention or release.

Thermodynamic equilibrium modelling of Colombian coal and 70 % Colombian coal / 30 % paper sludge blend combustion suggested calcium, magnesium and iron arsenates could retain arsenic in ash at suspension-firing reactor temperatures (Figure 46, Figure 47). No other solid arsenic compounds were predicted.

The lack of enrichment of arsenic on sinter ash (Figure 45) makes it unlikely that significant amounts of these arsenates formed from volatilised arsenic. The formation of magnesium and calcium arsenates perhaps limited by the need for reaction between two arsenic atoms and three of the minor element.

Arsenate formation in the solid phase does seem possible, here reactants could be in much more intimate contact. Iron would be especially favoured in this regard as arsenic in coal often occurs with pyrite [FeS_2] (Swaine, 1990). Iron arsenate, however, was only predicted to survive below approximately 850 °C.

Probably, most arsenic retained in ash has been prevented from volatilising by its mode of occurrence in the fuels or because of the formation of minor metal arsenate compounds. Most of the arsenic that was released from the fuel appears to exit the suspension reactor with the flue gas, rather than recondense.

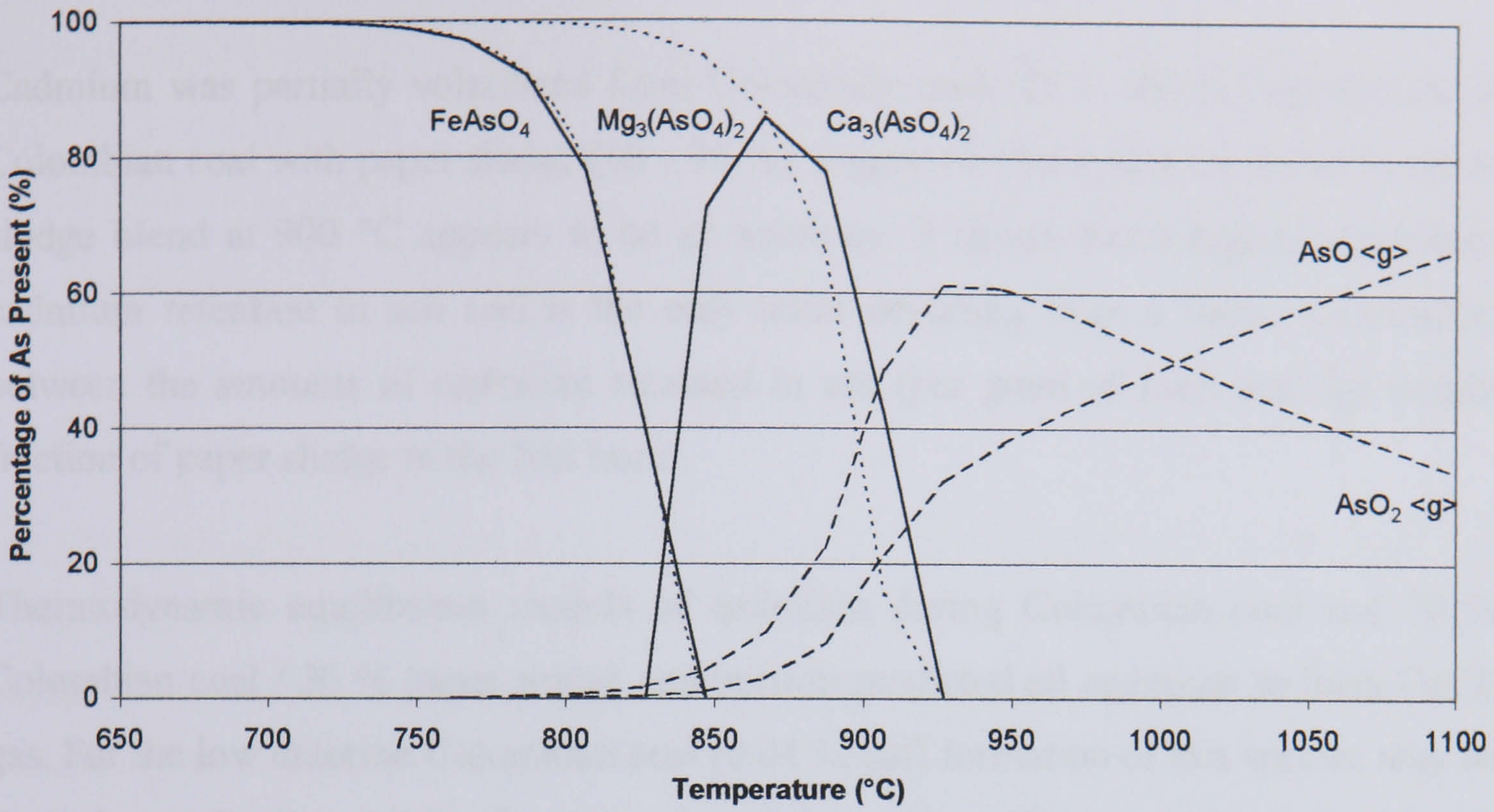


Figure 46 Thermodynamic Equilibrium Prediction for Arsenic During Colombian Coal Combustion

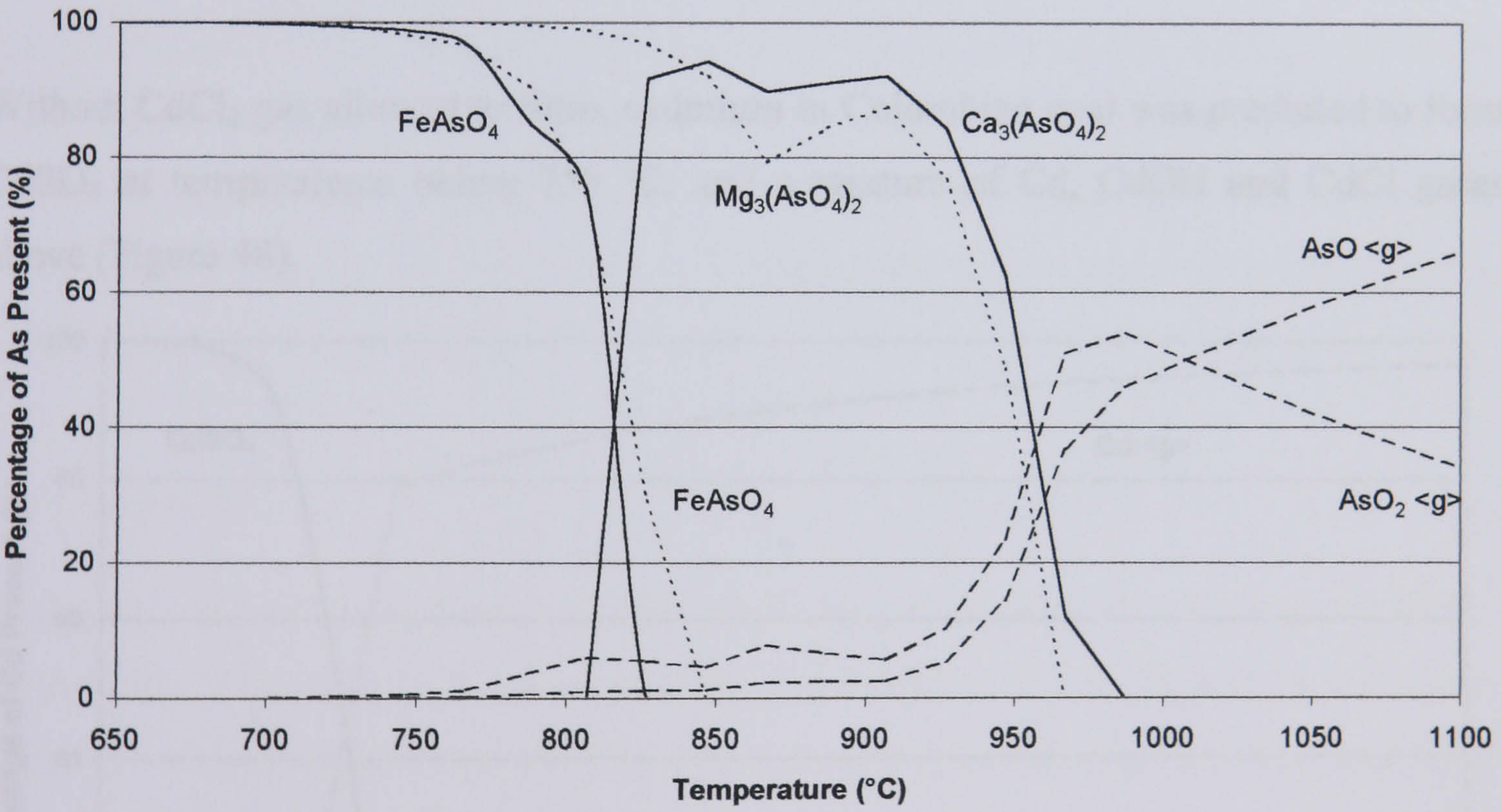


Figure 47 Thermodynamic Equilibrium Prediction for Arsenic During 70 % Colombian Coal / 30 % Paper Sludge Combustion

5.3.2 Cadmium

Cadmium was partially volatilised from Colombian coal (25 – 100 %) and blends of Colombian coal with paper sludge (40 – 95 %), Figure 44. The result for the 10 % paper sludge blend at 900 °C appears to be an anomaly. It shows much higher percentage cadmium retention in ash and is the only point deviating from a linear relationship between the amounts of cadmium retained in ash (per gram of fuel) and the weight fraction of paper sludge in the fuel burnt.

Thermodynamic equilibrium models of cadmium during Colombian coal and 70 % Colombian coal / 30 % paper sludge combustion predicted all cadmium to form $CdCl_2$ gas. For the low chlorine Colombian coal (0.04 % daf) formation of this species may be limited (see Section 5.2.2). To determine the possible influence of the low chlorine content, the thermodynamic model for Colombian coal was re run without $CdCl_2$ gas. This step was not taken with the higher (0.17 %) chlorine content 70 % Colombian coal / 30 % Paper sludge blend.

Without $CdCl_2$ gas allowed to form, cadmium in Colombian coal was predicted to form $CdSO_4$ at temperatures below 750 °C, and a mixture of Cd, CdOH and CdCl gases above (Figure 48).

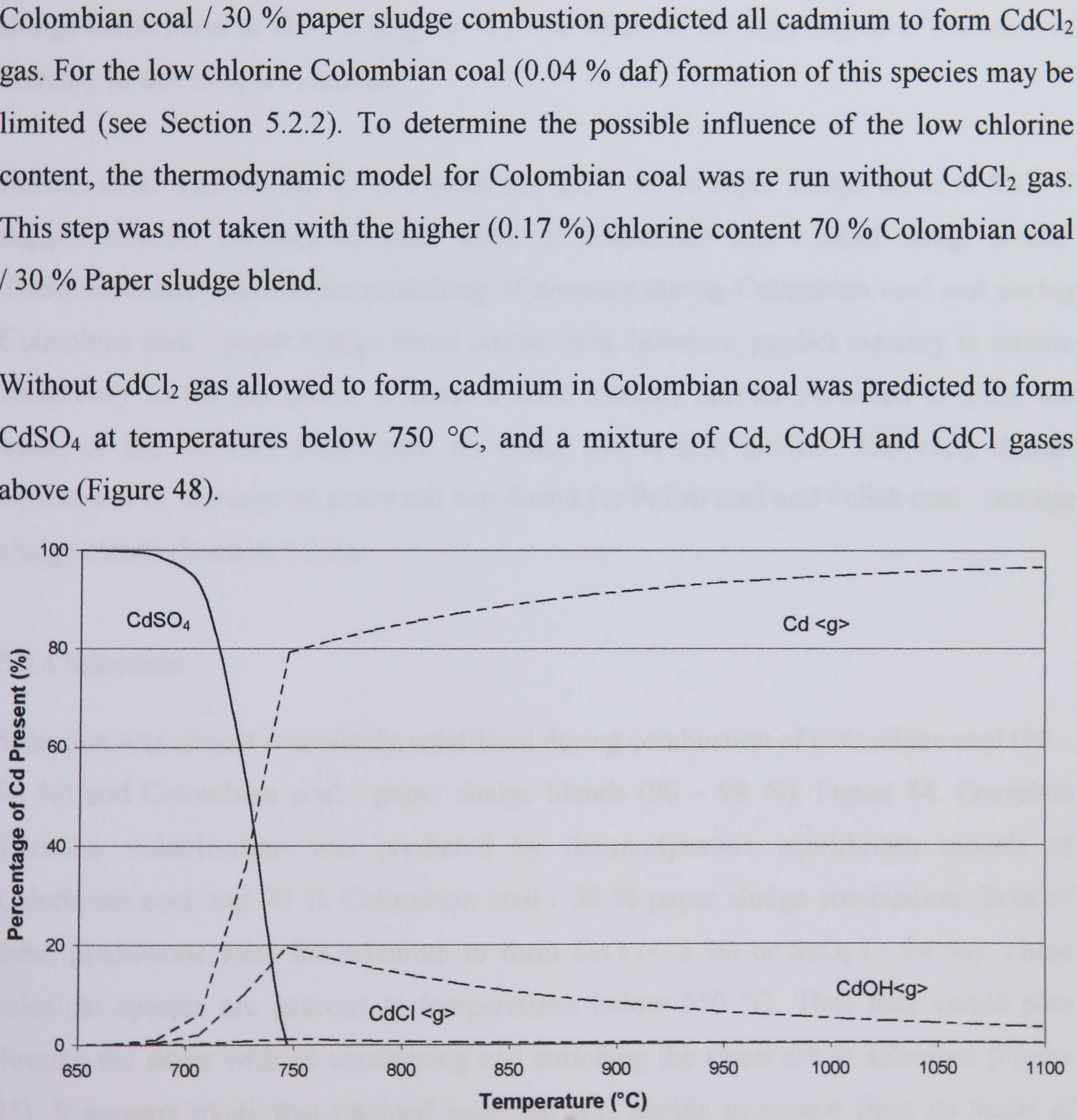


Figure 48 Thermodynamic Equilibrium Prediction for Cadmium During Colombian Coal Combustion

The cadmium sulphate was not predicted to high enough temperatures to have caused the cadmium enrichment on Colombian coal sinter ash at 900 °C (Figure 45). This must have been caused by the formation of a species not included in the MTDATA database. Possibly the formation of the cadmium alumino silicate species found by Lachas (1999) and Scotto et al (1993) that were discussed in section 5.2.2.

5.3.3 Mercury

Mercury was almost completely volatilised (90 – 95 %) from Colombian coal and Colombian coal / paper sludge blends, except the 90 % Colombian coal / 10 % paper sludge blend burnt at 800 °C (Figure 44). The cause of the high degree of retention of mercury in this sample is unclear.

Results other than for the 90 % Colombian coal / 10 % paper sludge blend at 800 °C suggest mercury enriches on sinter ashes of Colombian coal / paper sludge blends. Thermodynamic equilibrium modelling of mercury during Colombian coal and during Colombian coal / paper sludge blend combustion, however, predict mercury to remain completely in the gas phase. Without a solid mercury species predicted to form, the cause of the mercury enrichment on sinter ash is also unclear. However, similar enrichment of mercury on sinter ash was found for Polish coal and Polish coal / sewage sludge blends (Section 5.2.3).

5.3.4 Selenium

Selenium was almost completely volatilised during combustion of Colombian coal (90 – 98 %) and Colombian coal / paper sludge blends (90 – 98 %), Figure 44. Complete selenium volatilisation was predicted by thermodynamic equilibrium models of Colombian coal and 70 % Colombian coal / 30 % paper sludge combustion. Both of these predictions were for selenium to form SeO (< 2 %) or SeO_2 (> 98 %). These selenium species are gaseous to temperatures below 650 °C. Thus they would pass through the sinter without condensing and enriching the sinter ash in selenium (Figure 45). It appears likely that retained selenium was unable to escape from its mode of occurrence in either fuel (Section 5.0.2).

5.3.5 Lead

Lead was almost completely retained in Colombian coal ash (Figure 44). When paper sludge was mixed with the Colombian coal, lead retention was reduced. There does not however, appear to have been any synergy for lead retention or release between these fuels, a plot of the amount of lead retained (per gram of fuel) against the weight fraction of paper sludge in the blend was linear.

A thermodynamic equilibrium model of lead during the combustion of 70 % Colombian coal / 30 % paper sludge suggested lead was volatilised from the suspension reactor as $PbCl_2$ gas. Most of the volatilised lead in the Colombian coal / paper sludge blends probably formed $PbCl_2$ gas A similar prediction was made for Colombian coal. The Colombian coal, however, has a low chlorine content (0.04 % daf). This may have reduced formation of $PbCl_2$ significantly because of the low probability of lead reacting with two Cl atoms. To investigate this effect the Colombian coal was modelled with the formation of the $PbCl_2$ prevented (Figure 49).

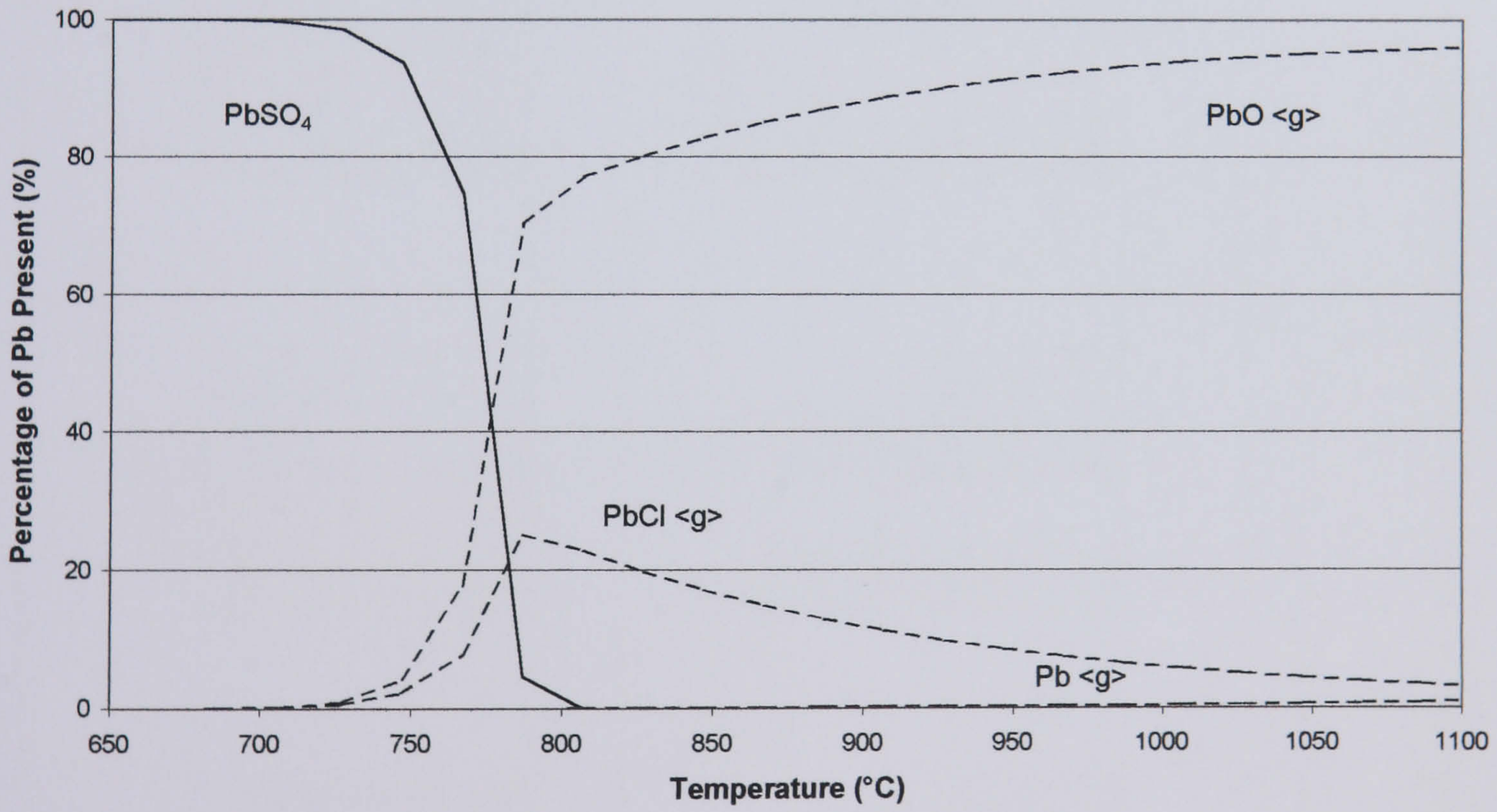
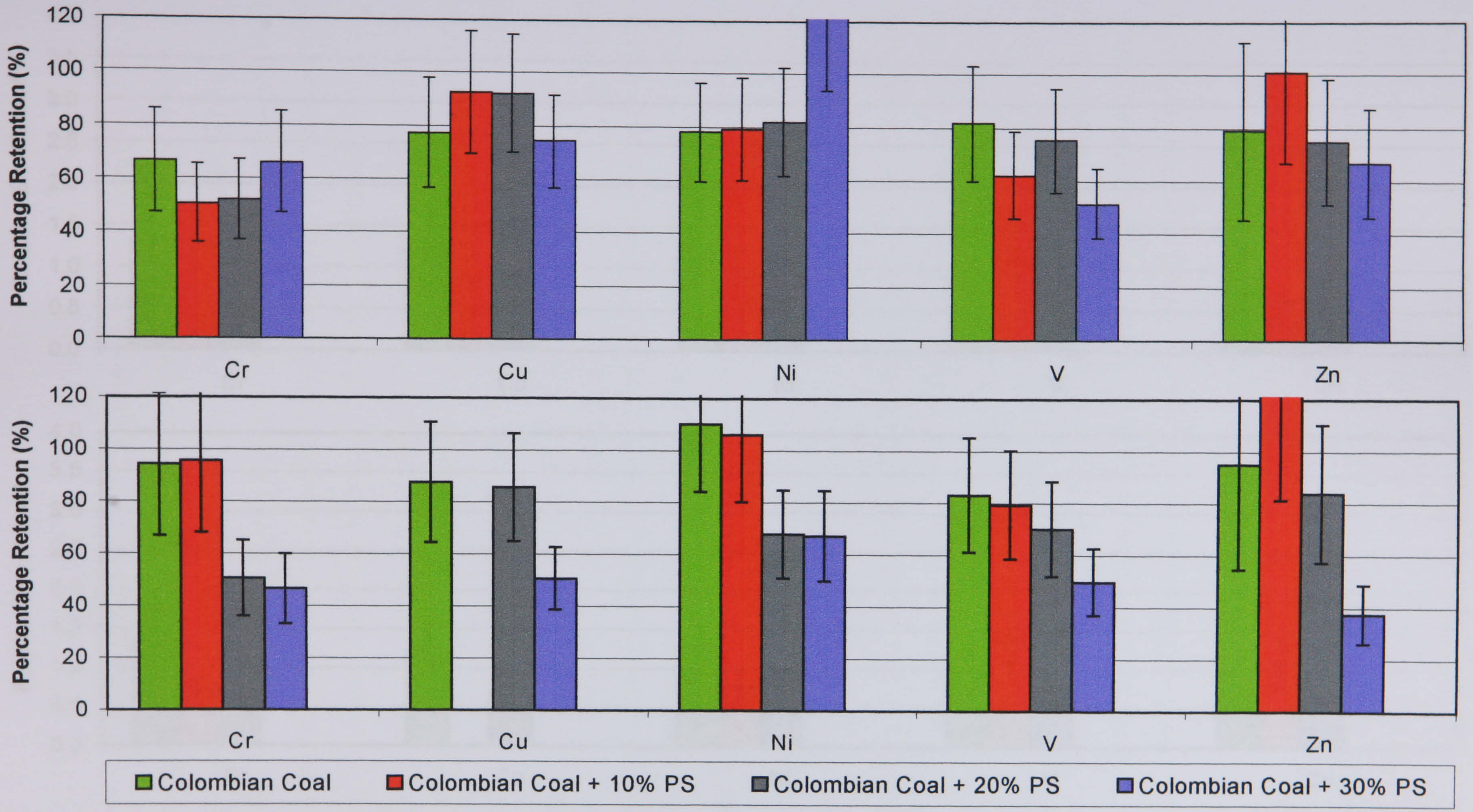


Figure 49 Thermodynamic Equilibrium Model for Lead During Colombian Coal Combustion

Thermodynamic equilibrium modelling suggests solid lead sulphate could form below 800 °C. This may have been the cause of lead enrichment on Colombian coal sinter ash at this temperature (Figure 45). Lead sulphate was not predicted to exist at a high

enough temperature to have caused the enrichment of lead on sinter ash at 900 °C. This enrichment must have been caused by formation of a compound not included in the MTDATA model. Possibly silicate or alumino silicate minerals in the ash have captured the volatilised lead as found by Lachas (1999) and Scotto (1993). The products of these reactions would not be predicted by thermodynamic equilibrium modelling, as no thermodynamic data was available.



Trace Element Concentration in raw fuels (ppm):	Cr	Cu	Ni	V	Zn
Colombian Coal	11 ± 2	5.8 ± 1.0	6.5 ± 0.8	12 ± 2	18 ± 7
Paper Sludge	11 ± 2	16 ± 2	2.9 ± 0.9	2.3 ± 0.2	132 ± 26

Figure 50 Percentage Retention of Cr, Cu Ni, V and Zn During Colombian Coal / Paper Sludge Co-Combustion

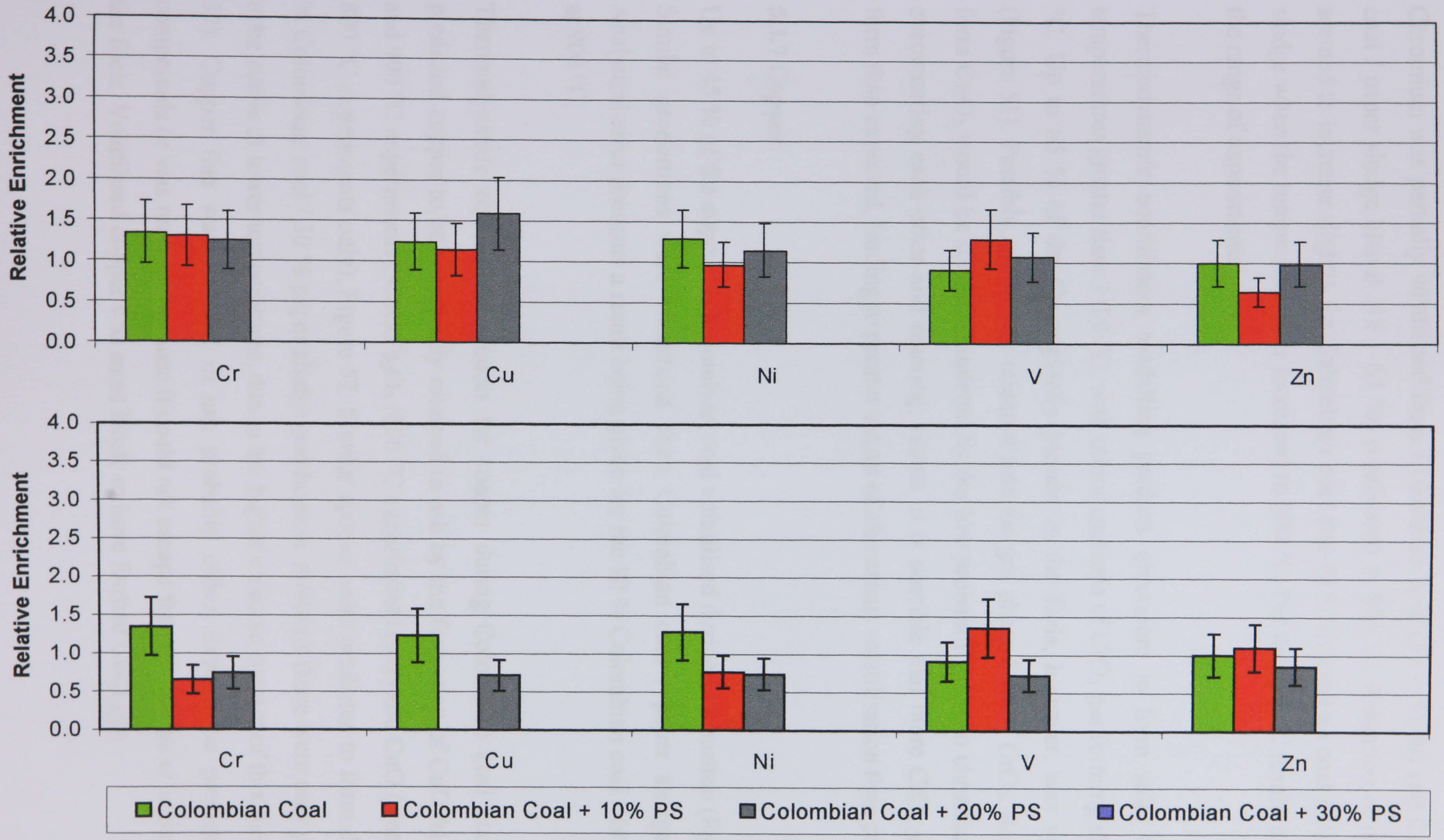


Figure 51 Relative Enrichments of Cr, Cu, Ni, V and Zn in Sinter Ash During Combustion of Colombian Coal and Paper Sludge

Note: A relative enrichment of one corresponds to that element being found in equal concentrations in the sinter and bottom ashes

5.3.6 Chromium

Chromium was partially volatilised from Colombian coal (15 – 55 %) and Colombian coal / paper sludge blends (15 – 65 %) combusted at 800 °C. Retention of chromium seemed to increase slightly for Colombian coal and 90 % Colombian coal / 10 % paper sludge when the temperature was increased to 900 °C, but the 800 °C results are within the range of experimental error.

Thermodynamic equilibrium modelling predicts chromium to form solid Cr_2O_3 to temperatures greater than 1100 °C, with minor amounts of CrO_3 gas forming above 930 °C. Up to 65 % of the Cr originally present in the fuels, however, was volatilised (Figure 51). Possibly, chromium released into the gas phase formed CrO_3. Reaction to form Cr_2O_3 would be severely hindered by the low probability of two chromium atoms encountering each other and reacting. Hence, it is possible that more CrO_3 gas could form than expected, leading to greater extent of chromium volatilisation than predicted.

5.3.7 Copper

Up to 45 % of the copper in Colombian coal volatilised during combustion (Figure 50). Similar proportions were volatilised from Colombian coal / paper sludge blends. Analytical error prevents a result being given for the 90 % Colombian coal / 10 % burnt at 900 °C.

Thermodynamic equilibrium models for copper during Colombian coal combustion predicted copper to be completely retained in ash by the formation of $CuO.Al_2O_3$ (800 and 900 °C experiments), $CuO.Fe_2O_3$ (800 °C experiments only) and CuO (sinter ash of 800 °C experiments only), Figure 52. Similar species were predicted to form during 70 % Colombian coal / 30 % paper sludge combustion, although these were only predicted to be stable at lower temperatures, due to the higher chlorine content of this fuel (Figure 53). Copper that was retained in ash probably either formed the predicted solid compounds or was retained because it could not escape from its modes of occurrence in the fuels. Volatilised copper was most likely to have formed CuCl gas.

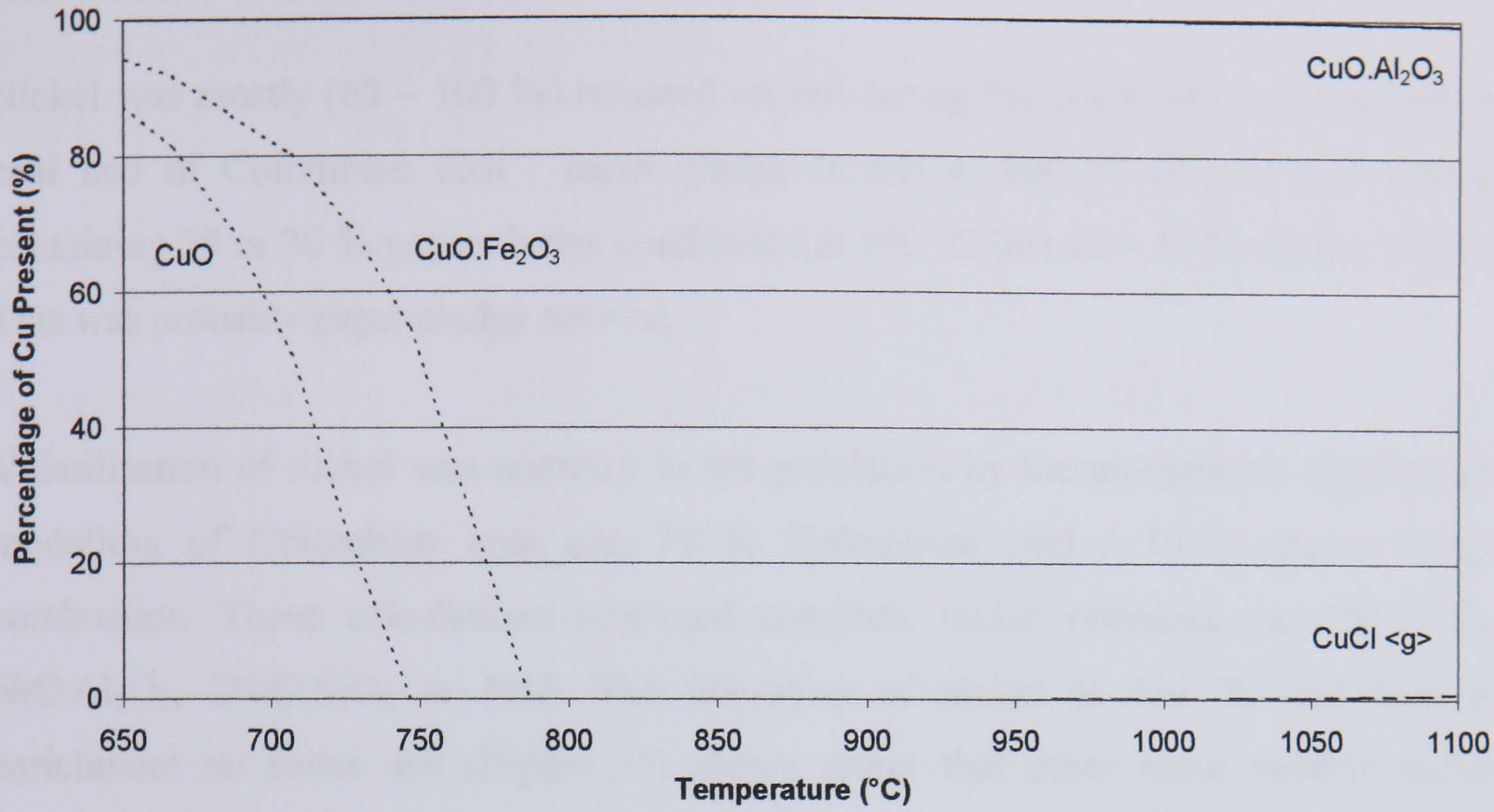


Figure 52 Thermodynamic Equilibrium Prediction for Copper During Colombian Coal Combustion

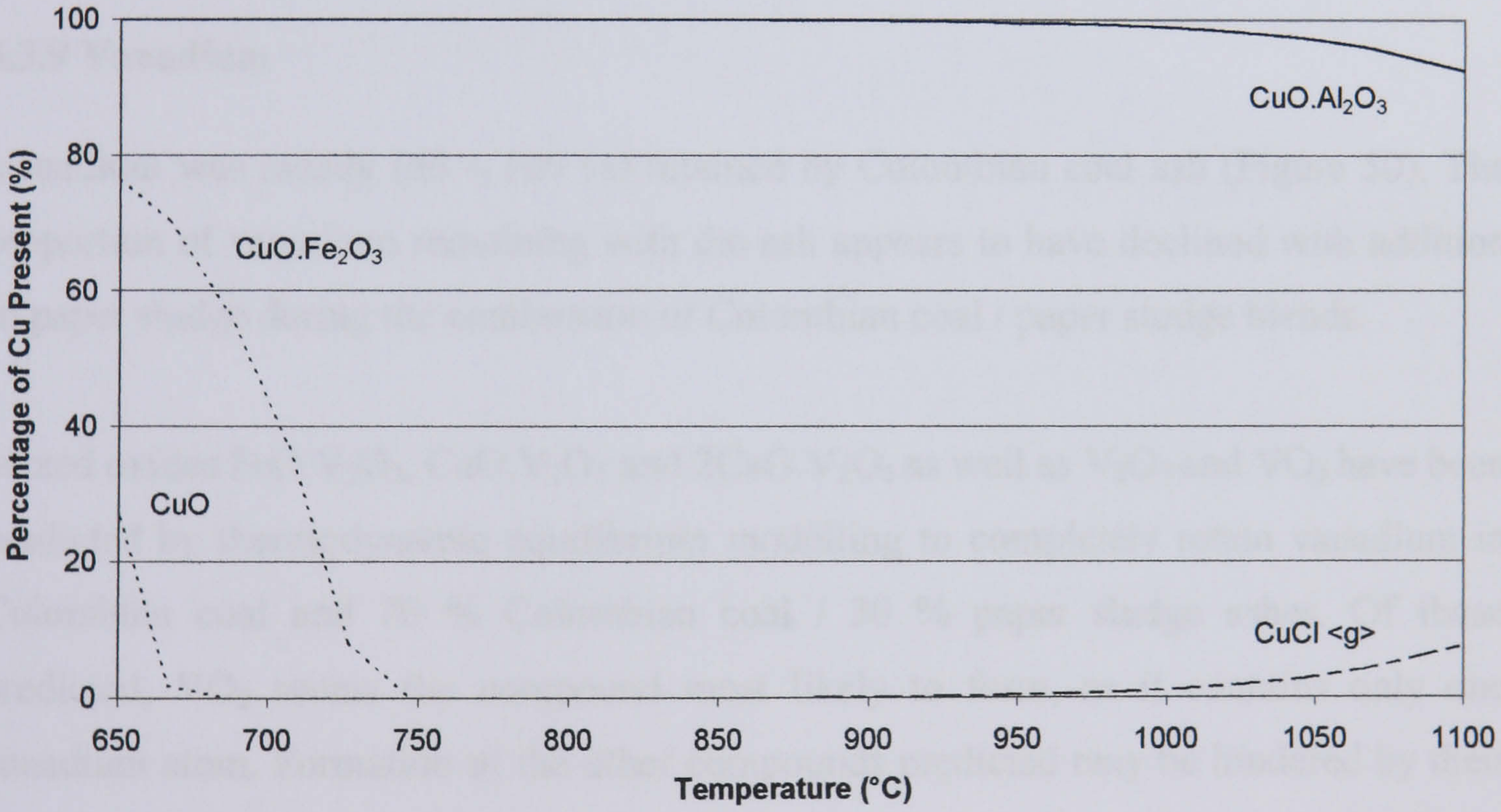


Figure 53 Thermodynamic Equilibrium Prediction for Copper During 70 % Colombian Coal / 30 % Paper Sludge Combustion

5.3.8 Nickel

Nickel was mostly (60 – 100 %) retained on ash during the combustion of Colombian coal and of Colombian coal / paper sludge blends at 800 °C (Figure 50). Blends containing 20 or 30 % paper sludge combusted at 900 °C lost 15 – 50 % of their nickel. This was probably paper sludge derived.

Volatilisation of nickel was contrary to the prediction by thermodynamic equilibrium modelling of Colombian coal and 70 % Colombian coal / 30 % paper sludge combustion. These calculations predicted complete nickel retention, as $NiO.Fe_2O_3$, $NiO.Al_2O_3$, $2NiO.SiO_2$ or NiO. The liberation of nickel at 900 °C and lack of enrichment on sinter ash (Figure 51) shows either that other more volatile nickel compounds were actually formed, or that the released into the gas phase by combustion did not completely recondense (Section 5.0.3).

5.3.9 Vanadium

Vanadium was mostly (60 – 100 %) retained by Colombian coal ash (Figure 50). The proportion of vanadium remaining with the ash appears to have declined with addition of paper sludge during the combustion of Colombian coal / paper sludge blends.

Mixed oxides $FeO.V_2O_5$, $CaO.V_2O_5$ and $2CaO.V_2O_5$ as well as V_2O_5 and VO_2 have been predicted by thermodynamic equilibrium modelling to completely retain vanadium in Colombian coal and 70 % Colombian coal / 30 % paper sludge ashes. Of those predicted, VO_2 seems the compound most likely to form, as it contains only one vanadium atom. Formation of the other compounds predicted may be hindered by their requirement for two vanadium atoms, which were present at very low concentrations. Preliminary models also suggested the formation of V_4O_{10} gas; however, this compound was excluded from prediction as described in section 3.4.1.

The vanadium that was volatilised from the Colombian coal / paper sludge blends probably originated from the paper sludge, as vanadium was almost completely retained in ash when the Colombian coal was combusted alone. It is likely that the vanadium in the paper sludge was mostly released from its original modes of occurrence, although

predicted to form solid compounds. Probably, once in the gas phase, not all of the released vanadium could recondense before being swept out of the reactor by the suspension gas flow (Section 5.0.3).

5.3.10 Zinc

A high proportion of zinc contained in Colombian coal and blends of Colombian coal with up to 20 % paper sludge appears to be retained in ash (Figure 50). Addition of 30 % paper sludge to the Colombian coal seems to have increased zinc to volatilisation.

Thermodynamic modelling suggests that the volatilised zinc formed $ZnCl_2$ gas. Less than one percent of the zinc in the Colombian coal was predicted to form $ZnCl_2$ (Figure 54); this proportion was increased by addition of paper sludge with its high (0.39 % daf) chlorine content (Figure 55). Zinc retained on the ash has probably formed the predicted $ZnO.Al_2O_3$, $2ZnO.SiO_2$ and ZnO or was not released from its original modes of occurrence in the fuels (Section 5.0.2).

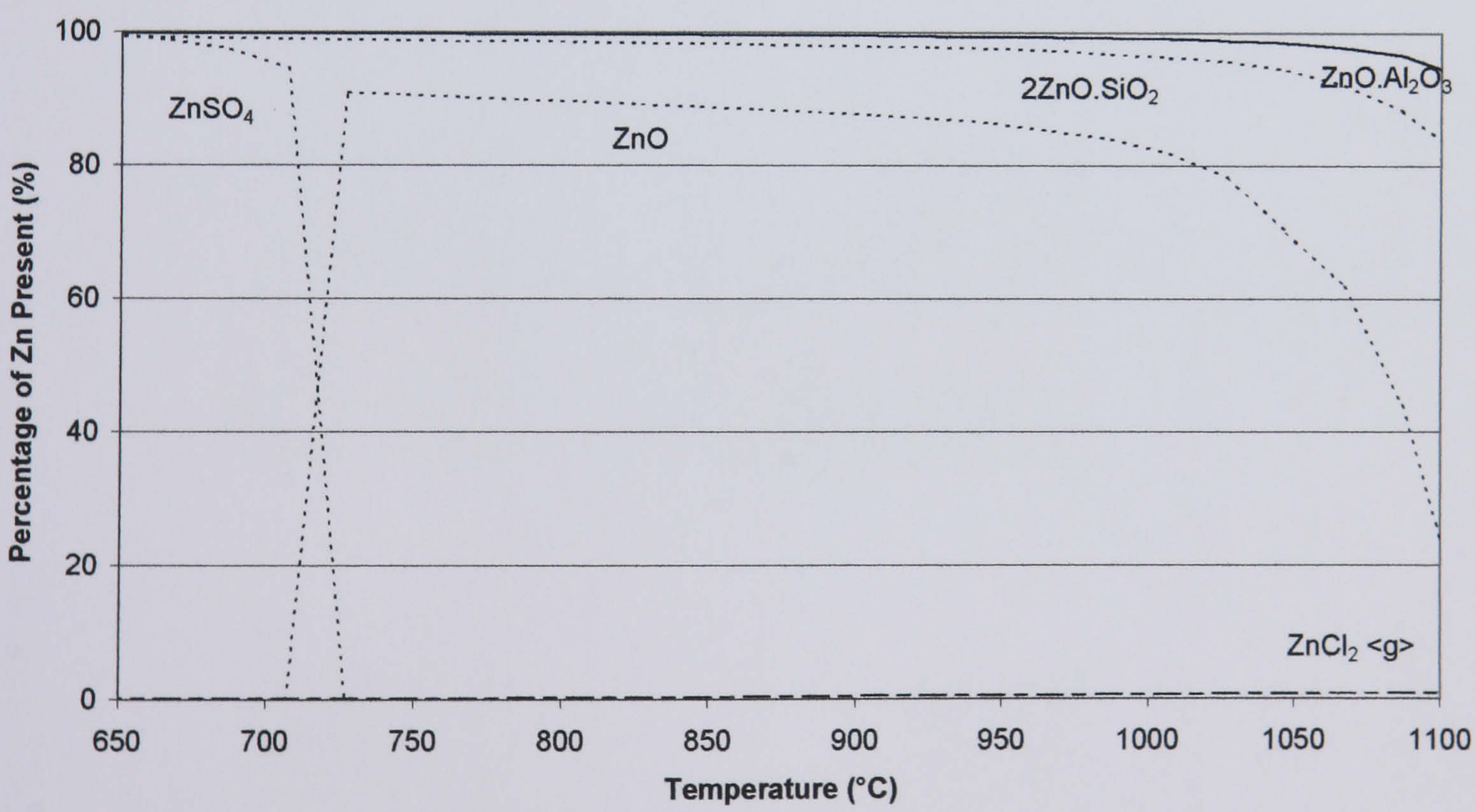


Figure 54 Thermodynamic Equilibrium Prediction for Zinc During Colombian Coal Combustion

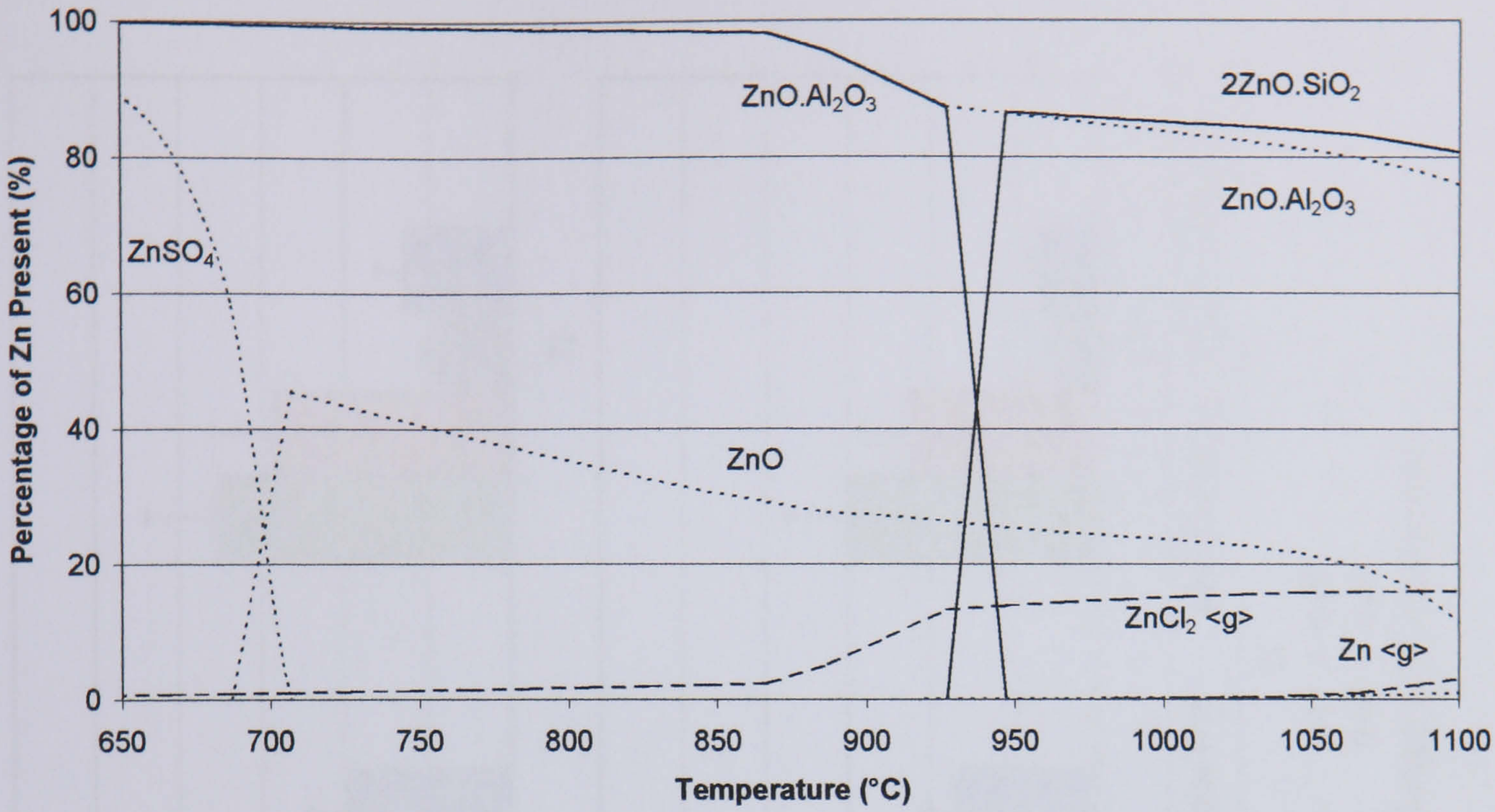
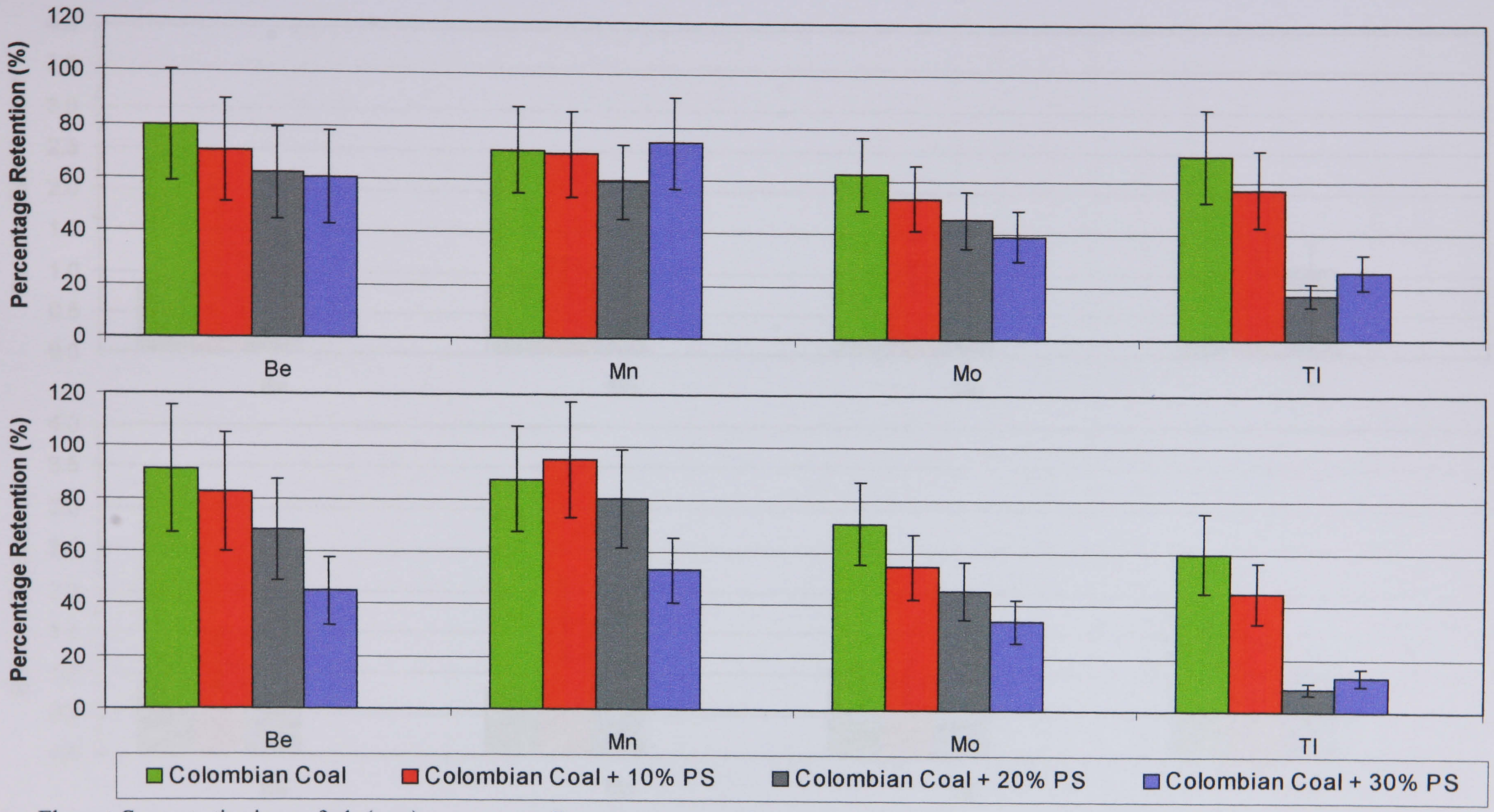


Figure 55 Thermodynamic Equilibrium Prediction for Zinc During 70 % Colombian Coal / 30 % Paper Sludge Combustion



Trace Element Concentration in raw fuels (ppm):	Be	Mn	Mo	Tl
Colombian Coal	0.40 ± 0.07	27 ± 3	1.51 ± 0.14	0.11 ± 0.02
Paper Sludge	0.05 ± 0.03	62 ± 8	1.2 ± 0.3	0.01 ± 0.00

Figure 56 Percentage Retention of Be, Mn, Mo and Tl in Ash After Colombian Coal / Paper Sludge Co-Combustion

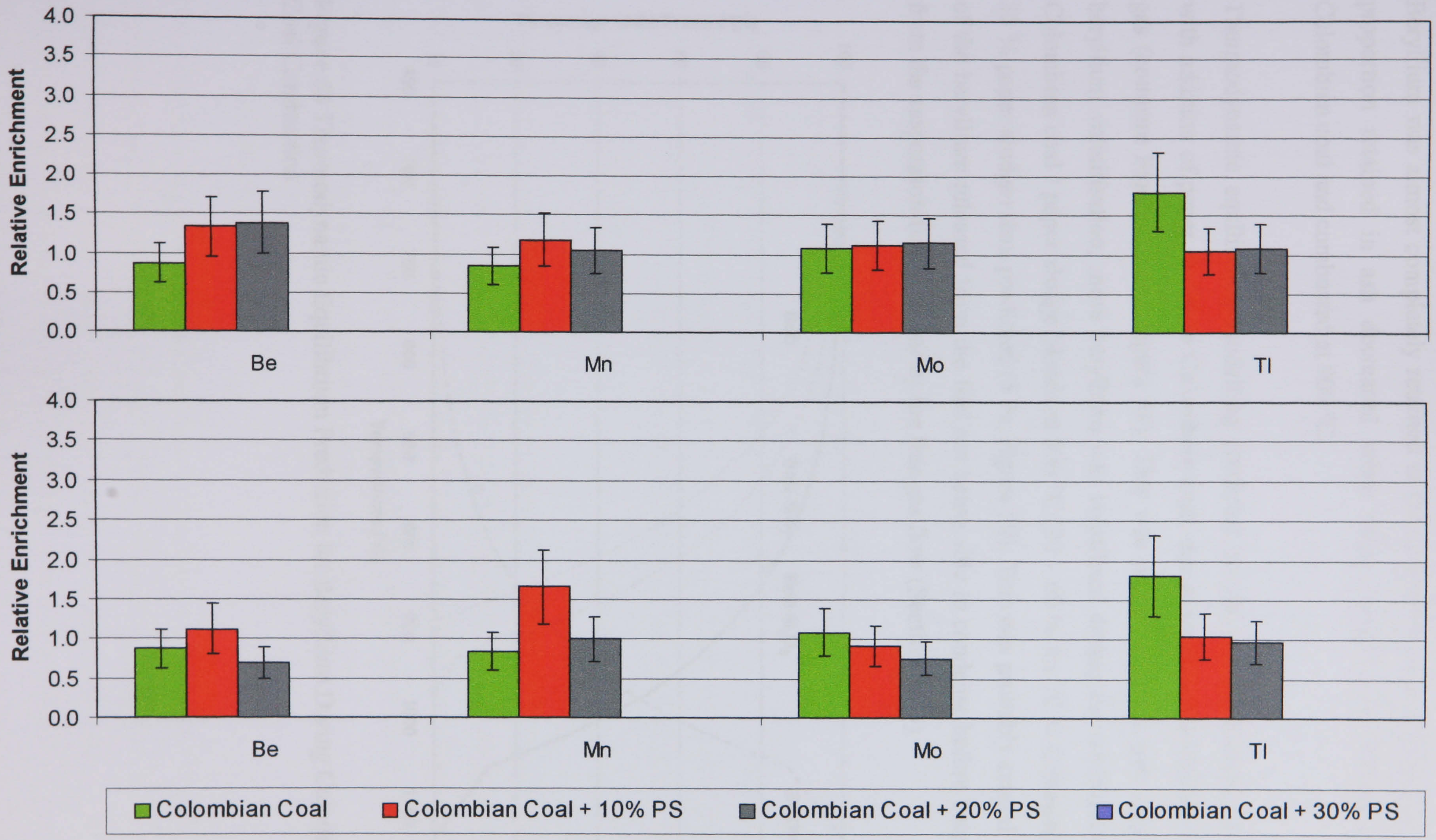


Figure 57 Relative Enrichments of Be, Mn, Mo and Tl in Sinter Ash During Colombian Coal / Paper Sludge Co-Combustion
Note: A relative enrichment of one corresponds to that element being found in equal concentrations in the sinter and bottom ashes

5.3.11 Beryllium

Beryllium was almost completely retained in the Colombian coal ash (Figure 56). The proportion retained in ash decreased when paper sludge was blended with the Colombian coal and combusted at 900 °C.

Thermodynamic equilibrium modelling predicted beryllium volatilisation to increase with addition of paper sludge to Colombian coal, due to increased formation of BeOH gas (compare Figure 58 and Figure 59). This was probably only a part cause of the beryllium volatilisation; more beryllium was volatilised during the combustion of the Colombian coal / paper sludge blends at 800 °C (20 – 60 % for 70 % Colombian coal / 30 % paper sludge) than predicted (5 %, Figure 59). This was probably caused by some of the beryllium released from the fuel not being able to condense before being swept from the suspension-firing reactor by the flue gas flow (Section 5.0.3).

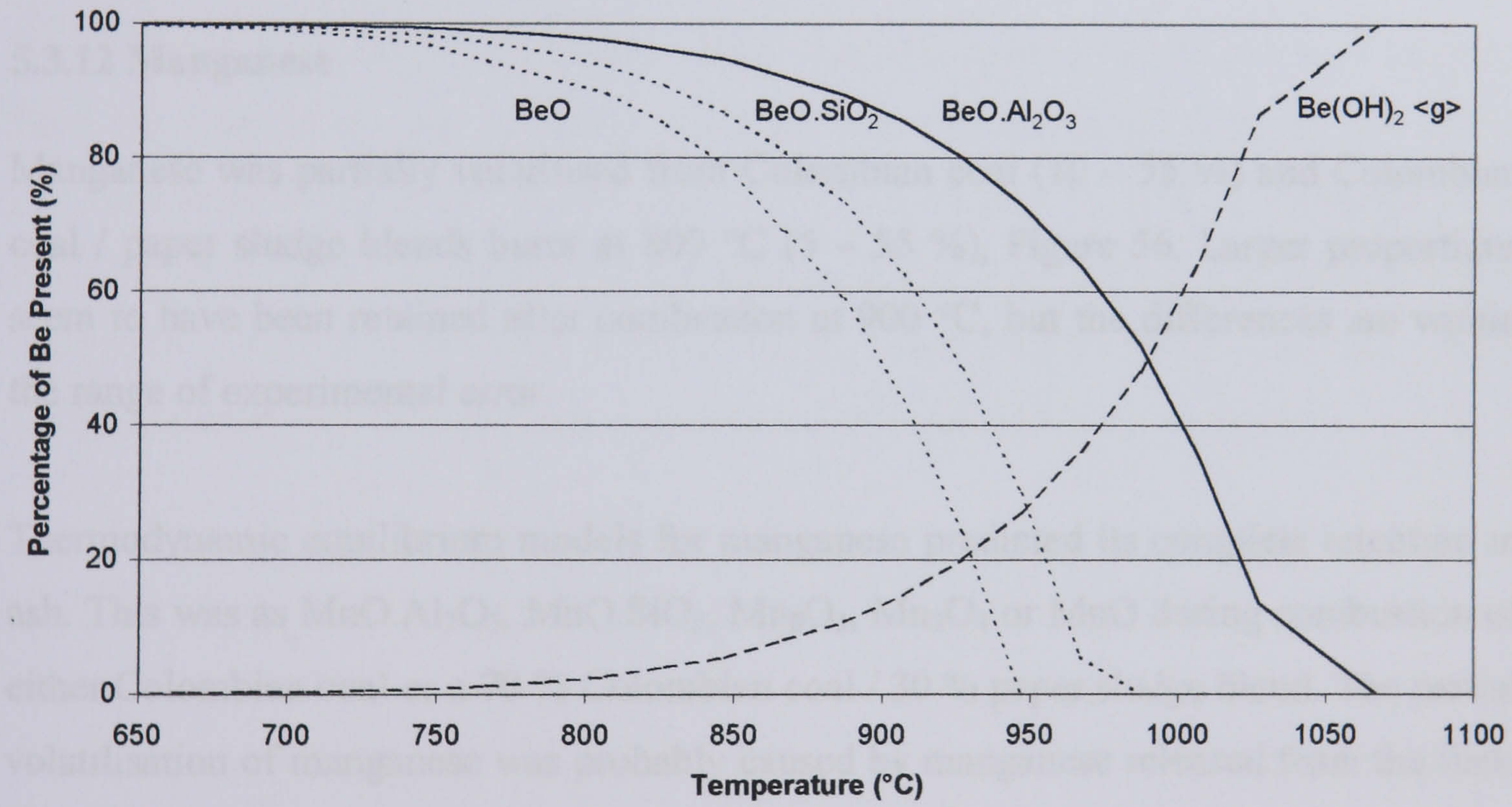


Figure 58 Thermodynamic Equilibrium Prediction for Beryllium During Colombian Coal Combustion

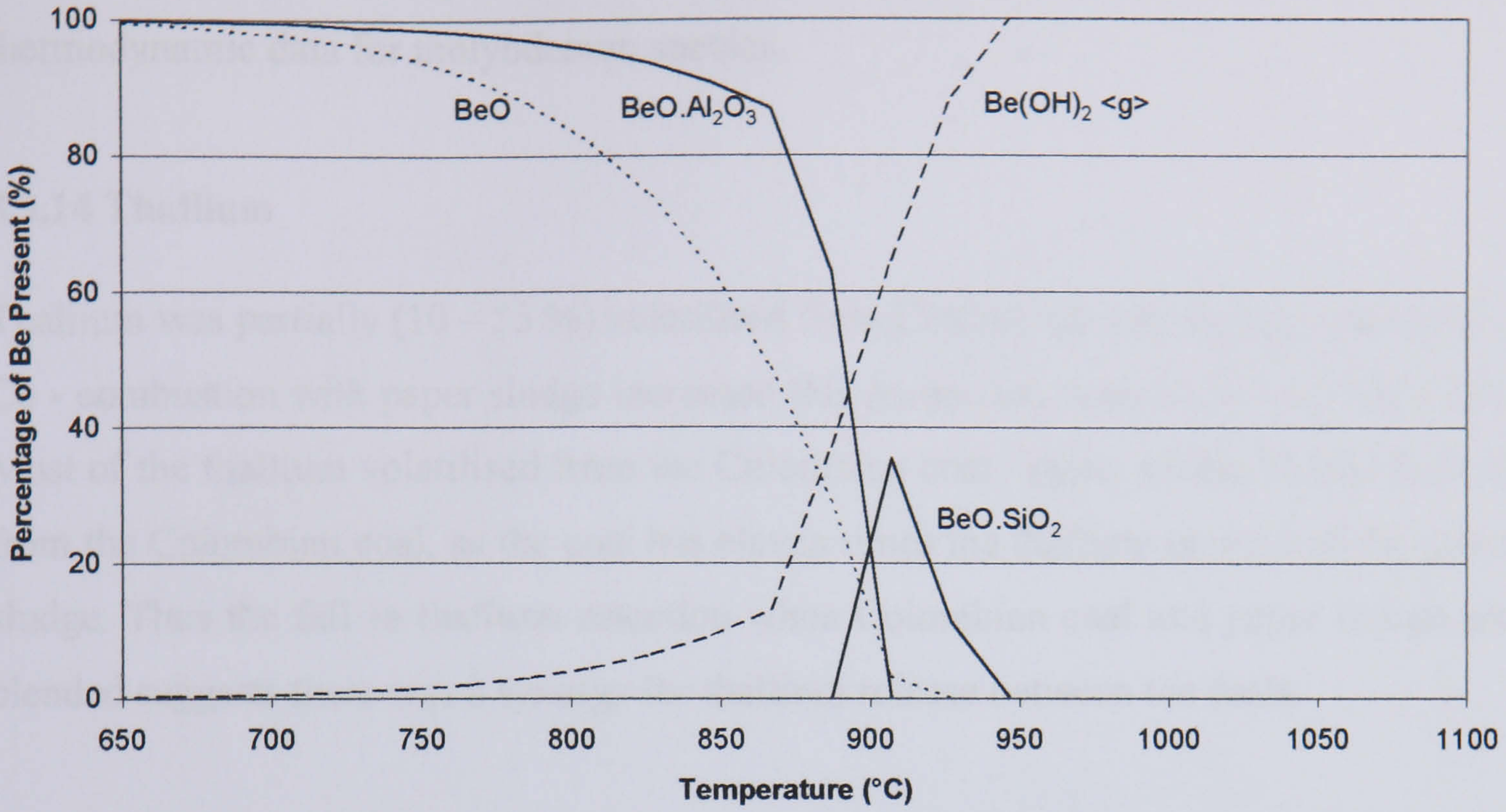


Figure 59 Thermodynamic Equilibrium Prediction for Beryllium During 70 % Colombian Coal / 30 % Paper Sludge Combustion

5.3.12 Manganese

Manganese was partially volatilised from Colombian coal (10 – 55 %) and Colombian coal / paper sludge blends burnt at 800 °C (5 – 55 %), Figure 56. Larger proportions seem to have been retained after combustion at 900 °C, but the differences are within the range of experimental error.

Thermodynamic equilibrium models for manganese predicted its complete retention in ash. This was as $MnO.Al_2O_3$, $MnO.SiO_2$, Mn_2O_3, Mn_3O_4 or MnO during combustion of either Colombian coal or a 70 % Colombian coal / 30 % paper sludge blend. The partial volatilisation of manganese was probably caused by manganese released from the fuels incompletely recondensing on ash, as described in Section 5.0.3.

5.3.13 Molybdenum

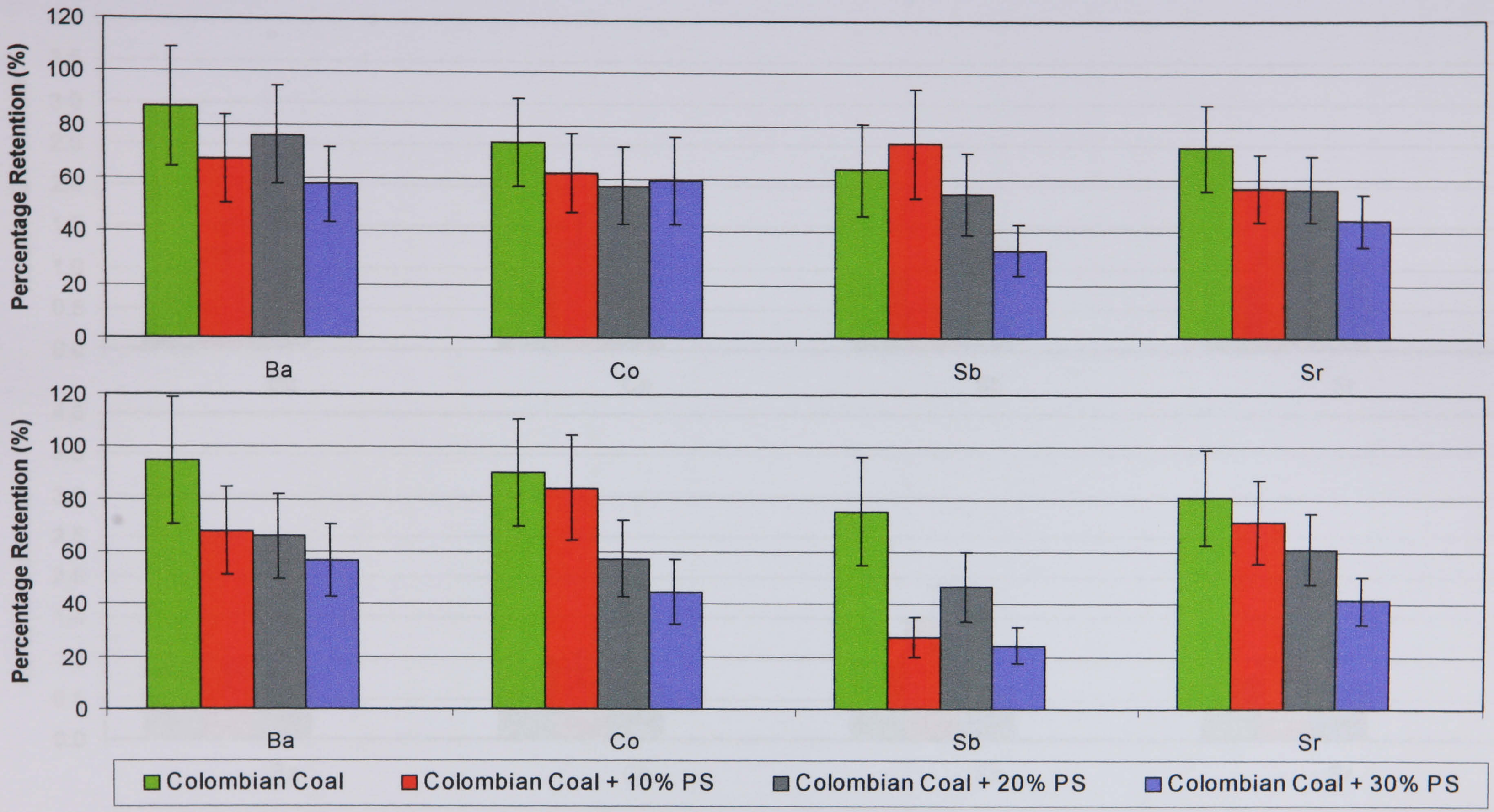
Molybdenum was partially volatilised from Colombian coal (25 – 50 %) and blends of Colombian coal with paper sludge (35 – 75 %), Figure 56. The proportion volatilised increased with the paper sludge content of the blend. Possibly, this is due to the high chlorine content of the paper sludge (0.39 % daf), or to differences in the proportion of molybdenum released from each fuel. It was not possible to compare this behaviour

with a thermodynamic equilibrium modelling prediction, however, due to a lack of thermodynamic data for molybdenum species.

5.3.14 Thallium

Thallium was partially (10 – 55 %) volatilised from Colombian coal during combustion. Co - combustion with paper sludge increased this proportion to up to 90 % (Figure 56). Most of the thallium volatilised from the Colombian coal / paper sludge blends derived from the Colombian coal, as the coal has eleven times the thallium content of the paper sludge. Thus the fall in thallium retention when Colombian coal and paper sludge are blended suggests there was a synergy for thallium release between the fuels.

Thermodynamic equilibrium modelling does not suggest a cause for this synergy. All thallium was predicted to be volatilised as a mixture of TlCl and TlOH gases during combustion of either the Colombian coal or a 70 % Colombian coal / 30 % paper sludge blend. Possibly, chlorine in the paper sludge caused increased volatilisation of thallium from the Colombian coal. However, thallium was also enriched on sinter ash during combustion of Colombian coal (Figure 57). This suggests that an unidentified solid thallium compound formed during combustion of this fuel. Perhaps chlorine prevents this unidentified compound from forming, during combustion of Colombian coal / paper sludge blends Colombian coal derived thallium may form TlCl gas instead.



Trace Element Concentration in raw fuels (ppm):	Ba	Co	Sb	Sr
Colombian Coal	49 ± 8	1.6 ± 0.2	0.57 ± 0.10	22 ± 2
Paper Sludge	143 ± 17	0.89 ± 0.41	6.6 ± 1.3	16 ± 1.5

Figure 60 Partitioning of Ba, Co, Sb and Sr During Colombian Coal and Paper Sludge Co-Combustion

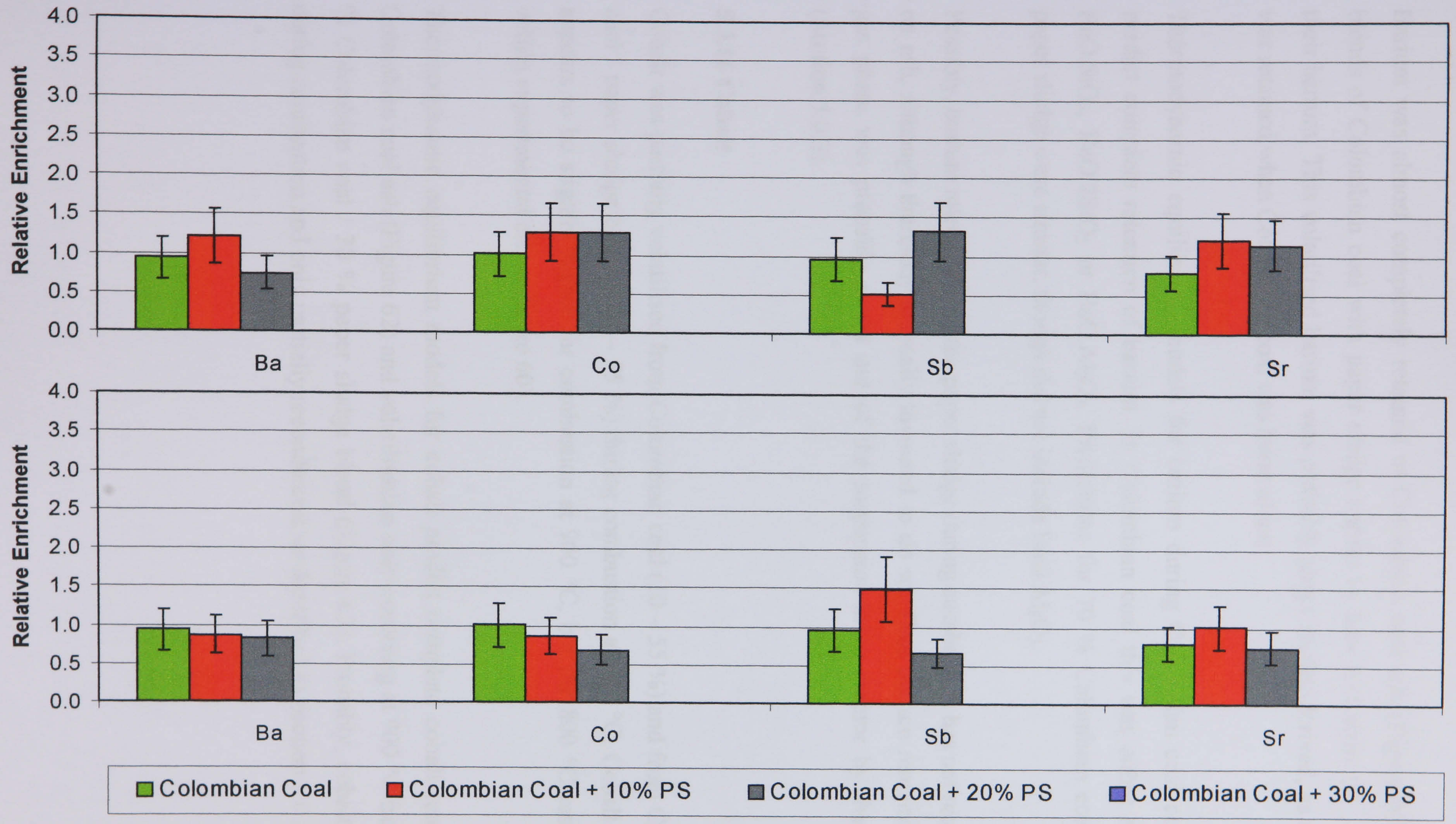


Figure 61 Relative Enrichments of Ba, Co, Sb, and Sr in Sinter Ash During Combustion of Colombian Coal and Paper Sludge

Note: A relative enrichment of one corresponds to that element being found in equal concentrations in the sinter and bottom ashes

5.3.15 Barium

Barium was almost completely retained in Colombian coal ash (Figure 60). Whilst, blends of Colombian coal with paper sludge appear to have lost some (5 – 60 %) of their barium. This volatilised barium was probably paper sludge derived, as almost all was retained when Colombian coal was burnt alone.

Thermodynamic equilibrium models for barium during Colombian coal combustion predict complete retention of barium. In Colombian coal this was either as $BaSO_4$, $BaO.SiO_2$, $BaO.2SiO_2$ or $BaO.Al_2O_3$. Predictions for 70 % Colombian coal / 30 % paper sludge were similar, though did not include $BaO.Al_2O_3$.

Possibly, barium released from the paper sludge during combustion has not recondensed on ash, although thermodynamically favoured to do so. Thus barium remaining in the gas phase was probably swept out of the suspension-firing reactor by the flue gas (Section 5.0.3).

5.3.16 Cobalt

Cobalt was partially volatilised from Colombian coal (10 – 55 %) and from Colombian coal / paper sludge blends (20 – 55 %) during combustion at 800 °C. Cobalt retention appears to be slightly higher for combustion at 900 °C, but the 800 °C results were within experimental error (Figure 60).

Thermodynamic equilibrium models for cobalt predict complete cobalt retention by Colombian coal ash (Figure 62) and volatilisation only occurring at 900 °C from the 70 % Colombian coal / 30 % paper sludge blend (Figure 63). Probably, cobalt released during combustion and only partially recondensed, as described in Section 5.0.3.

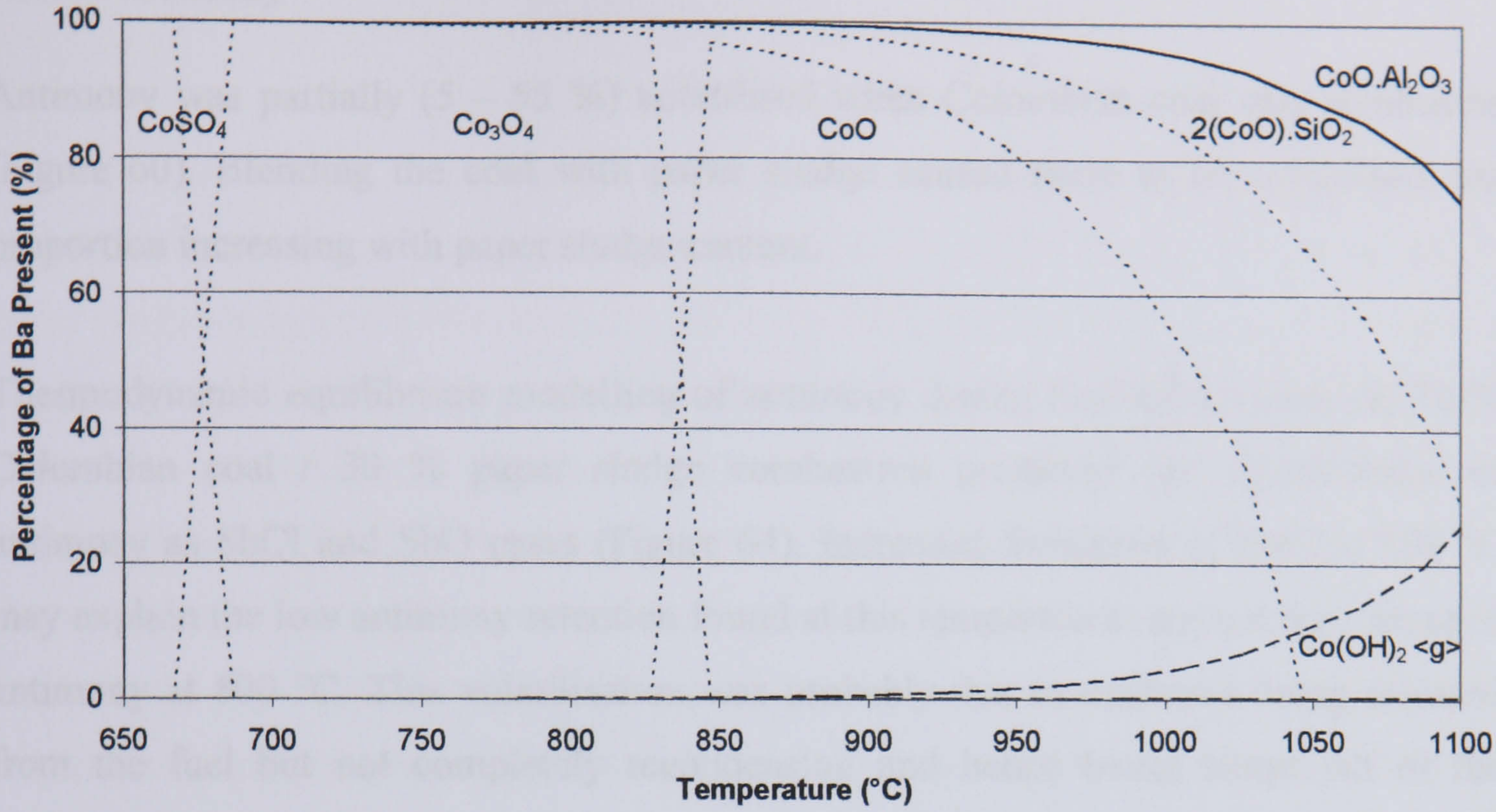


Figure 62 Thermodynamic Equilibrium Prediction for Cobalt During Colombian Coal Combustion

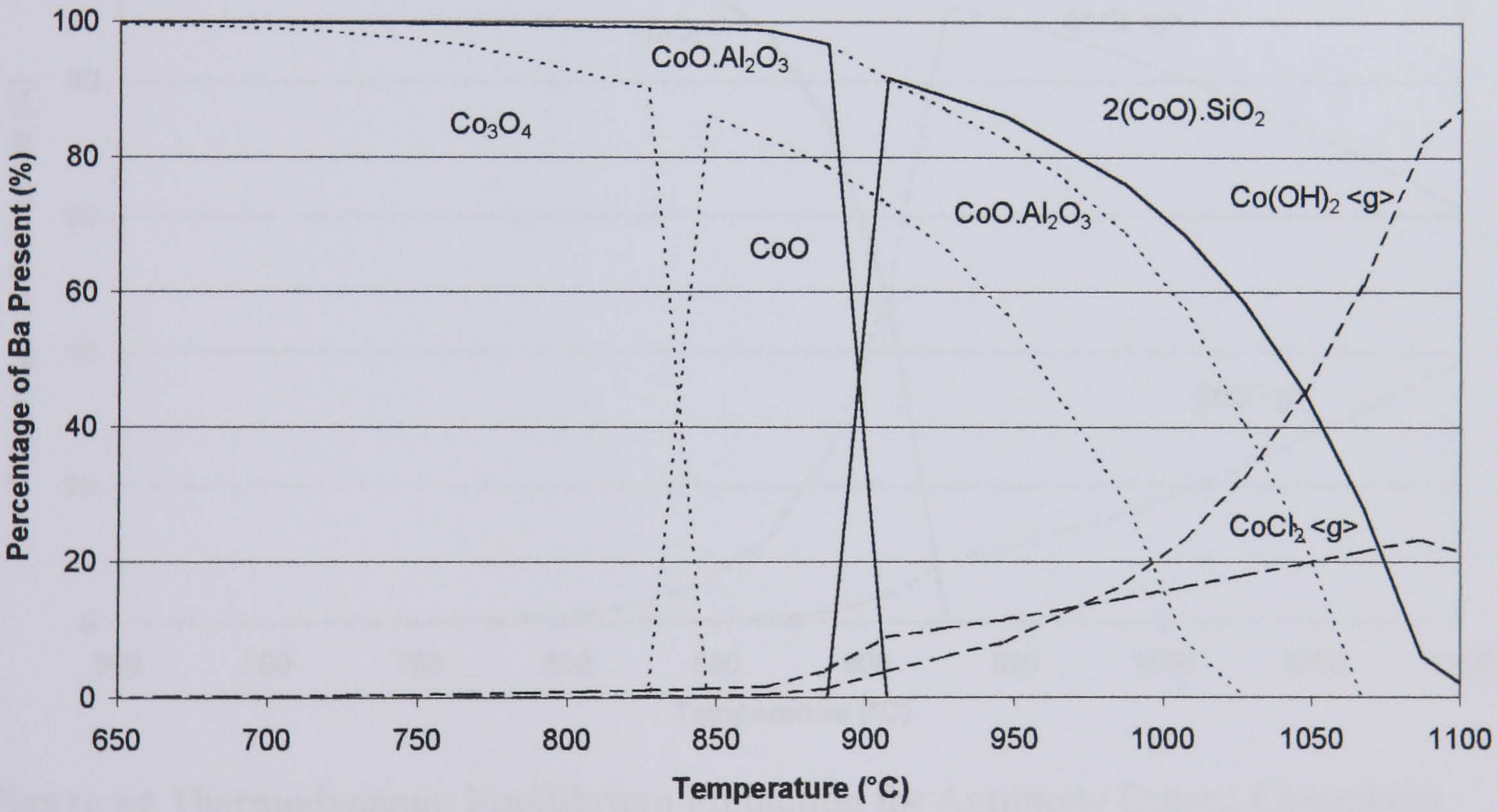


Figure 63 Thermodynamic Equilibrium Prediction for Cobalt During 70 % Colombian Coal / 30 % Paper Sludge Combustion

5.3.17 Antimony

Antimony was partially (5 – 55 %) volatilised when Colombian coal was combusted (Figure 60). Blending the coal with paper sludge caused more to be volatilised, the proportion increasing with paper sludge content.

Thermodynamic equilibrium modelling of antimony during Colombian coal and 70 % Colombian coal / 30 % paper sludge combustion predicted the volatilisation of antimony as SbCl and SbO gases (Figure 64). Increased formation of SbCl at 900 °C may explain the low antimony retention found at this temperature, but not the release of antimony at 800 °C. This volatilisation was probably due to antimony being released from the fuel but not completely recondensing and hence being swept out of the suspension-firing reactor in the flue gas (Section 5.0.3).

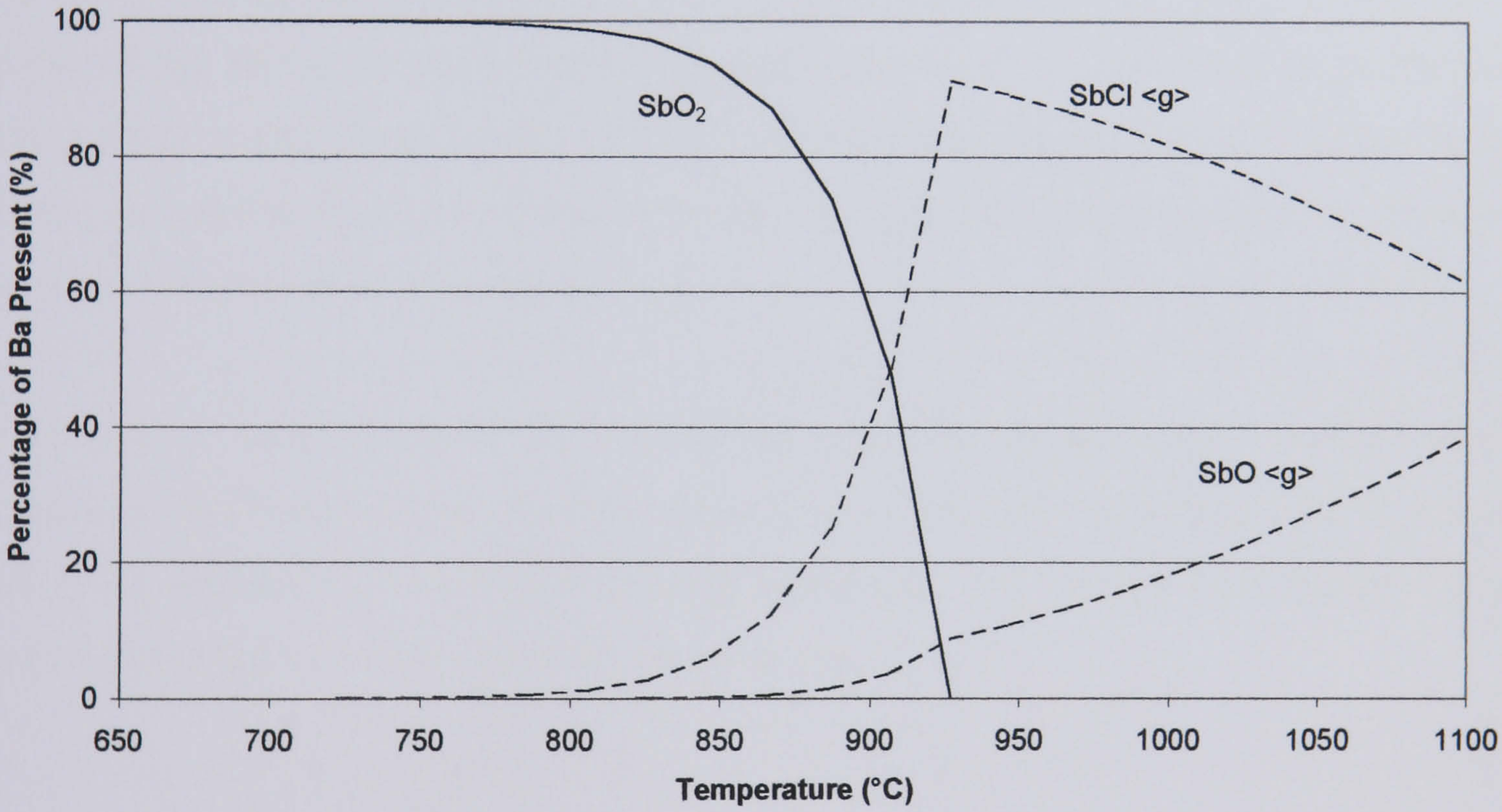


Figure 64 Thermodynamic Equilibrium Prediction for Antimony During Colombian Coal Combustion

5.3.18 Strontium

Strontium was partially volatilised from Colombian coal (20 – 55 %) at 800 °C. It was probably also partially volatilised at 900 °C, where the percentage retention appears higher, but within experimental error of the 800 °C results (Figure 60). Addition of paper sludge to Colombian coal increased the volatilisation of strontium, with up to 70 % released from the 70 % Colombian coal / 30 % paper sludge blend. Thermodynamic predictions for strontium suggest it should have been completely retained in ash, forming $SrSO_4$, $SrO.SiO_2$ or $SrO.2SiO_2$. Probably the strontium volatilised from the Colombian coal and paper sludge was released into the gas phase by transformation of its mode(s) of occurrence, especially organically bound strontium. Part of this volatised strontium has probably recondensed, the remainder being lost from the reactor with the flue gas (Section 5.0.3).

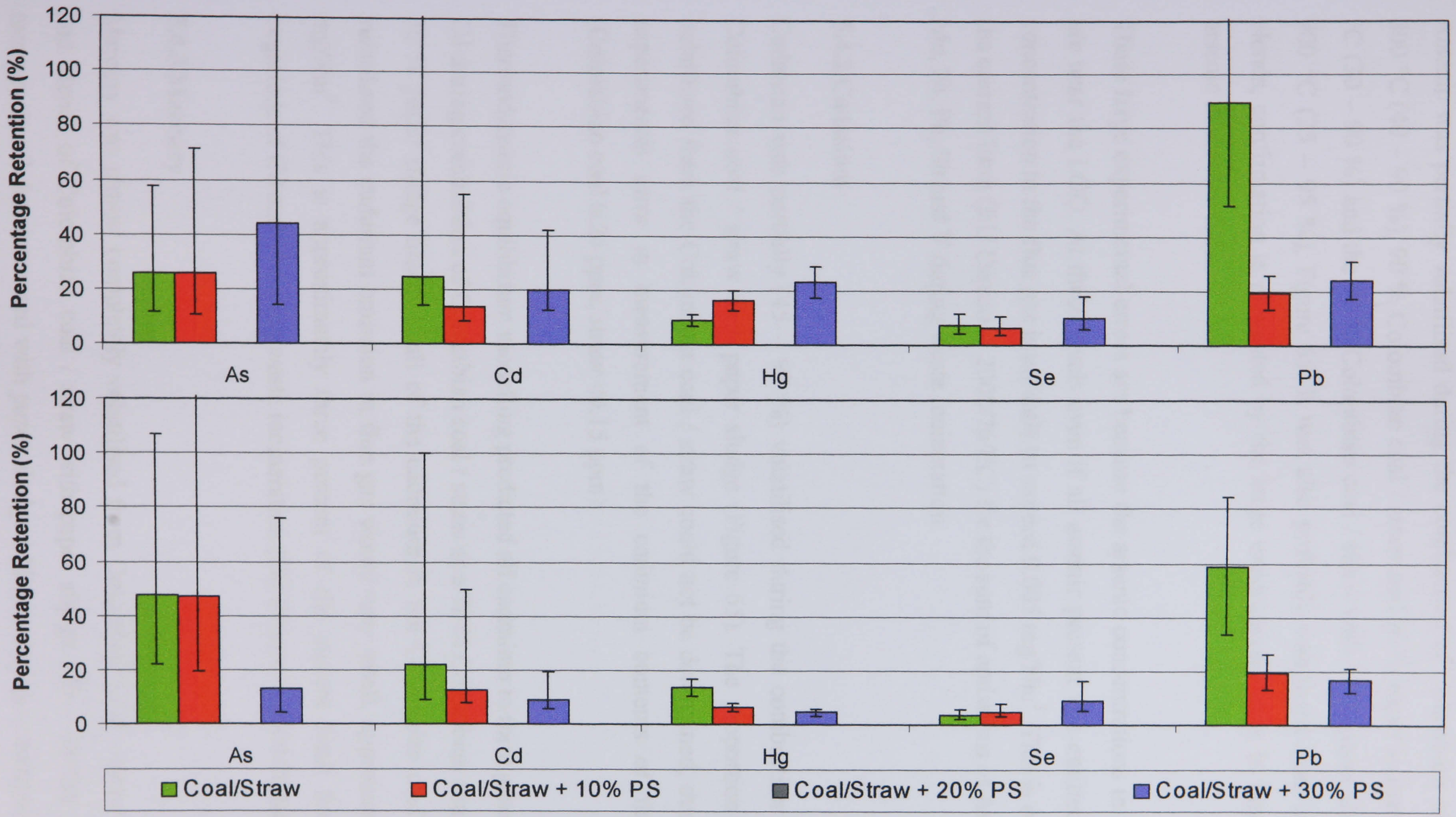
5.4 Colombian Coal, Straw and Paper Sludge Co combustion

Blends of bituminous coal and straw are already being burnt in the 79 MW_{th} bubbling fluidised bed combustor at Grenå, Denmark. Midtkaft, the power station owners would like to increase the spectrum of fuels burnt in this combustor by using paper sludge from a nearby paper mill. This section and the previous section (5.3) investigate the behaviour of trace elements during co-combustion of paper sludge with the fuel normally burnt at Grenå with paper sludge.

A 50:50 mixture (energy basis) of Colombian coal and Danish wheat straw has been chosen to represent the normal fuel burnt at Grenå. This mixed fuel was combusted alone and with 10 and 30 % paper sludge (energy basis).

As mentioned for Colombian coal – paper sludge blends, due to difficultly in feeding paper sludge to the suspension-firing reactor on its own, no runs could be performed using paper sludge alone as fuel. Without trace element results for paper sludge burnt alone, the possibility of determining whether a synergy exists between the fuels for trace element retention or release was limited.

Furthermore, combustion of the Colombian coal / straw and paper sludge blends produced insufficient sample for separate analysis of the sinter and bottom ash (a mixed ash being analysed). As a result there is no information available for these blends on the relative enrichment of trace elements in sinter ash.



Trace Element Concentration in raw fuels (ppm):		As			Cd			Hg			Se			Pb	
Colombian Coal	1.72	±	1.15	0.26	±	0.25	0.031	±	0.001	4.3	±	1.0	1.9	±	0.5
Straw			<0.1			<0.15	0.009	±	0.002			<0.2	2.6	±	1.1
Paper Sludge	0.63	±	1.33	0.77	±	0.19	0.08	±	0.02			<0.8	21.1	±	3.2

Figure 65 Percentage Retention of As, Cd, Hg, Se and Pb in Ash After Colombian Coal / Straw and Paper Sludge Co -Combustion

5.4.1 Arsenic

Arsenic was partially volatilised during the combustion of Colombian coal / straw at 800 °C (40 – 90 %), 90 % Colombian coal / straw and 10 % paper sludge blend at 800 °C (30 – 90 %) and the 70 % Colombian coal / straw with 30 % paper sludge blend at 900 °C (25 – 95 %), Figure 65. It was also probably volatilised from the other fuel blends, confirmation is prevented by the large experimental error in measurement of arsenic in the raw fuels.

These large experimental errors are because the arsenic concentrations in the raw fuels are near the LOQ. At these levels even if all arsenic present was emitted, the arsenic concentration in the flue gas is unlikely to exceed 0.005 mg/Nm^3. This is one percent of the current limit (EU Directive 2000/76/EC) for the sum of emissions of As, Co, Cr, Cu, Mn, Ni, Pb, Sb and V during waste incineration.

5.4.2 Cadmium

Cadmium was partially (45 – 95 %) volatilised during the combustion of blends of Colombian coal / straw with paper sludge (Figure 65). The proportion of cadmium volatilised from the Colombian coal / straw could not be determined, due to the large experimental error in measurement of the cadmium contents of the raw fuels (Colombian coal 0.26 ppm, straw <0.15 ppm).

Thermodynamic equilibrium modelling predicted all cadmium to form gaseous $CdCl_2$ or Cd during combustion of Colombian coal / straw or a 70 % Colombian coal / straw with 30 % paper sludge blend. If all of the cadmium in the Colombian coal / straw was volatilised the cadmium emission in flue gas would very small, approximately 0.0015 mg/Nm^3. This is approximately three percent of the current limit for the sun of emissions of Cd and Tl during waste incineration (EU Directive 2000/76/EC).

5.4.3 Mercury

Mercury was almost completely volatilised from Colombian coal / straw (85 - 95 %) and blends of Colombian coal / straw with paper sludge (70 – 98 %). Retention of mercury in ash has increased with paper sludge addition during combustion at 800 °C,

but declined with its addition at 900 °C.

The cause of these trends is not clear, as thermodynamic equilibrium modelling predicted all mercury to be present in the gas phase, either as Hg (> 98 %) or HgO (< 2 %) gases. The small amount of mercury remaining in the ash was possibly not released from its modes of occurrence in the fuels or formed an unknown solid mercury compound, as suggested in section 5.2.3.

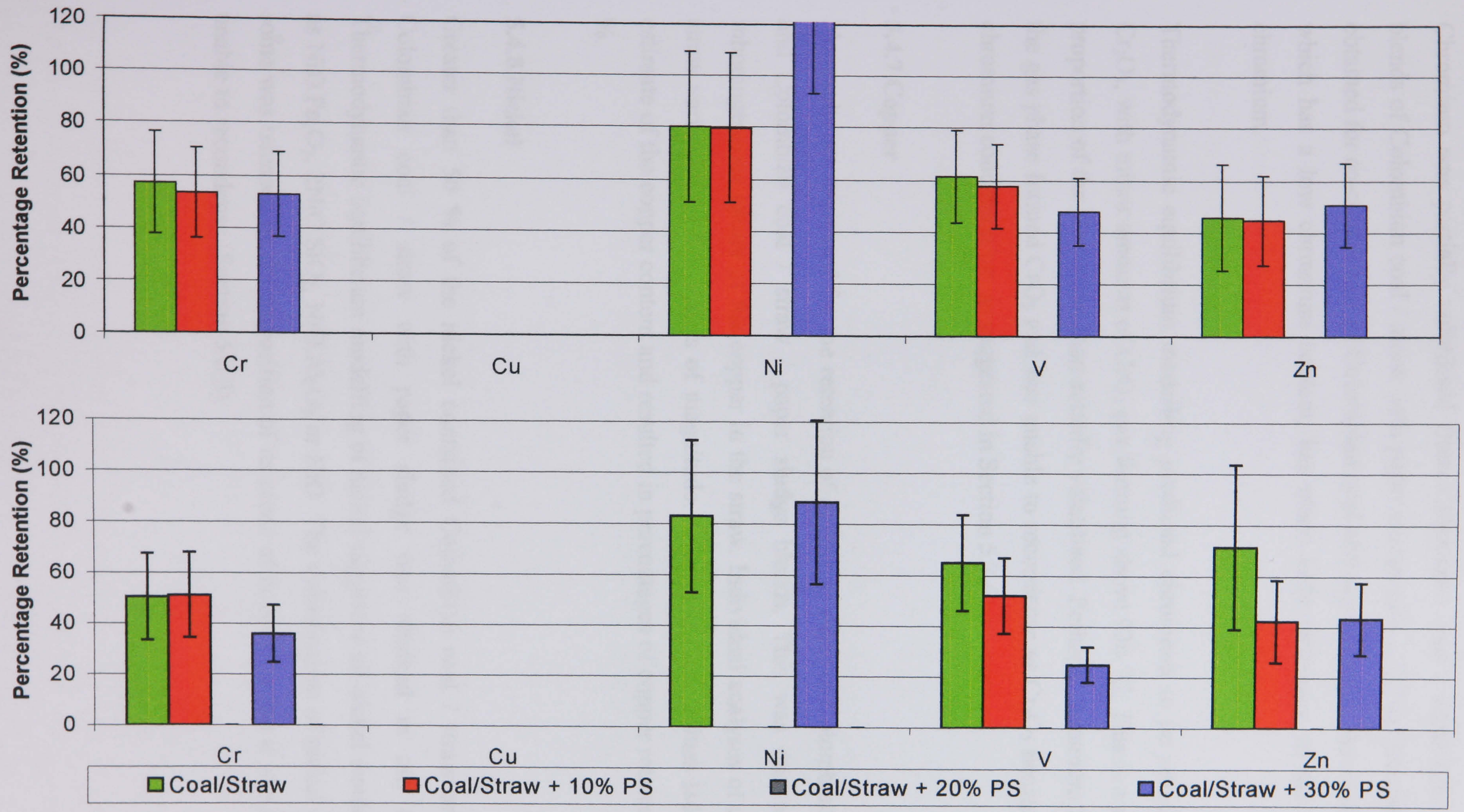
5.3.4 Selenium

Selenium was almost completely (80 – 98 %) volatilised during the combustion of Colombian coal / straw and blends of this fuel with paper sludge (Figure 65). This was predicted by thermodynamic equilibrium predictions for selenium, which were for it to completely volatilise as SeO_2 (> 98 %) and SeO (< 2 %) gases in the suspension reactor.

5.4.5 Lead

Lead was partially (15 - 65 %) volatilised by Colombian coal / straw combustion at 900 °C. Blending the Colombian coal / straw with paper sludge increased the proportion lost, with only 10 – 30 % remaining in ash. Thermodynamic equilibrium modelling predicted all lead to be lost in the gas phase during Colombian coal / straw and 70 % Colombian coal / straw with 30 % paper sludge combustion.

Most of the lead in the Colombian coal / straw / paper sludge blends was derived from the paper sludge. This lead appears to have volatilised as predicted. Possibly lead in the other fuels is contained in modes of occurrence that did not allow it to be released into the gas phase during combustion (Section 5.0.2).



Trace Element Concentration in raw fuels (ppm):	Cr	Cu	Ni	V	Zn
Colombian Coal	11.1 ± 2.3	5.8 ± 1.0	6.5 ± 0.8	12 ± 2	18 ± 7
Straw	2.5 ± 1.1	3.2 ± 1.6	0.9 ± 1.0	0.8 ± 0.4	31 ± 13
Paper Sludge	11 ± 2	16 ± 2	2.9 ± 0.9	2.3 ± 0.2	132 ± 26

Figure 66 Percentage Retention of Cr, Cu Ni, V and Zn in Ash After Colombian Coal / Straw and Paper Sludge Co-Combustion

5.4.6 Chromium

Chromium was partially volatilised from Colombian coal / straw (25 – 65 %) and blends of Colombian coal / straw with paper sludge (30 – 75 %). Similar results were obtained for co-combustion of Colombian coal and paper sludge. The addition of straw, which has a low chromium content, has made little difference to the behaviour of chromium.

Thermodynamic equilibrium modelling predicted chromium to be retained in ash as Cr_2O_3, with minor amounts of CrO_3 gas forming above 930 °C. This is a much smaller proportion of the chromium than actually volatilised. Perhaps, chromium liberated into the gas phase formed CrO_3 and was unable to recondense as Cr_2O_3 because of the low chromium concentration, as suggested in Section 5.2.6.

5.4.7 Copper

No results are presented for the retention of copper in ashes of Colombian coal / straw and Colombian coal / straw / paper sludge blends. This was due to the highly inhomogeneous nature of the copper in the straw. Individual analyses of copper in the straw varied over three orders of magnitude. Averaging these values led to an under estimate of the copper content and resulted in percentages of copper retained above 100 %.

5.4.8 Nickel

Greater than 50 % of the nickel contained Colombian coal / straw and blends of Colombian coal / straw with paper sludge was retained in ash (Figure 66). Thermodynamic equilibrium modelling of nickel suggested all nickel would be retained as $NiO.Fe_2O_3$, $2NiO.SiO_2$, $NiO.Al_2O_3$ or NiO. The volatilisation of nickel suggests that some was released by decomposition of its mode of occurrence but it was subsequently unable to recondense (Section 5.0.3).

5.4.9 Vanadium

Vanadium was partially volatilised from Colombian coal / straw (20 – 45 %) and from blends of Colombian coal / straw with paper sludge (25 – 80 %). During combustion at 900 °C retention of vanadium fell as the paper sludge content of the fuel blend was increased (Figure 66). The same trend may be present in results for combustion at 800 °C, but at this temperature any fall in vanadium retention was smaller than the range of experimental error.

The fall in vanadium retention with paper sludge addition was not explained by thermodynamic equilibrium modelling. Mixed oxides $FeO.V_2O_5$, $CaO.V_2O_5$, $2CaO.V_2O_5$ and $2MgO.V_2O_5$ as well as V_2O_5 and VO_2 were predicted to form and retain all vanadium in ash after combustion of Colombian coal / straw and of 70 % Colombian coal / straw with 30 % paper sludge.

Vanadium retention when paper sludge was added to Colombian coal also fell without straw (section 5.3.9). This was attributed to vanadium in the paper sludge incompletely recondensing on ash after being mostly released from its modes of occurrence (Section 5.0.3). For the Colombian coal / straw / paper blends percentage retention of vanadium appeared lower than for Colombian coal / paper sludge blends, suggesting that vanadium in the straw was also volatilised, like that in the paper sludge.

5.4.10 Zinc

Zinc was partially volatilised from Colombian coal / straw combusted at 800 °C (35 – 75 %) and probably also at 900 ° C (up to 60 %). Blending Colombian coal / straw with paper sludge made little change to the proportion of zinc volatilised, with between 40 and 75 % lost (Figure 66). Most zinc in the Colombian coal / straw / paper sludge blends was derived from the paper sludge. When this fuel was co-combusted with Colombian coal, but without straw the percentage retention of zinc in ash appeared to be higher (Section 5.3.10).

Perhaps, increased volatility of zinc results from the increased chlorine content of the fuel due to the straw (Cl content: 0.26 % daf). Zinc was predicted by thermodynamic equilibrium modelling to form $ZnCl_2$ gas during combustion of Colombian coal / straw

(Figure 67) and of 70 % Colombian coal / straw with 30 % paper sludge (Figure 68). Only minor amounts were predicted during Colombian coal combustion (section 5.3.10). Thus, it seems that while Colombian coal and paper sludge blends retained most of their zinc, the additional chlorine from the straw caused the volatilisation of zinc in Colombian coal / straw / paper sludge blends.

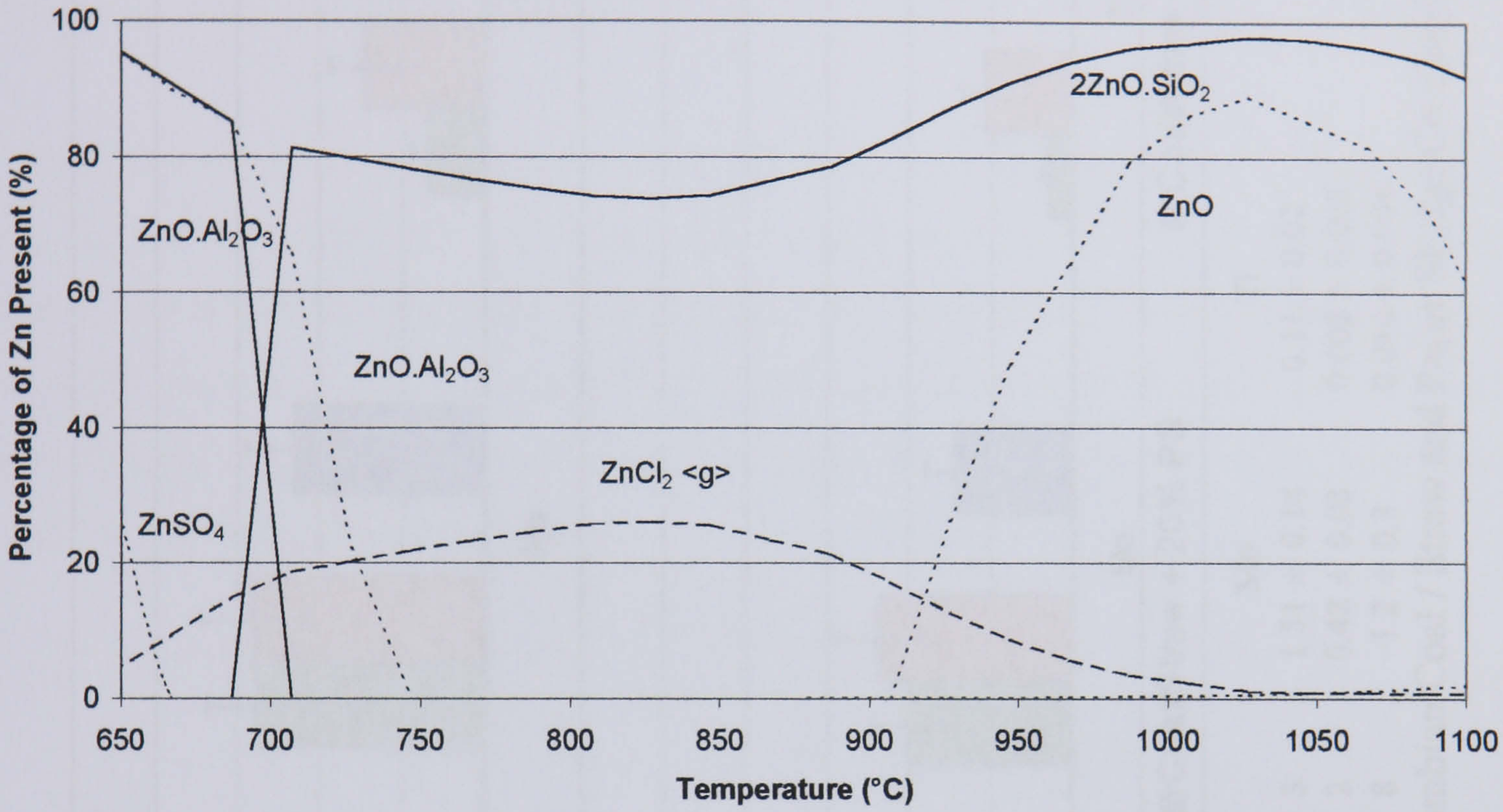


Figure 67 Thermodynamic Equilibrium Prediction for Zinc During Colombian Coal / Straw Combustion

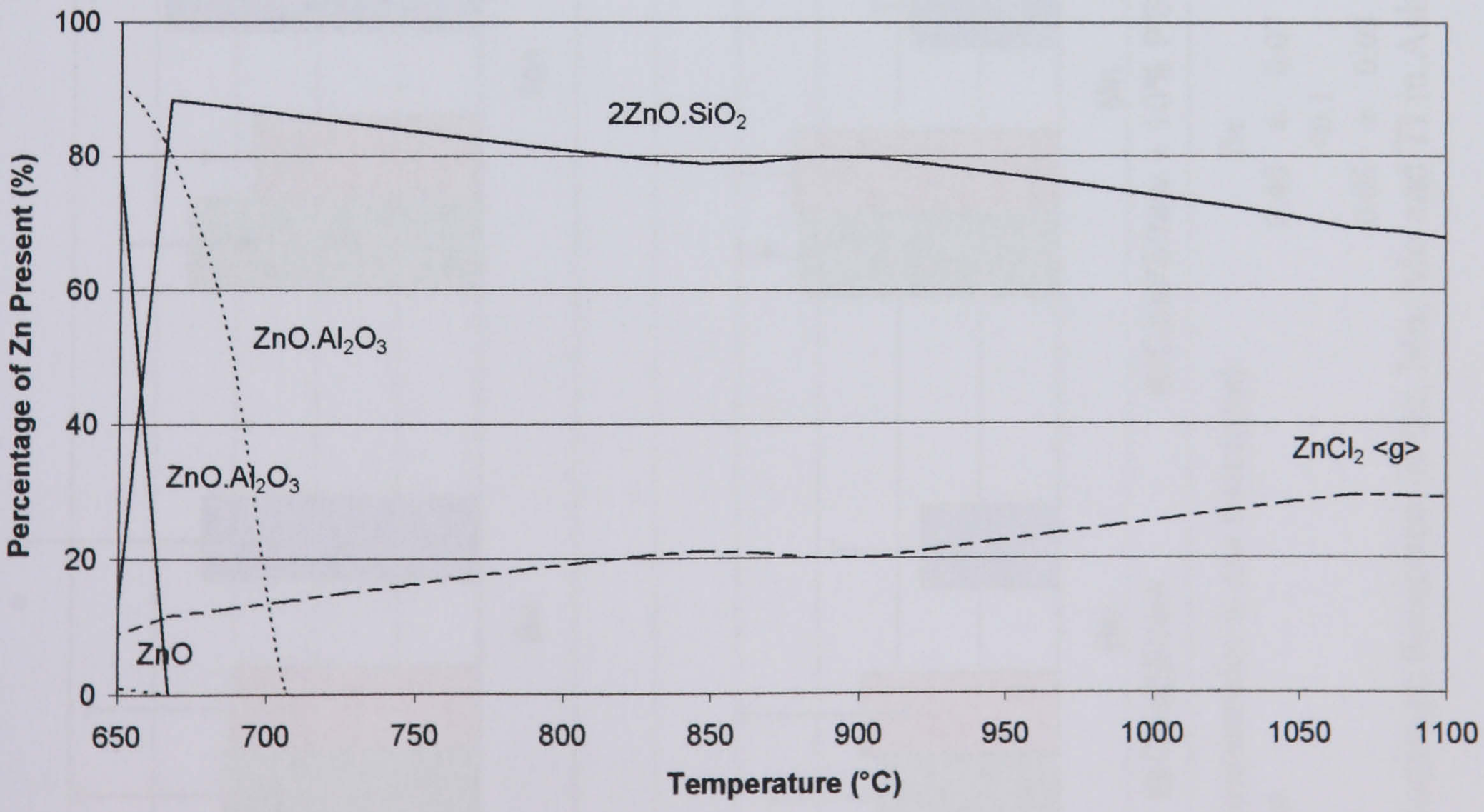
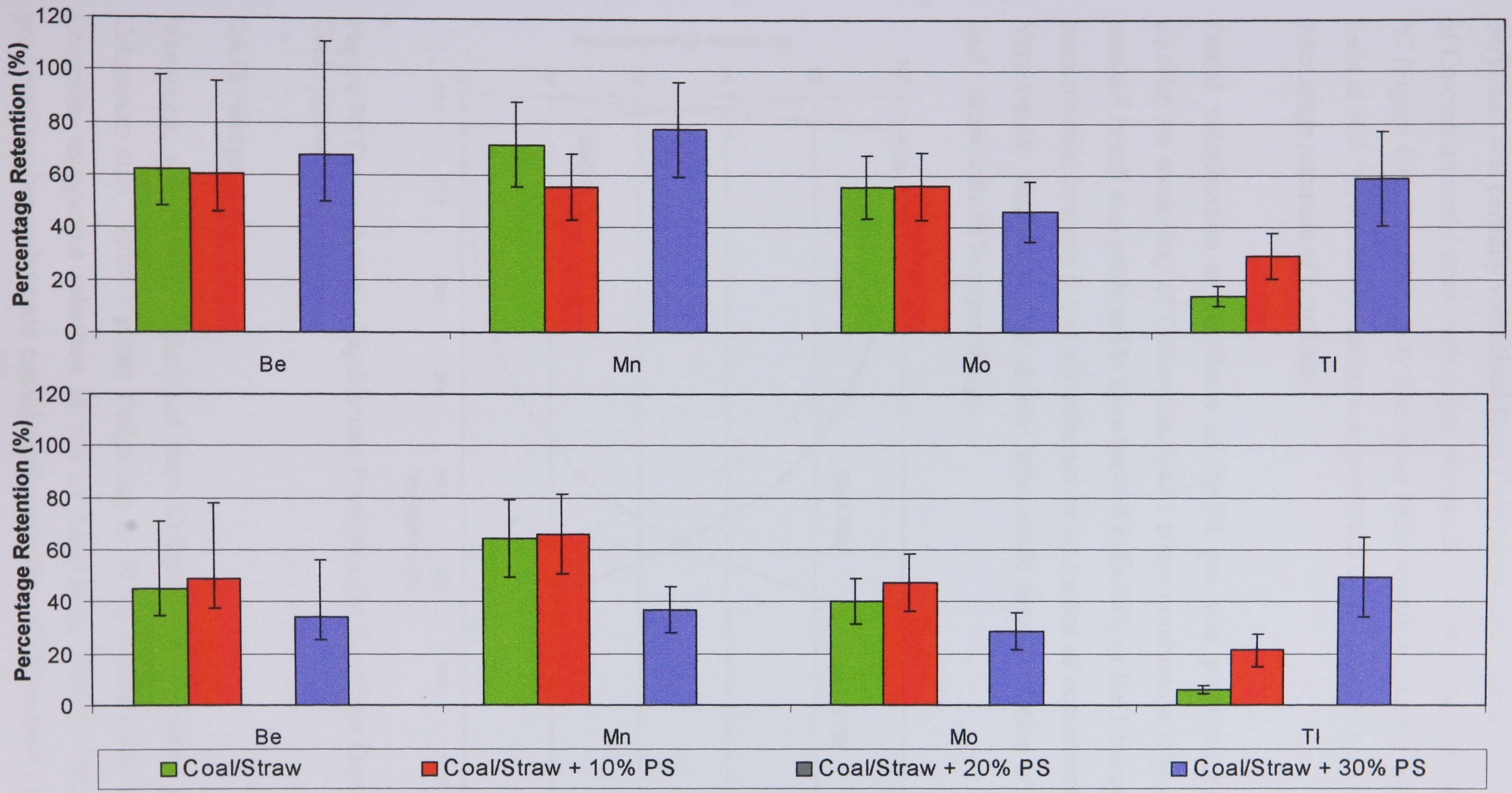


Figure 68 Thermodynamic Equilibrium Prediction for Zinc During Combustion of 70 % Colombian Coal / Straw with 30 % Paper Sludge



Trace Element Concentration in raw fuels (ppm):	Be	Mn	Mo	Tl
Colombian Coal	0.40 ± 0.07	27 ± 3	1.51 ± 0.14	0.11 ± 0.02
Straw	<0.1	20 ± 2	0.42 ± 0.03	0.002 ± 0.005
Paper Sludge	0.05 ± 0.03	62 ± 8	1.2 ± 0.3	0.010 ± 0.004

Figure 69 Percentage Retention of Be, Mn, Mo and Tl in Ash After Colombian Coal / Straw and Paper Sludge Co-Combustion

5.4.11 Beryllium

Beryllium was partially volatilised from Colombian coal / straw (30 – 65 %) and blends of Colombian coal / straw with paper sludge (20 – 75 %) when either was burnt at 900 °C (Figure 69). Beryllium may also have been volatilised during combustion of these fuels at 800 °C, but confirmation was prevented by the large experimental error on the percentage retention of beryllium.

Partial volatilisation of beryllium as BeOH gas was predicted by thermodynamic equilibrium modelling of Colombian coal / straw combustion (Figure 70). Beryllium retained in ash was predicted to have formed $BeO.SiO_2$ or BeO, though some may have been retained because it was not released by its modes of occurrence in the raw fuels. Very similar predictions (not shown) were made for combustion of 70 % Colombian coal / straw with 30 % paper sludge.

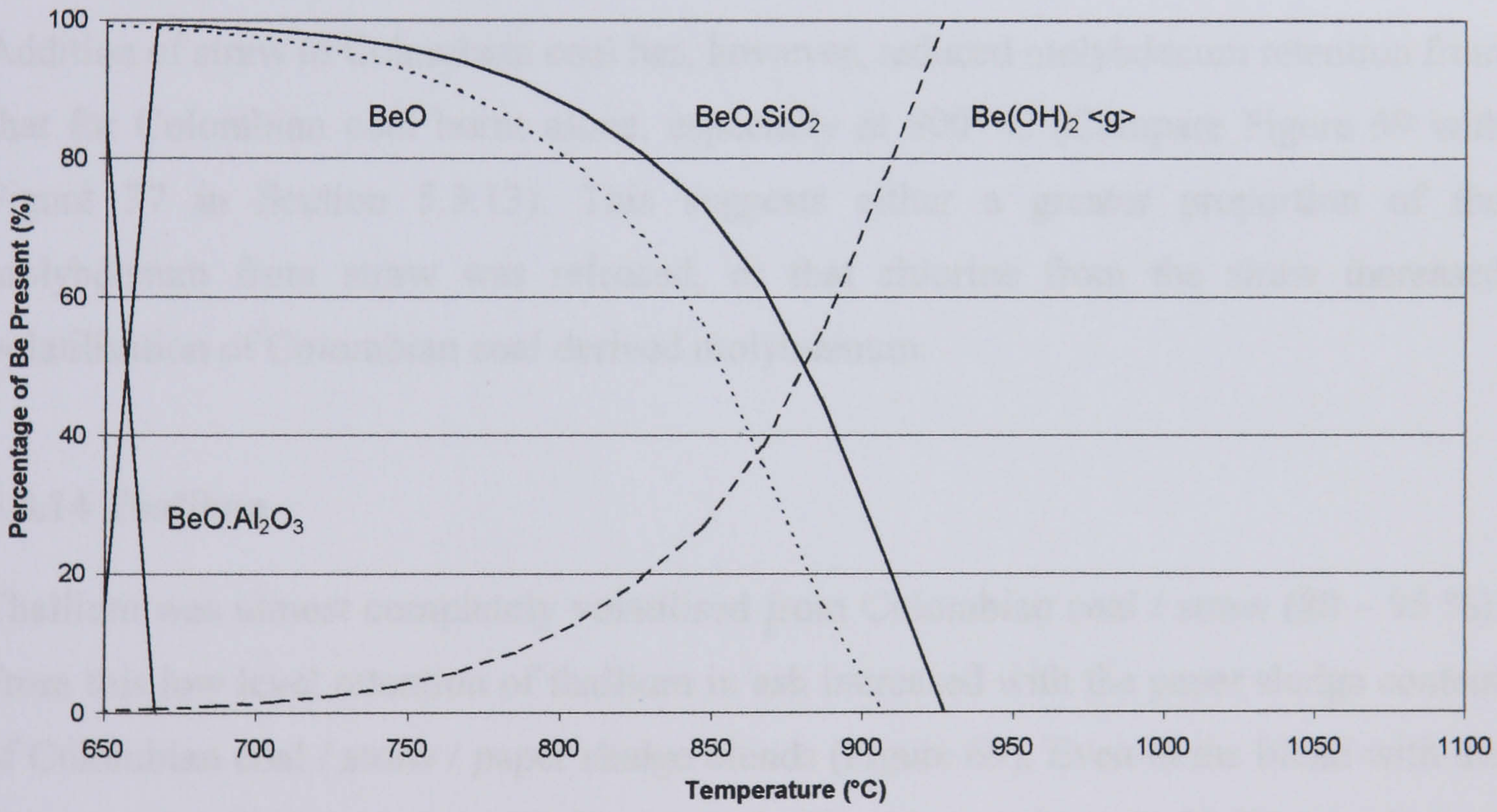


Figure 70 Thermodynamic Equilibrium Prediction for Beryllium During Colombian Coal / Straw Combustion

5.4.12 Manganese

Manganese was partially volatilised from Colombian coal / straw (10 – 50 %) and Colombian coal / straw / paper sludge (up to 70 %) during combustion (Figure 69). Complete manganese retention in ash as $MnO.SiO_2$, Mn_2O_3, Mn_3O_4 or MnO was predicted by thermodynamic equilibrium modelling of Colombian coal / straw and of

the 70 % Colombian coal / straw with 30 % paper sludge blend.

The volatilisation of manganese from Colombian coal / straw / paper sludge blends may be explained by a large proportion of the manganese in the fuels being released into the gas phase during combustion. This manganese is likely to have formed the predicted compounds (especially MnO), but, may not have had sufficient time to recondense on ash (Section 5.0.3).

5.4.13 Molybdenum

Molybdenum was partially (35 – 70 %) volatilised from Colombian coal / straw during combustion (Figure 69). Blending paper sludge with the Colombian coal / straw did not appear to change the proportion of molybdenum retained in ash, with between 30 and 80 % of that in the fuel blends released.

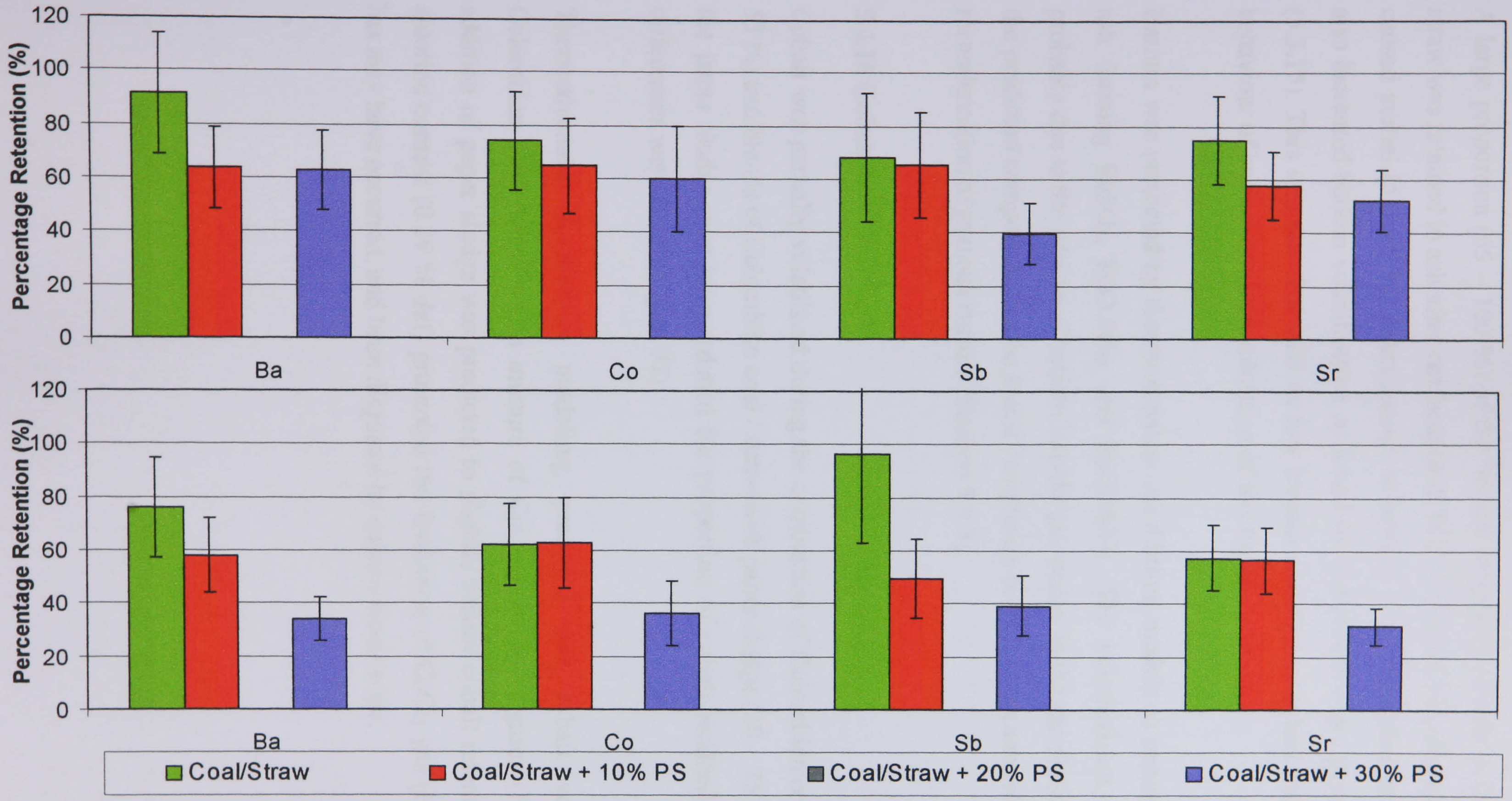
Addition of straw to Colombian coal has, however, reduced molybdenum retention from that for Colombian coal burnt alone, especially at 900 °C (Compare Figure 69 with Figure 37 in Section 5.3.13). This suggests either a greater proportion of the molybdenum from straw was released, or that chlorine from the straw increased volatilisation of Colombian coal derived molybdenum.

5.4.14 Thallium

Thallium was almost completely volatilised from Colombian coal / straw (80 – 95 %). From this low level retention of thallium in ash increased with the paper sludge content of Colombian coal / straw / paper sludge blends (Figure 69). Even in the blend with the highest paper sludge content (30 %), most thallium (approximately 70 %) was derived from Colombian coal. This Colombian coal derived thallium volatilised when Colombian coal was burnt with straw. However, not all of it has when the 70 % Colombian coal / straw with 30 % paper sludge blend was combusted. The high retention of thallium in Colombian coal / straw / paper sludge blends seems to be an effect of adding straw. When Colombian coal and paper sludge were burnt without straw, thallium retention fell with paper sludge addition (Section 5.3.14).

Thermodynamic equilibrium modelling of the combustion of Colombian coal / straw

and of 70 % Colombian coal / straw with 30 % paper sludge did not predict formation of any solid thallium compound. All thallium was predicted to be gaseous, mostly as TlCl, with a minor amount of TlOH gas. It seems an unknown thallium compound has formed when the Colombian coal, straw and paper sludge were combusted together, as there was when thallium was enriched on sinter ash of Colombian coal (Section 5.3.14).



Trace Element Concentration in raw fuels (ppm):	Ba	Co	Sb	Sr
Colombian Coal	49 ± 8	1.6 ± 0.2	0.57 ± 0.10	22 ± 2
Straw	13 ± 2	0.08 ± 0.05	0.08 ± 0.06	12 ± 1
Paper Sludge	143 ± 17	0.89 ± 0.41	6.6 ± 1.3	17 ± 1

Figure 71 Percentage Retention of Ba, Co, Sb and Sr in Ash After Colombian Coal / Straw and Paper Sludge Co-Combustion

5.4.15 Barium

A large proportion (65 – 100 %) of the barium originally present in Colombian coal / straw was retained in ash after combustion at 800 °C (Figure 71). Combustion at 900 °C caused partial (5 – 45 %) volatilisation of barium. Co-combustion with paper sludge also increased barium volatilisation, as found for Colombian coal / paper sludge blends (5.3.15). This suggests that with its low barium content, straw had little influence the behaviour of barium during combustion of this blend.

Barium was predicted by thermodynamic equilibrium models to remain completely in ash forming $BaSO_4$, $BaO.SiO_2$ and $BaO.2SiO_2$. The volatilisation of barium was probably due to the release of barium into the gas phase. In the gas phase it may be form the predicted compounds, but be found completely in the ash because of the incomplete recondensation of gaseous barium (Section 5.0.3).

5.4.16 Cobalt

Cobalt was partially volatilised during the combustion of Colombian coal / straw (10 – 55 %) and blends of Colombian coal / straw with paper sludge (20 – 75 %). Addition of the paper sludge may have reduced the proportion of cobalt retained in ash, though differences were small (Figure 71).

Thermodynamic equilibrium modelling predicted that cobalt volatilised from Colombian coal /straw was a mixture of $CoCl_2$ and CoOH gases (Figure 72). The addition of paper sludge was predicted to slightly reduce cobalt retention, as its high chlorine content (0.39 % daf) promoted the formation of $CoCl_2$ gas (Figure 73). This has may have occurred, and been disguised by experimental error.

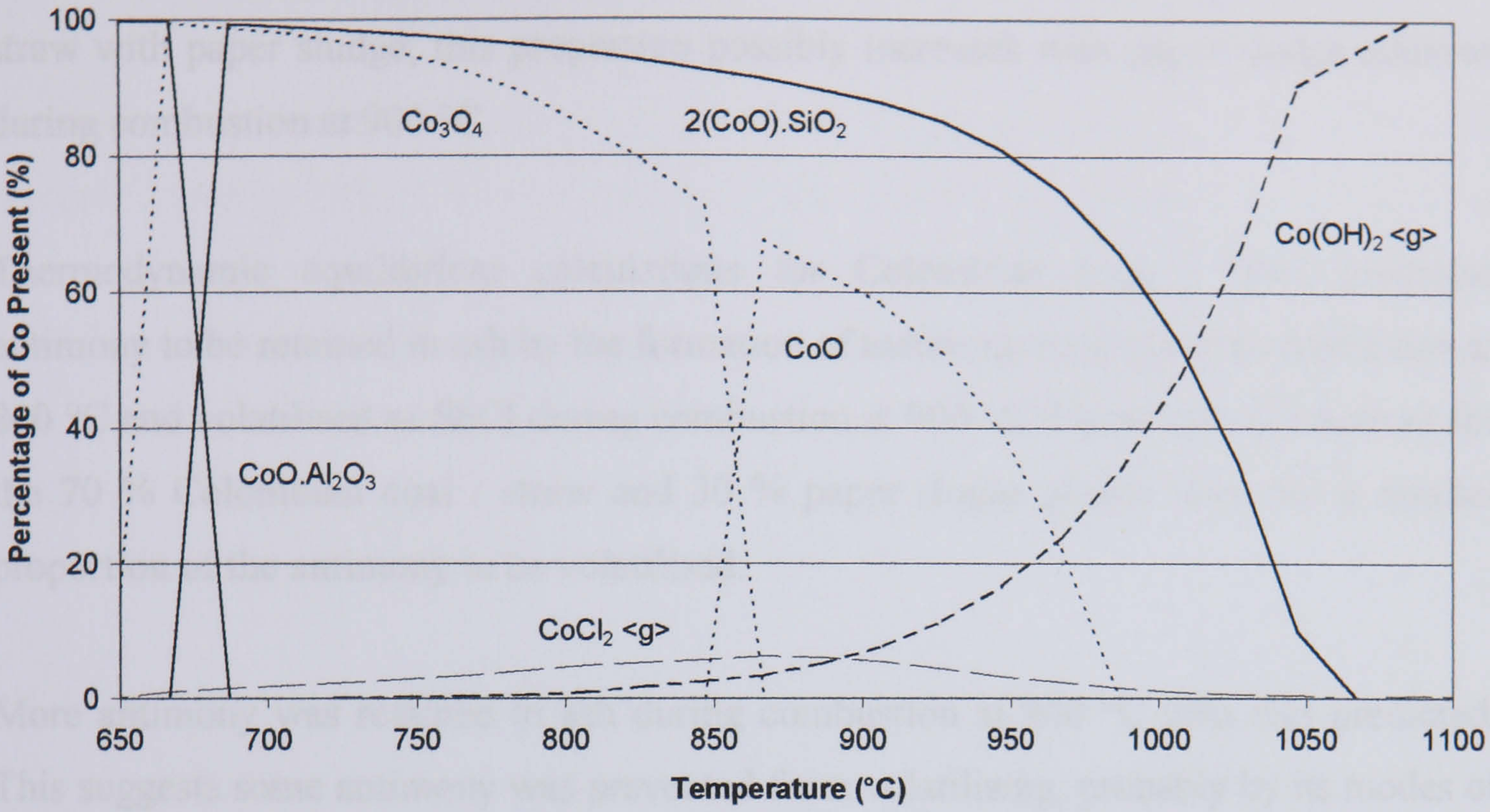


Figure 72 Thermodynamic Equilibrium Prediction for Cobalt During Colombian Coal / Straw Combustion

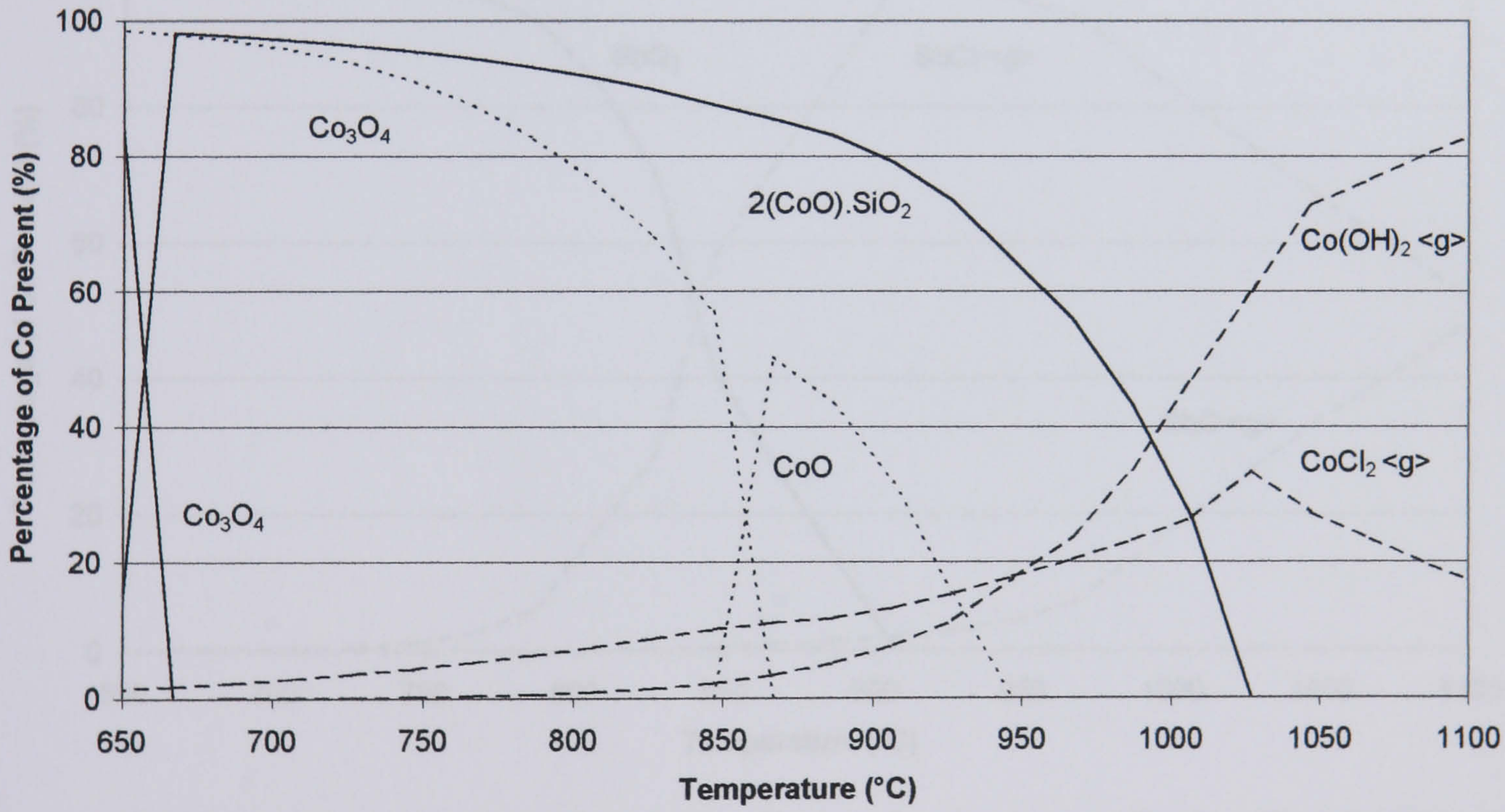


Figure 73 Thermodynamic Equilibrium Prediction for Cobalt During 70 % Colombian Coal / Straw with 30 % Paper Sludge Combustion

5.4.17 Antimony

Antimony was partially volatilised (10 – 30 %) from Colombian coal / straw during combustion at 800 °C. A higher proportion of antimony seems to have been retained after combustion at 900 °C, though the difference is within experimental error.

Antimony was also partially (15 – 70 %) volatilised from blends of Colombian coal / straw with paper sludge, this proportion possibly increases with paper sludge addition during combustion at 900 °C.

Thermodynamic equilibrium calculations for Colombian coal / straw predicted antimony to be retained in ash by the formation of antimony oxide during combustion at 800 °C and volatilised as SbCl during combustion at 900 °C (Figure 74). Predictions for the 70 % Colombian coal / straw and 30 % paper sludge blends were for a smaller proportion of the antimony to be volatilised.

More antimony was retained in ash during combustion at 900 °C than was predicted. This suggests some antimony was prevented from volatilising, probably by its modes of occurrence in the fuels (Section 5.0.2).

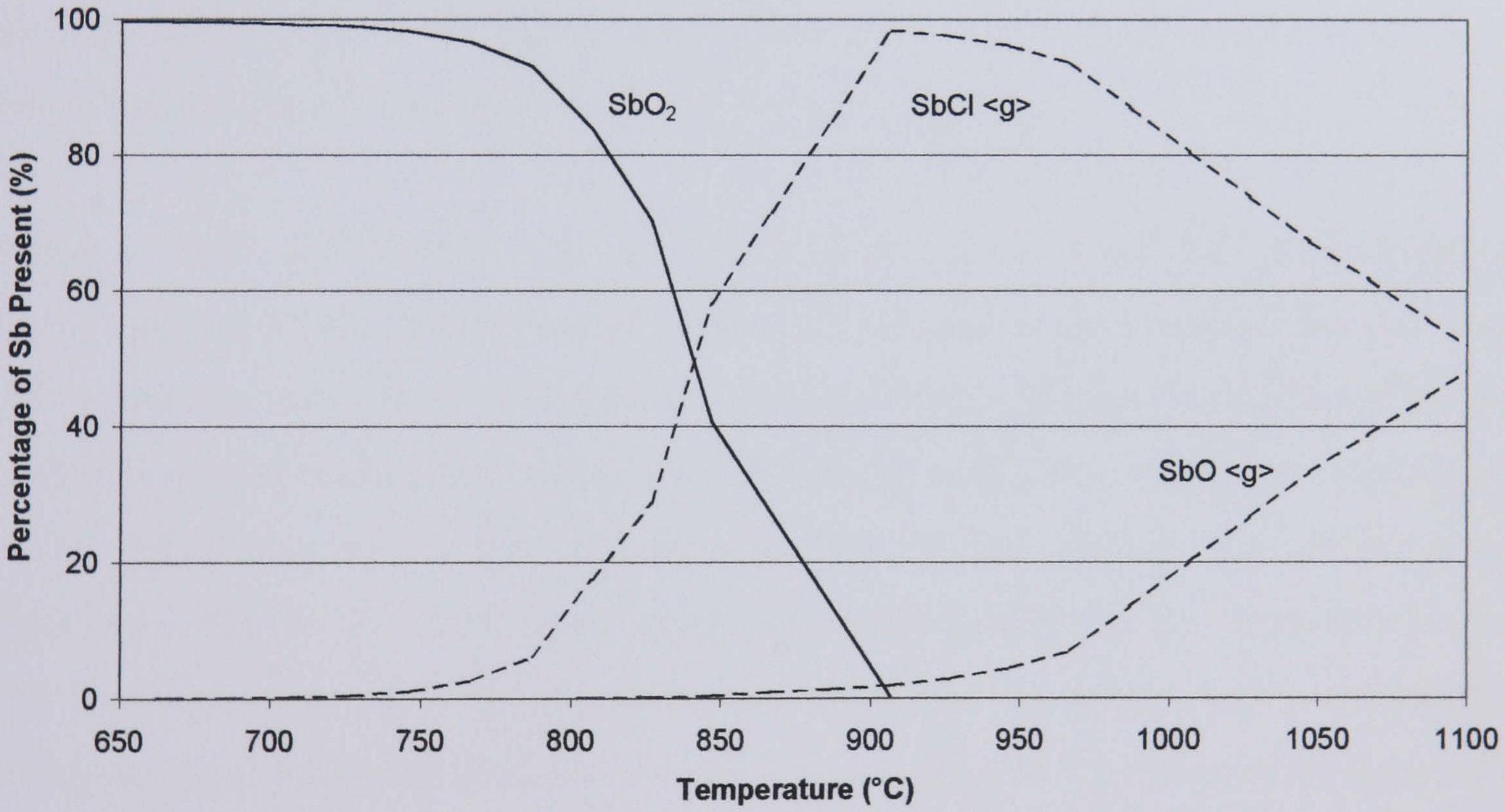


Figure 74 Thermodynamic Equilibrium Prediction for Antimony During Combustion of Colombian Coal / Straw

5.4.18 Strontium

Strontium was partially volatilised from Colombian coal / straw (10 – 55 %) and blends of Colombian coal / straw with paper sludge (30 – 75 %), Figure 71. The proportion volatilised appears to have increased with paper sludge addition, which was also found when Colombian coal and paper sludge were co-combusted without straw (section

5.3.18).

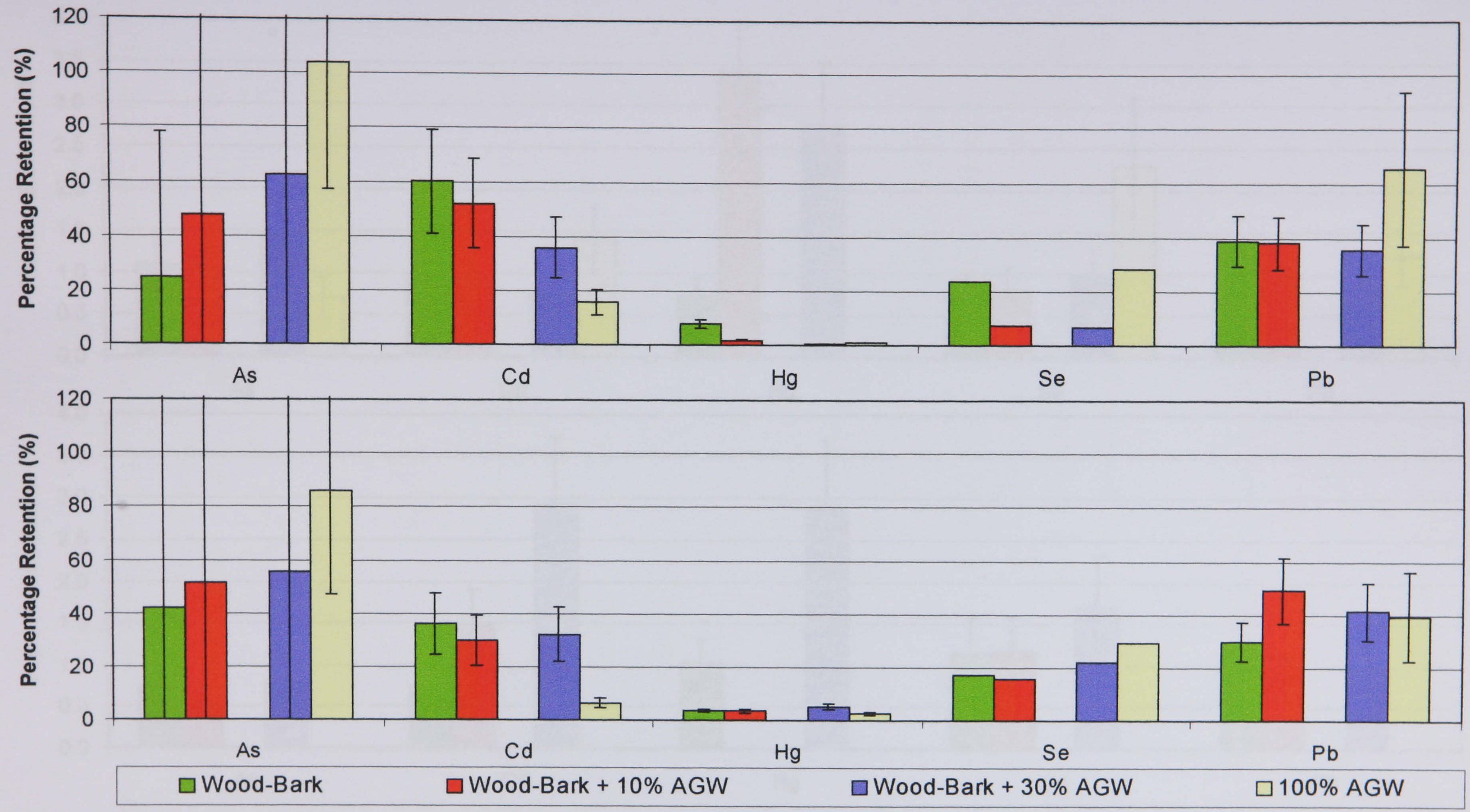
Strontium was predicted by thermodynamic equilibrium calculations to be completely retained in ash as $SrSO_4$, $SrO.SiO_2$ or $SrO.2SiO_2$. Perhaps strontium was released into the gas phase by transformation of its mode(s) of occurrence, especially organically bound strontium. Part of this volatised strontium probably recondensed, as predicted, but the remainder lost from the suspension-firing reactor with the flue gas (section 5.0.3).

5.5 Wood-Bark and Agricultural Waste Co-Combustion

Combustion is a potential method for the disposal of agricultural waste, greatly reducing the volume of waste and simultaneously recovering a considerable amount of energy, in this case, 15.7 MJ/kg. Agricultural waste combusted in this study was a mixture of wood chips and chicken manure from a henhouse in Finland. This type of fuel has been classified as waste by the EU, so emissions from its combustion are regulated by the waste incineration directive (2000/76/EC) thereby putting significant emission monitoring requirements on the incinerator operator.

Agricultural waste is a demanding fuel to burn because its ash has a tendency to sinter through the formation of alkali silicates (Aho 2001). These could cause the bed material of a fluidised bed combustor to agglomerate and defluidise. To reduce the possibility of this happening, agricultural waste must be co-combusted with a material of different ash characteristics. In this study, wood-bark, a waste product from debarking of logs prior to pulping in a paper mill has been used.

During several preliminary runs with fuel blends containing high proportions of agricultural waste, the feeder tube blocked at the tip, just prior to entry of the fuel into the combustion zone. Shortening the length of uncooled feeding tube extending into the combustion zone considerably reduced this problem but did not eliminate it completely. When agricultural waste was burnt alone at 900 °C fuel feeding was stopped by a blockage at the hot tip of the feeder tube. Unfed fuel from the feed hopper and feeder tube was recovered and weighed and the amount of fuel fed determined by difference. As less ash was recovered from this run; to have enough ash for trace element analysis, the bottom and sinter ash fractions were mixed together. As a result there were no relative enrichment on sinter ash data for agricultural waste burnt on its own at 900 °C.



Trace Element Concentration in raw fuels (ppm):	As	Cd	Hg	Se	Pb
Wood-Bark	0.44 ± 0.95	0.20 ± 0.05	0.033 ± 0.001	<0.8	3.1 ± 0.4
Agricultural Waste	0.34 ± 0.13	0.36 ± 0.09	0.95 ± 0.03	<0.8	0.9 ± 0.3

Figure 75 Percentage Retention of As, Cd, Hg, Se and Pb in Ash After Wood-Bark / Agricultural Waste Co-Combustion

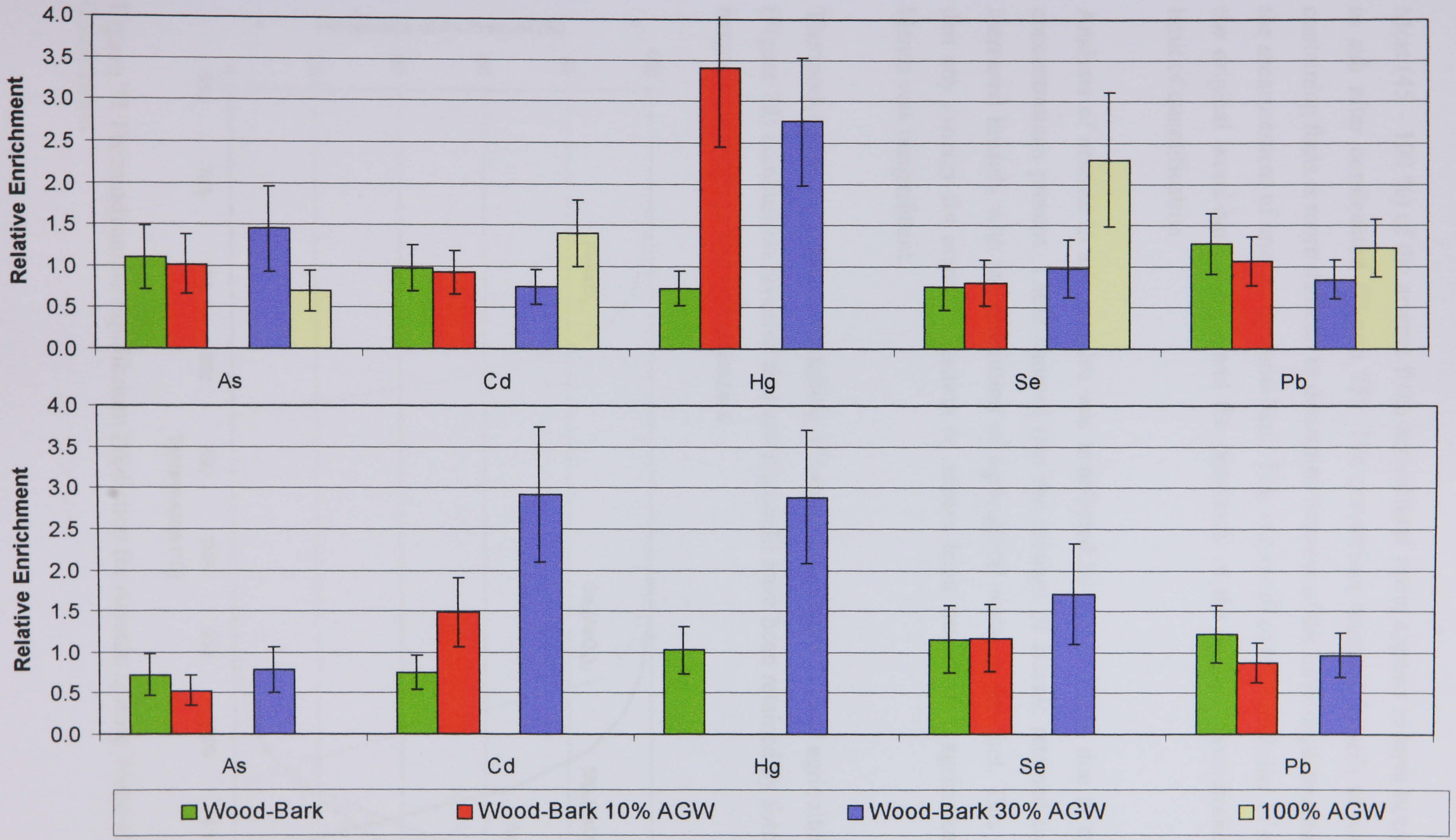


Figure 76 Relative Enrichment of As, Cd, Hg, Se and Pb in Sinter Ash During Wood-Bark / Agricultural Waste Co- Combustion

Note: A relative enrichment of one corresponds to that element being found in equal concentrations in the sinter and bottom ashes

5.5.1 Arsenic

Most (45 – 100 %) of the arsenic from agricultural waste appears to have been retained in ash after combustion (Figure 75). The proportion retained by ash of wood-bark containing fuels is more difficult to determine because of the large experimental error in the measurement of arsenic in wood-bark. This is a result of the variability of arsenic in the original wood-bark sample and the proximity of the arsenic concentration to the limit of quantification.

Analysis of arsenic in ash samples was unaffected by this problem, due to the higher concentrations present. These showed that the amount of arsenic retained by the ash increased linearly with the proportion of agricultural waste in the fuel. This indicates that any synergy for arsenic retention or release from wood-bark / agricultural waste blends was insignificant.

Thermodynamic equilibrium modelling of wood-bark (Figure 77) and agricultural waste (Figure 78) combustion revealed that arsenic could have been retained by formation of magnesium, calcium and iron arsenates.

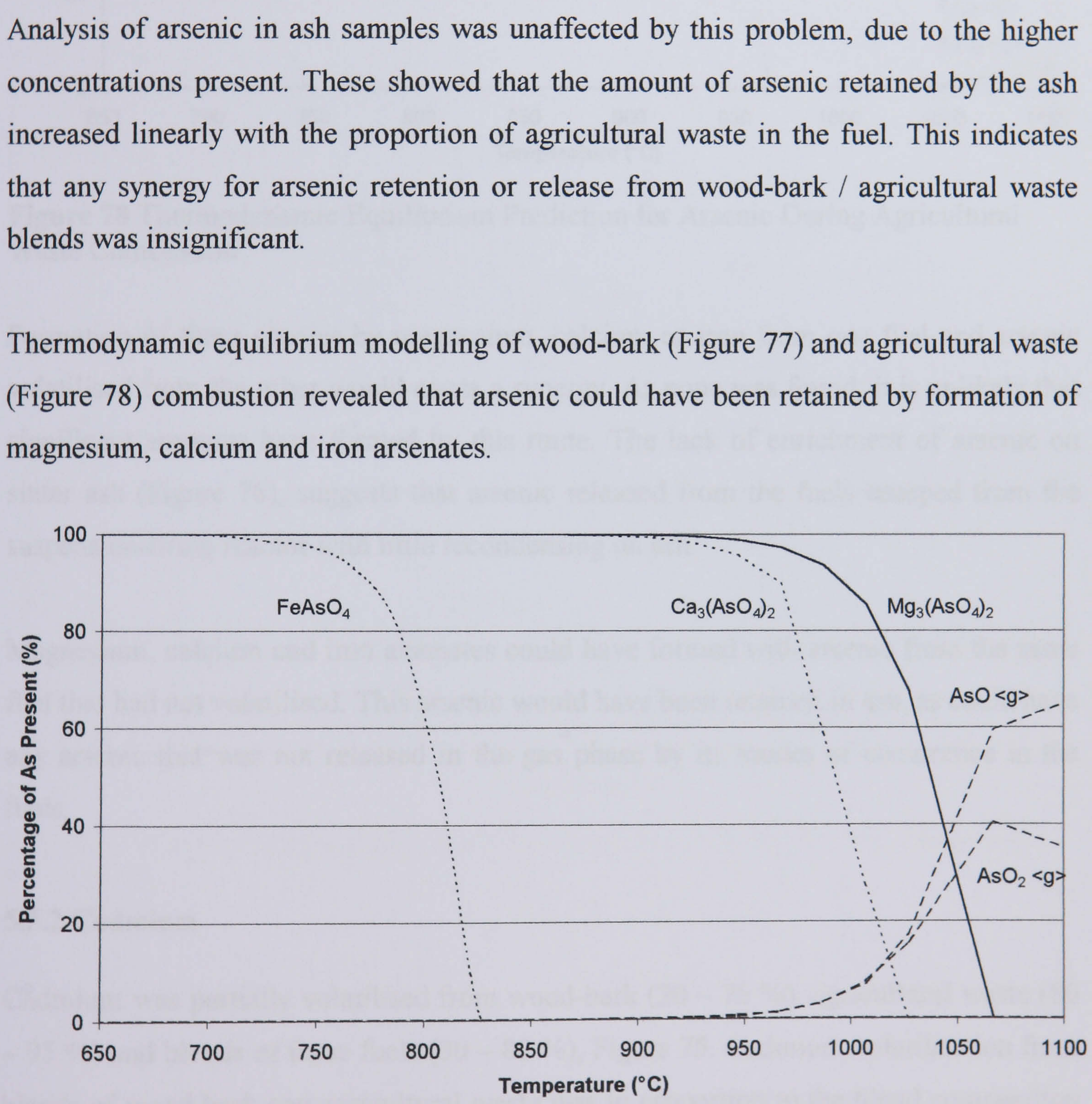


Figure 77 Thermodynamic Equilibrium Prediction for Arsenic During Wood-Bark Combustion

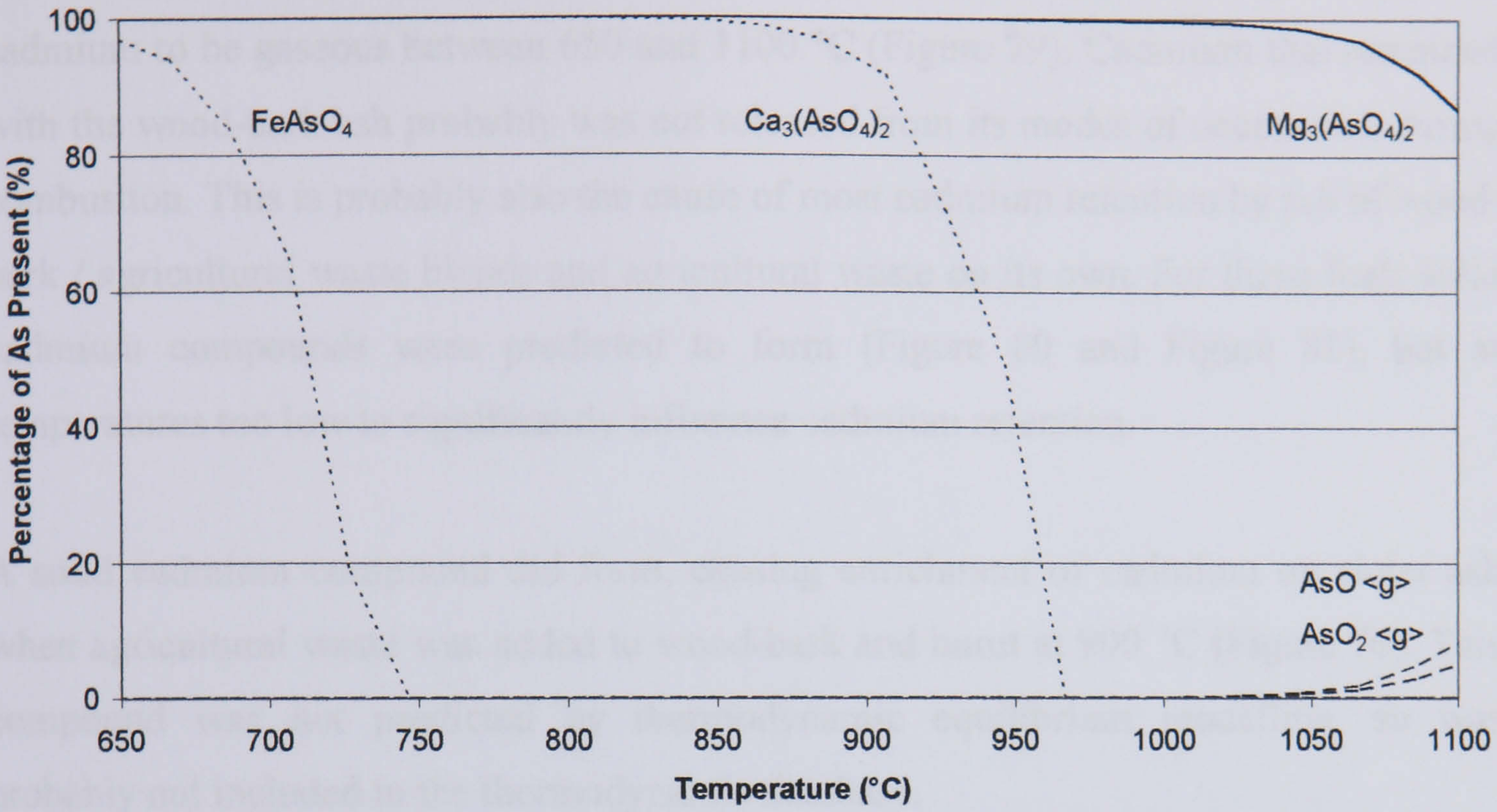


Figure 78 Thermodynamic Equilibrium Prediction for Arsenic During Agricultural Waste Combustion

Formation of these species by magnesium, calcium or iron from one fuel and arsenic volatilised from the other would cause a synergy. As none was found, it is unlikely that significant amounts have formed by this route. The lack of enrichment of arsenic on sinter ash (Figure 76), suggests that arsenic released from the fuels escaped from the suspension-firing reactor with little recondensing on ash.

Magnesium, calcium and iron arsenates could have formed with arsenic from the same fuel that had not volatilised. This arsenic would have been retained in ash, as could have any arsenic that was not released in the gas phase by its modes of occurrence in the fuels.

5.5.2 Cadmium

Cadmium was partially volatilised from wood-bark (20 – 75 %), agricultural waste (80 – 95 %) and blends of these fuels (30 – 80 %), Figure 75. Cadmium volatilisation from blends of wood-bark and agricultural waste was in proportion to the blend composition and the proportion of cadmium released by the constituent fuels. There was no significant synergy for cadmium release or retention.

Thermodynamic equilibrium modelling of wood-bark combustion predicted all cadmium to be gaseous between 650 and 1100 °C (Figure 79). Cadmium that remained with the wood-bark ash probably was not released from its modes of occurrence during combustion. This is probably also the cause of most cadmium retention by ash of wood-bark / agricultural waste blends and agricultural waste on its own. For these fuels solid cadmium compounds were predicted to form (Figure 80 and Figure 81), but at temperatures too low to significantly influence cadmium retention.

A solid cadmium compound did form, causing enrichment of cadmium on sinter ash when agricultural waste was added to wood-bark and burnt at 900 °C (Figure 76). This compound was not predicted by thermodynamic equilibrium modelling, so was probably not included in the thermodynamic database.

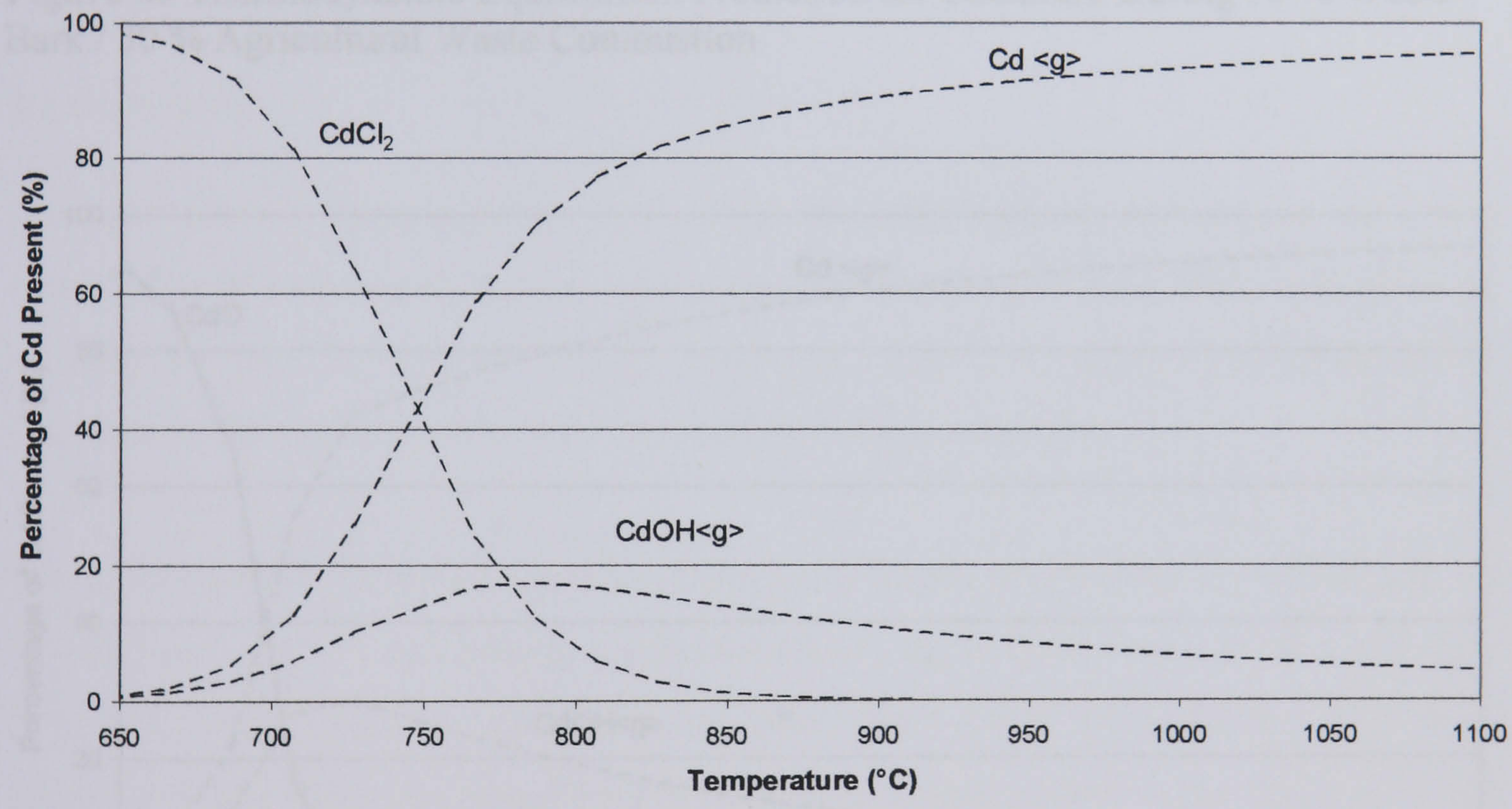


Figure 79 Thermodynamic Equilibrium Prediction for Cadmium During Wood-Bark Combustion

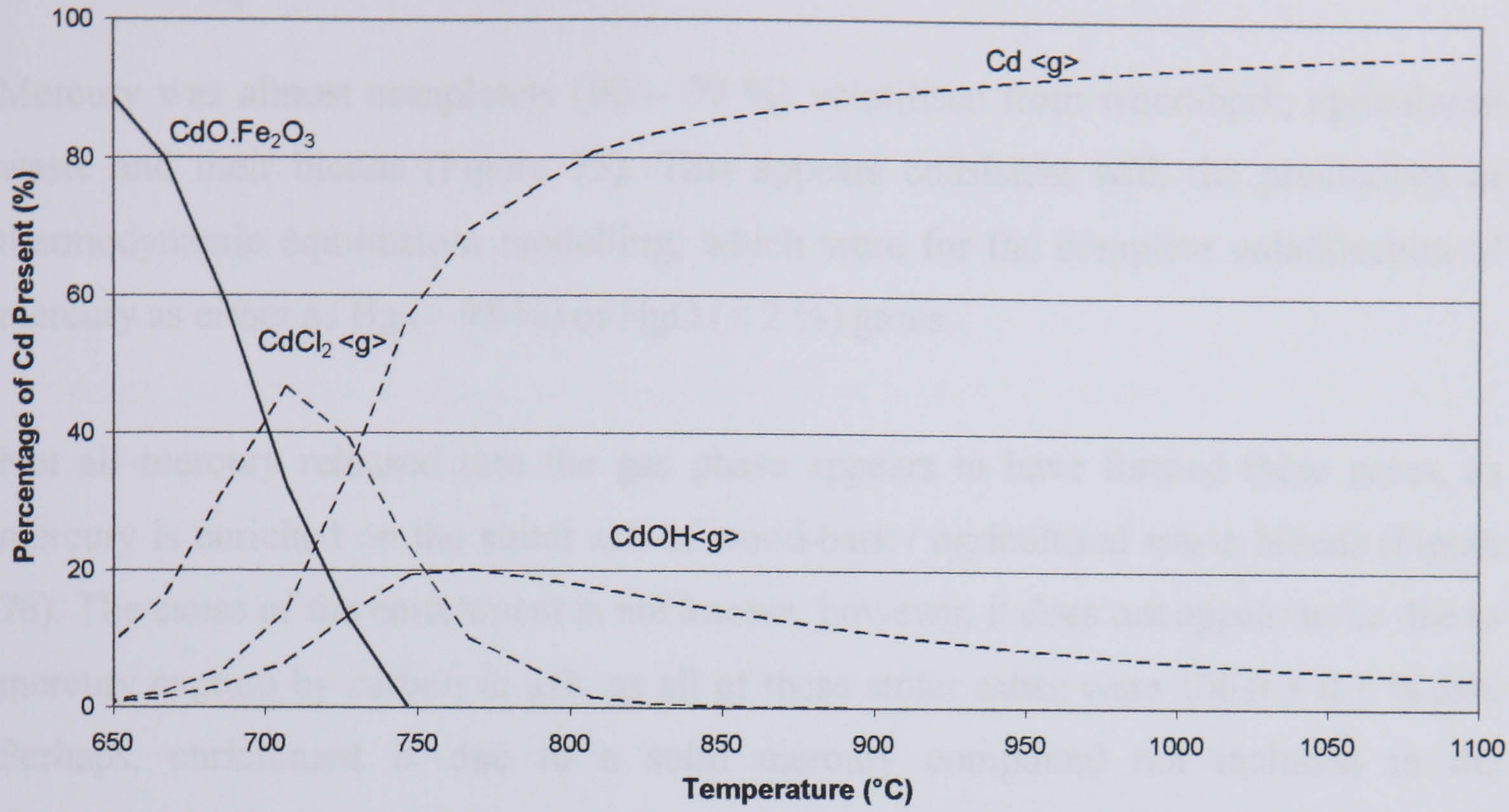


Figure 80 Thermodynamic Equilibrium Prediction for Cadmium During 70 % Wood-Bark / 30 % Agricultural Waste Combustion

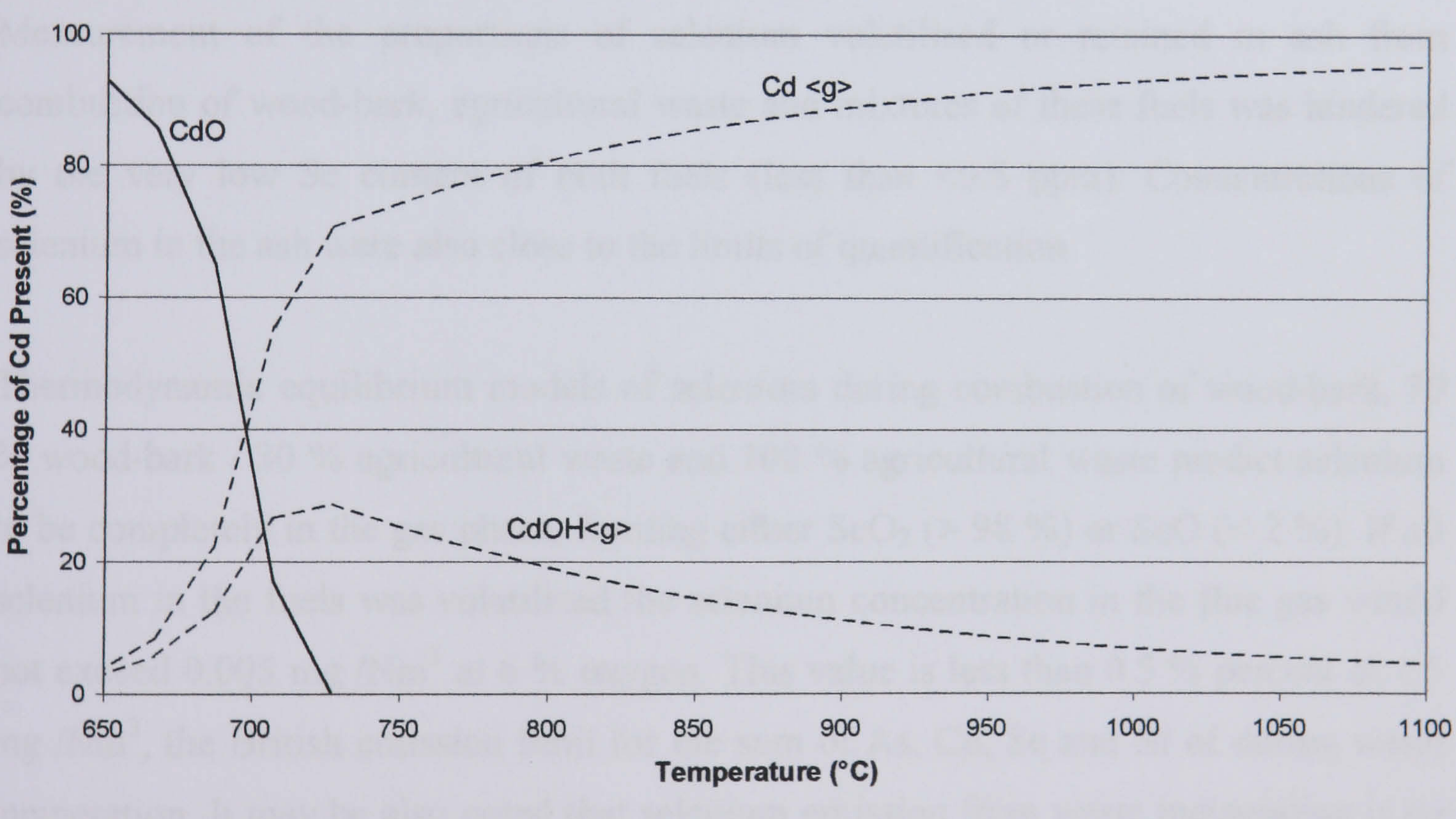


Figure 81 Thermodynamic Equilibrium Prediction for Cadmium During Agricultural Waste Combustion

5.5.3 Mercury

Mercury was almost completely (90 – 99 %) volatilised from wood-bark, agricultural waste and their blends (Figure 75). This appears consistent with the predictions of thermodynamic equilibrium modelling, which were for the complete volatilisation of mercury as either as Hg (> 98 %) or HgO (< 2 %) gases.

Not all mercury released into the gas phase appears to have formed these gases, as mercury is enriched on the sinter ash of wood-bark / agricultural waste blends (Figure 76). The cause of the enrichment is not known, however, it does not appear to be due to mercury capture by carbon in ash, as all of these sinter ashes were 100.0 ± 0.1 % ash. Perhaps, enrichment is due to a solid mercury compound not included in the thermodynamic model, as suggested in section 5.2.3.

5.5.4 Selenium

Measurement of the proportions of selenium volatilised or retained in ash from combustion of wood-bark, agricultural waste and mixtures of these fuels was hindered by the very low Se content of both fuels (less than <0.8 ppm). Concentrations of selenium in the ash were also close to the limits of quantification.

Thermodynamic equilibrium models of selenium during combustion of wood-bark, 70 % wood-bark / 30 % agricultural waste and 100 % agricultural waste predict selenium to be completely in the gas phase, forming either SeO_2 (> 98 %) or SeO (< 2 %). If all selenium in the fuels was volatilised the selenium concentration in the flue gas would not exceed 0.005 mg /Nm^3 at 6 % oxygen. This value is less than 0.5 % percent of 1.5 mg /Nm^3, the British emission limit for the sum of As, Co, Se and Ni of during waste incineration. It may be also noted that selenium emission from waste incineration is no longer regulated by the European union.

5.5.5 Lead

Percentage retention of lead in ash varied little between combustion of wood-bark (20 – 50 % retained), and blends of wood-bark with agricultural waste (25 – 60 %). Slightly more lead may have been retained in ash when agricultural waste was burnt alone (Figure 75). With similar proportions of lead retained by the pure fuels and blends, there was no synergy for lead retention or release between wood-bark and agricultural waste blends.

Complete lead volatilisation was predicted by thermodynamic equilibrium modelling of wood-bark (Figure 82), a 70% wood-bark / 30% agricultural waste blend and 100 % agricultural waste combustion. These thermodynamic results and the lack of lead enrichment on sinter ash (Figure 76) suggest lead released from the fuel did not recondense on ash and was lost from the suspension-firing reactor with the flue gas. Lead that was retained in ash was probably not released from its original modes of occurrence in the fuels (Section 5.0.2).

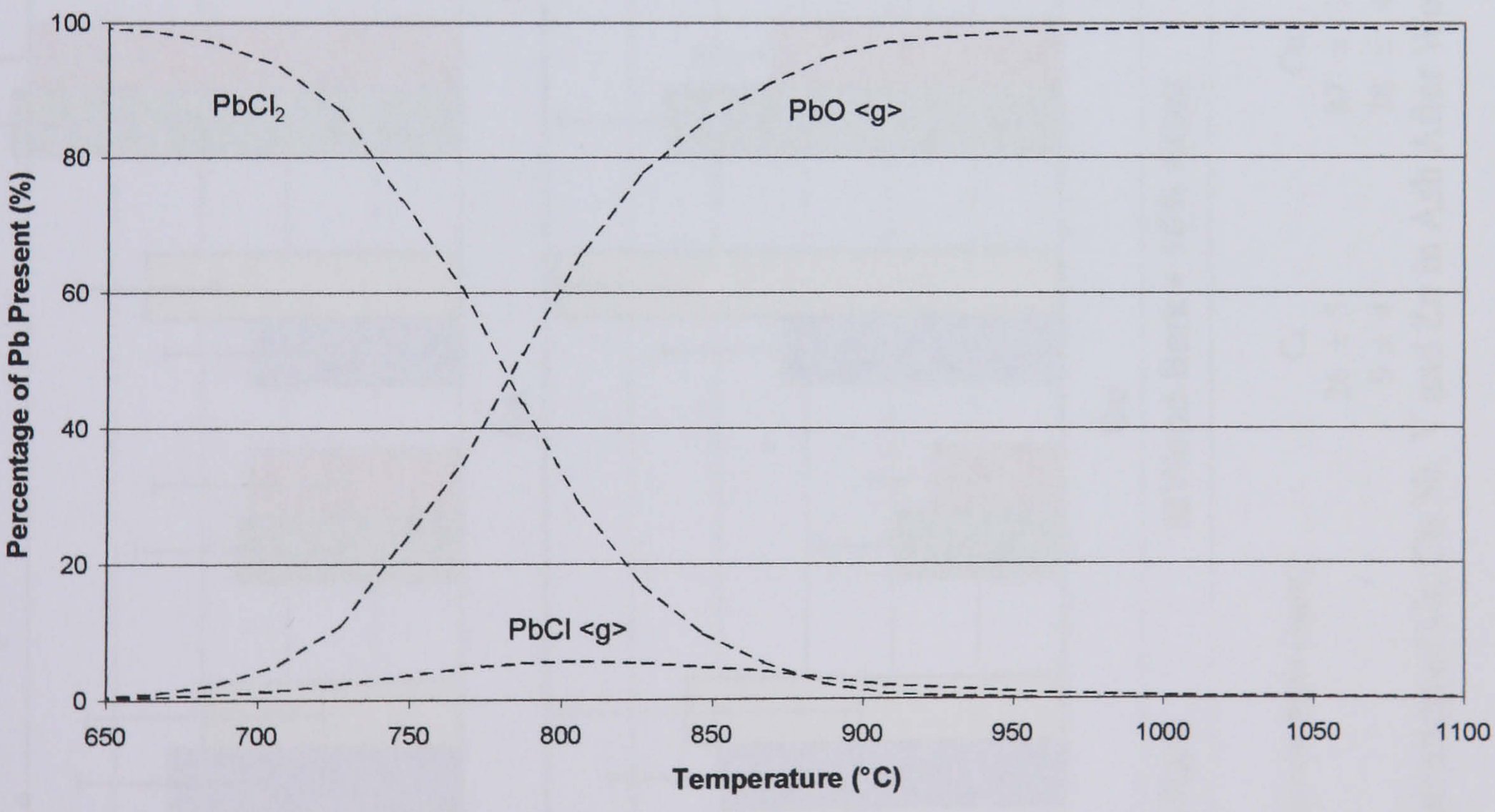
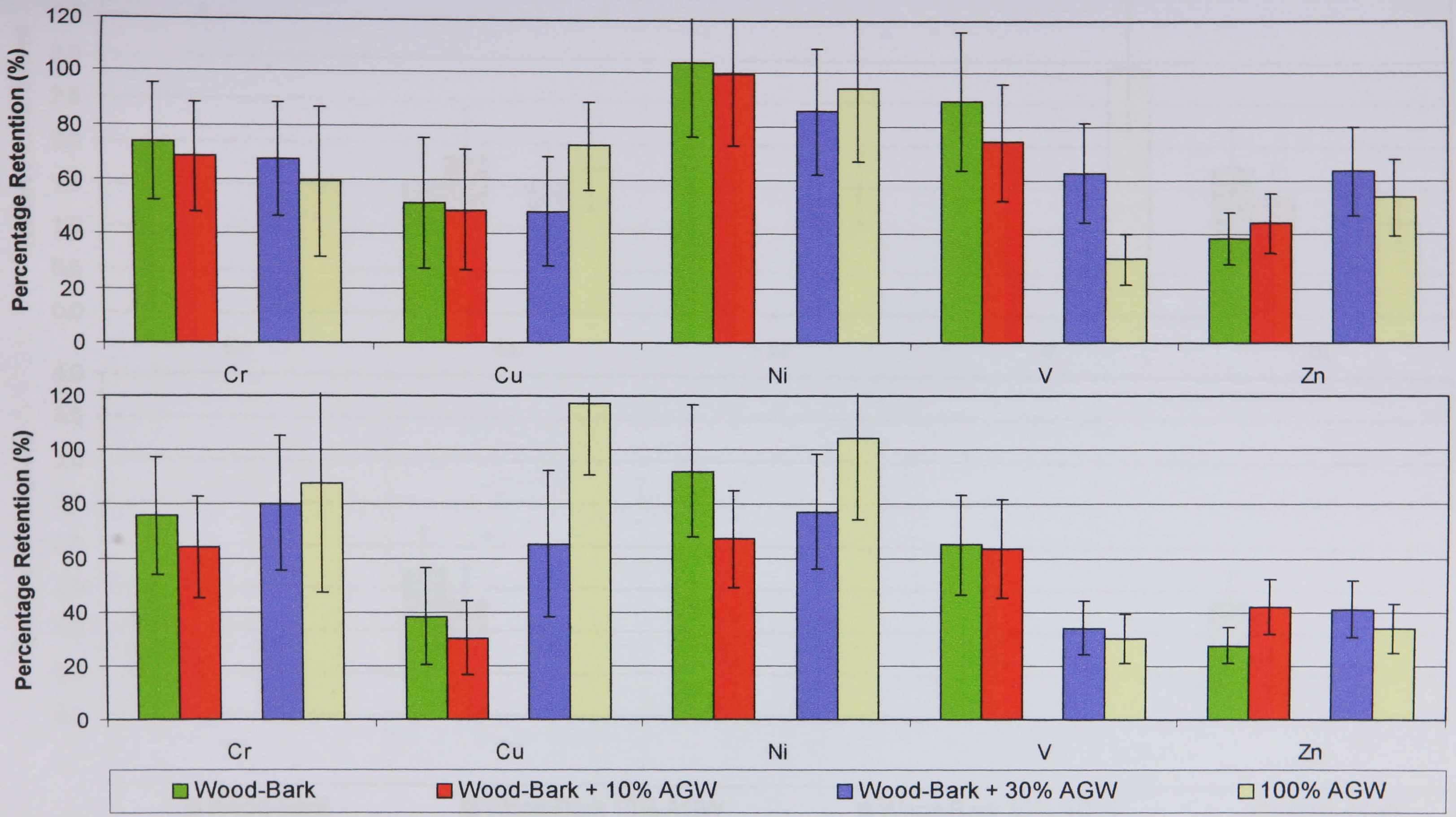


Figure 82 Thermodynamic Equilibrium Predictions for Lead During Wood-Bark Combustion



Trace Element Concentration in raw fuels (ppm):	Cr	Cu	Ni	V	Zn
Wood-Bark	26 ± 5	87 ± 37	10 ± 2	2.8 ± 0.6	150 ± 21
Agricultural Waste	9 ± 4	38 ± 4	11 ± 2	4.2 ± 1.0	252 ± 44

Figure 83 Percentage Retention of Cr, Cu Ni, V and Zn in Ash After Wood-Bark / Agricultural Waste Co-Combustion

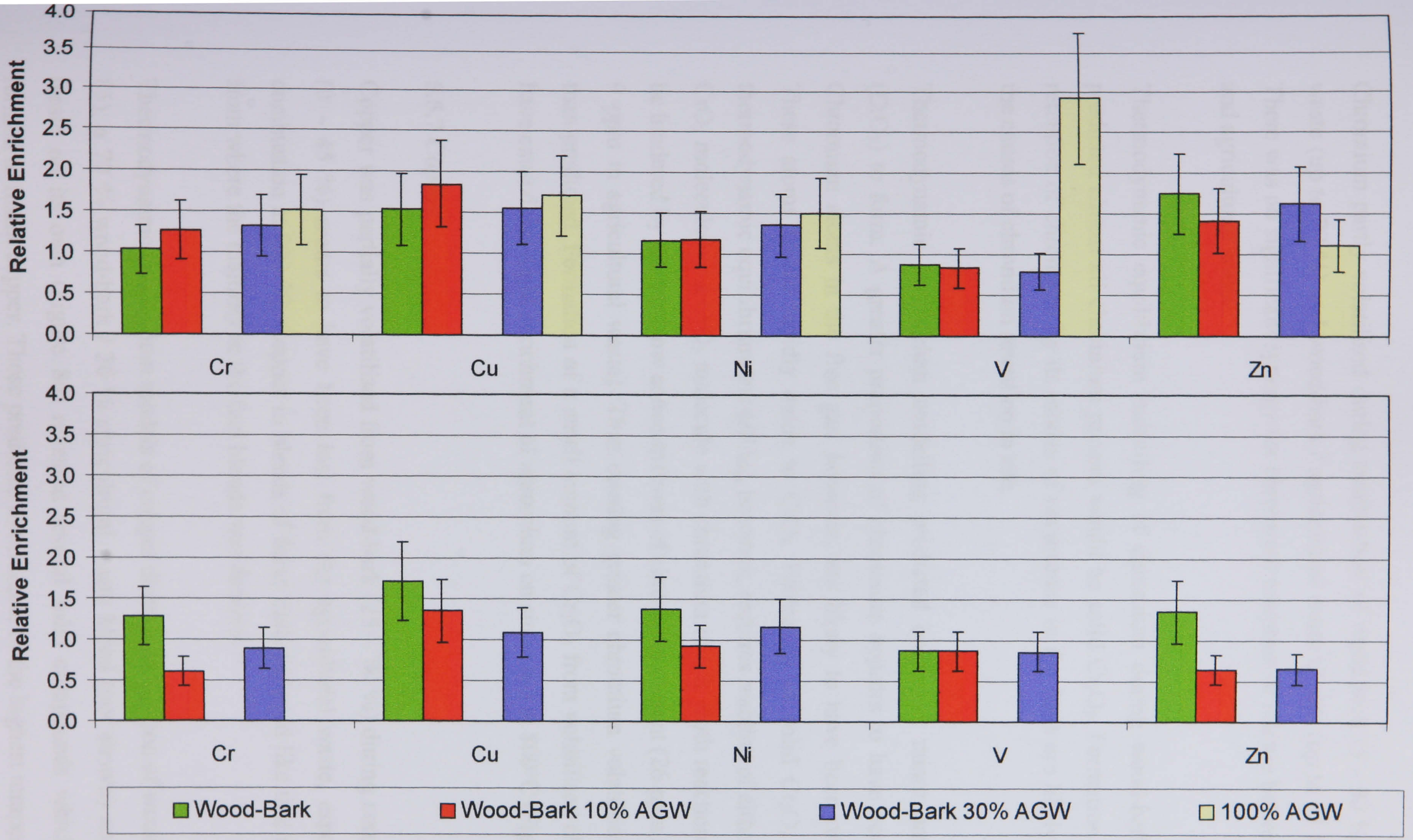


Figure 84 Relative Enrichment of Cr, Cu, Ni, V and Zn in Sinter Ash During Wood-Bark / Agricultural Waste Combustion

Note: A relative enrichment of one corresponds to that element being found in equal concentrations in the sinter and bottom ashes

5.5.6 Chromium

Chromium partly volatilised during combustion of wood-bark (5 - 50 %), agricultural waste (up to 70 %) and wood-bark / agricultural waste blends (up to 55 %), Figure 83. There was no significant synergy for chromium retention or release between wood-bark and agricultural waste.

Thermodynamic equilibrium modelling of chromium during wood-bark combustion predicted almost all chromium present would be solid Cr_2O_3. Formation of Cr_2O_3 and retention of chromium by its modes of occurrence in the fuels are likely to have been the causes of chromium retention in ash.

Thermodynamic equilibrium modelling predicted only very minor amounts of gas (CrO_3) to form. A greater proportion of chromium appears to have been volatilised. Chromium atoms in the flue gas, however, are likely to have been released singly. These atoms would rapidly oxide to CrO_3. Formation of solid Cr_2O_3 predicted by thermodynamic equilibrium modelling, however, requires reaction of either two gaseous CrO_3 molecules or a CrO_3 molecule with chromium in ash. Both reactions are likely to be hindered by the very low concentrations of chromium present (26 ppm in wood-bark, 9 ppm in agricultural waste). Thus causing greater chromium volatilisation as Cr_2O_3 than predicted. Formation of a small amount of Cr_2O_3 from volatilised chromium may have caused the slight enrichment of chromium on sinter ash at 800°C (Figure 84).

5.5.7 Copper

Copper was partially volatilised from wood-bark (25 – 80 %) during combustion. Less (0 – 45 %) seems to have been lost from the agricultural waste, especially during combustion at 900 °C. Copper in blends of these fuels behaved like that in wood-bark, from where the majority in the fuel blends was derived.

Thermodynamic equilibrium models of copper during combustion of wood-bark (Figure 85), a 70 % wood-bark / 30 % agricultural waste blend (not shown) and agricultural waste on its own (Figure 86) revealed several solid compounds which could have formed to retain copper. Those predicted to be stable to the highest temperatures during

wood combustion ($CuO.Al_2O_3$, $Cu_2O.Fe_2O_3$, CuO.FeO and CuO. Fe_2O_3) contained minor metals as well as copper. These were present at relatively low concentrations; a lack of sufficient contact between them and copper may prevented their formation in equilibrium concentrations. Where the minor element - copper compounds did not form to the extent predicted, CuO and at higher temperatures, Cu_2O were predicted instead.

Volatilised copper was predicted to have formed CuCl gas. The predicted formation of this species was reduced with agricultural waste addition to the wood-bark, not because of a lower chlorine content (agricultural waste Cl 0.39 % daf, wood-bark 0.01 % daf), but because of the very high concentration of potassium in the agricultural waste (27.1 g of K / kg of fuel). This reacts with chlorine preferentially to copper, forming KCl.

More copper was volatilised from wood-bark and wood-bark / agricultural waste blends that predicted to form CuCl gas. The additional volatilised copper was probably released from the fuels and formed CuO on contact with oxygen. Some of this CuO would have recondensed on ash, perhaps causing enrichment of copper on sinter ash (Figure 84). The remainder of the CuO was probably been swept out of the reactor by the flue gas, as described in Section 5.0.3.

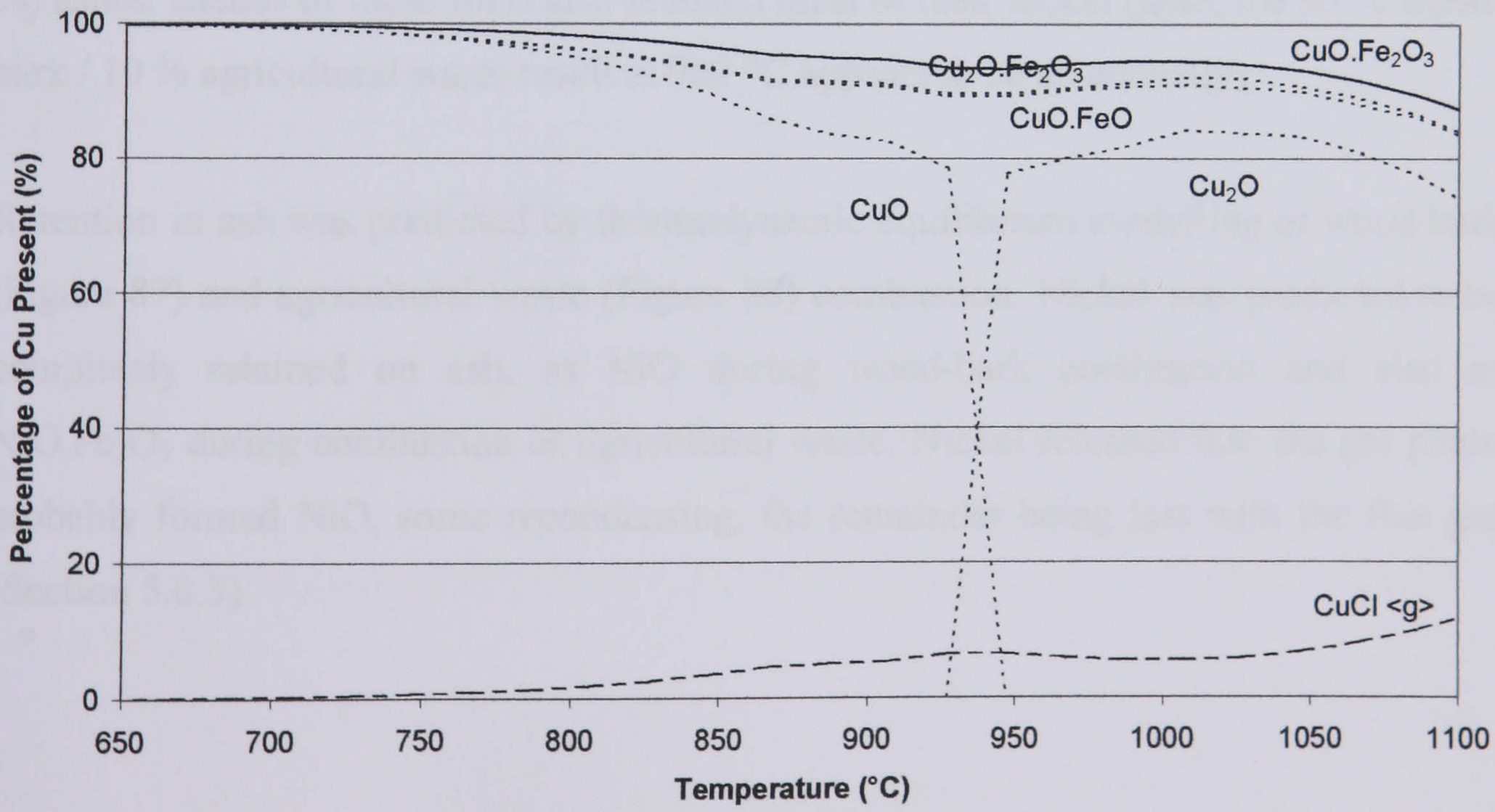


Figure 85 Thermodynamic Equilibrium Model of Copper During Wood-Bark Combustion

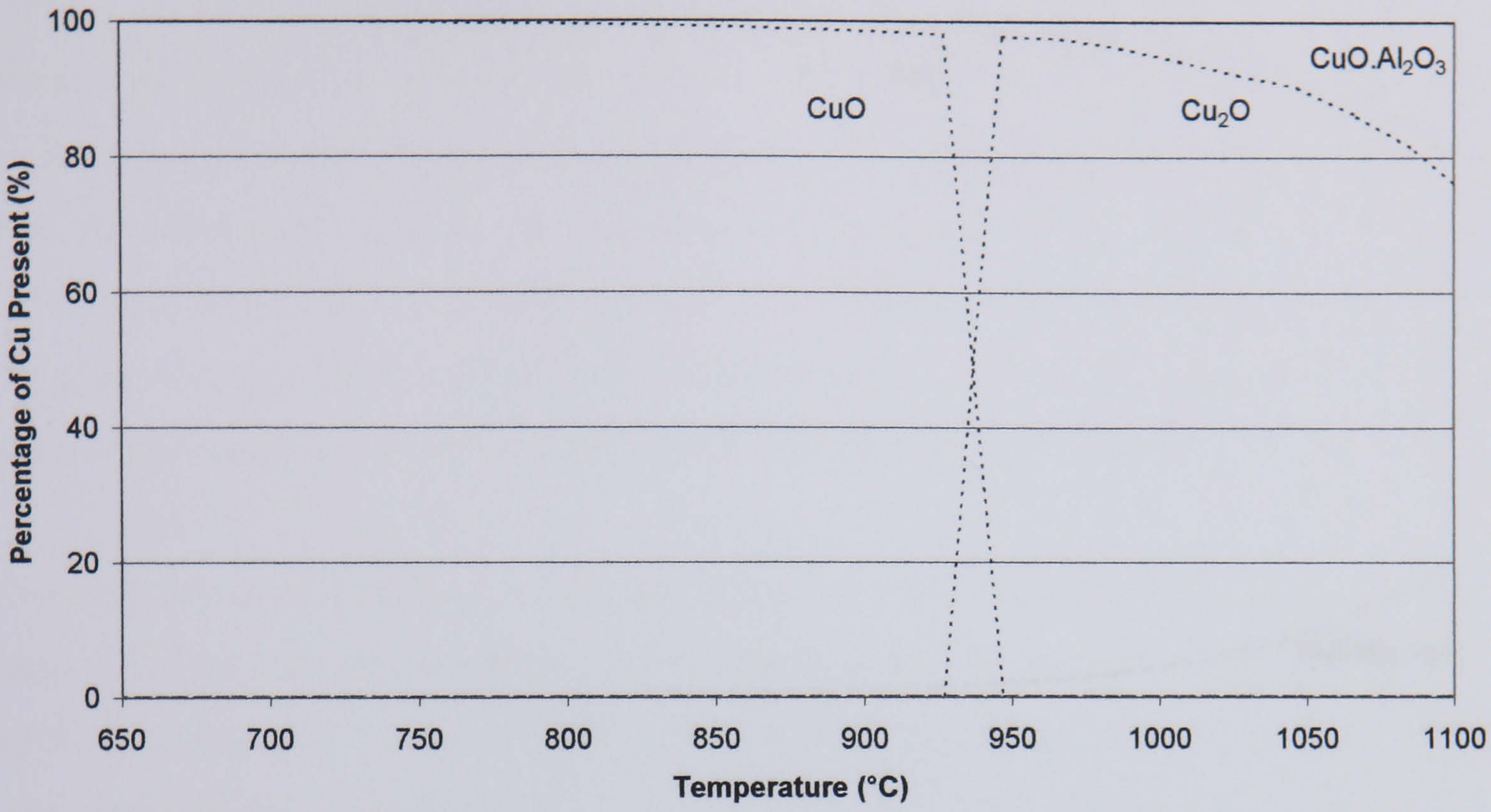


Figure 86 Thermodynamic Equilibrium Model of Copper During Agricultural Waste Combustion

5.5.8 Nickel

Nickel was mostly retained in wood-bark (65 – 100 %) and agricultural waste (65 – 100 %) ashes. Blends of these fuels also retained most of their nickel (note, the 90 % wood-bark / 10 % agricultural waste result at 900 °C appears to be an anomaly).

Retention in ash was predicted by thermodynamic equilibrium modelling of wood-bark (Figure 87) and agricultural waste (Figure 88) combustion. Nickel was predicted to be completely retained on ash, as NiO during wood-bark combustion and also as $NiO.Fe_2O_3$ during combustion of agricultural waste. Nickel released into the gas phase probably formed NiO, some recondensing, the remainder being lost with the flue gas (Section 5.0.3).

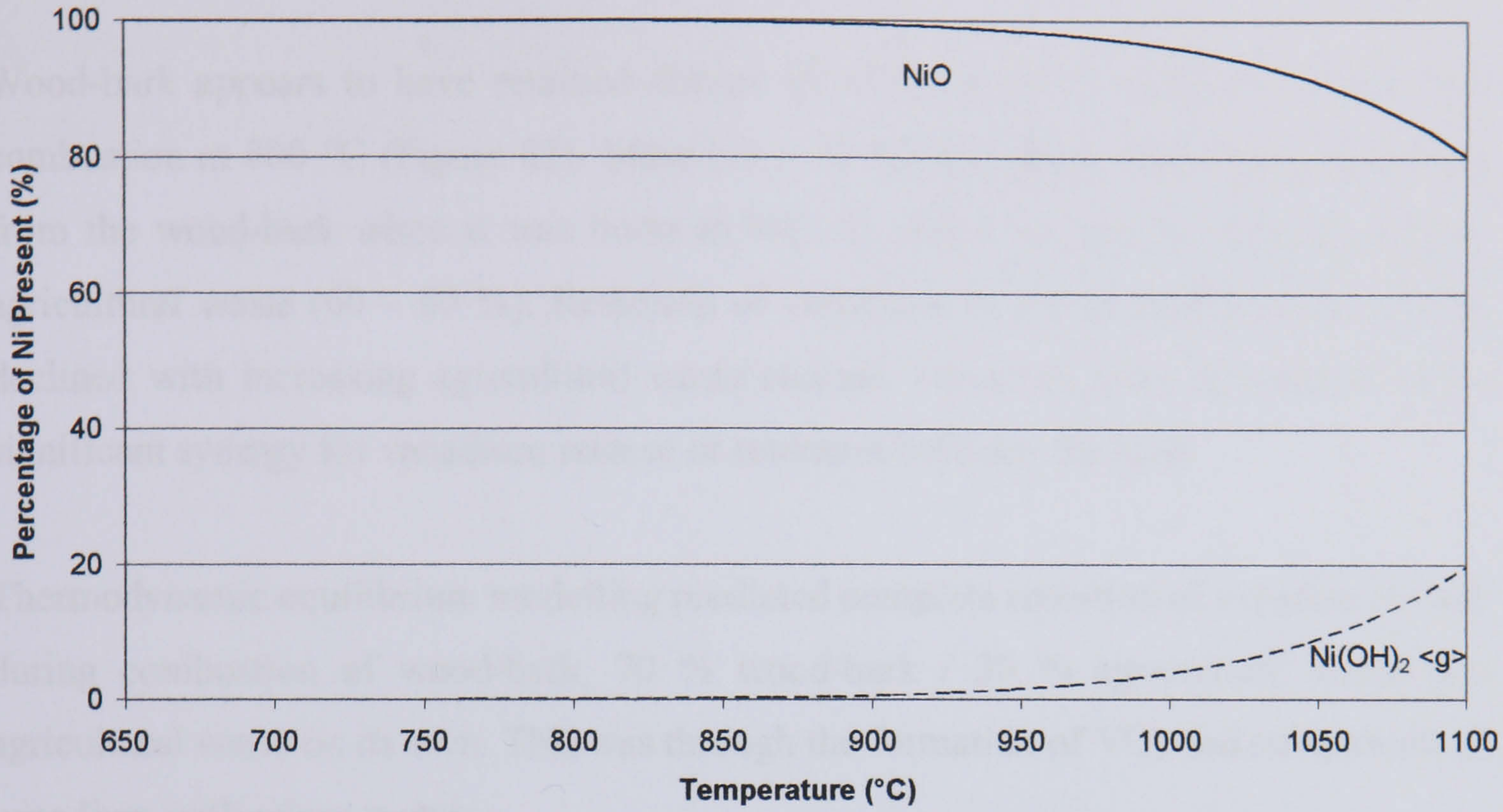


Figure 87 Thermodynamic Equilibrium Model of Nickel During Wood-Bark Combustion

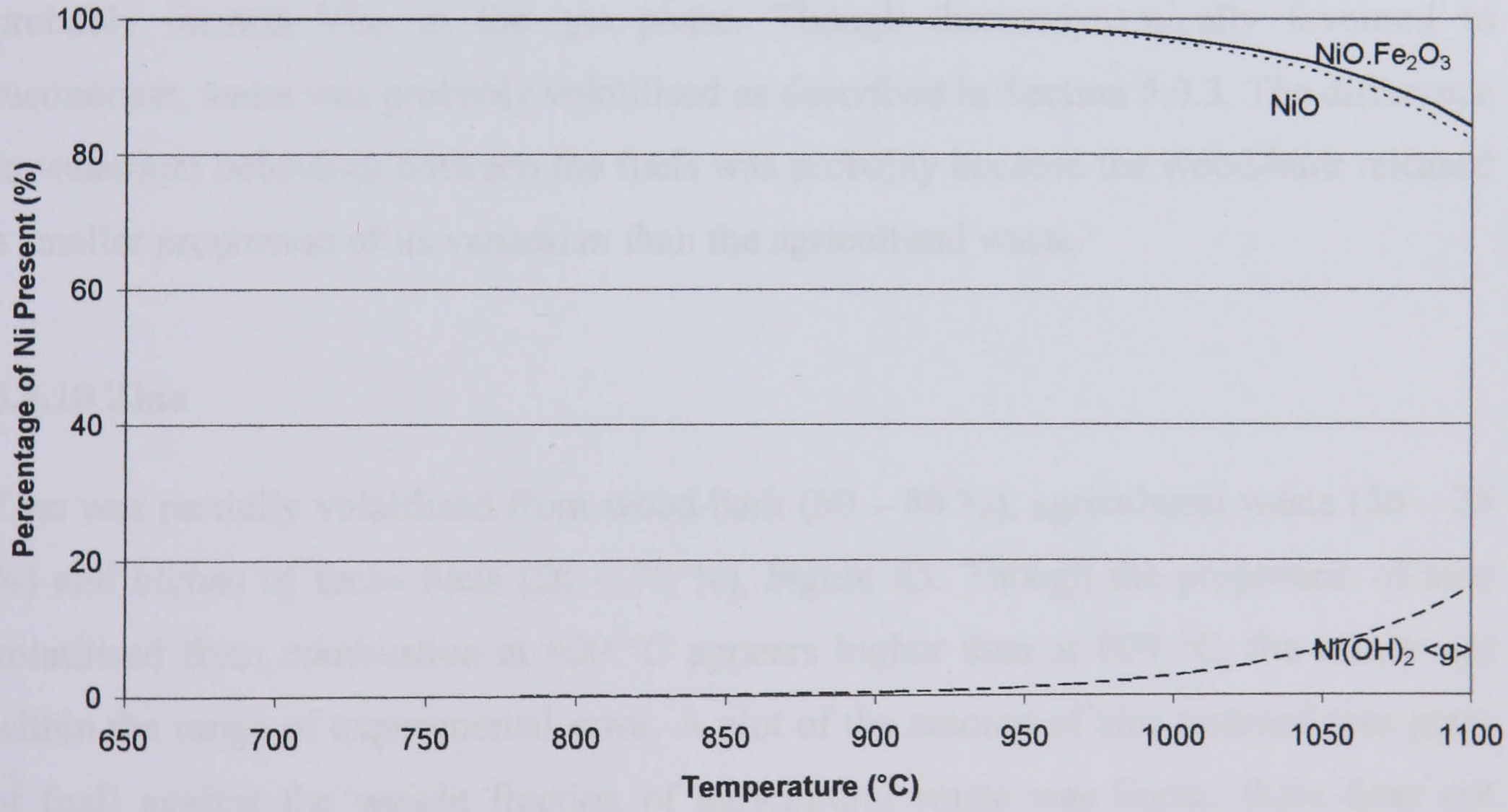


Figure 88 Thermodynamic Equilibrium Model of Nickel During Agricultural Waste Combustion

5.5.9 Vanadium

Wood-bark appears to have retained almost all of its original vanadium in ash after combustion at 800 °C (Figure 83). More (15 – 55 %) appears to have been volatilised from the wood-bark when it was burnt at 900 °C, and a far greater proportion from agricultural waste (60 – 80 %). Retention of vanadium in ash of blends of these fuels declined with increasing agricultural waste content. However, there appears to be no significant synergy for vanadium release or retention between the fuels.

Thermodynamic equilibrium modelling predicted complete retention of vanadium in ash during combustion of wood-bark, 70 % wood-bark / 30 % agricultural waste and agricultural waste on its own. This was through the formation of VO_2 and compounds of vanadium with minor metals.

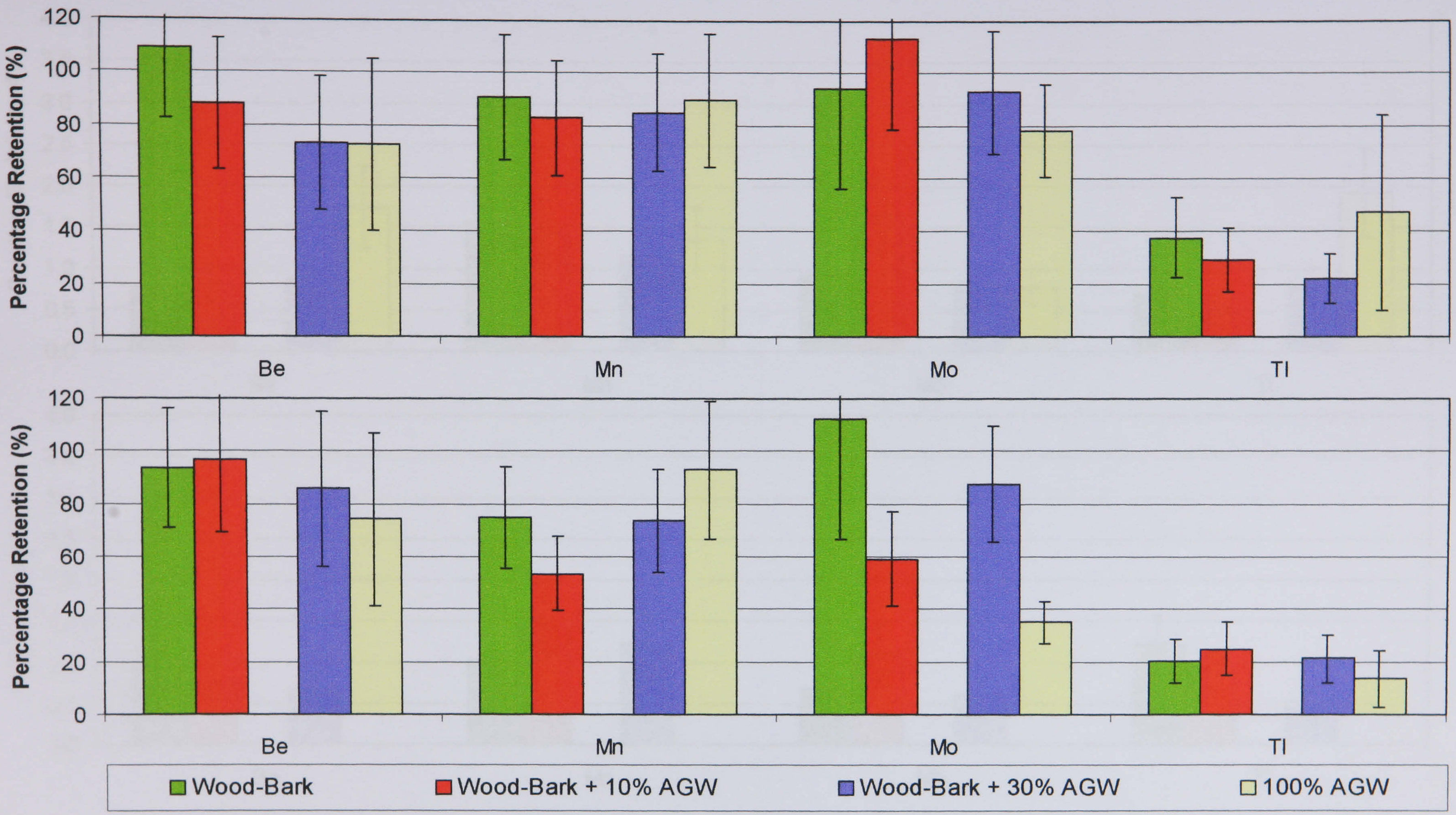
Vanadium, however, has partially volatilised. Vanadium released by combustion probably formed VO_2 in the gas phase. Though thermodynamically favoured to recondense, some was probably volatilised as described in Section 5.0.3. The difference in vanadium behaviour between the fuels was probably because the wood-bark released a smaller proportion of its vanadium than the agricultural waste.

5.5.10 Zinc

Zinc was partially volatilised from wood-bark (50 – 80 %), agricultural waste (30 – 75 %) and blends of these fuels (20 – 70 %), Figure 83. Though the proportion of zinc volatilised from combustion at 900 °C appears higher than at 800 °C, the results are within the range of experimental error. A plot of the amount of zinc retained (per gram of fuel) against the weight fraction of agricultural waste was linear, there does not appear to be a synergy for zinc retention in ash or volatilisation from blends of wood-bark and agricultural waste.

Zinc volatilisation was not predicted by thermodynamic equilibrium models of wood-bark, 70 % wood-bark / 30 % agricultural waste blend or 100 % agricultural waste combustion. For these fuels zinc was predicted to be retained in ash, as $ZnO.Al_2O_3$, $2ZnO.SiO_2$ or ZnO. However, zinc was volatilised during combustion. Probably this

zinc formed ZnO in the gas phase. Partial recondensation of this zinc possibly caused the enrichment on sinter ash (Figure 84). The remainder of the zinc was probably lost in the gas phase, as described in Section 5.0.3.



Trace Element Concentration in raw fuels (ppm):	Be	Mn	Mo	Tl
Wood-Bark	0.07 ± 0.01	414 ± 68	1.3 ± 0.4	0.09 ± 0.03
Agricultural Waste	0.18 ± 0.07	240 ± 48	9.1 ± 0.9	0.01 ± 0.01

Figure 89 Percentage Retention of Be, Mn, Mo and Tl in Ash After Wood-Bark / Agricultural Waste Co-Combustion

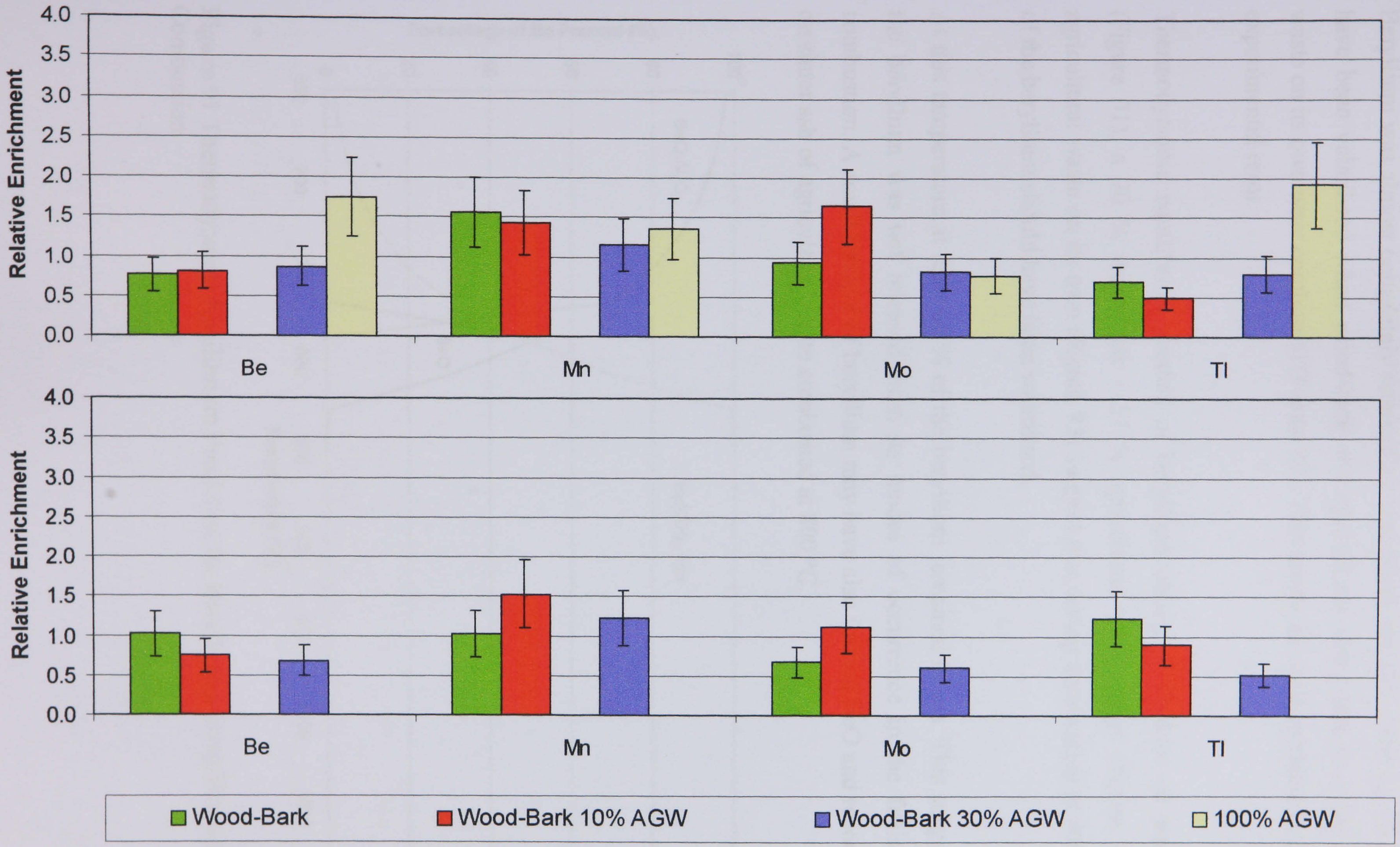


Figure 90 Relative Enrichment of Be, Mn, Mo and Tl in Sinter Ash During Combustion of Wood-Bark and Agricultural Waste

Note: A relative enrichment of one corresponds to that element being found in equal concentrations in the sinter and bottom ashes

5.5.11 Beryllium

Beryllium was almost completely retained by wood-bark ash (70 – 100 %). Some may have been volatilised when wood-bark and agricultural waste blends or agricultural waste on its own were combusted (Figure 89). This cannot be confirmed due to the large experimental error.

Thermodynamic equilibrium models of beryllium during combustion of wood-bark (Figure 91), a 70 % wood-bark / 30 % agricultural waste blend (Figure 92) and agricultural waste on its own (Figure 93) suggest that during combustion at 900 °C all of the beryllium should have been volatilised.

At this temperature at least 40 % of the beryllium remained in ash. This suggests that the beryllium was not released from its modes of occurrence in the fuels during combustion. A small amount of beryllium may have also formed BeO and recondensed on sinter ash of agricultural waste combusted at 800 °C.

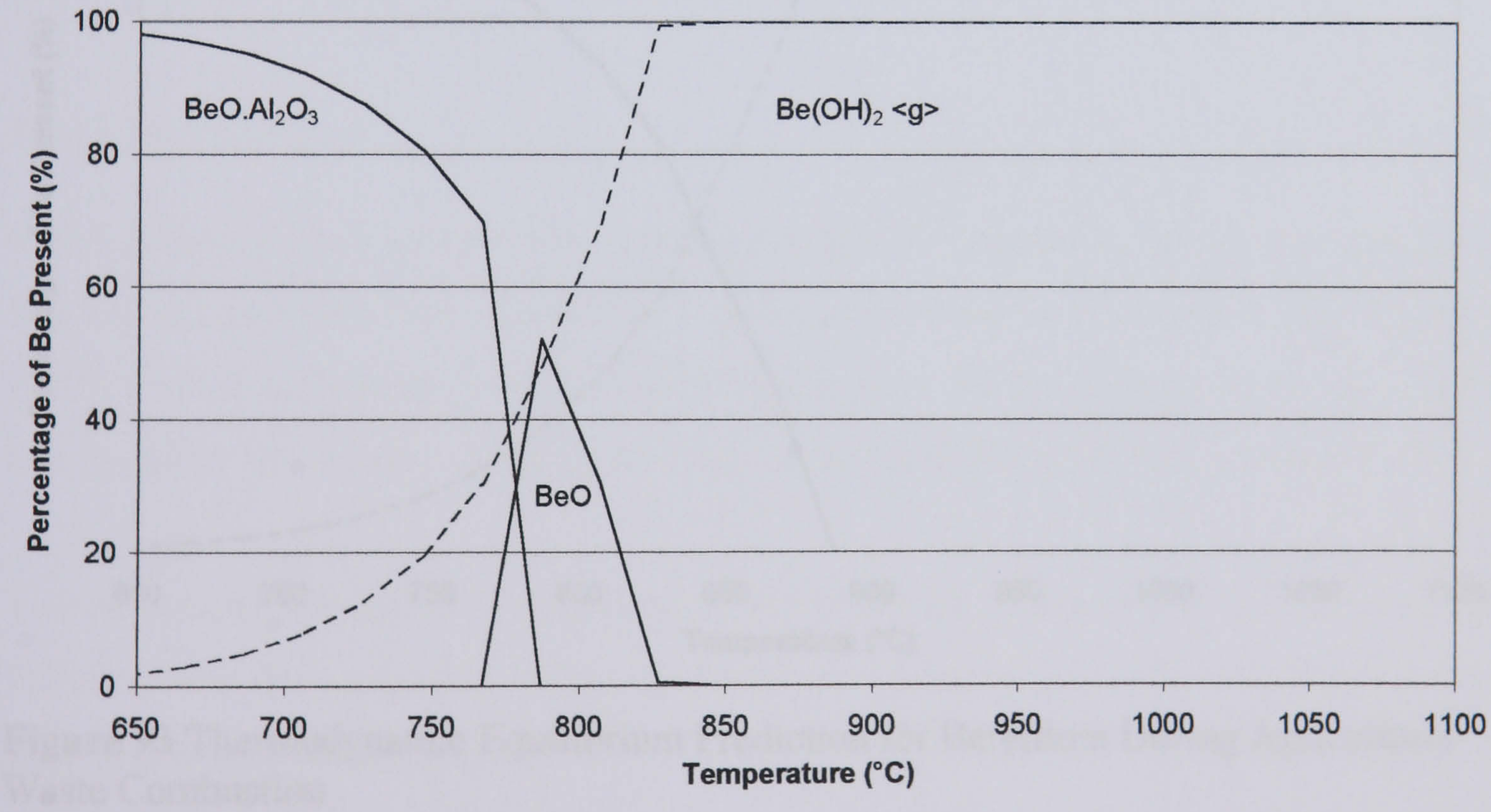


Figure 91 Thermodynamic Equilibrium Prediction for Beryllium During Wood-Bark Combustion

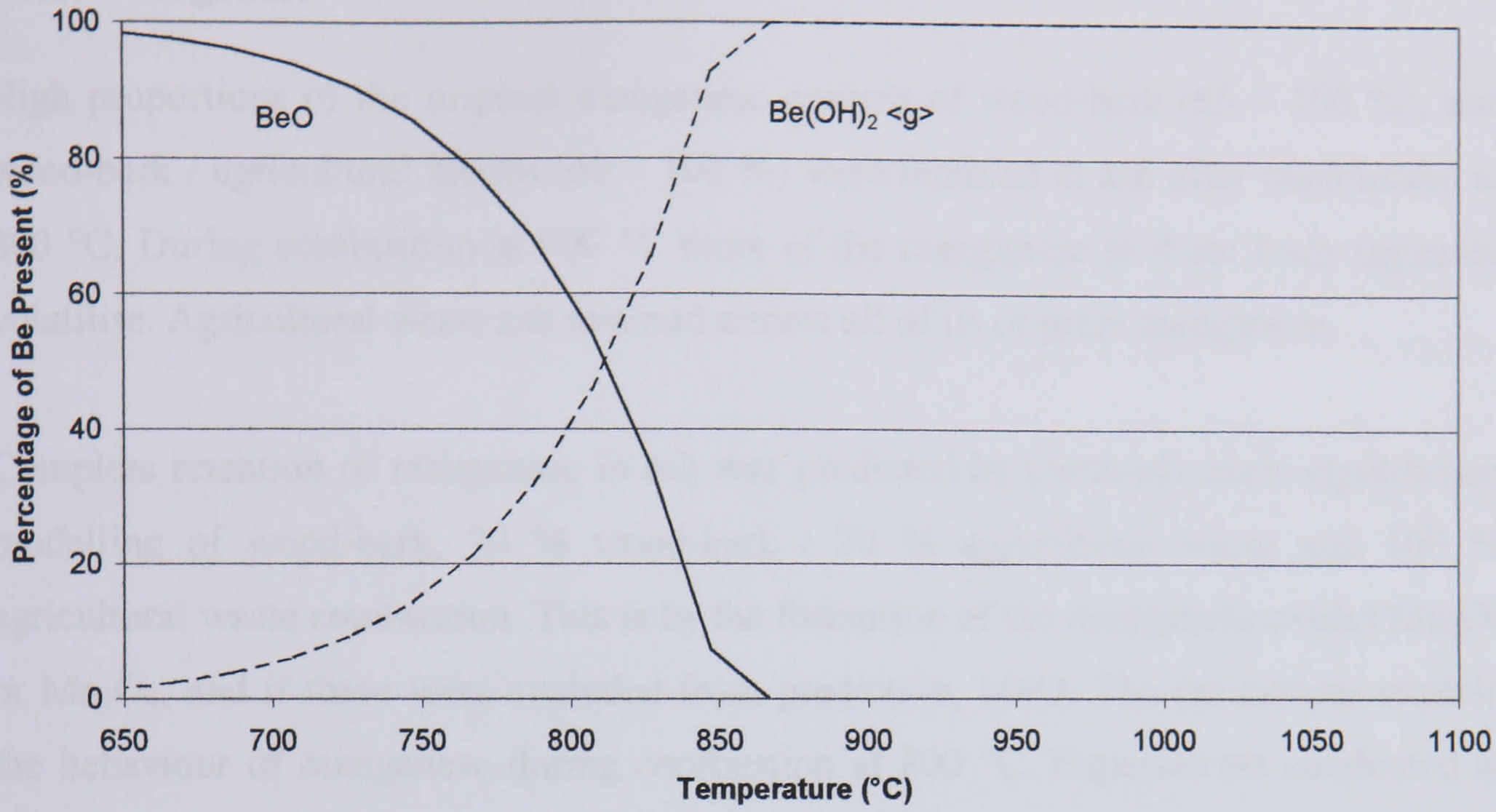


Figure 92 Thermodynamic Equilibrium Prediction for Beryllium During 70 % Wood-Bark / 30 % Agricultural Waste Combustion

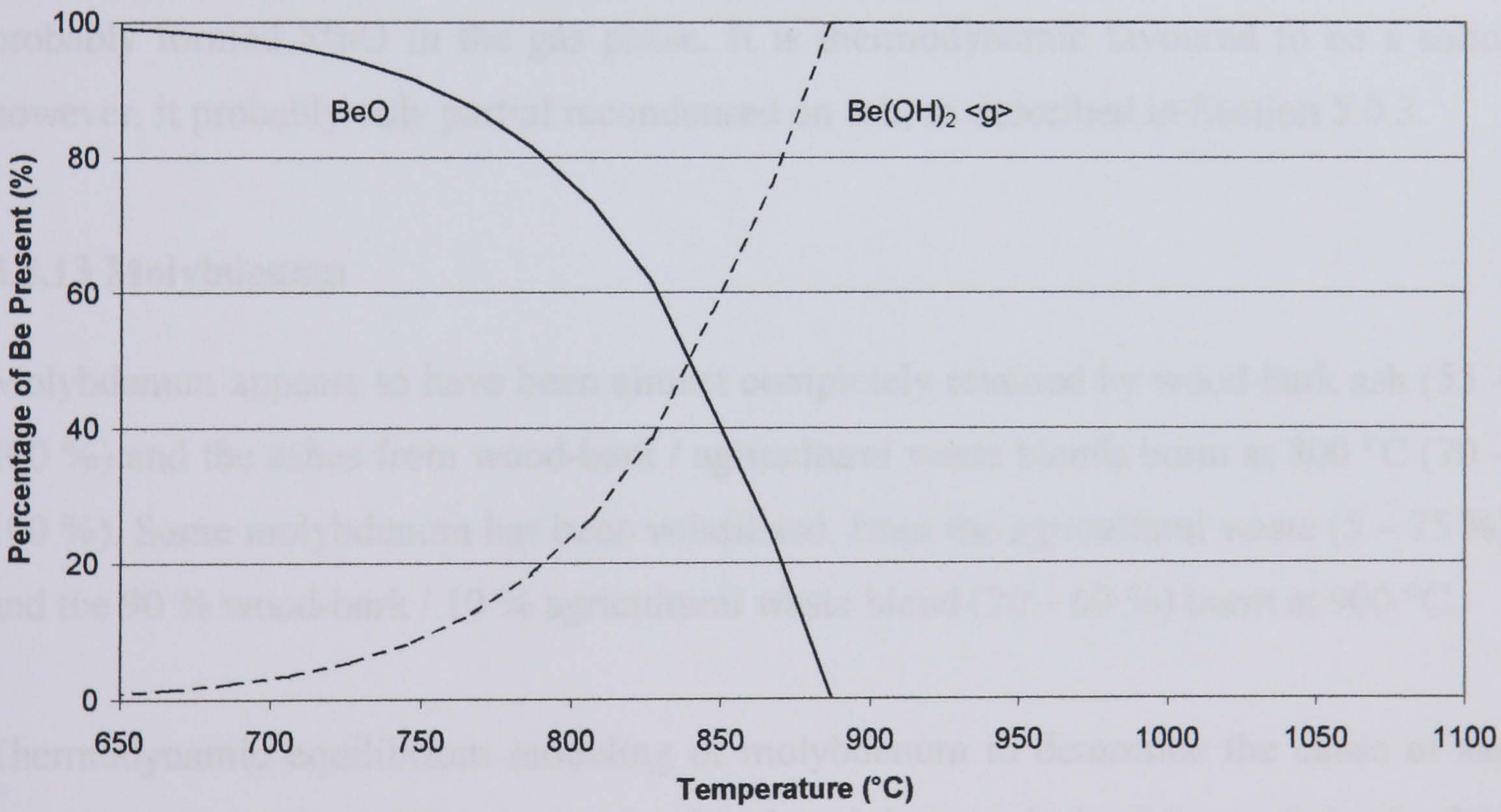


Figure 93 Thermodynamic Equilibrium Prediction for Beryllium During Agricultural Waste Combustion

5.5.12 Manganese

High proportions of the original manganese content of wood-bark (65 – 100 %), and wood-bark / agricultural blends (60 – 100 %) were retained in ash after combustion at 800 °C. During combustion at 900 °C more of the manganese in these fuels appeared volatilise. Agricultural waste ash retained almost all of its original manganese.

Complete retention of manganese in ash was predicted by thermodynamic equilibrium modelling of wood-bark, 70 % wood-bark / 30 % agricultural waste and 100 % agricultural waste combustion. This is by the formation of the manganese oxides Mn_2O_3 or Mn_3O_4, and if these were excluded from prediction, MnO. The predictions explain the behaviour of manganese during combustion at 800 °C. Experiments conducted at 900 °C, however, have shown some volatilisation of manganese.

Some manganese was released from the fuels during combustion. This manganese has probably formed MnO in the gas phase. It is thermodynamic favoured to be a solid, however, it probably only partial recondensed on ash, as described in Section 5.0.3.

5.5.13 Molybdenum

Molybdenum appears to have been almost completely retained by wood-bark ash (55 – 100 %) and the ashes from wood-bark / agricultural waste blends burnt at 800 °C (70 – 100 %). Some molybdenum has been volatilised, from the agricultural waste (5 – 75 %) and the 90 % wood-bark / 10 % agricultural waste blend (20 – 60 %) burnt at 900 °C.

Thermodynamic equilibrium modeling of molybdenum to determine the cause of the retention was attempted, but had to be abandoned due to a lack of thermodynamic data for molybdenum compounds.

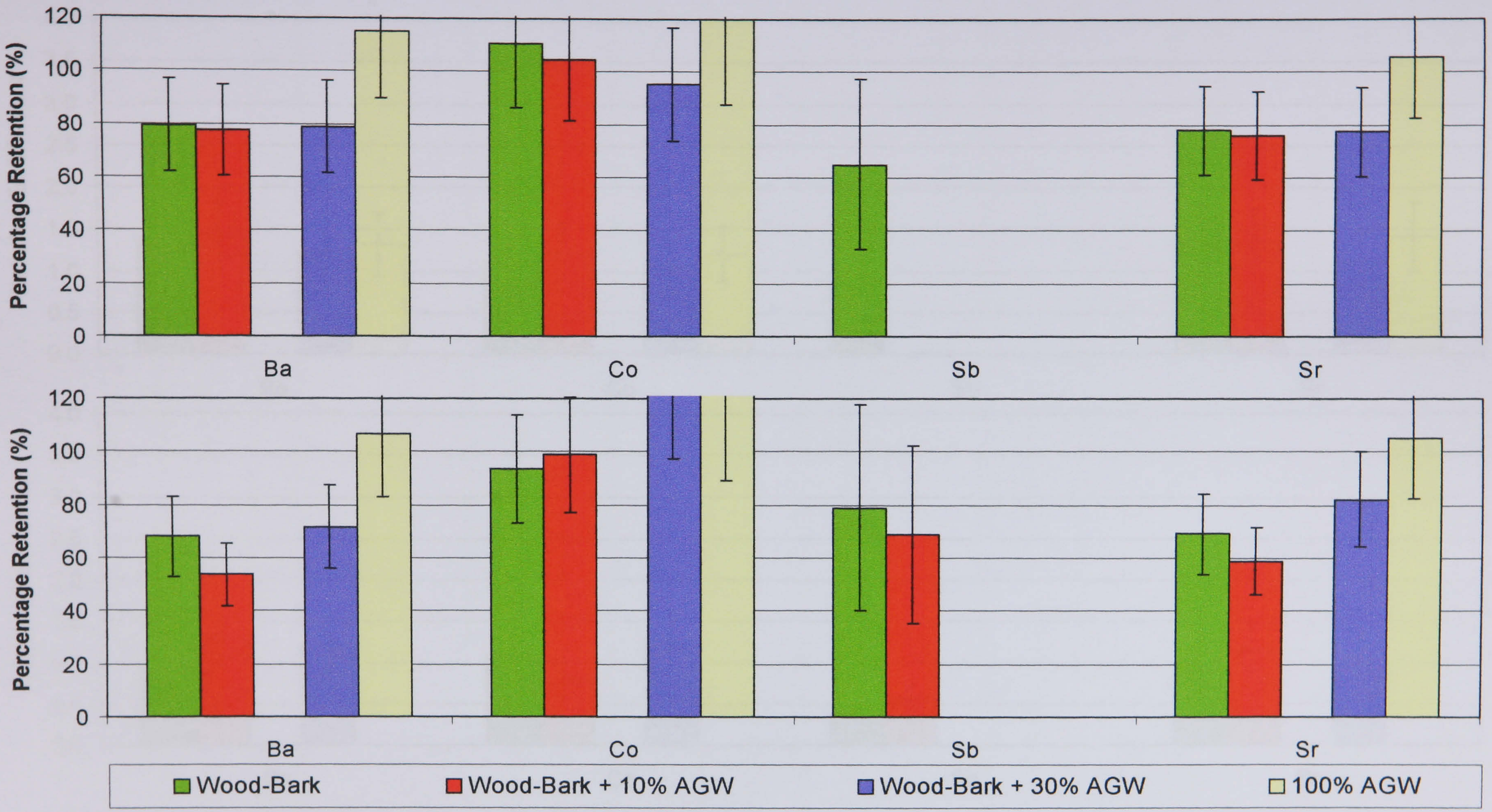
5.5.14 Thallium

Thallium was partially volatilised from wood-bark (45 – 90 %), agricultural waste (15 – 95 %) and blends of these fuels (60 – 85 %). The proportion of thallium retained by the blends was not measurably different from that retained by ash of the pure fuels. Plotting

the amount of thallium retained (per gram of fuel) against the proportion of agricultural waste, however, the 800 °C results suggest that there could be a small synergy for thallium release between the fuels.

Thermodynamic modelling suggests all thallium should have been volatilised. All thallium was predicted to form TlCl, TlOH or Tl gas during wood-bark, 70 % wood-bark / 30 % agricultural waste blend or 100 % agricultural waste combustion. Most thallium retention by ash was probably because it was contained in modes of occurrence in the fuels that prevented its volatilisation during combustion.

This is not true for all of the thallium, however, as it was enriched on the sinter ash of agricultural waste burnt at 800 °C (Figure 90). Therefore there must have been a solid thallium compound (not included in the thermodynamic model) formed. This compound could have caused the retention of some thallium in ash of other fuels, and may be responsible for the slight synergy for thallium release.



Trace Element Concentration in raw fuels (ppm):	Ba	Co	Sb	Sr
Wood-Bark	156 ± 14	0.72 ± 0.06	0.21 ± 0.10	51 ± 4
Agricultural Waste	13 ± 1	0.40 ± 0.07	0.08 ± 0.02	19 ± 2

Figure 94 Percentage Retention of Ba, Co, Sb and Sr in Ash After Wood-Bark / Agricultural Waste Co-Combustion

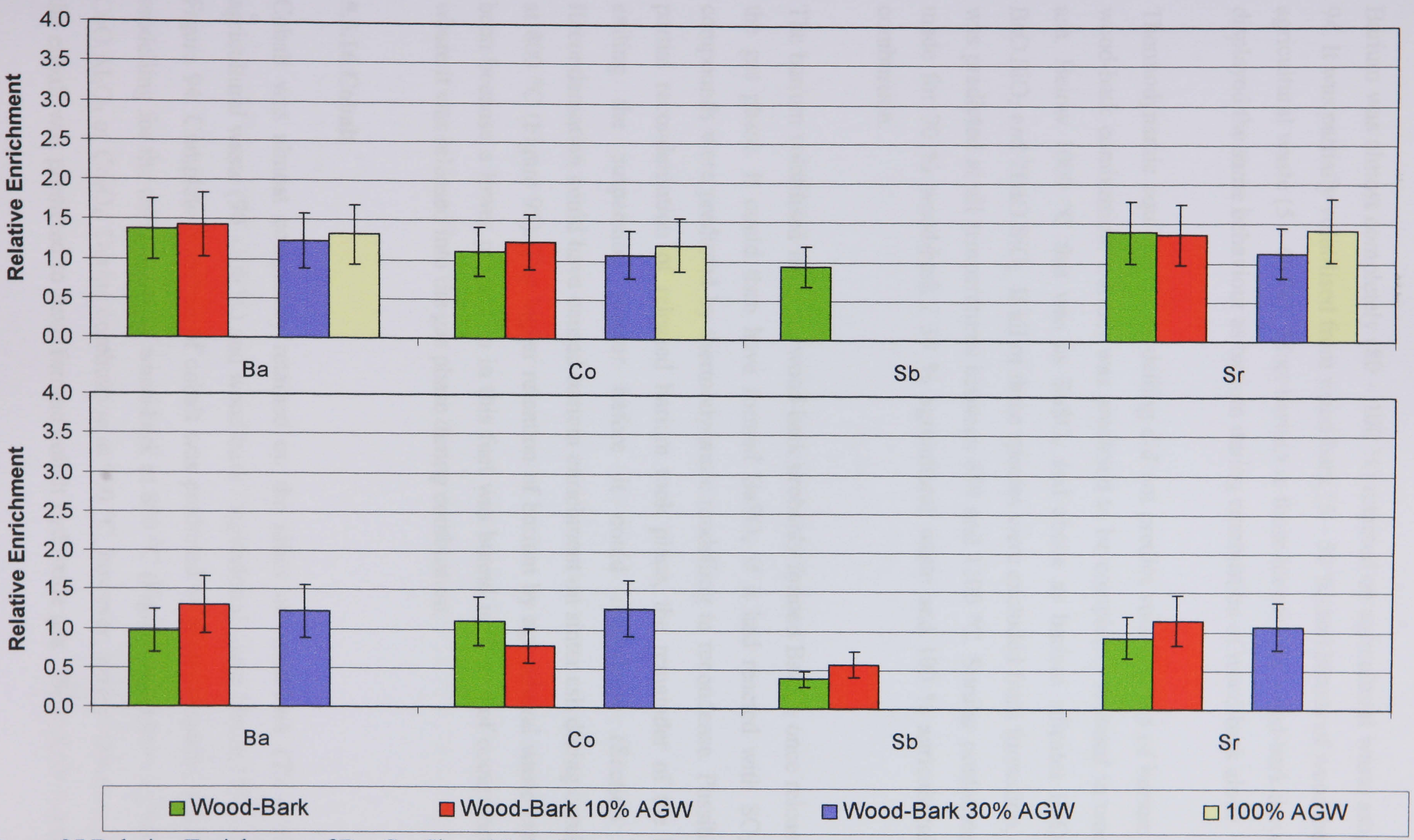


Figure 95 Relative Enrichment of Ba, Co, Sb and Sr in Sinter Ash During Wood-Bark / Agricultural Waste Co-Combustion

Note: A relative enrichment of one corresponds to that element being found in equal concentrations in the sinter and bottom ashes

5.5.15 Barium

Barium was almost completely (80 – 100 %) retained on agricultural waste ash, Figure 94. It was partially volatilised from wood-bark (5 – 50 %) and blends of wood-bark with agricultural waste (5 – 60 %). Most barium in those blends was wood-bark derived and displayed the same behaviour as barium during combustion of wood-bark alone.

Thermodynamic equilibrium modelling did not predict volatilisation of barium during wood-bark combustion. Barium was predicted to be completely retained in wood-bark ash. Below 1000 °C this was as $BaSO_4$ and above as barium silicates $BaO.2SiO_2$, $BaO.SiO_2$ and $2BaO.SiO_2$. If all of these species were excluded from formation, $BaCO_3$ was predicted at all temperatures between 650 and 1100 °C. Similar predictions were made for 70 % wood-bark / 30 % agricultural waste and 100 % agricultural waste combustion.

The barium volatilised from the wood-bark probably formed $BaCO_3$ once released into the gas phase. It could then have formed $BaSO_4$ if it had reacted with SO_2. Both compounds were predicted by thermodynamic modelling to recondense. Possibly only partial recondensation of released barium took place, the remainder of the barium exiting the suspension reactor before it could recondense (Section 5.0.3). Recondensation could have caused barium enrichment on sinter ash during combustion at 800 °C (Figure 95). The higher retention of barium by agricultural waste may have been because a lower proportion in this fuel was bound in modes of occurrence from where it was released into the gas phase during combustion.

5.5.16 Cobalt

Cobalt was almost completely retained on the ashes of wood-bark (75 – 100 %), agricultural waste (90 –100 %) and wood-bark / agricultural waste blends (75 – 100 %), Figure 94. Complete retention of cobalt was predicted by thermodynamic equilibrium modelling for the combustion of wood-bark at 800 °C (Figure 96), where it could form $CoO.Al_2O_3$ or Co_3O_4. During combustion at 900 °C, however, around fifteen percent of the cobalt was predicted to have formed cobalt hydroxide gas. This cobalt would have

escaped from the reactor. It cannot be determined if whether this has occurred, due to experimental error.

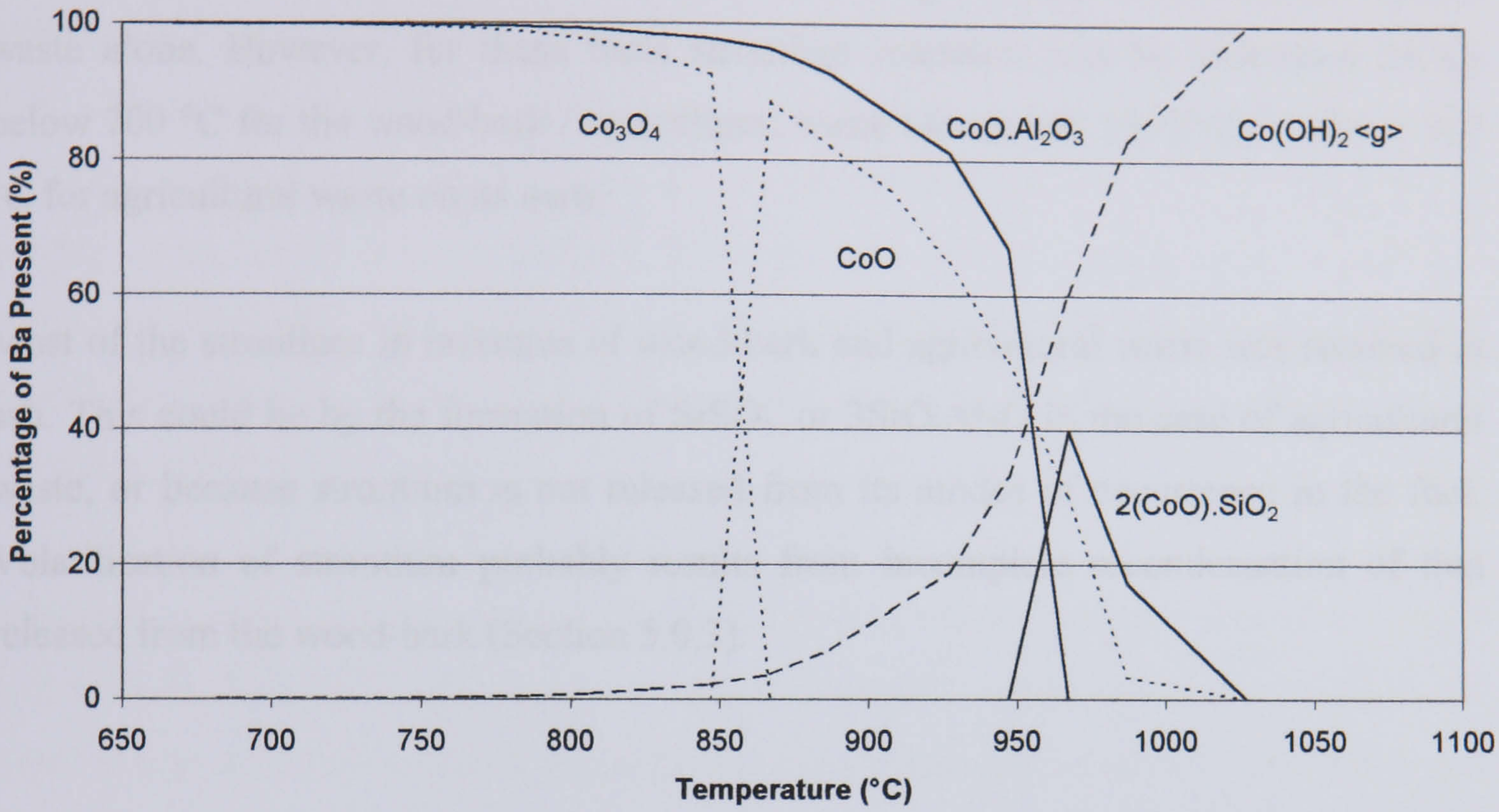


Figure 96 Thermodynamic Equilibrium Prediction for Co During Wood-Bark Combustion

5.5.17 Antimony

Antimony appears to have been partially volatilised from wood-bark (up to 70 %), however the wide range of experimental error prevents confirmation (Figure 94). Analytical error has prevented retention results for any more than one of the wood-bark / agricultural waste blends. In this result antimony was probably also partially volatilised (up to 65 %) however again the wide range of experimental error prevents confirmation.

5.5.18 Strontium

Strontium was almost completely retained on agricultural waste ash (80 – 100 %), but partially volatilised from wood-bark (5 – 50 %). Strontium in wood-bark / agricultural waste blends was mostly wood-bark derived and was partially (5 – 55 %) volatilised, like that in wood-bark. These results are very similar to those obtained for barium (Section 5.5.15, above).

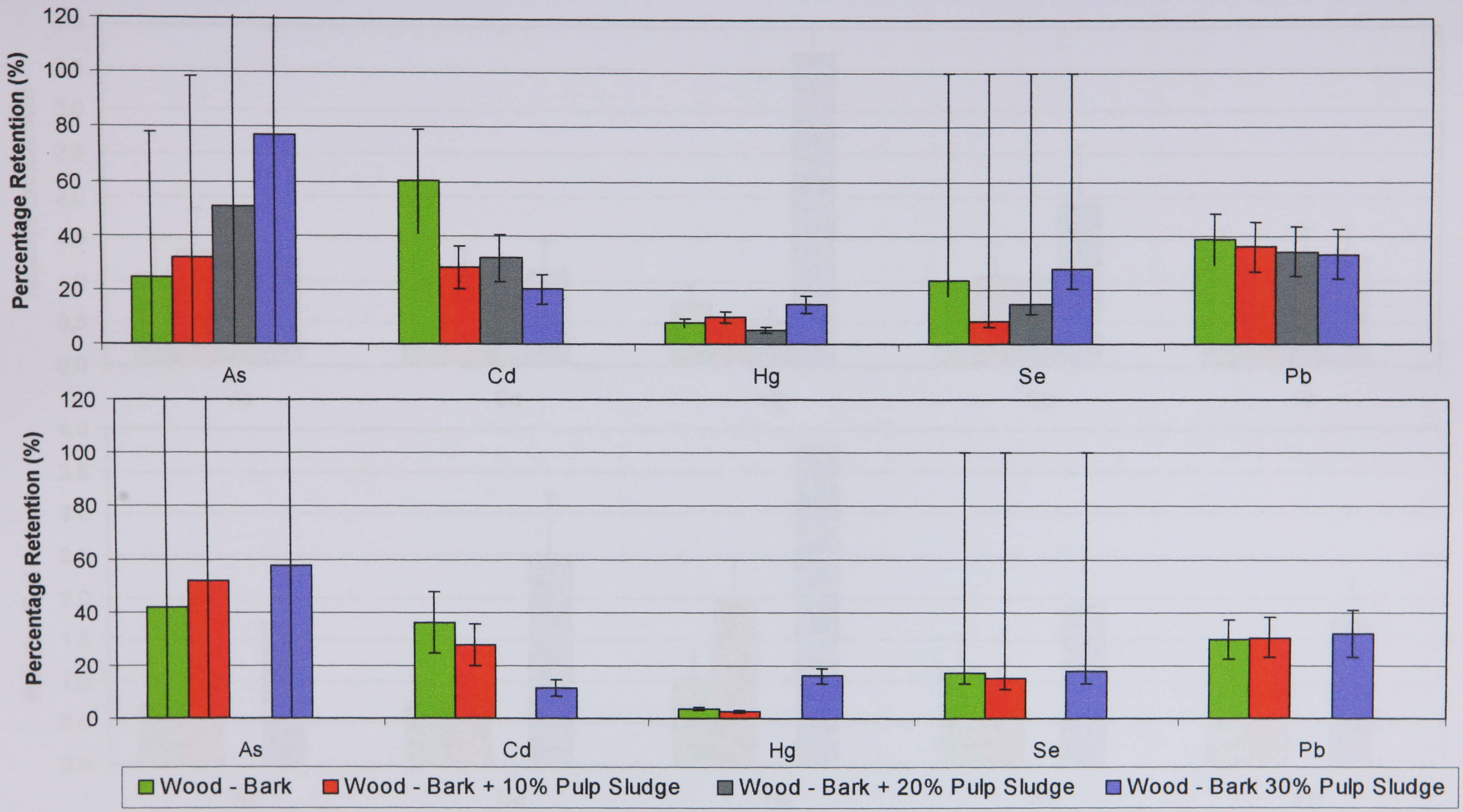
Thermodynamic equilibrium models for strontium during wood-bark combustion predicted complete retention by formation of strontium sulphate. This was also predicted for combustion of 70 % wood-bark / 30 % agricultural waste and agricultural waste alone. However, for these fuels strontium retention was by formation $SrCO_3$ below 700 °C for the wood-bark / agricultural waste blends and $3SrO.Al_2O_3$ above 900 °C for agricultural waste on its own.

Most of the strontium in mixtures of wood-bark and agricultural waste was retained in ash. This could be by the formation of $SrSO_4$, or $3SrO.Al_2O$ in the case of agricultural waste, or because strontium is not released from its modes of occurrence in the fuel. Volatilisation of strontium probably results from incomplete recondensation of that released from the wood-bark (Section 5.0.3).

5.6 Co-combustion of Wood – Bark and Pulp Sludge

Pulp sludge is another waste material from papermaking. It has a low ash content, so combustion is a very good method of disposing of it. Pulp sludge also has a very low bulk density, which makes transportation over long distances uneconomic. The preferred option is to burn it at the site of production, with other waste from paper making, such as wood-bark stripped from the logs before pulping. This solution is particularly desirable since both of these uncontaminated wood-based wastes have been classified as biomass by the EU for the purpose of setting combustion emission limits (2000/76/EC).

Pulp sludge used in this study was supplied by Kvaerner Pulping Oy from their paper mill at Oulu, Finland. It was mostly wood and is similar in appearance and origin to the paper sludge also used in this study. Like the paper sludge, it could only be fed into the suspension-firing reactor from the feed hopper if mixed with another fuel. Therefore again, the absence of results for the amount of each trace element retained when firing pulp sludge ash alone, limits the possibility of identifying a synergy for retention or release of a trace element in co-firing.



Trace Element Concentration in Raw Fuels (ppm):	As	Cd	Hg	Se	Pb
Wood-Bark	0.44 ± 0.95	0.20 ± 0.05	0.033 ± 0.001	<0.8	3.1 ± 0.4
Pulp Sludge	0.50 ± 0.46	1.99 ± 0.32	0.083 ± 0.004	<0.8	2.3 ± 0.8

Figure 97 Percentage Retention of As, Cd, Hg, Se and Pb in Ash After Wood-Bark / Pulp Sludge Co-Combustion

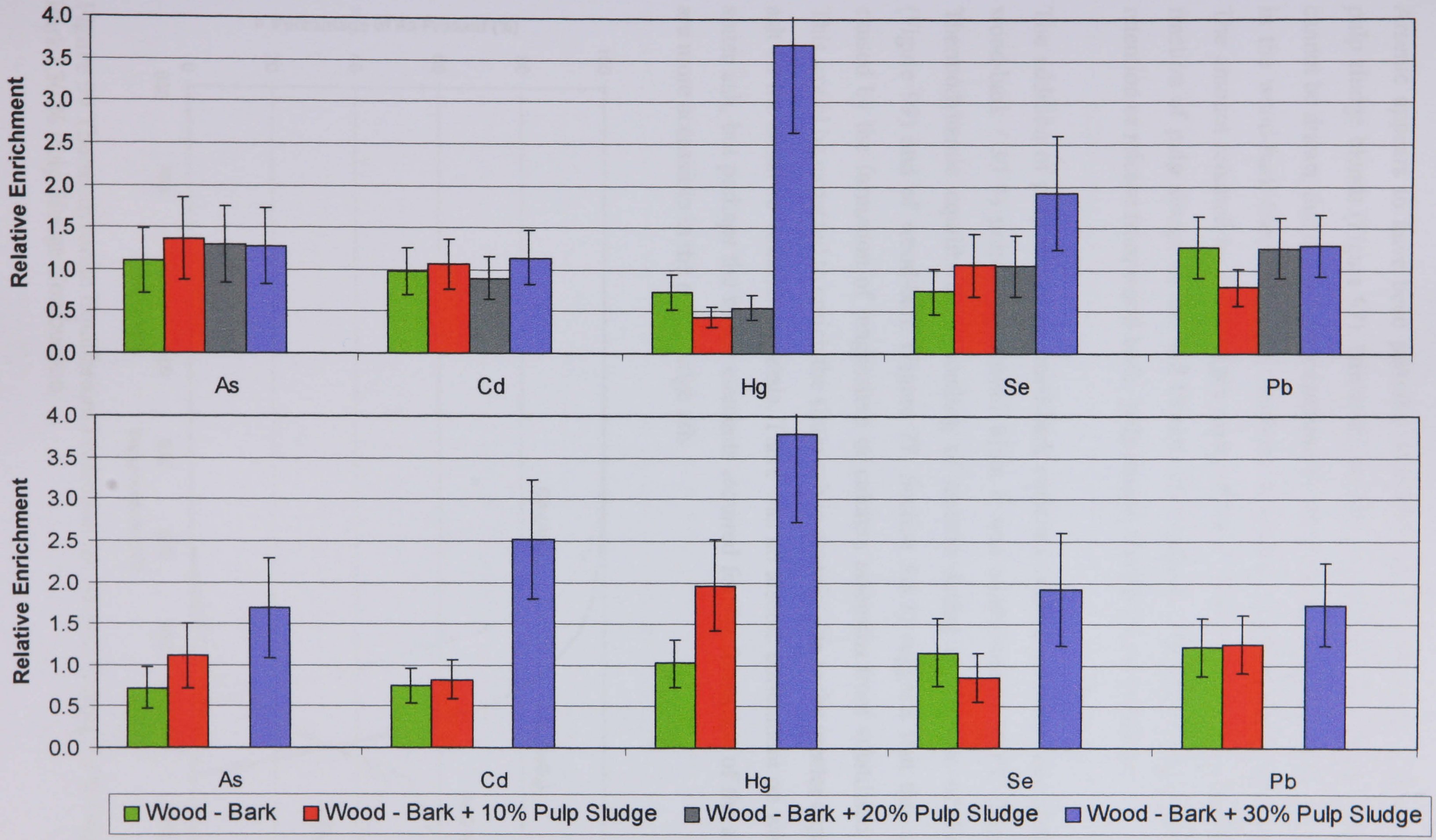


Figure 98 Relative Enrichment of As, Cd, Hg, Se and Pb in Sinter Ash During Wood-Bark / Pulp Sludge Co-Combustion

Note: A relative enrichment of one corresponds to that element being found in equal concentrations in the sinter and bottom ashes

5.6.1 Arsenic

Arsenic appears to have been partially volatilised from wood-bark, and wood-bark / pulp sludge blends (Figure 97). However, definite conclusions on arsenic volatilisation cannot be drawn, due to the large experimental error measurement of the arsenic content in the wood-bark (Section 5.5.1). Analysis of arsenic in ash samples was unaffected. The amount retained by the ash (per gram of fuel) increased linearly with the weight fraction of pulp sludge in the fuel blends. This indicates that any synergy for arsenic retention or release from wood-bark / pulp sludge blends was insignificant

The addition of pulp sludge to wood-bark enriched arsenic on sinter ash of the 70 % wood-bark / 30 % pulp sludge blend when it was combusted at 900°C (Figure 98). Thermodynamic equilibrium modelling of arsenic during combustion of this blend (Figure 99) and of wood-bark (Figure 77, Section 5.5.1) suggests that this could be caused by the formation of magnesium or calcium arsenates from volatilised arsenic. This would be expected to enrich the sinter ash in arsenic, due to the greater exposure of ash on the sinter to volatilised metals. There was no arsenic enrichment on wood-bark sinter ash, but perhaps the minor elements required for the formation of the arsenates are more accessible in the pulp sludge ash.

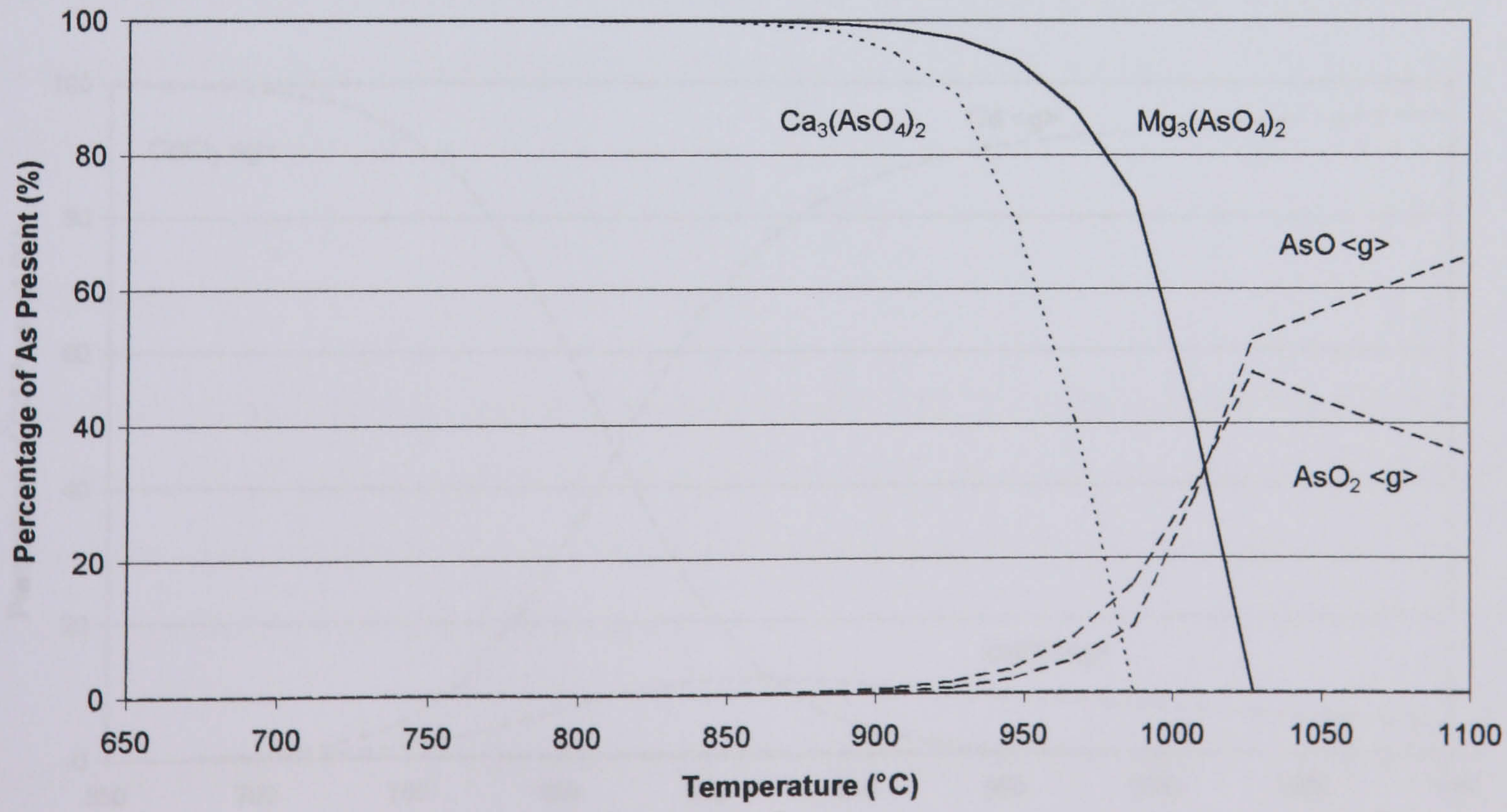


Figure 99 Thermodynamic Equilibrium Prediction for Arsenic During 70 % Wood-Bark / 30 % Pulp Sludge Combustion

5.6.2 Cadmium

Cadmium appears to have been partially (20 – 75 %) volatilised from wood-bark during combustion (Figure 97). Blending pulp sludge with the wood-bark increased the proportion of cadmium volatilised to up to 90 %. However, the linear relationship between the amount of cadmium retained in ash (per gram of fuel) and the weight fraction of pulp sludge suggests any synergy between these fuels for cadmium release was insignificant.

Thermodynamic equilibrium models for cadmium during the combustion of wood-bark (Figure 79, Section 5.5.2) and of 70 % wood-bark / 30 % pulp sludge (Figure 100) predict all cadmium to have been in the gas phase. Cadmium that was retained in the ash was probably not released from its mode(s) of occurrence in the fuels. Hence, the fall in the proportion of cadmium retained in ash with increasing pulp sludge content was probably the result of greater cadmium release from pulp sludge than wood-bark.

Some cadmium does appear to have recondensed on sinter ash, causing enrichment for the 70 % wood-bark / 30 % pulp sludge blend burnt at 900 °C. The cadmium compound that has recondensed here is unknown, but may have also formed during combustion of other wood-bark / pulp sludge blends, though not in significant amounts.

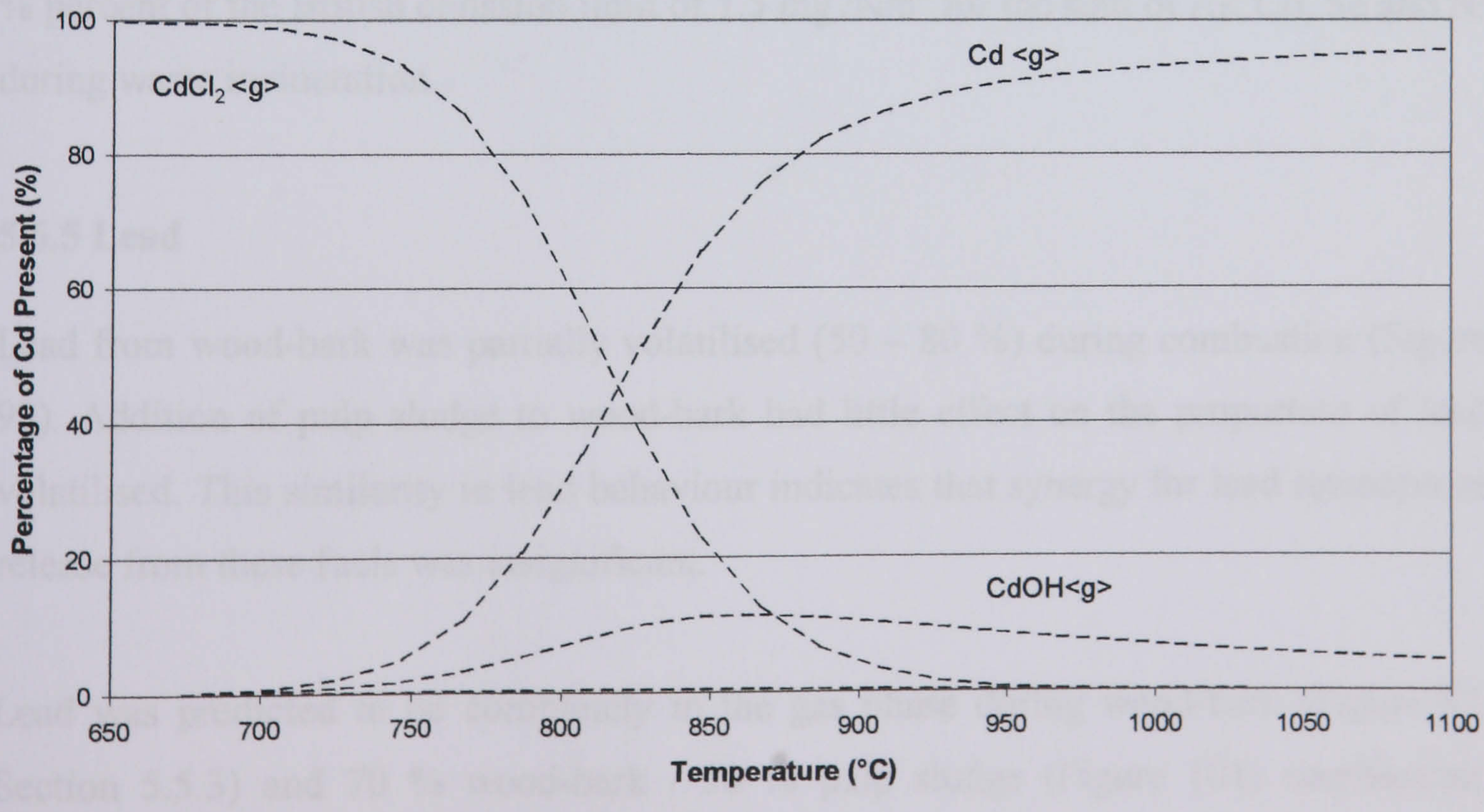


Figure 100 Thermodynamic Equilibrium Prediction for Cadmium During 70 % Wood-Bark / 30 % Pulp Sludge Combustion

5.6.3 Mercury

Mercury has been almost completely volatilised from wood-bark (90 – 95 %) and from wood-bark / pulp sludge blends (80 – 98 %) during combustion (Figure 97). The proportion retained seems to have increased slightly with pulp sludge addition, as has enrichment on sinter ash during combustion at 900 °C (Figure 98). The cause of this enrichment is unclear. All mercury was predicted to be gaseous as Hg or HgO during combustion of wood-bark and wood-bark / pulp sludge blends. Perhaps an unknown solid mercury compound has formed, as suggested in Section 5.2.3.

5.6.4 Selenium

Measurement of the proportion of selenium retained in ash of wood-bark and wood-bark / pulp sludge blends was hindered by the very low selenium content of both fuels (less than <0.8 ppm). Concentrations of selenium in the ash were also close to the limits of quantification.

Complete selenium volatilisation was predicted by thermodynamic equilibrium models of wood-bark, 70 % wood-bark / 30 % agricultural waste and 100 % agricultural waste combustion. If all selenium in these fuels was volatilised the selenium concentration in the flue gas would not exceed 0.005 mg /Nm^3 at 6 % oxygen. This value is less than 0.5 % percent of the British emission limit of 1.5 mg /Nm^3 for the sum of As, Co, Se and Ni during waste incineration.

5.6.5 Lead

Lead from wood-bark was partially volatilised (50 – 80 %) during combustion (Figure 97). Addition of pulp sludge to wood-bark had little effect on the proportion of lead volatilised. This similarity in lead behaviour indicates that synergy for lead retention or release from these fuels was insignificant.

Lead was predicted to be completely in the gas phase during wood-bark (Figure 82, Section 5.5.3) and 70 % wood-bark / 30 % pulp sludge (Figure 101) combustion. Without a solid lead species forming above the sinter temperature (approximately 750 °C during 800 °C experiments) all lead released from the fuel is expected to have passed

through the sinter and been lost. Thus most retained lead was probably not released from its modes of occurrence in the fuels, preventing its volatilisation.

Lead was however, slightly enriched on sinter ash of the 70 % wood-bark / 30 % pulp sludge blend burnt at 900 °C (Figure 98). This is unexpected and shows a condensed lead compound (not included in the thermodynamic database) formed at high temperatures. This compound may have also formed during the combustion of other wood-bark / pulp sludge blends but not to a measurable extent.

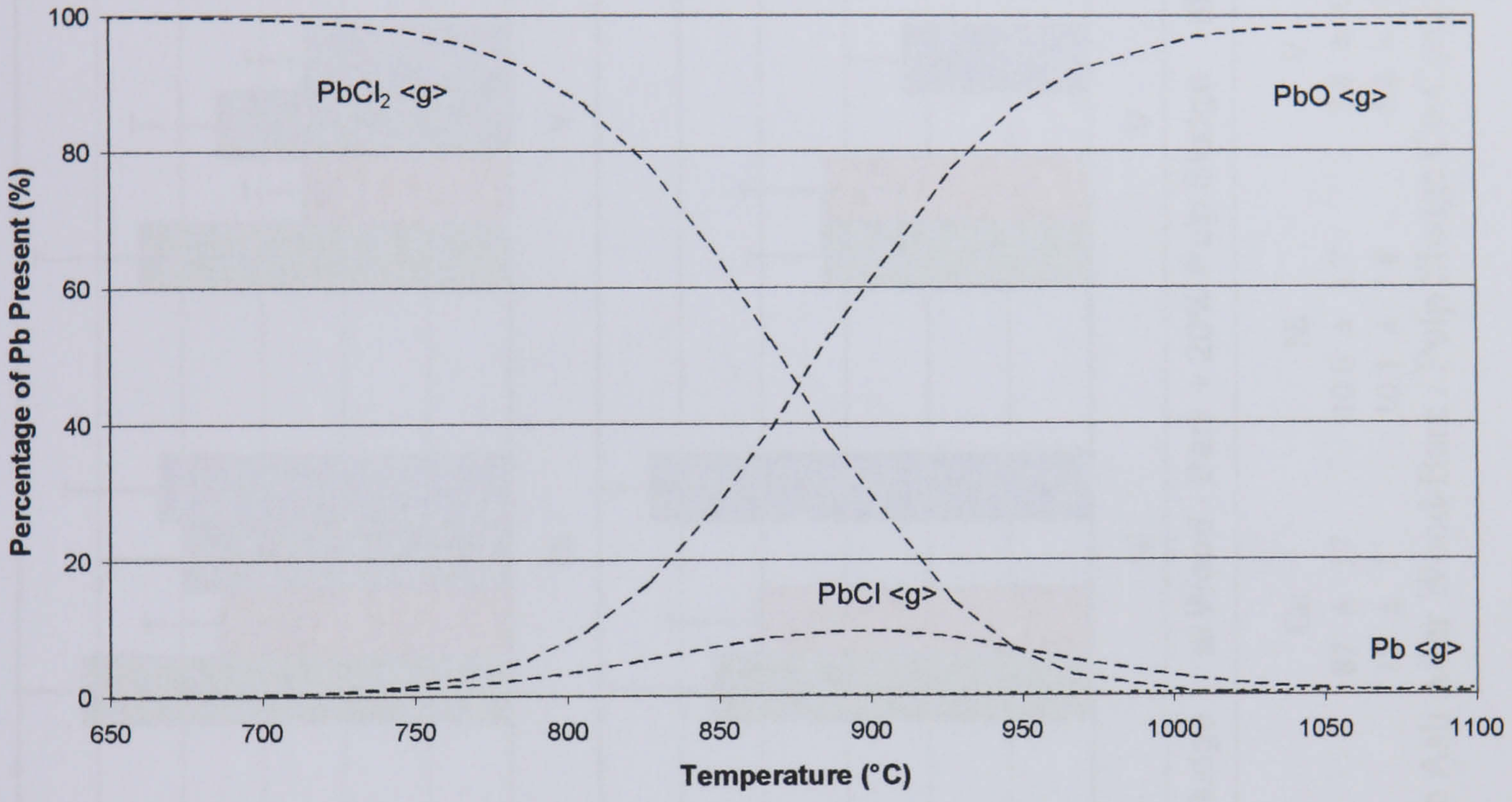
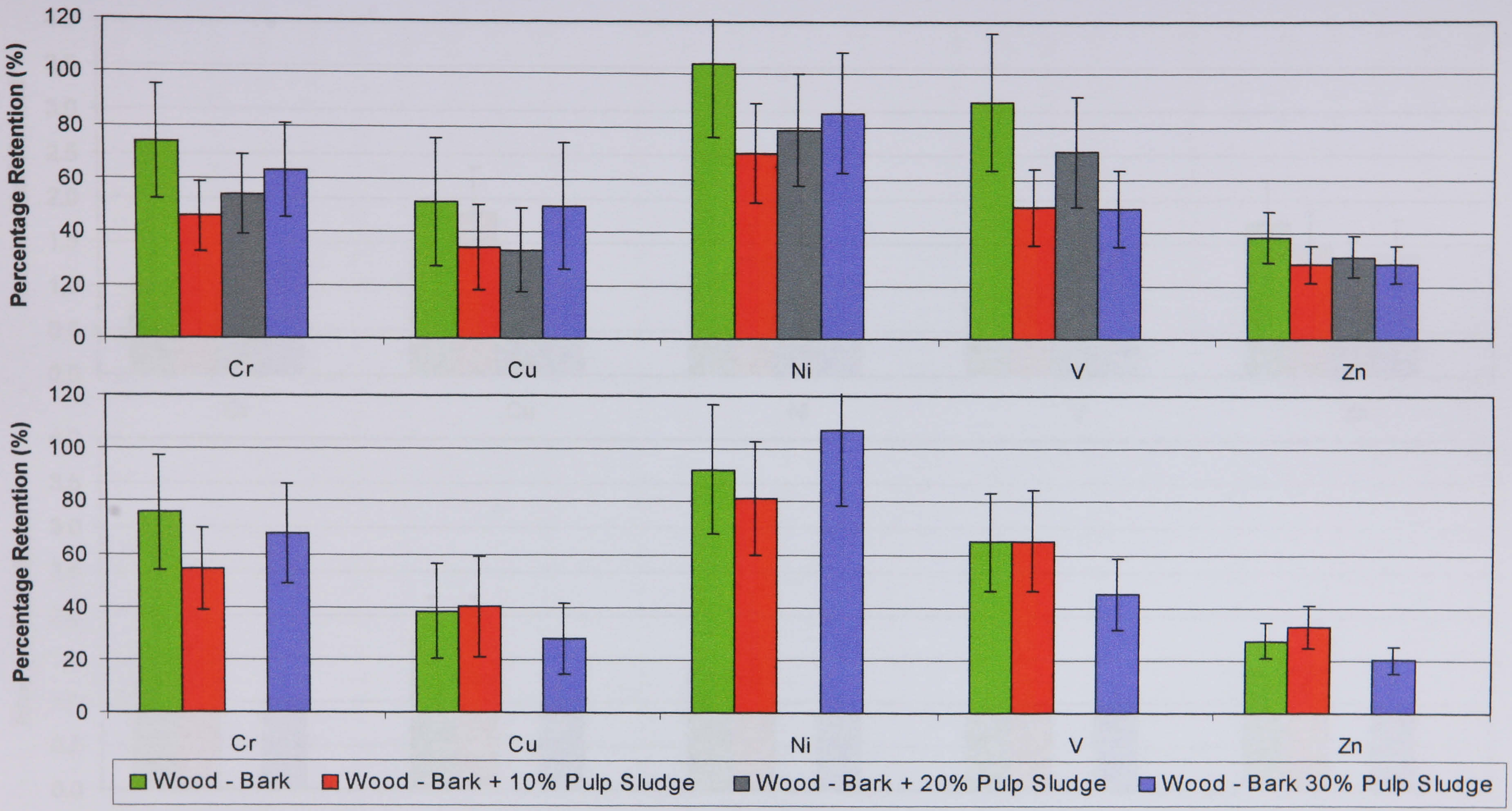


Figure 101 Thermodynamic Equilibrium Prediction for Lead During 70 % Wood-Bark / 30 % Pulp Sludge Combustion



Trace Element Concentration in raw fuels (ppm):	Cr	Cu	Ni	V	Zn
Wood-Bark	26 ± 5	87 ± 37	10.0 ± 1.7	2.8 ± 0.6	150 ± 21
Pulp Sludge	25 ± 4	15 ± 7	10.1 ± 1.8	5.2 ± 1.2	200 ± 31

Figure 102 Percentage Retention of Cr, Cu, Ni, V and Zn in Ash After Wood-Bark / Pulp Sludge Co-Combustion

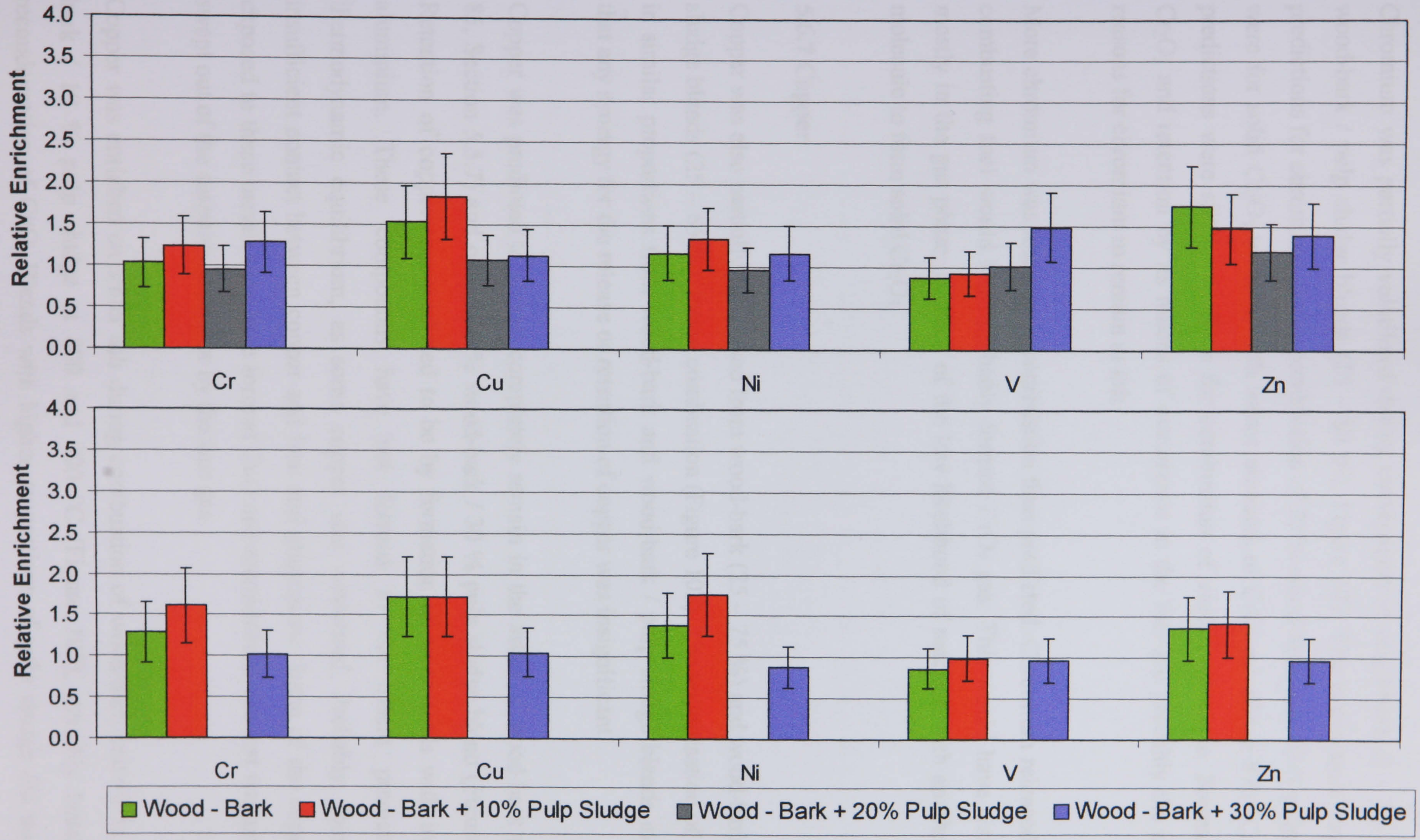


Figure 103 Relative Enrichment of Cr, Cu, Ni, V and Zn in Sinter Ash During Wood-Bark / Pulp Sludge Co-Combustion

Note: A relative enrichment of one corresponds to that element being found in equal concentrations in the sinter and bottom ashes

5.6.6 Chromium

Chromium was partially volatilised during combustion of wood-bark (2 – 50 %) and wood-bark / pulp sludge blends (25 – 80 %), Figure 102. Thermodynamic modelling predictions for chromium during combustion of 70 % wood-bark with 30 % pulp sludge were for solid Cr_2O_3 to form, with minor amounts of CrO_3 gas above 870 °C. These predictions were similar to those for combustion of wood-bark alone. Formation of Cr_2O_3 and retention by its modes of occurrence in the fuel are probably the primary reasons for chromium to remain in ash.

More chromium was lost during combustion than predicted. Chromium released by the combusting fuel would have probably formed CrO_3 gas. This would have remainder mostly in the gas phase, because of the low likelihood of reaction with another CrO_3 molecule to form solid Cr_2O_3.

5.6.7 Copper

Copper was also partially volatilised from wood-bark (25 – 75 %) and wood-bark / pulp sludge blends (25 – 65 %) during combustion (Figure 102). The volatilisation of copper in similar proportions from wood-bark and wood-bark / pulp sludge blends indicates that any synergy for the release or retention of copper was insignificant.

Copper was predicted to almost completely remain in the ashes of wood-bark (Figure 85, Section 5.5.7) and of the 70 % wood-bark / 30 % pulp sludge blend (Figure 104). Retention of copper was predicted to be by formation of compounds with iron and aluminium. These compounds have not formed to the extent predicted by thermodynamic equilibrium, as some copper was volatilised. Probably, there was insufficient contact between copper and iron and aluminium. Some of the copper not exposed to these metals may have formed CuO and recondensed, the rest was probably swept out of the suspension reactor by the flue gas.

Copper was enriched on sinter ash during combustion of wood-bark and 90 % wood-bark / 10 % pulp sludge at 800 and 900 °C (Figure 103), possibly because of recondensation of CuO. Blends with higher proportions of pulp sludge did not show

copper enrichment on sinter ash. Possibly, the high chlorine content of the pulp sludge (0.39 % daf) promoted formation of CuCl gas from copper in the gas phase instead of CuO. CuCl would not recondense at the temperature of the sinter (minimum temperature 750 °C) and thus not cause enrichment on sinter ash.

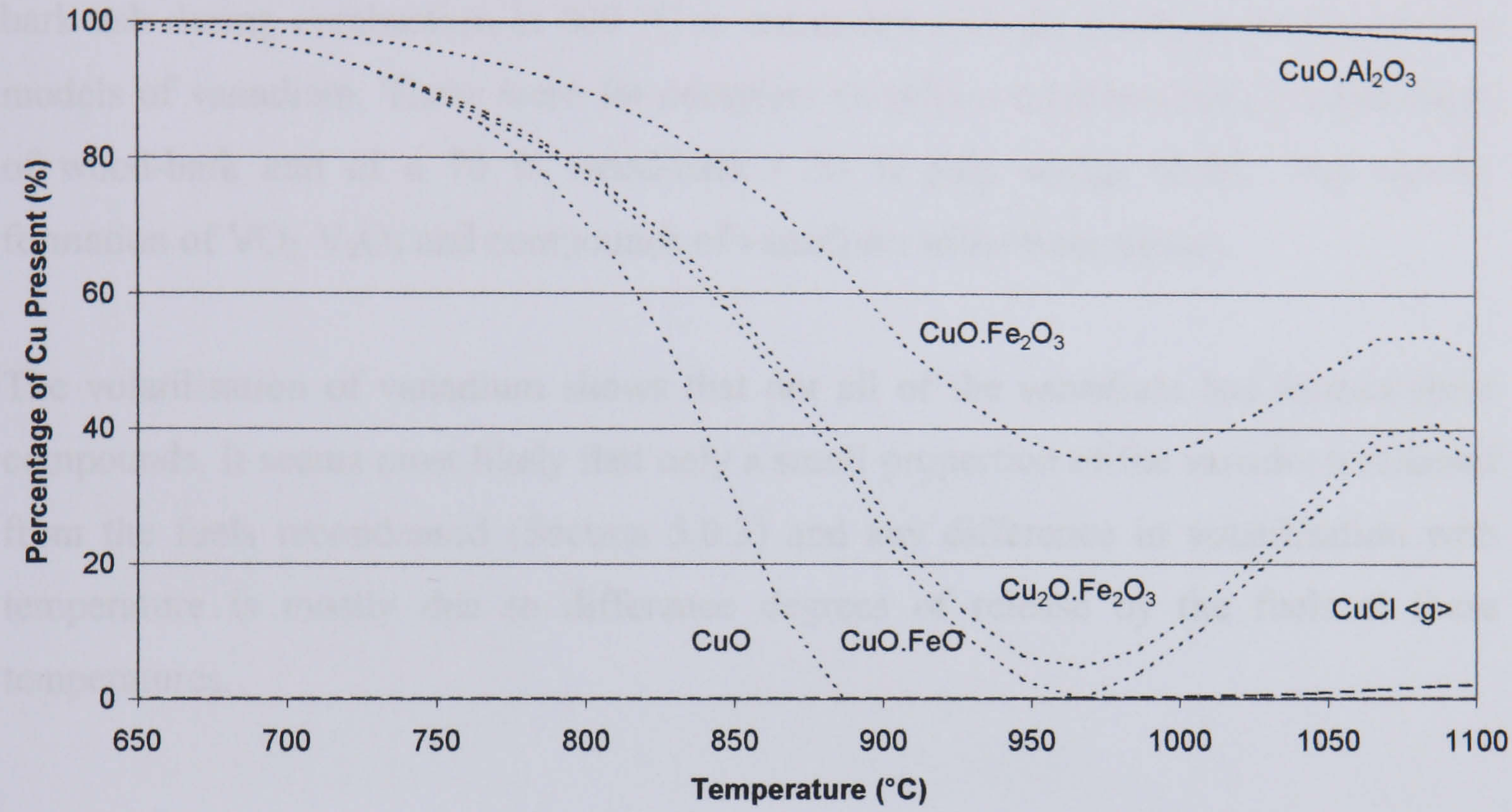


Figure 104 Thermodynamic Equilibrium Model of Copper During Combustion of 70 % Wood-Bark / 30 % Pulp Sludge

5.6.8 Nickel

Nickel was almost completely retained by wood-bark ash (65 – 100 %) and appears also to have been by the ash of wood-bark / pulp sludge blends (50 – 100 %), apart from the 90 % wood-bark / 10 % pulp sludge result at 800 °C, which was probably an anomaly.

Thermodynamic equilibrium modelling predicted complete nickel retention in wood-bark (Figure 87, Section 5.5.8) and 70 % wood-bark / 30 % pulp sludge (not shown) ashes. Retention on wood-bark ash was by formation of NiO, whilst $NiO.Fe_2O_3$ and $2NiO.SiO_2$ were predicted for the 70 % wood-bark / 30 % pulp sludge blend. The formation and recondensation of NiO from volatilised nickel may have caused the slight nickel enrichment on sinter ash (Figure 103).

5.6.9 Vanadium

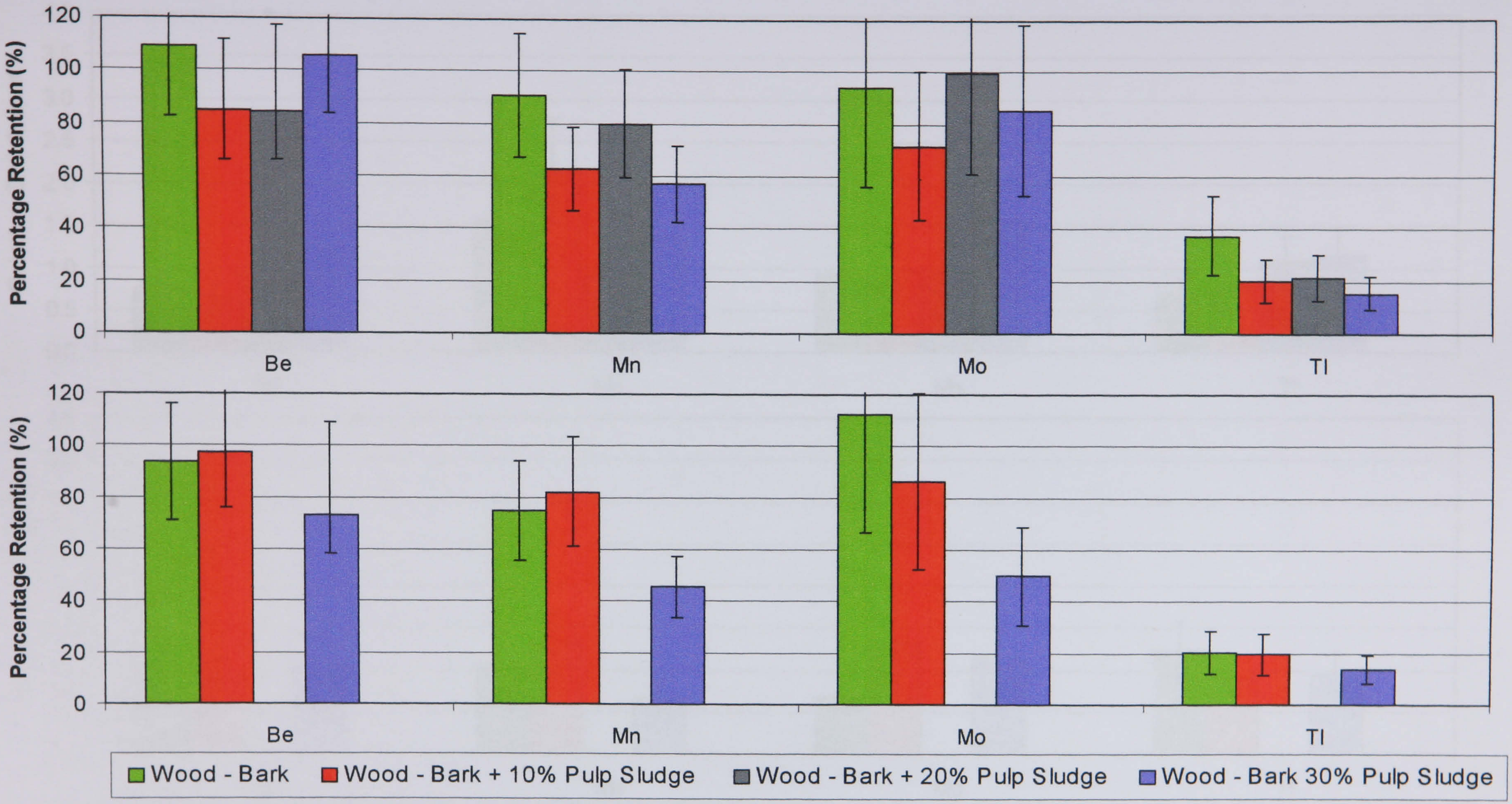
Most vanadium was retained on wood-bark ash after combustion at 800 °C (Figure 102). More (15 – 55 %) appeared to be liberated by combustion at 900 °C and by blending the wood-bark with pulp sludge (10 – 65 %). Vanadium retention by wood-bark ash during combustion at 800 °C is consistent with thermodynamic equilibrium models of vanadium. These were for complete vanadium retention during combustion of wood-bark and of a 70 % wood-bark / 30 % pulp sludge blend. This was by formation of VO_2, V_2O_5 and compounds of vanadium with minor metals.

The volatilisation of vanadium shows that not all of the vanadium has formed these compounds. It seems most likely that only a small proportion of the vanadium released from the fuels recondensed (Section 5.0.3) and any difference in volatilisation with temperature is mostly due to difference degrees of release by the fuels at these temperatures.

5.6.10 Zinc

Zinc was partially volatilised from wood-bark (50 – 80 %) and wood-bark / pulp sludge blends (60 – 85 %). Complete zinc retention in ash was predicted by thermodynamic equilibrium modelling. During combustion of wood-bark or a 70 % wood-bark / 30 % pulp sludge blend this was by the formation of $ZnO.Al_2O_3$, ZnO and $2ZnO.SiO_2$ (wood-bark only).

These compounds have not formed to the extent predicted, as up to 85 % of the zinc originally present has been volatilised. Possibly a large proportion of the zinc in these fuels was released during combustion. Once in the gas phase it would oxide to ZnO, possibly some of this zinc recondensing and causing enrichment on sinter ash (Figure 103). The remaining zinc was probably lost as described in section 5.0.3.



Trace Element Concentration in raw fuels (ppm):	Be	Mn	Mo	Tl
Wood-Bark	0.07 ± 0.01	414 ± 68	1.26 ± 0.44	0.09 ± 0.03
Pulp Sludge	<0.03	137 ± 22	1.0 ± 0.2	0.13 ± 0.04

Figure 105 Percentage Retention of Be, Mn, Mo and Tl in Ash After Wood-Bark / Pulp Sludge Co-Combustion

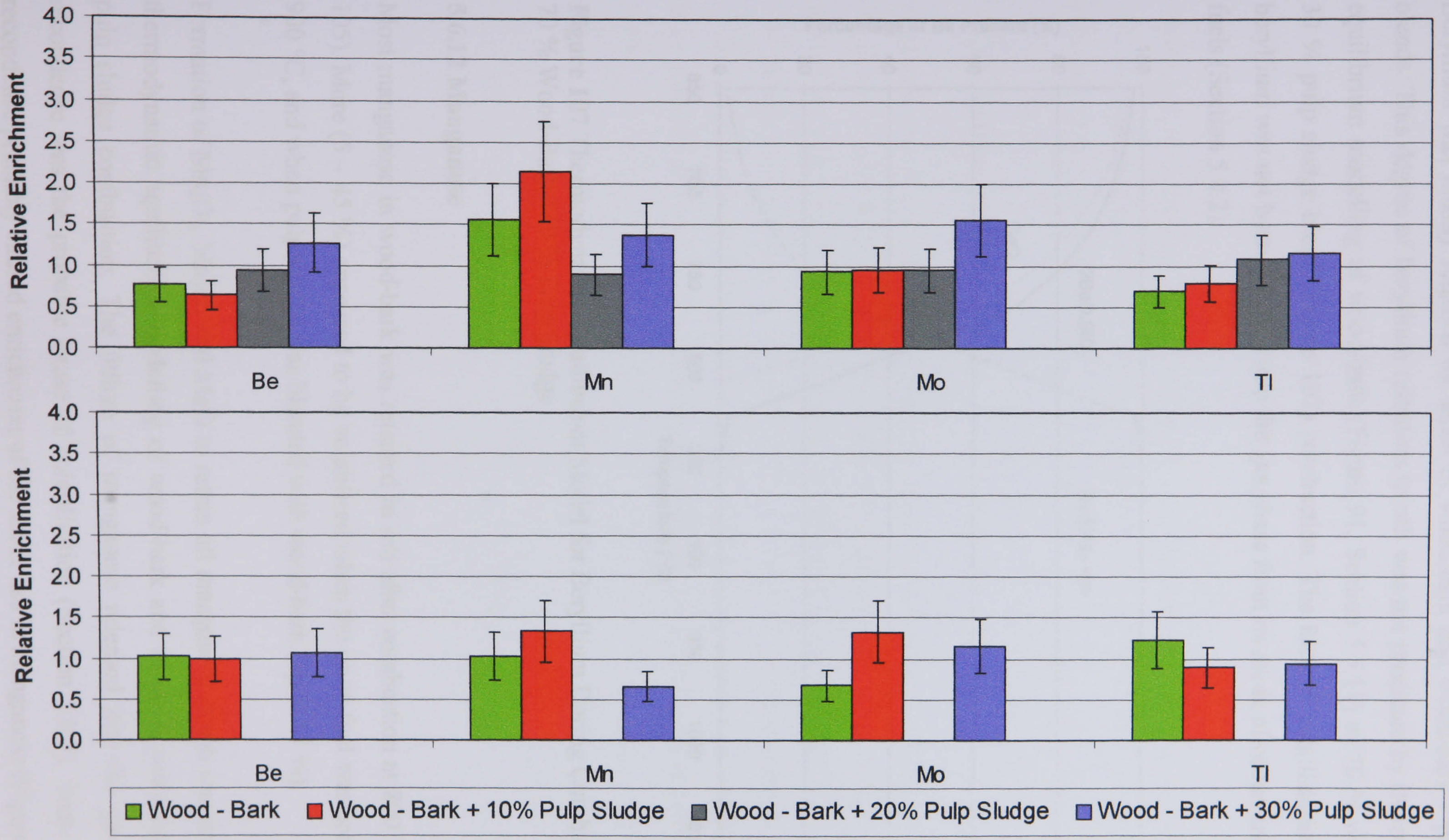


Figure 106 Relative Enrichment of Be, Mn, Mo and Tl in Sinter Ash During Wood-Bark / Pulp Sludge Co-Combustion

Note: A relative enrichment of one corresponds to that element being found in equal concentrations in the sinter and bottom ashes

5.6.11 Beryllium

Beryllium was mostly retained by ashes of wood-bark and wood-bark / pulp sludge blends. This degree of beryllium retention in ash was not predicted by thermodynamic equilibrium modelling of wood-bark (Figure 91, Section 5.5.11) or 70 % wood-bark / 30 % pulp sludge blend (Figure 107) combustion. The lack of volatilisation suggests beryllium was not been released into the gas phase from its mode of occurrence in these fuels (Section 5.0.2).

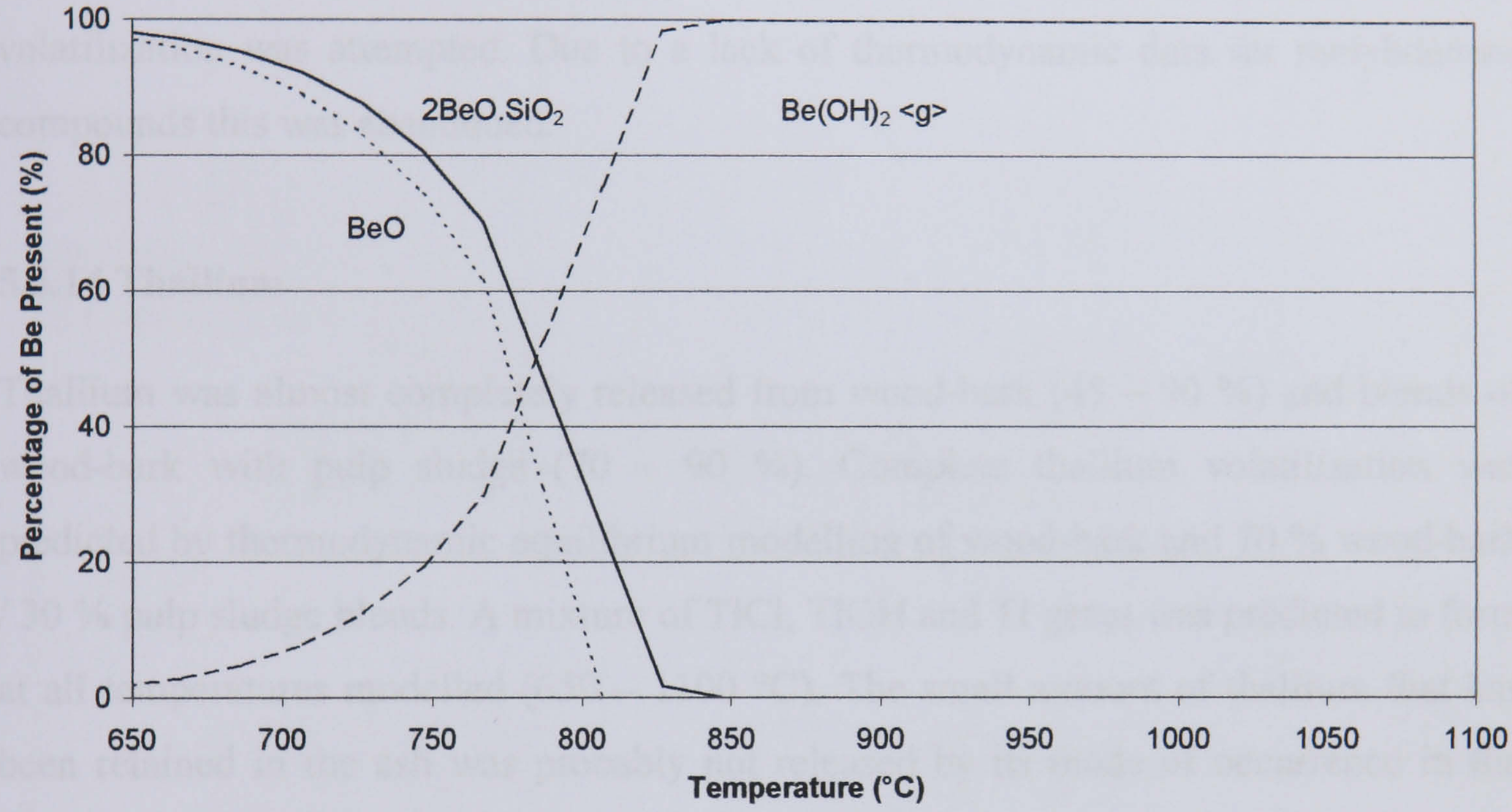


Figure 107 Thermodynamic Equilibrium Model for Beryllium During Combustion of 70 % Wood-Bark / 30 % Pulp Sludge

5.6.12 Manganese

Most manganese in wood-bark was retained in ash after combustion at 800 °C (Figure 105). More (5 – 45 %) appeared to be volatilised when the same fuel was combusted at 900 °C, and when pulp sludge was blended with wood-bark (up to 65 %).

Formation of Mn_2O_3, Mn_3O_4 and MnO to retain all manganese in ash was predicted by thermodynamic equilibrium modelling of wood-bark and of 70 % wood-bark / 30 % pulp sludge combustion. The failure of manganese released into the gas phase to recondense was the probable cause of volatilisation (Section 5.0.3). That which did recondense probably caused enrichment of the sinter ash in manganese (Figure 106).

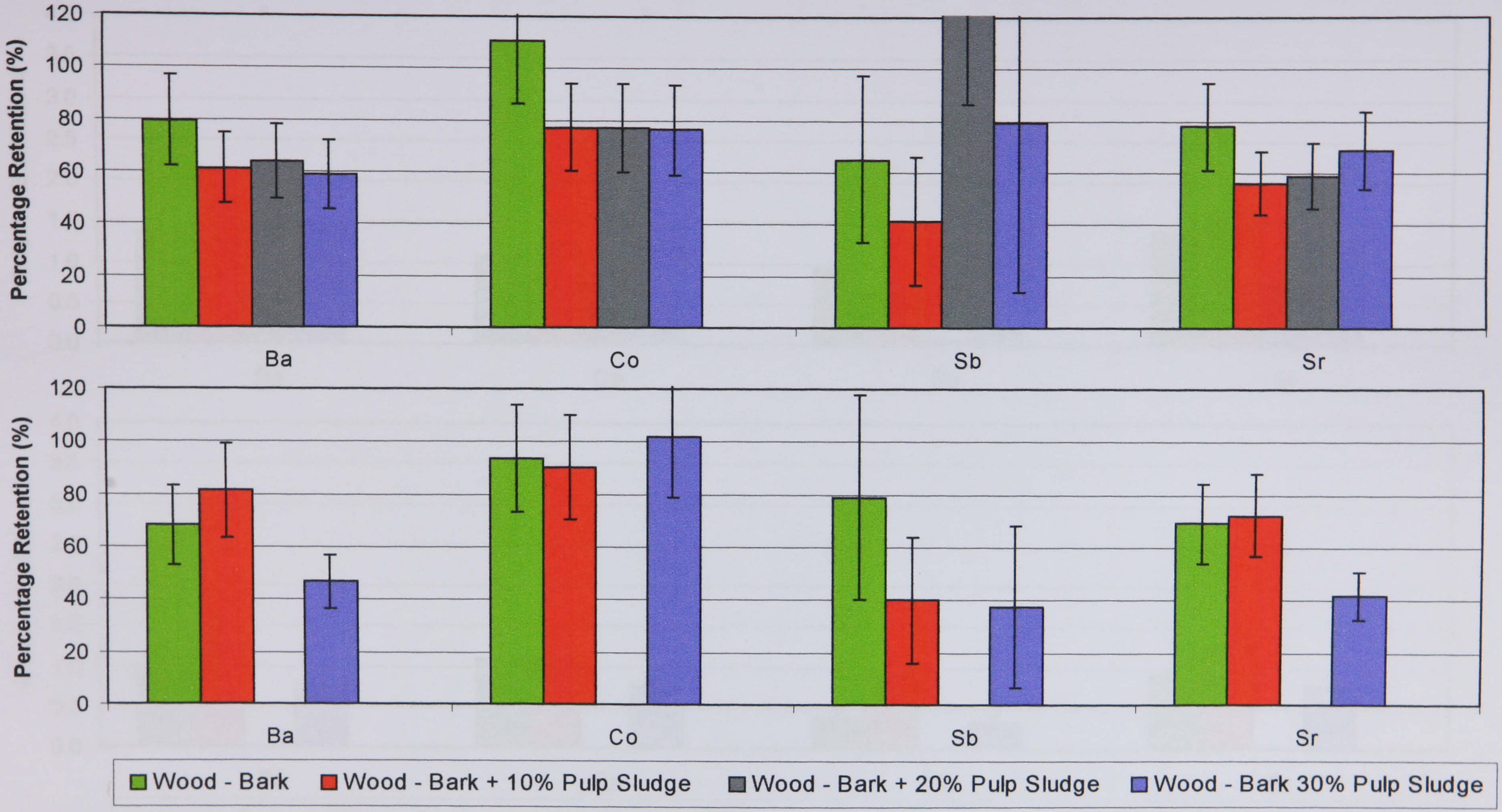
5.6.13 Molybdenum

Molybdenum was mostly retained in ashes from combustion at 800 °C of wood-bark (55 – 100 %) and wood-bark / pulp sludge blends (45 – 100 %), Figure 105. Combustion of wood-bark / pulp sludge blends at 900 °C appears to have caused molybdenum to volatilise, the proportion increasing with the fraction of pulp sludge.

Thermodynamic equilibrium modeling of molybdenum to determine the cause of this volatilization was attempted. Due to a lack of thermodynamic data for molybdenum compounds this was abandoned.

5.6.14 Thallium

Thallium was almost completely released from wood-bark (45 – 90 %) and blends of wood-bark with pulp sludge (70 – 90 %). Complete thallium volatilisation was predicted by thermodynamic equilibrium modelling of wood-bark and 70 % wood-bark / 30 % pulp sludge blends. A mixture of TlCl, TlOH and Tl gases was predicted to form at all temperatures modelled (650 – 1100 °C). The small amount of thallium that has been retained in the ash was probably not released by its mode of occurrence in the fuels.



Trace Element Concentration in raw fuels (ppm):	Ba	Co	Sb	Sr
Wood-Bark	156 ± 14	0.72 ± 0.06	0.2 ± 0.1	51 ± 4
Pulp Sludge	45 ± 6	0.45 ± 0.08	0.08 ± 0.02	11 ± 15

Figure 108 Percentage Retention of Ba, Co, Sb and Sr in Ash After Wood-Bark / Pulp Sludge Co-Combustion

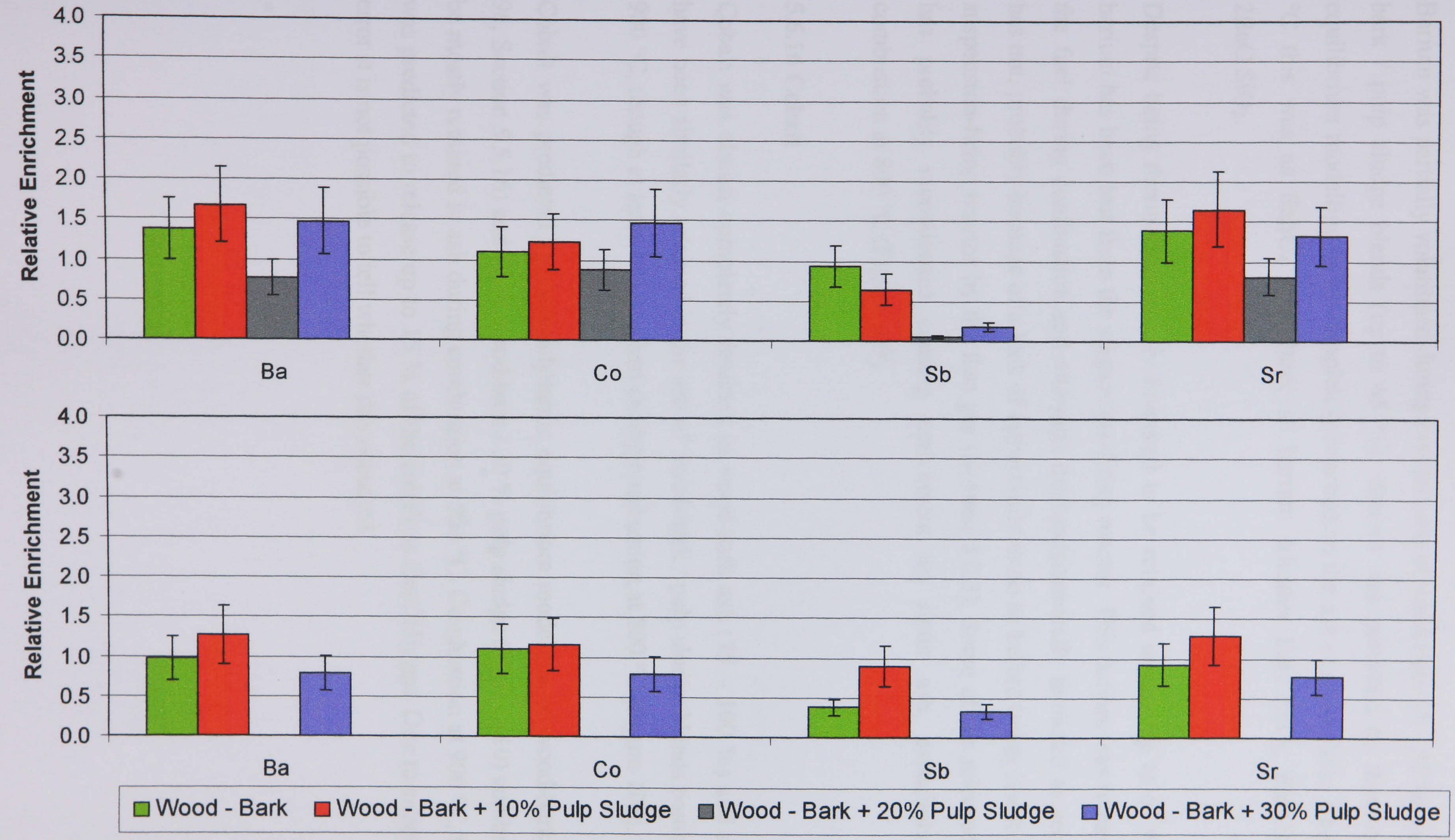


Figure 109 Relative Enrichment of Ba, Co, Sb and Sr in Sinter Ash During Wood-Bark / Pulp Sludge Co-Combustion

Note: A relative enrichment of one corresponds to that element being found in equal concentrations in the sinter and bottom ashes

5.6.15 Barium

Barium was partially volatilised during combustion of wood-bark (5 – 50 %) and wood-bark / pulp sludge blends (up to 65 %). Barium was predicted by thermodynamic equilibrium modelling to be completely retained on the ash of these fuels. Below 1000 °C this was as $BaSO_4$ and above as barium silicates $BaO.2SiO_2$, $BaO.SiO_2$ and $2BaO.SiO_2$.

Despite being thermodynamically favoured to be retained in ash, up to 65 % of the barium has been lost from the suspension-firing reactor. This barium was released from the fuel during combustion and although thermodynamically favoured to recondense has not, probably because of a lack of opportunity to do so before being swept from the suspension-firing reactor by the flue gas (Section 5.0.3). Some of the released barium has probably recondensed causing enrichment on sinter ash, especially during combustion at 800 °C (Figure 109).

5.6.16 Cobalt

Cobalt was almost completely retained in wood-bark ash (75 – 100 %) and seems to have been similarly retained in the ash of wood-bark / pulp sludge blends combusted at 900 °C, though at least 5 % was lost during combustion at 800 °C (Figure 108).

Cobalt was predicted by thermodynamic equilibrium modelling of wood-bark (Figure 96, Section 5.5.16) and 70 % wood-bark / 30 % pulp sludge (Figure 110) combustion to be mostly retained in ash during combustion at 800 °C. Combustion at 900 °C, however was predicted to release up to 15 % of the cobalt as $Co(OH)_2$ gas. Due to experimental error it is not possible to tell whether this occurred.

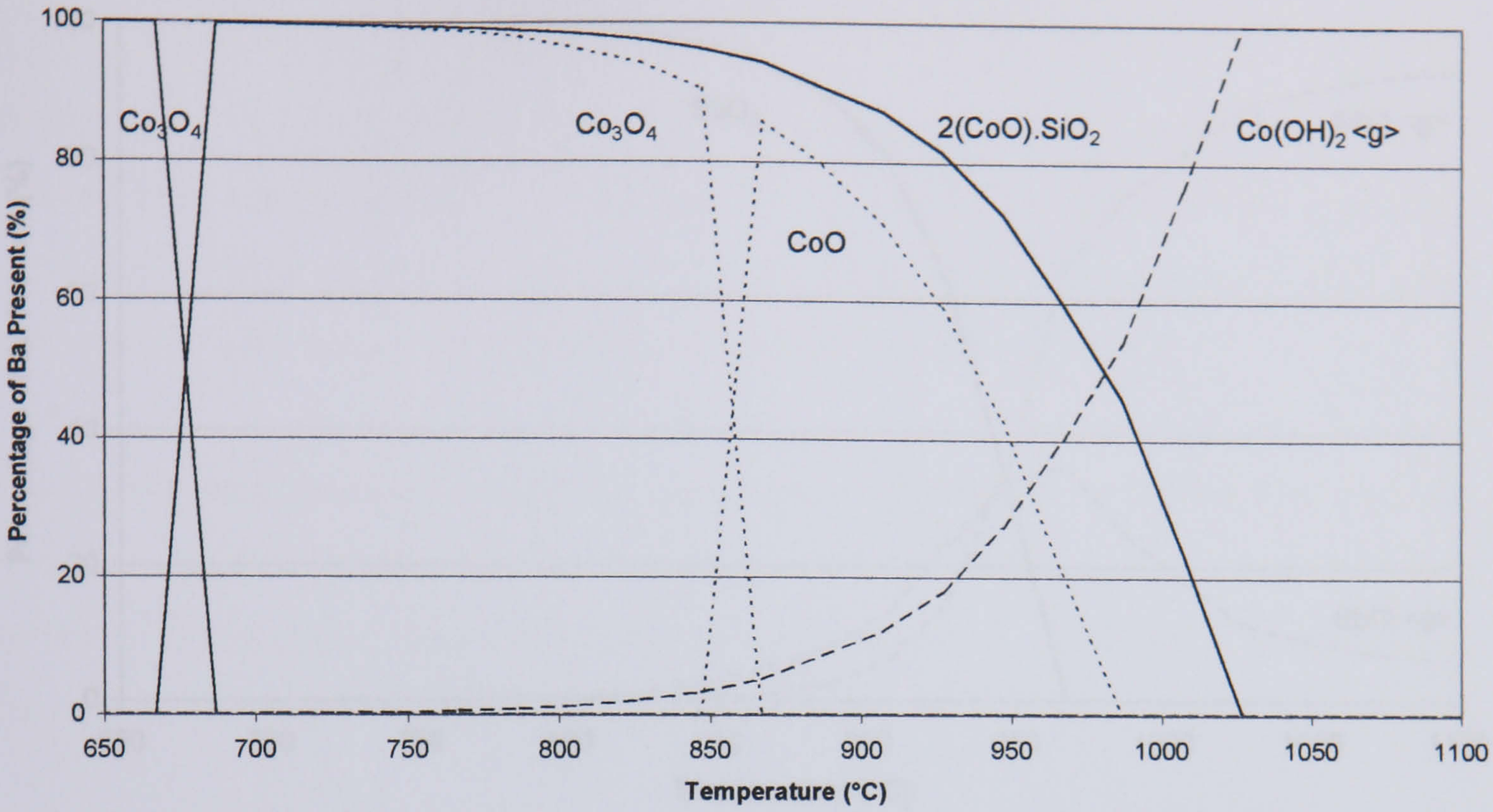


Figure 110 Thermodynamic Equilibrium Prediction for Cobalt During 70 % Wood-Bark / 30 % Pulp Sludge Combustion

5.6.17 Antimony

Antimony appears to have been partially volatilised from wood-bark (up to 70 %), however the wide range of experimental error prevents confirmation (Figure 108). It was volatilised from wood-bark / pulp sludge blends burnt at 900 °C (30 – 95 %) and from the 90 % wood-bark / 10 % pulp sludge blend burnt at 800 °C (35 – 80 %).

Thermodynamic equilibrium modelling of antimony during wood-bark (not shown) and 70 % wood-bark / 30 % pulp sludge (Figure 111) combustion predicted antimony to be completely retained in ash during combustion at 800 °C. Volatilisation of antimony at 800 °C indicates that not all antimony has been retained as SbO_2, as predicted. This was probably caused by the non-recondensation of antimony released from the fuel, as described in 5.0.3.

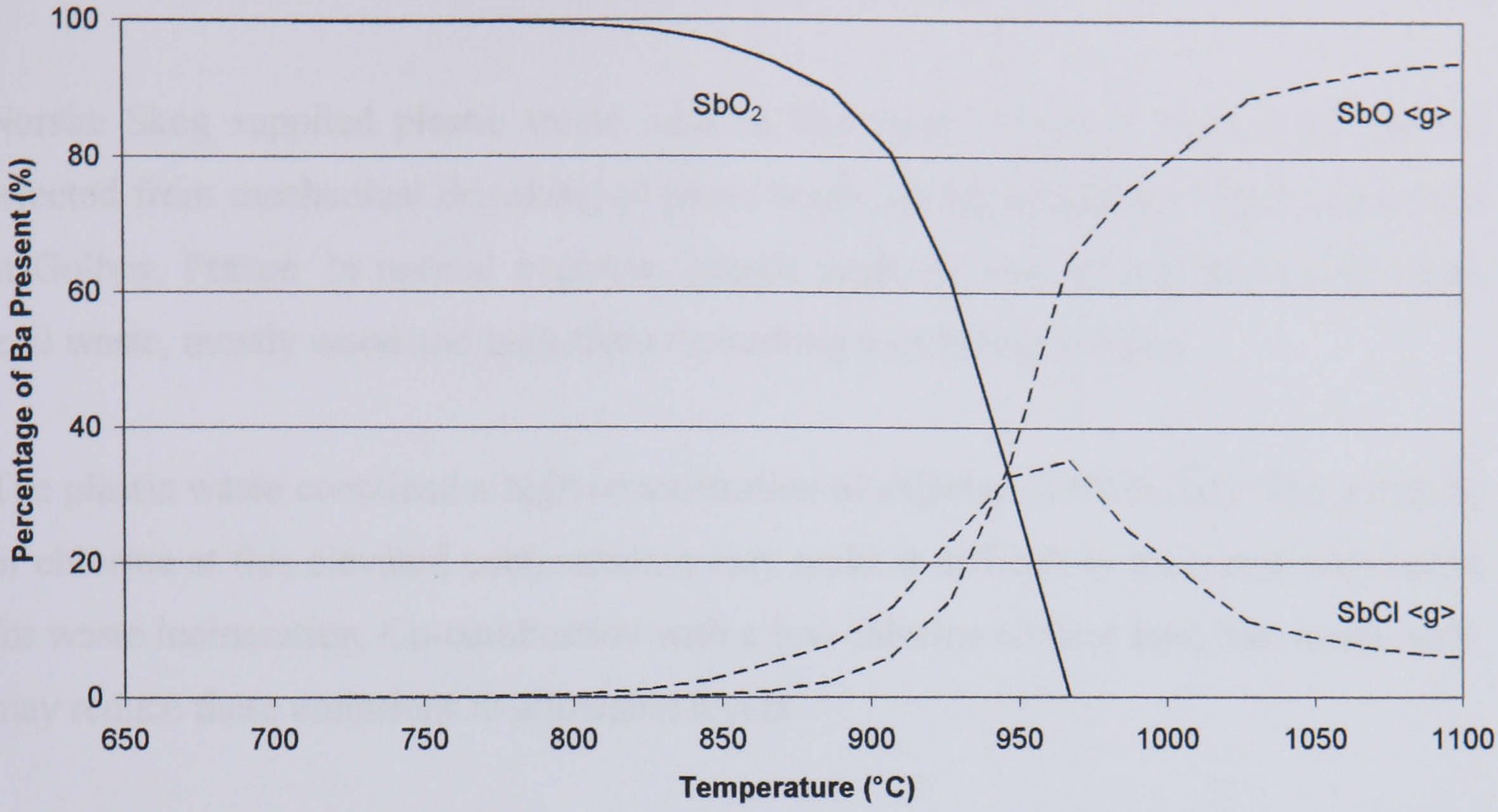


Figure 111 Thermodynamic Equilibrium Prediction for Antimony During 70 % Wood-Bark / 30 % Pulp Sludge Combustion

5.6.18 Strontium

Strontium was partially (5 – 45 %) volatilised during wood-bark combustion (Figure 108). Blending the wood-bark with pulp sludge made little difference to the proportion of strontium volatilised at 800 °C, but this proportion appears to have increased with pulp sludge addition during combustion at 900 °C. The results appear very similar to those for barium, above (Section 5.6.15).

Thermodynamic equilibrium modelling of the strontium during combustion of wood-bark and of 70 % wood-bark / 30 % pulp sludge predicted strontium to have been completely retained in ash as $SrSO_4$.

Release of strontium from the fuel, formation of $SrSO_4$ in the gas phase and subsequent recondensation may explain the enrichment of strontium on sinter ash (Figure 109). However not all of the released strontium has recondensed, probably because it lacked the opportunity (Section 5.0.3).

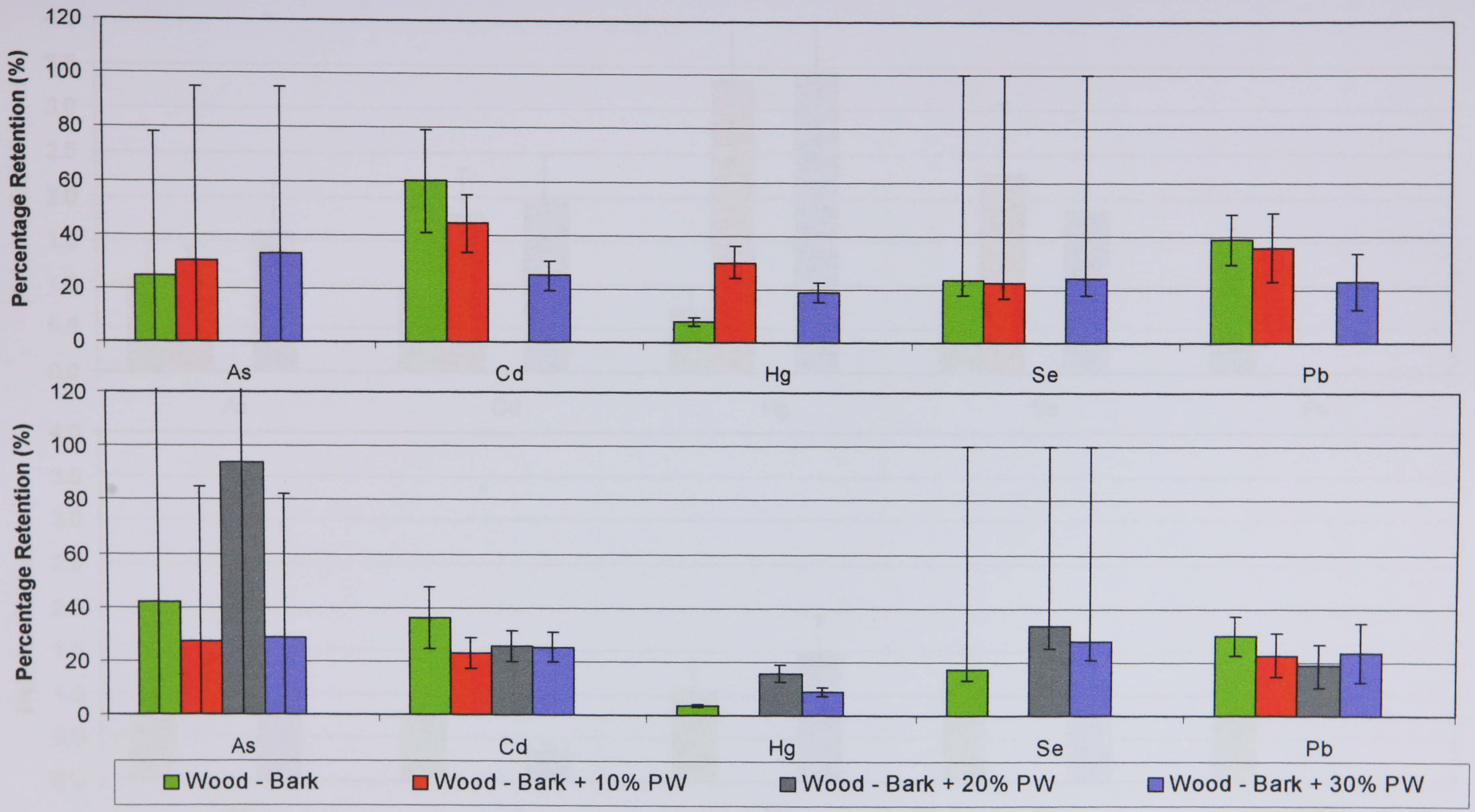
5.7 Co- Combustion of Wood-Bark and Plastic Waste

Norske Skog supplied plastic waste used in this study. It was a mixture of plastics rejected from mechanical de-inking of paper waste during recycling at their paper mill at Golbey, France. In normal operation plastic waste is crushed and burnt with other mill waste, mostly wood and bark from de-barking logs before pulping.

The plastic waste contained a high concentration of chlorine (0.98 % daf). The presence of chlorine at this elevated concentration may make it difficult to meet emission limits for waste incineration. Co-combustion with a low chlorine content fuel, like wood-bark, may reduce these emissions to allowable levels.

Co-combustion of wood-bark with plastic waste produced little sinter ash. In several runs the amount was insufficient to carry out measurements of the trace element concentrations. For these runs, bottom and sinter ash were mixed and analysed together. The results for these runs allow calculation of the percentage of each element retained in the total ash, but not the relative enrichment of the trace elements on sinter ash.

Plastic waste could not be burnt on its own in the suspension-firing reactor due to blocking of the short section of feeder tube prior to the combustion zone. Without results for the retention of trace elements in plastic waste ash, determination of the presence of any synergies in trace element behaviour during co-combustion was more difficult.



Trace Element Concentration in raw fuels (ppm):	As	Cd	Hg	Se	Pb
Wood-Bark	0.44 ± 0.95	0.20 ± 0.05	0.033 ± 0.001	<0.8	3.1 ± 0.4
Plastic Waste	0.31 ± 0.02	4.1 ± 0.23	0.055 ± 0.003	<0.8	35 ± 18

Figure 112 Percentage Retention of As, Cd, Hg, Se and Pb in Ash After Wood-Bark / Plastic Waste Co-Combustion

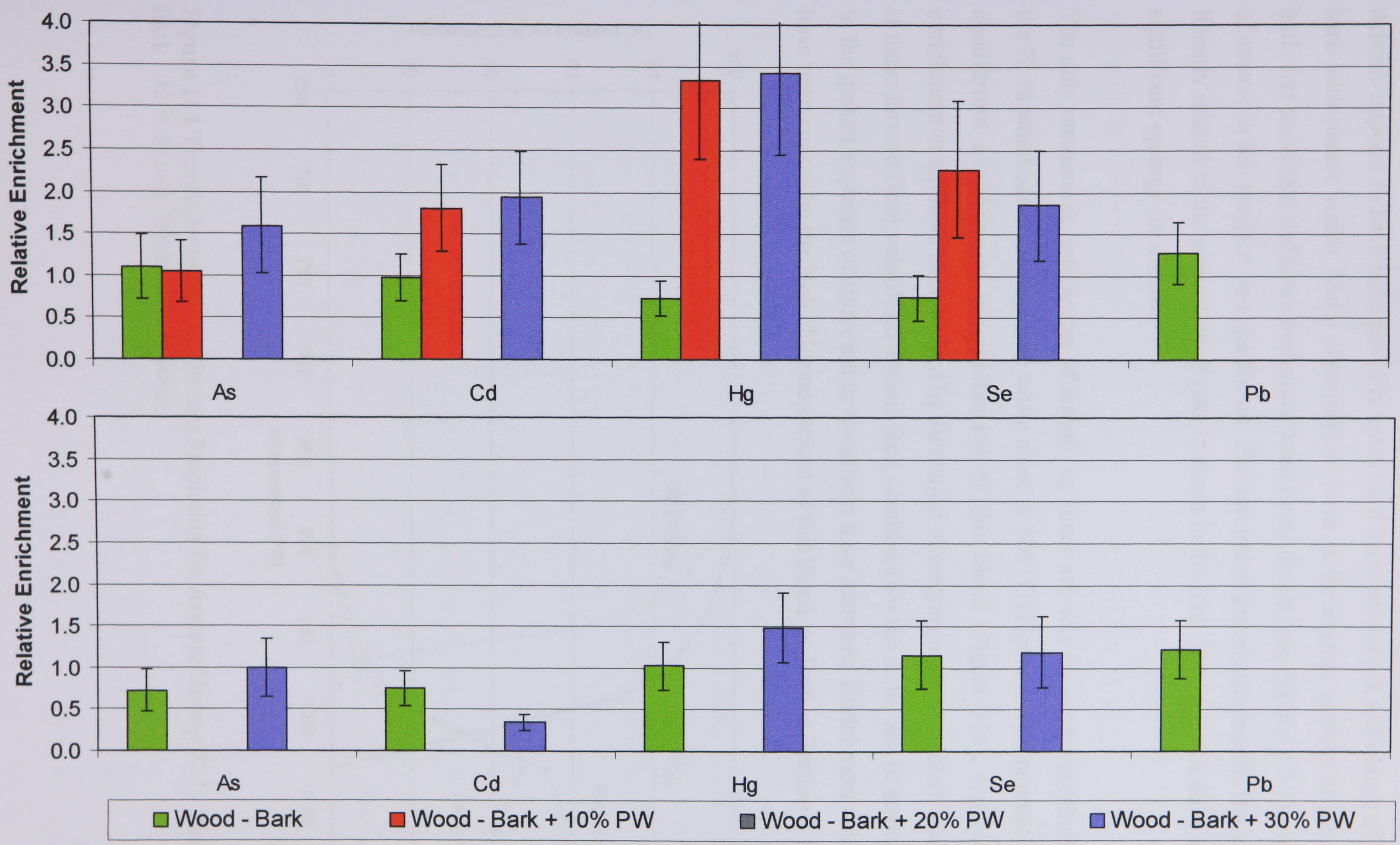


Figure 113 Relative Enrichment of As, Cd, Hg, Se and Pb in Sinter Ash During Wood-Bark / Plastic Waste Co-Combustion
Note a relative enrichment of one corresponds to that element being found in equal concentration in the sinter and bottom ashes

5.7.1 Arsenic

Arsenic appears to have been partially volatilised from wood-bark and blends of wood-bark with plastic waste. Large experimental error in the arsenic content of the wood-bark, has prevented definite conclusions from being drawn (see Section 5.5.1). Analysis of arsenic in ash samples was unaffected. The amount of arsenic retained by the ash was linearly related to the proportion of plastic waste in the fuel. This suggests there was no significant synergy for arsenic.

The only measurable enrichment of arsenic on sinter ash was during the combustion of the 70 % wood-bark / 30 % plastic waste blend at 800 °C (Figure 113). Thermodynamic equilibrium modelling of the combustion of this blend (Figure 114), suggests that enrichment could have been caused by formation of magnesium and calcium arsenates. If these formed from volatilised arsenic they would enrich the sinter ash in arsenic, due to the greater exposure of sinter ash to volatilised trace elements. Enrichment could also have been caused by the high chlorine content of this blend, as fond in Section 5.8.1.

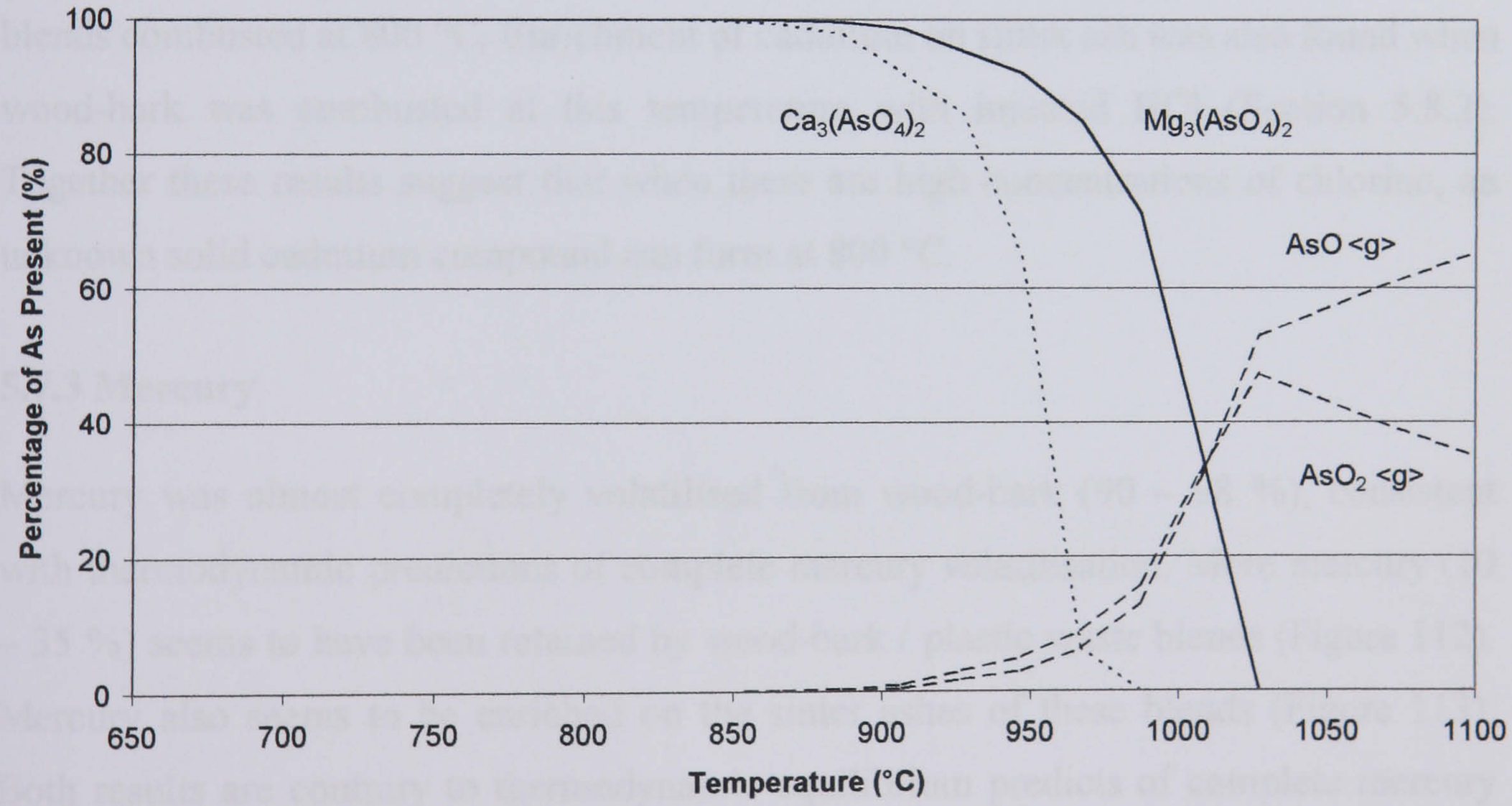


Figure 114 Thermodynamic Equilibrium Prediction for Arsenic During 70 % Wood-Bark / 30 % Plastic Waste Combustion

5.7.2 Cadmium

Cadmium was partially (20 – 75 %) volatilised from wood-bark during combustion (Figure 112). Blending plastic waste with the wood-bark caused a decline in the proportion of cadmium retained after combustion at 800 °C. At 900 °C lower cadmium retention by wood-bark ash made the proportions retained similar. There did not appear to be synergy for cadmium release or retention between the fuels. This suggests that chlorine from the plastic waste had little influence over the behaviour of cadmium derived from the wood-bark.

Thermodynamic equilibrium modelling predicted all cadmium was to be in a gaseous mixture of $CdCl_2$, CdOH and Cd during wood-bark and 70 % wood-bark / 30 % plastic waste blend combustion. As any cadmium released from the fuel could have formed these gases and been lost from the suspension-firing reactor as a gas, most cadmium retained in ash was probably not released from its modes of occurrence in the fuels.

Some released cadmium has recondensed on sinter ash of wood-bark / plastic waste blends combusted at 800 °C. Enrichment of cadmium on sinter ash was also found when wood-bark was combusted at this temperature with injected HCl (Section 5.8.2). Together these results suggest that when there are high concentrations of chlorine, an unknown solid cadmium compound can form at 800 °C.

5.7.3 Mercury

Mercury was almost completely volatilised from wood-bark (90 – 98 %), consistent with thermodynamic predictions of complete mercury volatilisation. More mercury (10 – 35 %) seems to have been retained by wood-bark / plastic waste blends (Figure 112). Mercury also seems to be enriched on the sinter ashes of these blends (Figure 113). Both results are contrary to thermodynamic equilibrium predicts of complete mercury volatilisation. Perhaps mercury is retained to a greater extent by its modes of occurrence in the plastic waste. The enrichment of mercury on sinter ash may be due to the formation of an unknown solid mercury compound (see Section 5.2.3).

5.7.4 Selenium

The proportion of selenium retained in ash during the combustion of wood-bark and wood-bark / plastic waste blends was not possible to determine, due to the very low level of Se in both fuels (<0.8 ppm). Concentrations of selenium in the ashes were also either close to, or below the limits of quantification. In cases where it was below the LOQ, selenium measurements by microwave analysis were used. For the 90 % wood-bark / 10 % plastic waste blend burnt at 900 °C, both sets of results were below their LOQs. With so few results it was not possible to ascertain whether a synergy for selenium retention or release was present.

Selenium was predicted to be completely in the gas phase by thermodynamic equilibrium modelling of wood-bark, 70 % wood-bark / 30 % agricultural waste and 100 % agricultural waste combustion. This was by the formation of either SeO_2 (>99 % of all Se present) or SeO (<1 %) gases.

Addition of plastic waste to wood-bark has caused Se to be enriched on sinter ash at 800 °C (Figure 113). This suggests a condensed selenium compound not included in the thermodynamic database has formed. With the high calcium concentration of both fuels, one possible compound is $CaSeO_4$, suggested by Clements et al (1999) to capture selenium in high calcium coal fly ash.

5.7.5 Lead

Between 20 and 50 % of the lead originally present in the wood-bark and 10 and 50 % of that in wood-bark / plastic waste blends remained in the ash (Figure 112). Complete volatilisation of lead was predicted by thermodynamic equilibrium models of wood-bark (Figure 82, Section 5.5.5) and of 70 % wood-bark / 30 % plastic waste blend (Figure 115) combustion. Without solid lead compounds predicted to form it seems likely that lead retained in ash was not released from its modes of occurrence in the fuels.

It was not possible to determine whether lead had formed a solid and recondensed on sinter ash. Wide differences between duplicate measurements of the lead concentration in this ash prevented determination of a trend in lead enrichment (Figure 113).

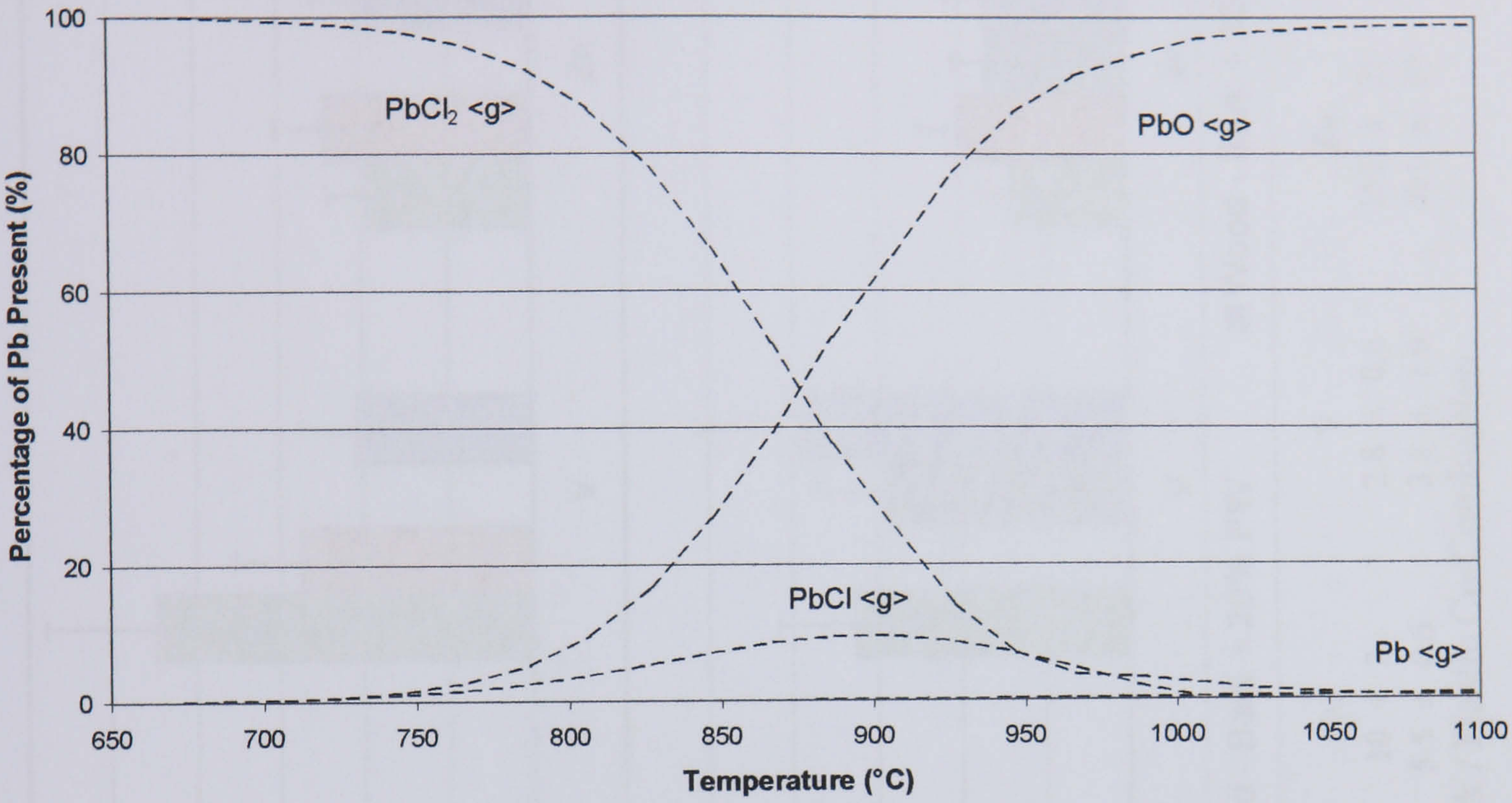
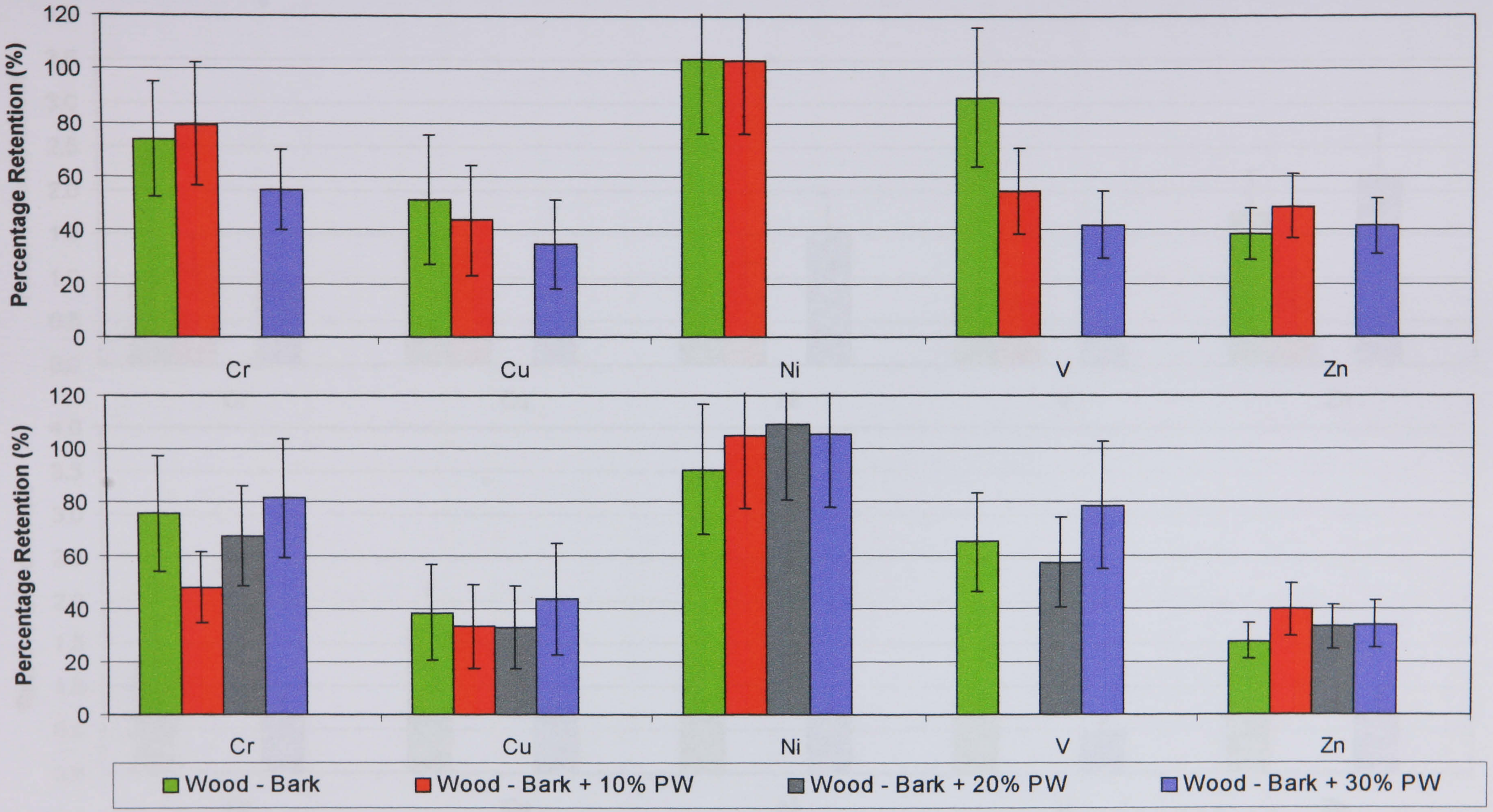


Figure 115 Thermodynamic Equilibrium Prediction for Lead During 70 % Wood-Bark / 30 % Plastic Waste Combustion



Trace Element Concentration in raw fuels (ppm):	Cr	Cu	Ni	V	Zn
Wood-Bark	26 ± 5	87 ± 37	10 ± 2	2.8 ± 0.6	150 ± 21
Plastic Waste	33 ± 4	65 ± 31	5.5 ± 0.6	3.2 ± 1.0	501 ± 85

Figure 116 Percentage Retention of Cr, Cu Ni, V and Zn in Ash After Wood-Bark / Plastic Co-Combustion

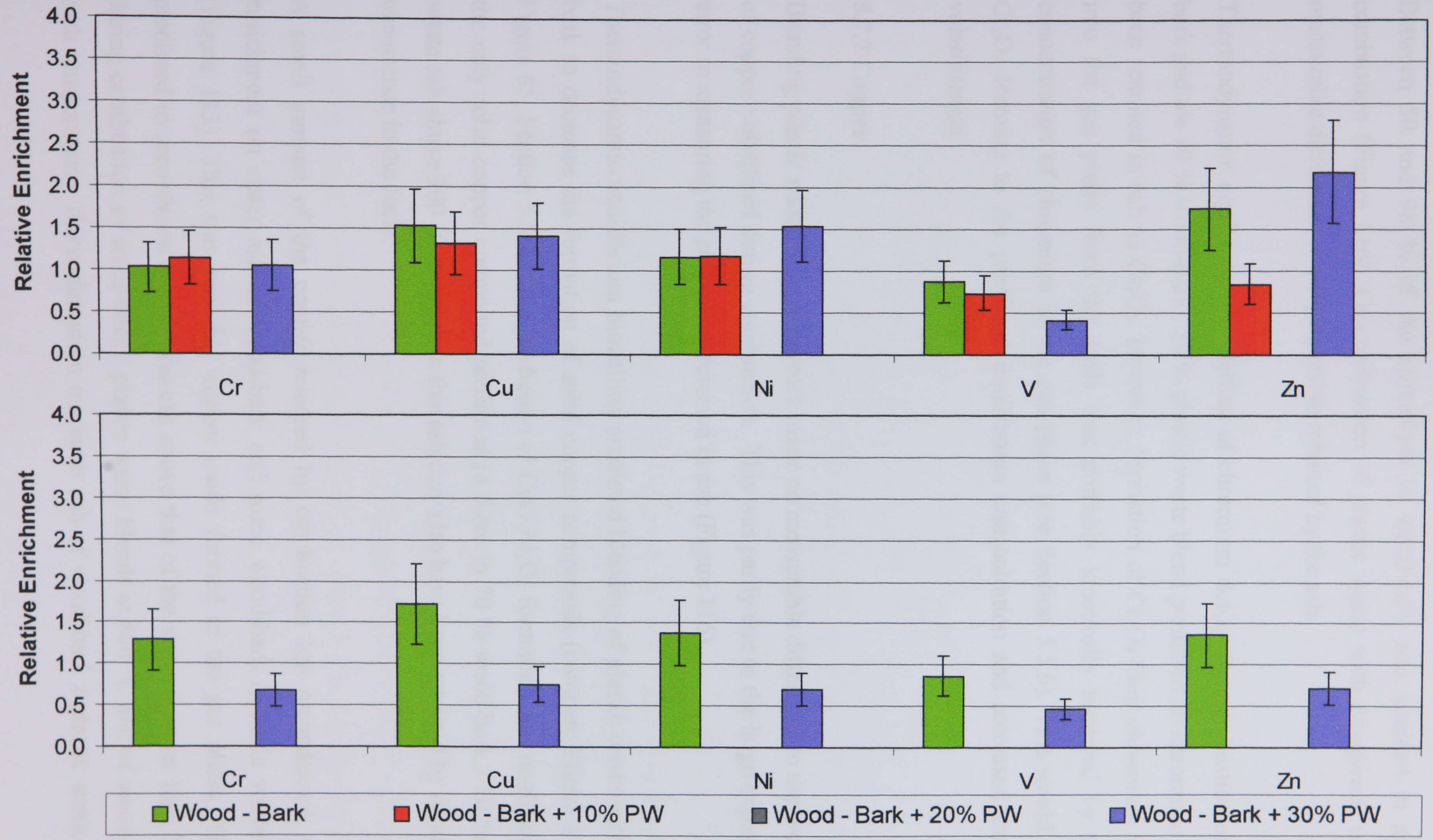


Figure 117 Relative Enrichment of Cr, Cu, Ni, V and Zn in Sinter Ash During Wood-Bark / Plastic Waste Co-Combustion
Note a relative enrichment of one corresponds to that element being found in equal concentration in the sinter and bottom ashes

5.7.6 Chromium

Between 50 and 98 % of the chromium in wood-bark was retained in ash after combustion (Figure 116). Co-combustion of plastic waste with wood-bark made no measurable difference to the proportion retained by the ash.

Thermodynamic equilibrium modelling of chromium during the combustion of wood-bark and the 70 % wood-bark / 30 % plastic waste blend predicted all chromium to have been retained in ash as Cr_2O_3. However, formation of Cr_2O_3 from chromium released into the gas phase from the fuels was probably kinetically hindered by the low concentration of chromium in the gas phase (see Section 5.5.6). This would prevent Cr_2O_3 forming to the predicted equilibrium concentration and increased chromium volatilisation.

5.7.7 Copper

Blending plastic waste with wood-bark made no measurable difference to the proportion of copper volatilised during combustion. This was partly due to the large experimental error in measuring the proportion retained in ash (Figure 116).

Thermodynamic equilibrium modelling predicted blending of plastic waste with wood-bark to decrease the formation of solid copper compounds (compare Figure 118 with Figure 85, Section 5.5.7). The prediction of $CuO.Al_2O_3$ formation was unaffected. It is the only solid copper compound predicted to form in 70 % wood-bark / 30 % plastic waste ash above 900 °C. Copper in this ash may also have been retained by its modes of occurrence in the fuels.

A small amount of the copper released by combustion has recondensed, causing enrichment on sinter ash of wood-bark and some wood-bark / plastic waste blends (Figure 113). This was probably copper oxide formed in the gas phase. This was predicted to recondense at temperatures above that of the sinter (greater than 750 °C) during combustion of wood-bark / plastic waste blends at 800 °C and of wood-bark at both temperatures. Recondensation on sinter ash of wood-bark / plastic waste blends

combusted at 900 °C was probably prevented by the high chlorine concentrations of plastic waste causing CuCl formation.

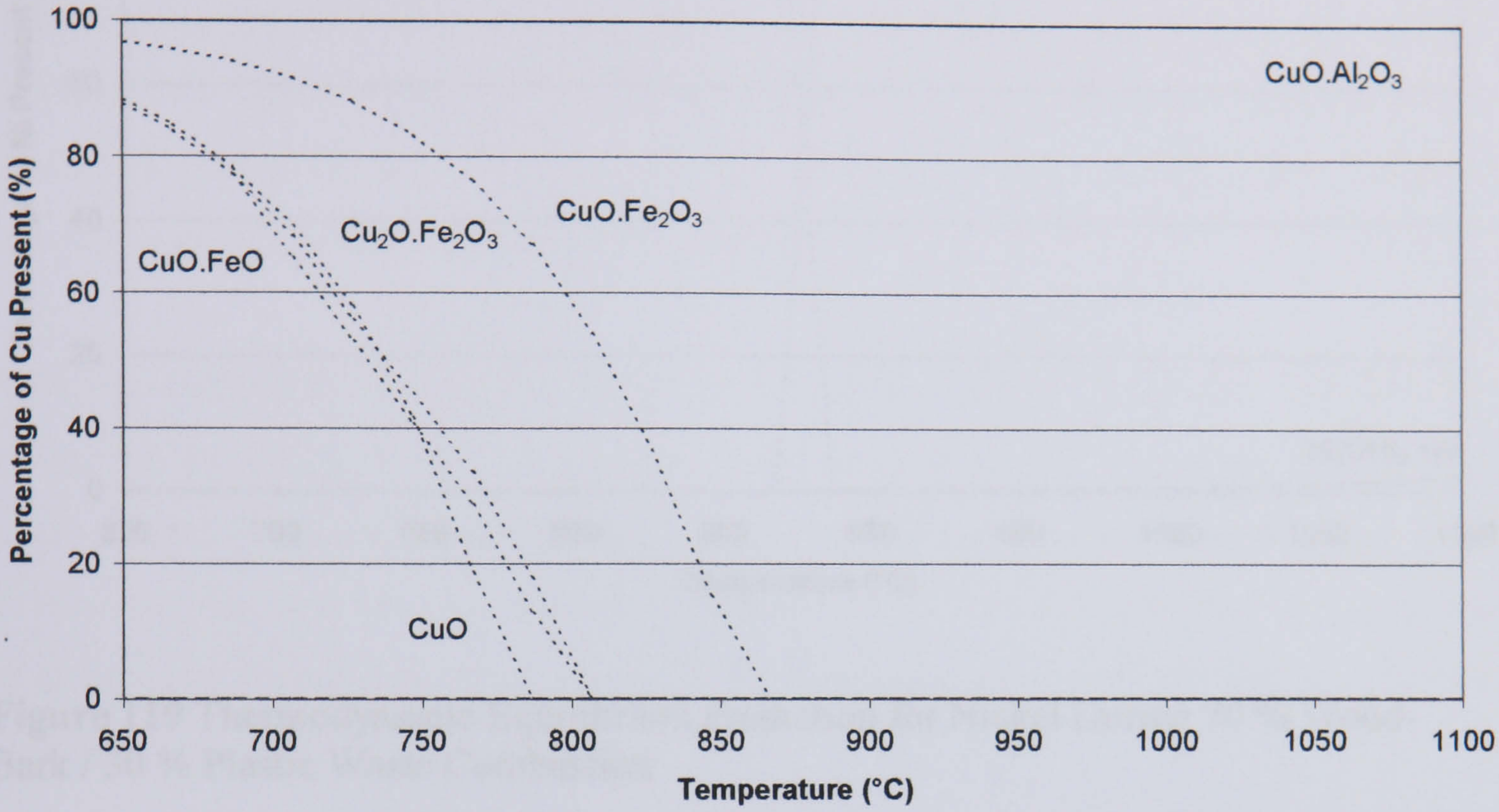


Figure 118 Thermodynamic Equilibrium Prediction for Copper During 70 % Wood-Bark / 30 % Plastic Waste Combustion

5.7.8 Nickel

Nickel was almost completely retained by wood-bark ash (65 – 100 %) and ashes from co-combustion of plastic waste with wood-bark (75 – 100 %), Figure 116. No result has been reported for the 70 % wood-bark / 30 % plastic waste blend burnt at 800 °C due to analytical error.

Complete retention of nickel in ash was predicted by thermodynamic equilibrium models for wood-bark (Figure 87, Section 5.5.8) and 70 % wood-bark / 30 % plastic waste blend (Figure 119) combustion. In both of these models nickel was predicted to remain completely in the ash by forming either $NiO.Fe_2O_3$, NiO or $NiO.Al_2O_3$. Nickel may also have been retained in ash because it was not released from its modes of occurrence in the fuels.

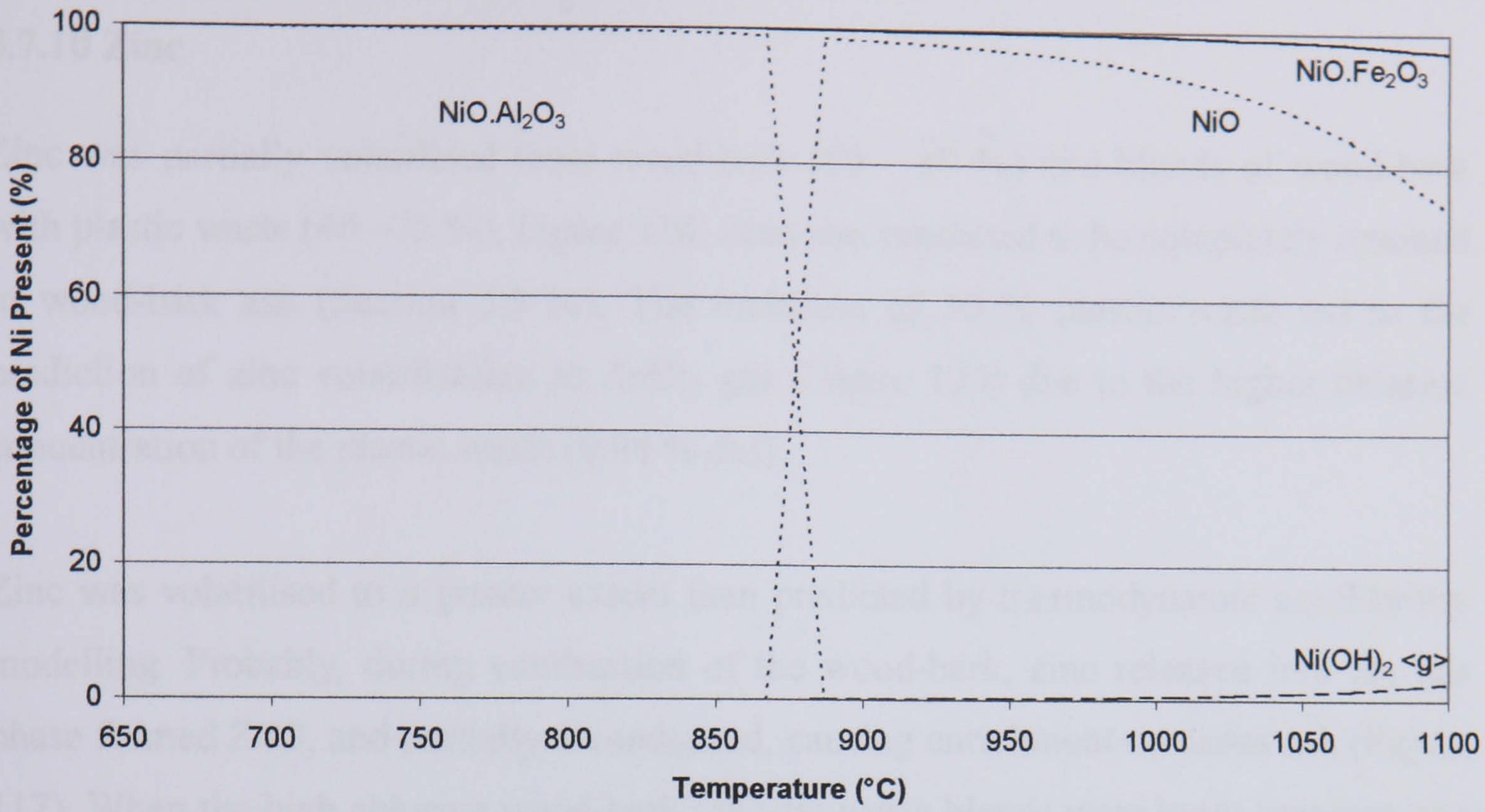


Figure 119 Thermodynamic Equilibrium Prediction for Nickel During 70 % Wood-Bark / 30 % Plastic Waste Combustion

5.7.9 Vanadium

Vanadium was almost completely (65 – 100 %) retained in wood-bark ash after combustion at 800 °C (Figure 116). Increasing the combustion temperature to 900 °C appears to have increased vanadium volatilisation. The addition of plastic waste to the wood-bark also caused vanadium volatilisation during combustion seemingly to a greater degree at 800 °C than 900 °C.

The thermodynamic equilibrium prediction for vanadium during combustion of the 70 % wood-bark / 30 % plastic waste blend was similar to that for combustion of wood-bark alone (Section 5.5.9). Condensed vanadium dioxide was predicted to form at all temperatures between 650 and 1100 °C. Calcium and sodium can also form compounds with vanadium, which at some temperatures were favoured over the VO_2.

Vanadium has however, been volatilised. This vanadium released from the fuel probably formed VO_2 in the gas phase, and only partially recondensed as described in Section 5.0.3.

5.7.10 Zinc

Zinc was partially volatilised from wood-bark (50 – 80 %) and blends of wood-bark with plastic waste (40 –75 %), Figure 116. Zinc was predicted to be completely retained in wood-bark ash (Section 5.5.10). The inclusion of 30 % plastic waste led to the prediction of zinc volatilisation as $ZnCl_2$ gas (Figure 120) due to the higher chlorine concentration of the plastic waste (0.98 % daf).

Zinc was volatilised to a greater extent than predicted by thermodynamic equilibrium modelling. Probably, during combustion of the wood-bark, zinc released into the gas phase formed ZnO, and partially recondensed, causing enrichment on sinter ash (Figure 117). When the high chlorine wood-bark / plastic waste blends were burnt however, the released zinc probably formed $ZnCl_2$ gas instead and was lost from the suspension reactor.

Zinc retained in ash may have formed the $ZnO.Al_2O_3$, $2ZnO.SiO_2$ or ZnO thermodynamic equilibrium modelling predicted. The remainder of the zinc was probably present in modes of occurrence from which it was not released during combustion.

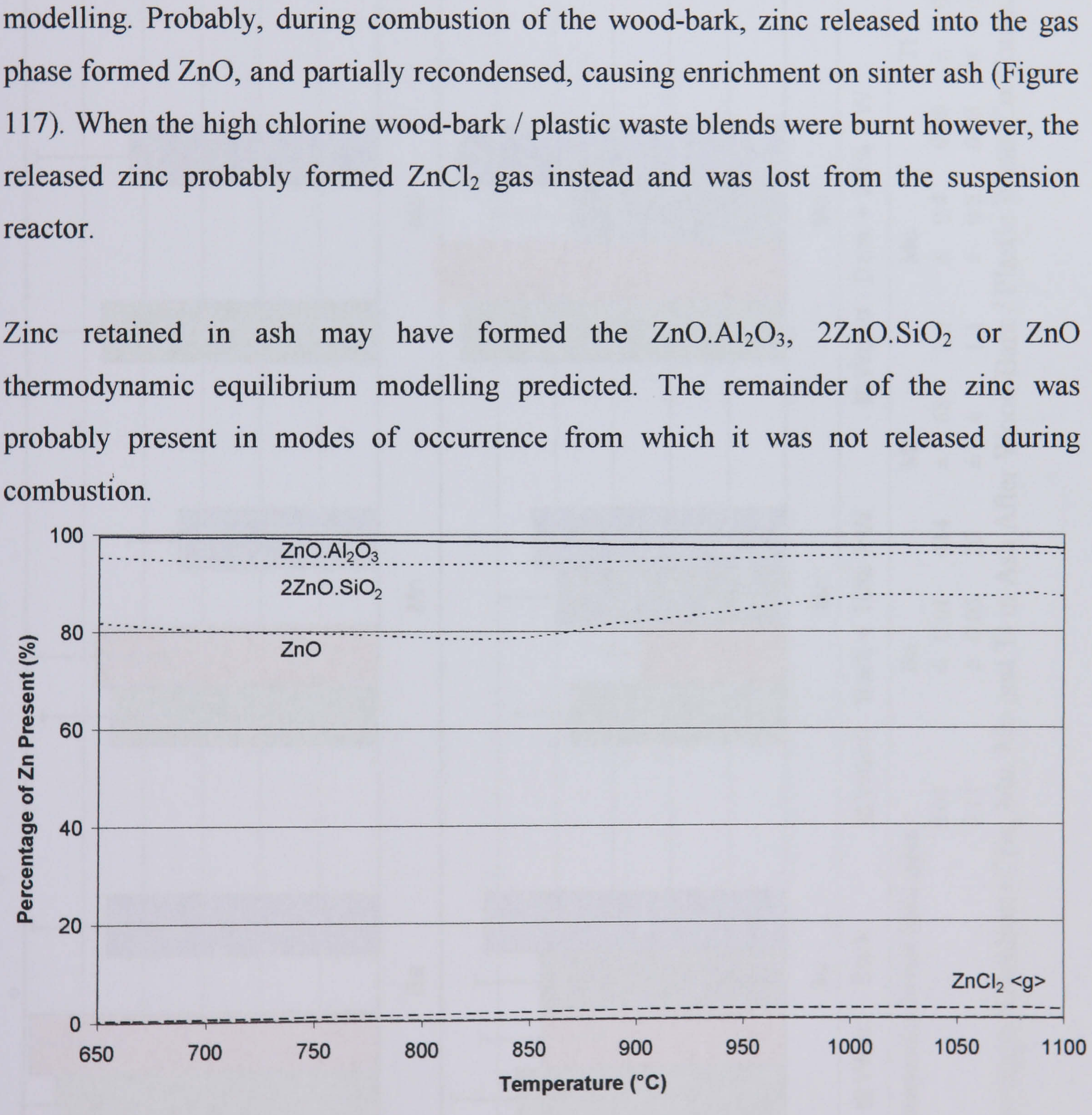
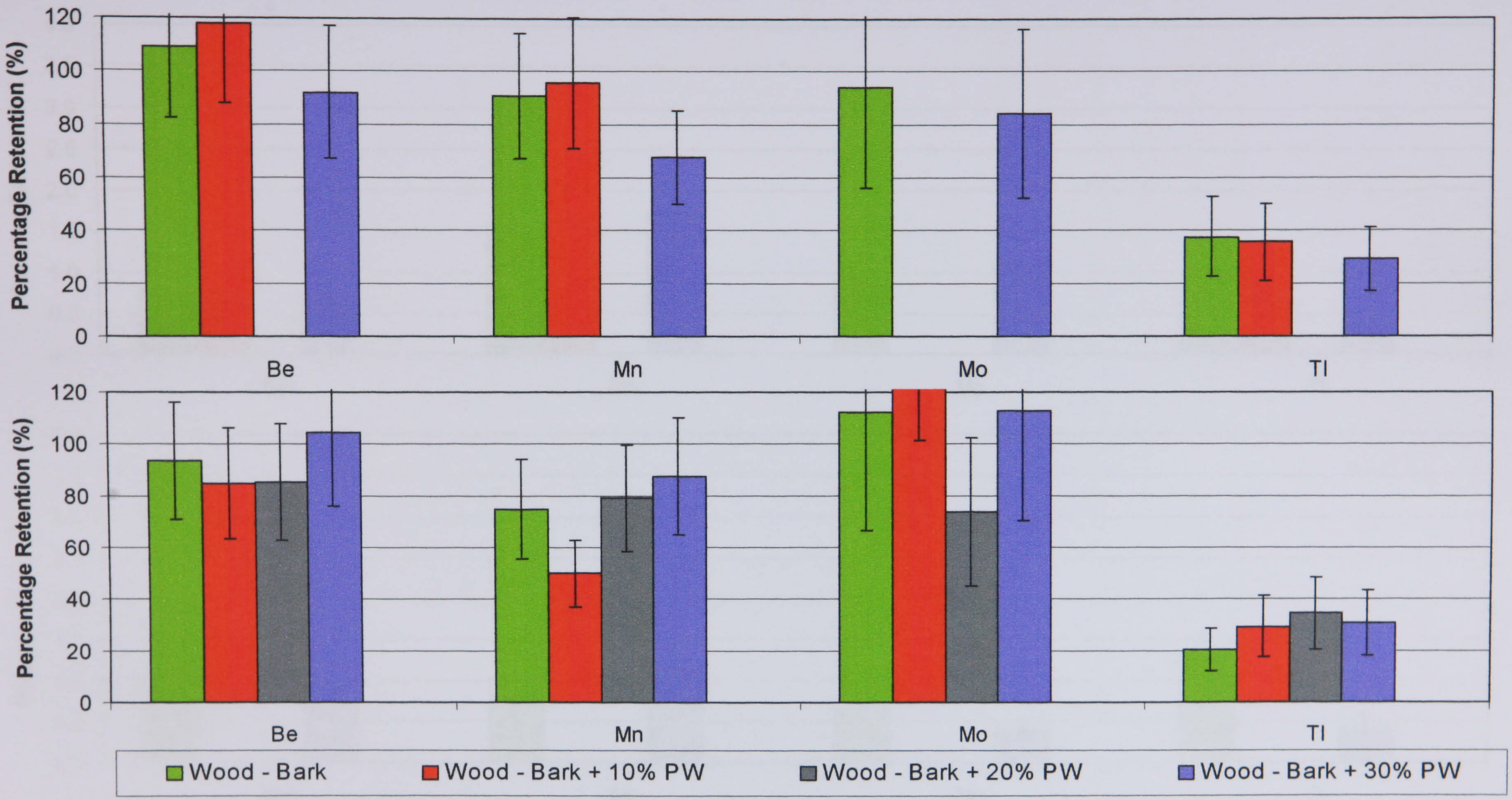


Figure 120 Thermodynamic Equilibrium Prediction for Zinc during 70 % Wood-Bark / 30 % Plastic Waste Combustion



Trace Element Concentration in raw fuels (ppm):	Be		Mn		Mo		Tl	
Wood-Bark	0.07	± 0.01	414	± 68	1.3	± 0.4	0.09	± 0.03
Plastic Waste	0.11	± 0.03	26	± 4	1.1	± 0.2	0.03	± 0.01

Figure 121 Percentage Retention of Be, Mn, Mo and Tl in Ash After Wood-Bark / Plastic Waste Co-Combustion

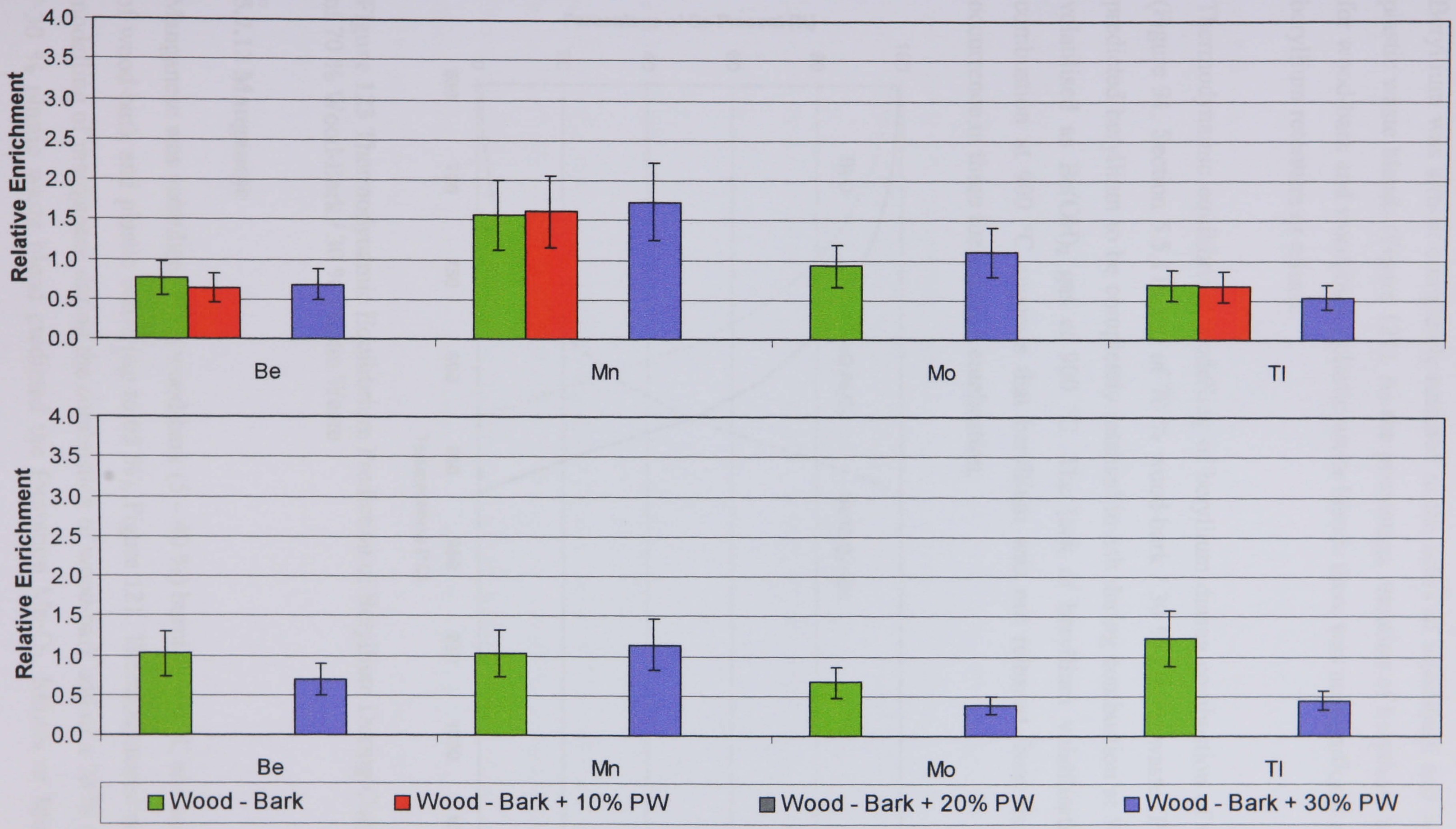


Figure 122 Relative Enrichment of Be, Mn, Mo and Tl in Sinter Ash Wood-Bark and Plastic Waste Co-Combustion

Note a relative enrichment of one corresponds to that element being found in equal concentration in the sinter and bottom ashes

5.7.11 Beryllium

Beryllium was almost completely retained in the ashes of wood-bark and wood-bark / plastic waste blends (Figure 121). As the percentage retention of beryllium was similar for wood-bark and wood-bark / plastic waste blends there was no significant synergy for beryllium retention or release.

Thermodynamic equilibrium modelling of beryllium during combustion of wood-bark (Figure 91, Section 5.5.11) and of 70 % wood-bark / 30 % plastic waste (Figure 123) predicted beryllium to be completely retained in ash during combustion at 800 °C, but volatilised as $Be(OH)_2$ gas at 900 °C. The lack of beryllium volatilisation during combustion at 900 °C suggests that beryllium was not released from its modes of occurrence in these fuels during combustion.

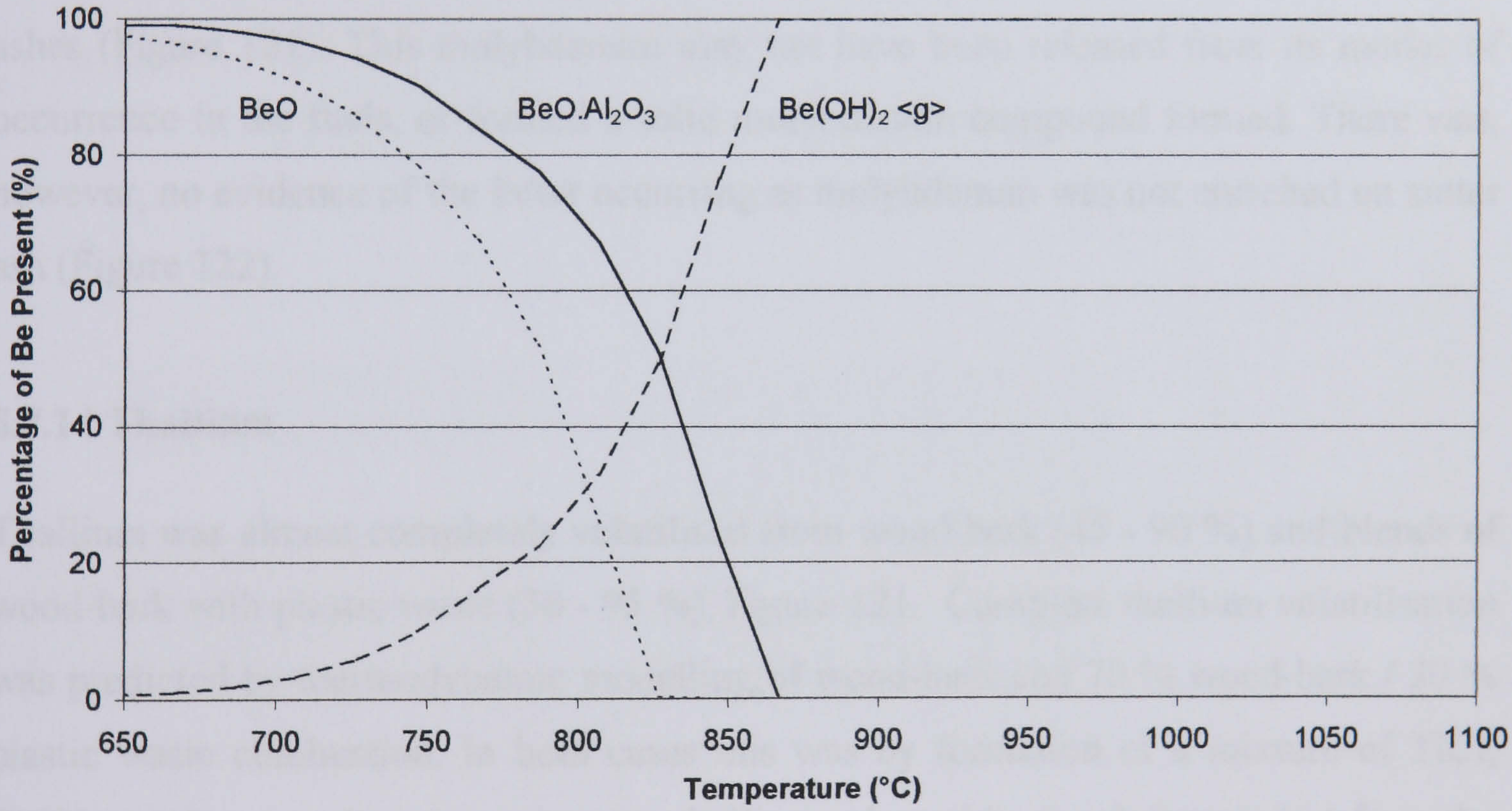


Figure 123 Thermodynamic Equilibrium Prediction of Beryllium During Combustion of 70 % Wood-Bark / 30 % Plastic Waste

5.7.12 Manganese

Manganese was volatilised from wood-bark (5 – 40 %) burnt at 900 °C and some blends of wood-bark and plastic waste (up to 65 %), Figure 121. Thermodynamic equilibrium modelling of manganese during the combustion of wood-bark and of a 70 % wood-bark / 30 % plastic waste blend predicted the formation Mn_2O_3, Mn_3O_4 or $MnO.SiO_2$ to

completely retain manganese in ash. When these species were excluded from the model MnO was predicted to form.

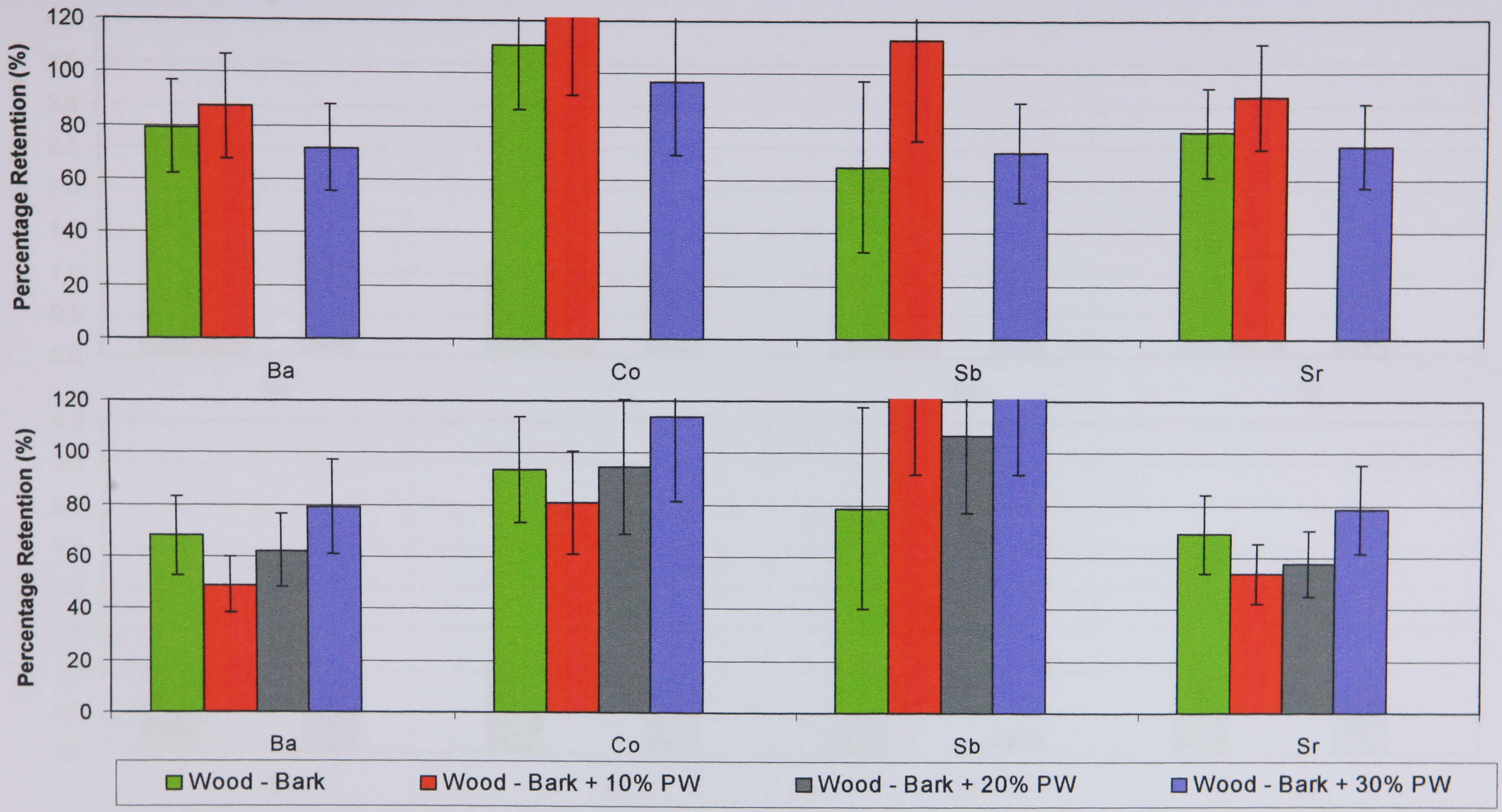
The difference between the experimental and predicted results was probably due to manganese released from the fuels during combustion forming MnO in the gas phase but only partially recondensing on ash (Section 5.0.3). This partial recondensation probably caused the enrichment of manganese on sinter ash at 800 °C (Figure 122). The remainder of the manganese probably exited the reactor with the flue gas (Section 5.0.3).

5.7.13 Molybdenum

A large proportion of the molybdenum originally contained in the wood-bark and wood-bark blends with plastic waste appears to have been almost completely retained in the ashes (Figure 121). This molybdenum may not have been released from its modes of occurrence in the fuels, or formed a solid molybdenum compound formed. There was, however, no evidence of the latter occurring as molybdenum was not enriched on sinter ash (Figure 122).

5.7.14 Thallium

Thallium was almost completely volatilised from wood-bark (45 - 90 %) and blends of wood-bark with plastic waste (50 - 95 %), Figure 121. Complete thallium volatilisation was predicted by thermodynamic modelling of wood-bark and 70 % wood-bark / 30 % plastic waste combustion. In both cases this was by formation of a mixture of TlCl, TlOH and Tl gases. It appears that any thallium released by the fuels was lost from the suspension-firing reactor. That which remained with the ash was probably not released from its mode of occurrence in the fuels (Section 5.0.2).



Trace Element Concentration in raw fuels (ppm):		Ba		Co		Sb		Sr
Wood-Bark	156	± 14	0.72	± 0.06	0.21	± 0.10	51	± 4
Plastic Waste	263	± 39	4.61	± 1.26	3.5	± 0.4	17	± 2

Figure 124 Percentage Retention of Ba, Co, Sb and Sr in Ash After Wood-Bark / Plastic Waste Co-Combustion

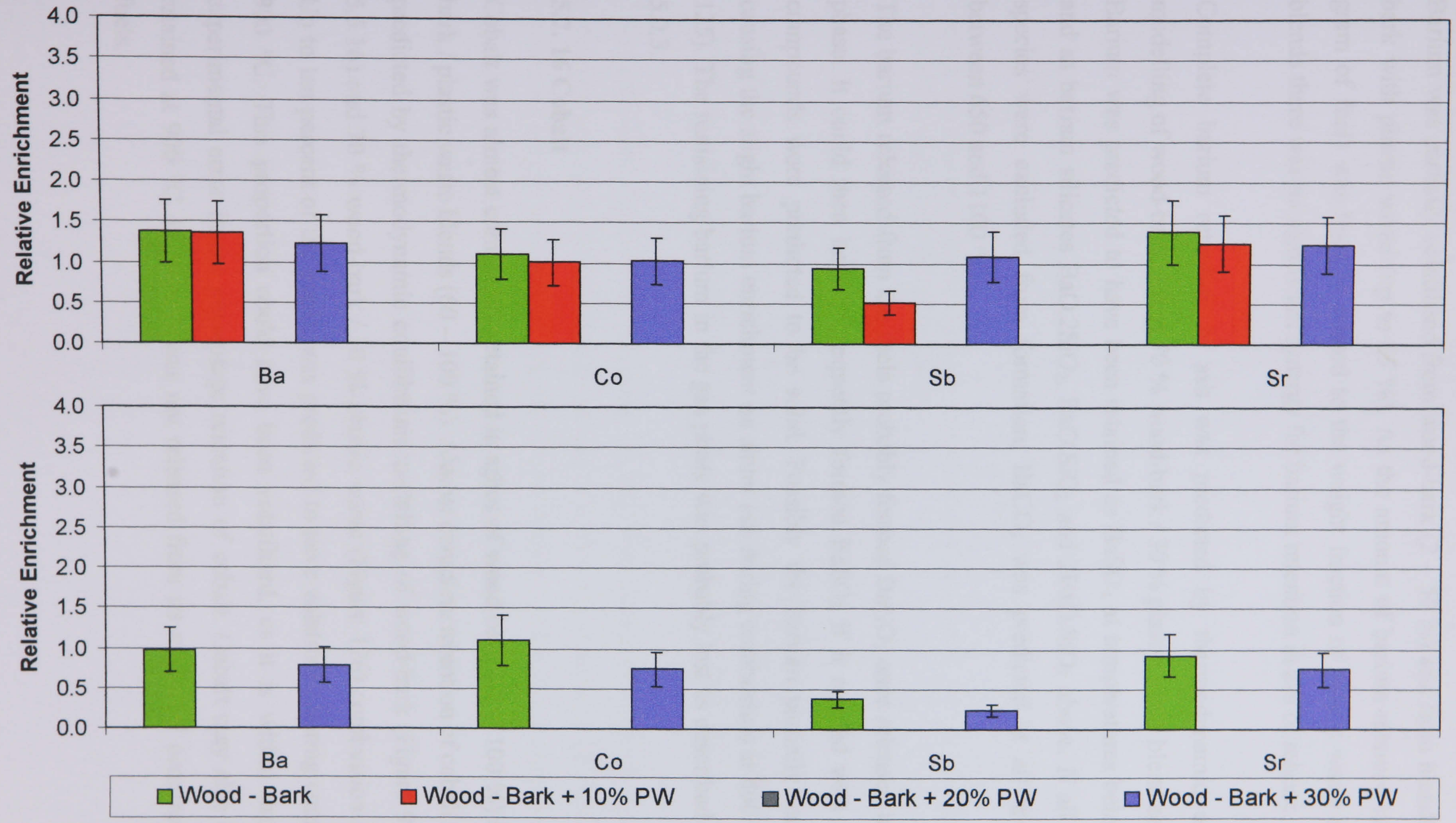


Figure 125 Relative Enrichment of Ba, Co, Sb and Sr in Sinter Ash During Wood-Bark / Plastic Waste Co-Combustion
Note a relative enrichment of one corresponds to that element being found in equal concentration in the sinter and bottom ashes

5.7.15 Barium

Barium was partially volatilised from wood-bark (2 – 50 %) and from blends of wood-bark with plastic waste (up to 65 %). As the amount of barium retained in ash (per gram of fuel) was linearly related to the weight fraction of plastic waste in the fuel blends there was no significant synergy for barium retention in ash or release.

Complete barium retention in ash was predicted by thermodynamic equilibrium modelling of wood-bark and of 70 % wood-bark / 30 % plastic waste blend combustion. Barium was predicted to have been retained as $BaSO_4$ at temperatures below 1000°C and as barium silicates $BaO.2SiO_2$, $BaO.SiO_2$ and $2BaO.SiO_2$ above. If all the above species were excluded from formation, $BaCO_3$ was predicted at all temperatures between 650 and 1100 °C.

The barium released from the fuels probably formed $BaCO_3$ once released into the gas phase. It could then have subsequently formed $BaSO_4$ if it reacted with SO_2. Both compounds were predicted to be solid. Possibly the barium partially recondensed, causing the slight barium enrichment on sinter ash during combustion at 800 °C (Figure 125). The remaining barium in the gas phase was probably lost as described in Section 5.0.3.

5.7. 16 Cobalt

Cobalt was almost completely retained in ashes of wood-bark (75 – 100 %) and wood-bark / plastic waste blends (60 – 100 %). Almost complete retention of cobalt in ash was predicted by thermodynamic equilibrium modelling of wood-bark (Figure 96, Section 5.5.16) and 70 % wood-bark / 30 % plastic waste (Figure 126) combustion at 800 °C. Up to ten percent of the cobalt was predicted to have volatilised during combustion at 900 °C. This proportion could have been volatilised, as it is within the range of experimental error in the percentage retention of cobalt. Cobalt may also have been retained at 900 °C, because it was not released from its modes of occurrence in the fuels.

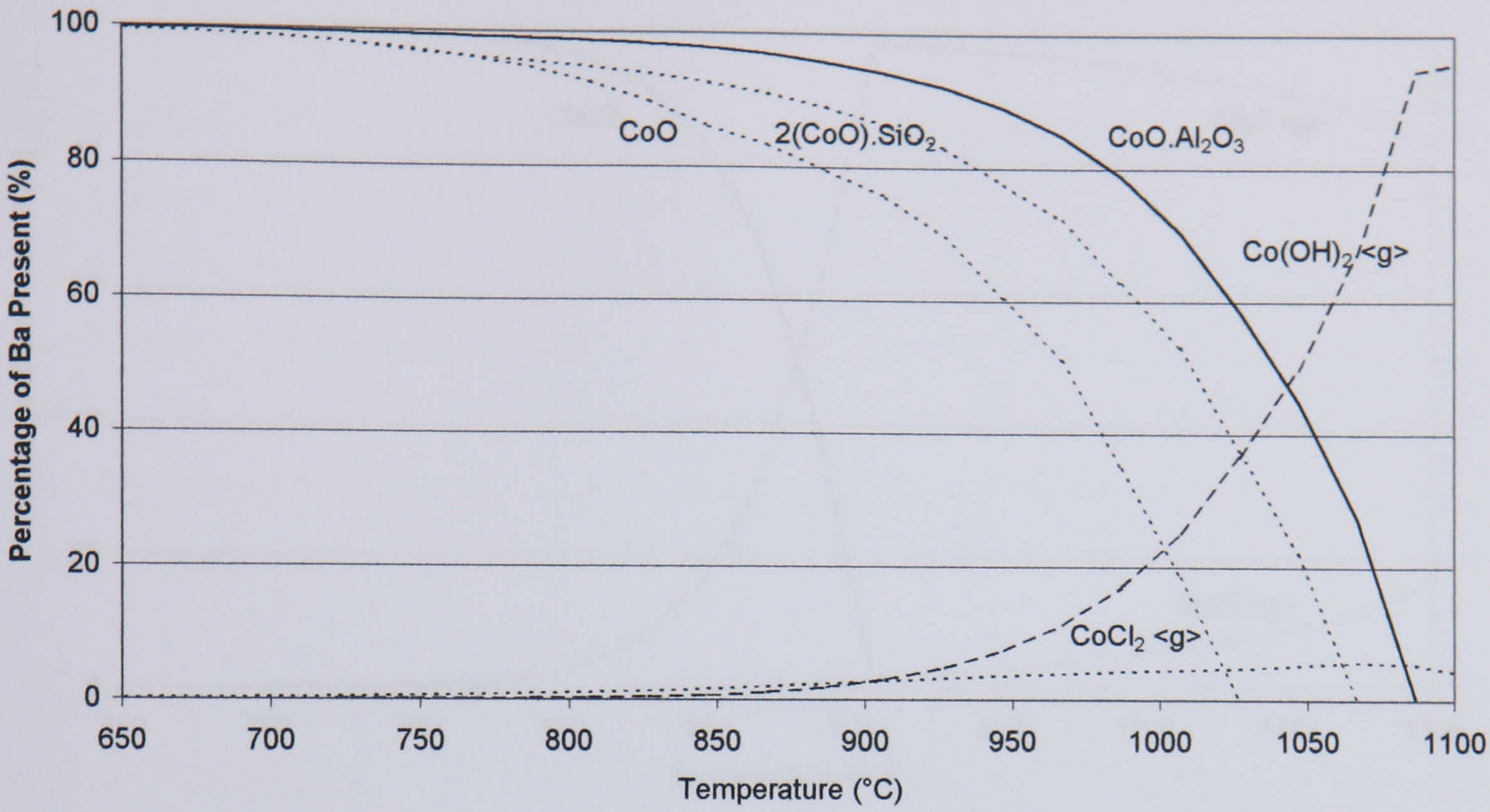


Figure 126 Thermodynamic Equilibrium Prediction for Cobalt During Combustion of 70 % Wood-Bark / 30 % Plastic Waste

5.7.17 Antimony

The large experimental error in the measurement of the antimony in the raw fuels makes it difficult to draw conclusions on antimony retention in ash (Figure 124).

Thermodynamic equilibrium modelling of antimony during combustion of wood-bark predicted antimony to be mostly retained in ash by formation of SbO_2. Similar predictions for the combustion of a 70 % wood-bark / 30 % plastic waste blend (Figure 127) however the SbO_2 was predicted to be less stable and antimony almost completely in the gas phase at 900 °C.

Most antimony was retained during combustion of the 70 % wood-bark / 30 % plastic waste blend at 900 °C. This suggests that antimony was not released from its modes of occurrence in the fuels, or an unknown solid antimony compound formed.

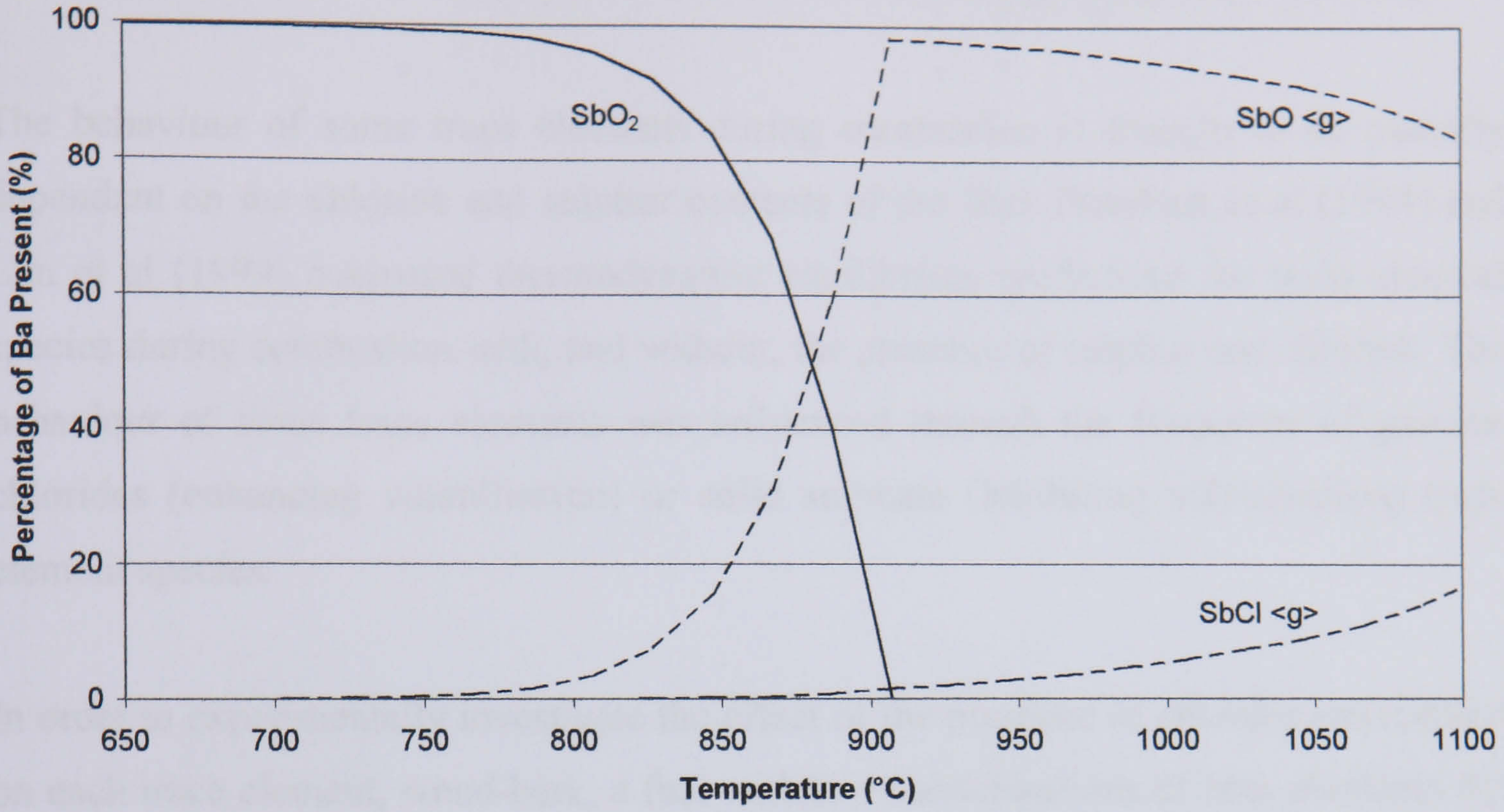


Figure 127 Thermodynamic Equilibrium Prediction for Antimony During 70 % Wood-Bark / 30 % Plastic Waste Combustion

5.7.18 Strontium

Strontium was partially volatilised by combustion of wood-bark (5 – 45 %) and wood-bark / plastic waste blends (up to 60 %), Figure 124. Strontium was predicted to remain completely in ash after combustion of wood-bark and of the 70 % wood-bark / 30 % plastic waste blend. This was by the formation of strontium sulphate, or strontium carbonate. Probably, the volatilised strontium was probably released from the fuel by combustion but incompletely recondensed on ash (described in Section 5.0.3). Strontium that did recondense probably caused the slight strontium enrichment on sinter ash shown in Figure 125.

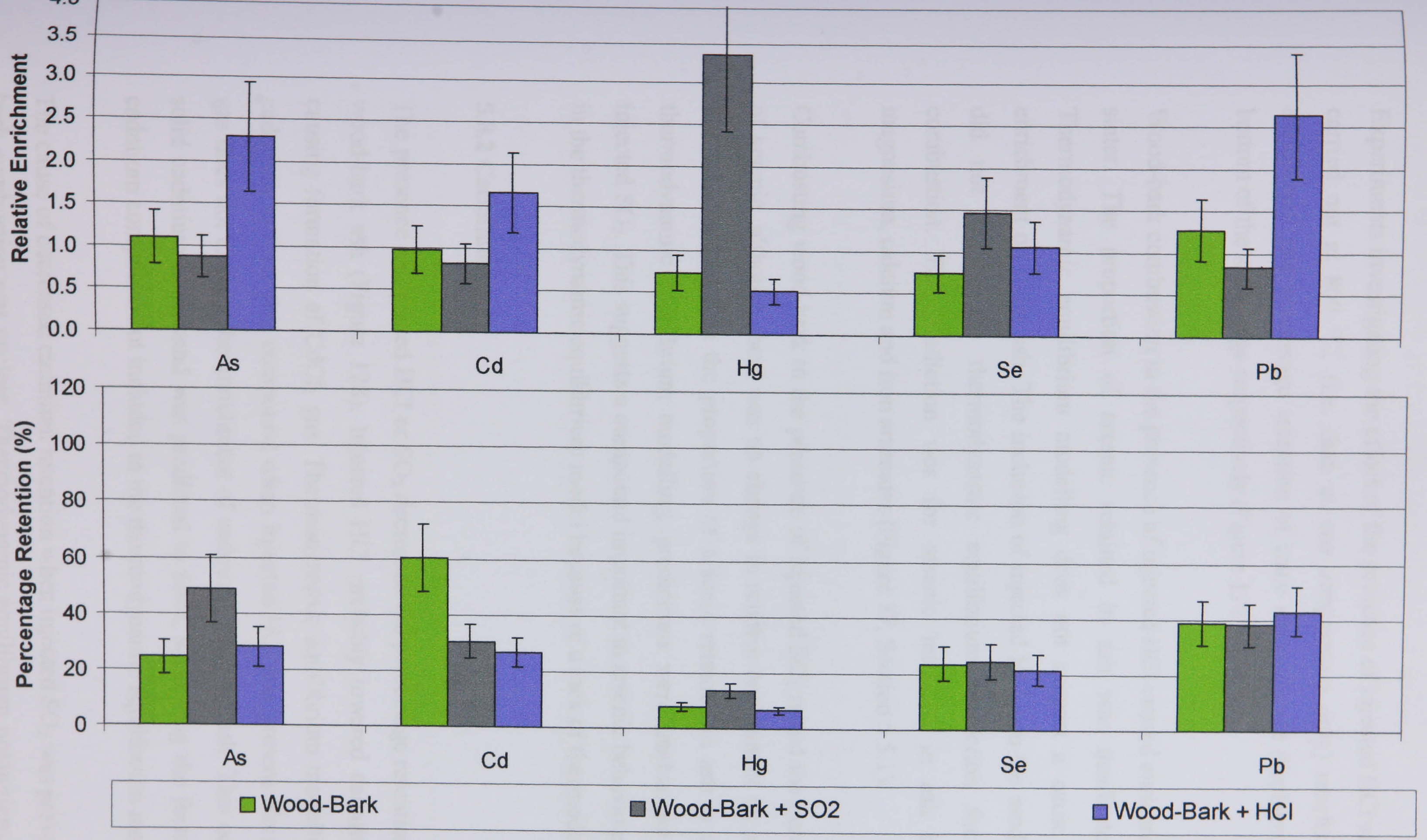
5.8 Combustion of Wood-Bark in the Presence of Injected HCl and SO_2

The behaviour of some trace elements during combustion is thought to be partially dependant on the chlorine and sulphur contents of the fuel. Frandsen et al (1994) and Lim et al (1999) compared thermodynamic equilibrium predictions for trace element species during combustion with, and without, the presence of sulphur and chlorine. The behaviour of some trace elements was influenced through the formation of gaseous chlorides (enhancing volatilisation) or solid sulphate (inhibiting volatilisation) trace element species.

In order to experimentally investigate the effect of the presence of chlorine and sulphur on each trace element, wood-bark, a fuel with low concentrations of both elements (Cl 0.01 %, S 0.07 % daf) was selected. This was burnt in the presence of injected HCl and separately in the presence of injected SO_2. The behaviour of trace elements was compared with the average of that from two blank runs, where wood-bark was combusted without either gas being injected.

Combustion was carried out at a temperature of 800 °C and at an air / fuel ratio of 1.2. In separate experiments, HCl and SO_2 were added to the suspension gas flow to obtain concentrations of approximately 5000 and 3300 ppm respectively. The amount of HCl added during the experiment was equivalent to a chlorine content of 4 % in the wood-bark. When SO_2 was added the amount was equivalent to a sulphur content of 2.5 % in the wood-bark.

Wood-bark was the fuel for all experiments examining the effect of the presence of injected HCl and SO_2 on trace element behaviour. Thus, trace element concentrations in the fuel were the same for all experiments. The only significant source of experimental error was in measuring the trace element concentrations in the ash. In other sections of this thesis percentage retention includes the contribution from the measurement of the raw fuel trace element contents. However, as it is the same for all experiments in this section, here it can be neglected. The calculation of experimental error in percentage retention and relative enrichment is described in section 3.6.



Trace Element Concentration (ppm):	As	Cd	Hg	Se	Pb
Wood-Bark	0.44 ± 0.95	0.20 ± 0.05	0.033 ± 0.001	<0.8	3.1 ± 0.4

Figure 128 The Effect of HCl and SO_2 on the Behaviour of As, Cd, Hg, Se and Pb During Combustion of Wood-Bark at 800 °C

5.8.1 Arsenic

Experiments investigating the effect of the presence of injected HCl and SO_2 were only carried out at 800 °C, (i.e. data at one temperature only) results for the relative enrichment and percentage retention of trace elements are displayed on the top and bottom of the same page respectively (Figure 128).

Wood-bark combustion in the presence of injected HCl caused enrichment of arsenic on sinter. The proportion of arsenic retained in ash was unaffected (Figure 128). Thermodynamic equilibrium modelling does not suggest a cause for the arsenic enrichment on sinter ash. The inclusion of injected HCl into the model for wood-bark did not change the thermodynamic equilibrium prediction for arsenic during combustion. This prediction was for arsenic retention in ash by formation of magnesium, calcium and iron arsenates (Figure 77, Section 5.5.1).

Combusting wood-bark in the presence of injected SO_2 raised the percentage retention of arsenic, although there was no change in relative enrichment on sinter ash (Figure 128). The increase in the proportion of arsenic retained in ash is not explained by thermodynamic equilibrium modelling, predictions were unchanged by inclusion of injected SO_2. This suggests a compound important to arsenic behaviour was not present in the thermodynamic equilibrium model because of a lack of thermodynamic data.

5.8.2 Cadmium

The presence of injected HCl or SO_2 decreased the percentage retention of cadmium in wood-bark ash (Figure 128). Injected HCl probably lowered cadmium retention by causing formation of $CdCl_2$ gas. Thermodynamic equilibrium modelling predicted all cadmium to form this compound when injected HCl was present. Formation of $CdCl_2$ gas does not explain the enrichment of cadmium on sinter ash. This occurred when no solid cadmium compound was predicted to form, suggesting the formation of a solid cadmium compound not included in the thermodynamic equilibrium model.

The cause of decreased cadmium retention when injected SO_2 was present during wood-bark combustion was unclear. Thermodynamic equilibrium predictions suggested there

would have been a slight increase in cadmium retention when SO_2 was injected due to recondensation of cadmium sulphate on sinter ash (Figure 129).

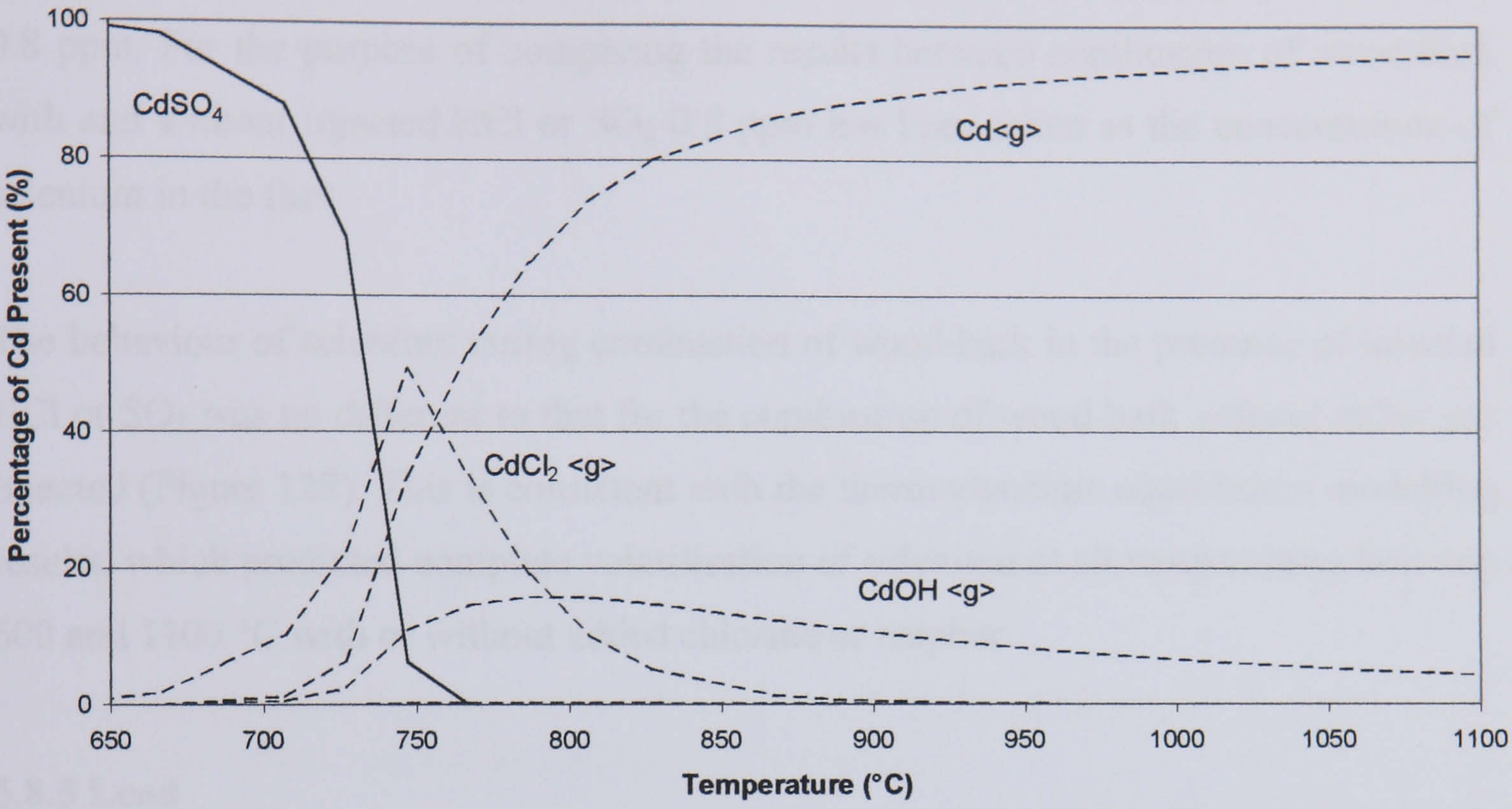


Figure 129 Thermodynamic Equilibrium Prediction for Cadmium During Wood-Bark Combustion in the Presence of Injected Sulphur Dioxide

5.8.3 Mercury

The presence of injected HCl during combustion of wood-bark made no measurable change to the behaviour of mercury (Figure 128). This is consistent with the thermodynamic equilibrium prediction for mercury to completely volatilise with or without injection of HCl.

Injection of SO_2 during combustion of wood-bark marginally increased the retention of mercury, but highly increased its relative enrichment on sinter ash (Figure 128). This was probably not due to mercury capture by carbon, as the sample was 100.0 ± 0.1 % ash. Neither this result nor the HCl result were predicted by thermodynamic equilibrium modelling, suggesting an unknown mercury compound has formed.

5.8.4 Selenium

The selenium concentration in the raw wood-bark was below the limit of quantification, 0.8 ppm. For the purpose of comparing the results between combustion of wood-bark with and without injected HCl or SO_2 0.8 ppm has been taken as the concentration of selenium in the fuel.

The behaviour of selenium during combustion of wood-bark in the presence of injected HCl or SO_2 was no different to that for the combustion of wood-bark without either gas injected (Figure 128). This is consistent with the thermodynamic equilibrium modelling results, which predicted complete volatilisation of selenium at all temperatures between 600 and 1100 °C with or without added chlorine or sulphur.

5.8.5 Lead

Thermodynamic equilibrium modelling predicted the presence of injected HCl to volatilise all of the lead as $PbCl_2$ gas at temperatures between 650 and 1100 °C. There was no reduction in lead retention in ash when HCl was injected (Figure 128). This suggests that all of the lead that could possibly be volatilised was lost from the wood-bark without HCl injection. Lead that remained with the ash was probably contained in modes of occurrence from which it could not be released during combustion.

Lead enriched on sinter ash when wood-bark was combusted in the presence of injected HCl gas. This is not explained by thermodynamic equilibrium models, which predicted all lead to be gaseous. This result suggests an unknown solid lead compound formed.

Combustion of wood-bark in the presence of injected SO_2 had no measurable difference to the behaviour of lead. This was unexpected; thermodynamic equilibrium predictions suggested that more lead should have been retained on ash because of the formation of lead sulphate, a solid (Figure 130). Possibly another volatile lead compound not included in the thermodynamic equilibrium model has formed instead of $PbSO_4$, preventing an increase in lead retention.

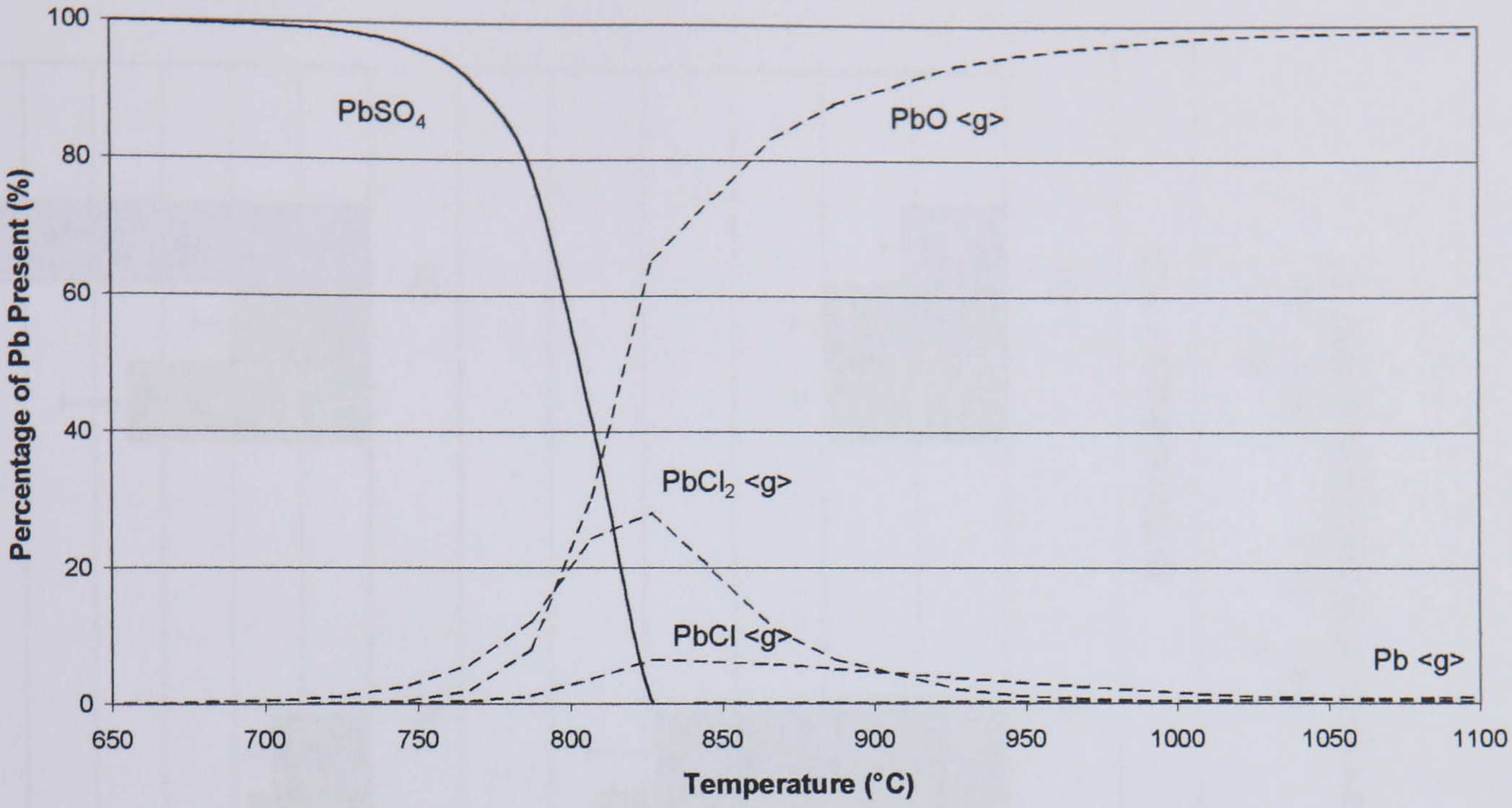
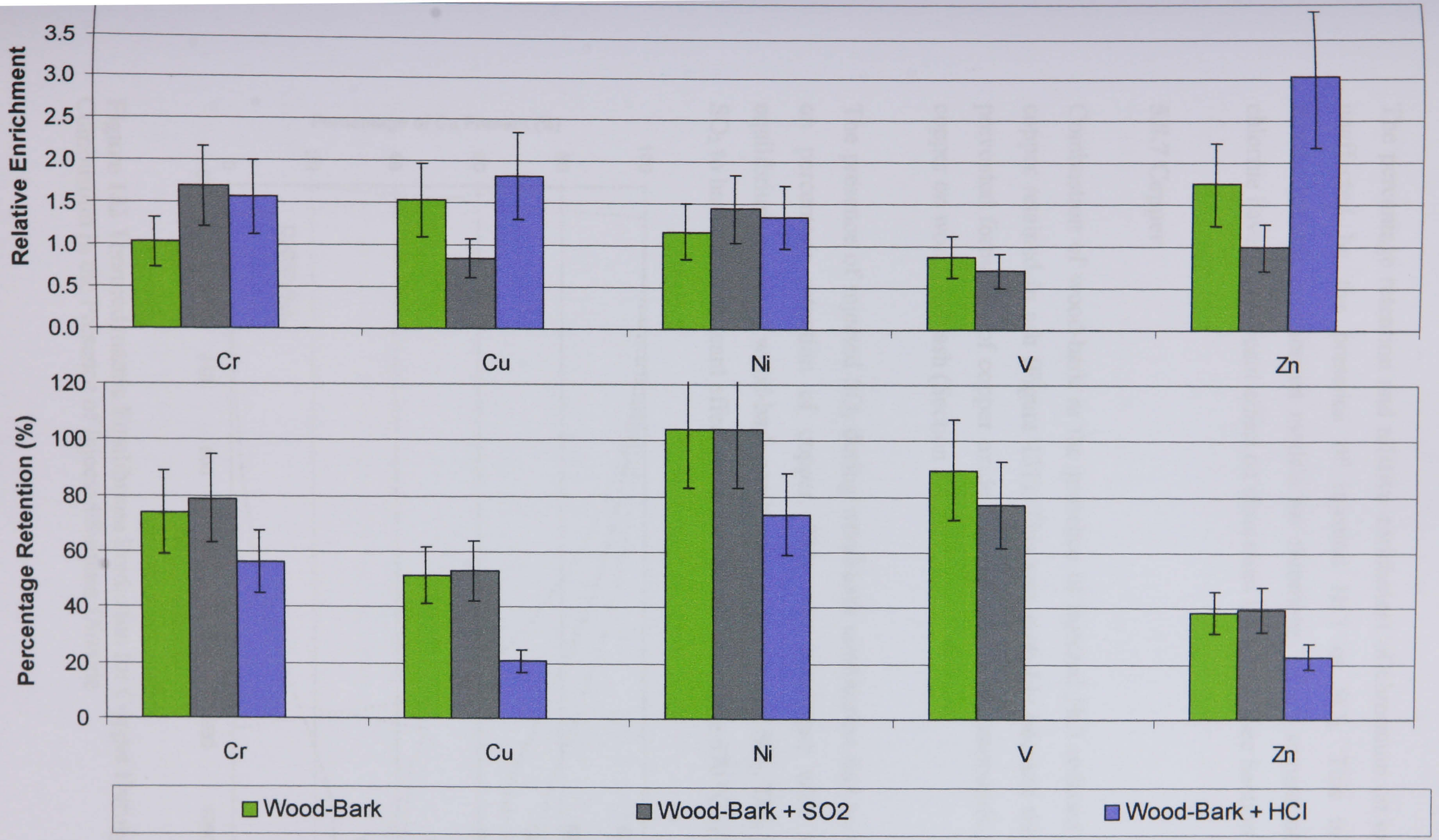


Figure 130 Thermodynamic Equilibrium Prediction for Lead During Wood-Bark Combustion in the Presence of Injected Sulphur Dioxide



Trace Element Concentration (ppm):	Cr	Cu	Ni	V	Zn
Wood-Bark	26 ± 5	87 ± 37	10 ± 2	2.8 ± 0.6	150 ± 21

Figure 131 The Effect of HCl and SO_2 on the Behaviour of Cr, Cu, Ni, V and Zn During Combustion of Wood-Bark at 800 °C

5.8.6 Chromium

The percentage retention and relative enrichment of chromium on wood-bark ash was unaffected by the presence of injected HCl or SO_2. This is consistent with thermodynamic equilibrium models for chromium, which suggest neither sulphur nor chlorine have a significant effect on chromium behaviour (see Section 5.56).

5.8.7 Copper

Combustion of wood-bark in the presence of injected HCl reduced the proportion of copper retained in ash (Figure 131). This was probably because the injection of HCl prevented formation of copper oxide and copper – iron compounds, which may retain copper on wood-bark ash (Section 5.5.7).

The presence of injected SO_2 during wood-bark combustion had no measurable effect on percentage retention of copper. This was consistent with a thermodynamic equilibrium model of wood-bark combustion with injected SO_2. This predicted injected SO_2 to have no significant effect on copper behaviour above 670 °C (Figure 132).

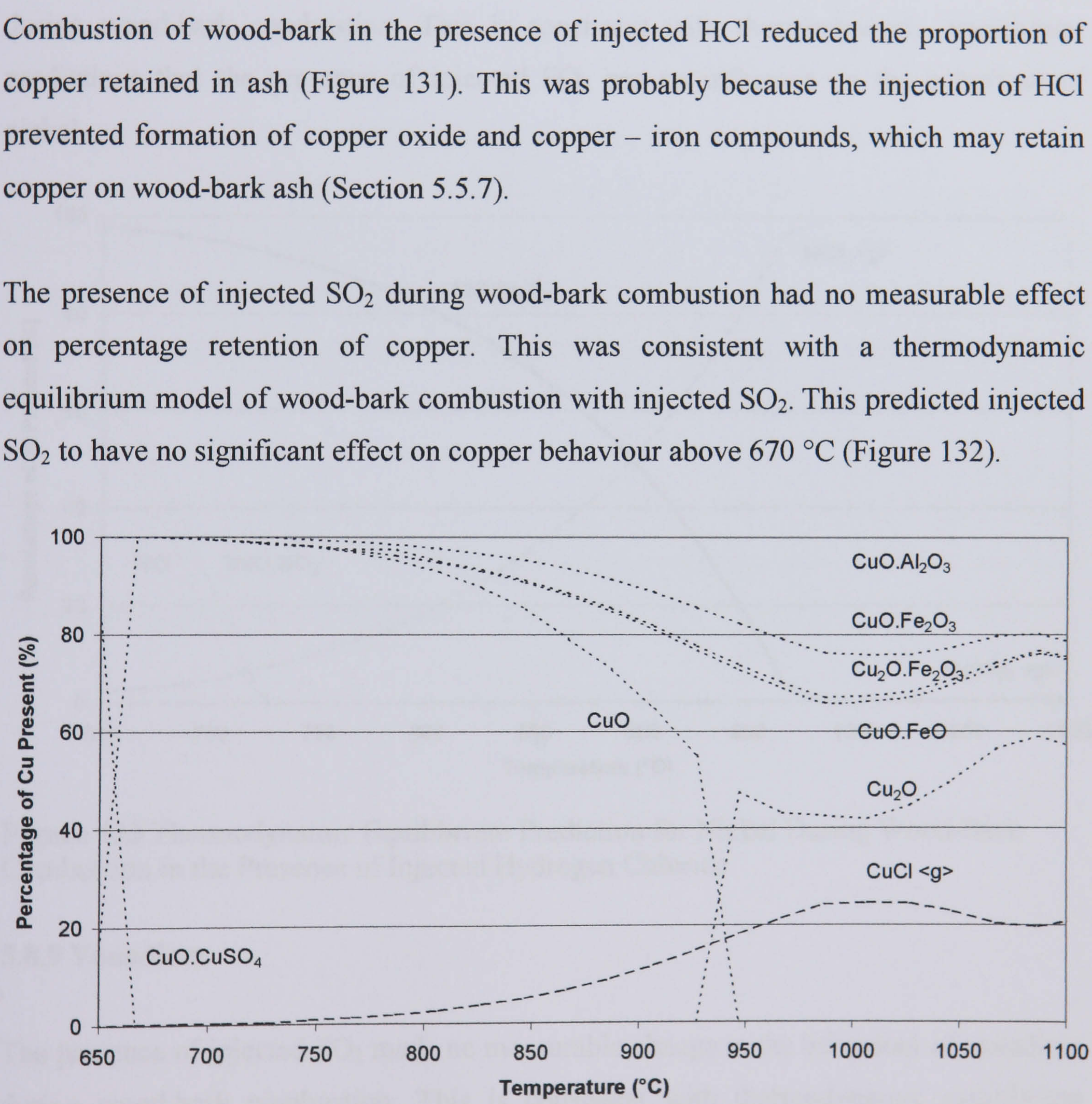


Figure 132 Thermodynamic Equilibrium Prediction for Copper During Wood-Bark Combustion in the Presence of Injected Sulphur Dioxide

5.8.8 Nickel

Combustion of wood-bark in the presence of injected HCl or SO_2 did not alter the retention of nickel in ash outside the range of experimental error (Figure 131). Thermodynamic equilibrium modelling of wood-bark combustion in the presence of injected HCl (Figure 133) suggest that around 20 % of the nickel would be volatilised. This may have occurred, but cannot be distinguished due to experimental error.

Nickel was almost completely retained in ash regardless of whether SO_2 was injected during wood-bark combustion. This is consistent with thermodynamic equilibrium predictions that the presence of injected SO_2 has no influence on the behaviour of nickel.

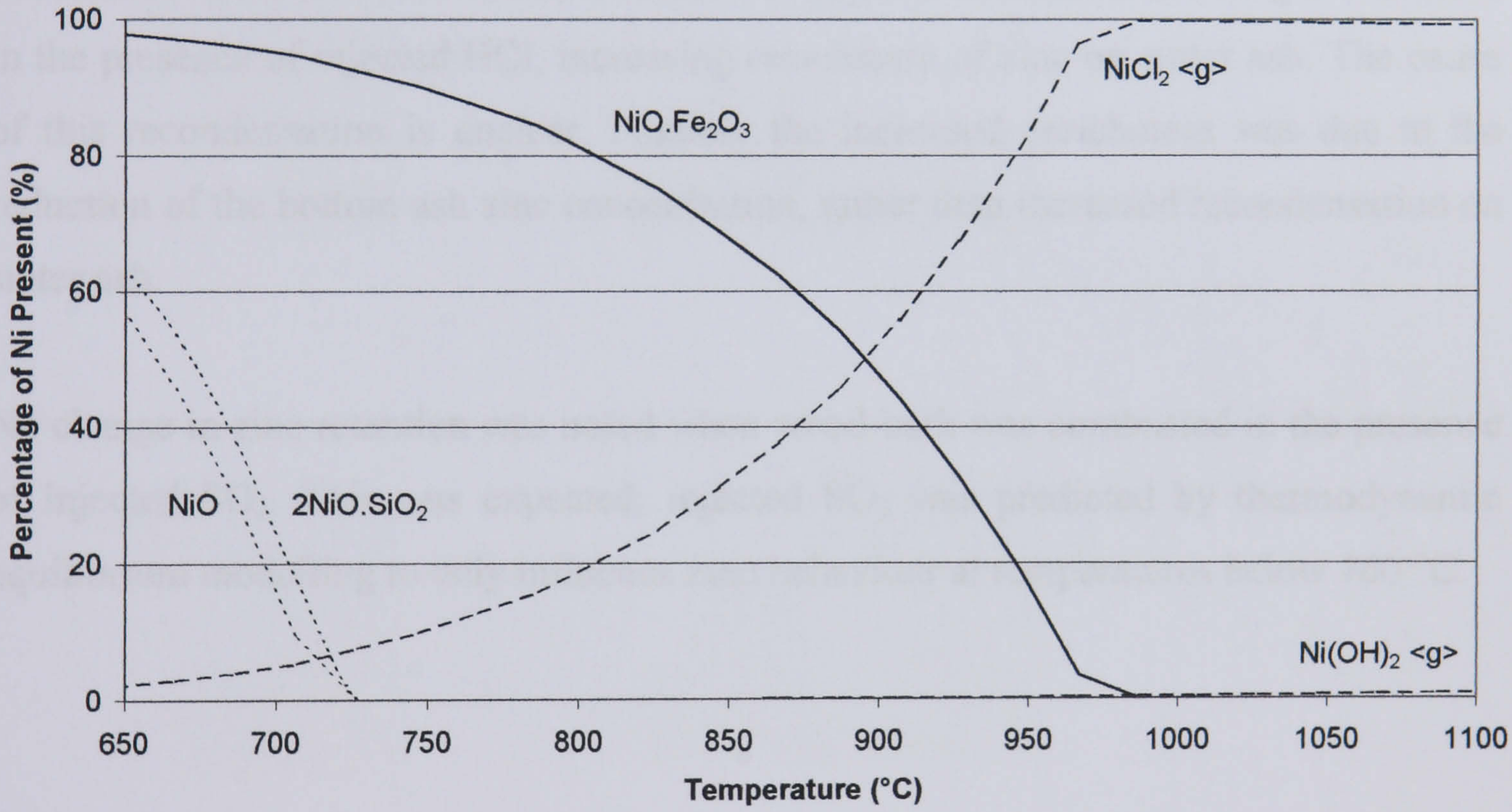


Figure 133 Thermodynamic Equilibrium Prediction for Nickel During Wood-Bark Combustion in the Presence of Injected Hydrogen Chloride

5.8.9 Vanadium

The presence of injected SO_2 made no measurable change to the behaviour of vanadium during wood-bark combustion. This is consistent with thermodynamic equilibrium predictions that also showed SO_2 injection to have no influence of on vanadium behaviour.

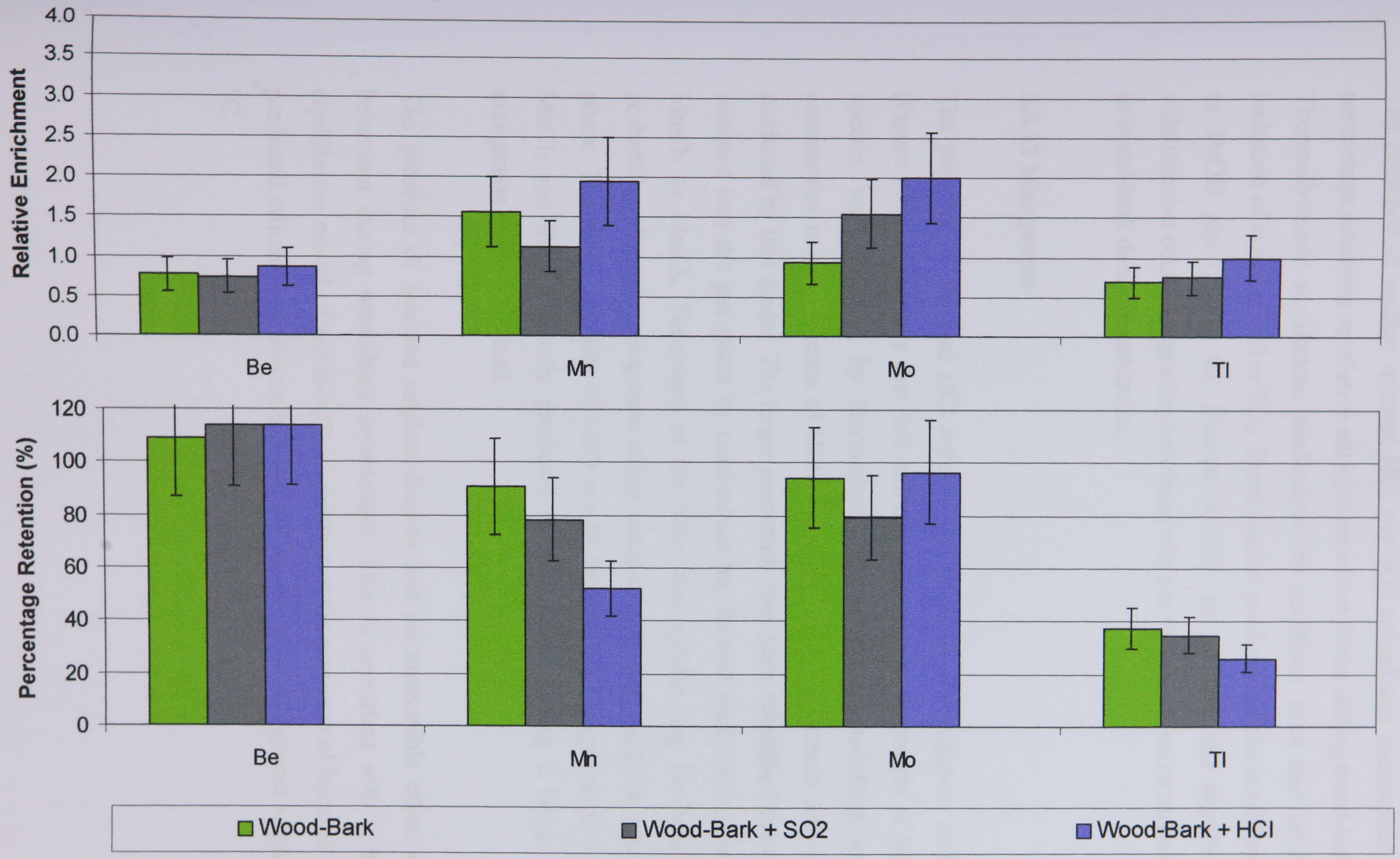
No results have been reported in the present study for vanadium during combustion of wood-bark in the presence of injected HCl, because of analytical error in measuring the concentration of vanadium in this ash sample.

5.8.10 Zinc

Combustion of wood-bark in the presence of injected HCl decreased zinc retention in ash (Figure 131). It is likely that the increased volatilisation was caused by formation of $ZnCl_2$ gas. In the presence of injected HCl, thermodynamic equilibrium modelling predicted all zinc to form $ZnCl_2$ at temperatures between 650 and 1100 °C.

Most of the zinc that remained in the ash was probably not released from its mode of occurrence in the raw fuel. A small amount of zinc has recondensed during combustion in the presence of injected HCl, increasing enrichment of zinc on sinter ash. The cause of this recondensation is unclear. Possibly the increased enrichment was due to the reduction of the bottom ash zinc concentration, rather than increased recondensation on sinter ash.

No change in zinc retention was noted when wood-bark was combusted in the presence of injected SO_2. This was expected; injected SO_2 was predicted by thermodynamic equilibrium modelling to only influence zinc behaviour at temperatures below 760 °C.



Trace Element Concentration (ppm):	Be	Mn	Mo	Tl
Wood-Bark	0.07 ± 0.01	414 ± 68	1.3 ± 0.4	0.09 ± 0.03

Figure 134 The Effect of HCl and SO_2 on the Behaviour of Be, Mn, Mo and Tl During Combustion of Wood-Bark at 800 °C

5.8.11 Beryllium

The presence of neither injected HCl nor SO_2 caused any measurable change to the percentage retention or relative enrichment of beryllium during wood-bark combustion. Thermodynamic equilibrium predictions for beryllium were also unchanged by the inclusion of injected HCl or SO_2. These models predicted partial beryllium volatilisation as BeOH gas (Figure 91, Section 5.5.11). In no case did significant beryllium volatilisation occur, suggesting beryllium was not released from its modes of occurrence in wood-bark during combustion.

5.8.12 Manganese

The presence of injected HCl reduced the retention of manganese in wood-bark ash (Figure 134). It is likely that this reduction was due to formation of $MnCl_2$ gas. This species was predicted by thermodynamic equilibrium modelling to form during combustion in the presence of HCl. However, more manganese was volatilised than predicted by this model. The larger proportion may have volatilised because manganese released into the gas phase by combustion has formed MnO instead of the predicted Mn_2O_3 or Mn_3O_4. Formation of the latter two species may be limited by the low probability of single manganese atoms encountering each other for reaction in the gas phase. The lower stability of MnO would allow more manganese to be converted to $MnCl_2$ gas than originally predicted (Figure 135), causing a larger proportion of manganese to be volatilised.

The presence of injected sulphur dioxide had no measurable effect on manganese behaviour during wood-bark combustion. This is consistent with a thermodynamic equilibrium model of wood-bark combustion in the presence of injected SO_2. The only predicted influence of SO_2 on Mn was the formation of manganese sulphate below 700 °C.

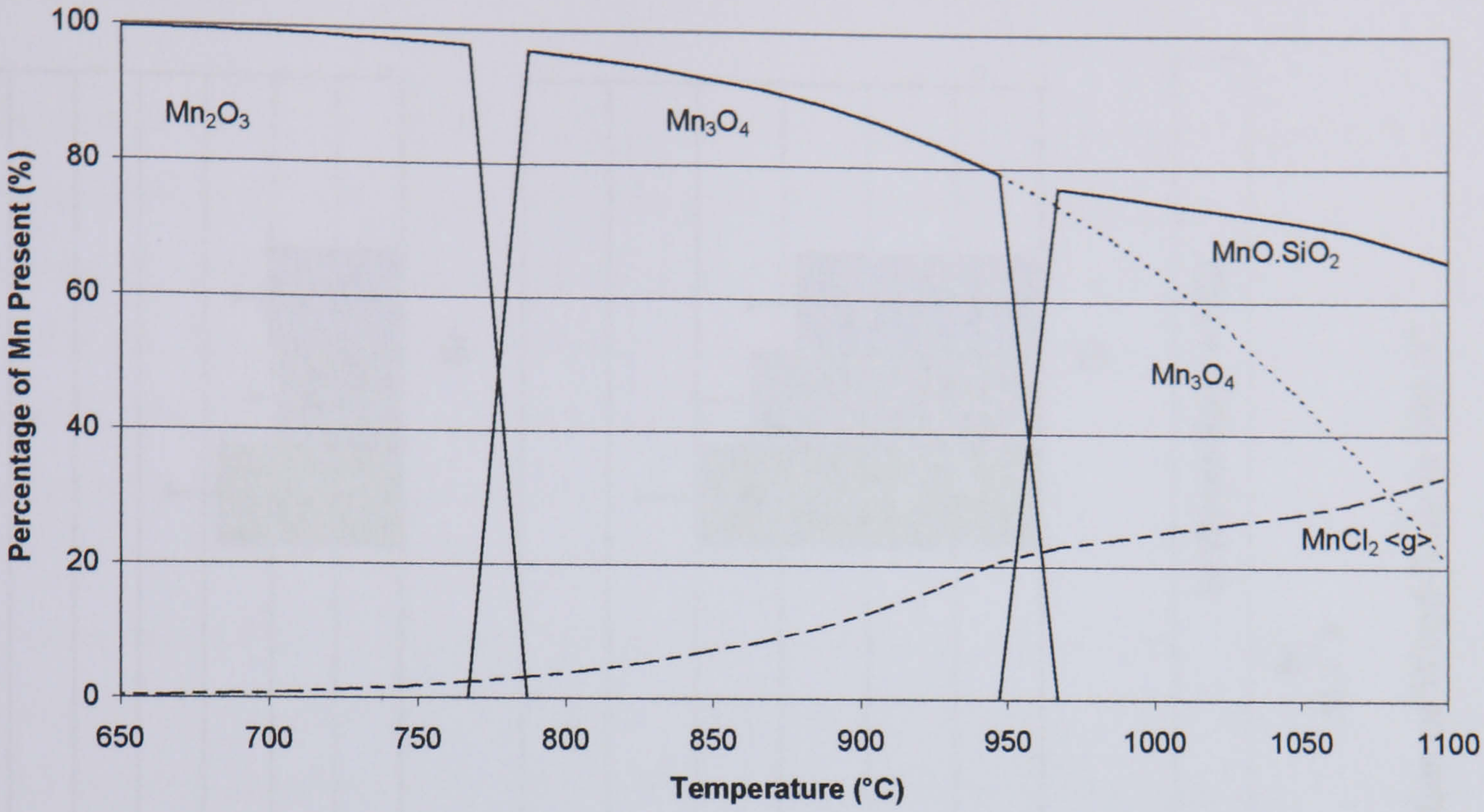


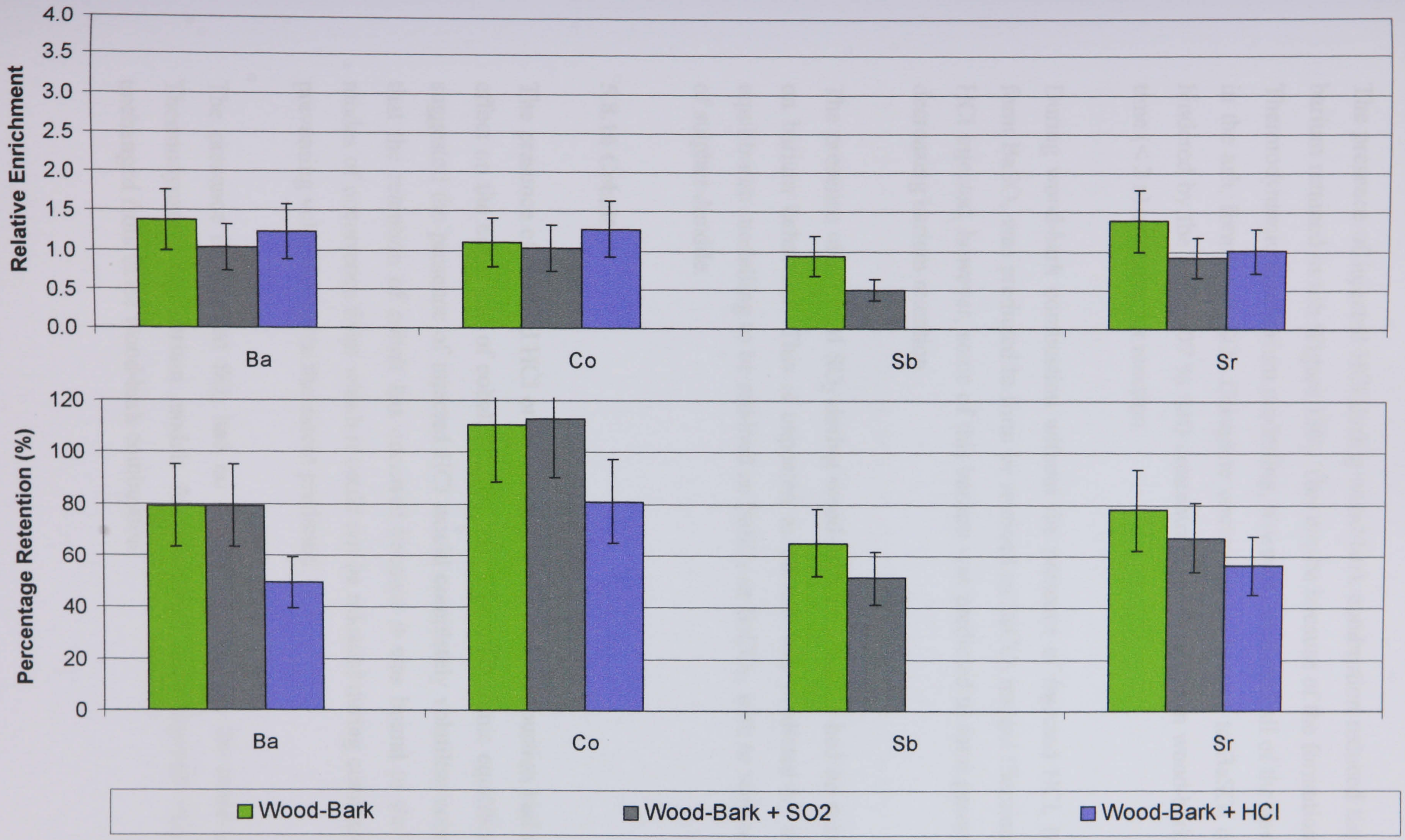
Figure 135 Thermodynamic Equilibrium Prediction for Manganese During Wood-Bark Combustion in the Presence of Injected Hydrogen Chloride

5.8.13 Molybdenum

The presence of injected HCl or SO_2 made no measurable difference to the proportion of molybdenum retained on wood-bark ash (Figure 134). Injected HCl has influenced molybdenum behaviour, causing its enrichment on sinter ash. Due to a lack of thermodynamic data for molybdenum compounds in the database, it is not possible to suggest any cause of this result.

5.8.14 Thallium

The behaviour of thallium in wood-bark was not influenced by the presence of either injected HCl or SO_2 during combustion. Regardless of whether injected HCl or SO_2 were present, thermodynamic equilibrium modelling predicted thallium to be completely volatilised. It is likely that the 20 – 45 % of thallium remaining in the ash was not released from its mode of occurrence in the wood-bark.



Trace Element Concentration (ppm):	Ba	Co	Sb	Sr
Wood-Bark	156 ± 14	0.72 ± 0.06	0.21 ± 0.10	51 ± 4

Figure 136 The Effect of HCl and SO_2 on the Behaviour of Ba, Co, Sb and Sr During Combustion of Wood-Bark at 800 °C

5.8.15 Barium

The presence of injected HCl during wood-bark combustion reduced the proportion of barium retained in ash (Figure 136). This maybe because of the formation of $BaCl_2$ gas. Thermodynamic equilibrium modelling, however, predicted all of the barium to remain in the ash, forming $BaSO_4$. Complete conversion of barium to $BaSO_4$ may have been hindered by the low (0.07 % daf) concentration of sulphur in wood-bark and the short time (< 2 s) available for reaction.

During wood-bark combustion without the presence of injected HCl, barium did not form $BaSO_4$ was predicted to form be retained as $BaCO_3$ instead (Section 5.5.15). With HCl injected, however, some of this barium was predicted to form gaseous $BaCl_2$, thus decreasing barium retention.

The presence of injected SO_2 during wood-bark combustion had no measurable effect on barium behaviour. This is expected as barium was predicted by thermodynamic equilibrium modelling to be retained as $BaSO_4$ or $BaCO_3$, with or without the injection of sulphur dioxide.

5.8.16 Cobalt

The presence of injected HCl or SO_2 during wood-bark combustion had no measurable effect on the behaviour of cobalt (Figure 136). Thermodynamic equilibrium modelling suggested the presence of injected HCl would completely volatilise cobalt. It is likely that the retention of cobalt has occurred because it was bound to the wood-bark in modes of occurrence from which it could not be released during combustion, therefore preventing volatilisation to the extent predicted.

The presence of injected SO_2 had no significant effect on the behaviour of cobalt. Thermodynamic equilibrium models for wood-bark with injected SO_2, which were unchanged from those wood-bark combustion.

5.8.17 Antimony

The presence of injected SO_2 during wood-bark combustion made no measurable difference to the behaviour of antimony. A slight increase in antimony retention was predicted by thermodynamic equilibrium modelling, but this difference was smaller than experimental error in the measurement of percentage retention.

No results have been reported in the present study for antimony during combustion of wood-bark in the presence of injected HCl (Figure 136). This is due to analytical error in determining the antimony content of the bottom ash sample.

5.8.18 Strontium

The influence of injected HCl or SO_2 on strontium retention in ash after the combustion of wood-bark was not measurable (Figure 136). This is consistent with thermodynamic equilibrium models for strontium, which predicted no change in the behaviour of strontium when either gas is injected.

5.9 NOx AND N_2O EMISSIONS FROM CO-COMBUSTION

Nitrogen oxide emissions from co - combustion in the suspension reactor have been measured. Main fuels (Polish coal, Colombian coal, Colombian coal / straw and wood - bark) were combusted on their own and blended with various auxiliary fuels. Where a combination of fuels was co – combusted, blends were prepared with 10, 20 or 30 % of the total calorific value of the blend supplied by the auxiliary fuel. The weight fraction of auxiliary fuel in these blends is presented in Table 14.

Table 14 Weight Fractions of Auxiliary Fuels in Combusted Blends

		Proportion of Auxiliary Fuel in Blend (Energy Basis)		
Main Fuel	Auxiliary Fuel	10%	20%	30%
Polish Coal	Sewage Sludge	0.252	0.431	0.564
Colombian Coal	Paper Sludge	0.134	0.259	0.375
Colombian Coal / Straw	Paper Sludge	0.105	0.208	0.311
Wood-Bark	Agricultural Waste	0.116	0.229	0.337
Wood-Bark	Pulp Sludge	0.102	0.204	0.305
Wood-Bark	Plastic Waste	0.065	0.136	0.213

Note: Colombian Coal / Straw is a 50:50 energy basis mixture of these fuels (37:63 on weight basis)

Each fuel blend was combusted in the suspension-firing reactor at 800 and 900 °C. The rate of fuel addition was controlled to ensure an air / fuel ratio of 1.2 (see section 3.3.7) with the oxygen in the 5 lpm flow of suspension air (BOC zero grade). A 0.5 lpm flow of nitrogen (BOC oxygen free) was used to push the feed down the feeder tube. These conditions were the same as used in the experiments on trace element behaviour (Section 3.2). Flue gas samples from the suspension-firing reactor were dried using a packed bed of magnesium perchlorate before analysis. NOx and N_2O concentrations in the flue gas were unchanged by this treatment.

NOx emitted from the reactor was measured by chemi-luminescence in a Signal Series 4000 NOx meter. Samples for N_2O analysis were analysed immediately (< 10 s) in a dedicated gas chromatograph (Carlo Erba Strumentazione Frato Vap 4160). Rapid

analysis avoided N_2O generation by NO, SO_2 and H_2O prior to analysis (Muzio and Kramlich, 1988). The oxygen content of the flue gas was measured using a Telegan Tempest fuel cell based analyser. All of these measurement techniques have been described in Section 3.3.3.

Concentrations of NOx have been expressed in this study in units of milligrams of NO_2 per normal cubic meter of flue gas (mg/Nm^3), as per EU directive (2000 / 76 / EC). To calculate this value all NOx was counted as its ultimate oxidation product, NO_2. Most NOx measured was probably actually NO. NO_2 is formed by the oxidation of NO, a reaction that occurs slowly. Nitrous oxide concentrations have been reported as milligrams of N_2O per normal cubic meter of flue gas (mg/Nm^3).

Combustion at a 1.2 air / fuel ratio resulted in oxygen concentrations in the flue gas of approximately 4 %. This varied slightly with the fuel ultimate analysis. Where the flue gas oxygen concentration was higher than this value, NOx and N_2O concentrations would have been diluted by extra oxygen and nitrogen, compared to those obtained with 4 % oxygen in flue gas. The reverse would have been true when the oxygen concentration was below this level. To allow comparison of results obtained at different flue gas oxygen contents all results have been converted to the basis of 6 % oxygen in flue gas.

Results presented for NOx emissions are average values from between two and six measurements, usually taken from more than one experimental run. The experimental error in these average values has been estimated at ± 15 % for Polish coal, Colombian coal, Colombian coal / straw and blends containing these main fuels. A higher experimental error of ± 20 % has been estimated for wood-bark and wood-bark containing blends, due to greater fluctuations in measured NOx levels when this fuel was burnt. Estimates of experimental error were based the 95 % confidence interval of five or more measurements of NOx emissions from the main fuels.

Analysis of the N_2O concentrations in flue gas takes much longer than NOx measurements; therefore fewer determinations of N_2O could be made during an experimental run. For N_2O individual data points have been plotted, and the

experimental error in their measurement has been estimated at ± 25 % from fuels where multiple measurements were made.

5.9.1 Polish Coal and Sewage Sludge Blends

NOx emissions from co-combustion of Polish coal / sewage sludge blends at 800 °C were similar to those from combustion of Polish coal on its own at this temperature (Figure 137). Raising the combustion temperature to 900 °C changed emissions little, except for increasing those from the 70 % Polish coal / 30 % sewage sludge blend.

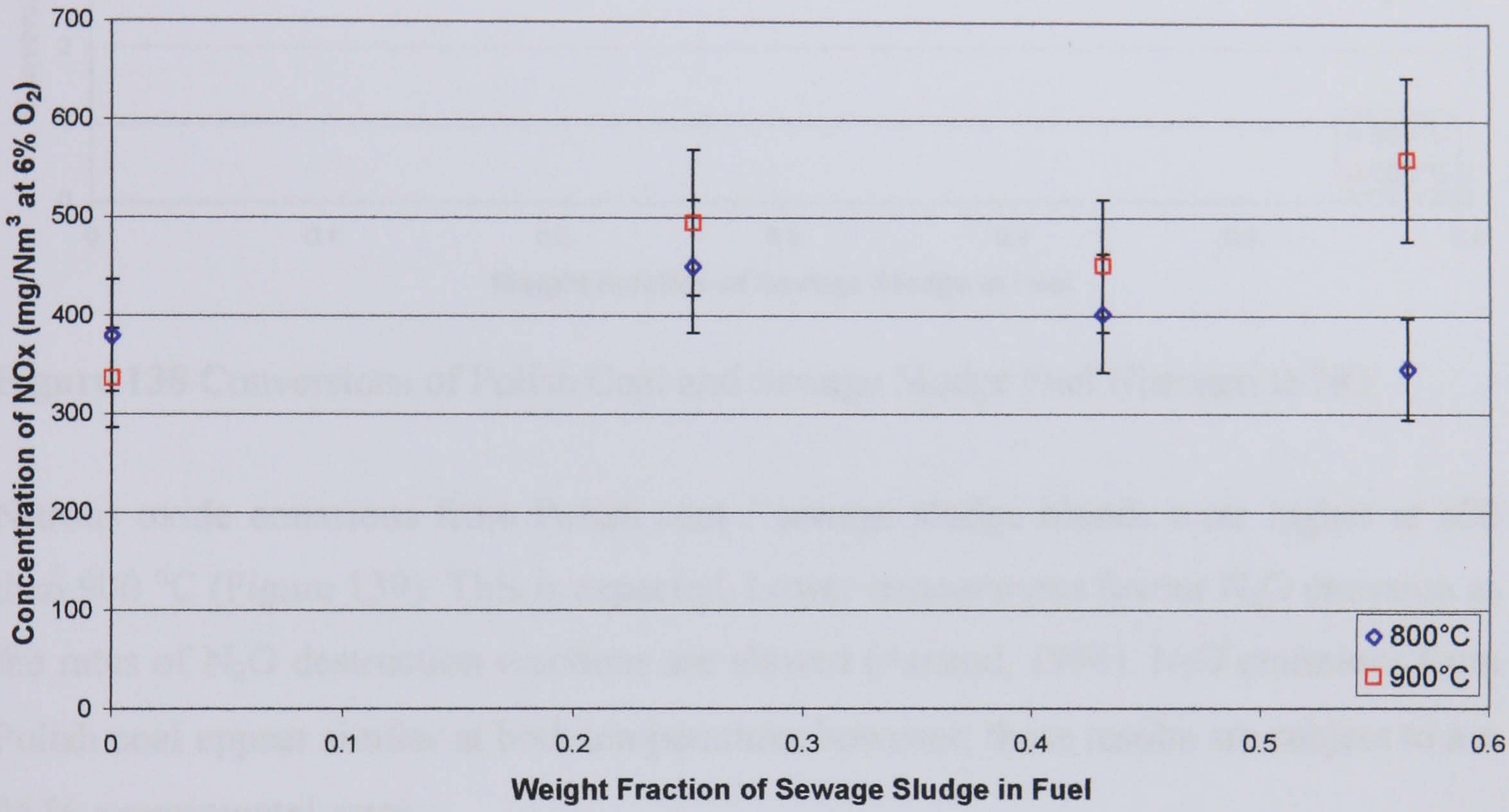


Figure 137 NOx Emissions from Polish Coal and Sewage Sludge Co-Combustion

NOx emissions from the Polish coal / sewage sludge blends was not proportional to their fuel nitrogen content. Conversion of fuel nitrogen to NO fell with sewage sludge addition (Figure 138). These results suggest that between 6 – 7 % of the nitrogen in Polish coal became NOx, while only 2 – 4 % of that derived from sewage sludge was converted.

The low conversion of sewage sludge fuel nitrogen to NO could be related to this fuel's high volatile matter content (93.5 % daf) and loose, open structure. Sewage sludge entering the combustion zone of the suspension-firing reactor would have quickly heated and devolatilised. This would have created a concentrated fuel rich cloud. Here

sewage sludge NO could be reduced by reaction with CO and other devolatilisation products, hence reducing conversion of fuel nitrogen to NO.

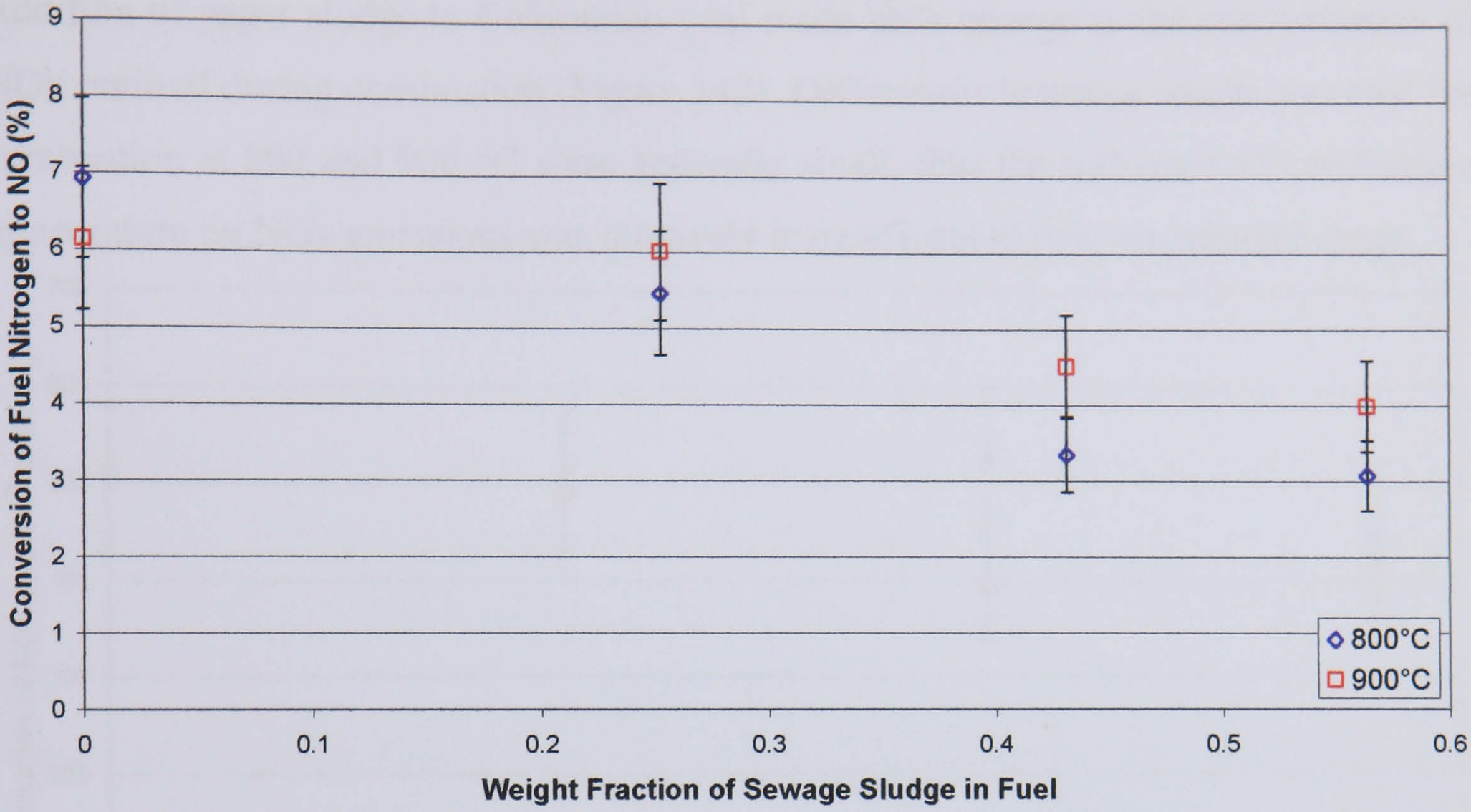


Figure 138 Conversions of Polish Coal and Sewage Sludge Fuel Nitrogen to NO

Nitrous oxide emissions from Polish coal / sewage sludge blends were higher at 800 than 900 °C (Figure 139). This is expected. Lower temperatures favour N_2O emission as the rates of N_2O destruction reactions are slowed (Amand, 1994). N_2O emissions from Polish coal appear similar at both temperatures however; these results are subject to a ± 25 % experimental error.

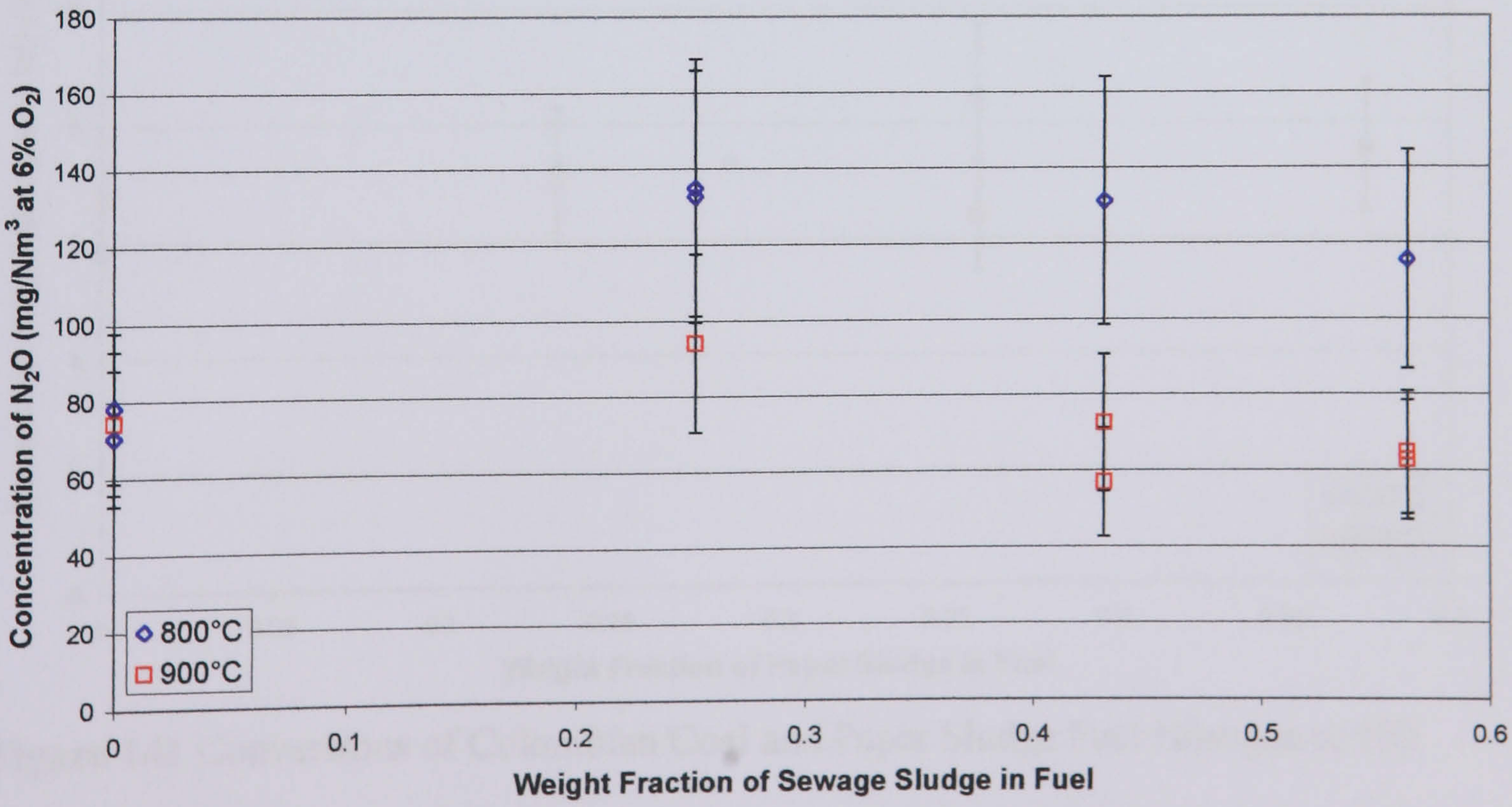


Figure 139 N_2O Emissions from Polish Coal and Sewage Sludge Co-Combustion

5.9.2 Colombian Coal and Paper Sludge Blends

Addition of paper sludge to Colombian coal made little change to the concentration of NOx emitted during combustion (Figure 140). Differences between results reported for combustion at 800 and 900 °C were generally small, thus the influence of combustion temperature on NOx emissions was relatively insignificant in this temperature range.

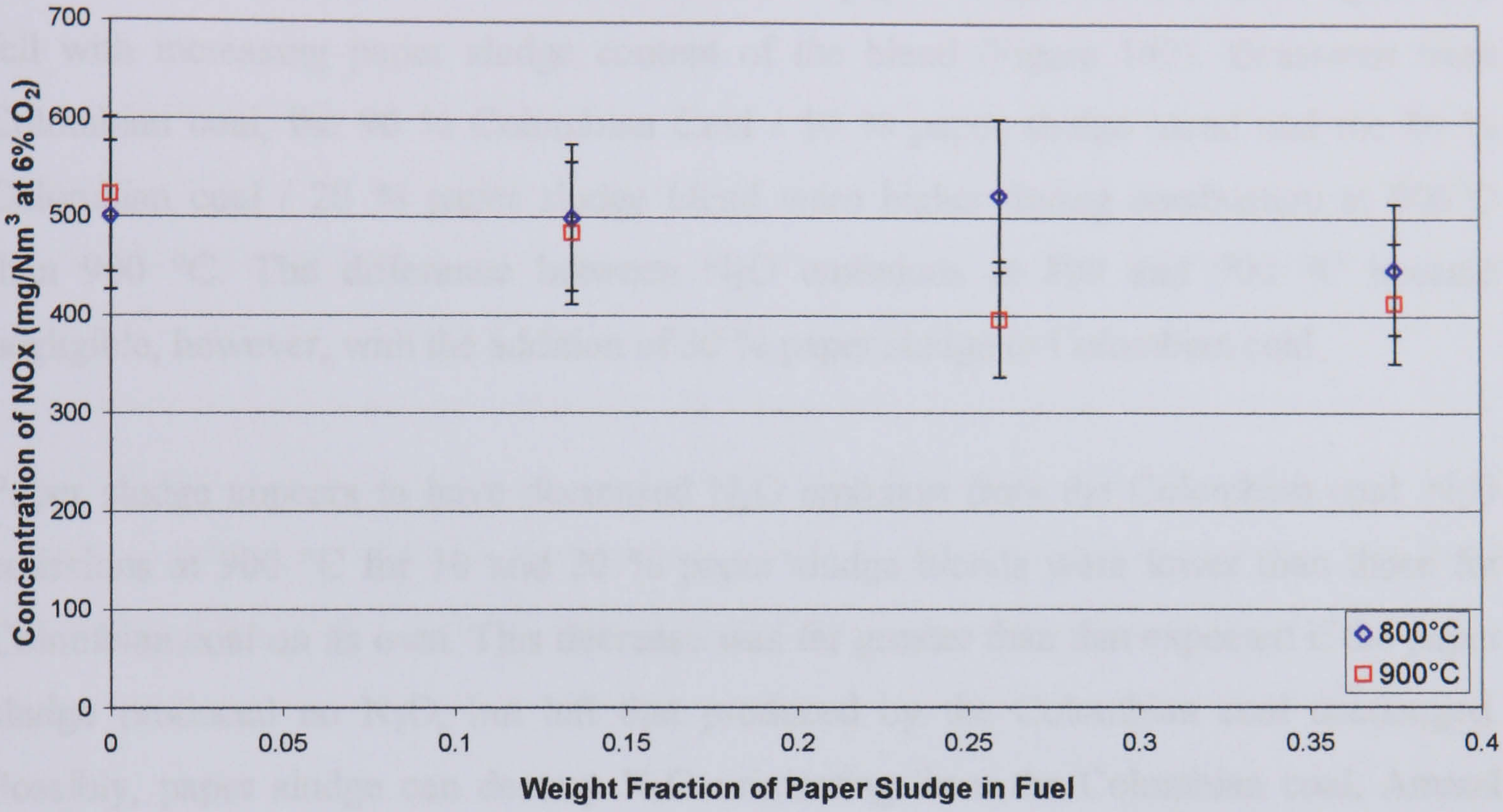


Figure 140 NOx Emissions from Colombian Coal and Paper Sludge Co-Combustion

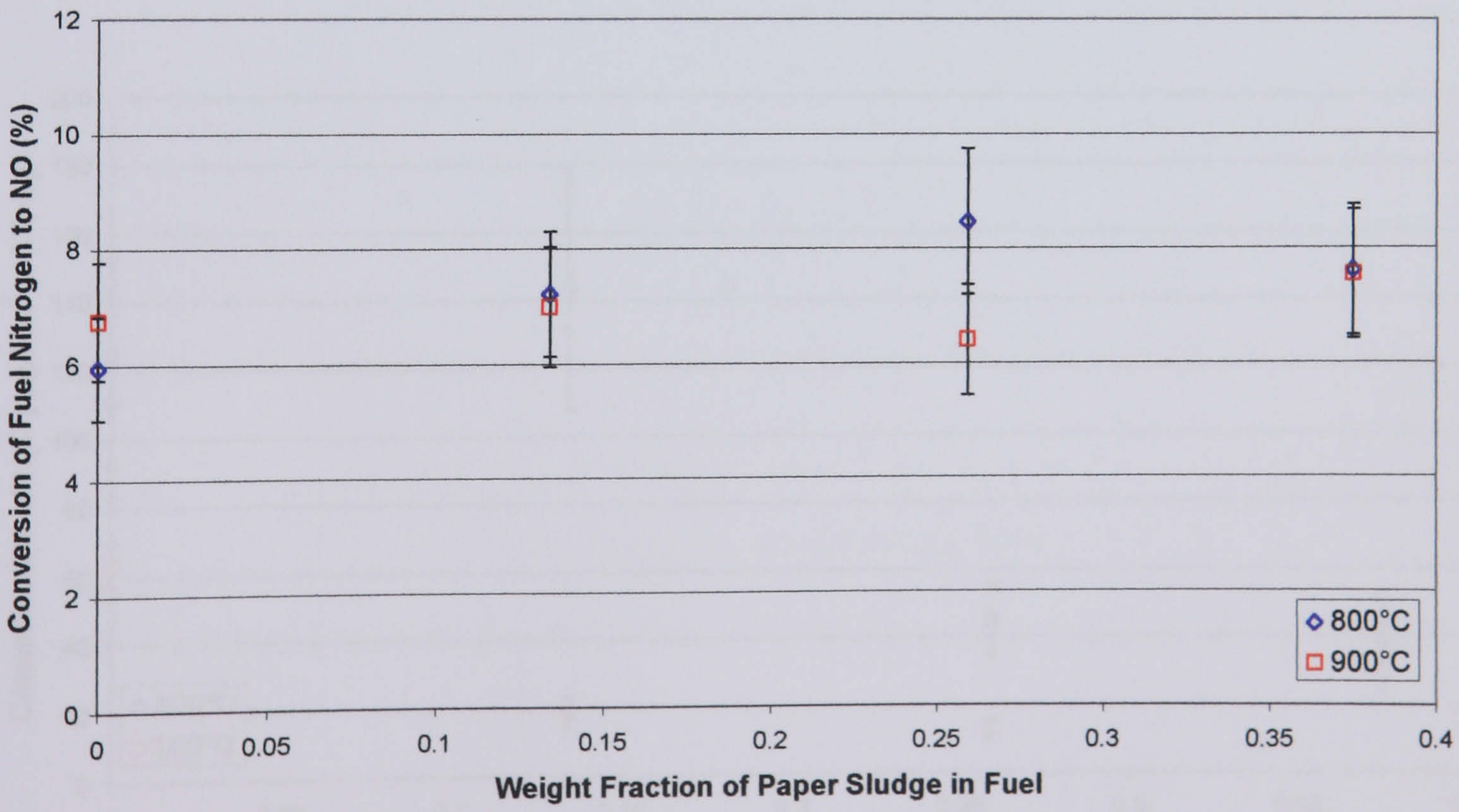


Figure 141 Conversions of Colombian Coal and Paper Sludge Fuel Nitrogen to NO

The proportion of fuel nitrogen from Colombian coal / paper sludge blends converted to NO was similar for all blend compositions (Figure 141). Extrapolating the conversion of fuel nitrogen to the case of burning only paper sludge suggests, 7 - 9 % of paper sludge fuel nitrogen was converted to NO during combustion.

Nitrous oxide emissions from Colombian coal / paper sludge co-combustion generally fell with increasing paper sludge content of the blend (Figure 142). Emissions from Colombian coal, the 90 % Colombian Coal / 10 % paper sludge blend and the 80 % Colombian coal / 20 % paper sludge blend were higher during combustion at 800°C than 900 °C. The difference between N_2O emissions at 800 and 900 °C became negligible, however, with the addition of 30 % paper sludge to Colombian coal.

Paper sludge appears to have decreased N_2O emission from the Colombian coal. N_2O emissions at 900 °C for 10 and 20 % paper sludge blends were lower than those for Colombian coal on its own. This decrease was far greater than that expected if the paper sludge produced no N_2O, but left that produced by the Colombian coal unchanged. Possibly, paper sludge can destroy N_2O originating from the Colombian coal, Amand (1993) found wood, the parent material of the paper sludge, could do to N_2O added to the primary air of a fluidised bed combustor.

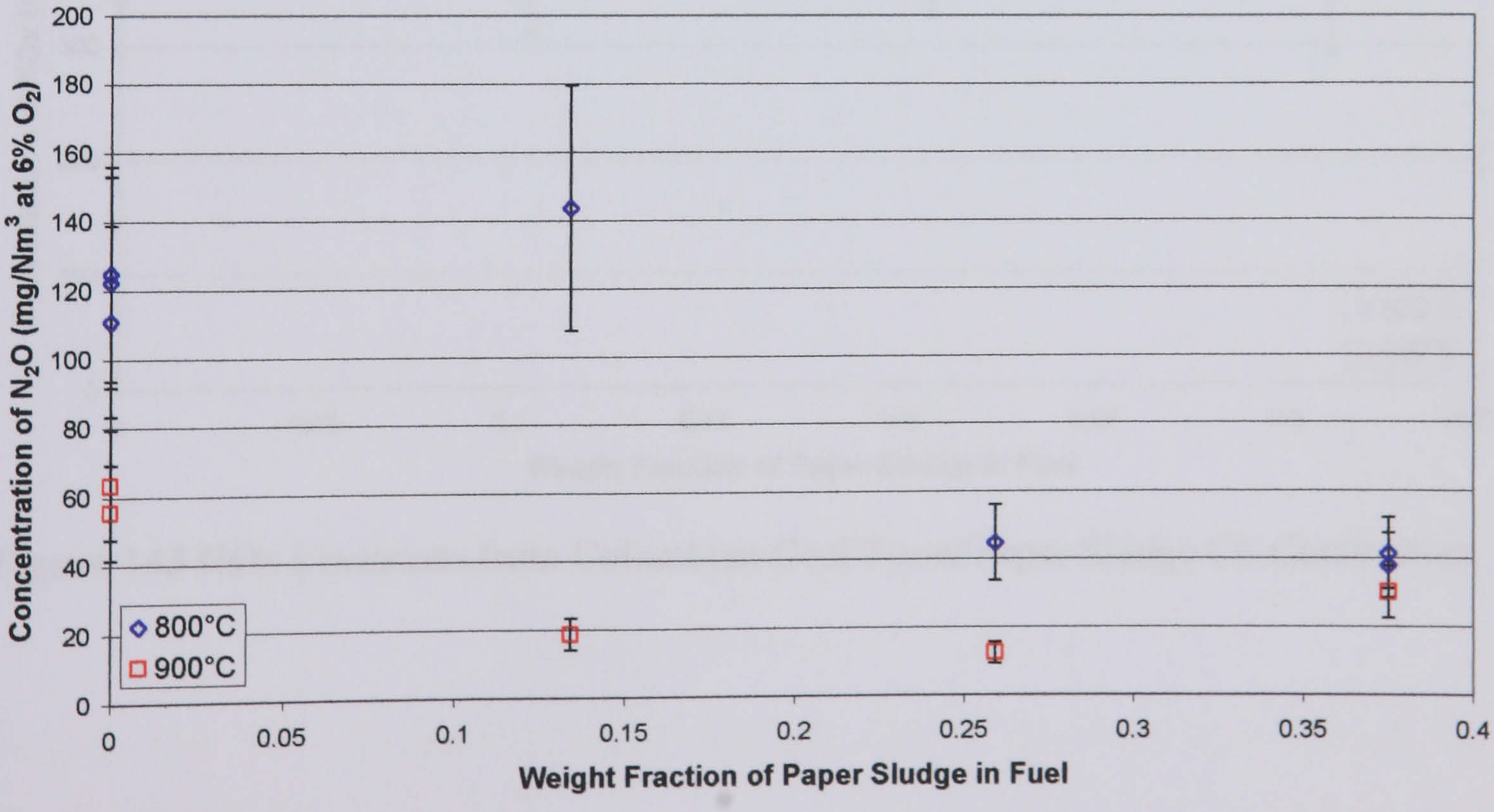


Figure 142 N_2O Emissions from Colombian Coal and Paper Sludge Co-Combustion

5.9.3 Colombian Coal/Straw and Paper Sludge Blends

Adding paper sludge to Colombian coal / straw (50:50 blend on energy basis) made little difference to NOx emissions compared to those from combustion of the Colombian coal / straw mixture on its own (Figure 143). The combustion temperature (800 or 900 °C) also had little influence on NOx emissions.

Co - combustion of Colombian coal with straw decreased NOx emission (compare Figure 141 with Figure 143). This decrease was expected as the straw had a lower nitrogen content (0.60 % as received) than the Colombian coal (1.40 % as received). This decrease has been partially offset by increased conversion of fuel nitrogen to NO (Figure 144). Possibly, this was due to less NO reduction on char. Less char was generated during combustion of this blend because the straw contained more volatile matter than the Colombian coal (89.9 % daf). Addition of paper sludge to Colombian coal / straw made no significant change to fuel nitrogen conversion to NO.

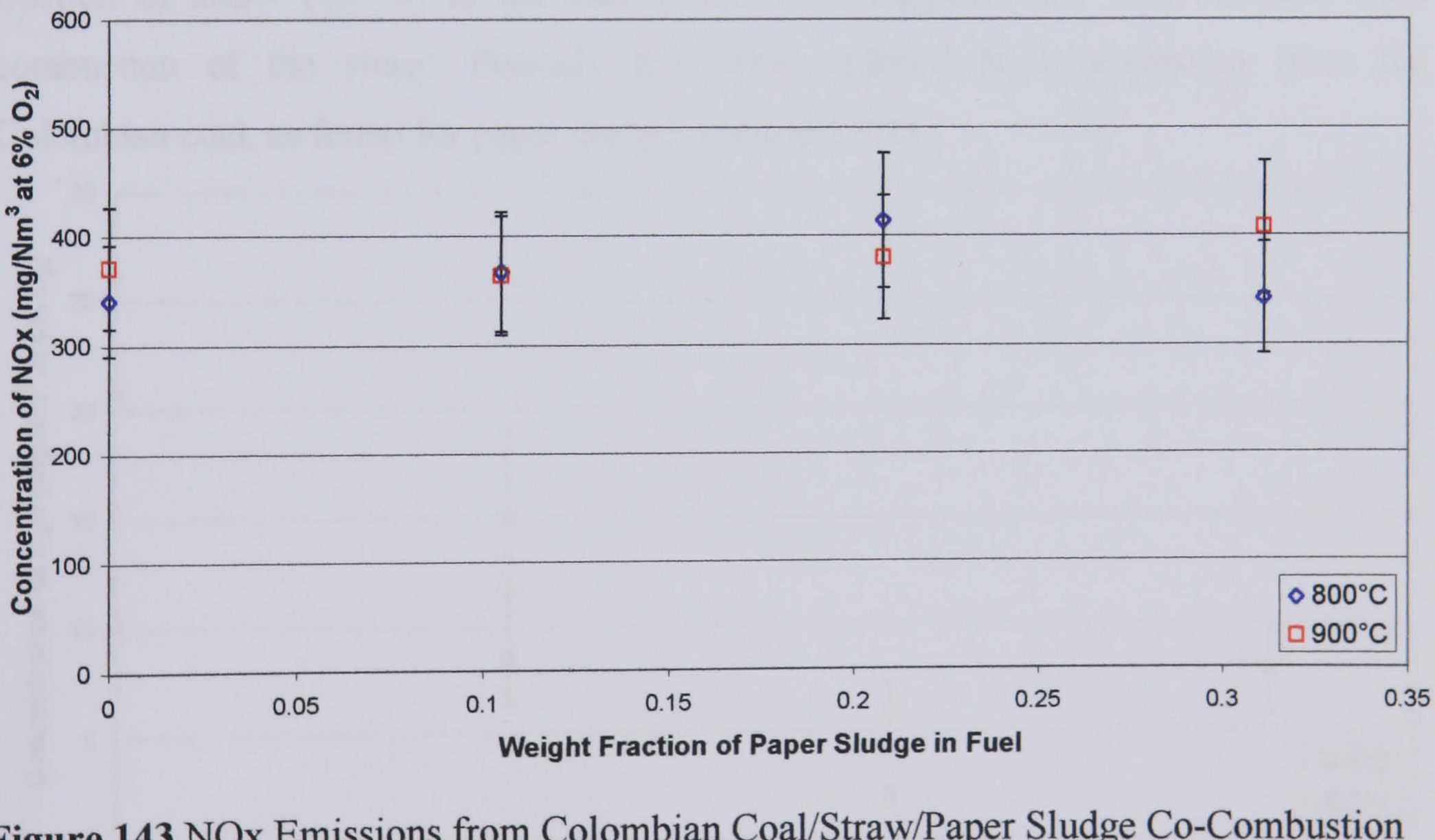


Figure 143 NOx Emissions from Colombian Coal/Straw/Paper Sludge Co-Combustion

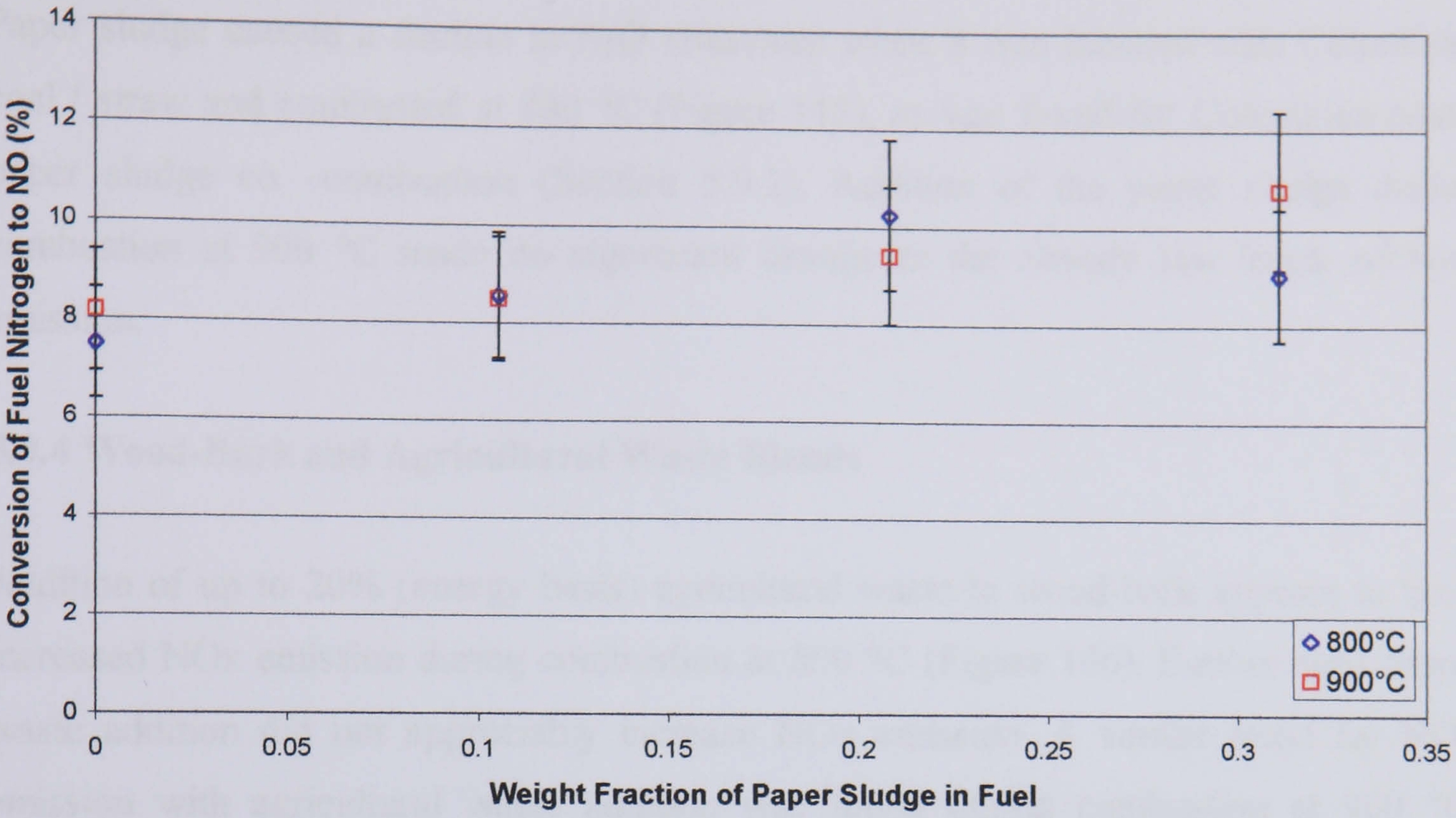


Figure 144 Conversion of Colombian Coal / Straw / Paper Sludge Fuel Nitrogen to NO

Co-combustion of Colombian coal with straw decreased N_2O emissions by approximately 75 % (Figure 145). The reduction was slightly greater than the weight fraction of straw (63 %) in the fuel blend. This suggests little N_2O resulted from combustion of the straw. Possibly the straw reduced N_2O originating from the Colombian coal, as found for paper sludge (section 5.9.2).

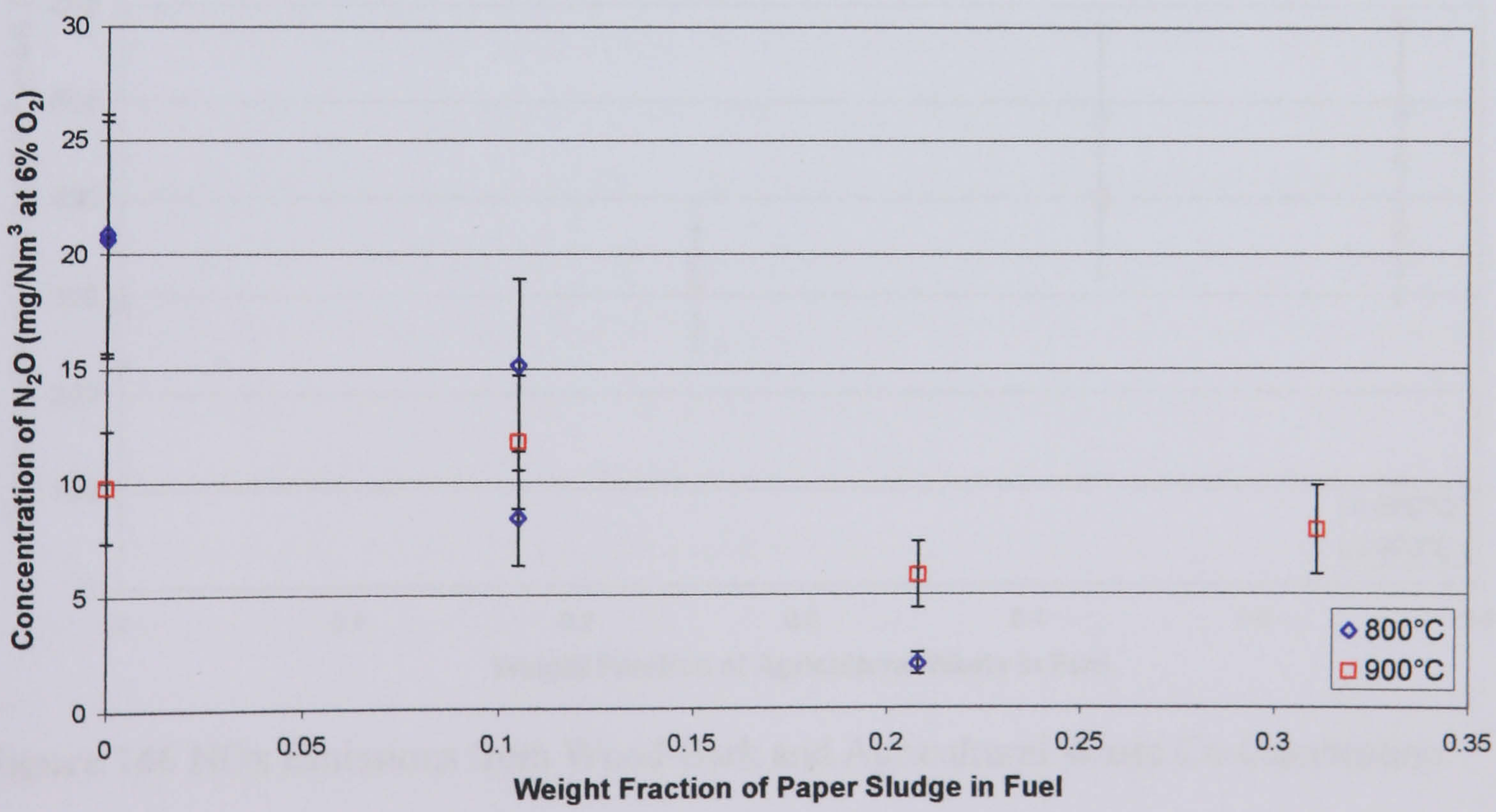


Figure 145 N_2O Emissions from Colombian Coal / Straw / Paper Sludge Co-Combustion

(Note: N_2O emission from combustion of Colombian Coal/Straw with 30% Paper sludge at 800 °C was below the detection limit of 2 mg/Nm^3)

Paper sludge caused a decline in N_2O emissions when it was blended with Colombian coal / straw and combusted at 800 °C (Figure 145), as was found for Colombian coal / paper sludge co –combustion (Section 5.9.2). Addition of the paper sludge during combustion at 900 °C made no significant change to the already low levels of N_2O emission.

5.9.4 Wood-Bark and Agricultural Waste Blends

Addition of up to 20% (energy basis) agricultural waste to wood-bark appears to have increased NOx emission during combustion at 800 °C (Figure 146). Further agricultural waste addition did not appreciably increase NOx emission. A similar trend for NOx emission with agricultural waste addition was found during combustion at 900 °C, though weaker, and within the range of experimental error.

There was no significant effect of combustion temperature on NOx emissions from combustion of wood-bark / agricultural waste blends, all differences were inside the range of experimental error.

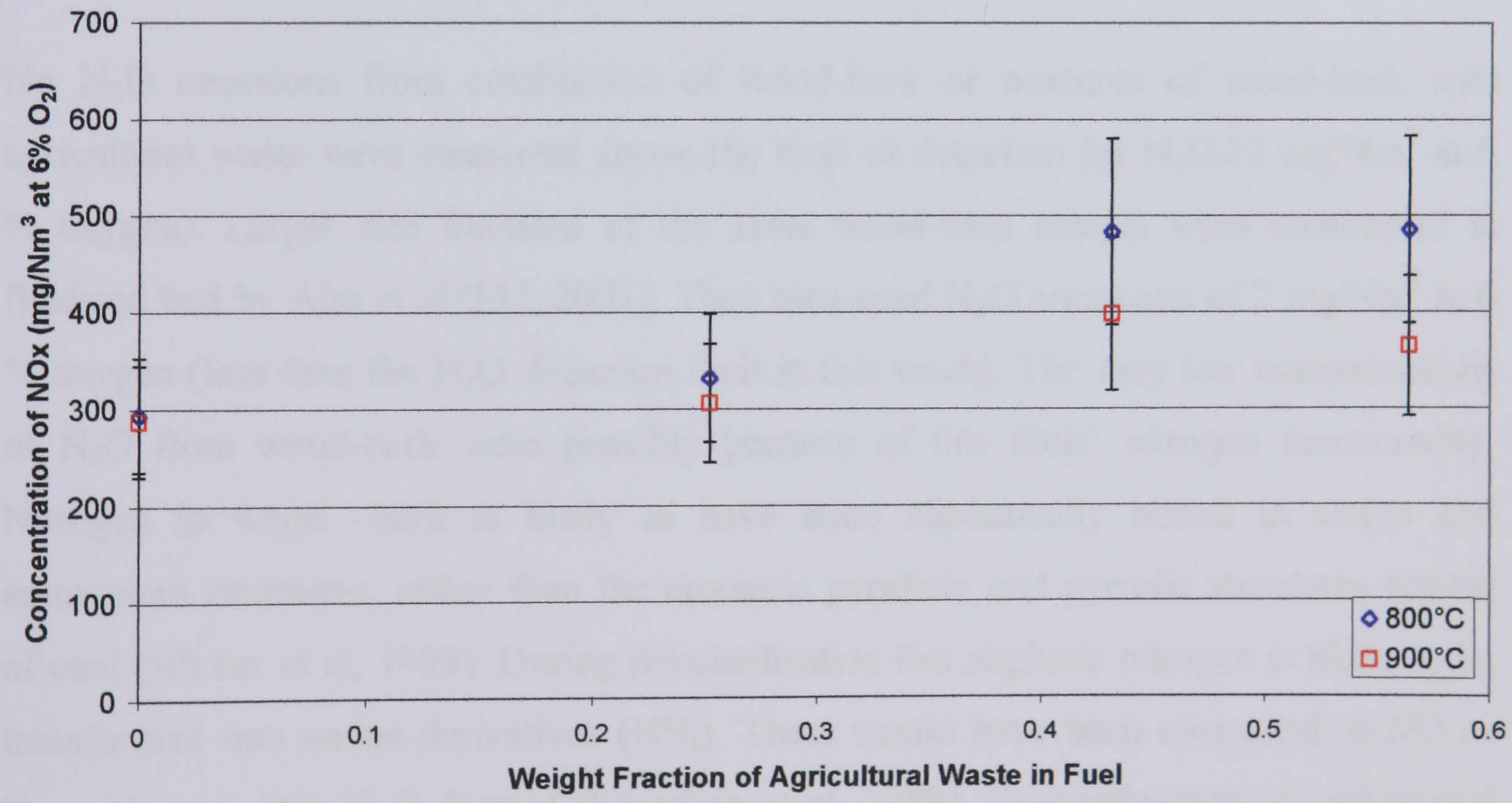


Figure 146 NOx Emissions from Wood-Bark and Agricultural Waste Co-Combustion

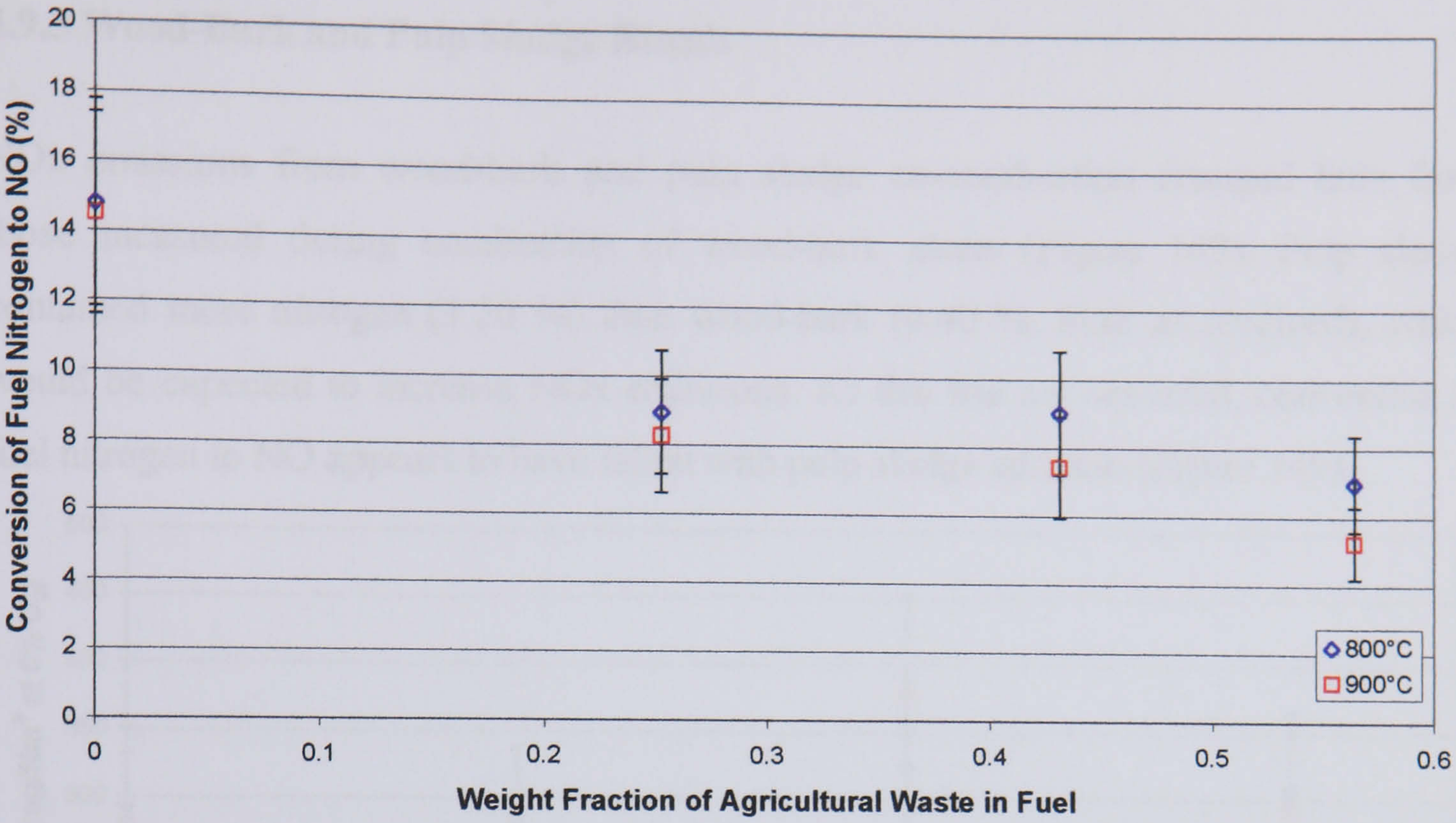


Figure 147 Conversion of Wood-Bark and Agricultural Waste Fuel Nitrogen to NO

Though NOx emissions rose with the addition of up to 20 % agricultural waste, the conversion of fuel nitrogen to NO fell (Figure 147). This result is similar to that obtained for the Polish coal / sewage sludge blends (section 7.1).

No N_2O emissions from combustion of wood-bark or mixtures of wood-bark with agricultural waste were measured above the limit of detection for N_2O (3 mg/Nm^3 at 6 % oxygen). Larger size fractions of the same wood-bark sample were combusted in fluidised bed by Aho et al (EU, 2001). They measured N_2O emissions of 2 mg/Nm^3 at 6 % oxygen (less than the N_2O detection limit in this work). The very low concentrations of N_2O from wood-bark were possibly because of this fuels' nitrogen functionality. Nitrogen in wood –bark is likely to have been aliphatically bound in amino and ammonium structures, rather than the aromatic pyridinic and pyrrolic structures typical of coal (Winter et al, 1999). During devolatilisation this aliphatic nitrogen is likely to be transformed into amine derivatives (NH_i). These would have been converted to NO or N_2, with very little N_2O formed (Kramlich et al, 1989). Co-combustion of agricultural waste with wood-bark did not produce measurable N_2O emissions. This could have been because of the nitrogen functionality in this fuel. Alternatively, agricultural waste derived N_2O may have also been destroyed by the wood-bark. This would be similar to the results found for paper sludge in this study (Section 5.9.2), and by Amand et al (1991) when they injected N_2O into the fluidising air of a FBC burning wood.

5.9.5 Wood-Bark and Pulp Sludge Blends

NOx emissions from wood-bark and pulp sludge co-combustion changed little from those measured during combustion of wood-bark alone (Figure 148). Pulp sludge contained more nitrogen (1.20 %) than wood-bark (0.40 %, both as received), which would be expected to increase NOx emissions. As this has not occurred, conversion of fuel nitrogen to NO appears to have fallen with pulp sludge addition (Figure 149).

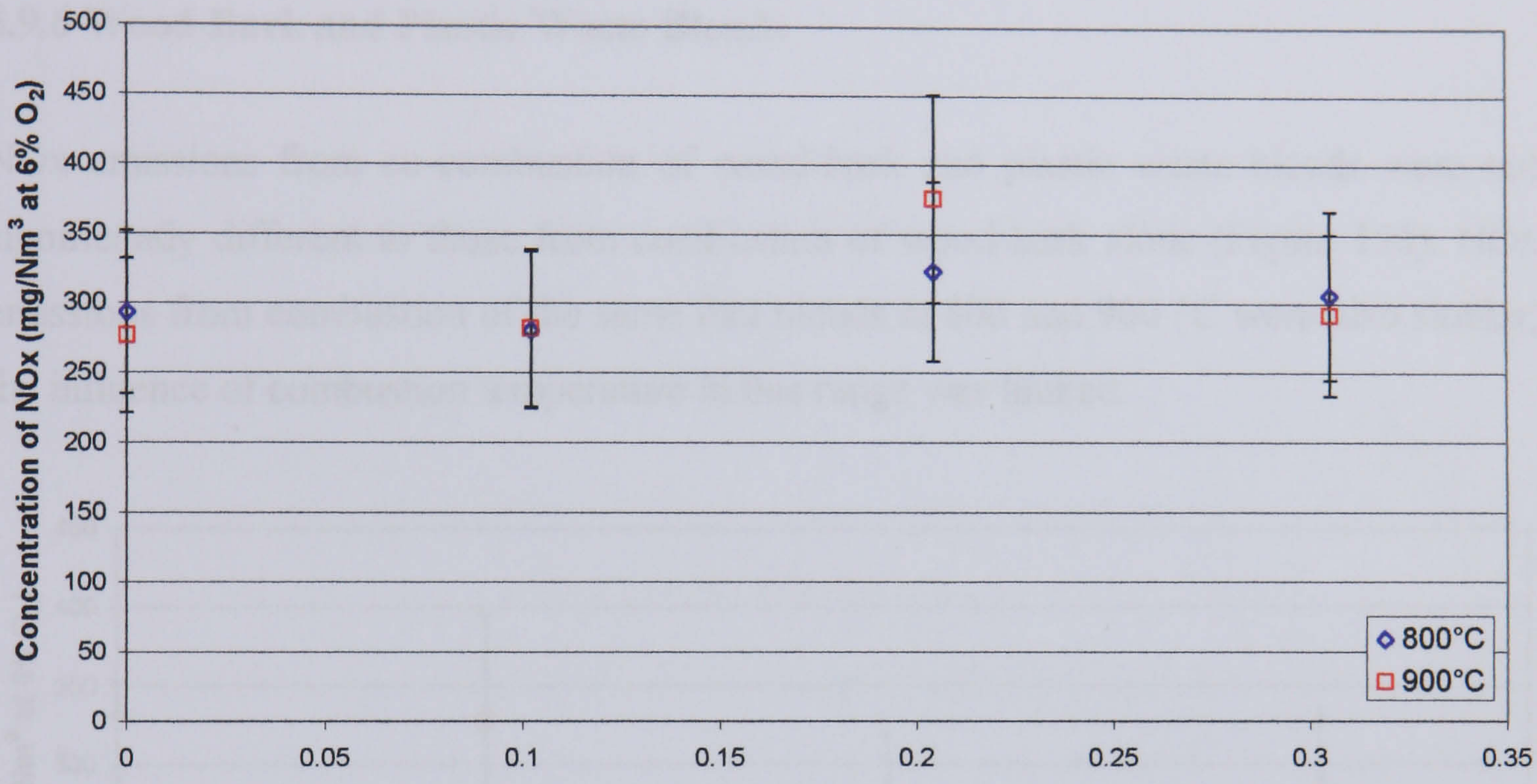


Figure 148 NOx Emissions Wood-Bark and Pulp Sludge from Co-combustion

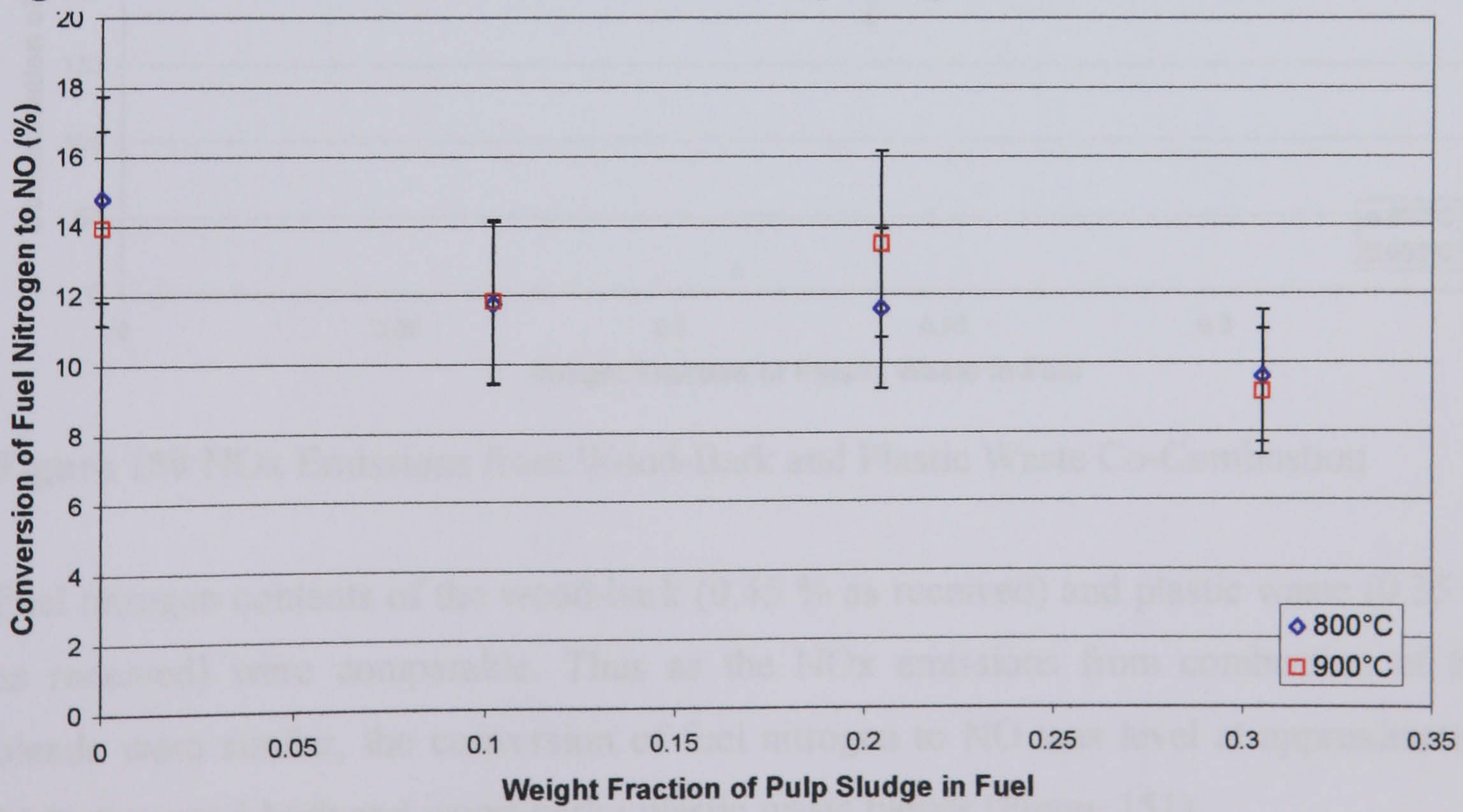


Figure 149 Conversion of Wood-Bark and Pulp Sludge Fuel Nitrogen to NO

No emissions of N_2O from wood-bark and pulp sludge blends were measured above the N_2O detection limit of 3 mg/Nm^3. Low N_2O emissions were possibly because of the nitrogen functionality in the wood-bark (section 5.9.4). This could also be the cause of the low N_2O emissions from wood-bark / pulp sludge blends. The organic fraction of the pulp sludge is essentially wood and its nitrogen functionalities are unlikely to have changed from those in the parent wood material.

5.9.6 Wood-Bark and Plastic Waste Blends

NOx emissions from co-combustion of wood-bark and plastic waste blends were not significantly different to those from combustion of wood-bark alone (Figure 150). NOx emissions from combustion of the same fuel blends at 800 and 900 °C were also similar; the influence of combustion temperature in this range was limited.

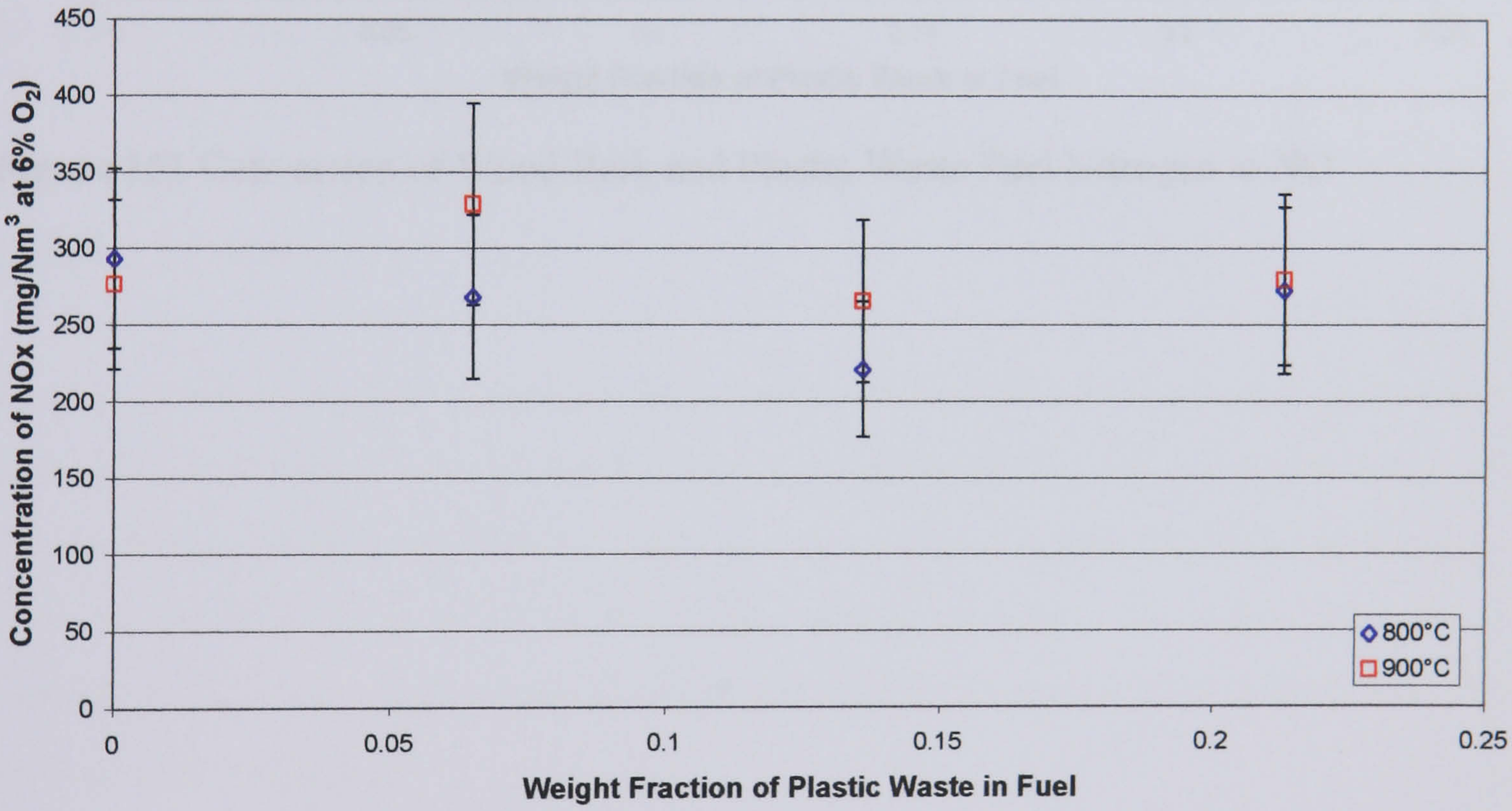


Figure 150 NOx Emissions from Wood-Bark and Plastic Waste Co-Combustion

Fuel nitrogen contents of the wood-bark (0.45 % as received) and plastic waste (0.35 % as received) were comparable. Thus as the NOx emissions from combustion of the blends were similar, the conversion of fuel nitrogen to NO was level at approximately 14 % for wood-bark and wood-bark / plastic waste blends (Figure 151).

No emissions of N_2O above the limit of detection (3 mg/Nm^3) were measured from co combustion of wood-bark and plastic waste blends. Possible reasons for low N_2O

emission from wood-bark were discussed in section 5.9.4. These could be applicable to plastic waste also, as nitrogen in plastic waste is unlikely to occur in the pyridinic or pyrrolic groups found in coal, but to be aliphatically bound as in common nitrogen containing plastics nylon and polyacrlonitrile.

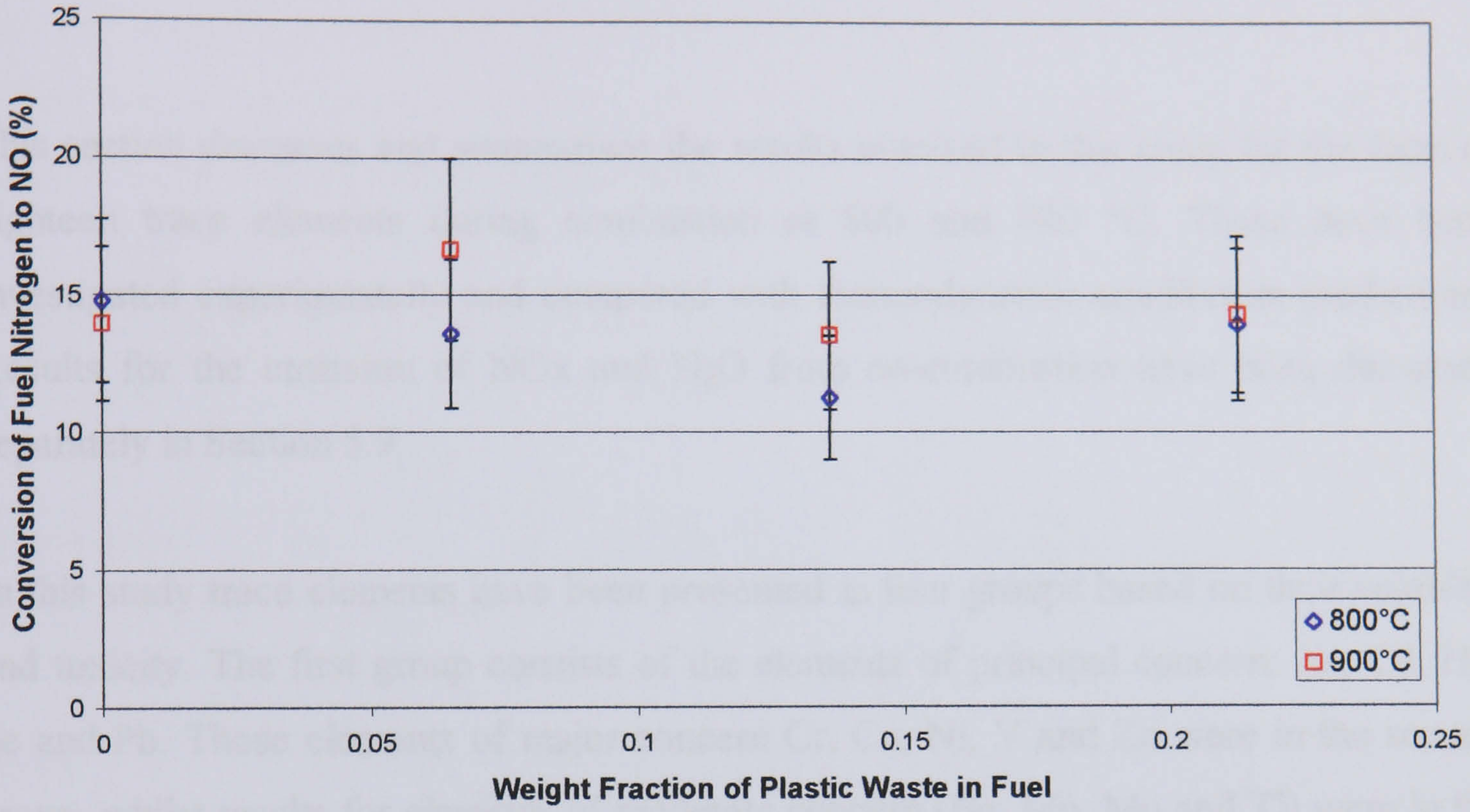


Figure 151 Conversion of Wood-Bark and Plastic Waste Fuel Nitrogen to NO

6.0 SUMMARY AND DISCUSSION OF TRACE ELEMENT RESULTS

This section discusses and summarises the results obtained in this study for the fates of eighteen trace elements during combustion at 800 and 900 °C. These have been investigated experimentally and compared with thermodynamic equilibrium predictions. Results for the emission of NOx and N_2O from co-combustion have been discussed separately in Section 5.9.

In this study trace elements have been presented in four groups based on their volatility and toxicity. The first group consists of the elements of principal concern: As, Cd, Hg, Se and Pb. Those elements of major concern Cr, Cu, Ni, V and Zn were in the second group, whilst results for elements of moderate concern (Be, Mn, Mo and Tl) were in the third. Other elements studied (Ba, Co, Sb and Sr) were presented in the fourth group, elements of minor concern.

Measurements of the trace element concentrations in the raw fuels and ashes were made by ICP-MS, ICP-AES (Mn, V and Zn) and Leco analyser (Hg only). Measurements of the percentage retention of trace elements in ash were in general subject to experimental error levels of at least ± 25 %. Variations above or below this error range were encountered: the actual experimental error varied with the raw fuel combusted and the trace element measured.

In the summary presented below, percentage retention in ash of trace elements after combustion has been divided into three categories. The first category consists of elements considered as almost completely volatilised during combustion, where less than 20 % of the amounts originally present in the fuel were retained in ash. In the second category were elements considered as having been almost completely retained; these were those with greater than 80 % retention in the ash. In the final category were elements that were partially volatilised. These were retained in proportions intermediate to the other two categories.

6.1 Trace Element Contents of the Raw Fuels

Sewage sludge had the highest trace element content of the fuels studied (Table 15). It contained the highest concentrations of As, Co, Cr, Cu, Hg, Ni, Mo, Sr and Zn. Straw had the lowest trace element content, with concentrations of As, Be, Cd and Se all falling below the limits of quantification. Trace element contents of the other fuel samples were broadly similar to each other.

Table 15 Trace Element Concentrations in the Raw Fuels

Fuel	Less than 1 ppm	1 to 10 ppm	10 – 100 ppm	Greater than 100 ppm
Wood-Bark	As, Be, Cd, Co, Hg, Se, Sb, Tl	Ni, Mo, Pb, V	Cr, Cu, Sr	Ba, Mn, Zn
Straw	As, Be, Cd, Co, Hg, Ni, Mo, Sb, Tl, V	Cr, Cu, Pb	Ba, Mn, Zn	
Colombian Coal	Be, Cd, Hg, Sb, Tl	As, Co, Cu, Ni, Mo, Pb, Se	Ba, Cr, Mn, Sr, V, Zn	
Polish Coal	Cd, Hg, Mo, Tl	As, Be, Co, Sb, Se	Cr, Cu, Ni, Pb, Sr, V, Zn	Ba, Mn
Sewage Sludge	Be, Hg, Tl	As, Cd, Co, Sb	Ni, Mo, Pb, V	Ba, Cr, Cu, Mn, Sr, Zn
Paper Sludge	As, Be, Cd, Co, Hg, Se, Tl	Ni, Mo, Sb, V	Cr, Cu, Mn, Pb, Sr	Ba, Zn
Agricultural Waste	As, Be, Cd, Co, Hg, Pb, Sb, Se, Tl	Cr, Mo, V	Ba, Ni, Sr, Cu	Mn, Zn
Pulp Sludge	As, Be, Co, Hg, Mo, Sb, Se, Tl	Cd, Pb, V	Ba, Cr, Cu, Ni, Sr	Mn, Zn
Plastic Waste	As, Be, Hg, Se, Tl	Cd, Co, Ni, Mo, Sb, V	Cr, Cu, Mn, Pb, Sr	Ba, Zn

6.2 Behaviour of Trace Elements During Co-Combustion

6.2.1 The Effect of Combustion Temperature

For most of the trace elements investigated in this study, the difference in the proportion of trace element retained in ash after combustion at 800 and 900 °C was smaller than experimental error. Thus, no significant influence of combustion temperature on percentage retention could be found by experimenting in this range. The few cases where the 100 °C temperature difference was important are mentioned in the discussion of the behaviour of that particular trace element.

6.2.2 Retention of Trace Elements Predicted to Volatilise

Some of the trace elements were predicted by thermodynamic calculations to volatilise much more than was found experimentally. However, any of the trace elements studied could have been retained in the ash because of the way that they were bound in the original fuel. Certain components of the mineral matter may not transform thermally, preventing release of their trace element inventories at the experiment temperatures used here. The limitation may also have been kinetic, the time allowed not being sufficient for the original or intermediate form to decompose. The mode of occurrence in the fuel is therefore an important factor in the behaviour of almost all trace elements. The possible modes of occurrence of each trace element are numerous and complex. Their determination in the original fuels is an important topic for further study.

6.2.3 Volatilisation of Trace Elements Predicted to Remain Completely in Ash

Some elements were volatilised during combustion, contrary to the prediction of thermodynamic equilibrium modelling. This is likely to occur where the trace element was partly held in the organic matrix of the raw fuel. During combustion the organic matrix would burn away and trace elements contained (dispersed) inside that matrix would be released into the gas phase. The released trace element may immediately recondense on ash particles, if it is thermodynamically favoured to form a solid. Recondensation, however, appears to be kinetically constrained. There is only a short

time (< 2 s) for it to occur. Any atoms of the trace element that have not recondensed will exit the suspension-firing reactor with the flue gas.

Trace elements bound in inorganic matrices may similarly be volatilised if these original forms decompose during combustion (e.g. pyrite). The extent to which parent inorganic matrices decompose is likely to be smaller than that of organic matrices so they may not release trace elements trapped within to the same extent.

6.2.4 Elements of Principal Concern (As, Cd, Hg, Pb, Se)

Arsenic was partially volatilised during the combustion of coal containing fuels, except for sewage sludge and Polish coal / sewage sludge blends combusted at 900 °C. Here there appeared to be a synergy for the retention of arsenic in the ash, possibly due to the formation of magnesium arsenate. This compound, along with iron and calcium arsenates was predicted by thermodynamic equilibrium modelling to retain arsenic in the ash of all fuels. Partial volatilisation of arsenic from coal containing fuels shows that these compounds did not form to the extents predicted.

The synergy in arsenic retention between Polish coal and sewage sludge could have also been caused by the high sulphur content of the sewage sludge. When SO_2 was injected during the combustion of wood-bark, this increased arsenic retention in ash. The compound that formed to increase arsenic retention in this case is unknown. It does not appear to have been included in the thermodynamic database. Formation of this compound may also have caused arsenic enrichment on the sinter ash of the wood-bark and pulp sludge blends.

Enrichment of arsenic on wood-bark sinter ash was also increased by the combustion of wood-bark in the presence of injected HCl. This was not predicted by thermodynamic equilibrium modelling, but may have also happened during combustion of the high chlorine content wood-bark / plastic waste blends. These results again suggest formation of an unknown arsenic compound not included in the database.

Cadmium was partially volatilised from all fuel samples and blends except Colombian coal / straw, where measurement of the proportion volatilised was precluded by

experimental error. Thermodynamic equilibrium predictions suggested complete volatilisation of cadmium in the suspension reactor for all fuels except sewage sludge, where $CdO.SiO_2$ was predicted to form at up to 850 °C. Cadmium was enriched on the sinter ash of sewage sludge, Colombian coal and some blends of wood-bark with agricultural waste, pulp sludge and plastic waste. For sewage sludge this enrichment could have been through the formation of $CdO.SiO_2$. However, for the other fuels no solid cadmium compounds were predicted to form. For Colombian coal at least, enrichment of cadmium on sinter ash could have been through reaction with mineral matter. Kaolin was found by Lachas (1999) to capture volatilised cadmium, as was bauxite and alumina (Scotto et al, 1993). Other mineral matter may also have been active in capturing volatilised cadmium.

The presence of injected SO_2 or HCl during combustion decreased the percentage retention of cadmium in wood-bark ash. When HCl was injected this was probably because of increased $CdCl_2$ gas formation. The cause of increased cadmium volatilisation when SO_2 was injected was not clear.

Mercury was almost completely volatilised during combustion of almost all fuel samples. Thermodynamic equilibrium models for all fuels predicted this. Mercury retention in ash was increased by the injection of SO_2 during wood-bark combustion, although this was not predicted by thermodynamic equilibrium modelling. Mercury was also enriched on the sinter ash of many fuels, at temperatures where mercury is normally thought to be completely gaseous. These results suggest that a solid mercury compound (or compounds) can retain mercury at high temperatures. Identifying these compounds may lead to a way of reducing the volatilisation of mercury from power plant.

Selenium was almost completely volatilised during combustion of all fuel samples, except sewage sludge and Polish coal / sewage sludge blends. It was almost completely retained by sewage sludge ash while retention increased with the sewage sludge proportion in Polish coal / sewage sludge blends. Complete selenium volatilisation, as SeO and SeO_2 gases was predicted by thermodynamic equilibrium models of all fuels and blends. Selenium retained in ash may not have been released from its mode of

occurrence in the fuels, or was retained by formation of $CaSeO_4$, suggested by Clements et al (1999) to retain selenium in ashes of high calcium coals.

Lead was partially volatilised during combustion of all fuel samples, except Colombian coal, Colombian coal / straw burnt at 800 °C and Polish coal / sewage sludge blends also burnt at 800 °C, where it was almost completely retained in ash. Between Polish coal and sewage sludge, there appeared to be a synergy for lead retention. This could have been caused by lead sulphate formation, predicted by thermodynamic equilibrium models of the combustion of these fuels and for Colombian coal. Lead may also have been retained in Colombian coal ash by reaction of lead with silicate and alumino silicates. Alumino silicate compounds were found by Scotto et al (1993) and Lachas (1999) to react with volatilised lead at temperatures similar to those in the suspension reactor.

Thermodynamic equilibrium models for other fuels suggested that lead would be completely volatilised, as Pb, PbO and $PbCl_2$ gases. Injection of HCl during wood-bark combustion however, had no influence on lead retention in ash. Probably all of the lead that could be liberated from the wood-bark was released regardless of whether the HCl was injected.

6.2.5 Elements of Major Concern (Cr, Cu, Ni, V, Zn)

Chromium was partially volatilised during the combustion of most fuel samples. Thermodynamic equilibrium modelling suggested that almost all chromium would be retained in ash as Cr_2O_3. This was not the case. Its volatilisation took place to a greater degree than predicted by thermodynamic equilibrium modelling. Volatilisation of chromium was attributed to single chromium atoms released from the fuel forming CrO_3 gas. Few of these molecules would be able to react and form Cr_2O_3 because of the low chromium concentration in the gas phase. Chromium in wood-bark was unaffected by injection of HCl or SO_2 during combustion, consistent with chromium preferentially forming oxides during combustion.

Copper was partially volatilised from all fuels where measurements could be made, except Colombian coal, sewage sludge, Polish coal / sewage sludge blends and

agricultural waste burnt at 900 °C, where it was almost completely retained in ash. Thermodynamic equilibrium modelling predicted almost complete copper retention in ash by formation of aluminium or iron containing copper compounds. Where copper was volatilised these compounds did not form to the extent predicted. This may have been due to the limited opportunity for copper to react with aluminium or iron. Injected HCl lowered the retention of copper in wood-bark ash, probably also because it prevented formation of CuO and the iron – copper species otherwise predicted and increased the formation of the volatile $CuCl_2$ species.

Nickel was partially volatilised from blends of Colombian coal with paper sludge and of Polish coal with sewage sludge (900 °C only). Nickel was almost completely retained in the ash of the other fuel samples. Complete nickel retention in ash was predicted by thermodynamic equilibrium modelling for all fuel samples and blends.

Vanadium was partially volatilised from Colombian coal / straw and fuels containing wood-bark or paper sludge. Other fuel samples retained almost all of their original vanadium in the ash. Thermodynamic equilibrium modelling predicted complete vanadium retention in the ashes of all fuels. This was by formation of VO_2, V_2O_5 and compounds with calcium, iron and magnesium. Partial volatilisation may have been because vanadium was released from the fuels (possibly from the organic fraction) and incompletely recondensed on ash. Vanadium remaining in the gas phase would have exited the suspension-reactor with the gas flow, as described in 6.2.3.

Zinc was partially volatilised during combustion of Colombian coal / straw and fuels containing wood-bark or paper sludge. For other fuel samples it was almost completely retained in ash. Complete zinc retention in ash was predicted for all fuels except Colombian coal / straw and those containing paper sludge. For these fuels thermodynamic modelling predicted $ZnCl_2$ gas formation. $ZnCl_2$ formation may have also caused the decrease in zinc retention seen when wood-bark was combusted in the presence of injected HCl. Zinc volatilised from fuels where its complete retention in ash was predicted, probably incompletely recondensed after release from the fuel (section 6.2.3).

6.2.6 Elements of Moderate Concern (Be, Mn, Mo, Tl)

Beryllium was partially volatilised from Polish coal, Colombian coal / straw and blends containing paper sludge. Other samples appeared to retain most of their beryllium in the ash. Thermodynamic equilibrium modelling predicted beryllium to remain in the ashes of all fuels combusted at 800 °C and Colombian coal, Polish coal, sewage sludge and Polish coal / sewage sludge blends burnt at 900 °C. For Polish coal, more beryllium was volatilised than predicted. This was attributed to beryllium released from the fuel not fully recondensing on the ash (section 6.2.3). For wood-bark and blends of wood-bark with pulp sludge and plastic waste, beryllium retention was higher than predicted. Beryllium was probably held in these fuels by modes of occurrence from which it was not released during combustion.

Manganese was partially volatilised during the combustion of all fuels except agricultural waste. Thermodynamic equilibrium modelling, however, predicted manganese to remain completely in the ash. It is likely that the volatilisation of manganese is the result of its incomplete recondensation after release into the gas phase during combustion (section 6.2.3). Partial recondensation on sinter ash of wood-bark blends caused manganese enrichment. Retention of manganese in wood-bark ash was decreased by the injection of HCl during the combustion. This was thought to have occurred because of the formation of $MnCl_2$ gas

Molybdenum was partially volatilised from most fuels, with the exception of wood-bark, wood-bark / plastic waste blends, sewage sludge burnt at 800 °C and wood-bark / pulp sludge blends also burnt at 800 °C. For these fuels molybdenum appeared to be completely retained in ash.

Thallium was almost completely volatilised from Colombian coal / straw whilst almost completely retained by sewage sludge ash. It was partially volatilised from all other fuels. There appeared to be slight synergies for thallium release between Colombian coal and paper sludge and between wood-bark and agricultural waste. Thermodynamic equilibrium models of all fuels predicted complete thallium volatilisation. If this had occurred there would not be any synergy. An unknown solid thallium compound (or compounds) appears to have retained thallium on some ashes.

6.2.7 Elements of Minor Concern (Ba, Co, Sb, Sr)

Barium was partially volatilised from wood-bark, Colombian coal / straw burnt at 900 °C and blends containing wood-bark or paper sludge. All other fuels retained almost all of their barium in the ash. Complete retention of barium in ash was predicted for all fuels by thermodynamic equilibrium modelling. Partial volatilisation of barium was probably because it did not completely recondense after release from these fuels (Section 6.2.3). Barium was sensitive to chlorine, but only where it was present in very high concentrations. Its retention in wood-bark ash was reduced by the presence of injected HCl, probably because of the formation of $BaCl_2$ gas.

Cobalt partially volatilised from Colombian coal at 800 °C, Colombian coal / straw and some blends containing pulp or paper sludge. Otherwise cobalt was almost completely retained in ash. Complete retention of cobalt in ash was predicted for all fuels by thermodynamic equilibrium modelling. Where cobalt was volatilised this was attributed to its incomplete recondensation after release into the gas phase, as described in Section 6.2.3, above.

Antimony was partially volatilised from all fuels and blends where measurements of percentage retention could be made, except sewage sludge and Polish coal / sewage sludge blends burnt at 800 °C. Partial antimony volatilisation at 900 °C was predicted by thermodynamic equilibrium modelling of all fuels except sewage sludge, wood-bark and wood-bark / pulp sludge blends. The higher volatilisation than predicted for some fuels was thought to be due to only partial recondensation of antimony released from the fuel during combustion (Section 6.2.3).

Strontium was partially volatilised from all fuels except agricultural waste, sewage sludge and Polish coal / sewage sludge blends. It was almost completely retained in the ashes of these fuels. Thermodynamic equilibrium modelling predicted complete strontium retention in ashes of all fuels. Volatilised strontium was probably that unable to recondense in the short (<2 s) time available (Section 6.2.3).

6.3 Influence of Fuel Type on Trace Element Retention

Retention of trace elements depended partially on fuels from which they were derived; thus it is likely that the modes of occurrence of trace elements in the fuels influenced their behaviour during combustion (Table 16).

Table 16 Retention of Trace Elements in Ash

Fuel	Percentage of Trace Element Retained in Ash				
	0 – 20 %	21 – 40 %	41 – 60 %	61 – 80 %	81 – 100 %
Wood-Bark	Hg	As, Pb, Tl, Zn	Cd, Cu	Ba, Cr, Mn, Sb, Sr, V	Be, Co, Mo, Ni
Colombian Coal / Straw	Hg, Se, Tl	As, Cd	Be, Cr, Mo, Zn	Co, Mn, Pb, Sr, V	Ba, Ni, Sb,
Colombian Coal	Hg, Se	As, Cd,		Cr, Mn, Mo, Sb, Sr, Tl	Ba, Be, Pb, Co, Cu, Ni, V, Zn
Polish Coal	Hg, Se	Tl	As, Cd, Pb, Sb	Ba, Cr, Cu Mo, Sr	Be, Co, Mn, Ni, V, Zn
Sewage Sludge	Hg	Cd		As, Cr, Mo, Ni, Pb	Ba, Be, Co, Cu, Mn, Sb, Se, Sr, Tl, V, Zn
Paper Sludge	Cd, Hg, Se	As, Mo, Pb, V, Sr	Ba, Be, Co, Cr, Mn, Sb, Zn	Cu	Ni
Agricultural Waste	Cd, Hg	V, Tl	Pb, Zn	Be, Cr, Cu	As, Ba, Co, Mn, Ni, Sr
Pulp Sludge	Cd, Hg, Tl	Cu, Pb, Zn	Ba, Mn, Sr, V	Be, Cr, Mo, Sb	Co, Ni,
Plastic Waste	Hg	Cd, Cu, Pb, Tl, Zn	V	Cr, Ba, Mn, Sr	Be, Co, Mo, Ni

Average of 800 and 900 °C results displayed. Results for paper sludge, pulp sludge and plastic waste estimated from the behaviour of these fuels in blends.

Paper sludge released the largest proportion of its trace elements, including Ba, Co and Sr which were retained to a much greater degree by the other fuels. By contrast, sewage sludge retained its trace elements to the greatest degree of all the fuels tested. Some of the sewage sludge (< 5 %) melted during combustion of this fuel on its own, although this was not thought to have affected trace element behaviour significantly.

The trace elements investigated in this study have been ranked based on their average retention in ash. This ranking is presented, descending from most volatile to least volatile, in Table 17. Where elements have been placed in the same group they are listed in order of decreasing volatility. Although the proportions each trace elements retained in ash vary significantly with each fuel (above), the average result is similar to that reported by Clarke and Sloss (1992) for trace elements in pulverised coal combustion (Figure 2, Section 2.3). The only notable difference between the average results and the diagram of Clarke and Sloss was the observed increased volatility of manganese.

Table 17 Relative Volatility of Trace Elements During Combustion of the Present Set of Fuels at Temperatures Between 800 and 900 °C

Most Volatile	Hg, Se
	Cd, Tl, Pb, As
	Zn, Sb, Cr, V, Cu, Sr, Mo, Mn, Ba
Least Volatile	Be, Co, Ni

6.4 Possible Problematical Trace Element Emissions during Combustion

Results from the suspension-firing reactor indicate the maximum possible release of trace elements from the fuels during fluidised bed combustion. In actual fluidised bed combustors lower proportions of the trace elements would be released, due to their recondensation on fly ash as the flue gas cools. Taking into account trace element concentrations in the fuel (Table 15), the proportions volatilised (Table 16) and potential toxicity, several trace element – fuel combinations that could be problematical in fluidised bed combustion have been identified as follows (Table 18):

Table 18 Potentially Problematic Fuel - Trace Element Combinations

Fuel	Trace Element
Wood-Bark	Cu, Zn
Colombian Coal / Straw	Se
Colombian Coal	Se
Polish Coal	As, Pb
Sewage Sludge	Cd, Hg
Paper Sludge	Cr, Pb, Zn
Agricultural Waste	Hg, V, Zn
Pulp Sludge	Cd, Cu, Zn
Plastic Waste	Cd, Cu, Pb, Zn

7.0 CONCLUSIONS

7.1 Trace Element Contents of the Raw Fuels

Sewage sludge had the highest trace element content of the fuels studied and straw the lowest. Trace element contents of the other fuels samples were broadly similar.

7.2 Trace Element Behaviour During Co-Combustion

The trace elements investigated in this study were ranked based on their relative retention in the ashes of the fuel samples. Hg and Se were found to be the most volatile elements, followed by Cd, Tl, Pb and As. A majority of the Zn, Sb, Cr, V, Cu, Sr, Mo, Mn and Ba contents of the fuels were retained in ash. Be, Co and Ni were retained to the highest degree.

In this study, the behaviour of trace elements were investigated experimentally and simulated mathematically, using a thermodynamic prediction package (MTDATA). Comparison of results led to three conclusions relevant to the behaviour of most trace elements.

1. For most trace elements, there was no significant difference in the proportion retained in ash after combustion at 900 °C and that remaining after combustion at 800 °C.

2. For many trace elements (Be, Cd, Hg, Pb, Sb, Se, Tl and Zn) a proportion of the element appeared to be retained in the ash despite the thermodynamic prediction of volatility. The fractions of the trace elements that are retained are probably incorporated in the parent fuel in modes of occurrence that either do not allow escape during combustion or, at least, have insufficient time to decompose during combustion.

3. Some trace elements (including Ba, Be, Co, Mn, Sr and V) were volatilised from the fuels contrary to the prediction of the thermodynamic equilibrium model. These elements are thought to be associated with the organic matrix or some other easily volatilisable mode of occurrence of the parent fuel. Some proportion of the trace element liberated from the fuel would have been expected to recondense. However, this process was probably kinetically hindered, since the time available for recondensation is short (<2 s), and a significant proportion of the released element would thus be swept out of the suspension reactor by the gas flow.

7.3 Influence of Fuel Type on Trace Element Retention

Retention of trace elements in ash depended partially on the fuel from which the elements were derived. Paper sludge released the largest proportion of its trace elements and, in particular, Ba, Co and Sr which were retained to a much greater degree by the other fuels. Whereas sewage sludge retained more of its trace elements than any of the other fuels tested. Therefore, to some extent, trace element release appears to depend on the structure and composition of the parent fuel.

7.4 Possible Problematical Trace Elements Emissions from Combustion

The trace element–fuel combinations that could be problematical in fluidised bed combustion were identified, taking into account the original trace element concentrations in the fuel, the degree of volatilisation observed and the potential toxicity. The principal potential problems were emissions of Cu and Zn from the combustion of wood-bark, emissions of As and Pb from Polish coal, and emissions of Cd and Hg from sewage sludge. Cr, Pb and Zn emissions from combustion of paper sludge were also thought to be potentially problematic, as was Se from Colombian coal and from Colombian coal / straw blends. Emissions of Hg, V and Zn from agricultural waste were also identified as potentially problematic, as were those of Cd, Cu and Zn from pulp sludge combustion and the same elements and Pb from plastic waste.

7.5 NOx and N_2O Emissions from Co-Combustion

NOx

1. Raising the combustion temperature from 800 to 900 °C had no significant effect on NOx emission for any fuel except the 70 % Polish coal / 30 % sewage sludge blend, where the NOx emission increased from 350 to 580 mg/m^3.

2. Addition of sewage sludge to Polish coal increased NOx emission from 350 to 580 mg/m^3 during combustion at 900 °C. However, there was no significant change in NOx emissions, from 380 mg/m^3, when sewage sludge was added to Polish coal at 800 °C.

3. NOx emissions from Colombian coal (500 mg/m^3) or Colombian coal / straw (350 mg/m^3) combustion were not significantly effected by blending these fuels with paper sludge.

4. NOx emissions were increased from approximately 290 mg/m^3 up to 500 mg/m^3 by the addition of agricultural waste to wood-bark. Addition of pulp sludge or plastic waste to wood-bark had no significant effect on the NOx emissions.

N_2O

1. The highest N_2O emission was from a Polish coal / sewage sludge blend (140 mg/m^3) followed by Colombian coal (120 mg/m^3), and Colombian coal / straw (20 mg/m^3). Wood-bark and blends containing wood bark produced little (<2 mg/Nm^3) N_2O when combusted.

2. N_2O emissions from combustion at 800 °C were similar to or higher than those from combustion at 900 °C.

3. Paper sludge was effective in decreasing N_2O emissions from Colombian coal, possibly because of a synergy between these fuels.

8.0 RECOMMENDATIONS FOR FUTURE WORK

Several results from this study of trace element release and NOx and N_2O emissions from co-combustion merit further exploration.

1. The mode in which a trace element occurs in the raw fuel appears to be one of the important factors determining its behaviour at fluidised bed combustion temperatures (800 – 900 °C). Identification of the trace element modes of occurrence in each of the fuels combusted in this study would allow better interpretation of the observed behaviour of trace element between the different fuels.

2. A large proportion of the mercury contained in fuel for power stations escapes with the flue gas. However, mercury enrichment on sinter ash has been observed here for several fuel blends and when wood-bark was combusted in the presence of injected SO_2. Mercury has thus recondensed on ash at temperatures where it would normally be gaseous. Identification of the mechanism by which this mercury was retained on the ash may lead to a way of reducing its emission in the gas phase from commercial combustors.

3. Improvement of the modelling of trace element behaviour could perhaps be achieved by utilising a computation fluid dynamic (CFD) model of combustion inside the reactor, in tandem with the thermodynamic equilibrium model. Utilisation of a CFD model would allow properties such as the local temperature and gas composition to vary inside the reactor thereby defining conditions within the combustion volume more precisely. The calculation of the reaction of species could then be done by thermodynamic equilibrium modelling, as employed in this study or, where chemical kinetic data permitted, by a reaction system model.

REFERENCES

Aho (2001) "Reduction of toxic emissions from co-combustion of coal, biomass and waste in fluidised beds", Final Report, EU Project JOR3-CT97-0191.

Amand, L.E.and S. Anderson (1989) "Emissions of Nitrous Oxide (N_2O) from fluidized bed boilers" Proc. 10th Int. Conference on Fluidized Bed Combustion, San Francisco, p49.

Amand, L.E.and Leckner, B. (1993) "Reduction of N_2O in a circulating fluidised bed combustor", *Fuel*, 73(9), p1389-1397.

Angelidis, M. and Gibbs, R.J. (1989) "Chemistry of metals in anaerobically treated sludges", *Water Research*, 23(1), p 29-33.

Bailey, J.H.E. and Reeve, D.W. (1994) "Spatial distribution of trace elements in black spruce by imaging microprobe secondary ion mass spectrometry", *J. Pulp and Paper Sci.*, 20(3), p J83-87.

Bailey, J.H.E. and Reeve, D.W. (1994) "Determination of the spatial distribution of trace elements in jack pine, pinas banksiana Lamb., by imaging microprobe secondary ion mass spectrometry", *J. Pulp and Paper Sci.*, 22(8), p J275-279.

Bonn, B., Pelz, G. and Baumann, H. (1995) "Formation and Decomposition of N_2O in Fluidized Bed Boilers" *Fuel* 74(2) p165-171.

Bool, L.E. and Helble, J.J.(1995) " A laboratory study of the partitioning of trace elements during pulverised coal combustion" *Energy and Fuels*, 9, p880-887.

Cai, H. (1995) "Fast Pyrolysis of Coals and Char Characterisation in Relation to Pulverised Coal Combustion", PhD thesis, Imperial College.

Cenni,R., Frandsen, F., Gerhardt, T., Spliethoff, H. and Hein, K.R.G. (1998) "Study on trace metal partitioning in pulverized combustion of bituminous coal and dry sewage sludge" *Waste Management*, 18, p433-444.

Chu, C.W., Poon C.S. and Cheung, R.Y.H. (1998) "Characterisation of raw sewage, chemically modified sludge and aerobically digested sludge in Hong Kong", *Water Sci. Tech.*, 38(2), p25-32.

Clarke, L.B. and Sloss, L.L. (1992) "Trace elements - emissions from coal combustion and gasification", Report IEACR/49, IEA Coal Research, London UK.

Clements, A.H. Damiano, L.F. Gong, D. Matheson, T.W. (1999) "Partitioning behaviour of some toxic volatile elements during stoker and fluidised bed combustion of alkaline sub-bituminous coal" *Fuel*, 78, p1379-1385.

Conference on the North Sea (1990) "Ministerial Declaration of the Third International Conference on the Protection of the North Sea" The Hague.

Croiset, E, Heurtebise, C, Rouan, J-P and Richard, J-R. (1998) "Influence of Pressure on the Heterogeneous Formation and Destruction of Nitrogen Oxides during Char Combustion" *Combustion and Flame*, 112(1) p33-44.

Davison, R.M. (1993) "Organic sulphur in coal" IEA report IEACR/60, IEA Coal Research, London.

Davison, R.M. (1994) "Nitrogen in coal" IEA report IEAPER/08, IEA Coal Research, London.

De Soete, G.G.(1990) "Heterogeneous N_2O and NO Formation from bound nitrogen atoms during char combustion", *23rd Symposium (int.) on Combustion*, p1257 - 1264.

Delay, I., Swithenbank, J. and Argent, B.B. (1999) "Prediction of the distribution of alkali and trace elements between the condensed and gaseous phases generated during

clinical waste incinerations", *Proceedings of the 2nd Int. Symp. on Incineration and Flue Gas Treatment Technologies*, Sheffield University p 14.

Durlak, S.K., Biswas, P. and Shi, J. (1997) "Equilibrium analysis of the effect of temperature, moisture and sodium content on heavy metal emissions from municipal soild waste incinerators", *J. Hazardous Materials*, 56, p 1 - 20.

Fenimore, C.P. (1971) "Formation of nitric acid in premixed hydrocarbon flames", *13th Int. Symp. On Combustion.* The Combustion Institute, Pittsburgh, PA, p 373.

Finkelman, R.B. (1994) "Modes of occurrence of potentially hazardous elements in coal: levels of confidence", *Fuel Processing Technology*, 39, p21-34.

Fisher, G.L., Chrisp, C.E. and Raabe, O.G. (1979) *Science,* 204, p 879.

Frandsen, F. Dam-Johansen, K. and Rasmussen, P (1994) "Trace elements from combustion and gasification of coal - an equilibrium approach", *Prog. Energy Combust. Sci.* 20, p115-138.

Gulyurtlu (1995) "A comparison of NOx levels from research and development studies with valves measured at different plants", *Fuel,* 74(2), p253 – 257.

Handcock, M and Rothon, R.N., (1995) "Principal types of particle fillers", in Particulate-Filled Polymer Composites, Rothon, R Editor, Longman Scientific and Technical, London.

Hassett, D.J. and Eylands, K.E. (1999) "Mercury capture on coal combustion fly ash", *Fuel*, 78, p 243 – 248.

Hoy, H.R. and Gill, D.W. (1987) "Combustion of coal in fluidised beds" In Principals of Combustion Engineering for Boilers, Lawn C.J. ed; Academic Press: London, pp544.

Huggins, F.E. Zhao, J Shah, N. Huffman, G.P. (1994) "Modes of occurrence of trace elements in coal from XAFS spectroscopy", *ACS Division of Fuel Chemistry Preprints*, 39(2), p504-508.

Hulgaard, T. Glarborg, P. and Dam-Johansen, K.(1991), *1991 Fludized Bed Combustion,* ed. E.J. Anthony ASME, New York, 2, p991.

Inhat, M. and Fernandes, L. (1996) "Trace element characterisation of composted poultry manure", *Bioresource Tech.*, 57, p 143 – 156.

Jones, J.M., Patterson, P.M., Pourkashanian, M. and Williams, A (1999) "Approaches to modelling heterogeneous char NO formation / destruction during pulverised coal combustion", *Carbon*, 37(10), p 1545 – 1552.

Kawasaki, A., Kimura, R. and Arai, S.(2000) "Fractionation of trace elements in wastewater treatment sludges" *Commun. Soil. Sci. Plant Anal.*, 31(11-14), p 2413 – 2423.

Kendrick, M.J., May, M.T., Plishka, M.J. and Robinson, K.D. (1992) "Metals in biological systems", Ellis Harwood.

Khraisha, Y. (1998) PhD Thesis, University of London.

Kilpinen, P and Hupa, M. (1991) "Homogeneous N2O Chemistry at Fluidised Bed Combustion Conditions: A Kinetic Modelling Study" *Combustion and Flame* 85 p94-104.

Kramlich, J.C., Cole, J.A., McCarthy, J.M., Lanier, W.S. and McSorley, J.A., (1989) "Mechanisms of NO formation in coal flames", *Combustion and Flame*, 77, p375.

Lachas, H.; Richaud, R.; Jarvis, K.E.; Herod, A.A.; Dugwell, D.R.; Kandiyoti, R.(1999) "Determination of 17 trace elements in coal and ash reference materials by ICP-MS applied to milligram sample sizes", *The Analyst*,124, pp177-184.

Lachas, H. (1999) "Trace element partitioning and emission control during coal gasification", PhD Thesis, University of London.

Landsberger, S., Chicester, D.L. (1995) "Characterisation of household plastics for heavy metals using neutron activation analysis", *J. Radioanalytical and Nuclear Chem.*, 192(2), p 287 – 297.

Latva-Somppi, J., Kauppinen, E.I., Valmeri, T., Ahonen, P., Gurav, A.S., Kodas, T.T. and Johanson, B. (1988) "The ash formation during co-combustion of wood and sludge in industrial fluidised bed boilers", *Fuel Proc. Tech.*, 54, p 74 – 94.

Linak, W.P. and Wendt, J.O.L. (1994) "Trace metal transformation mechanisms during coal combustion" *Fuel Processing Tech.*, 39, p173-198.

Lind, T. Kauppinen, E.I. and Jokiniemi, J.K. (1994) "A field study on the trace element behaviour in atmospheric circulating fluidised bed coal combustion" *25th Int. Symp. on Combustion*, p201-209.

Mascia, L. (1974) "The role of additives in plastics" Edward Arnold Publishers, London.

Miller, J.A., and Bowman, C.T. (1989) "Mechanism and modelling of nitrogen chemistry in combustion", *Prog. Energy. Combust. Sci.*, 15, p287.

Mojtahedi, W. (1989) "Trace metals volatilisation in fluidised bed combustion and gasification of coal", *Combustion Sci. and Tech.*, 63, p209-227.

Molina, A., Eddings, E.G., Pershing, D.W. and Sarofim, A.F. (year) "Char nitrogen conversion: implications to emissions from coal-fired utility boilers", *Prog. Energy and Combust. Sci.*, 26, p 507 - 531.

Moritomi, H., Y. Suzuki, N. Kido, Y. Ogisu (1991), "NOx Formation Mechanism of circulating fluidised bed combustion", *Proc. 11th Int. Conf. On Fluidised Bed Combustion*, Montreal, p1005.

Morrison, G.F. (1980) "Nitrogen oxides from combustion- abatement and control" Report no. ICTIS/TR11, IEA Coal Research, London, p13.

Muzio, L.J. and Kramlich, J.C. (1988) "An Artifact in measurement of N_2O from combustion sources", *Geophys. Res. Lett.*, 15, p1369.

Nomura, D.H., Mateus, S.F., Saiki, M. and Bode, P. (2000) "Characterisation of inorganic compounds in plastic materials", *J. Radio and Analytical Chem.*, 244(1), p 61 – 65.

Raask, E. (1985) "The mode of occurrence and concentration of trace elements in coal", *Prog. Energy Combust. Sci.*, 11, p97-118.

Reed, G.P., Dugwell, D.R. and Kandiyoti, R. (2001) "Control of trace elements in a gasifier hot gas filter: a comparision with predictions from a thermodynamic equilibrium model", Submitted to Energy and Fuels.

Richaud, R, (1999) PhD Thesis, University of London.

Richaud, R. Lazaro, M-J. Lachas, H. Miller, B.B. Herod, A.A. Dugwell, D.R. and Kandiyoti, R. (1999a) "Identification of organically associated trace elements in wood and coal by ICP-mass spectrometry" *Rapid Commun. In Mass Spectrometry*, 14, p 317 - 328.

Richaud, R., Lachas, H., Healey, A.E., Reed, G.P., Haines, J., Mason, P., Herod, A.A., Dugwell, D.R. and Kandiyoti, R. (1999b), "Trace element analysis of gasification plant samples by ICP-MS: validation by comparison of results from two laboratories," Fuel (accepted for publication).

Roby, R.J. and Bowman, C.T. (1987) "Formation of N_2O in Laminar, premixed, fuel rich flames", *Combustion and Flame*, 70, p119.

Scotto, M.V., Uberoi, M., Peterson, T.W., Shadman, F., Wendt, J.O.L. (1994) "Metal capture by sorbents in combustion Processes", *Fuel Proc. Tech.*, 39, p 357 – 372.

Skipperand, L., Salbu, B., Hagebø, E. (1998) "Transfer, pathways, enrichment and discharge of trace elements in the pulp industry measured by means of neutron activation analysis" *The Sci. of the Total Environ.*, 216, p 133 – 146.

Sunderman, F.W. J. Boil. Trace Element Res., vol 1, p63, 1979.

Swaine, D.J. (1990) "Trace elements in coal", Butterworths, London.

Swaine, D.J. (1994) "Trace elements in coal and their dispersal during combustion", *Fuel Processing Technology*, 39, p.121-137.

Thompson, D and Argent, BB (1995) "The use of thermodynamic computation packages to predict the reactions occurring during combustion and gasification in fluidised beds" *3rd Int. Conf. on Combustion Technologies for a Clean Environment*, Lisbon, paper 16-1, p1-10.

US National Research Council (1980) "Trace element geochemistry of coal resource development related to environmental quality and health", PECH Report, National Academy Press, Washington DC.

Watt R.G. (1997) "Engineering Response to Global Climate Change", CRC Press, New York p109.

Wiese, R.G. Muir, I.J. Fyfe, W.S. (1990) "Trace-element siting in iron sulfides in Ohio coals determined by secondary ion mass spectroscopy (SIMS)", *Int. J. of Coal Geology*, 14, p 155-174.

Winter, F., Wartha, C., Hofbauer, H. (1999) "NO and N2O formation during the combustion of wood, straw, malt waste and peat" *Bioresource Tech.*, 70, p 39 – 49.

Yousif, S (2000), PhD Thesis, University of London.